63rd ANNUAL

HIGHWAY GEOLOGY SYMPOSIUM

PROCEEDINGS

Redding, California

May 7th - 10th, 2012

www.HighwayGeologySymposium.org

Hosted By

The California State Department of Transportation

The California Geological Survey

63rd ANNUAL
HIGHWAY GEOLOGY SYMPOSIUM
Table of Contents

63rd ANNUAL
HIGHWAY GEOLOGY SYMPOSIUM

Redding, California
May 7th – 10th, 2012

Local Organizing Committee Members

Bill Webster CEG	Caltrans, Engineering Geologist
Roy Bibbens GE	Caltrans, Chief, Office of Geotechnical Design North
Charlie Narwold CEG	Caltrans, Senior Engineering Geologist
John D. Duffy CEG	Caltrans, Senior Engineering Geologist
Thomas Whitman CEG	Caltrans, Senior Engineering Geologist
Brian Hinman PE	Caltrans, Senior Transportation Engineer
Brandon Badeker CEG	Caltrans, Engineering Geologist
Chris Koepke CEG	Caltrans, Engineering Geologist
Scott Lewis CEG	Caltrans, Engineering Geologist
Richard Rusnak PE	Caltrans, Transportation Engineer
Chris Wills CEG	California Geological Survey, Supervising Engineering Geologist
Chris Higgins PG	California Geological Survey, Senior Geologist

Special Thanks:

John Parrish PG	California Geological Survey, State Geologist
James Davis PE	Caltrans, Acting Division Chief, Division of Engineering Services
Phil Stolarski PE	Caltrans, Chief Materials Engineering & Testing and Geotechnical Services
John Bulinski PE	Caltrans, District 2 Director
Stephen Most	Keynote Speaker

HIGHWAY GEOLOGY SYMPOSIUM
National Steering Committee Officers

Jeff Dean –
CHAIRMAN
Oklahoma Department of Transportation
200 NE 21st St.
Oklahoma City, OK 73105
Phone: (405) 522-0988
Fax: (405) 522-4519
Email: jdean@odot.org

Vanessa Bateman -
VICE-CHAIRMAN
Term: 7/2011 until 2013
USACE
Email: vanessa.c.bateman@usace.army.mil

Tom Eliassen -
SECRETARY
State of Vermont, Agency of Transportation
Materials & Research Section
National Life Building, Drawer 33
Montpelier, VT 05633
Phone: (802) 828-6916
Fax: (802) 828-2792
Email: tom.eliassen@state.vt.us

Russell Glass –
TREASURER
(Publications & Proceedings)
NCDOT (Retired)\
100 Wolf Cove
Asheville, NC 28804
Phone: (828) 252-2260
Email: frgeol@aol.com

HIGHWAY GEOLOGY SYMPOSIUM
National Steering Committee Members

Ken Ashton –
(Membership)
West VA Geological Survey
P.O. Box 879
Morgantown, WV 26507-0879
Phone: (304) 594-233
Fax: (304) 594-2575
Email: ashton@geosrv.wvnet.edu

Vanessa Bateman –
VICE-CHAIRMAN
Term: 7/2011 until 2013
USACE
Email: vanessa.c.bateman@usace.army.mil

Jim Coffin –
Wyoming Department of Transportation
Geology Program
5300 Bishop Blvd.
Cheyenne, WY 82009-3340
Phone: (307) 777-4205
Fax: (307) 777-3994
Email: jim.coffin@dot.state.wy.us

Richard Cross –
Golder Associates
RD 1 Box 183A
Sloansville, NY 12160
Phone: (518) 868-4820
Cell: (603) 867-4191
Email: dick_Cross@juno.com

Jeff Dean –
CHAIRMAN
Oklahoma Department of Transportation
200 NE 21st St.
Oklahoma City, OK 73105
Phone: (405) 522-0988
Fax: (405) 522-4519
Email: jdean@odot.org

John D. Duffy –
Caltrans
50 Higuera St.
San Luis Obispo, CA 93401
Phone: (805) 527-2275
Fax: (805) 549-3297
Email: John_D_Duffy@dot.ca.gov

Tom Eliassen –
SECRETARY
State of Vermont, Agency of Transportation
Materials & Research Section
National Life Building, Drawer 33
Montpelier, VT 05633
Phone: (802) 828-6916
Fax: (802) 828-2792
Email: tom.eliassen@state.vt.us

Russell Glass –
TREASURER
(Publications & Proceedings)
NCDOT (Retired)
100 Wolf Cove
Asheville, NC 28804
Phone: (828) 252-2260
Email: frgeol@aol.com

Bob Henthorne –
Materials and Research Center
2300 Van Buren
Topeka, KS 66611-1195
Phone: (785) 291-3860
Fax: (785) 296-2526
Email: roberth@ksdot.org

Peter Ingraham –
Golder Associates
670 North Commercial Street, Suite 103
Manchester, New Hampshire 03101-1146
Phone: (603) 668-0880
Fax: (603) 668-1199
Email: pingraham@golder.com

HIGHWAY GEOLOGY SYMPOSIUM
National Steering Committee Members

Daniel Journeaux –
Email: daniel@acadiafarm.com

Richard Lane –
NHDOT, Bureau of Materials and Research
5 Hazen Drive
Concord, NH 03301
Phone: (603) 271-3151
Fax: (603) 271-8700
Email: lanetrisbr@hotmail.com

Henry Mathis –
(By-Laws)
H. C. Nutting Co. / Terracon
561 Marblerock Way
Lexington, KY 40503
Cell: (859) 361-8362
Fax: (859)455-8630
Email: hmathis@iglou.com

Harry Moore –
(Historian, Appt.)
Tennessee DOT (Retired)
Golder Assciates
302 McKinney Road
Blaine, TN 37709
Phone: (770) 496-1893
Cell: (865) 603-7652
Fax: (770) 934-9476
Email: HLMoore@golder.com

John Pilipchuk –
NCDOT Geotechnical Engineering Unit
5253 Z-Max Blvd
Harrisburg, NC 28075
Phone: (704) 455-8902
Fax: (704) 455-8912
Email: jpilipchuk@ncdot.gov

Victoria Porto –
PA DOT Bureau of Construction and Materials
(Retired)
1080 Creek Road
Carlisle, PA 17015
Phone: (717) 805-5941
Email: vamporto@aol.com

Nick Priznar –
Arizona D.O.T.
121 N. 21st Ave. 068R
Phoenix AZ, 85009
Phone: (602) 712-8089
Fax: (602) 712-8138
Email: npriznar@azdot.gov

Erik Rorem –
Geobrugg North America, LLC
22 Centro Algodones
Algodones, New Mexico 87001
Phone: (505) 771 4080
Fax: (505) 771 4081
Email: erik.rorem@geobrugg.com

HIGHWAY GEOLOGY SYMPOSIUM
National Steering Committee Members

Christopher A. Ruppen –
(Connections) (YAA)
Michael Baker Jr., Inc.
4301 Dutch Ridge Rd.
Beaver, PA 15009-9600
Phone: (724) 495-4079
Cell: (412) 848-2305
Fax: (724) 495-4017
Email: cruppen@mbakercorp.com

Jim Stroud (Appt.) –
4541 Araby Lane
East Bend, NC 27018
Phone: (336) 699-2217
Cell: (336) 416-3656
Email: gemsjims@hotmail.com

John F. Szturo –
HNTB Corporation
715 Kirk Drive
Kansas City, MO 64105
Phone: (Direct Line) (816) 527-2275
Cell: (913) 530-2579
Fax: (816) 472-5013
Email jszturo@hntb.com

Michael P. Vierling –
(YAA)
Canal Design Bureau
New York State Thruway Authority
200 Southern Blvd
Albany, NY 12209
Phone: (518) 471-4378
Fax: (518) 436-3060
Email: michael_vierling@thruway.state.ny.us

Stephen Senior –
Ministry of Transportation, Ontario
1201 Wilson Ave.
Rm 220, Building C
Downsview, ON M3M IJ6
Canada
Phone: (416) 235-3734
Fax: (416) 235-4101
Email: stephen.senior@ontario.ca

Steven Sweeney –
New York State Canal Corporation
21 Woodlake Road, Apt. 1
Albany, NY 12203
Phone: (518) 334-2511
Email: ssweeney2@nycap.rr.com

Robert Thommen –
Rotec International, LLC
P.O.Box 31536
Sante Fe, NM 87594-1536
Phone: (505) 989-3353
Fax: (505) 984-8868
Email: thommen@swcp.com

Terry West –
(Medallion, Emeritus)
Earth and Atmospheric Science Dept.
Purdue University
West Lafayette, IN 47907-1297
Phone: (765) 494-3296
Fax: (765)496-1210
Email: trwest@purdue.edu

HIGHWAY GEOLOGY SYMPOSIUM
History, Organization, and Function

Established to foster a better understanding and closer cooperation between geologists and civil engineers in the highway industry, the Highway Geology Symposium (HGS) was organized and held its first meeting on March 14, 1950, in Richmond Virginia. Attending the inaugural meeting were representatives from state highway departments (as referred to at that time) from Georgia, South Carolina, North Carolina, Virginia, Kentucky, West Virginia, Maryland, and Pennsylvania. In addition, a number of federal agencies and universities were represented. A total of nine technical papers were presented.

W.T. Parrott, an engineering geologist with the Virginia Department of Highways, chaired the first meeting. It was Mr. Parrott who originated the Highway Geology Symposium.

It was at the 1956 meeting that future HGS leader, A.C. Dodson, began his active role in participating in the Symposium. Mr. Dodson was the Chief Geologist for the North Carolina State Highway and Public Works Commission, which sponsored the 7th HGS meeting.

Since the initial meeting, 62 consecutive annual meetings have been held in 32 different states. Between 1950 and 1962, the meetings were east of the Mississippi River, with Virginia, West Virginia, Ohio, Maryland, North Carolina, Pennsylvania, Georgia, Florida, and Tennessee serving as host state.

In 1962, the symposium moved west for the first time to Phoenix, Arizona where the 13th annual HGS meeting was held. Since then it has alternated, for the most part, back and forth from the east to the west. The Annual Symposium has moved to different location as listed on the next page.

Unlike most groups and organizations that meet on a regular basis, the Highway Geology Symposium has no central headquarters, no annual dues and no formal membership requirements. The governing body of the Symposium is a steering committee composed of approximately 20 - 25 engineering geologist and geotechnical engineers from state and federal agencies, colleges and universities, as well as private service companies and consulting firms throughout the country. Steering committee members are elected for three-year terms, with their elections and re-elections being determined principally by their interests and participation in and contribution to the Symposium. The officers include a chairman, vice chairman, secretary, and treasurer, all of whom are elected for a two-year term. Officers, except for the treasurer, may only succeed themselves for one additional term.

A number of three-member standing committees conduct the affairs of the organization. The lack of rigid requirements, routing and relatively relaxed overall functioning of the organization is what attracts many participants.

Meeting sites are chosen two to four years in advance and are selected by the Steering Committee following presentations made by representatives of potential host states. These presentations are usually made at the steering committee meeting, which is held during the Annual Symposium. Upon selection, the state representative becomes the state chairman and a member pro-tem of the Steering Committee.

List of Highway Geology Symposium Meetings

No.	Year	HGS Location	No.	Year	HGS Location
1st	1950	Richmond, VA	2nd	1951	Richmond, VA
3rd	1952	Lexington, VA	4th	1953	Charleston, WV
5th	1954	Columbus, OH	6th	1955	Baltimore, MD
7th	1956	Raleigh, NC	8th	1957	State College, PA
9th	1958	Charlottesville, VA	10th	1959	Atlanta, GA
11th	1960	Tallahassee, FL	12th	1961	Knoxville, TN
13th	1962	Phoenix, AZ	14th	1963	College Station, TX
15th	1964	Rolla, MO	16th	1965	Lexington, KY
17th	1966	Ames, IA	18th	1967	Lafayette, IN
19th	1968	Morgantown, WV	20th	1969	Urbana, IL
21st	1970	Lawrence, KS	22nd	1971	Norman, OK
23rd	1972	Old Point Comfort, VA	24th	1973	Sheridan, WY
25th	1974	Raleigh, NC	26th	1975	Coeur d'Alene, ID
27th	1976	Orlando, FL	28th	1977	Rapid City, SD
29th	1978	Annapolis, MD	30th	1979	Portland, OR
31st	1980	Austin, TX	32nd	1981	Gatlinburg, TN
33rd	1982	Vail, CO	34th	1983	Stone Mountain, GA
35th	1984	San Jose, CA	36th	1985	Clarksville, TN
37th	1986	Helena, MT	38th	1987	Pittsburg, PA
39th	1988	Park City, UT	40th	1989	Birmingham, AL
41st	1990	Albuquerque, NM	41st	1991	Albany, NY
43rd	1992	Fayetteville AR	44rd	1993	Tampa, FL
45th	1994	Portland, OR	46th	1995	Charleston, WV
47th	1996	Cody, WY	48th	1997	Knoxville, TN
49th	1998	Prescott, AZ	50th	1999	Roanoke, VA
51st	2000	Seattle, WA	52nd	2001	Cumberland, MD
53rd	2002	San Luis Obispo, CA	54th	2003	Burlington, VT
55th	2004	Kansas City, MO	56th	2005	Wilmington, NC
57th	2006	Breckinridge, CO	58th	2007	Pocono Manor, PA
59th	2008	Santa Fe, NM	60th	2009	Buffalo, NY
61st	2010	Oklahoma City, OK	62nd	2011	Lexington, KY
63rd	2012	Redding, CA			

The symposia are generally scheduled for two and one-half days, with a day-and-a-half for technical papers plus a full day for the field trip. The Symposium usually begins on Wednesday morning. The field trip is usually Thursday, followed by the annual banquet that evening. The final technical session generally ends by noon on Friday. In recent years this schedule has been modified to better accommodate climate conditions and tourism benefits.

The field trip is the focus of the meeting. In most cases, the trips cover approximately 150 to 200 miles, provide for six to eight scheduled stops, and require about eight hours. Occasionally, cultural stops are scheduled around geological and geotechnical points of interests.

To cite a few examples: in Wyoming (1973), the group viewed landslides in the Big Horn Mountains; Florida's trip (1976) included a tour of Cape Canaveral and the NASA space installation; the Idaho and South Dakota trips dealt principally with mining activities; North Carolina provided stops at a quarry site, a dam construction site, and a nuclear generation site; in Maryland, the group visited the Chesapeake Bay hydraulic model and the Goddard Space Center. The Oregon trip included visits to the Columbia River Gorge and Mount Hood; the Central mine region was visited in Texas; and the Tennessee meeting in 1981 provided stops at several repaired landslide in Appalachia regions of East Tennessee.

In Utah (1988) the field trip visited sites in Provo Canyon and stopped at the famous Thistle Landslide, while in New Mexico, in 1990, the emphasis was on rockfall treatments in the Rio Grande River canyon and included a stop at the Brugg Wire Rope headquarters in Santa Fe.

Mount St, Helens was visited by the field trip in 1994 when the meeting was in Portland, Oregon, while in 1995 the West Virginia meeting took us to the New River Gorge Bridge that has a deck elevation of 876 feet above the water.

In Cody, Wyoming the 1996 field trip visited the Chief Joseph Scenic Highway and the Beartooth Uplift in northwest Wyoming. In 1997 the meeting in Tennessee visited the newly constructed future I-26 highway in the Blue Ridge of East Tennessee. The Arizona meeting in 1998 visited the Oak Creek Canyon near Sedona and a mining ghost town at Jerrome, Arizona. The Virginia meeting in 1999 visited the “Smart Road” Project that was under construction. This was a joint research project of the Virginia Department of Transportation and Virginia Tech University. The Seattle Washington meeting in 2000 visited the Mount Rainier area. A stop during the Maryland meeting in 2001 was the Sideling Hill road cut for I-68 which displayed a tightly folded syncline in the Allegheny Mountains.

The California field trip in 2002 provided a field demonstration of the effectiveness of rock netting against rock falls along the Pacific Coast Highway. The Kansas City meeting in 2004 visited the Hunt Subtropolis which is said to be the “world’s largest underground business complex”. It was created through the mining of limestone by way of the room and pillar method. The Rocky Point Quarry provided an opportunity to search for fossils at the North Carolina meeting in 2005. The group also visited the US-17 Wilmington Bypass Bridge which was under construction. Among the stops at the Pennsylvania meeting were the Hickory Run Boulder Field, the No.9 Mine and Wash Shanty Museum, and the Lehigh Tunnel.

The New Mexico field trip in 2008 included stops at a soil nailed wall along US-285/84 north of Santa Fe and a road cut through the Bandelier Tuff on highway 502 near Los Alamos where rockfall mesh was used to protect against rockfalls. The New York field trip in 2009 visited the Niagara Falls Gorge and the Devil’s Hole Trail.

At the technical sessions, case histories and state-of- the- art papers are most common; with highly theoretical papers the exception. The papers presented at the technical sessions are published in the annual proceedings. Some of the more recent papers may be obtained from the Treasurer of the Symposium.

Banquet speakers are also a highlight and have been varied through the years.

A Medallion Award was initiated in 1970 to honor those persons who have made significant contributions to the Highway Geology Symposium. The selection was and is currently made from the members of the national steering committee of the HGS.

A number of past members of the national steering committee have been granted Emeritus status. These individuals, usually retired, resigned from the HGS Steering Committee, or are deceased, have made significant contributions to the Highway Geology Symposium. A total of 30 persons have been granted Emeritus status. Ten are now deceased.

Several Proceedings volumes have been dedicated to past HGS Steering Committee members who have passed away. The 36th HGS Proceedings were dedicated to David L. Royster (1931 - 1985, Tennessee) at the Clarksville, Indiana Meeting in 1985. In 1991 the Proceedings of the 42nd HGS held in Albany, New York were dedicated to Burrell S. Whitlow (1929 - 1990, Virginia).

HIGHWAY GEOLOGY SYMPOSIUM
Emeritus Members of the Steering Committee

Emeritus Status is granted by the Steering Committee

R.F. Baker*
John Baldwin
David Bingham
Virgil E. Burgat*
Robert G. Charboneau*
Hugh Chase*
A.C. Dodson*
Walter F. Fredericksen
Brandy Gilmore
Robert Goddard
Joseph Gutierrez
Richard Humphries
Charles T. Janik
John Lemish
Bill Lovell
George S. Meadors, Jr.*
Willard McCasland
David Mitchell
W.T. Parrot*
Paul Price*
David L. Royster*
Bill Sherman
Willard L. Sitz
Mitchell Smith
Steve Sweeney
Sam Thornton
Berke Thompson*
Burrell Whitlow*
W.A. "Bill" Wisner
Earl Wright
Ed J. Zeigler

(* Deceased)

HIGHWAY GEOLOGY SYMPOSIUM
Medallion Award Winners

The Medallion Award is presented to individuals who have made significant contributions to the Highway Geology Symposium over many years. The award, instituted in 1969, is a 3.5 inch medallion mounted on a walnut shield and appropriately inscribed. The award is presented during the banquet at the annual Symposium.

Hugh Chase*	1970
Tom Parrott*	1970
Paul Price*	1970
K.B. Woods*	1971
R.J. Edmondson*	1972
C.S. Mullin*	1974
A.C. Dodson*	1975
Burrell Whitlow*	1978
Bill Sherman	1980
Virgil Burgat*	1981
Henry Mathis	1982
David Royster*	1982
Terry West	1983
Dave Bingham	1984
Vernon Bump	1986
C.W. "Bill" Lovell	1989
Joseph A. Gutierrez	1990
Willard McCasland	1990
W.A. "Bill" Wisner	1991
David Mitchell	1993
Harry Moore	1996
Earl Wright	1997
Russell Glass	1998
Harry Ludowise*	2000
Sam Thornton	2000
Bob Henthorne	2004
Mike Hager	2005
Joseph A. Fischer	2007
Ken Ashton	2008
A. David Martin	2008
Michael Vierling	2009
Richard Cross	2009
John F. Szturo	2010

(*Deceased)

HIGHWAY GEOLOGY SYMPOSIUM
Young Author Award Winners

Ryan Turner	2012
Ethan Thomas	2012 Runner Up

HIGHWAY GEOLOGY SYMPOSIUM
Previous, Present, and Future Symposium Contact List

2011	Kentucky	Henry Mathis	859-455-8530	hmathis@iglou.com
2012	California	Bill Webster	916-227-1041	bill_webster@dot.ca.gov
2013	New Hampshire	Dick Lane		DLane@dot.state.nh.us
		Krystle Pelham		KPelham@dot.state.nh.us
2014	Wyoming			

63rd ANNUAL
HIGHWAY GEOLOGY SYMPOSIUM
Sponsors

The following companies have graciously contributed toward the sponsorship of the Symposium. The HGS relies on sponsor contributions for refreshment breaks, field trip lunches and other activities. We gratefully appreciate the contributions made by these sponsors.

Bentley
685 Stockton Drive
Exton, PA 19341, United State
1-800-BENTLEY (1-800-236-8539)
Outside the United States
+1 610-458-5000
www.bentley.com/en-US/Solutions

Bentley delivers 2D/3D architecture and engineering design software solutions for the entire lifecycle of the infrastructure asset, tailored to the needs of the various professions - the engineers, architects, planners, contractors, fabricators, IT managers, operators and maintenance engineers - who will work on and work with that asset over its lifetime. Comprised of integrated applications and services built on an open platform, each solution is designed to ensure that information flows between workflow processes and project team members to enable interoperability and collaboration.

Gannett Fleming Inc.
P.O. Box 67100
Harrisburg, PA 17106-7100
Phone: (717) 763-7211
(800) 233-1055
Fax: (717) 763-7059
www.gannettfleming.com

Our Vision
Gannett Fleming is a driving force in improving our communities and sustaining our world through an uncompromising commitment to growth, innovation, ethics and technical excellence.
Our Mission
Amaze our clients with our responsiveness and innovation and become their trusted advisor, promote a rewarding work environment and provide a fair return on investment.

63rd ANNUAL HIGHWAY GEOLOGY SYMPOSIUM
Sponsors

Geobrugg North America, LLC.
22 Centro Algodones
Algodones, New Mexico 87001
Phone: (505) 771 4080
Fax: (505) 771 4081
www.geobrugg.com

Geobrugg North America, LLC has manufactured natural hazard protection systems for nearly 25 years. We provide protection systems for slope and rock instabilities, shallow landslides, debris flow, rockfall, avalanche, mine protection including open pit and underground support, sink holes and more. Our GBE rockfall systems are fully approved with CE markings—the quality is certified!

Golder Associates, Inc.
300 Friberg Parkway
Westborough, MA 01581
Phone: (508) 366-5366
Fax: (508) 366-5966
www.golder.com

Golder Associates is an international group of science and engineering companies. The employee-owned group of companies provides comprehensive consulting services in support of environmental, industrial, and natural resources and civil engineering projects. Founded in 1960, **Golder Associates** now has nearly 6,000 employees in over 150 offices worldwide and has completed projects in more than 140 countries.

63rd ANNUAL HIGHWAY GEOLOGY SYMPOSIUM
Sponsors

Hi-Tech Rockfall Construction, Inc.
PO Box 674
Forest Grove, Oregon 97116
Phone: (503) 357-6508
Fax: (503) 357-7323
www.hitechrockfall.com

HI-TECH Rockfall Construction Inc. specializes in rockfall safety problems on highways, railroads, dams, construction sites and many other locations. The principals of **HI-TECH** have over 50 years of combined experience in the rockfall industry. Our highly skilled employees have extensive experience in all types of rockfall drapery systems, rockfall barriers, debris flow barriers, rock scaling, rock bolting, and shotcrete. Commendations for safety excellence from the Associated General Contractors of America and SAIF Corporation indicates the level of attention that **HI-TECH** imparts to all of our employees in this very specialized field.

Landslide Solutions Inc.
9362 Cedarview Way,
Elk Grove, CA 95758
Phone: (916) 698-5133
www.landslidesolutions.com

Landslide Solutions Inc. is the leading design, build, and warranty landslide repair and Geostabilization company in California and Nevada, with its in house expertise and national partner company **Soil Nail Launcher Inc.** **Landslide Solutions Inc.** can repair virtually any landslide in any geologic setting. Key Areas of Service:

- Landslide repair
- Bluff Stabilization and Restoration
- Temporary Geostabilization Systems
- Permanent Geostabilization Systems
- Micropiles and Ground Anchors
- Rockfall Mitigation
- Retaining Walls and Abutments

63rd ANNUAL HIGHWAY GEOLOGY SYMPOSIUM

Sponsors

Michael Baker Corp.
Airside Business Park
100 Airside Drive
Moon Township, PA 15108
(412) 269-6300 or (800) 553-1153
www.mbakercorp.com

As a leader in transportation design beginning with the U.S. domestic interstate highway boom of the 1950s, Baker understands the complexity of today's transportation planning, design, construction and maintenance challenges. Consistently ranked by *Engineering News-Record* as a Top 20 transportation firm, we offer clients an integrated team of professionals versed in all aspects of transportation planning, design, permitting, and construction management and inspection. In addition, Baker is a recognized leader in the practical aspects of operating and maintaining a safe and efficient transportation infrastructure.

Maccaferri, Inc.
8651 Morrison Creek Drive
Sacramento, CA. 95828
Phone: (916) 371 5805
Fax: (916) 371 0764
www.maccaferri-usa.com

Maccaferri is a world leader in engineered environmental solutions: our expertise includes solutions in erosion control, retaining walls, roads and pavements, slope reinforcement, slope revetment, rockfall protection, coastal protection, fiber reinforced concrete, and green engineering.

As part of a worldwide industrial group, **Maccaferri** has more than 130 years experience in soil stabilization. Our range of gabions, Reno mattresses, soil-reinforcement and erosion control products are field proven to be the best in the industry. **Maccaferri** strives to provide a cost effective and dependable environmental solution to each and every project, helping you to save time and money. Our team of highly trained professional is available to offer *free* advice, guidance, and design soultions for all **Maccaferri** products.

63rd ANNUAL HIGHWAY GEOLOGY SYMPOSIUM

Sponsors

Zonge International, Inc.
7711 W. 6th Ave. Suite G
Lakewood, Co 80214
Phone: (720) 962-4444
Fax: (720) 962-0417
www.zonge.com

Still an Employee-Owned company with the same ownership and management, **Zonge International** continues to provide innovative geophysical field services and instrumentation, specializing in electrical and electromagnetic methods. Starting with minerals exploration in the 1970's, Zonge has since expanded into hydrological, hydrocarbon, environmental, engineering, and unexploded ordnance applications and extended our capabilities to include potential field and seismic surveys.

Zonge International's success has been the result of a continuous commitment to the development of new geophysical tools and the integration of the Engineering and Field Service groups, leading to effective and innovative tools. The development of the receiver and transmitter systems has resulted in adaptation of these tools to numerous new applications and created the most versatile electrical and EM receivers available in the world today.

63rd ANNUAL HIGHWAY GEOLOGY SYMPOSIUM
Exhibitors

Thanks to all participating exhibitors.

The exhibit booths are in the Siskiyou, Trinity and Cascade Rooms

AIS Construction, Inc.
1110 Eugenia Place #200,
Carpinteria, CA 93013
Phone: (805) 684-4344
Fax: (805) 566-6534
www.aisconstruction.com

Bentley
685 Stockton Drive
Exton, PA 19341, United State
1-800-BENTLEY (1-800-236-8539)
Outside the United States
+1 610-458-5000
www.bentley.com/en-US/Solutions

Carlson's Construction
1910 Fort Jones Rd
Yreka CA 96097
Phone: 530-598-4640
www.carlsons-construction.com

Central Mine Equipment Company
4215 Rider Trail North,
Earth City, MO 63045
Phone: (314) 291-7700
Phone: (800) 325-8827
Fax: (314) 291-4880
www.cmeco.com

Chama Valley Productions
State Road 95 #265
HC75 Box 1317
Rutheron, NM, 87551
Phone: (575) 588-0332
Fax: (575) 588-0336
www.chamaproducts.com

Gannett Fleming Inc.
P.O. Box 67100
Harrisburg, PA 17106-7100
Phone: (717) 763-7211
Phone: (800) 233-1055
Fax: (717) 763-7059
www.gannettfleming.com

Geobrugg North America,LLC.
22 Centro Algodones
Algodones, New Mexico 87001
Phone: (505) 771 4080
Fax: (505) 771 4081
www.goebrugg.com

GEODAQ
3385 Lanatt St, Suite A
Sacramento, CA 95819
Phone: (916) 930-9800

Geokon, Inc.
48 Spencer Street
Lebanon, NH 03766
Phone: (603) 448-1562
Fax: (603) 448-3216
www.geokon.com

Golder Associates, Inc.
300 Friberg Parkway
Westborough, MA 01581
Phone: (508) 366-5366
Fax: (508) 366-5966
www.golder.com

Hi-Tech Rockfall Construction, Inc.
PO Box 674
Forest Grove, Oregon 97116
Phone: (503) 357-6508
Fax: (503) 357-7323
www.hitechrockfall.com

Horn and Associates, Inc.
216 North Main Street
Winchester, KY 40391
Phone: (859) 744-2232
Fax: (859) 744-5892
www.hornandassociates.com

Janod, Inc.
34 Beeman Way
P.O. Box 2487
Champlain, NY 12919
Phone: (518) 298-5226
Fax: (450) 424-2614
janod@janod.biz

KANE Geo Tech, Inc.
7400 Shoreline Drive, Suite 6
Stockton, CA 95219
Phone: (209) 472-1822
Fax: (209)0802
www.kanegeotech.com

Kleinfelder
5015 Shoreham Place
San Diego, Ca 92122
Phone: (858) 320-2000
Fax: 320-2001
www.kleinfelder.com

Landslide Solutions Inc.
9362 Cedarview Way,
Elk Grove, CA 95758
Phone: (916) 698-5133
www.landslidesolutions.com

Maccaferri, Inc.
8651 Morrison Creek Drive
Sacramento, CA. 95828
Phone: (916) 371 5805
Fax: (916) 371 0764
www.maccaferri-usa.com

Michael Baker Corp.
Airside Business Park
100 Airside Drive
Moon Township, PA 15108
(412) 269-6300 or (800) 553-1153
www.mbakercorp.com

Soil Nail Launcher, Inc.
PO Box 4709
Grand Junction, CO 81502
2841 North Avenue
Grand Junction, CO 81501
Phone: (970) 210-6170
Fax: (970) 245-7737
www.soilnaillauncher.com

Shannon & Wilson. Inc.
706 West Broadway 201
Glendale, CA 91204
Phone: (818) 543-4560
Fax: (818) 543-4565

Trumer Schutzbauten Canada Ltd
999 Broadway W Suite 720
Vancouver, BC V5Z 1K5, Canada
Phone: (604) 732-0325
www.trumerschutzbauten.com

Williams Form Engineering, Corp.
8165 Graphic Dr.
Belmont, MI 49306
Phone (616) 866-0815
Sales/Engineering Fax: (616) 866-1890
Administration Fax: (616) 866-1810
www.williamsform.com

Zonge International, Inc.
7711 W. 6th Ave. Suite G
Lakewood, Co 80214
Phone: (720) 962-4444
Fax: (720) 962-0417
www.zonge.com

63rd ANNUAL HIGHWAY GEOLOGY SYMPOSIUM
Agenda

Monday, May 7th

12:00 PM - 5:00 PM
Highway Geology Symposium: Registration - OPEN

12:00 PM - 5:00 PM
Transportation Research Board: Poster Board - OPEN
"Design and Construction of Rockfall Mitigation Systems"

12:30 PM - 4:15 PM
Transportation Research Board: Technical Session
"Design and Construction of Rockfall Mitigation Systems"
Location: Sierra Room

6:30 PM to 8:30 PM
Reception/Ice Breaker Social
Bar Sponsored by Zonge Geophysics
Food Sponsored by Hi-Tech Rockfall
Location: Siskiyou, Trinity & Cascade Rooms

Tuesday, May 8th

6:30 AM to 9:00 AM
Breakfast
Location: Coffee Shop

7:00 AM to 5:00 PM
Highway Geology Symposium: Registration - OPEN

7:00 AM to 5:00 PM
Transportation Research Board: Poster Board - OPEN
"Design and Construction of Rockfall Mitigation Systems"
Location: Sierra Room

8:00 AM to 5:00 PM
Highway Geology Symposium: Exhibitor Hall – OPEN
Location: Siskiyou, Trinity & Cascade Rooms

7:30 AM to 8:30 AM
Welcome & Opening Remarks
John Bulinski PE, Caltrans District 2 Director
John Parrish PG, California Geologic Survey, State Geologist
Jim Davis PE, Caltrans Acting Division Chief Department of Engineering Services
Phil Stolarski PE, Caltrans Chief METS/Geotechnical Services
Location: Sierra Room

Tuesday, May 8th (continued)

Technical Session I - Rockfall

8:30 AM to 8:50 AM

Rock Slope Protection Utilizing a New Washington State Department of Transportation (WSDOT) Designed Hybrid Drapery System in Conjunction with Traditional Stabilization Techniques
Author(s): Fish, Dobrey, Johnston, & Badger
Location: Sierra Room

8:50 AM to 9:10 AM

Rockfall and Debris Flow Barrier Post Foundation Design
Author(s): Kane & Shevlin
Location: Sierra Room

9:10 AM to 9:30 AM

Cable Anchors versus Solid Bar Anchors in Rockfall Protection Systems
Author(s): Ingram & Wagner
Location: Sierra Room

9:30 AM to 9:50 AM

Case Histories on Mitigating Geologic Hazards in Mountainous Areas of California's Intrastate Highway System
Author(s): Badeker
Location: Sierra Room

Break

9:50 AM to 10:10 AM

Morning Coffee Break
Co-sponsored by: Maccaferri & Michael Baker Corp.
Location: Siskiyou, Trinity & Cascade Rooms

Technical Session I - Rockfall (continued)

10:10 AM to 10:30 AM

Design Software for Secured Drapery
Author(s): Brunet & Giacchetti
Location: Sierra Room

10:30 AM to 10:50 AM

The Hyampom Road Project: Managing Geotechnical Risk in Difficult Mountainous Terrain
Author(s): Andrew & Haramy
Location: Sierra Room

Tuesday, May 8th (continued)

Technical Session I - Rockfall (continued)

10:50 AM to 11:10 AM

Rockfall and Rockslide Mitigation Options with Rocksheds and Real-time Slope Monitoring along Interstate 70 in Glenwood Canyon, Colorado
Author(s): Arndt & Ortiz
Location: Sierra Room

11:10 AM to 11:30 AM

Using LIDAR in Highway Rock Cuts
Author(s): Maerz, Otoo, Kassebaum, & Boyko
Location: Sierra Room

11:30 AM to 11:50 AM

Rockfall Mitigation for Conversion of a Contractor's Access Road to a Permanent Low-Volume Roadway
Author(s): Ruppen, Garced, Zuo, & Gaffney
Location: Sierra Room

Lunch

11:50PM to 1:00PM

Lunch
Co-sponsored by: Bentley Systems and Hi-Tech Rockfall Construction, Inc.
Location: Sundial Room

Technical Session I - Rockfall (continued)

1:00 PM to 1:20 PM

Rock Slope Catchment Ditch Effectiveness: An Assessment of Methods used for Rockfall Hazard Rating System (RHRS) Scoring
Author(s): Thomas & Eliassen
Location: Sierra Room

1:20 PM to 1:40 PM

Case Study: West Virginia US Highway 19 'The Narrows' Rockfall Mitigation
Author(s): Kane & Amend
Location: Sierra Room

1:40 PM to 2:00 PM

Geotechnical Design of Supplemental Rock Anchors, Wurts Street Suspension Bridge, Kingston, NY
Author(s): Duskin & Charles
Location: Sierra Room

Technical Session I - Rockfall (continued)

2:00 PM to 2:20 PM

Research into and Application of Attenuator Rockfall Protection Systems
Author(s): Mumma
Location: Sierra Room

2:20 PM to 2:40 PM

Cascade Subdivision Mile 010.20: Rockfall Analysis and Protection of Railway with Ring Net Attenuator and Rockfall Barrier
Author(s): Morris, Wyllie, Shevlin, & Harrison
Location: Sierra Room

Break

2:40 PM to 3:00 PM

Afternoon Refreshment Break
Sponsored by: Michael Baker Corp. & Gannet Flemming Inc.
Location: Siskiyou, Trinity and Cascade Rooms

Technical Session II - Site Investigations

3:00 PM to 3:20 PM

Geotechnical Investigation for the K-7 and I-70 Interchange in Bonner Springs, Kansas
Author(s): Halverson
Location: Sierra Room

3:20 PM to 3:40 PM

Practical Estimation of Mohr-Coulomb Shear Strength for Cemented Conglomeratic Deposits in the Arid Western United States
Author(s): Gates
Location: Sierra Room

3:40 PM to 4:00 PM

Measurement of Ground Movement during Seismic Events
Author(s): Hipley & Huang
Location: Sierra Room

4:00 PM to 4:20 PM

Field Methods of Measuring Discontinuities for Rock Slope Stability Analysis on Price Mountain, VA
Author(s): Farny & West
Location: Sierra Room

Tuesday, May 8th (continued)

Technical Session III - Roadway

4:20 PM to 4:40 PM

Presidio Parkway Project Phase 1
Author(s): Pokrywka, Salimi, Momenzadeh, Greguras, Sojourner, & Nguyen
Location: Sierra Room

4:40 PM to 5:00 PM

Multifaceted Approach for Evaluating and Treating Sinkhole Activity beneath Highways – Case Study: SR 0422 in Southeastern Pennsylvania
Author(s): McInnes & Krupansky
Location: Sierra Room

Field Trip Preview

5:00 PM to 5:15 PM

Field Trip Preview Presentation
Scott Lewis CEG Caltrans Engineering Geologist
Location: Sierra Room

5:30 PM to 6:30 PM

HGS National Steering Committee Meeting
Location: Sacramento Room

Wednesday, May 9th

6:30 AM to 9:00 AM

Breakfast
Location: Coffee Shop

8:00 AM to 4:00 PM

Highway Geology Symposium: Field Trip
Lunch Sponsored by Geobrugg
Afternoon Beverages Sponsored by Golder and Associates
Location(s): State Route 299

5:30 PM to 6:30 PM

Highway Geology Symposium: Social Hour
Sponsored by Zonge Geophysics
Location: Siskiyou, Trinity and Cascade Rooms

6:30 PM to 9:30 PM

Highway Geology Symposium: Banquet Dinner
Keynote Speaker: Stephen Most
Topic: “River of Renewal, Myth and History in the Klamath Basin”
Location: Sierra Room

Thursday, May 10th

6:30 AM to 9:00 AM

Breakfast
Location: Coffee Shop

8:00 AM to 12:00 PM

Highway Geology Symposium: Exhibitor Hall – OPEN
Location: Siskiyou, Trinity & Cascade Rooms

Technical Session IV - Landslides

8:00 AM to 8:20 AM

Dani Creek Landslide: Anchored Soldier Pile Wall in Franciscan Mélange
Author(s): Turner-Ryan
Location: Sierra Room

8:20 AM to 8:40 AM

Estimating Landslide Losses to State Highways: A General Approach for a Winter Storm Scenario
Author(s): Wills, Perez, & Branum
Location: Sierra Room

8:40 AM to 9:00 AM

Effects of Postfire Debris Flows on California State Route 395, Geologic Factors and Assessment Tools
Author(s): Lancaster
Location: Sierra Room

9:00 AM to 9:20 AM

Impacts of the Double Draw Landslide (Debris Flow) in Wyoming's Snake River Canyon Lincoln County, Wyoming
Author(s): Hood & Falk
Location: Sierra Room

9:20 AM to 9:40 AM

Challenges Faced during the Emergency Response to the Bear River Canal Failure
Author(s): Mack, Kennedy, Leung, & McManus.
Location: Sierra Room

9:40 AM to 10:00 AM

Case Studies in Innovative Roadway Landslide Repair and Rock Slope Stabilization in California
Author(s): Chinchiolo, Barrett, & Beard
Location: Sierra Room

Thursday, May 10th (continued)

Break

10:00 AM to 10:20 AM

Morning Coffee Break
Sponsored by: Landslide Solutions
Location: Siskiyou, Trinity and Cascade Rooms

Technical Session IV - Landslides (continued)

10:20 AM to 10:40 AM

I-40 along the Cumberland Escarpment Highway Instability, Historic Reviews, and Remedial Concepts
Author(s): Sneyd, Sak, Moore, Barker, & Oliver
Location: Sierra Room

10:40 AM to 11:00 AM

Distribution of Weathered Geologic Bedrock Controls on Slope Movement, Green Point Sink, State Route 299, Humboldt County, California
Author(s): McGuire
Location: Sierra Room

Technical Session V - Structures

11:00 AM to 11:20 AM

Rock-Socketed Shafts for the Bridge at Pitkins Curve
Author(s): Turner-John, Duffy, Buell, & Zheng
Location: Sierra Room

Potential Presentations

11:20 AM to 11:40 AM

Numerical Analysis of Rockfall Sheltering Structures
Author(s): Calvetti, Frenez, & Tondini
Location: Sierra Room

11:40 AM to 12:00 PM

WSNs for Rockfall Protection Assets, Tracking, and Maintenance
Author(s): Danzi
Location: Sierra Room

Symposium Adjournment

12:00 PM to 12:10 PM

Closing Remarks/Adjournment
Bill Webster
Location: Sierra Room

63rd ANNUAL HIGHWAY GEOLOGY SYMPOSIUM
Red Lion Hotel Layout

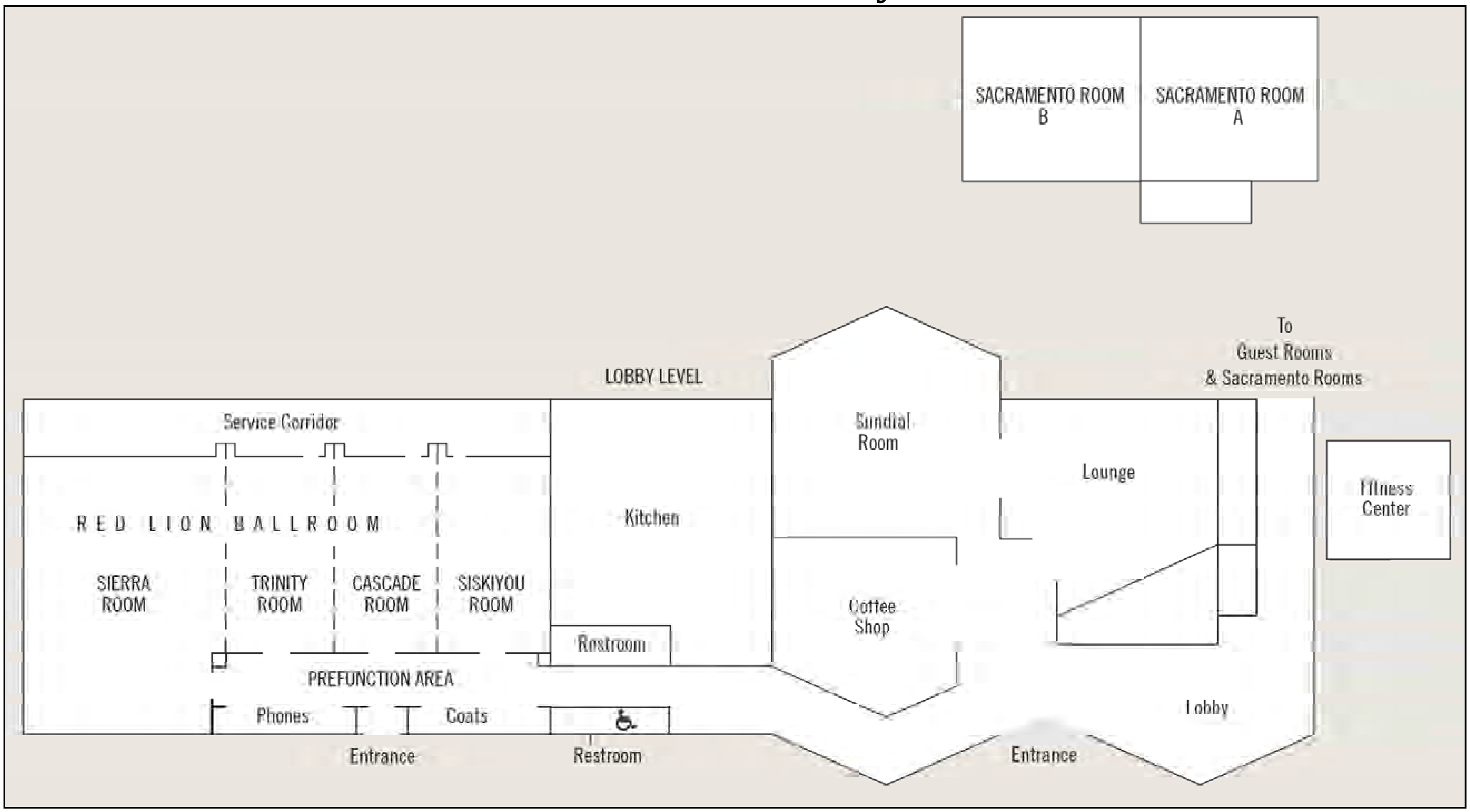

63rd ANNUAL HIGHWAY GEOLOGY SYMPOSIUM
Exhibitor Map

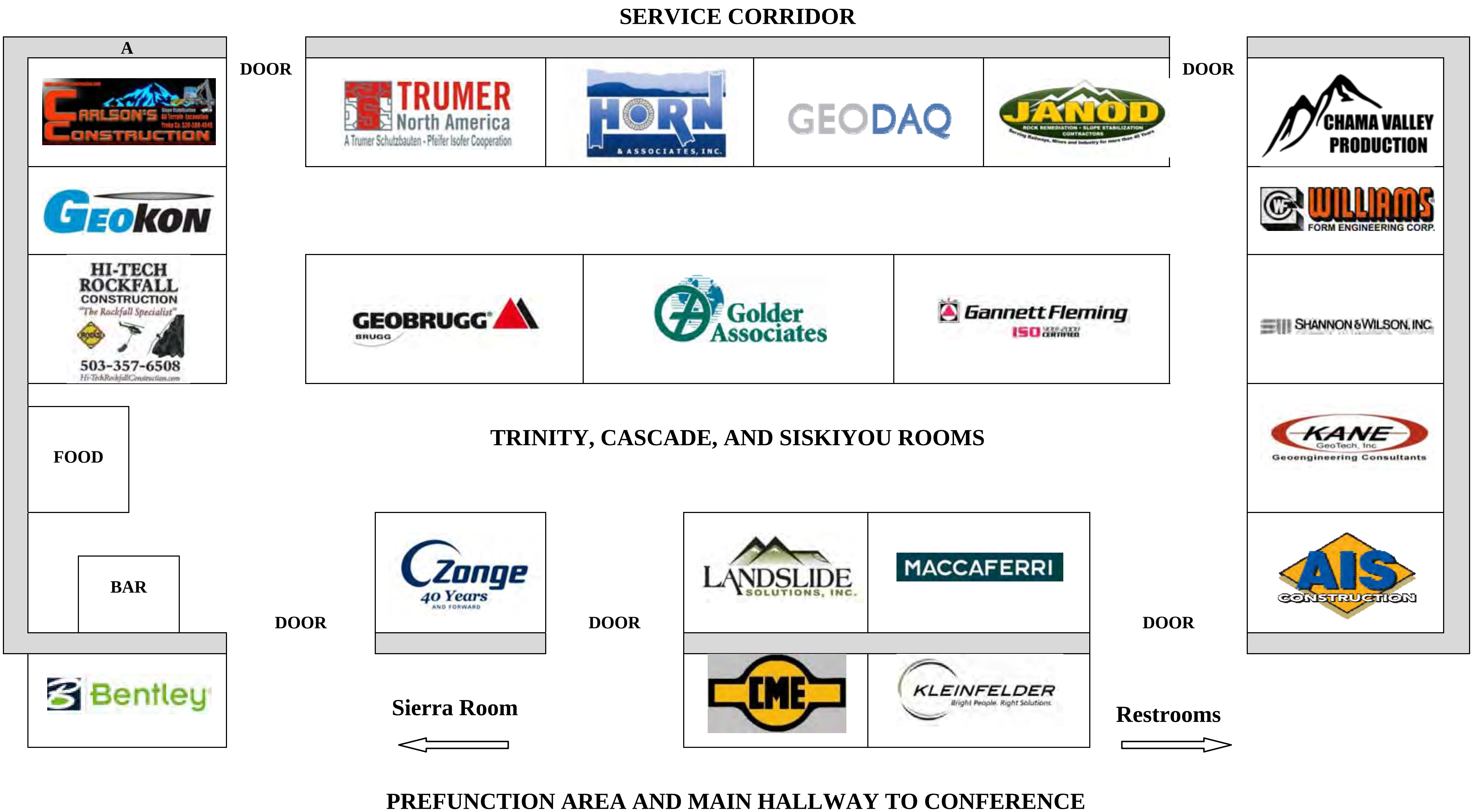

63rd ANNUAL HIGHWAY GEOLOGY SYMPOSIUM

TRANSPORTATION RESEARCH BOARD

Design and Construction of Rockfall Mitigation Systems

Redding, California

May 7th, 2012

Presided by

Duffy, John David
California Department of Transportation

Sponsored by:

Committee on Engineering Geology (AFP10)

Committee on Rockfall Management (AFP10(1))

63rd ANNUAL HIGHWAY GEOLOGY SYMPOSIUM

TRANSPORTATION RESEARCH BOARD

Design and Construction of Rockfall Mitigation Systems

This workshop will help practitioners and researchers understand the current state of rockfall mitigation design based on the different perspectives of both the design and construction sides of the issue. Presentations from the construction side will be given on mitigations such as flexible rockfall fences, drapery, anchored mesh systems, attenuators/hybrid systems and scaling. Following each presentation there will be discussions from both sides on each topic. The focus will be on achieving better and more practical designs and design elements that can be successfully constructed.

Chairman

John D Duffy
California Department of Transportation
50 Higuera Street
San Luis Obispo, CA 93401
805-549-3663
John_d_duffy@dot.ca.gov

Panel

AIS Construction
Andy Schafer
1110 Eugenia Place
Suite 200
Carpinteria, CA 93013
805-684-4344
andy@aisconstruction.com

Hi-Tech Rockfall Construction, Inc.
Chris Ingram
2328 HAWTHORNE STREET
FOREST GROVE, OR 97116
503-357-6508
htrockfall@aol.com

Janod, Inc.
Todd Reccord
190 Rue Valois, Vaudreuil-Dorion,
Quebec, Canada, J7V 1T4
Phone: (450) 455-1223
Fax: (450) 424-2614
toddr@janod.biz

Midwest Rockfall Inc.
Ryan Fetzer
10401East 102 nd Ave
Unit #3
Henderson, CO 80640
303-288-4970
ryan@midwestrockfall.com

63rd ANNUAL HIGHWAY GEOLOGY SYMPOSIUM

TRANSPORTATION RESEARCH BOARD

Design and Construction of Rockfall Mitigation Systems

AGENDA

Monday, May 7th

Subject	Speaker	Schedule	Time
Overview	**Chairman**	12:30 PM – 12:40 PM	10 minutes
Barriers	**Midwest**	12:40 PM – 12:55 PM	15 minutes
Group Discussion	All	12:55 PM – 1:05 PM	10minutes
Drapery	**Hi-Tech**	1:05 PM – 1:20 PM	15 minutes
Group Discussion	All	1:20 PM – 1:30 PM	10minutes
Attenuators/Hybrids	**Janod**	1:30 PM – 1:45 PM	15 minutes
Group Discussion	All	1:45 PM – 1:55 PM	10minutes
Anchored Mesh	**AIS**	1:55 PM – 2:10 PM	15 minutes
Group Discussion	All	2:10 PM – 2:20 PM	10minutes
Break	All	2:20 PM – 2:40 PM	20 minutes
Scaling	**Chairman**	2:40 PM to 2:50 PM	50 minutes
	Midwest	2:50 PM to 3:00 PM	
	Hi-Tech	3:00 PM to 3:10 PM	
	Janod	3:10 PM to 3:20 PM	
	AIS	3:20 PM to 3:30 PM	
Group Discussion	All	3:30 PM to 4:15 PM	45 minutes

63rd ANNUAL HIGHWAY GEOLOGY SYMPOSIUM

Abstracts & Notes

Redding, California

May 7th – 10th, 2012

Hosted By

The California Department of Transportation

The California Geological Survey

ROCK SLOPE PROTECTION UTILIZING A NEW WSDOT DESIGNED HYBRID DRAPERY SYSTEM IN CONJUNCTION WITH TRADITIONAL STABILIZATION TECHNIQUES

Marc Fish

Washington Department of Transportation
PO Box 47365, Olympia, WA
360-709-5498
E-mail: fishm@wsdot.wa.gov

Boyan Dobrev

Washington Department of Transportation
PO Box 47340, Olympia, WA
360-705-7191
E-mail: dobrevb@wsdot.wa.gov

Samuel Johnston

Washington Department of Transportation
PO Box 47365, Olympia, WA
360-709-5556
E-mail: johnstons@wsdot.wa.gov

Thomas C. Badger

Washington Department of Transportation
PO Box 47365, Olympia, WA
360-709-5461
E-mail: badgert@wsdot.wa.gov

Prepared for the 63rd Highway Geology Symposium, May 7-10, 2012

Acknowledgements

The authors would like to thank Rock & Co, Inc. for building the WSDOT designed project according to the plans. The project was completed on time and within budget.

Disclaimer

Statements and views presented in this paper are strictly those of the authors, and do not necessarily reflect positions held by their affiliations, the Highway Geology Symposium (HGS), or others acknowledged above. The mention of trade names for commercial products does not imply the approval or endorsement by HGS.

Copyright Notice

ABSTRACT

The US2 West of Leavenworth Slope Stabilization project was located on the eastern slope of the Cascade Mountains within a deeply incised valley named Tumwater Canyon. This project mitigated rockfall events along approximately 2500 feet of highway. Rockfall sources included bouldery colluvium that discontinuously mantled the bedrock on over-steepened slopes, and structurally controlled rock slope failures. To develop the mitigation designs, planar and wedge type failures, snow loading on cable net installations, rockfall bounce heights, and kinetic energies were evaluated. The mitigation work included rock slope scaling, debris removal, untensioned rock dowels, post-tensioned rock bolts, horizontal drains, shotcrete facing, cable net slope protection, and WSDOT's newly designed hybrid drapery system. This new design addresses rockfall with kinetic energies of up to 100 ft-tons and bounce heights of up to 18 ft. Lessons learned from this project included the need for a more defined procedure to locate posts and to determine post foundation types, the need for a new micropile post foundation type for posts constructed on steep colluvial slopes, the need for instructions to address alternative maximum post spacing, the need for specified minimum tension values or maximum sag on the post-support cables, the need for improved procedures for constructing grout pads and how to place post-support cable anchors, and needed plan revisions better defining termination and the lay of the cable nets on the slope. Post foundations will also now be bid as a separate item rather than included within a single bid item for the total installed square footage of cable nets.

INTRODUCTION

The US2 West of Leavenworth Slope Stabilization project mitigated rockfall events along approximately 2500 feet of highway at two locations, approximately 3 miles apart from one another (Figure 1). These slopes generated frequent rockfall involving structurally controlled rock slope failures (Figure 2) and over-steepened, bouldery colluvial slopes that discontinuously mantle the bedrock (Figure 3).

The project was located within the North Cascades physiographic province on the eastern slope of the Cascade Mountains within a deeply incised valley named Tumwater Canyon. This area is geologically complex and has developed through a series of tectonic environments. The Chiwaukum graben and the Leavenworth Fault zone are significant geologic features in this area (Figure 1). The Chiwaukum graben formed through deformation, uplift, and thrust faulting, and it separates most of the metamorphic rocks of the Chelan Mountains from the metamorphic and igneous rocks of the Ingalls Tectonic Complex and the Mount Stuart Batholith. The Leavenworth Fault zone trends from the northwest to the southeast, is located just to the east of the project site, and through tectonic compression has created a series of northwest to southeast trending anticlines and synclines with steeply dipping limbs. Exposed bedrock on Slope 1 consists of serpentinized peridotite rocks of the Ingalls Tectonic Complex, and at Slope 2 the exposed bedrock consists of tonalite bedrock of the Mount Stuart Batholith. Colluvial and mass wasting deposits are prominent on the valley walls and grade down valley and terminate at several locations within both slopes (Tabor, 1987).

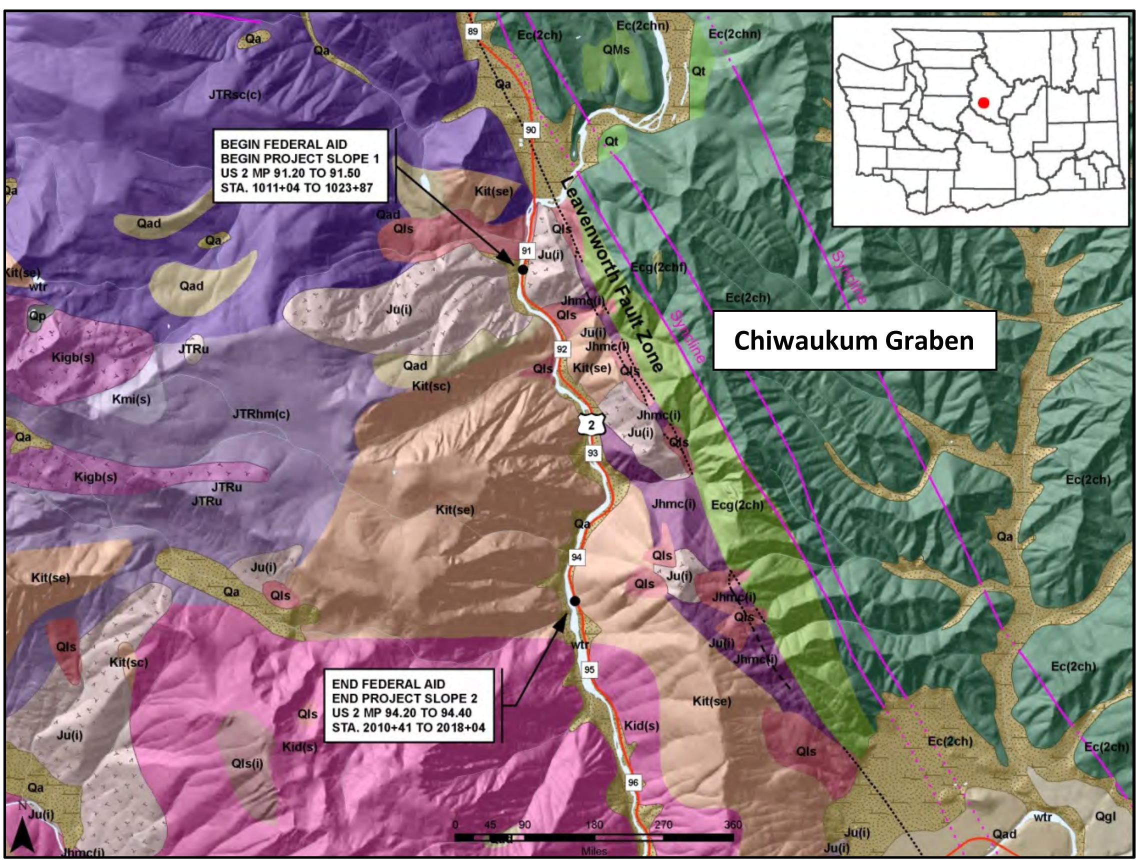

Figure 1: Location and geology map of project.

Figure 2: Rockfall initiates from structurally controlled rock slope failures.

Figure 3: Rockfall initiates from over-steepened colluvial slopes.

FIELD INVESTIGATION, ANALYSES, AND RECOMMENDATIONS

Our field investigation included photographing the slopes, performing geologic mapping of rock structure, measuring slope profiles, and measuring slope distances and heights with a tape to estimate cable net quantities. No subsurface investigation was conducted for this project.

Numerous bedrock discontinuity orientations were obtained through our geologic field mapping. We evaluated these orientations on a lower hemisphere stereonet and identified multiple wedge and planar-type features within each rock slope. To evaluate the stability of these features, we conducted numerous stability analyses under dry conditions to conservatively estimate shear strengths of critical discontinuities. This included back analyses of known rock fall locations. Through our analyses, reinforcement was designed to stabilize each (assumed) marginally stable block with a factor-of-safety greater than or equal to 1.25. To mitigate the raveling rocks within the over-steepened colluvial slopes and the smaller unstable blocks, cable net slope protection was proposed for multiple sections on each slope. Also, because rockfall is regularly generated from locations upslope of the highway cuts, many of the cable net systems were elevated with posts, which we refer to as hybrid drapery. To ensure adequate anchorage of the netting, we evaluated snow loading conditions on the nets where slope inclinations were less than 60 degrees. We also used the Colorado Rockfall Simulation Program v. 4 (CRSP) to estimate potential rockfall trajectories to determine the necessary post heights for the hybrid drapery.

Final geotechnical recommendations included hand scaling of loose blocks, reinforcing other unstable blocks with rock bolts and rock dowels, draining water from the slopes with horizontal drains, covering a weathered igneous dike with fiber-reinforced shotcrete, and covering portions of the slopes with either cable net or hybrid drapery. This project was WSDOT's second installation using a recently developed hybrid drapery system. Through this project, WSDOT installed about 85,000 square feet of post-supported cable nets on to 24 posts. The posts ranged between 6 and 18 feet in height and were spaced from 15 to 60 feet apart from one another.

Staging and traffic control were significant elements of this project. Average daily traffic through the project is approximately 2600 vehicles. There was little to no space beneath each slope to store equipment and supplies, and the closest staging area was approximately one mile away. Traffic control was also required for most of the slope stabilization work. One lane of alternating traffic remained open for the shotcrete application, for the drilling and grouting of the rock bolts, rock dowels, horizontal drains, and for the cable net and hybrid drapery system anchors. The highway was closed in both directions while the slope scaling occurred.

Based off of the contract plans and the Contractor's site assessment, it was the Contractor's responsibility to determine the quantity of each post type (end, connection, or intermediate) to manufacture and the amount and sizes of cable net panels to order. WSDOT was responsible for assisting the Contractor in field-locating the rock bolt and the rock dowel locations and for verifying the cable net and the hybrid drapery system post and anchor locations.

DESIGN OF A HYBRID DRAPERY SYSTEM

A *hybrid drapery system* (also referred to as an *attenuator system*) is a passive rockfall protection system consisting of a flexible, woven wire mesh or cable net fabric suspended from a horizontal top support cable that is raised off the ground by posts or by anchoring across a chute. No internal, side or bottom anchoring of the fabric is generally included, allowing for controlled deformation of the fabric and providing either full containment or attenuation of the rockfall trajectory at the base of the installation. Hybrid drapery addresses rockfall source areas, both underneath and upslope of the installation, and controls the rock's descent under the mesh, combining the performance of standard unsecured draperies and flexible rockfall fences. These systems have been extensively used for several decades in western North America, but until recently, these systems have been designed empirically in the absence of quantitative design data, full-scale field testing, or documented performance. This paper presents an overview of a new design completed by WSDOT of the supporting infrastructure, based on limited existing and recently completed studies documenting loading conditions on these systems (Badger and others, 2011). The objectives for this design were to:

- Incorporate new field test and modeling data on infrastructure loading
- Refine design requirements of the infrastructure based on current structural design codes~~,~~
- Diversify system attributes to accommodate varied loading and site conditions
- Reduce post vulnerability by maximizing post spacing and, where feasible, eliminating lateral support of the posts.

The *American Society of Civil Engineers (ASCE) 7-05 Minimum Design Loads for Buildings and Other Structures* publication was selected in calculating all the loads except for the falling rock load. The following loads were considered in the design:

1. Dead load (D) = 1.3 lbs/ft^2 for the 12-inch-grid cable net with double-twisted wire mesh (DTWM).
2. Ice load (D_i) = 5.7 lbs/ft^2 corresponds to approximately 1" diameter icing around the 5/16" cable net rope and the 0.106" (8x10) mesh wire.
3. Falling rock load (L) = 1.7 kip/ft applied over the middle 4-ft of the cable net support rope (6.8 kips total).
4. Snow load (S) = 0.7 lbs/ft^2 (54% of dead load).
5. Wind load (W) = 3.9 lbs/ft^2
6. Wind on ice load (W_i) = 4.0 lbs/ft^2.

Nine load combinations, based on ASCE 7-05, 2.4.1 (modified by 2.4.3) and *American Association of State Highway and Transportation Officials (AASHTO) Standard Specifications for Structural Supports for Highway Signs, Luminaires, and Traffic Signals, 5th ed.*, Table 3-1, were considered in the design. Fatigue was not considered due to the low-cyclic behavior of the system. The governing load combination was determined to be $D+0.7D_i+L$. While the falling rock load influenced the design, the ice load was the dominant load demand.

Three post heights (6 ft, 12 ft, and 20 ft) and three slope heights (100 ft, 200 ft, and 300 ft) were evaluated for design. Due to the different loading requirements, the end, connection, and intermediate posts were designed separately (Figure 4).

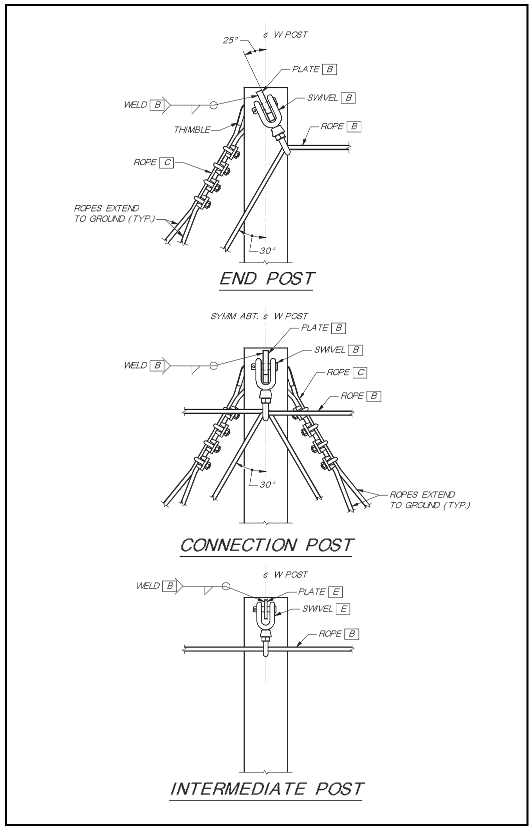

Figure 4: Post types.

The hybrid drapery system employs the following design assumptions:

1. A maximum post spacing of 40 ft.
2. Posts are inclined between 0° and 30° angle from vertical.
3. Posts are aligned with horizontal and vertical deflection angles of 30° or less (Figure 5).
4. Support ropes are attached at a 30° angle with respect to the longitudinal axis of the posts.
5. Wind, wind on ice, and rock loads act perpendicular to the posts. Dead, snow, and ice loads act at a 25° angle with respect to the longitudinal axis of the posts.
6. The cable net is vertical with no interface friction between the net and the ground.
7. The system is not designed for a direct impact on a post from a falling rock.

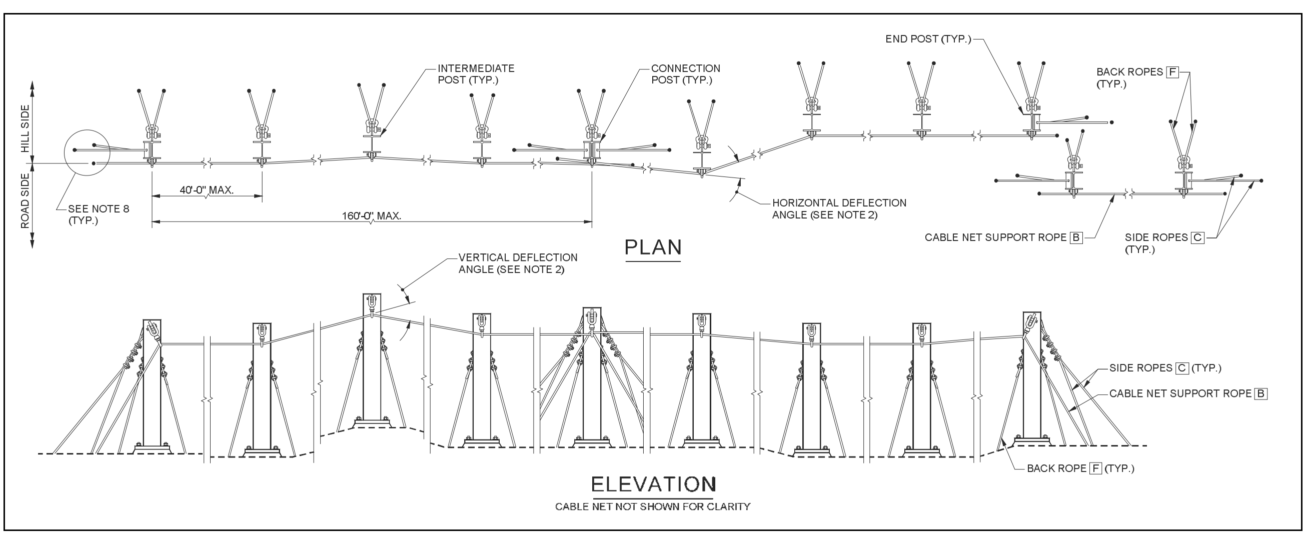

Figure 5: Hybrid drapery system plan and elevation views.

Theoretically, the length of the cable net support rope can be infinite provided the spacing between any two adjacent posts does not exceed 40 ft. However, the maximum rope length was set at 160 ft to limit system vulnerability. We designed the posts for a fixed rather than a pinned connection to simplify fabrication and construction requirements. The overall capacity of the posts was calculated from the interaction of the bilateral bending and axial compression capacities. The torsion in the end posts was ignored.

We created 3D models for the various post height and cable net length configurations using the structural analysis software SAP2000. All loads were applied as distributed loads along the cable net support rope. As a check, we verified certain model outputs with hand calculations. Building on previous work (Muhunthan and Radhakrishnan, 2007), a basic 3D ABAQUS model (two 6-ft-high posts suspending a 40-ft-wide by 100-ft-long cable net) was created as an additional tool to estimate an equivalent static rock load for our SAP2000 models, as well as to compare key structural outputs: deflections, axial, and bending forces. The results between ABAQUS and SAP2000 were comparable.

LESSONS LEARNED

With regards to our hybrid drapery system, there were several lessons WSDOT learned as a result of this project. These lessons will result in design modifications for future projects sites requiring posts with different sizes, multiple post foundation types, and post spacings of greater than 40 feet.

For this project, the contract plan sheets showed the approximate post locations superimposed on photographs of the slopes. They also stated the criteria for the post's maximum horizontal and vertical deflection angles, the maximum post spacing, the post heights, and the approximate slope heights at the location of the systems top horizontal rope. Based upon these plan sheets and on-slope measurements, the Contractor needed to site the posts and post anchor locations that met all the requirements of the contract. In addition, they needed to determine the quantity of different post types, the post foundation types to construct, and the quantity and sizes of cable net panels to order to fully cover the slope several weeks ahead of installation. To make certain that design changes are not warranted and that the proposed post locations are acceptable to the Engineer, an inspection needs to occur shortly after the mucking and scaling of the slope. This inspection helps ensure that the necessary cable net quantities and post types are ordered. Because WSDOT does not typically perform subsurface investigations for the post foundations, the Contractor must make assumptions in his bid for the expected foundation type. Even during construction, there were differences in opinion as to what type of post foundation should be constructed beneath each post. For these reasons, specification revisions need to be considered for a better defined procedure for locating the posts and to determine the post foundation type as early on as possible.

The contract plan sheets also identified two post foundation types for the hybrid drapery system. One type was for posts constructed on rock, which consists of four threaded bars, drilled and grouted approximately three feet in depth (Figure 6). A second type was for posts constructed in soil, which consists of a 3 ft x 3 ft x 3 ft concrete footing (Figure 7) with four threaded bars. Because of raveling ground conditions at several oversteepened post locations, it was determined that a third foundation type was needed. Because of the high axial loads (61 kips), a special micropile foundation was designed to satisfy bearing capacity and slope stability requirements. It consisted of a concrete footing with four 8-foot-long, 3-inch-diameter, fully grouted micropiles, two installed into the slope at approximately 90 degrees and two installed into the slope at approximately 30 degrees (Figures 8 & 9).


Figure 6: Four threaded bars grouted into rock for a post constructed on rock.


Figure 7: Concrete footing for a post constructed in soil.

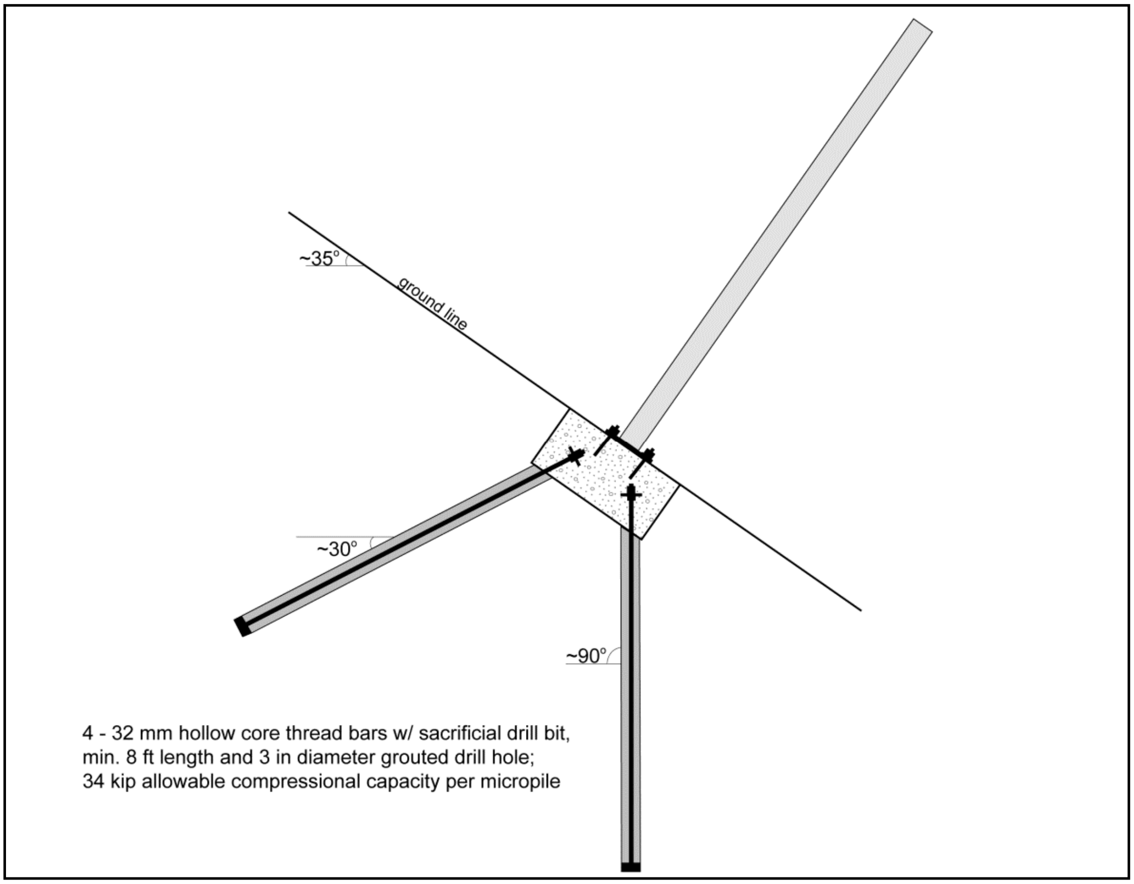

Figure 8: Typical micropile orientation.

Figure 9: Construction of a micropile foundation.

Both slopes on this project contained one or more chutes that channeled frequent rockfall, and several chutes had a width greater than the 40-foot-maximum plan post spacing (Figure 10). The plans were not specific as to how the Contractor should address post locations that fall in the middle of a rockfall chute or how to maintain the vertical deflection angle criteria on slopes with variable height over short distances. For future projects, better instructions for addressing alternative maximum post spacing are needed, including how to adjust post heights to meet the vertical deflection angle criteria while still conforming to the expected bounce heights.

Figure 10: Rockfall chute spanned by posts with an increased spacing of ~60 feet.

The contract plans also did not specify a minimum tension value or maximum sag for the post-support cables. A loose cable cannot carry its designed load prior to the post failing at its point of attachment to the ground (Figure 11). By specifying minimum tension values or maximum sag for post-support cables, the system will be able to perform as intended by the design. This could be done by measuring the tension value of each post-support cable with a tension meter device. Alternatively, a taut string could be used to measure the sag in a post-support cable. Measuring the sag would be a simpler procedure, yet not as reliable as using a tension meter, especially for the short cables.

Figure 11: Loose post-support cables.

The contract plans called for grout pads up to 3 inch thick to be placed beneath the post base plates. The purpose of the grout pad is to limit deflection of the post and excess stresses in the bearing plate during an impact. The construction of the grout pad is not as simple as it might appear. For posts constructed on steeper bedrock surfaces, such as the case on this project, either a thicker grout pad needs to be constructed or bedrock needs to be excavated in order for the posts to be oriented correctly. For this project, the Contractor chose to use nuts, approximately 1 ½ inches long, placed onto the threaded bars below the base plate to help orient the posts and to transfer energy from the system to the ground surface during an extreme event (Figure 12). The nuts were adjustable, and helped to orient the posts into a position whereby they could meet the horizontal deflection angle criteria as defined in the plans. The grout pads were then constructed beneath the post. While this is not the preferred option due to air pockets forming underneath the base plate, the use of thicker nuts and reinforced grout would mitigate the issue. For future projects on similarly steep slopes, considerations should also be given for allowing thicker grout pads with nuts placed beneath the post base plates. For pads thicker than 3 inches, fiber or steel reinforcement of the grout may also be necessary.

Figure 12: Nuts beneath the post base plate to help transfer energy from the post to the ground surface and to help orient the post.

Post and cable anchor placement is a critical aspect of the system. The anchors need to be installed at a location, where they can attain their designed capacity and where the attached post-support cables can also achieve their designed orientation. Some of the support cables need to be collinear; others have a specified angle with respect to each other. While the current plans address the general geometry of the support cables, future plans need to be more explicit about cable anchor spacings based on the ground conditions. Limited space for anchors is especially evident for short (6 ft) connection and end posts. If anchors are constructed too close to one another, they may not develop the requisite capacity.

In an attempt to better explain our design and to eliminate confusion with the Contractor, the contract documents should state that the cable nets need to lay as flat as possible on the slope and that, due to the use of a perimeter cable on the cable nets, excess netting should not be cut. Cable nets should also not be folded under but should be folded over to minimize the possibility of accumulating debris and overloading the system.

Considerations should also be given to having separate bid items for posts with each foundation type (i.e. rock, soil, or micropile) and for the total square footage of cable nets installed on the slope. Varying amounts of time and effort are required for constructing post foundations in bedrock as compared to constructing post foundations in soil or on steep colluvial slopes. Since there is a significant difference in time and effort, having separate bid items would allow more flexibility to the owner during construction and reduce the Contractor's risks.

CONCLUSION

This project took approximately 4½ months to build for a total cost of around 1.5 million dollars (Figure 13). The project required several project design revisions, one of which was a new micropile post foundation type for posts constructed on steep colluvial slopes. As a result of this project, we have incorporated some of the lessons learned into new plan details and revised specifications. These include: a new micropile post foundation type for posts constructed on steep colluvial slopes, more defined procedures to locate posts and to determine post foundation types, better instructions to address alternative maximum post spacing, specified minimum tension values or maximum sag on the post-support cables, improved procedures for constructing grout pads and how to place post-support cable anchors, and instructions on how and where the cable nets should terminate and how they should lay on the slope. From an administrative standpoint, post foundations will also now be bid as a separate item rather than included within a single bid item for the total installed square footage of cable nets.

Figure 13: Completed hybrid drapery installation on one of the slopes.

REFERENCES

Badger, T.C., B. Dobrev, M. Anderson, H. Radhakrishnan, and B. Mununthan, 2011, Structural design of a hybrid drapery system, in Moelk, M et al., eds., Proceedings for the Interdisciplinary Workshop on Rockfall Protection, Innsbruck, Austria, pp. 3-5.

Fish, M., Allen, T.M., May 2010, US 2 – West of Leavenworth Slope Stabilization Geotechnical Report MP 91.2 to 91.5, Washington State Department of Transportation, Olympia, Washington.

Fish, M., Allen, T.M., June 2010, US 2 – West of Leavenworth Slope Stabilization Geotechnical Report MP 94.2 to 94.4, Washington State Department of Transportation, Olympia, Washington.

Muhunthan, B., S. Shu, N. Sasiharan, O.A. Hattamleh, T.C. Badger, S.M. Lowell, and J.D. Duffy, 2005, Design Guidelines for Wire Mesh/Cable Net Slope Protection, Washington State Department of Transportation, Olympia, Washington, WA-RD 612.2.

Muhunthan, B., and H. Radhakrishnan, 2007, Finite Element Analysis of Hybrid Barrier for Rockfall Slope Protection, Final Report, Washington State University Dept. of Civil & Environ. Engineering, 13 p.

Tabor, R.W., Frizzell Jr., V.A., Whetten, J.T., Waitt, R.B., Swanson, D.A., Byerly, G.R., Booth, D.B., Hetherington, M.J., and Zartman, R.E., 1987. Geologic Map of the Chelan 30-Minute by 60-Minute Quadrangle, Washington Map I-1661, Department of the Interior, U.S. Geological Survey, scale 1:100,000.

Washington State Department of Transportation, 2010, Special Provisions, Details, and Plan Sheets for Type 2 Cable Nets.

Rockfall and Debris Flow Barrier Post Foundation Design

William F. Kane, PhD, PG, PE
President and Principal Engineer
KANE GeoTech, Inc.
7400 Shoreline Drive, Suite 6
Stockton, California 95219
209-472-1822
william.kane@kanegeotech.com

Timothy Shevlin, PG
Regional Manager, NW USA & Western Canada
Geobrugg North America, LLC
4676 Commercial St SE, PMB 174
Salem, OR 97302
503-423-7258
tim.shevlin@geobrugg.com:

Prepared for the 63rd Highway Geology Symposium, May 7-10, 2012

Acknowledgements

Disclaimer

Statements and views presented in this paper are strictly those of the author, and do not necessarily reflect positions held by their affiliations, the Highway Geology Symposium (HGS), or others acknowledged above. The mention of trade names for commercial products does not imply the approval or endorsement by HGS.

Copyright Notice

ABSTRACT

The design of post foundations for rockfall and debris flow barriers has received considerable attention especially by agencies and plan reviewers. This is despite the fact that relatively small foundations have shown to be effective at resisting the short-term dynamic loads of rockfall impacts. Reported post foundation failures for rockfall barriers have been rare. However, in the past few years, the development of debris flow barriers and the increase in rated energy capacity of rockfall barriers suggests that foundation design in soils for dynamic flexible barriers be evaluated more thoroughly. Additionally, rockfall barrier certification guidelines have become more stringent, and full-scale, instrumented certification tests for barrier have allowed for better determination of foundation loads.

There are several approaches for the design of post foundations in soil. These include micropiles, reinforced and unreinforced concrete blocks, and drilled shafts. Traditionally, an approximately 3-ft cubic concrete block has been used. Barrier manufacturers generally show a concrete block with one or two micropiles beneath it. This approach has been adopted by many engineers, although constructability of such foundations in soil is often difficult.

This paper reviews the current standard of design practice, the relative merits and drawbacks of current design practice, and makes recommendations for methodology and testing to obtain realistic and constructible foundation designs.

THE ROCKFALL POST FOUNDATION PARADOX

Rockfall barriers have been used for protecting infrastructure for many decades. Over time, barrier designs have evolved greatly while also becoming more regulated with standardized certification guidelines. Population growth and the scenic nature of mountainous regions have led to increased development in hazardous areas, making the need for rockfall protection more widespread. As the use of rockfall barriers has expanded beyond their initial use by a relatively small group of experts found mostly within the highway community, these barriers have begun to receive heightened scrutiny from the wide range of end-owner plan reviewers that now find themselves involved in rockfall mitigation projects. Sometimes these plan reviewers are qualified rockfall designers specifically hired for their expertise. More often, they are either an engineer unfamiliar with rockfall or a local building inspector.

Testing of many of the early rockfall barriers focused primarily on overall system performance and much less on analysis of individual component loading. As a result, detailed information regarding foundation loads was generally unavailable. Foundation design was rudimentary, often estimated, and largely based on empirical observations of field and testing experience. At this time, it became the standard of practice to construct a post foundation in soils that was approximately 1-m^3 of unreinforced concrete. Despite the absence of detailed design data, these foundations performed successfully for many years; and were used and accepted by many engineers and agencies qualified in the field of rockfall.

Over time, rockfall barrier testing has become more detailed and refined. This process has proceeded in line with the dramatic advancements seen in barrier design. The earliest test specifically on a rockfall barrier in the 1960’s resulted in an impact energy of 23 kJ. Barriers have now been designed and tested up to 8,000 kJ, with the testing providing detailed and accurate information regarding anchor and foundation forces. In addition to higher impact energies, other changes have occurred in barrier design that affected foundation loading. Many early systems incorporated a breakaway post connection that transferred most of the loading to the lateral and upslope anchors. These breakaway posts have been largely replaced by hinged posts that allow the post to rotate downslope with an impact, while still transferring loads to the rope anchors. A recent trend in barrier design has seen a movement toward more systems designed with rigid posts and no-upslope anchors. These types of systems are similar to the early designs, but they are now of much higher energies up to and even greater than 1,000 kJ. The post spacing used in barrier designs have also seen significant change. The earliest rockfall barriers typically had post spacing of up to 25-ft. Now the standard post spacing is approximately 40-ft. All of these changes in barrier design have affected both the magnitude of loads and the way loads are distributed to barrier foundations.

Regulation and oversight by owners, owner’s representatives, and others not familiar with rockfall and other natural hazards is now commonplace. This has brought a great deal of scrutiny to many projects. One such item of strict scrutiny is the design of the rockfall barrier post foundation. Structural engineers, not familiar with earth-structure interaction, often design massive, heavily reinforced post foundations for even the smallest (100 kJ) rockfall barriers. As a result, qualified project design engineers, suppliers, and contractors are held hostage by owner’s representatives and/or structural engineers not familiar with rockfall barrier design and function. Many experienced practitioners and contractors suggest that the purely structural solution is generally over-sized and results in unnecessarily expensive foundations. They offer as evidence the performance of earlier un-engineered foundations with their many years of effective performance on countless projects. The current codes, however, suggest that these simplified foundations cannot withstand the loading that results from a rockfall impact, hence the PARADOX. As is often the case, the truth is somewhere in the middle.

BACKGROUND

Rockfall barrier design considerations over the years have focused primarily on the impact energies in the net and the forces on support rope anchors. The primary purpose of the supporting posts in a rockfall barrier system has been to maintain the height of the catchment net. As such, foundation performance has not been as critical to the operation of the system as, for example, is anchor embedment. However, post foundations are subject to loading during an impact and should be designed accordingly to ensure limited maintenance after impact. This is especially important for foundations in soil.

Very little emphasis has been placed on the actual design of the concrete post foundation. The argument for the lack of emphasis has been that the posts serve only to hold the barrier to the design height during impact and therefore foundation performance is secondary to the other issues involved in protection system design. Indeed, many construction projects rely only on a 3-ft X 3-ft X 3-ft unreinforced and un-engineered concrete block without any analysis.

Some observations concerning this approach are as follows:

1. Rockfall impact results in dynamic loads < 1-sec in duration of loading
2. Foundation movement (ground deformation) is unknown and unpredicted
3. Current designs are based on limited or no geotechnical data. Therefore they are becoming more and more conservative
4. Maximum elongation of the rockfall barriers is now well known
5. Forces applied to the foundations, are now available from full scale tests to permit improvement of a barrier’s design and quality.

Design foundation forces during barrier impact are provided by rockfall barrier manufacturers. Although these loads may have been determined by direct measurement during testing, more likely by they are extrapolated based on support rope anchor loads. This is due to the difficulty involved in instrumenting the foundations during testing and the prevalent feeling that the foundations are not so important to warrant significant effort to determine their loads.

Post anchor bolts can be loaded in shear, tension, compression or a combination of loads. The type of post determines the design forces and moments that are applied on the foundation by the base plate. Fixed post foundations, Figure 1, must be designed to resist an applied moment, generally on the order of 170-kn-m to 410-kn-m, while the upslope foundation anchors must resist pull-out, about 160-kN to 300-kN, from the concrete. Pinned rockfall barrier posts, Figure 2 need only resist an applied shear force at the base plate, up to 600-kN.

European Approach

Berber (2001) described European guidelines for post foundations used for certification testing. Because it was recognized that foundations types depend on the actual barrier as well as the foundation material, no standard foundation was proposed. However, Berber did state that all pressures and forces acting on the foundation must be transmitted to the subsurface material. If the foundations are shallow, some method of transmitting these forces and moments must be incorporate and the foundation design must account for the earth-structure interaction effects of an applied dynamic load.

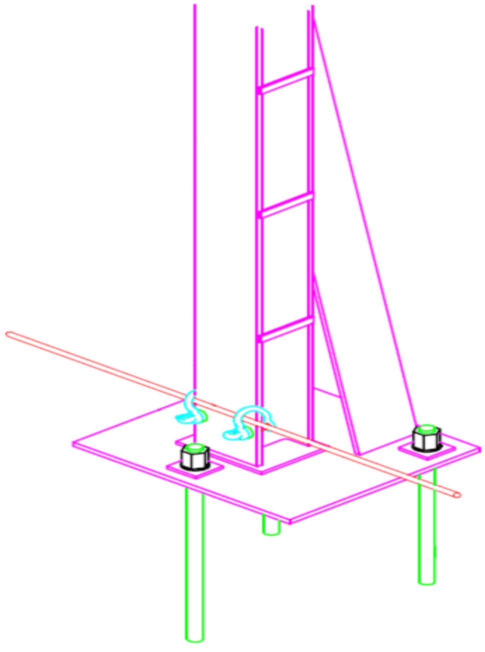

Figure 1. Fixed post base plate

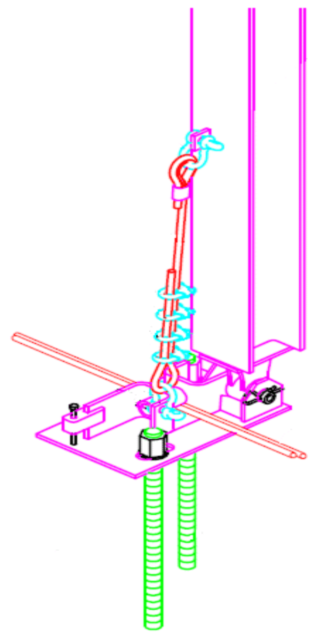

Figure 2. Pinned post base plate

In addition, Berber also stated that: "There is no reliable method of precisely calculating the forces on foundations and anchorages that result from the conversion of the kinetic energy of a rock into deformation energy of the construction." Therefore the European position is that only the force measurements determined during actual testing can be relied upon. Even in that case it was recommended that loads be increased by 30% from the measured loads for actual design.

TESTING

Actual published measurement data of loads on foundations are rare but directly govern design. Turner et al. (2009) published data from Diotallevi, et al. (2007) derived from an actual instrumented pinned post foundation. The loads were 33.6-kN (7.55-kips) in shear and 57.3-kN (12.88-kips) in compression.

Roth (2006) reported on foundation forces for an instrumented 100-KJ barrier with a fixed end connection. Three pressure cells were mounted to a baseplate. One cell was mounted beneath the plate on the compression anchor (downslope). The other two cells were mounted on the tension (upslope) anchors on top of the baseplate. Figure 3 shows a typical load cell test setup for a post foundation. A test at 110% of the barrier design energy resulted in a compression force of 41-kn on the downslope post anchor and tensile forces on the upslope anchors of 39-KN and 23-KN. The resulting calculated moment was 43.26-KN-m.

CURRENT PRACTICE

Figure 3. Typical foundation instrumentation set-up (Berber, 2007)

Presently, there is no accepted standard foundation design for rockfall barrier posts in soil. As described above, often the foundations are not designed using the prescribed forces for the intended barrier but, instead, are built to the satisfaction of the design engineer or even the contractor. As stated by Berber (2007), depending on the geomaterial present, the foundation type can vary. When installed on hard, competent bedrock, anchors are grouted directly into drilled holes. Generally, only the tension anchor must be checked for capacity. This can be done using the Post Tensioning Institute (1994) bond strengths for anchors. Details on foundation anchors in rock are beyond the scope of this paper.

Types of post foundations in current use in the United States are concrete blocks, drilled shafts, and concrete block/micropile combinations.

Unreinforced Concrete Block

Foundations in colluvial materials or soils can be either shallow concrete block foundations or drilled shafts. Turner et al. (2009) used Broms' (1964a; 1964b) approach, which is essentially a Rankine earth pressure approach, and the loads described above to design a foundation in cohesionless soil for a 1,000-KJ (350 ft-ton) barrier. The foundation size was a cubical 2.5-ft x 2.5-ft x 2.5-ft. They determined that the footing had a safety factor against sliding of 2.56.

This approach has the distinct advantage of simplicity using simple geotechnical design methodology and parameters. In weak soils at higher barrier energies and foundation loads, the width of the foundation becomes problematic as it relies only on the friction mobilized along the base and the passive resistance of the soil in front to resist failure.

Concrete Anchor Bolt Design

The adoption of the 2003, 2006, or 2009 International Building Code (IBC) by nearly all United States jurisdictions created a need to design anchors in concrete per the American Concrete Institute ACI 318 Appendix D. Design per this code accounts for breakout of anchors subject to dynamic loads. Many reviewers are now requiring that baseplate anchors meet Appendix D criteria.

The authors have calculated the size of an unreinforced concrete block necessary to meet Appendix D requirements. Using the shear force of 191-KN (43-kips) for a heavy duty barrier, the minimum width to prevent anchor bolt breakout was calculated to be 1.22-m (4-ft). These calculations suggest that a 1-m3 block cannot be used in all situations.

Drilled Shaft-type foundation

It appears that at very low energies or foundation anchor loads unreinforced concrete blocks may be used and that the foundation type depends more on constructability and preference. At higher foundation loads, calculated block sizes may become prohibitive. In that case a drilled shaft foundation may be the best option. The advantage of the shaft is that, because it is deeper, less rotation will occur on impact. At higher energies the size of a pier-type foundation becomes extremely wide in order to accommodate the high dynamic passive pressure placed on the subgrade. In these cases, a drilled shaft will most likely be more constructible.

Drilled shaft design for rockfall barriers can be done similar to Tuner, 2009 as shown by early design analysis for laterally-loaded piles also used Broms' Method. This approach treats the laterally-loaded pile foundation as either a 'fixed' or 'free' end condition. The hand calculation used determines the ultimate soil resistance to lateral loading. The Broms' method is limited to purely cohesive conditions or purely cohesionless conditions.

The p-y method analyzes the pile as an elastic beam and the soil is represented by a series of springs. This approach takes into account the nonlinear behavior of soil, pile geometry, pile material properties, and nature of loading on the pile. These parameters are used to determine deflection, bending moment, shear, and soil resistance as a function of Pile Length. The p-y curve is dependent on Soil Resistance (p) vs. Pile Deflection (y).

By defining the soil properties, the initial stiffness (EI) of the soil is determined based on soil classification. The variation of this soil stiffness can cause a significant change of the pile deflection.

Hetényi's beam on elastic foundation equation (Hetényi, 1946) is solved using the p-y curve for soil behavior.

$$EI^* \frac{d^4y}{dx^4} + P_x^* \frac{d^2y}{dx^2} - p - W = 0$$

P_x = Axial Load on Pile
y = Lateral Deflection of the pile at a point x along the length of the pile
p = Soil reaction per unit length
EI = Flexural Rigidity (stiffness)
W = Distributed load along the length of the pile

The computer program (LPILE) is used to solve the equation along the length of the foundation. The solution provides deflection, rotation, moment, shear, and soil resistance as a function of length along the pile.

Wagner and Kane (2010) repeated the design of a foundation using the loads and soil properties used by Turner et al. above. Instead of a block and using a deflection criterion of apporoximately 1-in at the top of the foundation, they designed a drilled shaft using the L-PILE (13) program. The solution yielded a shaft 5-ft deep x 2-ft in diameter with the same volume of concrete as the 2.5-ft cube, approximately 15.7-ft^3. Therefore, the required amount of steel reinforcement will be the same if the Turner et al. foundations were reinforced per concrete design criteria.

Further, the L-PILE analysis provides the estimated horizontal displacement under the manufacturer's published design load for the drilled shaft being 1.3-in (no damage to the foundation). Turner, et al. (2009) did not publish an estimated horizontal displacement after impact. It would be expected that the cubical foundation displacement would be much greater as it was only one half as deep. By taking into account foundation deflection the relatively small 1-m3 block of concrete can likely shown to be sufficient for many barriers and ground conditions.

Micropile Foundations

Rockfall protection system manufacturers also show typical foundations in their installation material. Figures 4 and 5 show typical drawings from two prominent manufacturers for post foundations in soil.

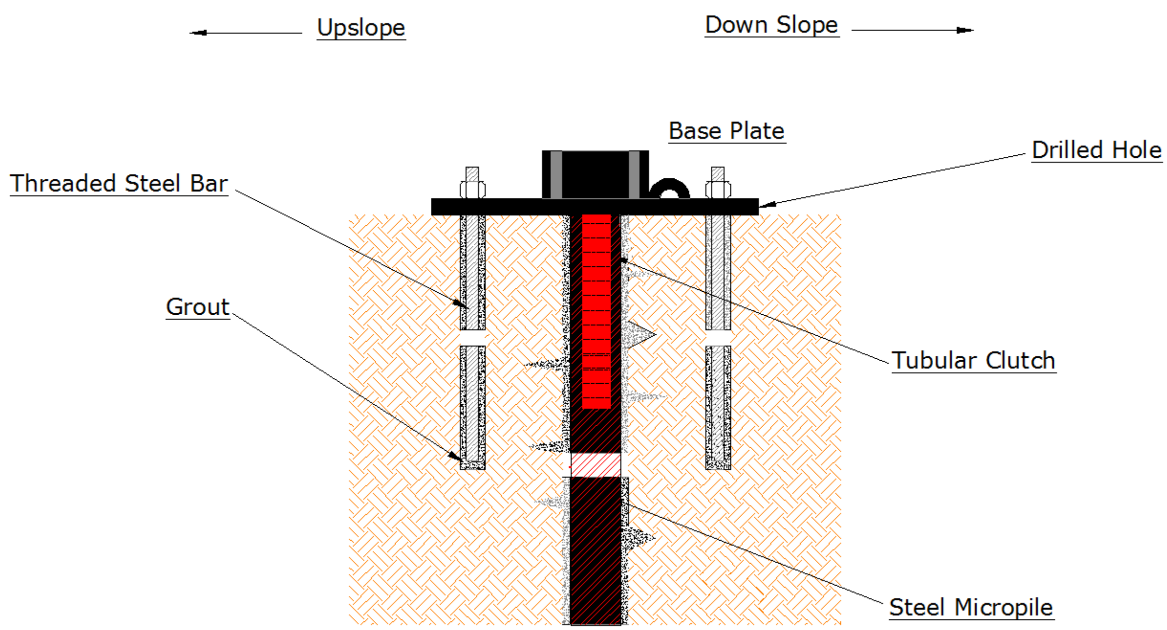

Figure 4. Schematic diagram from rockfall barrier manufacturer for a pinned post foundation on soil

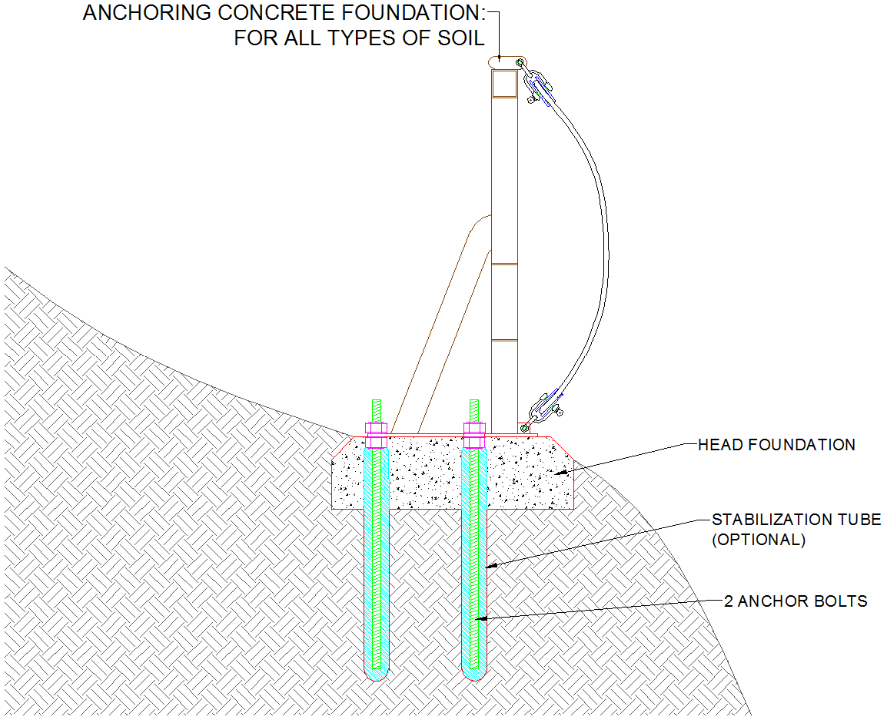

Figure 5. Schematic diagram from rockfall barrier manufacturer for affixed post foundation on soil

Design problems arise in Figure 4 because the foundation is pinned so that the applied load is in shear. A Broms/Rankine solution would be best as passive pressures against the foundation elements restrain the foundation. In addition, the depth of the central micropile is irrelevant as significant rotation of the baseplate on the soil would be necessary to mobilize a moment in the pile. To prevent horizontal displacement, it would have to be much wider, that is, approaching a block foundation. Installation of the central micropile would have to be by driving or drilling and grouting. In such a case, deep foundation design methodology would need to be employed and one would most likely use the approach of Reese et al (2004).

Figure 5 presents its own set of problems. The central design problem is an applied moment to the foundation. Relying on uplift and compressive forces on the anchors is unacceptable as this foundation design uses a concrete "head" or cap. The thickness and stiffness of the cap becomes part of the design mix making a straightforward calculation difficult.

CONCLUSIONS

For post foundations in soils, the following conclusions can be made:

1. Reinforcement of concrete is standard to foundations. The often used 3 x 3 x 3 block is probably good for relatively low energy barriers. As energies increase, the block will either fail structural or undergo undesirable lateral displacements.
2. As loads become greater block foundations become impractical
3. Micropile foundations in soil are difficult to analyze and construct

4. For higher energy barriers, drilled-shaft foundations are probably the most easily designed and constructed.

As engineers and geologists we have an obligation to protect and serve the public. While safety is the pre-eminent concern, using clients' funds wisely is also a very important aspect. Under-designed or un-engineered foundations place the public at risk while over-design, either from lack of experience or an extreme attempt to avoid liability, does no one any service. The authors have personally witnessed 500-KJ barrier post foundations in weathered rock/stiff soil with three 25-ft deep micropiles beneath a concrete block for each post! These foundations clearly did not take into account load transfer and foundation design principles, but also an inexplicable fear of deviating from an interpretation of a schematic sketch in the manufacturer's installation literature.

Field performance of rockfall barriers over the past decades has shown that unreinforced concrete post foundations can perform well during rockfall impacts. At the same time recent barrier post foundations have been designed based on accurate foundation loads and standard engineering practices to be larger and more complex than seen in the past. This paper is not a prescription for barrier foundation design, but it is hoped that this paper will help to provide a rational discussion of this one aspect of rockfall barrier design.

REFERENCES

American Concrete Institute (ACI) *318-08 (Appendix D) – Building Code Requirements for Structural Concrete and Commentary (Anchoring to Concrete),* American Concrete Institute, Farmington Hills, Michigan.

Broms, B.B., 1964a, Lateral Resistance of Piles in Cohesive Soils. Journal of the Soil Mechanics and Foundations Division, ASCE, Vol. 90, No. SM2, pp. 27-63.

Broms, B.B., 1964b, Lateral Resistance of Piles in Cohesionless Soils. Journal of the Soil Mechanics and Foundations Division, ASCE Vol. 90, No. SM3, pp. 123-156.

Berber, W., 2001, *Guideline for the approval of rockfall protection kits*, Swiss Agency for the Environment, Forests and Landscape, (SAEFL) and the Swiss Federal Research Institute WSL Berhe, pp. 32-33.

Diotallevi, P., P., Gottardi, G., Govoni, L., 2007, *High Resistance (Maccaferri) Rockfall Barrier, (500kJoule) CTR/05/07/B, Full Scale Impact Test Certification*, University Of Bologna, DISTART Department (Faculty of Engineering) and Consorzio Triveneto Rocciatori s.r.1 f Fonzaso, July 25, 2007.

Hetényi, M. (1946). *Beams on Elastic Foundations: Theory with Applications in the Fields of Civil and Mechanical Engineering*. University of Michigan Press, Ann Arbor.

International Code Council (ICC) – 2003, 2006, 2009 *International Building Code*, International Code Council, Washington, D.C.

Reese, L. C. and O'Neill, M. W. (1988). *Drilled Shafts: Construction Procedures and Design Methods*." Report prepared for the Federal Highway Administration, Mclean, Virginia.

Reese, L. C., Wang, S. T., Isenhower, W. M. Arréga, J. A., and Hendrix, J. (2004). "Computer Program *LPILE^{Plus} Version 5.0 User's Guide*." Ensoft, Inc., Austin, Texas.

Roth, A., 2006, *Summary Report on the Approval of the Geobrugg Rockfall Protection Barrier TXI-010 (100KJ)*, Colorado School of Mines, Department of Geology and Geological Engineering, Golden, Colorado.

Turner, R., Duffy, J. D., Turner, J. P., 2009, *Post Foundations for Flexible Rockfall Fences*, Proceedings of the 60th Highway Geology Symposium, pp. 125-139.

Wagner, D. A., and Kane, W. F., 2010, *Rockfall Mitigation Field Techniques and Design*, Proceedings, of the 61st Highway Geology Symposium.

Cable Anchors versus Solid Bar Anchors in Rockfall Mitigation Systems

Chris G Ingram
HI-TECH Rockfall Construction, Inc.
PO Box 674
Forest Grove, Oregon 97116
503-357-6508
Chris@hi-techrockfallconstruction.com

Dane Wagner, GIT
HI-TECH Rockfall Construction, Inc.
PO Box674
Forest Grove, OR 97116
(503)-357-6508
Dane@hi-techrockfallconstruction.com

Prepared for the 63rd Highway Geology Symposium, May, 2012

Disclaimer

Statements and views presented in this paper are strictly those of the authors, and do not necessarily reflect positions held by their affiliations, the Highway Geology Symposium (HGS), or others acknowledged above. The mention of trade names for commercial products does not imply the approval or endorsement by HGS.

Copyright Notice

Cable Anchors versus Solid Bar Anchors in Rockfall Mitigation Systems

Abstract

This is a comparison of different types of anchors used in rockfall mitigation systems across the US. For years the standard had been using a solid bar drilled and grouted into rock to support the upper cable in all rockfall drape systems. We also saw solid bars used for the tie-back and lateral anchors in rockfall barrier installations in the beginning stages of constructing these barriers in the US.

It was found during observation of the installed systems that, due to the impacts from the rockfall, the solid bar anchors used in rockfall barriers were not working as rocks were shearing off the top of the anchor bars as they rolled down the slopes prior to impacting the barriers resulting in post failures and reduced net heights, thus compromising the systems capacities before impact. We also found years ago that solid bar anchors for rockfall drapes were being compromised by using too small of an anchor rod. The forces that are transferred to the anchors in more in shear than the vertical pull-out direction that the anchors were tested in, thus reducing the capacities most engineers were requiring as the shear strengths in the solid bars were considerably less than the required pull-out strength.

In recent years, there has been some testing to determine the difference in strengths between cable anchors and solid bar anchors (WSDOT field test). This testing clearly showed that cable anchors are superior to solid bar anchors. When testing the anchors in the same direction as the loads that are stressing the anchors the pull-out strength increased substantially in cable anchors versus the standard vertical pull-out tests usually performed. It also showed that the solid bar anchors failed at or near the shear strength of the bar which was much less than the required pull-out strength for most anchoring systems designed using a solid bar anchor.

INTRODUCTION

This paper outlines the differences in strengths and capacities of cable anchors versus solid bar anchors in a variety of rockfall mitigation systems. In the beginning stages of rockfall mitigation work in the U.S. solid bar anchors were generally specified for use on all rockfall mitigation systems including rockfall barriers, wire mesh draperies, and cable net draperies. However, during observations of constructed systems in the field and continue field testing of systems, concerns arose. These concerns developed as observations of damage to the solid bar anchors occurred. In rockfall barriers damage occurred in the form of shearing off of anchors during rockfall events due to impacts from falling rocks. In wire mesh and cable net drapery systems excessive bending and breaking of anchors occurred during loading during rockfalls.

PREVIOUS WORK & METHODS

Muhunthan's research report, (Muhunthan, 2005) prepared for the Washington State Department of Transportation in cooperation with the U.S. DOT – Federal Highway Administration compiled data from the testing of five different types of anchors for rockfall systems including manta-ray, single cable anchor, double cable anchor, 1" solid bar anchor and 1" hollow core anchors with cable attachment. The anchors were installed in unconsolidated slope deposits consisting of moist, medium dense, silty gravel with sands, cobbles, and small boulders. The anchors were loaded both vertically and within 15 degrees of horizontal to determine the capacities in both directions.

The design and the capacity of the anchors in rockfall mitigation systems is one of the most important factors in assuring that the system performs as required and is also one of the most important factors in affecting the overall cost of the system. The installation of the anchors typically consists of approximately 35% of the labor costs in drapery systems and 30% of the costs of rockfall barriers. In the early stages of drapery rockfall mitigation systems in the U.S., anchoring systems used a 5/8" loop eye bolt installed to a depth of 1 meter (figure 1), with no criteria for pull-out strengths or any testing criteria.. In construction of rockfall barriers, 1" solid bar anchors were used and generally the specifications called for testing of a percentage of the anchors to a capacity recommended by the manufacturer.

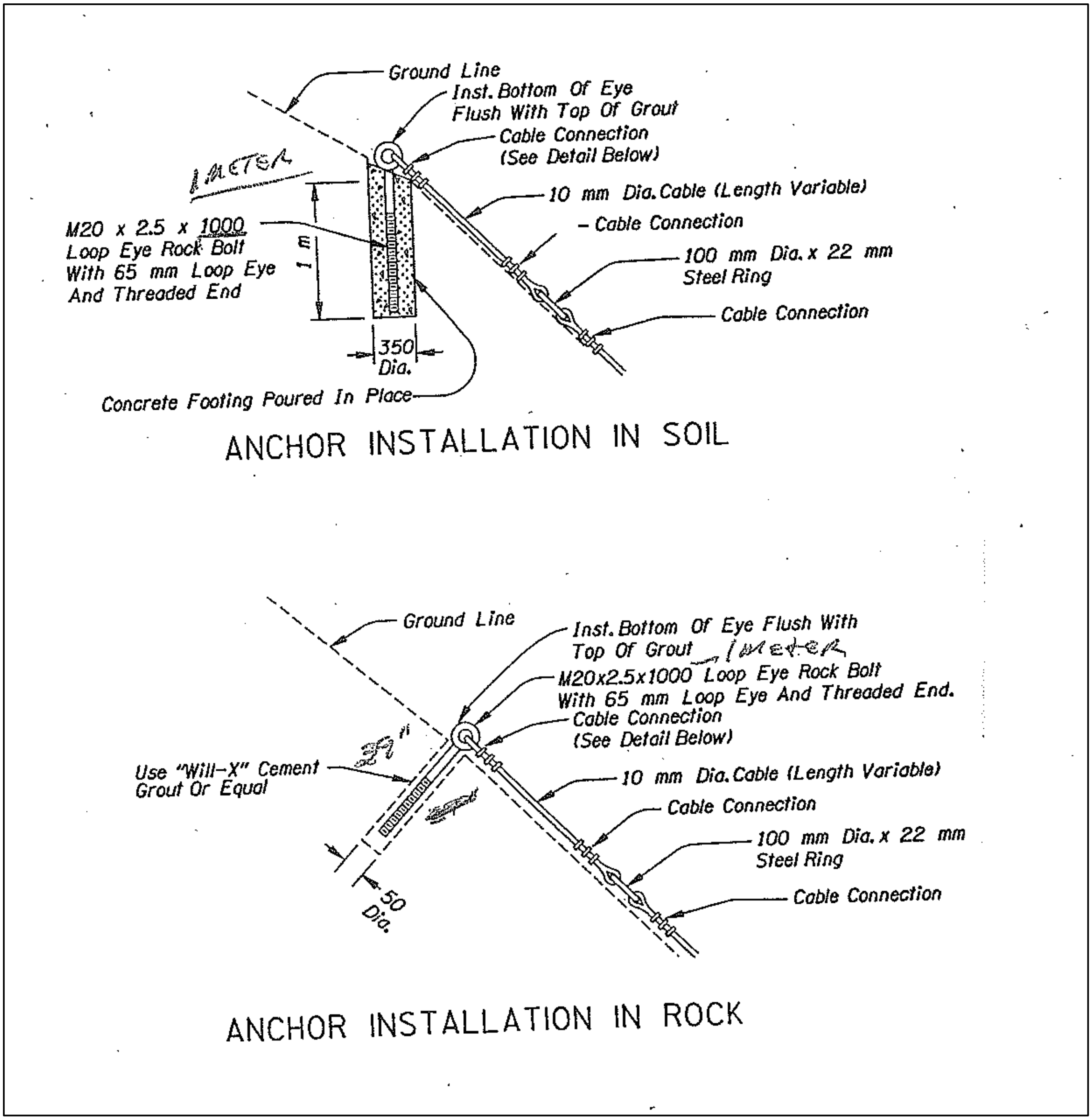

Figure 1. Early Solid Bar Anchor Design Detail for Drapery System.

As both barriers and drapery systems were constructed in the US, observations of the solid bar anchordamage were made. As the anchors became stressed or impacted by rockfall events, anchors began pulling out of the ground, bending in the direction of the applied force, and in some instances, breaking or shearing off at ground level due to loading or impacts from the falling rocks. Figure 2, displays a rockfall barrier anchor bending in the direction of the loading force.

Figure 2. Bent Solid Bar Rockfall Barrier Anchor After Barrier Impact.

The industry began a shift towards wire rope anchors in rockfall barriers in the late 1990's as it was observed that anchors were sheared off due to impacts from the falling rocks. The failures of these anchors were occurring during impacts that the barriers were designed to withstand. Shearing of the anchors in this situation compromised the integrity of the rockfall barriers. The loss of the anchors reduced the effective catchment height of the barrier as retaining ropes sagged and design energy dissipation was lost since energy transfer through retaining ropes to the ground was no longer available.

Rockfall drapes however during this time frame were still being specified for solid bar anchors across the United States even though anchor failures were ongoing. During this time typical anchor designs did change from the use of 5/8-inch rods to a 1-inch diameter bar. An increase anchor depth was also specified in the range of 5-feet to 6-feet. The range of the drapery support anchors, used at the top of the slope, varied greatly. Specifications for the anchor spacing ranged from 6-foot centers to 40-foot centers. Anchor proof testing criteria to verify capacities of the anchors was done on a percentage of the load for the installed anchors. The anchor capacities at this time were specified in the 15 to 20 ton range; this was due to a lack verifiable data or studies done to determine the actual loads placed on the anchors. Today, with available data there is the ability to determine the actual pull-out strengths that are required by the system. This can be done for both rockfall barriers and draperies by determining the load the anchor must support (Wagner and Kane, 2010). Anchor sizes and depths can also be calculated utilizing the known loading requirements with the aid of the Post Tensioning Institute (PTI) formula for prestressed rock and soil anchors (PTI, 2004).

CONTEMPORY METHODS

A study that was completed in April 2005 by WSDOT (Muhunthan, 2005) was instituted to develop a rational and broadly applicable design methodology, while ensuring optimal system performance and where possible construction of a more economical system. The study tested both solid bar anchors and cable anchors in similar ground conditions. The study compared pull-out strengths of both wire rope cable and the solid bar type anchors. The study provided results showing that when anchors were pull-tested vertically both anchor types were capable of loads exceeding 20,000 lbf (89kN) and all the loads were achieved with less than 2 inches of displacement. Of the anchors that were tested to failure a cable anchor achieved the highest load of 47,000 lbf (209kN).

While a vertical pull-out test is a representative strength of an anchor's capacity in the vertical(?) direction, rockfall systems loading forces occur in a direction sub-perpendicular to the ground surface (Figure 3). This is especially true for drapery systems where the load is applied to the anchor in a direction parallel to sub-parallel to the ground surface (Figure 4).

Figure 3. Rockfall Barrier with Typical Sub-Perpendicular Anchors.

Figure 4. Wire Mesh Drapery Support Anchor Conforming to the Slope Surface.

For these reasons tests were also done in a horizontal loading direction. The results of these test showed that the pull-out capacities increased. The tests utilized the same anchors installed at the same depths when the testing was performed and loads were applied in the actual direction by which the drapery systems would load the anchor. The testing results again proved that the cable type anchor out-performed the solid bar anchors. The solid bars required the highest amount of deflection while developing the lowest range of capacity. This occurs because the solid bar anchors are rigid. The rigid anchor prevents the load from being transferred directly to the ground through the anchor itself. Wire rope cable anchors, to the contrary, are flexible and conform to the ground surface which allows for the majority of the load to be transferred to ground anchor (Figure 5).

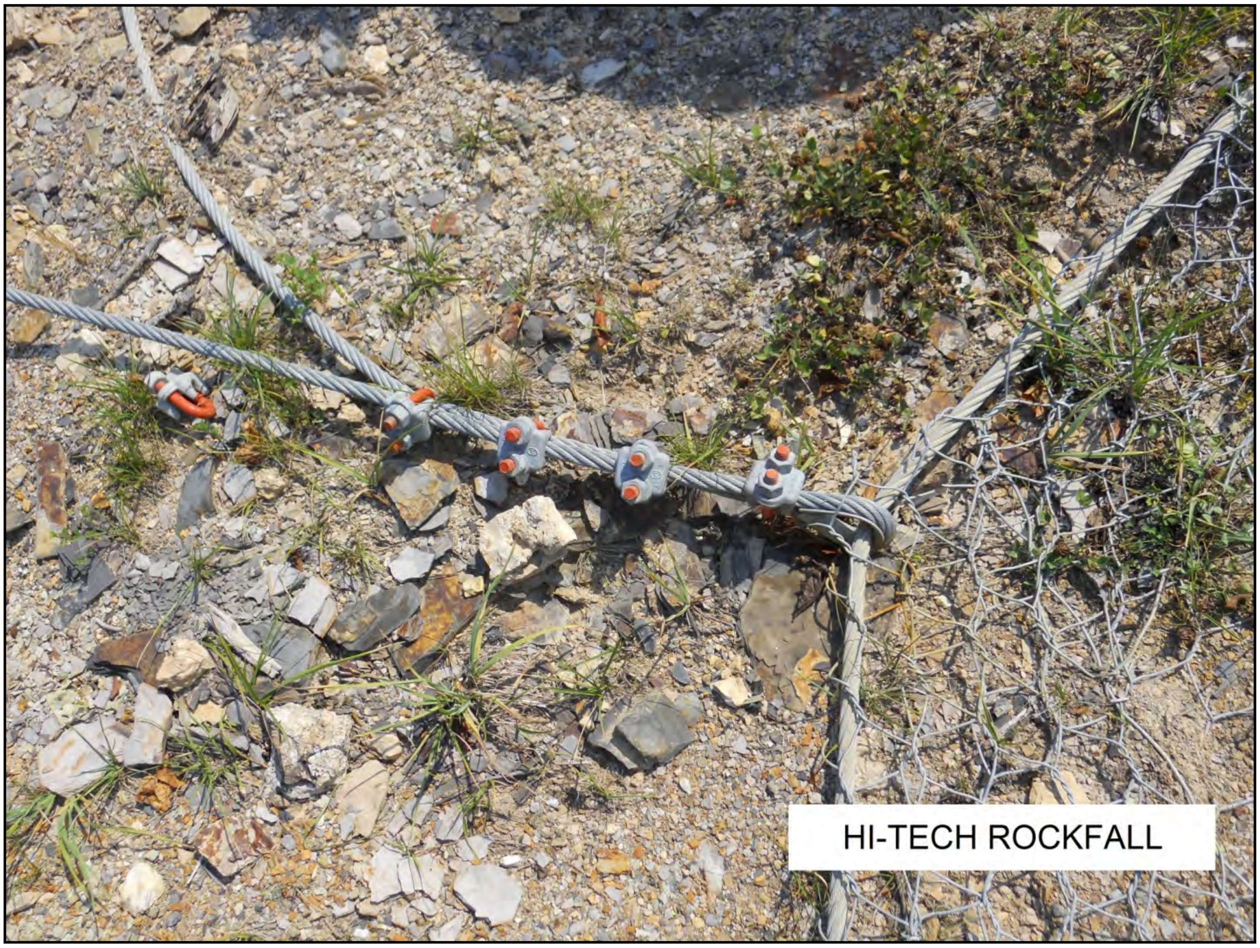

Figure 5. Loaded Wire Rope Cable Anchor.

CONCLUSIONS

During the last 25 years there have been a variety of anchor designs with a wide range of capacities, depths, and diameters. The design of the anchors is an important factor to assure that the system will perform as designed without compromise. In the past drapery systems utilizing solid bar anchors have ranged in depths and diameters from 2-inchs to 6-inchs in diameter, with depths from 6-feet to 25-feet, and with pull-out strengths from 6-tons to 20-tons. In extreme cases, anchors for drapery systems have required anchor depths which were longer in length than the exposed slope itself. When anchors are designed it is important to understand the overall effect the system has on the anchor, meaning an increased depth for a solid bar anchor may not increase the strength. As the WSDOT 2005 testing demonstrated, bar anchors loaded in a direction not in line with the ancho show signs of deformation. Additionally, observations of solid bar anchors sheared off near the ground surface showed that solid bar anchors can compromise the integrity of the system. Thus, anchor design can greatly affect the cost of the system, especially if repairs are needed to insure the system is working appropriately.

The use of cable anchors in the design of all rockfall mitigation systems allows for a greater degree of assurance that the anchor will not be compromised. This is true for impacts from falling rocks in barrier installations or potential shearing or bending when movement of rocks under a drapery system occurs. The use of a cable anchor also provides higher capacities in a similar depth and diameter holes than the use of solid bar anchors. Cable anchors conform to uneven ground conditions due to their flexibility. They can also flex in multiple directions during loading events, which allows for the transfer of load to the ground anchors. Thus insuring loads during rockfall events are transferred to the anchors and prevents damage to the systems. For these reasons wire rope cable anchors should be specified in all rockfall systems in lieu of solid bar anchors as they provide a better overall product than the solid bar anchors.

REFERENCES:

- Muhunthan, B., Shu, S., Sasiharan, N., Hattamleh, O., Badger, T., Lowell, S., Duffy, J. *Analysis and Design of Wire Mesh/Cable net Slope Protection*. Research Report. Washington State Department of Transportation and US DOT – Federal Highway Administration. April, 2005.

- Wagner, D. A. and W. F. Kane. Rockfall Mitigation Field Techniques and Design. In *Conference Proceedings 3: Slope Stabilization and Mitigation*, 61st Annual HGS, Highway Geology Symposium, Oklahoma City, OK. 2010.

- Post-Tensioning Institute, (2004). "Recommendations for Prestressed Rock and Soil Anchors." Post-Tensioning Institute. Phoenix, Arizona. 2004. 98 p.

Case Histories on Mitigating Geologic Hazards in Mountainous Areas of California's Intrastate Highway System

Brandon Badeker, CEG
California Department of Transportation
5900 Folsom Boulevard, Sacramento, California 95819
(916) 227-1046
E-mail: Brandon_Badeker@dot.ca.gov

Prepared for the 63rd Highway Geology Symposium, May 7-10, 2012

Acknowledgements

The author would like to thank fellow Engineering Geologists and Senior Engineering Geologists with the California Department of Transportation with their assistance in mitigating rock fall hazards throughout the State and their assistance with preparation of this report.

Disclaimer

Statements and views presented in this paper are strictly those of the author, and do not necessarily reflect positions held by their affiliations, the Highway Geology Symposium (HGS), or others acknowledged above. The mention of trade names for commercial products does not imply the approval or endorsement by HGS.

ABSTRACT

Maintenance of highways in the mountainous areas of California is challenged by a multitude of geologic hazards which include slumps (small scale rotational slides) and rock fall to deep seated failures comprised of landslides and rockslides. This paper primarily focuses on rock fall and the mitigation measures employed to reduce that hazard.

Various options are available to the Engineering Geologist at Caltrans (California Department of Transportation) to mitigate rock fall hazards in a cost efficient yet professionally suitable basis. Mitigation options selected for this review consist of temporary solutions such as hand scaling (removal of loose rock on a slope surface with hand operated equipment) as well as permanent solutions such as grading, blasting and realignment.

This paper will look at five locations, the rock fall hazards posed, and the measures employed to mitigate those hazards. The sites are presented from north to south and are situated in the Sierra Nevada and Basin and Range Geomorphic Provinces. The sites extend from Alpine County in the north through Kern County in the south, and from Inyo County in the east to Fresno County in the west. The locations include Highway 88 at Carson Pass where three projects have been performed to mitigate recurrent rock fall issues, as well as hand scaling of multiple slopes on Highway 198 east of Visalia to prevent weather induced rock fall. Other locations include an earthwork mitigation of a rockslide on Highway 168 east of Fresno; blasting to prevent a rockslide on Highway 180 in Kings Canyon, and realignment of Highway 190 at Towne Pass in Death Valley National Monument to mitigate recurrent rock fall.

The locations have been chosen to show a range in mitigation options for rock fall related hazards on California's highway transportation system in mountainous areas. Due to the short time frame (about 10 years) encompassed in this case history, as well as the localized area (primarily central and south Sierra), all mitigation methods currently employed by Caltrans could not be documented in this one area alone. Other mitigation options that are not discussed in this paper include wire mesh and cable net draperies, and flexible and rigid barriers.

INTRODUCTION

Maintenance of the State Highway System in the mountainous areas of California are challenged by numerous types of geologic hazards that effect the integrity of the roadway and the safety of the travelling public. Hazards include localized instabilities in the form of rock fall and slumps. Movement occurs at every scale along the transportation corridors, from the small slumps to large rotational and translational slides. Due to the complex geologic nature of California's mountainous areas, nearly every earth material type can be identified, from hard, competent rock to variably fractured and weathered rock and soil, alluvium and fill. This paper focuses on rock fall related hazards that have occurred in the last ten years depicting some of the mitigation measures available to the Engineering Geologist at The California Department of Transportation (Caltrans).

The majority of the sites are situated in the Sierra Nevada Geomorphic Province, typified by Mesozoic Granitic rocks although each site varies in exact species of granitic composition. The exception to this is the last location, Towne Pass, situated in Death Valley National Monument. Towne Pass is situated in the Basin and Range Geomorphic Province, and typical of extensional regimes, contains Tertiary volcanics, unconformably overlying Paleozoic marine sedimentary rocks.

Figure 1: Overview map of California showing the five locations used in the case history; (1) Carson Pass in Alpine County; (2) Auberry Slide in Fresno County; (3) Kings Canyon in Fresno County; (4) Kaweah Reservoir in Fresno County; and (5) Towne Pass in Inyo County. The map was adapted from Google© Maps.

CASE 1: CARSON PASS

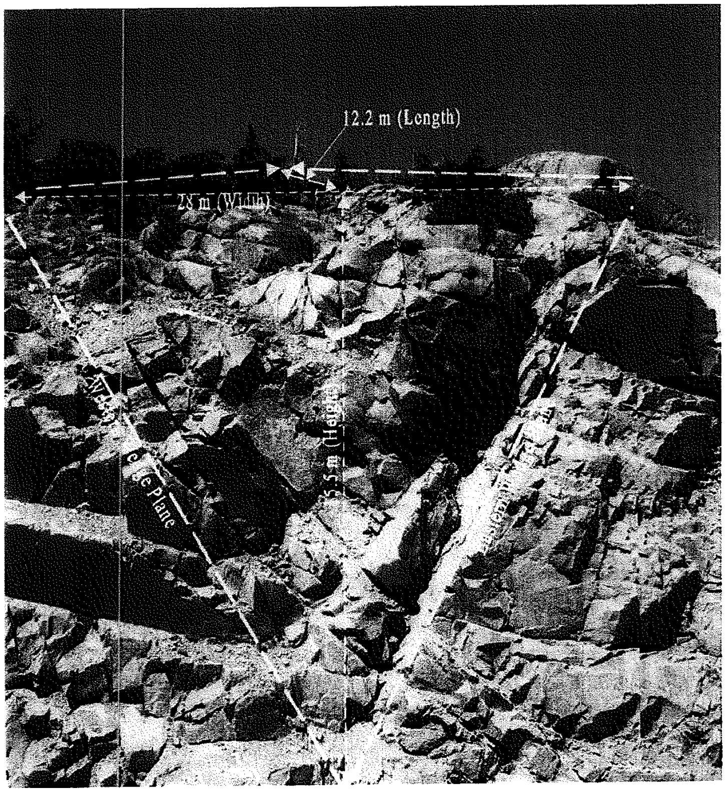

Figure 2a: Documents from the original investigation depicting the wedge shaped discontinuities as the primary mode of failure.

Carson Pass is on Highway 88 in Alpine County, about 50-miles east of the Sacramento Metropolitan area and southwest of Lake Tahoe. Highway 88 is an east-west trending highway, south of Highway 50, connecting the Town of Jackson, along the Highway 49 corridor to Highway 89 south of Lake Tahoe (Figure 1). Carson Pass has exhibited rock fall as the primary geologic hazard in which to be mitigated. Three separate projects have previously been initiated at different intervals to combat the rock fall hazard. The hazard in this area is intensified due to the fact that there are ski resorts in the area that see numerous visitors during the winter and spring seasons.

This location is situated in Mesozoic granitic rocks typical of the Sierra Nevada Geomorphic Province. Locally, the rock is moderately to highly fractured and slightly weathered creating large, competent boulders. The slopes were originally graded at about 0.5:1 (h:v) with maximum heights of about 80-feet.

At PM R5.6 (the westerly most portion of the Pass), rock fall occurred in 2006 closing the Highway. Engineering Geologists reconnoitered the site, and performed kinematic evaluation of the discontinuities. It was determined that the rock fall was induced by wedge failure (Figure 2a). After their evaluation, recommendations as to catchment and slope angle were devised resulting in an earthwork style mitigation strategy for this portion of the Pass. Their determination, due to the structure of the rock, was a slope ratio of 0.6:1 (h:v) with a 6-meter catchment, with a back-slope of 4:1 (Figure 2b). The new slope was constructed in 2011.

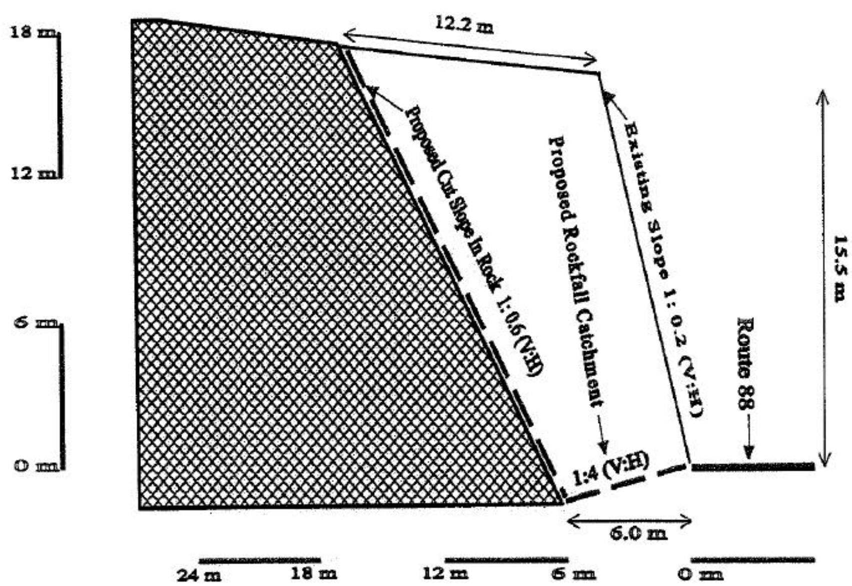

Figure 2b: Cross section schematic of the earthwork mitigation strategy at the westerly portion of Carson Pass showing a slope ratio of 0.6:1 (h:v) and a 6-meter backsloped catchment.

Approximately 500-feet east of the curve, a large semi-loose block was slowly creeping towards the highway as evidenced by an ever increasing tension crack visible from the roadway. A project was initiated to bolt the rock in place due to the fact that there were several large boulders behind the face that would have been dislodged if the boulders on the face were removed (Figure 2c).

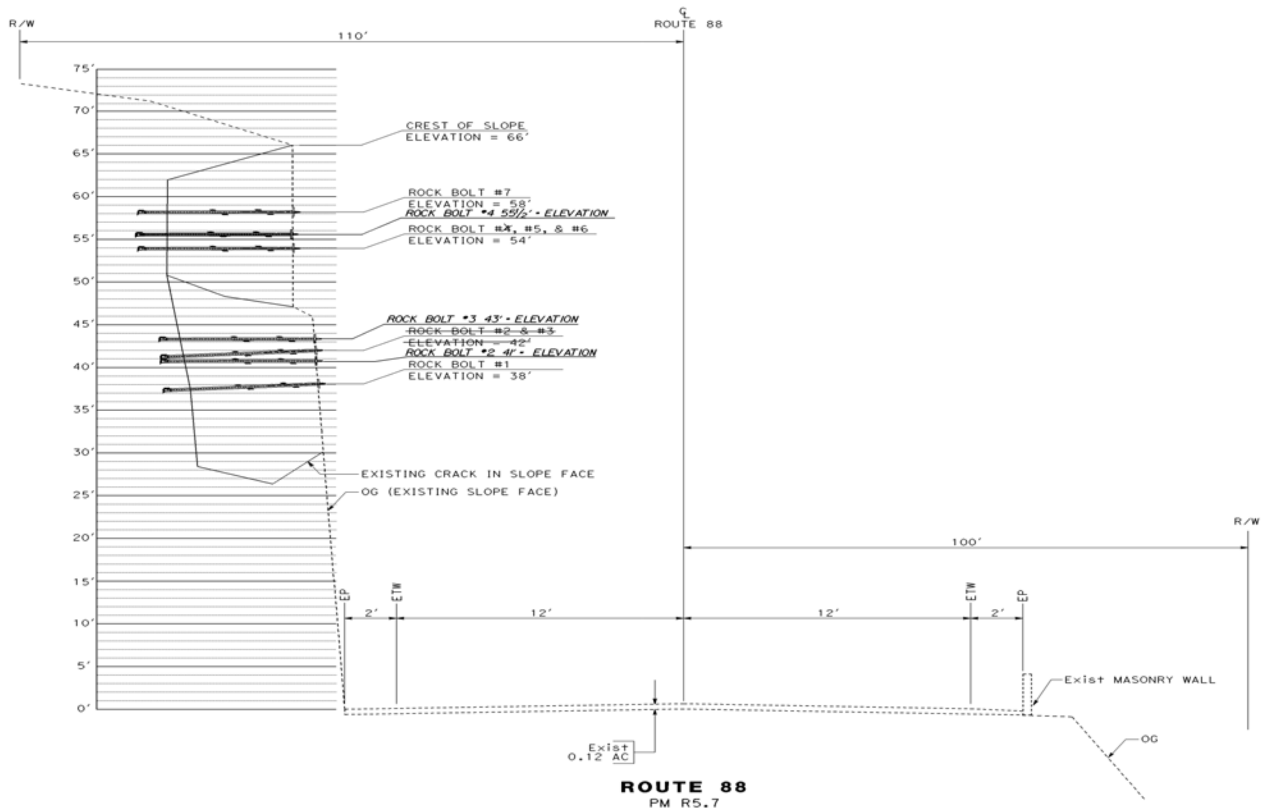

Figure 2c: Project document of the rocks that were bolted in the central portion of Carson Pass.

Figure 2d: Photograph of a boulder being dislodged from the slope and bouncing over the guardrail during emergency hand scaling operations performed on the easterly portion of the Pass.

Another 300-foot further east, a car made impact with a large boulder causing severe injury. An emergency project was initiated to hire a private scaling company to remove loose rock from approximately 150-feet of slope face. A crew of four men covered the 150-feet in two weeks, releasing approximately 180 cubic yards of material under the oversight of a Caltrans Engineering Geologist. The tools utilized included Kevlar air bags, pry bars and shovels (Figure 2d).

CASE 2: AUBERRY SLIDE

This location is situated on Highway 168 near PM L28.9, east of the town of Auberry, about 25-miles northeast of Fresno (Figure 1). In this location, the highway consists of four lanes. Slope ratios are consistent with those in California's mountainous areas at about 0.5:1 (h:v) with a maximal height of about 200-feet.

The geologic setting consists of Cretaceous granitic rocks that vary from very strong and hard with minor weathering and moderate fracturing to completely decomposed. The decomposed granite was observed primarily at the top of slope and along major discontinuities that allowed for subsurface water to infiltrate.

Figure 3a: Photograph showing Auberry Slide crossing the four lanes of Highway 168 in Fresno County, east of the Town of Auberry and west of Shaver Lake.

Figure 3b: Photograph showing some of the loose boulders remaining on the slope.

In February 2010, a mass wasting event forced the closure of the highway (Figure 3a). The overall length of the cut slope was about 1000-feet and failed along the easterly 250-feet. Upon investigation, it was found that additional rock material remained on the slope and had to be removed prior to reopening the roadway (Figure 3b). An emergency force account was initiated to remove the loose talus and rock material (Figure 3c). Immediately after the force account was initiated, the slope relaxed causing tension cracks to form above the head and laterally to the slide. Upon reinvestigation, it was determined to lay back the upper portion of the slope to remove the upper tension cracks. Due to the layout of the slope to the roadway, the lateral tension cracks were left in place as

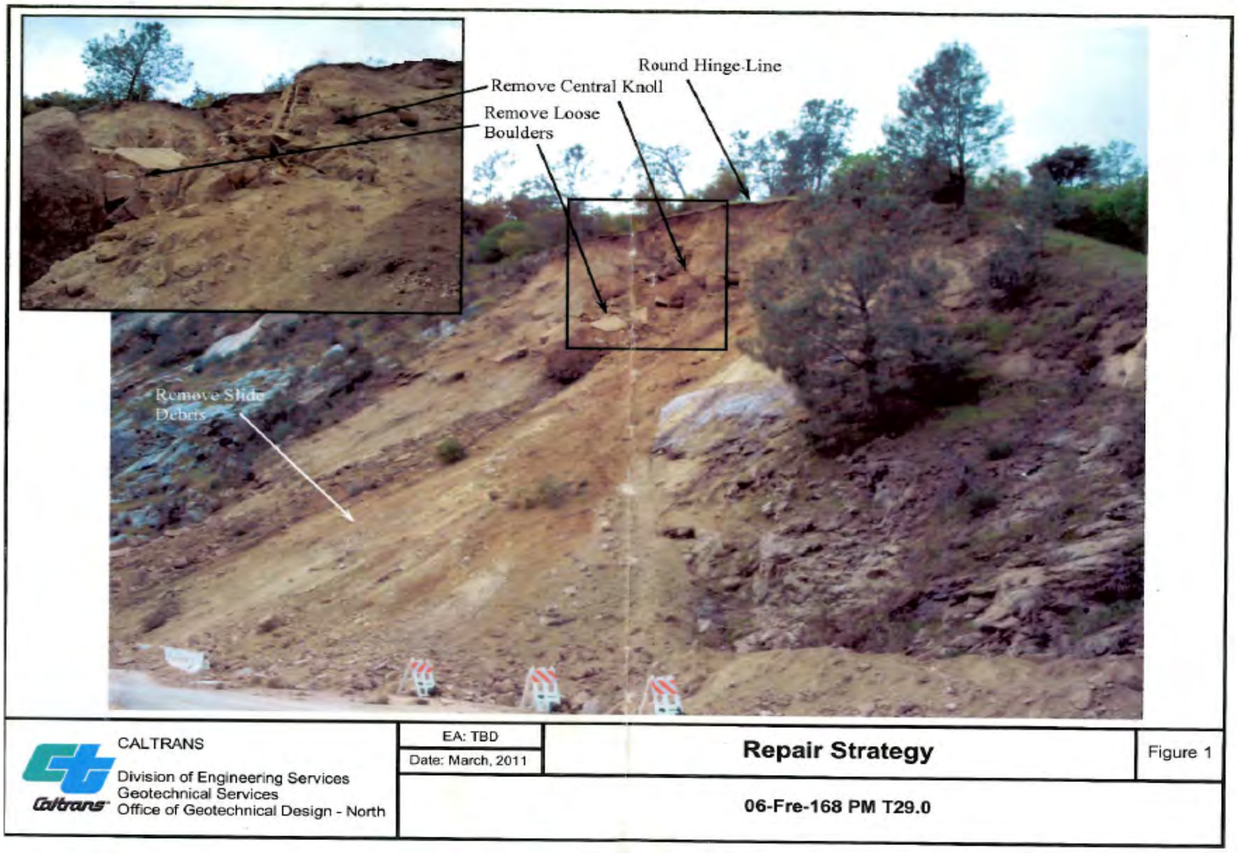

Figure 3c: Project document showing the repair strategy for the Auberry slide.

Figure 3d: Photograph showing the sompleted slope with landscape treatment.

it appeared that a failure in that area would be surficial in nature and not affect the roadway or any other facilities.

Earthwork commenced, cleaning the slide and restoring the roadway. The Highway opened approximately one-week after the slide, restoring traffic to that portion of Highway 168 (Figure 3d).

CASE 3: KINGS CANYON

Figure 4a: Photograph showing the original slide prior to investigation by Caltrans' Engineering Geologists at the Kings Canyon location on Highway 180 in Fresno County.

This site is located on Highway 180 at postmile 121.25 between Kings Canyon and Sequoia National Forests approximately 30 miles east of Fresno (Figure 1). The roadway in this area is narrow, contains numerous curves and little to no shoulders. Slope ratios vary from 0.5:1 (h:v) to 1:1. The rock type is typical of the Serra Nevada Geomorphic Province, hard Mesozoic granite with moderate fracturing (CGS, 1965).

The highway through this area is generally closed during the winter months due to heavy snow. Upon opening the highway, local maintenance forces routinely scale and blast rock that is near or on the roadway. During this period, in the week prior to opening in 2009, rocks became dislodged in an uncontrolled fashion, damaging equipment and concerning the local maintenance forces opening the road (Figure 4a). Caltrans' Engineering Geologists were called out to review the site. The only immediate hazard at that location consisted of one large block that was slowly creeping as a single 200-ton mass, held by several rocks on the bottom essentially keying the larger mass of rock in place (Figure 4c). It was decided to monitor the rock as removal would be extremely difficult by local personnel (Figure 4b).

Figure 4b: Photograph showing the monitoring plan implemented at the Kings Canyon location.

A few days after monitoring, the large mass of rock as well as the keystone blocks moved and rotated substantially. Since the large mass was acting as a whole slab it was decided to blast the rock in situ. A private blasting contractor was hired to drill and blast the rock (Figure 4d). The contractors utilized a drilling platform on a crane to access and drill the upper portion of rock. After the primary blast, a few smaller columns of rock remained on the slope, which was then hand scaled utilizing airbags, pry bars, shovels and feet by both private and State forces. Much of the rock removed during the primary blast had to be secondarily blasted in order to off haul the material.

The roadway was then patched, as substantial damage had occurred to the pavement section, and reopened one day later than originally anticipated prior to discovery of the rock fall hazard.

Figure 4c: Photograph showing the 200-ton boulder slowly creeping as one mass; note the orange marks denoting the locations for drilled holes for the explosives.

Figure 4d: Photograph showing the blasting of the 200-ton rock.

Figure 5a: Photograph the slope characteristics and the hand scaling techniques at the Kaweah Reservoir location on Highway 168 in Fresno County.

CASE 4: KAWEAH RESERVOIR

This location is on Highway 190 between postmiles 29.63 and 33.78, adjacent to Kaweah Reservoir in Fresno County, about 35 miles southeast of Fresno (Figure 1). Slope ratios are typically 0.5:1 (h:v) with heights up to about 120-feet. Benches were cut into the slopes at a height of about 80-feet above the roadway. The vast majority of the rock fall was generated in the cuts below the benches. There were several modes of local failure, from plan to wedge and topple.

Like the majority of sites presented herein, this location is situated in the Sierra Nevada Geomorphic Province, typified by Mesozoic Granitic rocks (CGS, 1965). The rock through this section is primarily very hard with moderate fracturing with weathered zones, presumably due to water infiltration.

The highway through this section consists of two and four lane sections as well as a bridge. Local Maintenance has had recurrent rock fall problems with several cut slopes throughout the years. As part of Caltrans' ongoing scaling program to reduce hazards associated with rock fall, Caltrans Geotechnical personnel assisted local maintenance forces in setting up a local hand scaling program. The coordination began with five slopes at this location essentially providing District Maintenance forces the tools for hand scaling slopes on their own with geotechnical oversight.

Figure 5b: Photograph showing some of the loose boulders being removed from the slope.

Figure 5c: Photograph showing ten Caltrans' employees hand scaling a slope near Kaweah Reservoir on Highway 168 in Fresno County.

Figure 5d: Photograph showing a rockslide on a nearby cut slope that was not scaled as part of the project

Up to fifteen Caltrans employees hand scaled the slopes removing a substantial quantity of loose rock over a four day period (Figures 5a,b,c). As stated previously, it was a coordinated effort between several departments within Caltrans, from Geotechnical Design to Maintenance Engineering and local Maintenance. The work of Caltrans staff directly affected the roadway making it safer that winter, as one of the slopes in the area that was not scaled released a bit of rock, closing one lane (Figure 5d).

CASE 5: TOWNE PASS

Towne Pass is situated in Death Valley National Monument, on Highway 190 at postmile 65 approximately 60 miles southeast of Bishop, 120 miles northeast of Los Angeles, and about 90 miles west of Las Vegas, Nevada (Figure 1). Highway 190 is a two lane highway with narrow shoulders on the cut slope side of the road. Turnoffs and guardrails line the embankment, or downhill side of the road. The location has had recurrent rock fall issues for decades.

Figure 6a: Panoramic photograph showing the entire rock cut slope on Highway 190 in Inyo County near Towne Pass in Death Valley National Monument.

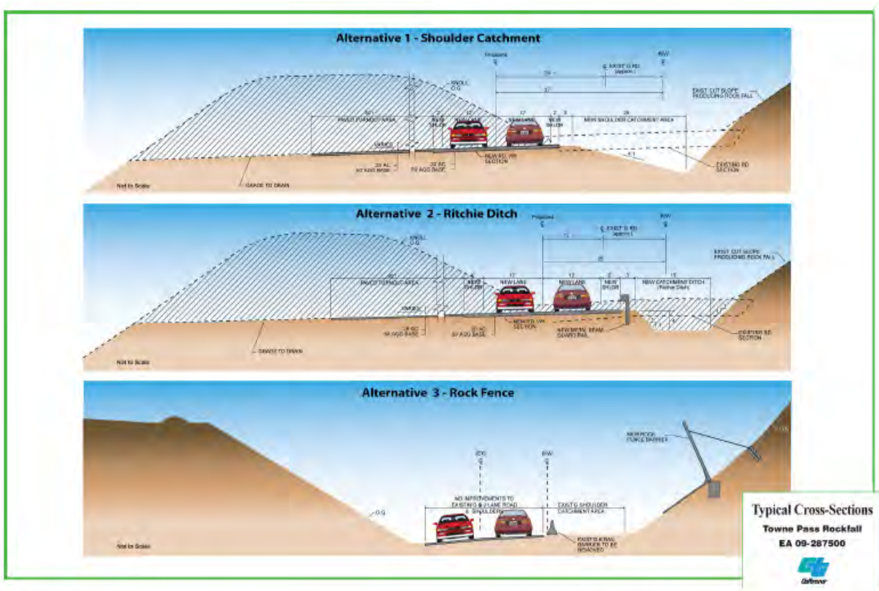

Figure6b: Conceptualized cross sections showing some of the alternatives proposed to mitigate the rockfall hazard.

The geology of this location is one of the more interesting. The site is situated in the basin and range Geomorphic Province, versus all of the previous locations situated in the Sierra Nevada Geomorphic Province. Due to the extensional regime of the area, the topography is broken into chains of parallel to eneschelon mountain ranges and valleys, textbook of the horst and graben topography (CGS, 1974). Locally in the area, Paleozoic marine sediments underlie younger scoriated basalt flows that contain substantial amygdules containing fine grained quartz. In the fractures, gypsum is prevalent and typical of the local, arid climate. Due to the extensional regime of the

Figure 6c: Project document showing the new layout for the realignment alternative.

area and the brittle nature of the rock contained in the cutslope, the rock has become substantially fractured causing the rock fall issue observed at the site.

The slope is over 200-feet in length paralleling the roadway. In 1989 the roadway was realigned and catchment added due to an accident involving a chartered bus. Later low energy fencing was added at the base of the slope, again in an effort to keep the rock from reaching the roadway. The fencing was destroyed and as an effort to create a catchment, Maintenance Forces installed portable concrete barriers at the edge of the highways travelled way. Rock fall continued forcing Caltrans to further evaluate the site (Figure 6a). Numerous alternatives were presented to the project team, each with advantages and disadvantages (Figure 6b). Again, realignment was the best scenario since there was room available to move the roadway (Figure 6c).

CONCLUSIONS

Out of the five locations presented in this case history, two of the locations had earthwork style mitigations to the rock fall hazard, Carson Pass, with the construction of a new slope face and catchment and the Auberry Slide with the removal of loose debris and revegetating the new competent slope face.

One location, Towne Pass in Death Valley National Monument, realignment of the roadway was the prevailing alternative.

Of the locations, three utilized hand scaling to help mitigate the rock fall hazard. This was either due to residual rock left on the slope as in the case of the Kings Canyon location, or was the most practical solution at the time given scaling is typically not a long term solution to mitigation rock fall. In the cases where hand scaling was the preferred option, all interested parties had the understanding that scaling may have to be performed at frequent intervals, depending on when loose rock develops on each slope.

Blasting was utilized at two of the locations; one, Carson Pass where blasting the rock was needed due to the strength of the rock and aid in excavation productivity, and two, Kings Canyon, where blasting was the only feasible way of removing the sliding 200-ton rock mass.

Rock bolting was utilized at one of the five locations, in one area of the Carson Pass location where removal of the rock would have allowed the relatively uncontrolled release of several blocks behind it. Since the underlying fracture plane was relatively shallow angled, there wasn't much force required to bolt the rock into place.

This report was not intended to show all of the mitigation measures employed throughout the State of California but was a sampling of techniques employed in a small area of the State.

REFERENCES

Strand, R.G. and Koenig, J.B., 1965, *Geologic map of California: Sacramento sheet*: California Geological Survey

Matthews, R.A. and Burnett, J.L., 1965, *Geologic map of California: Fresno sheet*: California Geological Survey

Streitz, R. and Stinson, M.C., 1974, *Geologic map of California: Death Valley sheet*: California Geological Survey

Design Software for Secured Drapery

Ghislain Brunet
Maccaferri, Inc
10303 Governor Lane Blvd.,
Williamsport, MD 21795-3116
Ph: 301-223-6910
gbrunet@maccaferri-usa.com

Giorgio Giacchetti
OFFICINE MACCAFERRI S.p.A.
Via Kennedy 10
40069 Zola Predosa
Ph: 01139051646000
giorgio.giacchetti@maccaferri.com

Prepared for the 63rd Highway Geology Symposium, May 7-10, 2012

Disclaimer

Statements and views presented in this paper are strictly those of the author, and do not necessarily reflect positions held by their affiliations, the Highway Geology Symposium (HGS), or others acknowledged above. The mention of trade names for commercial products does not imply the approval or endorsement by HGS.

ABSTRACT

A secured drapery system, consisting of rockfall netting and a systematic nailing scheme, is designed to stabilize surficial material on an exposed rock face. The design procedure can be very complicated because the geomechanical models are very complex or unrealistic, and obtaining accurate input data is rather problematic. This paper presents a simple design approach for secured a drapery system, which combines the field experience of geologists and engineers on one hand, and the results of full scale drapery field tests on the other.

The proposed calculations assume that the rock face exists in a limit equilibrium condition. With this approach, knowledge of parameters like cohesive strength and friction angle that are difficult to obtain is not required. The necessary input data are geometric measurement of the rock face and the main performance features of the anchors and mesh. The safety factors proposed in the calculations are based on considerations concerning the slope morphology, the weathering of the rock mass, and the presence of additional loads such as snow or ice. In this way the designer can easily input data and deal with uncertainties related to the real slope situation.

The calculation procedure allows for determining both the ultimate limit state (verification of breaking loads of the system components), and serviceability limit state (maximum permissible deformation of the facing).
The design analysis has been implemented in the MacRo 1 software package from Officine Maccaferri. Nevertheless, even if the software allows a quick and simple calculation approach, onsite observations are always recommended to achieve a good design, with the ultimate goal of protecting property and the public.

PRELIMINARY REMARKS

Protection against rockfall is frequently carried out with mesh facing and patterned nails; this system, known as secured drapery (or pin drapery, or surficial consolidation or cortical strengthening) is aimed at improving the rock face stability (Fig. 1). This kind of intervention is typically recommended where the number of unstable blocks is too large, and/or the unstable rock size is too small to allow the nailing of each single rock, so that the surficial portion of slope can be compared to a continuous unstable thickness. The unstable portion is usually thinner than 1.0 m (3 ft) and frequently ranges between 0.3-0.6 m (1-2 ft); it can be generally estimated by observing the thickness of the weathered / loose rock mass (typical size of the fallen blocks is also a good indication of the dimension). A more precise estimation approach would require a good geomechanical survey and an analysis with the Goodman & Shi theory (Goodman and Shi, 1985) in order to size the removable "area" and the average thickness of the unstable portion; A time consuming approach that often does not make sense in common practice.

Even if the secured drapery system could improve the global stability for slopes smaller than 1000 m^2 (11,000 ft^2), the solution should only be considered for surficial stability problems. That is why the designer's judgment is always required for identifying the extent and depth of the unstable rock face. In common practice, the secured drapery design is often dimensioned on the basis of experience and common sense when accurate data is not available.

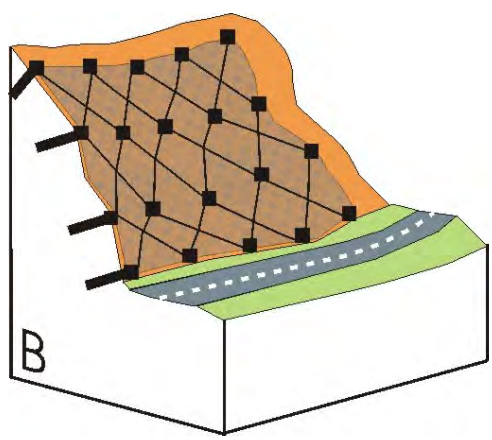

Fig. 1 – Secured drapery system: the intervention consists of a mesh facing and a pattern of nails. Diamond cable netting pattern is shown above.

PRINCIPALES OF SECURED DRAPERY WORKS

The stabilization of the rock face is mainly achieved by inserting reinforcement bars (nails) in the rock mass, which are then grouted and bonded to the rock mass for their entire length. The nailing mobilizes friction and shear force resistance along the entire length and contributes to the improvement of the stability. When there are displacements in the joints, nail resistance is passively generated (Fig. 2).

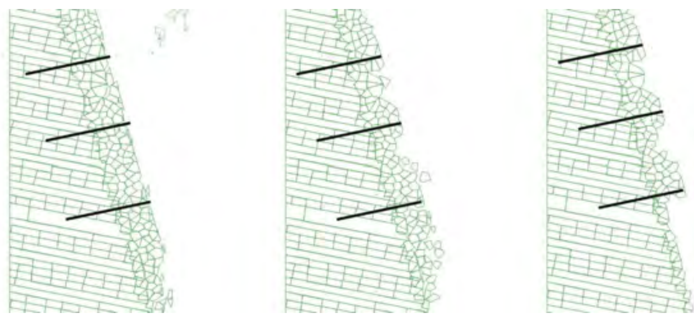

Figure 2 – Scheme of the nailed rock mass. The anchors support the whole unstable mass, including the net. The net has only to control the unstable rock portion between the anchors.

The stability of the exposed rock face, reinforced with nails, is obtained by the contribution of the steel mesh. The function of the mesh is to stabilize the material between the nails by limiting the bulging (which may also have an aesthetic function). the steel mesh facing has a flexible structural behavior, within the limits of its intrinsic deformability, and works in unison with the passive action of the nails. In fact, this type of stabilization cannot be considered as a stiff structure (e.g. shotcrete or precast elements), which limits the blocks displacement in an optimal approach. The design of the flexible structural facing requires a certain consideration in order to minimize any problems related to the intrinsic properties of the mesh and its limited applications. The punch testing method is fundamental for modeling the transition of the forces to the nails (Fig. 3).

Fig. 3 - Outdoor test facility at Pont Boset, developed by Technical University of Torino in cooperation with Officine Maccaferri (Bertolo et Al. 2009), where the behavior of several type of mesh restrained in a real condition has been measured. The results showed that the deformability depends on the pattern of the mesh, and that the mesh can work in unison with the nails when a stiff membrane is used.

In the past, several authors have carried out tests of samples with different sizes and restrained within different test frames (Ruegger R., & Flum D., 2000; Bonati & Galimberti, 2004; Muhunthan B. et Al., 2005). The most interesting tests have been developed in Pont Boset (Aosta – Italia), where a realistic restraint is formed by a pattern of 3.0 m x 3.0 m (10 ft x 10 ft) nails, similar to that frequently adopted for the consolidation of rock and soil slopes. A punch device plunging at 45° on the mesh plane (Fig. 4) was installed to reproduce rock movement (Bertolo et. al. 2007; Bertolo et. al. 2009).

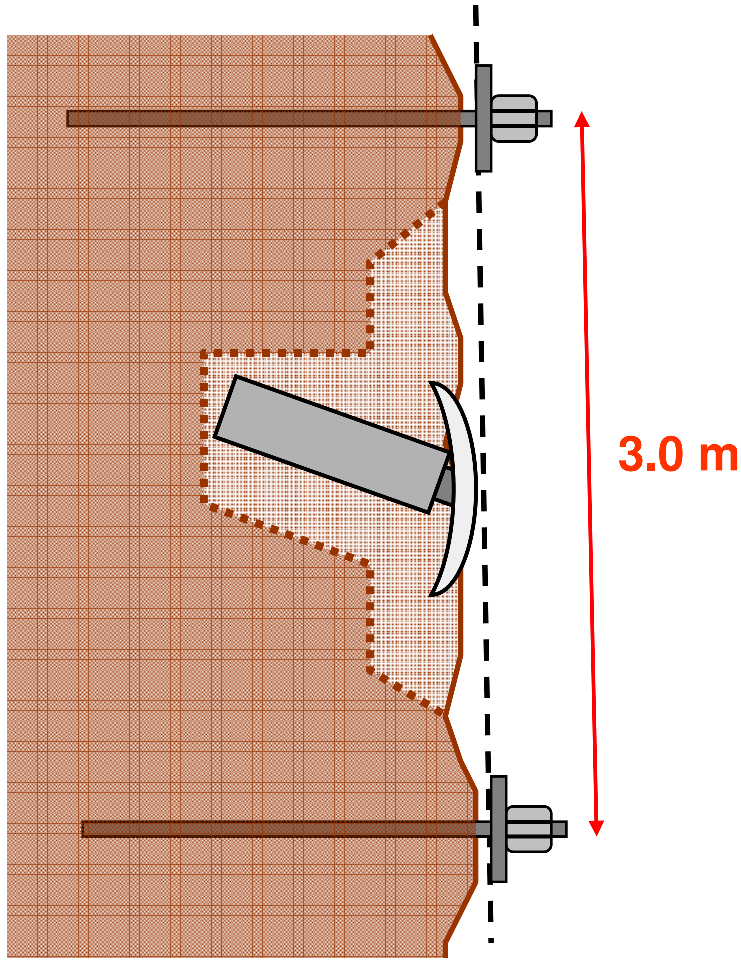

Fig. 4 - Punch device at Pont Boset test facility

The test results have demonstrated the poor correlation between laboratory tests with small size samples and real site behavior, highlighting the necessity to reproduce the real conditions in which the mesh is applied (Majoral et Al., 2008). Secondly, the results have demonstrated that certain meshes develop resistance appreciable forces only after they have reached a displacement of several decimeters (one or more feet) with negligible load. For example, the displacement of the punch device under load for hexagonal mesh, at 0.4 m (16 inches), is half that of a diamond mesh with high tensile resistance wire (Fig. 5). Given this behavior, it is obvious that the rock displacements engage nails in a passive intervention, where the facing elements do not yet offer a stabilizing contribution. Stabilizing will only start when the selected mesh generates load transfer to the nail, usually after few decimeters of displacement.

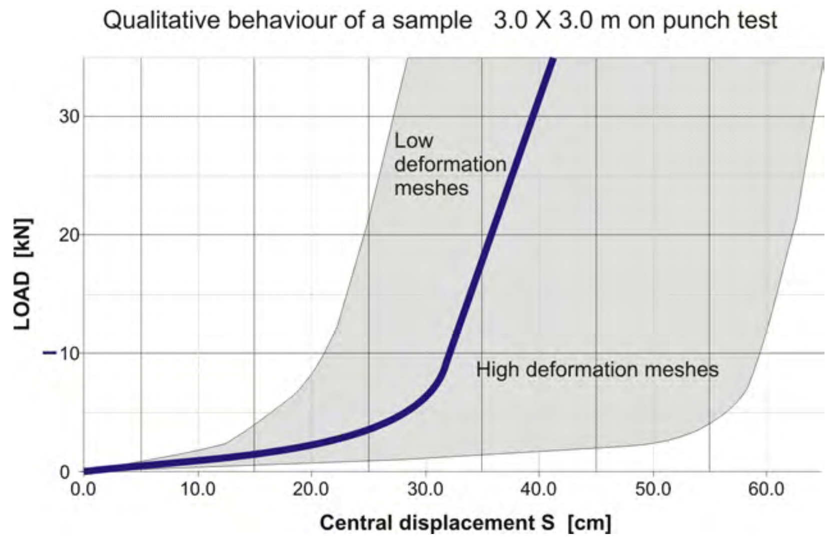

Figure 5 – Load-displacement curve of punch tests on 3.0 m x 3.0 m net samples. The non-linear behaviour can be clearly seen. For loads less than 10 kN, deformations are in the order of 200 to 600 mm, depending on the net type. This behaviour allows the gradual but continuous detachment of blocks from rock mass.

Despite a lack of evidence, it is often mistakenly assumed that pre-stretching of the facing allows active pressures to develop which contribute to stabilization of the slope. Pre-stretching of the facing is theoretically carried out by pre-tensioning the nails, which is done by screwing down the nut on the nail plate, so that the mesh is pushed into concavities of the ground surfaces, or by tangentially stretching the mesh on the edges of the revetment. In the first case, the nail tensioning does not provide advantages, since any pressure from the plate to the mesh or soil will necessarily generate equal and opposite forces, which will pull out the nail, so there is no stabilizing force developed in the system. In the second case, pre-stretching could be implemented on planar surfaces in principle, but if the nails are already installed, or if the ground surface is just uneven, tension is almost impossible to obtain because of the frictions on the asperities (Ferraiolo and Giacchetti, 2004). In both these cases, the intrinsic deformability of the mesh invalidates the effect of the pre-stretching.

Therefore, even if it was possible to pre-stretch the mesh, the forces developed would be tangential to the mesh plane, and some pressure could be developed only against the protuberance of the cavity next to the nail area. However, there are non-relevant pressures on the soil between the nails, so it is possible to lift the mesh from contact with the ground, simply by using the fingers.

SOME IMPLICATIONS

Some important implications for the design approach of the structural flexible facing came out as corollaries of the above:

- From the geomechanical point of view, the mesh has a passive behavior where it needs to be solicited before generating any resistance forces. It cannot be modeled as shotcrete which is made to transmit almost uniform pressures on the ground surface by means of the nails.

- The difference of behavior between meshes depends upon the way the fabric is manufactured and not upon the steel grade of the wire. The membrane stiffness plays a primary role into the facing choice; the higher the stiffness is, the more effective the facing is. Therefore, the tensile strength has marginal importance in the mesh choice, because the tensile stresses acting on the mesh are almost always 3 times lower than the nominal tensile strength of the mesh.

- The overlapping of a cable net on the mesh facing is always recommended. The cable netting, which is much stiffer than the mesh, reduces the membrane deformability and helps to distribute the stress on the mesh generated adjacent to the nails. That is why a mesh with cables woven into the fabric performs the best (Fig. 5).

- With flexible structural facing, the nails could have difficulty cooperating with each other in consolidation of the surface, which depends on mutual interlocking of the blocks near the nails; that is why nail spacing should never exceed 3.0 m, because with larger spacing, each anchor is working independently of the other.

Figure 5 – In-situ test on a net installed in real conditions, (Pont Boset Facility test). A stiffer mesh can be obtained by inserting cables in the netting.

THE SIMPLIFIED DIMENSIONING APPROCH OF MARCRO 1

The design of secured drapery is not at all easy because of numerous variables, including topography, rock mass properties, joint geometry and properties, mesh type and related restraint conditions. Often the solution to the problem may require complex numerical modeling which is not practical for every project, especially if the design is aimed at interventions of modest size and scope. Because of that, at the present, limit equilibrium models are the preferable design method; they can be simplified by estimating the rock mass displacement. Taking this into consideration and incorporating field experience, Officine Maccaferri has developed MacRo1, a limit equilibrium approach for the design of secured drapery. The procedure is quite rough, but it is sufficient when considering the low accuracy level of the input data, the reliability of the results and the speed of the calculations.

NAIL DIMENSIONING

Considering passive behavior, the nail calculation must assume the unstable portion of the slope lies in condition of limit equilibrium, where the safety factor is equal to 1.0. Therefore, the resisting forces have the same value of the driving forces and the following equation is true:

[1] $$\textit{Resisting forces} = W \sin\beta = \textit{driving forces}$$

where
W = weight of the unstable rock mass to be consolidated
β = inclination of the slope surface, where the sliding of the unstable rock mass can occur.

Using the resistance criteria of Barton-Bandis for the joints, equation [1] can be rewritten to describe the improved stability condition (Hoek and Brown, 1981):

[2] $$W \cdot \sin\beta - c \cdot \sin\beta \tan\phi + R \geq W(\sin\beta + c \cdot \cos\beta)$$

assuming

R = stabilizing contribution of the nails
c = seismic coefficients
ϕ = residual friction angle of the joint

Setting $\tan\phi \approx 1$ (friction angle = 45°), and posing the safety factors for reducing the stabilizing forces (γ_{RW}) and increasing the driving ones (γ_{DW}), the stability condition would be:

[3] $$W \cdot \sin\beta \cdot (1-c) / \gamma_{RW} + R \geq W \cdot \gamma_{DW} \cdot (\sin\beta + c \cdot \cos\beta)$$

or $$F_{Sslp} >= F_{Dslp}$$

assuming

$F_{Dslp} = (W \sin\beta + c \cos\beta)\, \gamma_{DW}$ = Sum of the driving forces
and
$F_{Sslp} = ((W \sin\beta)(1-c)) / \gamma_{RW} + R$ = Sum of stabilizing forces

Equation [3] allows for determining the nail force that consolidates a rock mass in the limit equilibrium state. It is a conservative equation and is simple to use since the only geotechnical variable is the inclination of the sliding plane. The safety coefficients (γ_{RW}, γ_{DW}) depend on several factors. The rock mass features affect the size of the stabilizing forces, so that their safety coefficient can be described as

$$\gamma_{RW} = \gamma_{THI}\ \gamma_{WG}\ \gamma_{BH}$$

where

- γ_{THI} describes the uncertainties in determining the surficial instability thickness s. Its value ranges between 1.20, when the estimation is based on a geomechanical survey, and 1.30, when it is based on rough estimation.

- γ_{WG} describes the uncertainties in the unitary weight determination of the rock mass. Usually it is assumed to equal 1.00, but if there are severe uncertainties (e.g. when the density is not homogeneous, as in flysch rock masses) it can be assumed to equal 1.05.
- γ_{BH} describes the uncertainties related to the rock mass behaviour. High erodibility of the rock surface can cause necking of the nails and weakness of the whole system. Usually the value is assumed to equal 1.00, but if there are severe environmental conditions or the rock mass is easily weathered, it can be assumed to equal 1.05.

External conditions, especially slope morphology, play an important role in the magnitude of the driving forces, whose safety coefficient is defined as

$$\gamma_{DW} = \gamma_{MO} \ \gamma_{OL}$$

where:

- γ_{MO} describes the uncertainties related to slope morphology. If the slope is very rough, then the mesh facing is not in good contact with the surface, and the unstable blocks can freely move; in that case a safety coefficient of 1.30 should be applied. If the slope surface is even, the mesh facing lies in better contact with the ground; in the case, the unstable block movement is limited, and a safety coefficient of 1.10 is used.
- γ_{OL} describes the uncertainties related to additional loads applied on the facing system. The additional loads could be related to the presence of ice and snow, or to vegetation growing on the slope. Usually it is assumed to equal 1.00, but if severe conditions are foreseen, it can be assumed to equal 1.20.

The reinforcing nail bars work principally in proximity to the sliding joint, where it is subjected to shear stresses together with tensile stresses. The resisting force R, due to the bar along the sliding plane, is derived utilising the maximum work principal:

[4]

$$R = \left[\frac{1 + \frac{m^2}{16}}{1 + \frac{m^2}{4}} \right]^{\frac{1}{2}} \cdot N_e$$

where:

$m = \text{cotg}\ (\varepsilon + \delta)$

ε = the angle between the bar axis and a line perpendicular to the sliding joint.

It is equal to

$\varepsilon = 90° - \beta - \theta_o$, where θ_o is the drilling inclination referenced to the horizontal.

δ = sliding surface dilatancy

N_e = bar strength (elasticity limit condition) = ESS σ_{adm} = ESS $\sigma_{ST} / \gamma_{ST}$

γ_{ST} = coefficient of reduction for the steel resistance.

ESS = effective area of the steel bar = $\pi / 4 ((fe - 2\ fc)^2 - fi^2)$

fe = external diameter of the steel bar

fc = thickness of corrosion on the external crown

fi = minor diameter of the steel bar

In accordance with the Barton – Bandis resistance criteria, the δ value is approximated as

$$\delta \approx \frac{JRC \cdot \log\left[\frac{JCS}{\sigma_{plan}}\right]}{3}$$

$$\sigma_{plan} = \frac{i_x \cdot i_y \cdot s \cdot \gamma \cdot \cos\alpha}{i_x \cdot i_y}$$

where:

α = inclination of the most unfavourable sliding plane

σ_{plan} = sliding plane tensile stress

JRC = joint roughness coefficient = $JRC_0 \cdot \left[\frac{L_g}{L_0}\right]^{(-0.02 \cdot JRC_0)}$

JCS = joint uni-axial compression resistance = $JCS_0 \cdot \left[\frac{L_g}{L_0}\right]^{(-0.03 \cdot JRC_0)}$

JCS_0 = joint compression strength referred to the scale joint sample

JRC_0 = roughness referred to scale joint sample

L_0 = joint length (assumed to be 0.1 m for lack of available data)

L_g = sliding joint length (assumed to be equal to vertical nail spacing of 1.0 m for lack of available data).

Please note that the roughness values and the uniaxial compression resistance should be estimated on the most unfavourable joints.

EVALUATION OF THE NAIL LENGTH

The evaluation of nail length considers the following:

a) The nail plays the most important role in superficial consolidation of the slope. Its length must be deeper than the instability thickness, and should allow the bar to reach into the stable section.

b) The steel bar and the grout are exposed to weathering actions (ice, rain, salinity, temperature variations, etc.).

The minimum theoretical length is derived by

$$L_t = L_s + L_i + L_p$$

assuming:

L_s = length in the stable part of the mass = $P / (\pi\ \phi_{drill}\ \tau_{lim} / \gamma_{gt})$

L_i = length in the weathered mass = $s / \cos \varepsilon\ \ \gamma_{dw}$

L_P = length of hole with plasticity phenomena in firm part of the rock mass. It is assumed to equal 0.3 m (1.0 ft).

With

ϕ_{drill} = diameter of the hole for the bar

τ_{lim} = adherence tension between grout – rock

γ_{gt} = safety coefficient of the adhesion grout – rock

P = pullout force; it is the greater of the following:

$P_{Mesh} = ((W_{Sbar} - W_{Dbar}) \cos(\alpha + \theta_o))\, i_x$ = pull out force due to the mesh

$P_{Rock} = (F_{Sslp} - R - F_{Dslp}) \cos(\beta + \theta_o)$ = pull out force due to the slope instability.

The length of the nail now has a preliminary value. The final suitable length of the bars has to be evaluated during drilling and confirmed with pull out tests.

MESH DIMENSIONING: ULTIMALE LIMIT STATE

Some secondary blocks could slide among the nails on a plane with inclination α, where α is smaller than the slope inclination β, and push on the mesh facing. The maximum block size pushing per horizontal linear meter of facing depends on the thickness s and the vertical spacing i_y between two nails.

Since the load pushing is asymmetric and the mesh deforms unevenly, the forces acting on the facing are represented with the following simplified scheme (see Figure 6):

- F - the force developed by the blocks sliding between the nails on a plane inclined at α.
- T - the force acting on the facing plane, which rises when the sliding blocks push on the facing. The force can develop because there is a large friction between mesh and blocks, and a pocket is formed. The facing, which is considered to be nailed on the upper part only, reacts to T with the tensile resistance of the mesh.

M – the punch force developed by the blocks perpendicular to the facing plane. The force is developed since there are several lateral restraints, like the nailing (strong restraint) and the next meshes (weak restraint). The magnitude of M largely depends on the stiffness of the mesh: the higher the membrane stiffness of the mesh is, the more effectiveness the facing is.

In the case of the mesh, the ultimate limit state is satisfied when

$$T_{adm} - T >= 0$$

where

T_{adm} = admissible tensile strength of the mesh

The admissible tensile strength of the mesh would be

$$T_{adm} = T_m / \gamma_{MH}$$

where

T_m = Tensile resistance of the mesh

γ_{MH} = safety coefficient for the reduction of the tensile resistance of the mesh. Taking into account the inhomogeneous stress state of the loaded mesh, the minimum safety coefficient should be not lower than 2.50.

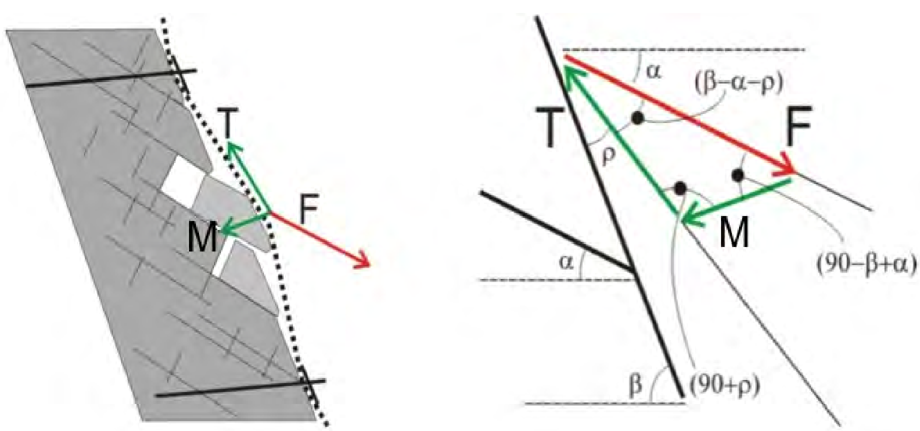

Fig. 6- Scheme of the forces acting on the mesh

The stress T on the mesh depends on the force pushing on the mesh (M – see figure 6), which can be calculated using the same principles as formula [3]

$$M = F \sin(\beta-\alpha)\, i_x = (M_{bdrv} - M_{bstb}) \sin(\beta-\alpha)\, i_x$$

Where:

$M_{bdrv} = (Mb \sin\alpha + c \cos\alpha)\, \gamma_{DW}$ = driving forces

$M_{bstb} = (Mb \sin\alpha\ (1- c))\, \gamma_{RW}$ = resisting forces

$Mb = V\ \gamma$ = weight of the unstable rock mass

V = maximum unstable volume between nails which is calculated by the following:

(Case A): if $\alpha \geq (\beta - \arctan(s/i_y))$ and $\alpha < \beta$ $\qquad V = \frac{1}{2} \cdot i_y{}^2 \cdot \tan(\beta-\alpha)$

(Case B): if $\alpha < (\beta - \arctan(s/i_y))$ $\qquad V = i_y \cdot s - \frac{1}{2} \cdot \frac{s^2}{\tan(\beta-\alpha)}$

(Case C): if $\alpha < (\beta - \mathrm{arctg}(s/i_y))$ $\qquad V = 0.5\, s^2 / \tan(\beta-\alpha)$

Finally

if $M/i_x / \sin(\beta-\alpha) - \rho p) < Mb \operatorname{sen}\beta$

then $\quad T = M / i_x / \sin(\beta-\alpha) - \rho_p \quad$ else $\quad T = Mb \operatorname{sen}\beta$

with

$\rho_p \approx \mathrm{arctg}(Z_{bulg} / 1.5)$ = angle of deformation of the mesh.

Z_{bulg} = displacement related to the punch load M. It is directly measured from Maccaferri's test experiences.

MESH DIMENSIONING: SERVICEABILITY LIMIT STATE

The serviceability limit state provides information concerning the following:

- required maintenance activity on the facing;
- risks of stripping because of anchor necking;
- interference between infrastructure and facing as consequence of excessive displacements.

The serviceability limit state is satisfied if

$$B_{ulg} - Z_{bulg} \quad >= 0$$

where

B_{ulg} $= D_{mbulg} / \gamma_{mbulg}$ = admissible displacement

D_{mbulg} = maximum design displacement

γ_{mbulg} = safety coefficient. Its value ranges between 1.50 (facing installed properly on a slope with an even surface) and 3.00 (facing installed improperly on a slope with uneven morphology).

Z_{bulg} = deformation of the facing as derived from the results of Maccaferri tests on the base due to punch force M.

CONCLUSION

Secured drapery is an effective consolidation system for rock slopes, and is recommended where the surficial weathered portion of slope can be compared to a continuous unstable thickness. Both laboratory testing and field performance give evidence that the secured drapery reacts to rock mass displacements, and that one of the most important properties of the mesh facing is the membrane stiffness. The calculation approach, which has necessarily been introduced with some simplification, has been implemented in the MacRo 1 software package, which uses safety coefficients related to field experience.

REFERENCES

AICAP, (1993): Anchor in soil and rock: recommendations (in Italian).

Bertolo P. , Giacchetti G., 2008 - An approach to the design of nets and nails for surficial rock slope revetment – in Interdisciplinary Workshop on Rockfall Protection, June 23-25 2008, Morshach, Switzerland.

Bertolo P., Ferraiolo F., Giacchetti G., Oggeri C., Peila D., e Rossi B., (2007): Metodologia per prove in vera grandezza su sistemi di protezione corticale dei versanti – GEAM Geoingegneria Ambientale e mineraria, Anno XLIV, N. 2, Maggio-Agosto 2007.

Bertolo P., Oggeri C., Peila D., 2009 – Full scale testing of draped nets for rock fall protection - Canadian Geotechnical Journal, No. 46 pp. 306-317.

Besseghini F., Deana M., Di Prisco C., Guasti G., 2008 – Modellazione meccanica di un sistema corticale attivo per il consolidamento di versanti di terreno, Rivista GEAM Geoingegneria ambientale e Mineraria, Anno XLV, N. III dicembre 2008 (125) pp. 25-30 (in Italian)

Bonati A., e Galimberti V., (2004): Valutazione sperimentale di sistemi di difesa attiva dalla caduta massi – in atti "Bonifica dei versanti rocciosi per la difesa del territorio" - Trento 2004, Peila D. Editor.

Castro D., 2008 – Proyetos de investigaciòn en la Universidad de Cantabria - II Curso sobre protecciòn contra caida de rocas – Madrid, 26 – 27 de Febrero. Organiza STMR Servicios técnicos de mecànica de rocas.

Cravero M., Iabichino G., Oreste P.P., e Teodori S.P. 2004: Metodi di analisi e dimensionamento di sostegni e rinforzi per pendii naturali o di scavo in roccia – in atti "Bonifica dei versanti rocciosi per la difesa del territorio" – Trento 2004, Peila D. Editor.

Ferraiolo F., e Giacchetti G., (2004): Rivestimenti corticali: alcune considerazioni sull'applicazione delle reti di protezione in parete rocciosa – in atti "Bonifica dei versanti rocciosi per la difesa del territorio" – Trento 2004, Peila D. Editor.

Ferrero A.M., Giani G.P., Migliazza M., (1997): Interazione tra elementi di rinforzo di discontinuità in roccia - atti "Il modello geotecnico del sottosuolo nella progettazione delle opere di sostegno e degli scavi" – IV Conv. Naz. Ricercatori universitari – Hevelius pp. 259 – 275.

Flumm D., Ruegger R. (2001): Slope stabilization with high performance steel wire meshes with nails and anchors – International Symposium Earth reinforcement, Fukuoka, Japan.

Goodman, R.E. and Shi, G. (1985), Block Theory and Its Application to Rock Engineering, Prentice-Hall, London.

Hoek E., e Bray J.W., (1981): Rock slope engineering - IMM – London.

Jacob V., (2009): Engineering, unpublished thesis, Technical University Torino.

LCPC, (2001) : Parades contre les instabilités rocheuses - Guide technique - Paris.

Majoral R., Giacchetti G., Bertolo P., 2008 – Las mallas en la estabilizaciòn de taludes – II Curso sobre protecciòn contra caida de rocas – Madrid, 26 – 27 de Febrero. Organiza STMR Servicios técnicos de mecànica de rocas (in Spanish).

Muhunthan B., Shu S., Sasiharan N., Hattamleh O.A., Badger T.C., Lowell S.M., Duffy J.D., (2005): Analysis and design of wire mesh/cable net slope protection - Final Research Report WA-RD 612.1 - Washington State Transportation Commission Department of Transportation/U.S. Department of Transportation Federal Highway Administration.

Pellet F., e Egger P., (1995): Analytical model for the behaviour of bolded rock joints and practical applications. In proceedings of international symposium Anchors theory and practice. Widmann R. Editor. A.A. Balkema.

Phear A., Dew C., Ozsoy B., Wharmby N.J., Judge J., e Barley A.D., (2005): Soil nailing – Best practice guidance - CIRIA C637, London, 2005.

Ruegger R., e Flumm D., (2000): High performance steel wire mesh for surface protection in combination with nails and anchors – Contribution to the 2nd colloquium “Contruction in soil and rock” – Accademy of Esslingen (Germany).

Saderis A., (2004): Reti in aderenza su versanti rocciosi per il controllo della caduta massi: aspetti tecnologici e progettuali – Tesi di Laurea in Ingegneria per l’Ambiente e il Territorio, unpublished thesis, Technical University Torino.

Torres Vila J.A., Torres Vila M.A., e Castro Fresno D., (2000): Validation de los modelos fisicos de analisis y diseno para el empleo de membranas flexibile Tecco G–65 como elemento de soporte superficial en la estabilizacion de taludes.

Valfrè A., (2007): Dimensionamento di reti metalliche in aderenza per scarpate rocciose mediante modellazioni numeriche – GEAM Geoingegneria Ambientale e mineraria, Anno XLIII, N. 4, Dicembre 2006.

Wyllie D.C., e Mah C.W., (2004): Rock slope engineering civil and mining - 4th edition – Spon Press London and New York.

The Hyampom Road Project:
Managing Geotechnical Risk in Difficult Mountainous Terrain

Richard Andrew, P.G.
Yeh and Associates, Inc.
5700 East Evans Ave.
Denver, CO 80222
Phone: (303) 781-9590
Email: (randrew@yeh-eng.com)

Khamis Haramy
CFLHD-FHWA
12300 Dakota Ave.
Lakewood, CO 80228
Phone: (720) 963-3521
Email: (khamis.haramy@dot.gov)

Prepared for the 63rd Highway Geology Symposium, May 7-10, 2012

Disclaimer

Statements and views presented in this paper are strictly those of the author, and do not necessarily reflect positions held by their affiliations, the Highway Geology Symposium (HGS), or others acknowledged above. The mention of trade names for commercial products does not imply the approval or endorsement by HGS.

ABSTRACT

Hyampom Road, also known as California Forest Highway 114, is located within Shasta-Trinity National Forest in northern California. It begins at California State Highway 3 (SR 3) in Hayfork, proceeds northwest and ends in the town of Hyampom at the intersection with Lower South Fork Road. The existing two-lane narrow winding roadway traverses canyon slopes with steep cuts excavated in bedrock and steep side-cast fills. The pre-construction template was comprised of a two-lane roadway with10-foot lane widths and some sections narrowing to a single lane. The roadway conditions were poor with marginally stable slopes, poor drainage, short sight distance, and other geometry issues that did not meet highway design standards. The roadway is primarily used for logging and commuter purposes and is the only year round publicly maintained access to the town of Hyampom.

Multiple landslides are present along the corridor and the orientation of the bedrock structure created zones of instability. During the course of project development, the alignment was adjusted through multiple iterations to balance project cost and risk. Risk assessment included the evaluation of geological hazards, roadway safety and the achievable roadway template. Major reconstruction and rehabilitation elements of the roadway included: 1) constructing retaining walls and rock cuts, where necessary, to provide a wider roadway complete with travel lane and shoulder in each direction; thereby, reducing the severity of the existing "hairpin" curves; 2) constructing landslide mitigation systems; and, 3) providing rockfall mitigation in specific locations.

INTRODUCTION

Hyampom Road (California Forest Highway 114, Trinity County Road 301) has long been the only County road providing year-round access to the town of Hyampom. The regional location of the project area is depicted in Figure 1. Other U.S. Forest Service resource roads provide seasonal access from Hayfork, State Route (SR) 36 to the south, and SR 299 to the north, but these roads are not regularly maintained in the winter months and are frequently closed during periods of heavy snowfall. Originally constructed in 1924, Hyampom Road once served as a stagecoach route between Hayfork and Hyampom. The route served the timber industry for many years, providing access to Forest Service lands and private timberlands, and a route to transport finished lumber from sawmills in Hyampom. Placer and lode gold mining activity and aggregate mining were also common, particularly in the early 20th century.

The roadway corridor is cut through steep terrain with frequent slope failures that have caused numerous road closures. The slides have required extensive repairs and constant monitoring. In addition, the annual freezing and thawing action, resource truck use and gradual wear and tear had lead to degradation of the road condition. Maintenance had been ongoing, but major reconstruction and minor realignment were needed to bring the aging resource road to current safety standards, and to maintain sufficient width for two-way traffic. In the steepest sections, the road was reduced to a single lane, and portions of the roadway width continued to be lost continuously to erosion of the near-vertical slopes and pockets of highly weathered rock.

The Hyampom Road Project consisted of reconstructing, repaving, widening, and modifying the alignment within the existing roadway corridor. The project included developing a consistent two 11-foot lane roadway with shoulders, reducing the severity of existing tight-radius curves, placing new and/or additional surface and subsurface drainage systems, constructing retaining walls, and placing guardrails in strategic locations. The specific purpose of the proposed Hyampom Road project was to:

- Provide a safe, year round, all weather access to Hyampom.
- Provide a consistent-width two-lane roadway alignment to enhance the safety for current and future traffic.
- Ensure mobility for emergency response, school buses, postal service, and other delivery vehicles.
- Reduce roadway maintenance concerns.
- Provide better access for administration of United States Forest Service lands.

In general, the project was implemented to address four types of needs; roadway deficiencies, maintenance, safety, and social and economic conditions.

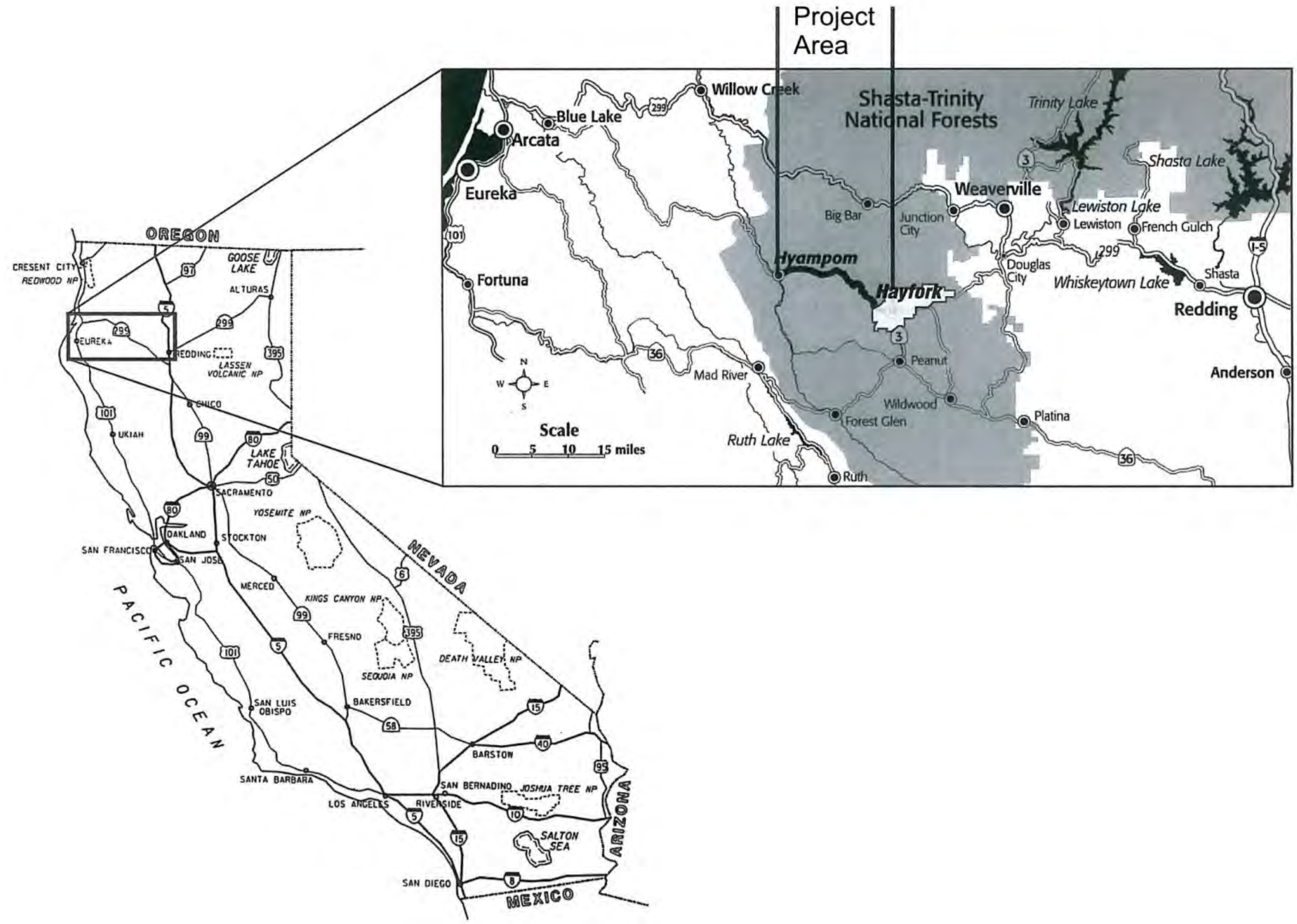

Figure 1. Project location map

REGIONAL GEOLOGIC SETTING

The project site is located in the Klamath Mountains Geologic Province of northwestern California (McClaughlin et al, 2000). Bedrock in this region is primarily accreted terranes composed of deformed oceanic sediments and igneous plutons. These fault-bounded blocks represent the accretionary history of the western continental subduction zone (McClaughlin et al, 2000). The bedrock occurring in the eastern portion of the project consists of Mesozoic plutonic rocks, primarily hornblende diorite of the Ironside Mountain Batholith (Strand, 1962). The bedrock occurring in the western portion of the project consists of pre-Cretaceous metamorphic rock of the Rattlesnake Terrane (Strand, 1962). The Rattlesnake Terrane is a mélange comprised of many different rock types; at this locality the rock type is a gray thinly bedded metasedimentary slate. (Figure 2).

There were no active faults identified within the project area with the closest active faults located near the California coastline. Based on maximum credible earthquakes from identified faults, the nearest faults are the Mad River and Trinidad faults, located approximately 25 miles west of the project site. These faults are capable of producing 6.75 to 7.5 – magnitude earthquakes. An inactive thrust fault occurs near the middle of the project limits as shown on the geologic map (Figure 2).

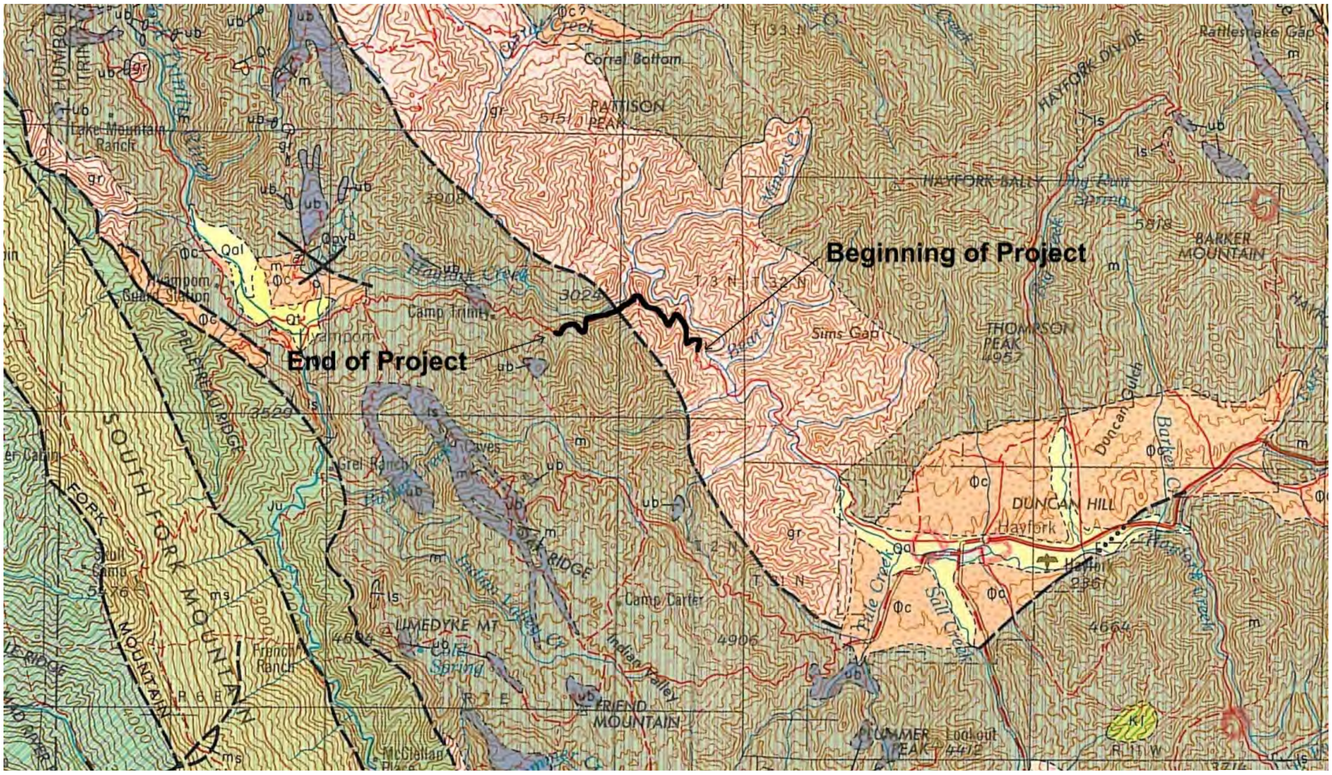

Legend:

gr — Mesozoic Granitic Rocks

m, ls — Pre-Cretaceous Metamorphic Rocks
Undifferentiated, ls=limestone and/or dolomite

Thrust fault

N

Figure 2. Localized Geologic Map of the project area. From Strand (1962); published by California Division of Mines and Geology.

SITE CONDITIONS AND GEOLOGICAL HAZARDS

The roadway alignment generally follows Hayfork Creek, which flows northwest towards the Trinity River in Hyampom. Within the project limits, the roadway is approximately 60-feet vertically above the creek. The terrain is mountainous with moderate to steep slopes above and below a majority of the road alignment. The undisturbed side slopes are heavily vegetated forest of oak, pine, and madrone. Several small, intermittent streams cross the roadway through culverts. Bedrock outcrops can be observed throughout the site. There was no evidence of recent debris flow activity within the stream channels. Instability within the cut slopes was evident along the alignment at several locations leading to rockfall and shallow rock slides.

Figure 3. Hyampom single-lane road configuration prior to construction

The varied and complex geologic and geomorphic process led to the development of the several zones of instability and marginal subsurface material. During the original construction of the road, many of these zones of instability were exposed and exacerbated by over-steepened cut and fill slopes. These areas experienced continual rockfall and large rock slides causing damage to the roadway and occasional road closures.

A segment within the roadway, identified as the Narrows, experienced the greatest frequency of rockfall. This is mainly attributed to the rock structure that dips at an orientation unfavorable to the roadway alignment. It appeared that the original highway construction encountered several failures causing the road through this area to be constructed to a single lane width (Figure 3). Because of the nature of the geology and height and steepness of the cuts and fills, this segment represented the greatest challenge for widening the road to the full two-lane template.

Several small soil-slumps in the cut slopes and shallow failures along the fill slopes were observed during the site investigation but few represented a serious risk of impacting the roadway. The shallow failures along the fill had worked into the shoulders as seen in Figure 3. A large dormant landslide was identified at the location of the thrust fault near the middle of the project. Although this feature was not shown in the 1962 geologic map (Figure 2), the loose and broken material common to large-scale failures was encountered through a large portion of the roadway.

THE PROJECT DEVELOPMENT PROCESS

From the project planning to final conception, some community residence posed continuing resistance to any improvements to the existing road. Concerns were raised ranging from potential environmental impacts to affects on local businesses from the construction activities to changing the character of the existing road. Through a series of stakeholder meetings, a process was established that incorporated the public, County, and Forest Service concerns and comments. This process followed many of the principles outlined in the FHWA Context Sensitive Solutions (CSS) Program. In CSS, the word "context" refers to a project's surroundings—its natural environment and its historical setting and role in the community (i.e., its use as a public space or thoroughfare). The CSS program promotes the development of principles and processes that can be used to improve the quality of transportation decision-making. This includes opportunities to enhance environmental protection and encourage partnerships that promote ecosystem conservation or encourage broader mitigation strategies.

Through the interaction with the stakeholders, the following basic design considerations were developed:

- Will the proposed improvements affect the general physical character of the area surrounding the project?
- Will the improvements affect the historic or scenic characteristics?
- What are the safety and cost concerns of the community?

The effect of incorporating the design considerations on the project has the potential for increasing risk due to tighter radius and reduced lane widths as compared to the full-build template. To help manage this risk, the design speed was selected at 25 mph throughout the project. AASHTO permits the use of specific design parameters on low-volume roads, particularly at low-risk locations, defined as those not near intersections, narrow bridges, railroad-highway grade crossings, sharp curves, or steep downgrades. Although the corridor contains numerous sharp curves and steep grades, the proposed project dramatically improved the geometry and lane configuration as compared to existing conditions.

RISK AND DESIGN CONSIDERATIONS

Transportation engineers and designers are trained to use accepted design criteria throughout project development. Striving to meet those criteria is the primary means by which high-quality roadways are produced. A highway or roadway that reflects full compliance with accepted design criteria decreases the probability that safety or traffic operational problems will develop. Therefore, using design values that lie within typical ranges provides a degree of quality control and a level of risk that transportation agencies consider acceptable.

Ideally, agencies would reduce or mitigate all potential risks associated with a project. But in reality, limited budgets coupled with increased demands on agency staffs necessitate prioritizing where resources will be concentrated. Risk management is the process of identifying, evaluating, prioritizing, and mitigating risks, which guides a coordinated approach to minimize, monitor, and control identified risks and their impacts on the project. Part of this process was assessing the probability with which certain risks could not be avoided. To the extent possible, risks were quantified, both on the basis of their probability and their potential consequences.

Risk management began during the early stages of project planning with identification and prioritization of various potential risks and the selection of the most critical risks to mitigate or alleviate during planning. The process continued throughout the project design and required knowledge of the project-specific risk factors and the exercise of sound professional judgment. Identifying risks involved analysis of all pertinent issues. The project's geographic, environmental, safety, and traffic conditions and the assumptions underlying the design standards were essential to understanding the risks associated with selecting and applying those standards. In most cases, the risks associated with a design element were mitigated with inclusion or enhancement of other features that could offset the risk. This is an accepted practice when identifying the design exceptions through the development of the project. Figure 4 illustrates the FHWA design exception process.

Figure 4. FHWA mitigation strategies for design exceptions
http://safety.fhwa.dot.gov/geometric/pubs

THE HYAMPOM DESIGN CONSIDERATIONS

Roadway Template

Within this constrained area, providing a cross section that fully meets the design criteria would have significantly increased the costs and impacts of the project on the surrounding land. Several iterations of the roadway section were considered up to a full template with 12-foot lanes and 4-foot shoulders. The cross section that was eventually selected narrowed the travel lanes on both sides by 12 inches to 11 foot lanes. The shoulder widths were narrowed to 2 feet with a 4 foot maximum ditch width. The resulting design represented a compromise in the lane, shoulder and ditch width values. The consensus was that although this design did not meet the standard design criteria, it would function well operationally and would most effectively use the available cross-sectional width to optimize safety and reduce costs.

Balancing Cut Slopes and Fill Walls

Several iterations were conducted to evaluate widening through the final alignment, from pushing the improvements all on fill to moving fully into the cut side. The fill-side alignment required the construction of extensive retaining walls with maximum heights reaching 40 feet. Several wall types such as mechanically stabilized earth (MSE), soldier piles with lagging, Shored MSE walls with truncated base, and micropiles walls were considered. Each type of wall possessed a certain constructability issues. Due to the steep terrain, meeting AASHTO guidelines for wall base embedment, reinforcement lengths and achieving an acceptable factor of safety for global stability and bearing capacity were difficult. Many of the new walls would require deep foundations to develop the necessary requirements for capacity and slope stability. Costs for the tall complex retaining structures significantly exceeded the project funds and more economical/higher risk options such as gaining road widths by moving the alignment into steep cuts were considered.

With the alignment moved into the hillside, cut slopes exceeding 200 feet in height, with near vertical slope ratios, were required. The extensive slope cuts would expose poor quality rock and adverse fractures creating unstable slope configurations. Combined with almost non-existing ditch widths, the risk from rockfall hazards (reaching the roadway) were determined unacceptable, even for a low volume road with existing rockfall hazards. Costs for stabilization and extensive rockfall mitigation were also beyond the scope for the project and the appearance of extensive rock cuts was unacceptable to the local community.

Figure 5. Construction of the MSE walls

The final alignment that balanced risk and cost incorporated both cut slope and fill wall structures. Fill walls were constructed using wire face mechanically stabilized earth walls (MSE) designed to a maximum height of 17 feet. The MSE wall reinforcement length and embedment depth were extended to accommodate achieve the desired factors of safety for global stability and bearing capacity.

To further narrow the roadway footprint, the guardrail was placed at a maximum distance of 2 feet from the back of post to the face of the wire-face MSE walls. Typically this distance is a minimum of 3 feet. To minimize deformation to the wall face during impact and to provide the necessary support to the guardrail posts, additional reinforcement was placed vertically at midpoints between wall reinforcements and extended ¾ the reinforcement lengths in the top 6 feet of each wall.

Rock Slope Design

The most challenging and highest risk portion of the project was the development of a stable rock slope design. The slope designs had to consider the stakeholders constraints, stay within the available project budget, reduce the maintenance demands, and minimize risk from rockfall and/or rock slides. Additionally, several rock slopes contained loose soil pockets and water seeps which made it more difficult to predict stability during construction. Due to the steepness of the terrain, several slopes were initially designed at steeper slope angles than would generally be recommended for the rock types and fracture orientation found along the corridor. It was determined that all of the rock cuts would be adjusted (if needed) in the field during construction as the rock conditions were uncovered. Although this was not ideal, it was a means of economizing the rock excavations and adjusting the slope angles to match the variations in the rock structure.

Figure 6. Shallow wedge failure common though the area.

During construction, many of the marginally stable slopes experienced shallow wedge and planar failures. Figure 6 is a typical wedge failure that developed shortly after excavating the slope. In these areas, the slope was laid back slightly with a long-reach excavator and hoe ram to adjust the unstable slope angle. This process of matching the slope angle to the dominate rock structure was very effective in achieving the most economical excavation with very slight changes to the geometry needed to create a stable slope. This was also very effective in creating slope rounding and warping techniques in the minor drainage channels and at the top of slopes to create more naturally appearing cuts. Slope warping is the process of rounding (or sculpting) the lateral ends of a cut slope to smooth its transition to the surrounding terrain

In the vicinity of the landslide deposits near the middle of the project, the slope angle was changed dramatically due to the presence of very loose material. Drilling and mapping in the area had indicated that hard bedrock with favorable rock structure should be present along the perimeter of the slide. When excavating the slope, this material was found to be large blocks of slide debris and required an extensive amount of excavation to maintain a stable slope.

Due to the ditch width requirements developed during planning, the rockfall catchment area was greatly reduced. In addition, the cut slope angles were steepened to minimize the excavation quantities and slope scaring. These factors, along with the rock structure, rock quality and rock type, were used to evaluate the stabilization and mitigation requirements.

Dark brown colored draped wire mesh was applied in select locations to minimize the rockfall hazards. The locations and amount of mesh were based the percentage material contained in the ditch using the Colorado Rockfall Simulation Program (CRSP). The objective for this project was determined to be 60% to 70% of rocks contained based on a design rock of 2 feet in diameter. Although not ideal for typical highway construction, these criteria represented a substantial improvement to the pre-build condition.

Figure 7. Completed Hyampom Road

CONCLUSIONS

The reconstruction of the most challenging portion of Hyampom Road has resulted in improvements to mobility and safety while achieving the objectives of the community. Through the process of involving stakeholders and implementing a flexible design procedure, risks were clearly defined and managed. The final alignment and roadway section was the result of an iterative process, balancing cost and risk.

One of the most important considerations on the project was developing a slope angles and configurations that fit within the context of the project setting. Rock slope configurations were adjusted to fit the conditions during construction and to achieve a more natural appearing slopes. Developing the proper slope angle with respect to the rock structure and roadway alignment will have a largest effect of the long-term stability of the cuts.

REFERENCES

FHWA, *Flexibility in Highway Design,* FHWA Pub. No. FHWA-PD-97-062.

McClaughlin, R.J., et al. 2000. *Geology of the Cape Mendocino, Eureka, Garberville, and Southwestern part of the Hayfork 30 x 90 Minute Quadrangles and Adjacent Offshore Area, Northern California.* U.S. Geological Survey Miscellaneous Field Studies MF-2336.

Strand, R.G. 1962. *Geologic Map of California, Redding Sheet—Olaf P. Jenkins Edition.* California Division of Mines and Geology Map Sheet, scale 1:250,000.

Rockfall and Rockslide Mitigation Options with Rocksheds and Real-time Slope Monitoring along Interstate 70 in Glenwood Canyon, Colorado

Ben P. Arndt
Yeh and Associates, Inc.
5700 East Evans Ave.
Denver, Colorado 80222
303-781-9590
barndt@yeh-eng.com

Ty Ortiz
Colorado Department of Transportation
4670 Holly St., Unit A
Denver, Colorado 80216
303-398-6588
ty.ortiz@dot.state.co.us

Prepared for the 63rd Highway Geology Symposium, May 7-10, 2012

Acknowledgements

The authors would like to acknowledge Mr. Joe Elsen, the CDOT Program Engineer for his valuable input and experience with the project; Mr. Ralph Trapani, Parsons Program Director, for his valuable input and experience with Glenwood Canyon and overall review of the project; Mr. John Duffy, CalTrans, for his review comments and experience with similar projects; Mr. Larry Olson, Olson Engineering, for his contributions for slope scanning; and Mr. Toshimitsu Nomura, PROTEC Engineering of Japan, and his associates for their collaboration on the rockshed designs and design energies for the project.

ABSTRACT

Interstate 70 is the primary east-west route across Colorado. The interstate crosses a multitude of geologic hazards, but mile marker 125 in Glenwood Canyon has been a site prone to large scale rockfall events resulting from rockslides. At this location, rockslides closed the interstate five times since 2003.

Closures ranged from partial lane closures to full closure of the interstate for two to three days; and the full costs of highway repairs and emergency response have exceeded $2,500,000. In two cases the westbound lanes of the interstate were closed for up to 60 days to allow for highway repairs. The westbound lanes at this location are supported on retaining walls and a steel girder bridge supports the eastbound lanes. The rockfall events have destroyed sections of the retaining wall and punctured holes ranging from 2 meters to 5 meters in diameter in the bridge deck. Detour routes when the interstate is closed consist of a 325 km long bypass. Consequently, indirect and safety costs from closures are significant, up to several hundred thousand dollars per day of closure.

March 2010 was the last incident that caused significant damage to the highway. This incident resulted in a 5 meter hole in the bridge deck and closed the highway for three days for rock mitigation. The westbound lanes were closed for nearly 60 days for bridge repairs.

After the event, which was repaired through FHWA Emergency Repair procedures, it was recommended that CDOT investigate long term rockfall and rockslide mitigation options. The investigation consisted of providing mitigation and management options for dealing with the ever present rockfall hazard. The investigation included lidar scanning of the slopes; remote mapping; two and three dimensional rockfall analysis; rock shed mitigation, design and evaluation; and remote slope stability radar (SSR) scanning that was conducted as a test for 22 hours. The results of the study outline of the mitigation options, and combination of mitigation and management of asset features are presented.

INTRODUCTION

This paper presents the abbreviated findings of the rockfall mitigation structure selection study for rockfall and rockslide hazards near mile post 125 along Interstate 70 (I-70) in Glenwood Canyon, Garfield County, Colorado. Since 2003, two major rockfall events and three smaller events at this location have caused significant or severe damage to the roadway; the total closure of I-70 was required for both the two major events. The Colorado Department of Transportation (CDOT) initiated this study for development of a long-term mitigation plan based on the feasibility, effectiveness, and required programming costs for various mitigation systems.

The project site is a 600 meter section of I-70 just west of the Hanging Lake Tunnel, at the bottom of the Canyon near the Colorado River. Here, the natural slopes above the highway which historically have generated rockfall are up to 450 vertical meters high.

The lower rock slopes generally consist of Pre-Cambrian age (590 Ma) biotite granite, range from 1H:1V to ¾H:1V in slope and extend approximately 260 meters vertically above the roadway. Vertical and near-vertical slopes of Cambrian age (505 to 590 Ma) Sawatch quartzite overlie the granite on an unconformity at the contact of the two units; these quartzite cliffs extend from approximately 260 to 450 meters above the roadway. Both the granite and the quartzite have generated significant rockfall events. Above the Sawatch quartzite are shallower slopes of sedimentary geologic units from Ordovician to Pennsylvanian in age, but they generally have not been noted for recent rockfall events. Natural drainage channels within the granite rock slopes form pathways which the rockfall and rockslide events descend. Figure 1 depicts the lower granites and upper quartzite geologic units.

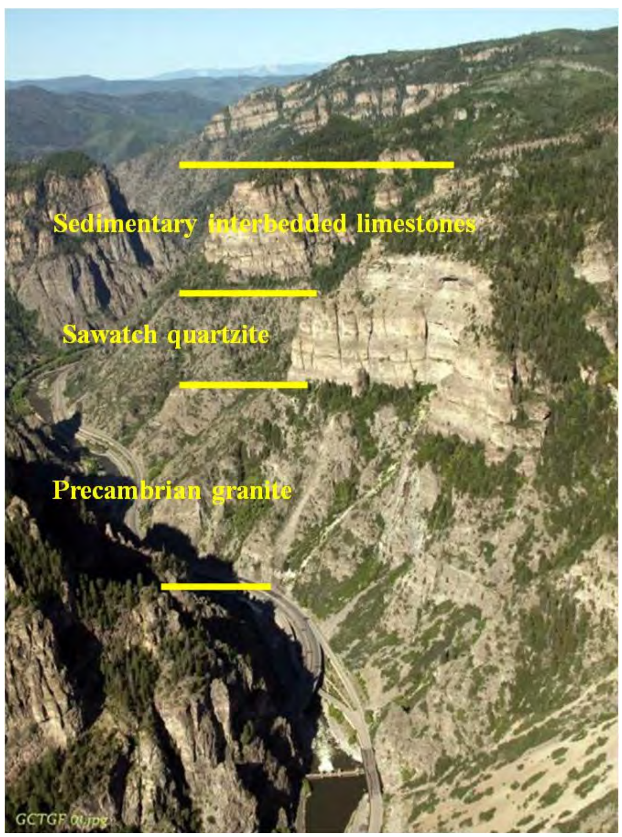

Figure 1.The contact between Pre-Cambrian granite, Cambrian Sawatch Quartzite, and Sedimentary units.

DISCUSSION

At the base of the slope, the highway consists of four lanes: two 3.6 meter wide eastbound lanes and two 3.6 meter wide westbound lanes, with 1 meter inside shoulders and 2.5 meter outside shoulders. Additionally, a single lane eastbound off-ramp and a single lane westbound on-ramp convey traffic to and from the Hanging Lake Rest Area, the Shoshone Dam, and the multi-use path which traverses through Glenwood Canyon. The eastbound lanes are supported by a steel-girder bridge structure with a concrete deck. The westbound lanes are constructed on a double-tee retaining wall, with part of the median cantilevered from the retaining wall. The concrete bridge deck for the eastbound lanes extends to abut the cantilevered median deck, providing a continuous concrete deck between the eastbound and westbound lanes. At the study location, the eastbound bridge structure is approximately 15 meters wide, and the retaining wall structure is approximately 12 meters wide. The roadway surface is about 10 meters above the Colorado River at this location (Figure 2).

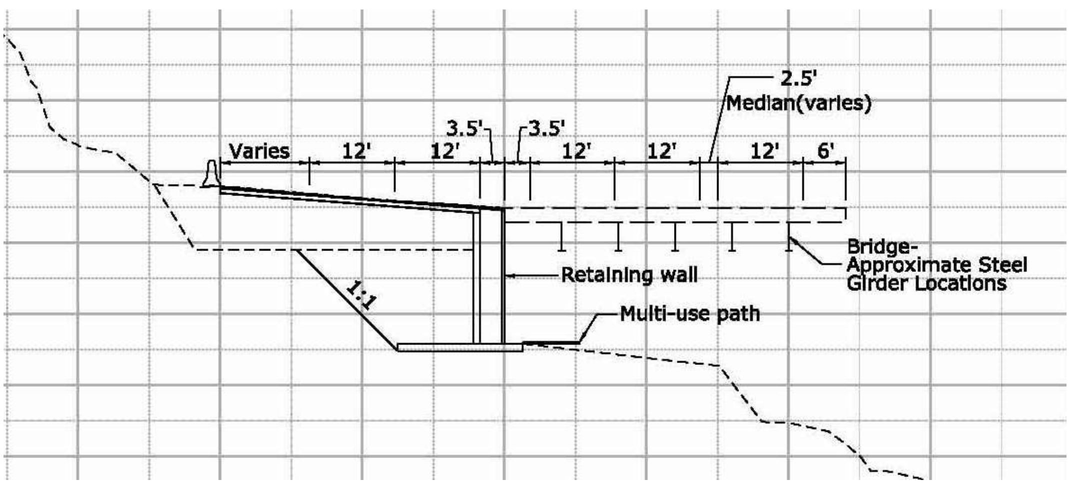

Figure 2. Typical section through roadway at project location.
(Units depicted in feet)

ROCKFALL EVENTS

Since 2003, two major rockfall events have caused severe damage to the I-70 roadway, resulting in complete closure of the highway for several days. In addition, three smaller events caused significant damage to the highway which did not require a complete closure; most of these were cleaned up and the highway repaired with only a single lane temporarily closed. All of these events impacted the westbound and eastbound lanes within an approximate 300 meter length of highway. Each rockfall event had a different source area, and generally consisted of multiple rocks damaging the roadway and supporting structures. The two largest events occurred on November 25, 2004 and March 8, 2010. The three events which resulted in only a partial highway closure occurred on January 21, 2003; January 1, 2006; and March 19, 2011. A brief summary of the January 21, 2003 through March 10, 2010 incidents follows.

January 2003

On January 21, 2003, a rock slope failure occurred approximately 180 meters above the roadway in the Precambrian granite. As a result of this slope failure, a large boulder approximately 2.5 meters in diameter impacted the westbound and eastbound lanes, forming large indentations in the concrete pavement of both, and crushed concrete median guardrails. It came to rest on the concrete guardrail between the east-bound lanes and the eastbound off-ramp. Smaller cobbles also came to rest on the roadway. No vehicles were involved. The eastbound lanes and off-ramp were closed for multiple days for repairs.

November 2004

On November 25, 2004 (Thanksgiving Day in the US), a large block of rock released from an overhanging layer of Sawatch Quartzite approximately 350 meters above the highway. The block was estimated to have a total volume between 1500 and 2000 cubic meters, and broke into several boulders before impacting the roadway. The largest boulder that landed on the highway, approximately 5 by 2.5 by 3meters, impacted the highway and continued rolling into the Colorado River. Rocks impacted the westbound and eastbound lanes, leaving several holes in the concrete bridge deck, the largest of which was approximately 6 meters by 3 meters. Relatively small areas of pavement in the westbound lanes were damaged. No vehicles were involved. Both directions of I-70 were closed for approximately 1½ days for scaling; and, the westbound lanes were closed for about two months for repairs.

January 2006

Several boulders ranging from 0.6 to 1.2meters in diameter released from the upper Precambrian granite slopes, approximately 250 meters above the roadway, on January 1, 2006. The rocks impacted the eastbound lanes of I-70, leaving a hole in the eastbound bridge deck approximately 1 meter in diameter. Some rocks also continued over the bridge railing, landing in the Colorado River. No vehicles were involved, and no injuries were reported. The left eastbound lane was closed for multiple days for repairs.

March 2010

On March 8, 2010, a large number of boulders ranging from 1 to 3 meter in diameter from the lower Precambrian granites impacted the highway in the westbound and eastbound lanes. The rocks released from Precambrian granite, approximately 180 vertical meters above the roadway. Rocks left several holes in the concrete pavement and bridge deck, the largest of which was approximately 5 meters by 3 meters, located in the bridge deck overhang under the left eastbound lane. Reinforcing steel was sheared off or became unbonded from adjacent concrete. In addition, the outer edge of the retaining wall under the left westbound lane was severely damaged, and steel and concrete guardrails at the median were destroyed. No vehicles were involved. Both directions of I-70 were closed for 4 days for rock stabilization, and intermittent closures occurred for the following 60 days for repairs. The rocks' final position was on the roadway and on the multi-use path below the eastbound bridge. Rocks most likely rolled into the river as well. Figure 3 depicts the rockfall site locations.

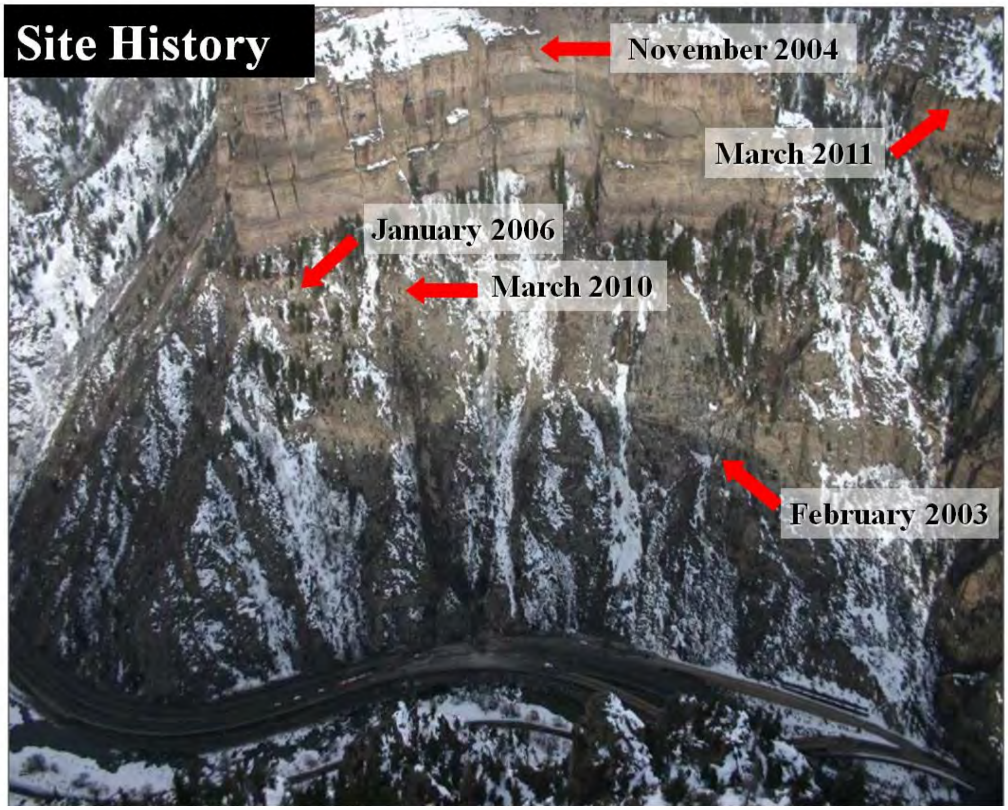

Figure 3.Rockfall Source Areas between 2003 and 2011.

Figure 4. Rocks damaged the bridge deck closing four (all) lanes of I-70 on March 8, 2010.

CDOT has estimated the daily operational cost of closing I-70 through Glenwood Canyon was US$980,000 per day during this closure, with a safety cost of US $225,000 per day for a total of over US $1.2 million per day.

Rockfall Modeling

During the study, a rockfall shed protection structure was the primary structural mitigation option considered. A rockfall shed would protect both motorists and the highway structures below the shed. In order to determine the feasibility of these options, rockfall energies and impact forces were evaluated using rockfall trajectory modeling.

Design Rockfall Event

In order to choose the “design rock” size for the structural mitigation, it was necessary to determine the relationship between rock size and estimated recurrence interval, based on discussions with personnel from the CDOT Rockfall Program, CDOT Region 3, and the design team. It is our understanding that other governmental agencies that have dealt with similar rockfall problems have attempted to assign risk and probability to a rockfall event with a given rock diameter and subsequent energy. For the purposes of this study, the design team concluded that data from past rockfall events was not adequate to do this, and assigning probability and risk to the traveling public for this area did not lend itself to reasonable estimates or calculations, given the five recent documented events at the site. Therefore, the CDOT Rockfall Program and CDOT Region 3 suggested rock sizes for evaluation, to provide the design team with a basis for the rockfall modeling. Based on past rockfall events, field observations, and experience, reasonable recurrence intervals for those rock sizes are:

Table 1. Rock size and estimated recurrence interval.

Rock size	Estimated Recurrence Interval
8x8x6 ft. block	3 -5 years
16x10x8 ft. block	5 - 10 years
16x16x16 ft. block	75 - 100 years

Part of this table was based on measurements of rocks currently located on the south bank of the Colorado River just below the study area. The largest of these from recent incidents was the rectangular block approximately 5 by 3 by 2.5meters, deposited during the November 2004 event. The event with a 5- to 10-year estimated recurrence interval is based on this size rock, which is also estimated to correlate to the size of event experienced in 2010.Although many rockfall events have been observed and recorded at this location, it is important to note the subjective nature of these recurrence interval values.

For the purposes of modeling rockfall, based on discussions with the CDOT Rockfall Program, the following two idealized rocks were chosen to facilitate trajectory modeling:

- A spherical rock 4.5 meters in diameter, and
- A rectangular rock 5x3x2.5 meters.

Modeling Methodology

Rockfall modeling was performed using two different computer programs: CRSP 4.0 (Jones et al., 1999) andRocFall4.054 (Rocscience, Inc., 2003). Each of these programs uses a different analysis method for defining the physical properties of the slope and for modeling the interaction between the falling rock and the slope. CRSP 4.0 is widely used in the US for rockfall trajectory and energy analysis, for the purpose designing mitigation features, such as rockfall fences and catchment areas. RocFall is also a well-established comparable software program, used in the US and Canada for similar purposes

Based on the rockfall events in 2004 and 2010,Yeh and Associates chose two rockfall paths for the modeling, and the rockfall source areas were taken as the approximate source areas from those events. These two paths are considered probable paths for future rockfall events. Preliminary modeling was performed using 1.5, 3, and 4.5 meter spherical rocks for both of these paths, with and without generalized rockfall shed geometries included in the model. These preliminary rock sizes do not correlate to the sizes in Table 1 above; they were chosen only to determine the relationship between rock size/mass and kinetic energy for this slope, and to verify the software's capabilities in modeling such large rocks. One of the two rockfall paths consistently resulted in higher energies and velocities, so this profile was used in all subsequent modeling.

Yeh and Associates determined that overall, the current state of practice for two dimensional rockfall modeling is very limited for rockfall diameters greater than 1.5 to 2.5 meters. CRSP 4.0 in particular did not yield reasonable velocity results for a 4.5 meter diameter rock. Although the results from RocFall for a 4.5 meter rock appeared reasonable, the results may still be unrepresentative or unreliable, as both CRSP and RocFall were calibrated with rock diameters of typically 1.2 to 1.8 meter or smaller. Because of these apparent inaccuracies, CRSP 4.0 was not utilized further for design purposes.

RocFall provided the most reasonable velocity and kinetic energy results for larger rocks; however, it also has the limitation of modeling the rock as a point with a large mass so when working with larger diameters the point of impact to a mitigation system is not the center of the rockfall diameter but rather the center of a point.

Based on the trajectory modeling, and after conferring with the CDOT Rockfall Program, it was agreed that 80 ft/sec was the practical upper limit on translational velocity. The evaluation was carried forward using this upper velocity limit and the anticipated rock masses listed in Table 1.

Modeling Results

As part of the project scope of work, PROTEC Engineering of Niigata, Japan was employed as a sub-consultant with extensive rockfall shed design experience in Japan, to determine whether a rockfall shed would be a feasible mitigation option at the study site. Based on discussions with the design team, PROTEC engineers recommended that "performance limit states" be determined for various kinetic energies which correlated with the estimated recurrence intervals. This would define the energy that a rockfall shed would be required to withstand while maintaining a specified level of structural performance, and maintenance requirements.

As a result of this recommendation, Yeh and Associates used rockfall modeling to determine the kinetic energies associated with each of the three rock sizes and recurrence intervals listed in Table 1. In addition, through discussions with the Design Team and CDOT, desired structural performance for each "limit state" was determined (Table 2).

Table 2. Performance limit states for a rockfall shed at the study site.

Energy Level	Rock size	Average Translational Kinetic Energy (kJ)	Maintenance Required after Impact	Estimated Recurrence Interval
1	8x8x6 ft. block	8,500	None	3 -5 years
2	16x10x8 ft. block	28,000	Replace EPS, no replacement of concrete or steel	5 - 10 years
3	16x16x16 ft. block	86,000	Deformation does not enter roadway zone, replacement required for EPS and structural elements	75 - 100 years

MITIGATION OPTIONS

Options Reviewed

Based on rock mass ratings and rockfall modeling, Yeh and Associates was asked to consider the feasibility of several mitigation options for the project area and to determine potential effectiveness and approximate costs for each option. Mitigation options evaluated as part of this effort included deflection structures, fences, barrier walls, rock scaling, rock bolting, cable lashing, roadway realignment options, rockfall monitoring/warning systems and a reinforced bridge deck "super-deck"; other, less effective options were also considered. Ultimately the rockfall shed and slope monitoring/warning options were evaluated to be carried forward.

Rockfall Sheds

Rockfall sheds are roofed structures over roadways, typically open-sided (on the downhill side), and sometimes with rock catchment areas or rock deflection structures on the roof over the protected road-way. Rockfall sheds are widely used in parts of Europe and Asia to allow falling rocks to pass over or be contained without impacting traffic or structures below the shed.

Rockfall sheds are typically limited to usage on narrow mountain roadways, because the shed is often constructed at a steep angle to deflect the moving rocks over the roadway without damaging the structure. The flatter the "roof" of the shed, the more easily a falling rock will damage or break a hole through the shed. For wider roads, the shed typically begins higher up the slope, which reduces the feasibility to reduced access and the need for very tall columns to support the shed roof.

Overall, based on evaluation by the design team and PROTEC Engineering, it appears that rockfall sheds are a feasible technical option at the Glenwood Canyon project site for Energy Levels 1 and 2 (Table 2). At Energy Level 3, we would expect the rockfall shed to be significantly damaged and likely in need of extensive repair and/or replacement.

Two rockfall shed options were proposed by PROTEC: a "half shed" across the westbound lanes with an MSE retaining structure on top, and a full shed design across both directions of I-70, without an MSE structure. Figures 5 and 6 depict the two rockfall shed conceptual designs.

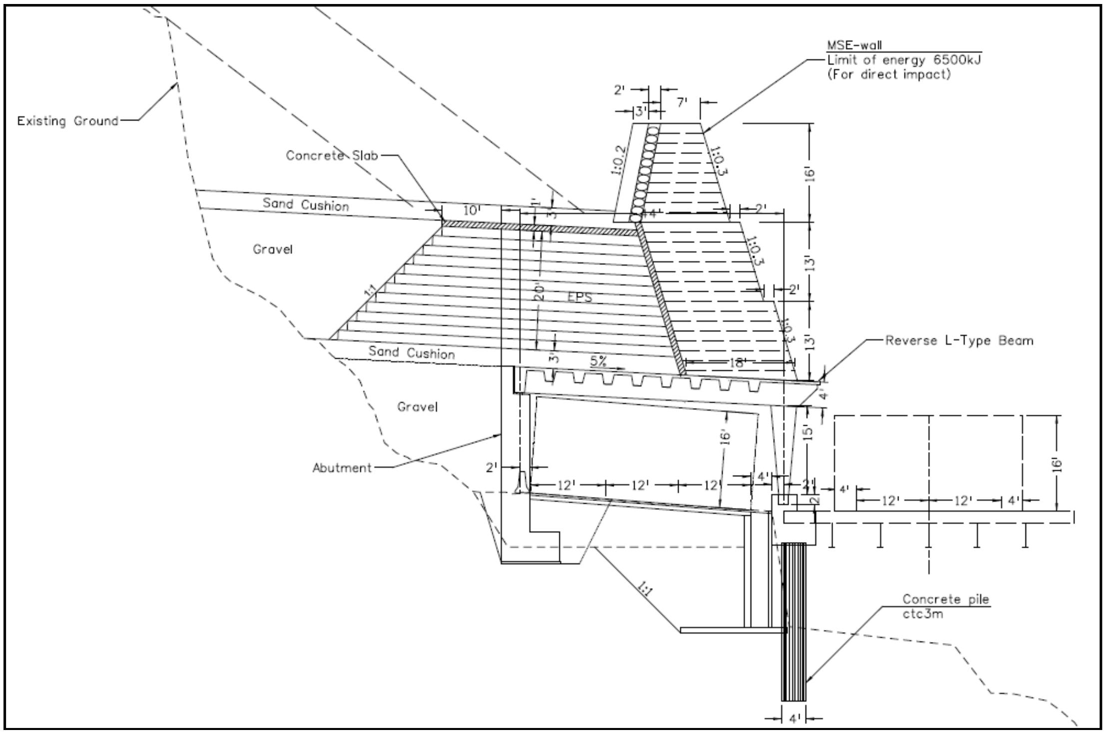

Figure 5.Half-shed rockshed across the westbound lanes only.

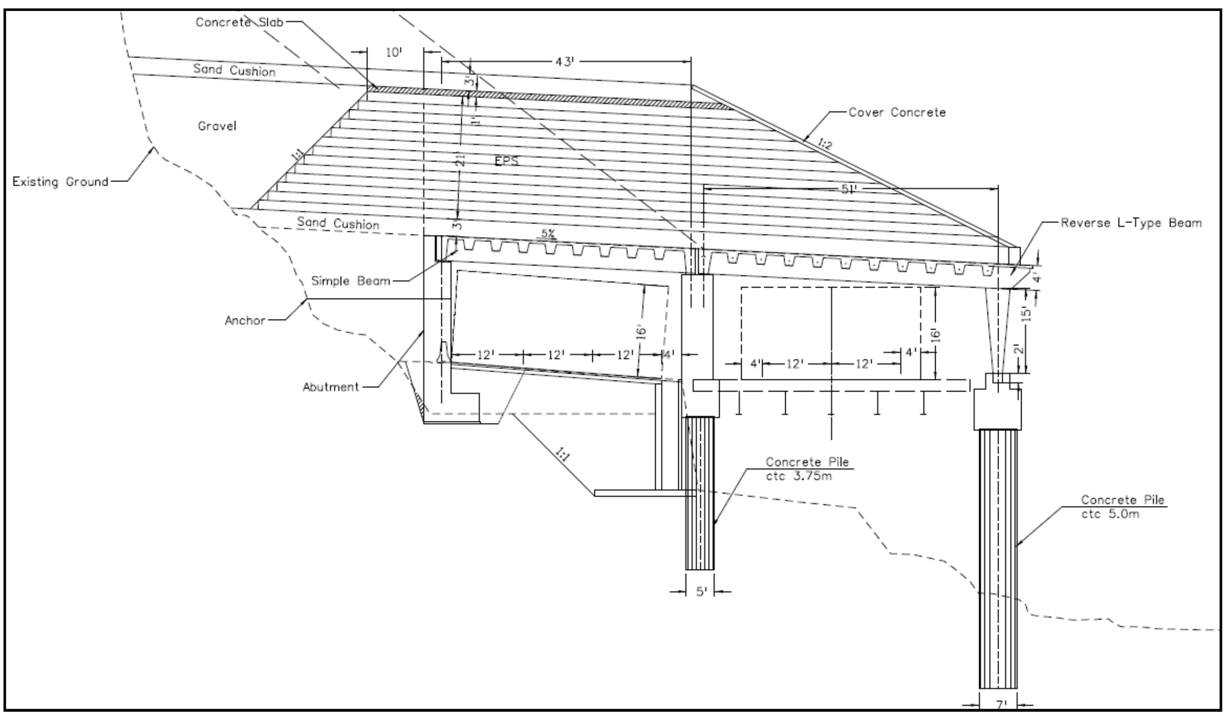

Figure 6. Full-shed rockfall shed across all four lanes of I-70.

Both of these rockfall shed designs include elements of energy-absorbing materials constructed on the roof of the shed, including Expanded Polystyrene (EPS). Based on conceptual rockfall shed design and estimated quantities of probable construction items (concrete, reinforcing, backfill, etc.), for a rockfall shed 135 meters long at the study location, the total construction cost would be in excess of $6-8 million for a shed covering only the westbound lanes, and costs would be in excess of $11-13 million for a shed covering all westbound and eastbound lanes. The location and length of 135 meters is based on a design approach of reducing the hazard from an event similar to the ones in 2004 and 2010. Note that with this shed length, segments of the study area would still be exposed to some hazard; for example, the events from 2003 and 2011 occurred outside of the proposed rockfall shed coverage area. To mitigate the hazard outside of the shed area, rockfall fences or barrier walls may be incorporated as additional mitigation measures for further hazard reduction beyond what the shed alone could provide.

Slope Monitoring/Warning Systems

Monitoring of rockfall slopes can consist of various degrees of complexity, from recording regular visual observations of rock slopes and rock cuts to using radar technologies that can determine real-time and prolonged rock deformations over time.

The CDOT Rockfall Program initiated a test slope scan at the Glenwood Canyon site using a version of Synthetic Aperture Radar (SAR) technology. The trial scan used an Interferometric Survey-Landslide (IBIS-L) system operated by Olson Engineering. Displacement measurements were made from the edge of a cliff on the south side of I-70 across the canyon from the study site. The IBIS-L system was evaluated and set up on the top of the south canyon edge by CDOT, Yeh and Associates, and Olson Engineering personnel by using a helicopter to access the site on multiple occasions. The slope monitoring was performed from approximately 11 am on March 2nd to 9 am on March 3rd, 2011. The system provided scan coverage across most of the study area, with the exception of the lower slope portion which was shadowed by the foreground cliff edge. The system operated with virtually no disturbance to the highway below or the adjacent Hanging Lake Tunnel.

The data was analyzed and graphically overlain on a Digital Terrain Model (DTM) to help visualize the displacements. Approximately 40,000 pixels were simultaneously monitored to measure movements less than sub-millimeter. Following analysis of the monitoring data, the maximum line-of-site displacements measured within the 22-hour testing period were approximately 7.5 to 12 millimeters. The time domain data can be differentiated to calculate the velocity of each measured pixel, which has been shown to be an indicator of imminent slope failure. Figure 7 depicts the DTM image obtained from the study, with slope displacements colored according to their magnitude.

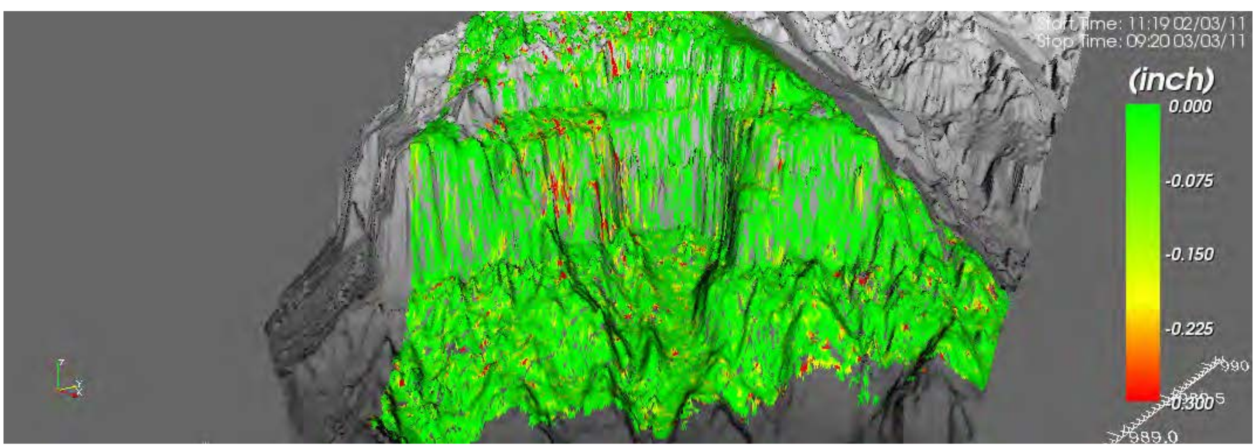

Figure 7.Displacements from the scanning study, on a DTM. (Olson Engineering)

Due to the limited data set from the trial scan, it was not possible to determine if any of the monitored movement actually indicates potential for imminent rockfall failure, but clear trends of displacement were detected on the monitored slope. Further, the noted displacement trends appeared to be influenced by daily temperature cycles of freezing and thawing. In particular, slope displacements were largest between late morning and late evening hours as temperatures approached 10ºC. As temperatures fell below freezing to nearly -7ºC, displacements slowed significantly. It should be noted that the main purpose of the test was to determine if the slope could be satisfactorily scanned from the south side of the canyon. The anticipate cost of implementing a SAR system is expected to be less than $3M.

CONCLUSIONS

Although impacts have been limited to date, the probability of vehicles being significantly affected by rock slope failures in this area exist. The study was undertaken to evaluate feasible rockfall mitigation options at the site and what approximate costs were associated with each option. Also, the study undertook using emerging technologies to monitor rockslope faces over a period of time in an effort to provide a warning system for rockfall events.

Overall, the rockfall shed options appeared to offer a reasonable mitigation alternative when and if funding sources are allocated in the future. Furthermore, the real-time rockslope scanning showed to be a technology that could be implemented in the canyon to provide an early warning or detection of rockslope movements.The three options that were to be carried forward include:

1. Rockfall Shed
   - Half rockfall shed over westbound lanes
   - Full rockfall shed over both eastbound and westbound lanes
2. Slope scanning in conjunction with warning system(s)
3. Realignment of I-70 with a tunnel through the subject site.

Table 3 depicts the approximate costs generated for the project.

Table 3.Approximate costs associated with Mitigation Options.

	Mitigation Option	Estimated Cost Range (Millions)
1	Rockfall shed	-
(a)	Half Shed over Westbound	$6 to $8
(b)	Full Shed over West and East	$11 to $13
2	Slope scanning systems	$2 to $3
3	Tunnel	$174 to $201

Using LIDAR in Highway Rock Cuts

Norbert H. Maerz, Ph. D., P. Eng,
Missouri University of Science and Technology,
1006 Kingshighway, Rolla, MO, 65401,
norbert@mst.edu, 573 341-6724

James Otoo, M. Sc.,
Missouri University of Science and Technology,
1006 Kingshighway, Rolla, MO, 65401,
norbert@mst.edu, 573 341-6724

Travis Kassebaum, B. Sc.,
Missouri University of Science and Technology,
1006 Kingshighway, Rolla, MO, 65401,
norbert@mst.edu, 573 341-6724

Ken Boyko, B. Sc.
Missouri University of Science and Technology,
1006 Kingshighway, Rolla, MO, 65401,
norbert@mst.edu, 573 341-6724

Prepared for the 63rd Highway Geology Symposium, May 7-10, 2012

Acknowledgements

The authors would like to thank the National Science Foundation for sponsoring some aspects of the work presented here. This is supported in part by the NSF CMMI Award #0856420 and #0856206. Other aspects of this work have been supported by the University of Missouri Research Board and the Center for Infrastructure Engineering and the National University Transportation Center at Missouri University of Science and Technology.

Disclaimer

Statements and views presented in this paper are strictly those of the author, and do not necessarily reflect positions held by their affiliations, the Highway Geology Symposium (HGS), or others acknowledged above. The mention of trade names for commercial products does not imply the approval or endorsement by HGS.

ABSTRACT

LIDAR is a relatively new technology that is being used in many aspects of geology and engineering, including researching the potential for rock falls on highway rock cuts. At Missouri University of Science and Technology we are developing methods for remotely measuring joint orientations and quantifying the raveling process. Measuring joint orientations along highways remotely is safer, more accurate, and can result in larger and more accurate data sets, including measurements from otherwise inaccessible areas. Measuring the nature of rock raveling will provide the data needed to begin the process of modeling the rock raveling process.

INTRODUCTION

LIDAR(LIght Detection And Ranging) is a relatively new technology that is being used in many aspects of geology and engineering. At Missouri University of Science and Technology we are developing methods for remotely measuring joint orientations and quantifying the raveling process, in addition to many other measurement capabilities. We are using LIDAR to measure discontinuity orientation (which governs certain types of instabilities) and to measure and research the rock raveling process (which in some jurisdictions is the major cause of instability in highway rock cuts.)

ROCK FALLS ON HIGHWAYS

Rock falls are a major geological hazard in many States with mountainous or hilly terrain. The safety and convenience of the motoring public demands that highway rock cuts be made as safe as possible, while expenditures on remediation are always limited by often shrinking budgets. Catastrophic failures of rock cuts can result in property damage, injury, and even death. Highways impeded by even small spills of rock material are an inconvenience for motorists. Rock fall hazard assessment in the USA has traditionally been a reactive process.
Highways that traverse through rocky terrains often require that artificial vertical slopes be cut by blasting techniques to facilitate the highway construction. A constant danger to the motoring public is for large blocks of rock to fall or slide down, at worst killing and injuring members of the motoring public, and at best blocking the highway and impeding traffic flow.

Discontinuity Controlled Rock Falls (Conducive to Quantitative Analysis)

Many of these failures result because of release along planar cracks or discontinuities in rock mass. Whether or not failure occurs will depend on the orientation of the cracks, individually or in combinations (Figure 1).The cracks or discontinuities tend to cluster in terms of their orientations, into typically three or more sets, which tend to be mutually orthogonal, or roughly at 90 degree to each other (Figure 2). Knowing the orientations of the discontinuities can lead to stability prediction based on well established analytical tools (Hoek and Bray, 1981).

Figure 1. Example of wedge, planar, and toppling failures along road cuts.

Figure 2: Orthogonal nature of joint sets. Measurements of the “cracks” or discontinuities are displayed in Figure 3.

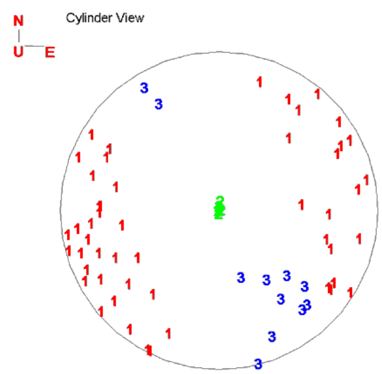

Figure 3. Projections of vectors normal to discontinuity plane on a unit lower hemisphere, clustered into three sets.

Figure 3 shows the time honored stereonet projection method [2] where each data point, consisting of a normal vector to an individual discontinuity plane, is assigned to a discontinuity set by using cluster analysis. Cluster analysis techniques are described in [3,4,5,6,7].

The orientations can be and have been traditionally measured using manual compass and clinometer methods. These methods are however slow, tedious and cumbersome, are in some cases dangerous because of potential falling rock, and are often limited to easily accessible locations like the base of the slope.

Once having identified the discontinuities traditional graphical or computational techniques can be used to determine the kinematic feasibility of failure (Figure 4) and standard modeling techniques such as limiting equilibrium analysis can be used to determine if failure will indeed take place (Figure 5) [1,8,9,10,11,12,13,14, 15,16,17].

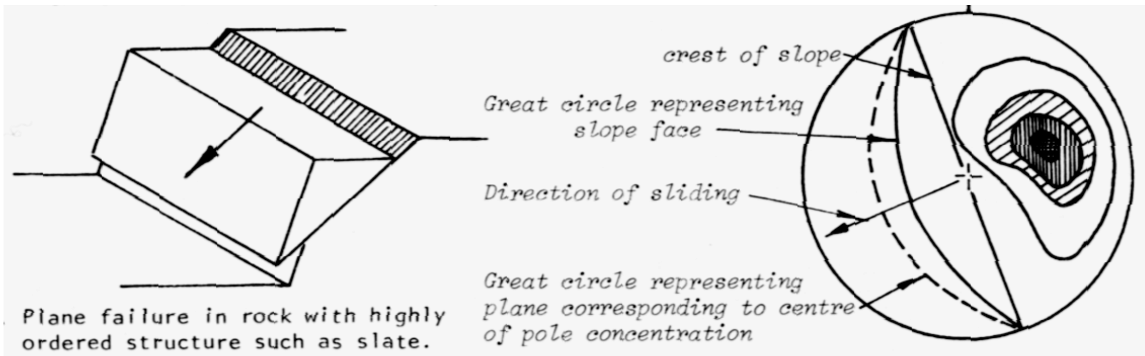

Figure 4: Planar failure geometry (left) and graphical method of determining if slide failure is kinematically possible (Hoek and Bray, 1981).

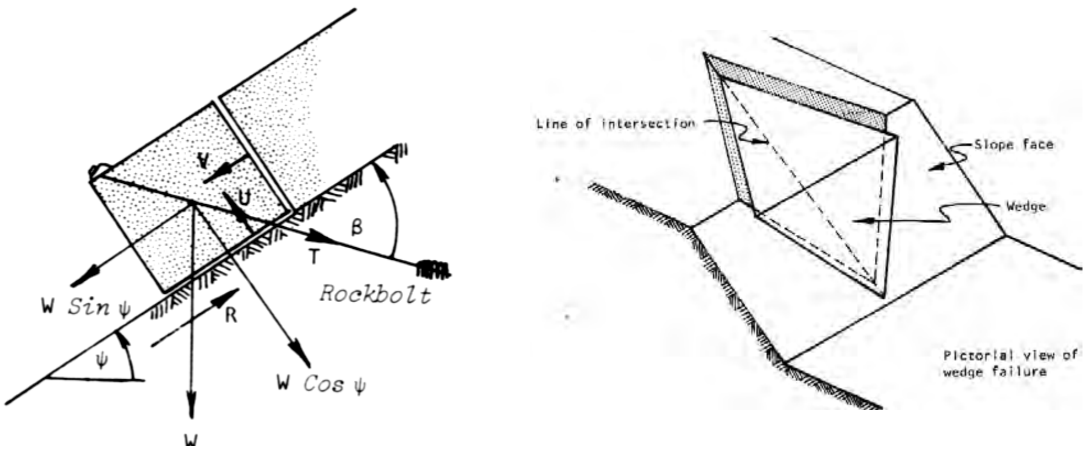

Figure 5: Limiting equilibriums analysis applied to planar features (left) and wedge features (right) after Hoek and Bray, [1].

Raveling Type Rock Falls (Not Conducive to Quantitative Analysis)

In many terrains the discontinuities are not oriented in such a way that they contribute to create wedge, planar sliding, or toppling failures or other easily analyzed failure mechanisms. Franklin and Senior [18] report that of 415 analyzed cases of failure in Northern Ontario, only 33% of failures involved these mechanisms (23% toppling, 8% planar sliding, 2% wedge sliding).

In the Northern Ontario study, 65% of the failures were of the "raveling" type. These included raveling (25%), overhang/undercutting failure (15%), ice jacking (14%), and rolling blocks (11%). In other terrains, most notably flat lying sedimentary rock, such as is found in much of the US, the predominant failure mechanism being of the raveling type is even greater.

Raveling failure, the most common type of rock failure is poorly understood. Analysis is mostly descriptive, and prediction of the amount of raveling is typically an empirical exercise in guessing based on extrapolation of visual evidence. Raveling failures are often usually slow and time dependent, but can also be catastrophic if they involve large blocks falling or many blocks releasing at once. Large blocks are often results of the collapse of overhanging ledges that have been undercut by raveling.

The literature abounds with mention of raveling [1,8,19,20]. Rock hazard rating systems use raveling as a parameter to determine the durability of rock cuts [21,22,23]. European research has investigated the processes and morphology of raveling, although in a qualitative observational way [23,24,25].In short there is no quantitative mechanism and model available to describe the raveling process, and consequently no predictive tools. Mitigation efforts make use of empirical observation and engineering judgement.

Figure 6.Example of raveling, undercutting, and rolling failures along road cuts.

TERESTRIAL LIDAR TECHNOLOGY

As a distance measuring device, LIDAR replaces traditional methods of laser surveying, which take individual measurements, and require reflective targets to measure distances and angles. LIDAR is more analogous to radar, in that the scanning laser can make thousands ofpoint measurements per second, reflecting off any surface, and returning a point cloud, which can be used by sophisticated software to create a very detailed 3-D surface map. The scanner uses either time of flight or phase shift sensors technology. The result is a million of points reflected from the surface. The points are represented by xyz coordinates, these xyz coordinates and their associated intensity values are known as a “Point cloud”. At Missouri S&T we have two LIDAR scanners (Figure 7). The Leica ScanStation II is a time of flight scanner capable of scanning up to 300 m at a maximum rate of 50,000 points per second. The Leica HDS6000 is a phase shift scanner capable of scanning up to 100 m at a maximum rate of 500,000 points per second. Both scanners have an accuracy of a bit less that 1 cm for a single measurement, but accuracy can be improved up to an order of magnitude for modeled surfaces, and even greater for in special circumstances. The ScanStation II in addition has a built in camera, so is capable of adding optical color information to the point cloud.

Figure 7: Left: Leica ScanStation II time of flight scanner with integrated optical camera. Right Leica HDS 6000 phase shift scanner on remote controlled robotic buggy.

Kemeny et al. characterized rock masses using LiDAR and automated point cloud processing, and also analyzed rock slope stability using LiDAR and digital images [27, 28], including measuring and clustering discontinuity orientations. LiDAR was used by Mikos et al. to study rock slope stability [29]. Lim et al used photogrammetry and laser scanning to monitor processes active in hard rock coastal cliffs [30]. High resolution LiDAR data was used by Sagy et al. to quantitatively study fault surface geometry [31]. Enge et al. illustrated the use of LiDAR to study petroleum reservoir analogues [32].

LIDAR DISCONTINUITY ORIENTATION MEASUREMENTS

To measure joint orientations LIDAR scans are taken of the joints to be measured (Figure 1). To simplify and speed up the process, no survey control is needed; it is simply required to measure the strike of a single sub-vertical feature in the scan. In addition, since only a single LIDAR scan is sufficient, no image registration is required. (In the case of the Leica ScanStation II, the optical image is automatically registered to the scanned point cloud.)Two types of rock faces/cuts are possible (Figure 8). In the first case some rock faces are composed almost exclusively of natural discontinuity surfaces. The orientation of each of these surfaces can be and should be measured. These are conducive to automatic or semi automated analysis such as described in [32,33,34,35,36,37,38]. Figure 9 shows an example of an automated analysis of such a rock face, in which the discontinuity measurements are clustered into sets and each resulting set is represented by a different color.

Figure 8: Left: Rock faces with 100% coverage of natural joint surfaces. Right:Rock faces with significant ambiguity as to the location of natural joint surfaces.

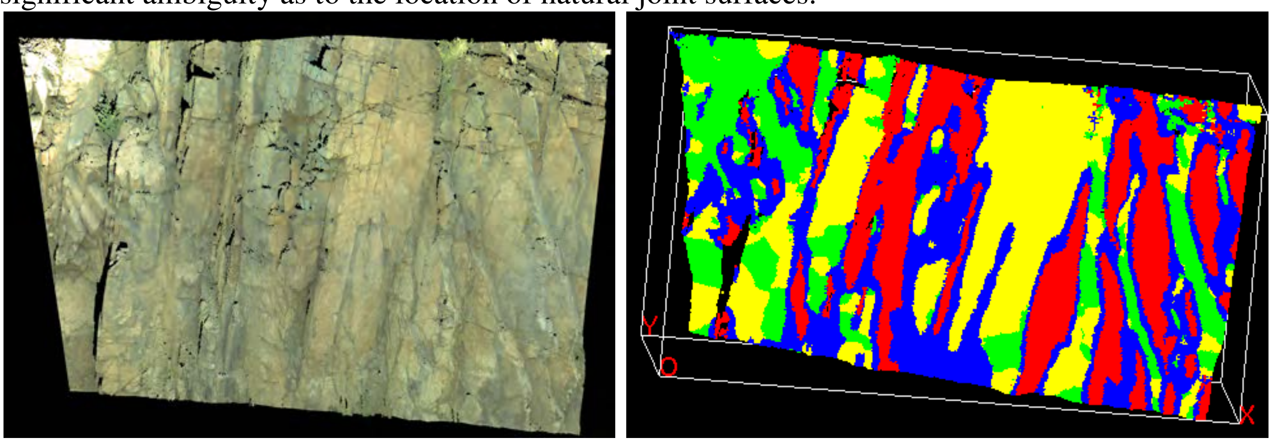

Figure 9: Left:Point cloud of a Missouri Rock cut in ignimbrite rock. Right: Identification of discontinuity orientations. Each different color represents discontinuities of similar orientations.

On the other hand for rock cuts that have sparse representation of natural joint surfaces, it is often easiest just to manually identify individual discontinuities on a LIDAR image viewer and pick (on the planar discontinuity surface) three co-planar non co-linear points. Figure 10 shows an example of using a point cloud viewer to select 3 points on a discontinuity surface. The discontinuity orientation can be determined by the classic 3-point solution [39].

Figures 11-12 show the results of a small verification study where LIDAR measurements are compared with manual measurements using a Brunton compass.

Figure 10: Picking three points on a discontinuity surface to calculate orientation.

Figure 11: Rock cut selected for verification study.

Dip Direction/ Dip Angle	
Field	LIDAR
008/51	011/54
108/85	112/87
006/07	008/09
198/63	200/65
159/85	162/87
102/87	105/86
158/78	156/77
101/82	112/88
021/47	023/48
218/61	215/60

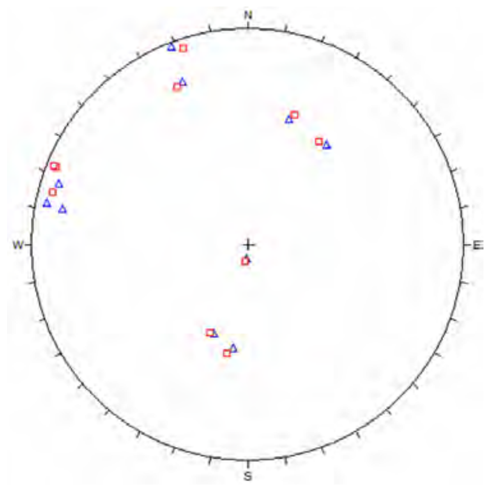

Figure 12: Results of verification study comparing manual measurements with LIDAR measurements. On the lower hemisphere projection, red points are LIDAR measurements, blue points are manual measurements.

RAVELING MEASUREMENTS

To quantify raveling of rock,scans of a raveling rock face are taken over a period of time. Again,to simplify and speed up the process, no survey control is needed, it is simply required to position the LIDAR unit in approximated the same place, and scan approximated the same area. Algorithms for automated registration are used to superimpose the two scanned sets, and then the volume differences between the two sets are measured and displayed. Figure 13 shows an example of a raveling rock cut in weathered dolomite. Figure 14 shows the results of 3 sequential measurements with the missing pieces highlighted for a six month pilot study.

Figure 13: Scan section of a rock face near a local quarry.

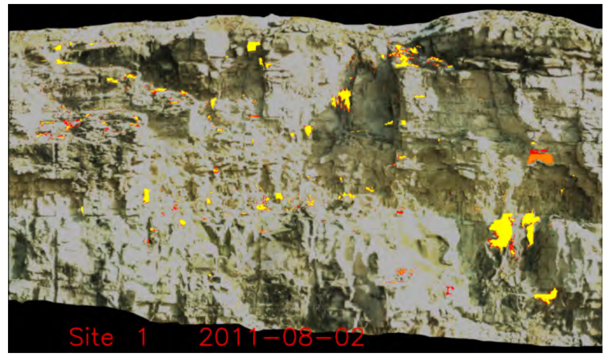

Figure 14: Point cloud of the scan and measured progressive raveling loss. Yellow, 7-15, orange 7/26, red 8/02.

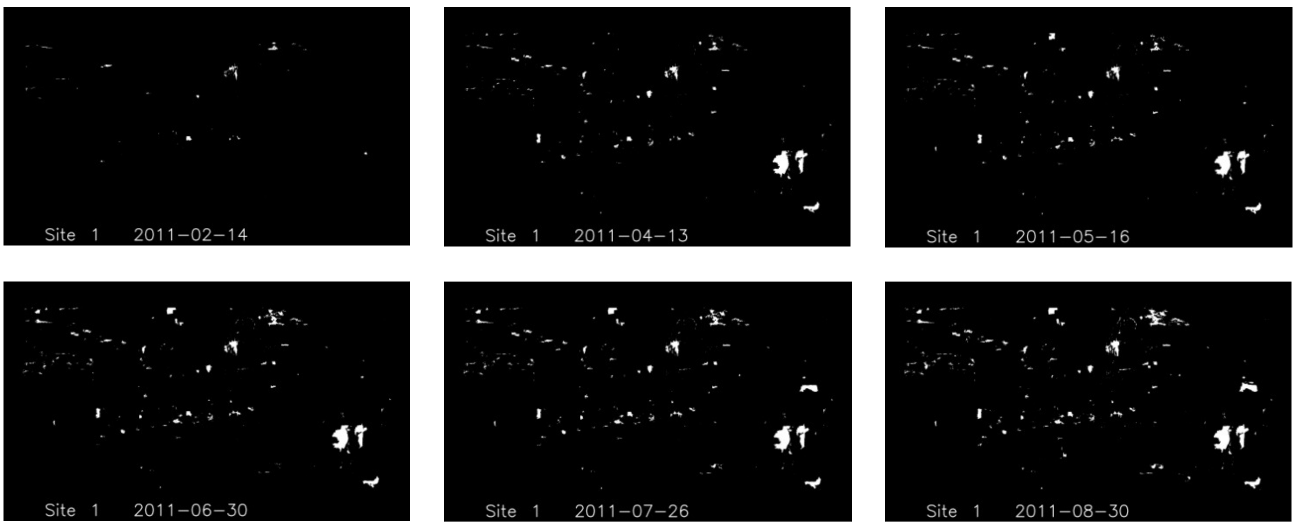

Figure 15.Part of the sequence of 16 images showing the increase in missing (fallen) blocks as a function of time.

To demonstrate the feasibility of the proposed technique, a small 6 month study was undertaken (Figure 15). Two small local rock cuts one in and one near a local quarry were imaged using LIDAR, 18 separate times over that period. At the same time measurements of rainfall and ground vibration from blasting were taken. Resolution was found to be 3 mm for site one and 8mm for site 2, with an average of 6.7 million data points per scan. The smallest rock that could be detected is 9 mm across.Software was developed to register the point clouds (with an average root mean square error of 2.5 mm) scanned at different times and measure the volume of the fallen rock. All software is developed in C++, compiled using the GNU G++ complier, and runs on Ubuntu® Linux. The processing sequence was as follows:

1. Pre-loading, determines the minimum and maximum ranges of the horizontal and vertical components of the observation set.
2. Load individual triplets (x,y,z), sort according to position.
3. Filling gaps by interpolating between triplets.
4. Register the image to know coordinate system using automatic algorithms.
5. Determine maximum common crop boundary for all temporal data sets
6. Crop the image so that each image consistently covers the same area.
7. Removal of vegetation and all non-rock artifacts.
8. Creation of a difference surface between any two scans.
9. Segmentation of individual (missing) rocks.
10. Volume calculation.

Preliminary correlations (Figure 16) between volume of blocks lost and freeze-thaw cycles, blasting episodes, and rainfall are somewhat tentative at this point. Site 2 seems significantly affected freeze-thaw cycles in correlating scan #2. In the area of scans #11-13, as the rainfall decrease to near zero the volume of blocks lost also trends to zero. Unanswered at this point is why the difference in scan #2 between the two sites which are very close together.

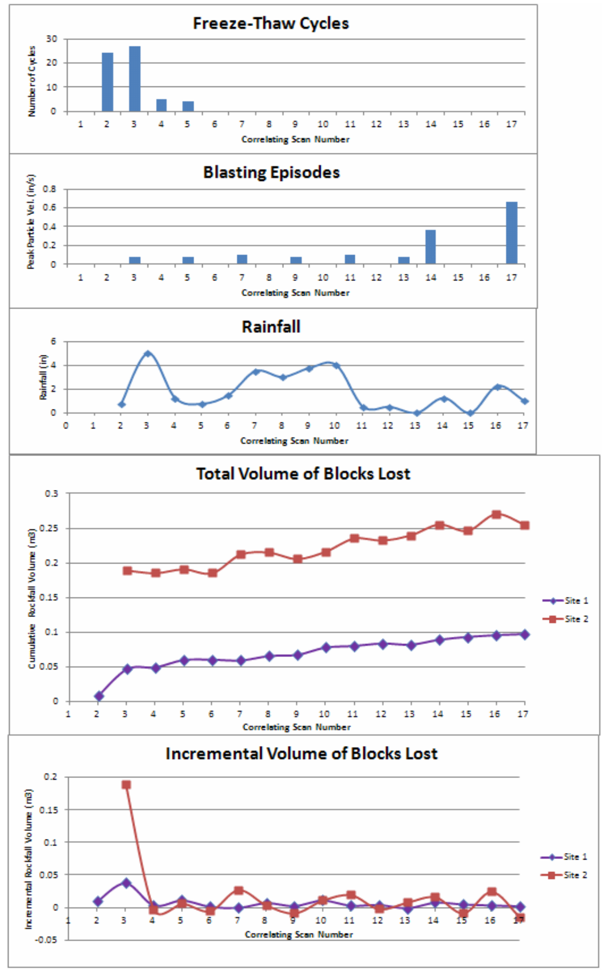

Figure 16: Results of the study: Correlation between volume loss and external stimuli including rainfall, freeze-thaw cycles, and the number of blasting episodes in a nearby quarry.

The results show that in some incremental scans there were some small volume gains. Observations suggest that this is real, and it is a result of small quantities of rock accumulating on ledges after having fallen from higher up. More work on the algorithms may increase the fidelity of the lost volume measurement.

Ultimately the goal of this work is to provide verification for numerical models that will be used to model the raveling process.

CONCLUSIONS

LIDAR technology provides tremendous new opportunities for measurement and characterization of rock cuts. Measurements using LIDAR are superior to manual measurements and older technologies in that they produce vast amounts of data, quickly, safely and with less sampling bias. What is required are algorithms, both simple and sophisticated, that use the LIDAR data to characterize the rock cuts and provide input to predictive tools.

REFERENCES

1. Hoek, E., and Bray, J., 1981, *Rock slope engineering*. The Institution of Mining and Metallurgy, 358 pp.Priest, S. D., 1985. Hemispherical Projection Methods in Rock Mechanics. George Alleu&Unwin, London, 124 pp.
2. Maerz, N. H., and Zhou, W., 1999, *Multivariate analysis of bore hole discontinuity data*. Rock Mechanics for Industry, Proceedings of the 37th US Rock Mechanics Symposium, Vail Colorado, June 6-9, 1999, v. 1, pp. 431-438.
3. Maerz, N. H., and Zhou, W., 2000, *Discontinuity data analysis from oriented boreholes*. Pacific Rocks; Proceedings of the Fourth North American Rock Mechanics Symposium, Seattle, Washington, July 31- Aug.1, 2000, pp. 667-674.
4. Zhou, W., and Maerz, N. H., 2001, *Multivariate clustering analysis of discontinuity data: implementation and applications.* Rock Mechanics in the National Interest; Proceedings of the 38th U.S. Rock Mechanics Symposium, Washington, D.C., July 7-10, 2001, pp 861-868.
5. Zhou, W., and Maerz, N. H., 2002, *Implementation of multivariate clustering methods for characterizing discontinuites from oriented boreholes.*Computers & Geosciences, v. 28, no. 7, pp. 827-839.
6. Maerz, H. H., and Zhou, W., 2005,*Multivariate clustering analysis of the ECRB cross drift discontinuities, Yucca Mountain Project.* Alaska Rocks, Proceedings of the 40th US Rock Mechanics Symposium, Anchorage Alaska, June 25-29, 2005, 10 pp.
7. Piteau, D. R., 1979a, *Engineering geology considerations and basic approach to rock slope stability analysis for highways.* Part A., Rock Slope Engineering Reference Manual: FHWA Report – FHWA-TS-79-208, 78 pp.
8. Piteau, D. R., 1979b, *Methods of obtaining geological, structural, strength and related engineering geology data*. Part B, Rock Slope Engineering Reference Manual: FHWA Report – FHWA-TS-79-208.,147 pp.
9. Piteau, D. R., 1979c, *Approach and techniques in geological structural analysis.* Part C, Rock Slope Engineering Reference Manual: FHWA Report – FHWA-TS-79-208.
10. Piteau, D. R., 1979d, *Slope stability analysis methods.* Part D, Rock Slope Engineering Reference Manual: FHWA Report – FHWA-TS-79-208.
11. Piteau, D. R., 1979e, *Rock slope stabilization, protection and warning-instrumentation measures and related construction considerations.* Part E, Rock Slope Engineering Reference Manual: FHWA Report – FHWA-TS-79-208.
12. Piteau, D. R., 1979f, *Blasting for rock slopes and related excavation considerations*. Part F, Rock slope Engineering Reference Manual: FHWA Report – FHWA-TS-79-208.
13. Piteau, D. R., 1979g, *Description of detail line engineering geology mapping method*. Part G, Rock slope engineering reference manual: FHWA Report – FHWA-TS-79-208, 29 pp.
14. Brawner, C. O., 1994,*Rockfall Hazard Mitigation Methods.* Participant Workbook: FHWA Report – FHWA-SA-93-085.
15. Konya, C.J., And Walter, E.J., 1991*, Rock blasting and overbreakcontrol*: FHWA Report – FHWA-HI-92-001.
16. Franklin, J. A., And Senior, S. A., 1987a*, Outline of RHRON, the Ontario rockfall hazard rating system:* Proceedings International Symposium on Engineering Geology and The Environment, Athens, Greece, pp. 647-656.
17. Franklin, J. A., And Senior, S. A., 1987b,*Rockfallhazards – Strategies for detection, assessment, and remediation:* Proceedings International Symposium on Engineering Geology and The Environment, Athens, Greece, pp. 657-663.
18. Walkinshaw, J., And Santi, P., 1996,*Shales and other degrable materials.* Landslides Investigation and Mitigation, TRB special report 247, pp. 555-576.
19. Kliche, C., 1999. *Rock Slope Stability*. Society for Mining, Metallurgy, and Exploration, 253 pp.

20. Pierson, L. A., And Van Vickle, R., 1993, *Rockfall hazard rating system* – Participants' Manual: FHWA Report: – FHWA-SA-93-057, 102 p.
21. Senior, S., 1999,*Rockfall hazard remediation along Ontario highways.* 50th Highway Geology Symposium, Roanoke, Virginia, May. 20-23, 1999, pp. 276-286.
22. Maerz, N. H., Youssef, A., AND LAUER, R., 2004, MORFH RS*: A rockcut rating system for Missouri highways.* 55th Highway Geology Symposium, Kansas City, Missouri, Sep. 7-10, 2004, pp 406-424.
23. Huisman, M, Hack, H., And Nieuwenhuis, J., 2004*, Observed rock mass degradation and resulting slope instability.* EURROCK 2004, 4 Pp.
24. Nicholson, D., 2003, *Breakdown mechanisms and morphology for man-made rockslopes in North West England.* North West Geography, v. 3. no. 1, pp. 12-26.
25. Kuhnel, R., 2002, *Driving forces of rock degradation*. Protection and Conservation of the Cultural Heritage of the Mediterranean cities, pp. 11-17.
26. Kemeny, J., Norton, B. and K. Turner. 2006,*Rock slope stability analysis utilizing ground-based lidar and digital image processing,*Felsbau – Rock and Soil Engineering, Nr. 3/06, pp 8-15, Invited publication.
27. Mikos, M., Vidmar, A., and Brilly, M., 2005*, Using a laser measurement system for monitoring morphological changes on the Strug rock fall, Slovenia*, Nat. Hazards Earth Syst. Sci., 5, 143–153.
28. Lim, M., Petley, D.N., Rosser, N.J., Allison, R.J., Long, A.J. and Pybus, D. 2005. *Combined digital photogrametry and time-of-flight laser scanning for monitoring cliff evolution*. Photogrammetry record, 20, 109-129.
29. Sagy, A., Brodsky, E.E. and Axen, G.J. 2007,*Evolution of fault-surface roughness with slip*. Geology, 35, 283-286.
30. Enge, H.D., Buckley, S.J., Rotevatn, A. and Howell, J.A., 2007,*From outcrop to reservoir simulation model: workflow and procedures*. Geosphere, 3, 469-490.
31. Donovan, J., Kemeny. J., and Handy, J., 2005,*The application of three-dimensional imaging to rock discontinuity characterization,* Alaska Rocks, Proceedings of the 40th US Rock Mechanics Symposium, Anchorage Alaska, June 25-29, 7 pp.
32. Feng, Q., 2001,*Novel methods for 3-D semi-automatic mapping of fracture geometry at exposed rock faces*. Ph.D. Thesis, Division of engineering geology, Royal Institute of Technology (KTH), Stockholm. ISBN 91-7283-113-8.
33. Feng, Q. H., and Roshoff, K., 2004, *In-situ mapping and documentation of rock faces using a full coverage 3D Laser Scanning Technique*. International Journal of Rock Mechanics and Mining Sciences, Volume 41, Issue 3, 6 pp.
34. Gigli, G., and Casagli, N., 2011,*Semi-automatic extraction of rock mass structural data from high resolution LIDAR point clouds.* International Journal of Rock Mechanics and Mining Sciences, Volume 48, Issue 2, February 2011, pp. 187-198.
35. Lato, M., Hutchinson, J., Diederichs, M, Ball, D., And Harrap, R., 2009,*Engineering monitoring of rockfall hazards along transportation corridors: using moble terrestrial LiDAR*. Nat. Hazards Earth syst. Sci. 9, pp. 935-946.
36. Otoo, J. N., Maerz, N., H., Xiaoling, L., and Duan, Y., 2011, *3-D discontinuity orientations using combined optical imaging and LiDAR techniques.* Proceedings of the 45th US Rock Mechanics Symposium, San Francisco California, June 26-29 2011, 9 pp.
37. Slob, S., and Hack, R., 2004,*3D Terrestrial laser scanning as a new field measurement and monitoring technique.*Engineering Geology for Infrastructure Planning in Europe, Vol. 104, 179–189.
38. Maerz, N.H., Youssef, A.M., Otoo, J.N., Kassebaum, T.J., Duan, Y. 2012,*A simple method of measuring discontinuity orientations from terrestrial lidar images.* Submitted to the Journal of Environmental and Engineering Geoscience.

Rockfall Mitigation for Conversion of a Contractor's Access Road to a Permanent Low-Volume Roadway

Chris Ruppen
Michael Baker Jr., Inc.
Beaver, PA
724-495-4079
E-mail: cruppen@mbakercorp.com

Greg Garced
Michael Baker Jr., Inc.
Arlington, TX
817-987-4917
E-mail: ggarced@mbakercorp.com

Gang Zuo
Michael Baker Jr., Inc.
Moon Township, PA
412-269-6069
E-mail: gzuo@mbakercorp.com

Don Gaffney
Michael Baker Jr., Inc.
Moon Township, PA
412-269-2967
E-mail: cruppen@mbakercorp.com

Prepared for the 63rd Highway Geology Symposium, May 7-10, 2012

Acknowledgements

The authors would like to thank the cooperation and consent of the U.S. Army Corps of Engineers in allowing presentation of this paper.

The authors acknowledge the cooperation of the U.S. Department of Homeland Security's Customs and Border Protection (CBP) and U.S. Border Patrol (USBP), especially during field visits.

The authors acknowledge the support of Geobrugg AG and its U.S. representatives during analysis and design.

Disclaimer

Statements and views presented in this paper are strictly those of the author, and do not necessarily reflect positions held by their affiliations, the Highway Geology Symposium (HGS), or others acknowledged above. The mention of trade names for commercial products does not imply the approval or endorsement by HGS.

ABSTRACT

The A-1 roadway was first constructed as a contractor's access road during construction of the Border Fence across a stretch of mountainous terrain east of San Diego, CA, and west of Monument 250. At the end of construction it was decided that the contractor did not have to reclaim the road. Instead it should remain for use by Border Patrol. However, to minimize risk to vehicles, improvements would have to be made to address rock falls from the slopes above the road.

Field reconnaissance, slope characterization, rock fall modeling, and mitigation analyses led to recommendations for a variety of treatments depending on the slope height, slope angle, and primary character of slope material over the entire length of the roadway. More than 80 discrete slopes were identified and characterized along the eight-mile roadway. Options investigated included concrete barrier, fences of various heights, and draped mesh. Factors considered in analyses included roadway and shoulder widths, traffic volume, and cost-benefits for risk minimization. Selected slope areas outside of the rock-fall treatments are planned for re-vegetation management, and the two types of improvements had to be coordinated.

The project, set for construction in 2012, will provide cost-effective, improved safety for Border Patrol agents. This paper presents an overview of the investigations and analyses leading to selection of these rock-fall treatments.

INTRODUCTION

The U.S. Department of Homeland Security's U.S. Customs and Border Protection (CBP) and the U.S. Border Patrol (USBP), through the U.S. Army Corps of Engineers (USCOE), contracted for construction of a segment of the U.S./Mexico border fence known as the PF 225 A-1 Project along the U.S./Mexico International Boundary in San Diego County, California. This project is located within the San Ysidro Mountains and the Otay Mountain Wilderness. Beginning at Puebla Tree at the Western end and extending to Border Monument 250 at its Eastern end, the Project's border length is about 3.28 miles. The A-1 construction access road is about 5.8 miles in length.

At the conclusion of border fence construction, CBP, USBP and their partners determined that the contractor's construction access roadway could provide continued access to the border through this rugged terrain. However, since the roadway was not initially constructed for this purpose, they recognized the need to plan, develop and implement measures that would improve slope stability, agent/driver safety, and enhance the vegetation cover for a portion of the ground disturbed by construction of the A-1 construction road and primary fence at the International Boundary.

A Design Concept Feasibility Study & Report (DCFSR) was prepared by Baker and used by USCOE and CBP's Facilities Management and Engineering (FM&E) to obtain funding and provide general construction recommendations to implement slope and driver safety measures along with revegetation of portions of the site. This DCFSR was then further developed by more detailed analysis and requirements into a set of contract documents for rockfall mitigation and slope revegetation activities. Construction is planned to begin in the spring of 2012 on the resulting contract.

This paper addresses the development of rockfall mitigation recommendations only, and does not discuss revegetation as the areas for the two treatment types are mutually exclusive.

GEOLOGY AND SOILS

From the ***Preliminary Geologic Map of El Cajon 30' x 60' Quadrangle, Southern California*** surficial geologic conditions present at the project site are commonly mapped as mildly metamorphosed volcanic, volcanoclastic and sedimentary rocks of Late Jurassic to Early Cretaceous age. The ***Geologic Map of Otay Mesa 7.5 minute Quadrangle, San Diego County*** describes the metavolcanics and metasediments as the Santiago Peak Formation. Recently deposited materials are generally classified as alluvial sands, gravels and cobbles with some boulders within drainage features. Based on National Resources Conservation Service (NRCS) data for the project area, a thin soil veneer ranging from about 1.0 to 2.5 feet thick generally overlays crystalline bedrock.

These veneer soils are described in the ***Soil Survey of San Diego County, California*** as predominantly sandy silt (ML) with an AASHTO classification of A-4 and sandy to gravelly fat clay (CH) with an AASHTO classification of A-7. The overburden soils are generally not cemented to weakly cemented. It is expected that the clay (CH) will be moderately to highly expansive. The somewhat thicker soil within washes and drainage features is typically comprised of sandy gravel with cobbles and boulders (GP and GW) with an AASHTO classification of A-1.

SITE RECONNAISSANCE AND SLOPE CHARACTERIZATION

Primary site reconnaissance was performed on December 8 and 9, 2010. A confirmatory reconnaissance was performed on June 21, 2011. The observations were primarily for evaluating rockfall potential from the cut slopes above the existing roadway alignment, and were based on surficial evidence. Current digital topography was obtained and all cut slopes were documented photographically. No detailed measurements (e.g.; rock strike and dip) were made and evaluation of the stability of deeper failure surfaces in the cut slopes along the road was not investigated.

The general site conditions observed are summarized below by Road and Cut Slopes:

<u>Road</u>

- The existing road generally ranged from about 24 feet to 40 feet in width and appeared to be in good condition. No specific measurements of roadway widths were taken during the site visit.
- The road was generally constructed with a gravel surface course of unknown thickness and with occasional massive rock formations visible on the road surface.
- A drainage ditch, typically 2 feet to 3 feet wide, was constructed on the inside of the roadway and typically contained varying quantities of rock debris. Most of the debris was less than 6 inches in diameter, but there also were some boulders as large as three to four feet in diameter.
- Concrete barrier is being used successfully to mitigate rockfalls at some locations along the road

<u>Cut Slopes</u>

- Cut heights range from a few feet to more than 90 feet in height based on visual observations and measurements from the topographic mapping. No field measurements of embankment height were taken during the site visit.
- Cut slopes generally ranged from about 1H (Horizontal):1V (Vertical) to about 0.5H:1V with the majority of the critical slopes in the 0.75H:1V range.
- Over 80 discrete slopes were defined and photographed.
- Material observed in the exposed cut face was categorized as follows:

Category 1 – Massive rock, fractured rock, or rock with soil seams; with the major component of the material being rock, cobbles or boulders (see Photographs 1 and 2).

Photograph 1. Example of Category 1

Photograph 2. Example of Category 1

Category 2 – Soil or soil with gravel, cobbles and boulders; with the major component being fine grained material consisting of clay, sand or silt, or a combination thereof (see Photographs 3 and 4 below).

Photograph 3. Example of Category 2

Photograph 4. Example of Category 2

ROCKFALL MODELING AND MITIGATION ANALYSIS

During design concept feasibility assessment, the cut slopes were evaluated based on cut angle, cut height, slope material composition, estimated volume of unstable debris (rock material approximately 3" or greater), and debris at base of slope. Areas with no cut slopes and slopes appearing to have little to no potential for rock fall events were not considered. The other slopes were then rated as having moderate, high, or very high potential to experience rock fall events. Concrete barrier, rockfall fence, and draped mesh were determined to be conceptually feasible to mitigate rockfalls for slopes with these respective ratings.

During analysis for preparation of construction documents, this same basic approach was followed as the slopes were evaluated in more detail and the mitigation concepts were refined. The Colorado Rockfall Simulation Program (CRSP) was used to model and analyze the rockfall hazards from the existing cut slopes above the road. The CRSP program provides a statistical analysis of probable rock fall behavior at defined locations by simulating the behavior and trajectories of the rockfalls. These results can then be used to evaluate the type, size and locations of mitigation systems most appropriate to confine the rockfall debris.

The input to the CRSP software includes the slope geometry, rock density and block size along with Tangential Coefficient, Normal Coefficient and Surface Roughness design parameters. The initiation zone, the portion of the slope where the rocks are to begin their decent, is also input. Input parameters used in the analysis for the A-1 road project were approximated from photographs and site notes obtained during the site reconnaissance.

The model applies equations of gravitational acceleration and conservation of energy to describe the motion of the falling rock. Empirically derived functions relating velocity, friction, and material properties are used to model the dynamic interaction of the rock and slope. Experimental verification and calibration of CRSP on similar projects has been conducted by others by analyzing videotapes of rocks traveling down a slope.

The statistical variation among rockfalls is modeled by randomly varying the angle at which a rock impacts the slope within limits of surface roughness. The program provides an estimated distribution (more specifically, mean and standard deviation for a normal distribution) of bounce height and kinetic energy at various locations using the results of simulations. Based on the estimated distribution, it is possible to design a rockfall barrier that can stop a falling rock with a given level of confidence.

The following assumptions were used in CRSP modeling and analysis of project slopes:

- Natural slopes are stable. Rockfall initiates from the cut slope only. Conservatively consider the rockfall initiation zone is limited to the upper half of the cut slope.
- Cut slopes are modeled as either Category 1 – rock or Category 2 – soil, as described above. Only one slope category is analyzed in each model; i.e., the cut slope is NOT divided into different zones with different slope categories.
- Cut slopes are modeled as a straight line (constant slope) with a slope roughness of 0.75 ft.
- All rocks are assumed to be spherical. Three different diameters of rocks were considered in each combination of slope and cut height, one-foot, three-foot and four-foot. The one-foot rock has the highest bounce height, while the four-foot rock has the highest kinetic energy.

- The rockfall barrier was assumed to be three feet from the toe of slope, where the drainage ditch typically met the roadway. The geometric feature of the drainage ditch is ignored, since the shallow ditch tends to be filled with debris.

These assumptions allowed use of simplified models for CRSP analysis, instead of investigating each slope individually. As presented in Figure 1, the cross section in analysis was modeled by two straight lines, with one representing the cut slope and another representing the patrol road. The rockfall barrier location was the analysis point at which the bounce height and kinetic energy would be statistically calculated.

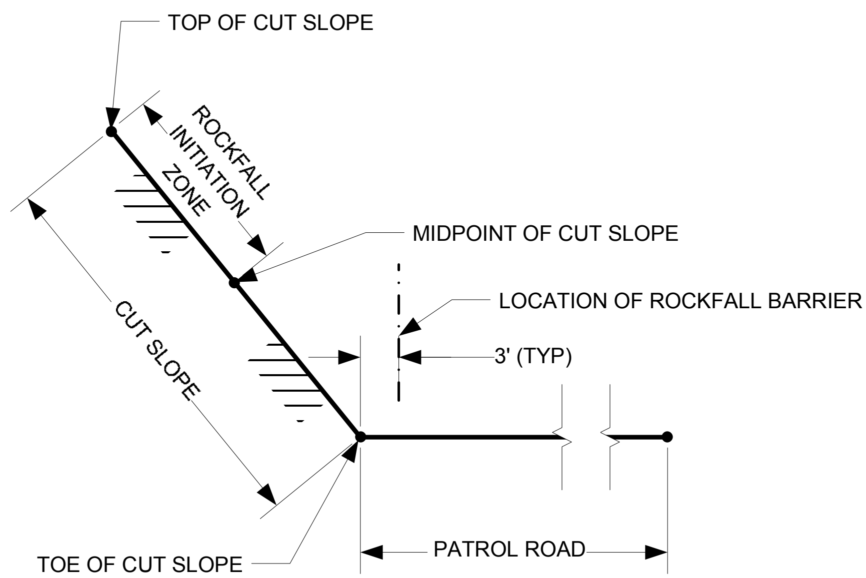

Figure 1. Simplified Cross Section for CRSP Analysis

Following parameters were used in CRSP models for this project:

Table 1. Parameters Used in CRSP

Slope Type	Tangential Coefficient	Normal Coefficient	Surface Roughness (feet)
Massive Rock	0.90	0.30	0.75
Soil (with gravel, cobbles and boulders)	0.80	0.20	0.75
Patrol Road	0.80	0.20	0.25

A parametric study was performed to obtain the distribution of bounce height and kinetic energy for different combinations of cut slope angle, height, and slope type that cover all the scenarios encountered for this project. For each combination, rockfall barrier options were assessed with target probabilities of less than or equal to ten percent for the rock to bounce over the barrier and for the kinetic energy of the rock to exceed the design rated energy of the barrier.

The probability with respect to kinetic energy was calculated using the average and standard deviation reported by CRSP. However, the probability of rock bounce height was determined directly from the histogram provided by CRSP after 1000 rock rolls, because an examination of the bounce height histograms indicate that the distribution of bounce height is highly skewed and the direct use of the average or geometric mean and standard deviation will yield an unreliable prediction.

Four different options were considered as rockfall barriers based on increasing severity:

1) Three-foot high concrete barrier
2) Five-foot high rockfall fence
3) Eight-foot high rockfall fence
4) Draped mesh

The following steps then were used in barrier type selection:

1. Compare barrier height with the bounce height, H_1, of 1-ft diameter rock with an occurrence less than 100 out of 1000 rolls:
   if $H_1 < 3$ ft, select concrete barrier;
   if 3 ft $\leq H_1 < 5$ ft, select 5- ft high rock fence;
   if 5 ft $\leq H_1 < 8$ ft, select 8- ft high rock fence;
   if $H_1 > 8$ ft, select draped mesh.

2. Compare barrier rated energy with the kinetic energy, E_1, above which the probability of occurrence is less than 10%. For the concrete barrier, compare rated energy with E_1 for a 3-ft diameter rock. For rockfall fences, compare rated energy with E_1 for a 4-ft diameter rock.
   For concrete barrier,
   if $E_1 \leq 30$ ft-tons (or 80 kJ), use of concrete barrier is confirmed;
   if $E_1 > 30$ ft-tons (or 80 kJ), a 5-ft rockfall fence is required.
   For 5-ft or 8-ft rockfall fence, compare E_1 with following rated energy, and select the lowest rated energy that meets the requirement:
   30 ft-tons (or 80 kJ),
   74 ft-tons (or 200 kJ),
   129 ft-tons (or 350 kJ),
   184 ft-tons (or 500 kJ),
   if $E_1 > 184$ ft-tons (or 500 kJ), change to draped mesh.

Table 2 summarizes the results of barrier type selection based on CRSP results and the above selection criteria for different combinations of cut slope angle, cut slope height and slope type.

Table 2. Selection of Barrier Type for Different Slope Types, Heights and Angles

		Rock Slope				**Soil Slope**								
		Cut Slope (H:1V)				Cut Slope (H:1V)								
		0.25	0.5	0.75	1	0.5	0.6	0.7	0.75	0.8	0.9	1	1.1	1.2
Cut Slope Height feet)	10	---	---	---	---	---	---	---	---	---	---	---	---	---
	20	---	K	K	---	---	---	---	---	K	K	K	---	K
	30	05-030	05-074	K	K	---	K	K	K	K	K	K	---	---
	40	---	08-074	05-074	---	---	---	K	K	K	---	K	---	---
	50	---	08-074	05-129	---	---	---	05-074	05-074	05-074	---	K	---	---
	60	---	D	08-129	---	---	---	---	05-129	05-129	---	---	---	---
	70	---	D	08-129	---	---	---	---	05-129	05-129	---	---	---	---
	80	---	D	08-184	---	---	---	---	08-129	05-129	---	---	---	---
	90	---	---	D	---	---	---	---	---	05-129	---	---	---	---

Notes:

1. K = Concrete Barrier.
2. XX-XXX = XX-foot Rockfall Fence with Rated Energy of XXX ft-tons.
3. D = Draped Mesh.

FINAL RECOMMENDATIONS AND CONSTRUCTION DOCUMENTS

Table 2 was used as the primary basis for selection of the barrier type for different reaches of the project. The cut type, height and angle of each individual cut slope on the project was tabulated and compared with the modeled results to identify the appropriate barrier type. This was "Step 1." "Step 2" was to evaluate the barrier selection in context. Table 3 is a partial sample of that table.

Context factors considered during barrier type selection include steepness of slope above the cut, surface irregularity of the cut, length of treatment, and adjacent treatments. For consistency, short lengths of weaker treatments adjacent to more robust treatments were replaced with the more robust treatment. For ease of construction, only one energy rating was specified, (184 ft-tons).

Table 3 was the basis for a tabular listing of rockfall treatments in the construction documents. Specifications, details, roadway profiles for rock fence areas, and general construction notes were also provided. The specifications and details were made compatible with available products from a variety of suppliers.

Table 3. Selection of Barrier Type for the Project

Station Limits		Approximate Embankment Geometry		Alternative Solutions				Slope Category		Combination Selection [1]				Barrier Selection (Step 1) [2][3]				Barrier Selection (Step 2)
Begin Station	End Station	Cut Height (feet)	Slope of Cut	Concrete Barrier	5-Ft Fence	8-Ft Fence	Draped Mesh			Category 1 (Rock Slope)		Category 2 (Soil Slope)		Category 1 (Rock Slope)		Category 2 (Soil Slope)		
22+50 RT	25+00 RT	23	0.87H : 1V	250				2				0.90-30	0.90-30			K	K	K
22+00 LT	26+00 LT	44	0.73H : 1V		400			1		0.75-50	0.75-50			05-129	05-129			5
26+00 LT	28+00 LT	17	1.23H : 1V	200				2				1.20-20	1.20-20			K	K	K
32+00 LT	34+50 LT	20	0.75H : 1V	250				1		0.75-20	0.75-20			K	K			K
63+00 LT	66+50 LT	30	0.64H : 1V		350			1		0.50-30	0.50-30			05-030	05-030			5
69+00 LT	70+50 LT	40	0.75H : 1V		150			1		0.75-40	0.75-40			05-074	05-074			5
70+50 LT	72+50 LT	20	0.75H : 1V	200				1		0.75-20	0.75-20			K	K			K
72+50 LT	76+00 LT	27	0.67H : 1V		350			1		0.50-30	0.50-30			05-030	05-030			5
76+00 LT	80+30 LT	37	0.75H : 1V		430			1		0.75-40	0.75-40			05-074	05-074			5
80+30 LT	80+70 LT	25	0.75H : 1V	40				1		0.75-30	0.75-30			K	K			K
80+70 LT	81+80 LT	20	0.75H : 1V	110				1		0.75-20	0.75-20			K	K			K
82+20 LT	83+70 LT	60	0.61H : 1V				150	1		0.50-60	0.50-60			D	D			D
83+70 LT	85+50 LT	50	0.5H : 1V			180		1		0.50-50	0.50-50			08-074	08-074			8
85+50 LT	85+90 LT	50	0.5H : 1V			40		1		0.50-50	0.50-50			08-074	08-074			8
85+90 LT	86+00 LT	74	0.57H : 1V				10	1		0.50-70	0.50-70			D	D			D
86+00 LT	92+80 LT	74	0.57H : 1V				680	1		0.50-70	0.50-70			D	D			D
92+80 LT	94+30 LT	25 - 30	0.75H : 1V	150				1		0.75-30	0.75-30			K	K			K
130+20 LT	131+00 LT	20	0.97H : 1V	80				2				1.00-20	1.00-20			K	K	K
134+00 LT	134+50 LT	40 - 45	0.9H : 1V				50	1		0.75-40	0.75-50			05-074	05-129			D[4]
134+50 LT	137+50 LT	45 - 80	0.6H : 1V				300	1		0.50-40	0.50-80			08-074	D			D
137+50 LT	138+50 LT	30 - 40	0.6H : 1V			100		1		0.50-30	0.50-40			05-030	08-074			8
138+50 LT	140+00 LT	30	0.6H : 1V		150			1		0.50-30	0.50-30			05-030	05-030			5
140+00 LT	144+00 LT	20 - 30	0.67H : 1V		400			1		0.50-20	0.50-30			K	05-030			5
145+50 RT	147+30 RT	20 - 35	0.65H : 1V			180		1		0.50-20	0.50-40			K	08-074			8
241+50 LT	242+50 LT	60 - 83	0.84H : 1V		100			2				0.80-60	0.80-90			05-129	05-129	5
242+50 LT	243+00 LT	25 - 50	1H : 1V	50				2				1.00-30	1.00-50			K	K	K
244+50 LT	245+00 LT	65	0.77H : 1V		50			2				0.75-70	0.75-70			05-129	05-129	5
245+00 LT	246+20 LT	65	0.77H : 1V			120		2				0.75-70	0.75-70			05-129	05-129	8[5]
246+20 LT	248+50 LT	65	0.77H : 1V		230			2				0.75-70	0.75-70			05-129	05-129	5
250+10 RT	252+00 RT	64	0.77H : 1V			190		1		0.75-70	0.75-70			08-129	08-129			8
253+40 RT	254+80 RT	20	0.75H : 1V	140				1		0.75-20	0.75-20			K	K			K
259+00 LT	260+00 RT	50 - 65	0.74H : 1V			100		1		0.75-50	0.75-70			05-129	08-129			8
260+00 RT	261+00 LT	40 - 50	0.74H : 1V		100			1		0.75-40	0.75-50			05-074	05-129			5
261+00 LT	262+00 LT	25 - 40	0.74H : 1V		100			1	2	0.75-30	0.75-40	0.75-30	0.75-40	K	05-074	K	K	5
262+00 LT	263+50 LT	20 - 25	0.74H : 1V	150				1	2	0.75-20	0.75-30	0.75-30	0.75-30	K	K	K	K	K
266+20 RT	268+50 RT	35	0.8H : 1V		230			1		0.75-40	0.75-40			05-074	05-074			5
272+30 LT	275+00 LT	20	0.75H : 1V	270				1		0.75-20	0.75-20			K	K			K
277+80 LT	282+00 LT	30	0.9H:1V	420				1		1.00-30	0.75-30			K	K			K

Notes:

1. The basis of barrier selection is the closest case (a combination of slope of cut and cut height) that was considered in CRSP analysis. The combination of slope of cut and cut height is given in the form of X.XX-XX. The number before "-" is the slope of cut in H:1V and the number after "-" is cut height in feet. For example, 0.75-50 means a 0.75H:1V slope with a cut height of 50 feet. Dual columns reflect range considered.
2. K = Concrete barrier; XX-XXX = XX-foot Rockfall Fence with Rated Energy of XXX ft-tons; D = Draped Mesh.
3. Select barrier type based on the summary table for CRSP analysis.
4. Short reach. Combine with the next reach.
5. Steep slope above cut.

CONCLUSIONS

This approach of using simplified modeling and statistics generated by CRSP was successfully applied to propose rockfall mitigation treatments that significantly improve the safety of the border patrol and other authorized users of this segment of roadway. It was a means of performing appropriate analyses covering many similar cut slopes without requiring analysis of each individual slope, resulting in a compressed design schedule and optimal use of government funds.

REFERENCES

Michael Baker Jr., Inc, 2011, *Design Concept Feasibility Study & Report for Site Stabilization, Re-vegetation, and Roadway Safety Improvements at the PF-225 A-1 Project Site*. Prepared for the Department of Homeland Security, Bureau of Customs and Border Protection, and the U.S. Army Corp of Engineers.

Todd, V.R., 2004, *Preliminary Geologic Map of El Cajon 30' x 60' Quadrangle, Southern California*, Open File Report 2004-1361, US Department of the Interior, US Geological Survey.

Tan, S. S. and Kennedy, M.P., 2002, *Geologic Map of Otay Mesa 7.5 minute Quadrangle, San Diego County, CA*, Department of Conservation, California Geological Survey.

National Resources Conservation Service, 2007, *Soil Survey of San Diego County, California*.

Andrew, R.D., Bartingale, R., and Hume, H, 2011, *Context Sensitive Rock Slope Design Solutions*, FHWA-CFL/TD-11-002

Pierson, L.A., Gullixson, C.F., and Chassie, R.G., 2001, *Rockfall Catchment Area Design Guide – Final Report*, FHWA-OR-RD-02-04

Rock Slope Catchment Ditch Effectiveness

An Assessment of Methods used for RHRS Scoring

Ethan Thomas
Vermont Agency of Transportation (Former VTrans Intern)
231 Montgomery Road
East Hardwick, VT 05836
(802) 472-3910

Thomas D. Eliassen, P.G.
Vermont Agency of Transportation
1 National Life Drive
Montpelier, VT 05633
(802) 828-6916
Tom.eliassen@state.vt.us

Prepared for the 63rd Highway Geology Symposium, May 7-10, 2012

Acknowledgements

The authors wish to express their gratitude to Christopher C. Benda, P.E., Vermont Agency of Transportation for his support of this work and to Michael Vierling, NY Thruway Authority, Peter Ingraham, P.E., Golder Associates and Brent Black, P.G., Landslide Technology, Inc for their critical review and welcomed comments. The pioneering work in rockfall evaluation by Arthur M. Ritchie and the participating States efforts in the pooled funded study Rockfall Catchment Area Design Guide cannot go unrecognized.

ABSTRACT

As a means of managing aging rock cuts, a number of states have developed Rockfall Hazard Rating Systems similar to that developed in the 1993 FHWA pooled funded study led by the state of Oregon. One of the parameters within those rating systems is Ditch Effectiveness. Ditch Effectiveness relates the ability of a ditch to retain fallen rock. Assignments of None, Limited, Moderate and Good are made and numeric values are chosen to represent the appropriate rating. In a review of other states RHRS reports, we have identified three existing methods for assigning these values. These methods include 1) Suggestive method - assigning a suggestive value, based on visual observations of the slope and ditch geometry, 2) Section Factor method - calculating a Section Factor whereby individual ditches are measured and compared to the ditch design of Ritchie and 3) RCAD method - comparing individual ditch geometries with design charts contained in the 2001 Oregon/FHWA pooled fund study Rockfall Catchment Area Design guide.

The Vermont Agency of Transportation proposes a fourth method, which involves taking detailed slope and ditch profiles and performing rockfall analyses to calculate a percentage of rocks retained in the catchment ditch. Percentage retained values are entered directly into a RHRS scoring system providing a more quantifiable way to characterize ditch effectiveness. As part of a VTrans periodic re-evaluation of their "A" ranked cuts, full length slope profiles and ditch geometries were measured, the information keyed into a rockfall computer simulation program and the resulting ditch effectiveness calculated. These results were compared to values generated using the Subjective, Section Factor, and RCAD methods.

INTRODUCTION

In 2011, the Vermont Agency of Transportation (VTrans) conducted a scheduled reevaluation of all RHRS "A" ranked rock slopes. During the initial RHRS study performed in 2007, VTrans had collected detailed profiles of all "A" rock slopes. It became apparent during the 2011 study that these detailed profiles (including ditch geometries) could be used in rockfall simulation programs to assist in estimating ditch effectiveness.

One key component of highway design is the roadside ditch. Ditches serve many purposes such as drainage, snow storage, recovery zones for errant vehicles and collection area for falling rock. One of the most efficient ways of mitigating rockfall hazards is the construction and use of properly designed catchment ditches. Catchment ditches are used to contain the debris from rockfalls as this prevents that debris from reaching the roadway, where it could cause damage to passing vehicles and/or risk of accident. Ditch effectiveness is one of the categories evaluated within the Preliminary Phase of most Rockfall Hazard Rating Systems (RHRS) and plays a vital role in determining the preliminary ranking for a rock slope. The effectiveness of a catchment ditch should be evaluated by qualified geotechnical engineers or geologists specializing in rock slope hazards/mitigation. Ditch effectiveness can also be empirically estimated from equations and charts found in published studies and evaluated semi-quantitatively by the use of rockfall simulation computer programs.

When using semi-quantitative values for determining ditch effectiveness, one needs to estimate the percentage of rocks, from a rockfall context, that reach the roadway or the amount of rock retained (percent retained) within the ditch and establish a range of values that can be used to determine what is "Good", "Moderate"," Limited", or " Poor" catchment. In many cases, it may not be possible to design a catchment ditch that would retain 100% of a rockfall due to right-of-way considerations or costly design constraints. Many State Departments of Transportation (DOT's) use either subjective (visual) methods to estimate ditch effectiveness or empirically derived methods such as Section Factor or the Oregon Rockfall Catchment Area Design Chart (RCAD) methods. It is important to note that Section Factor values, (which are based on Ritchie Design Criteria), and the RCAD charts, were created to be used as design charts for rock-slope construction. However, it is possible to use these charts to estimate the amount of rock that might be retained within a ditch (Ditch Effectiveness).

VTrans evaluated estimated ditch effectiveness by all three methods as well as a fourth method, a semi-quantitative method whereby actual ditch geometries and slope profiles were input into the rockfall analysis computer program RocFall, developed by Rocscience Inc. of Toronto, Canada. The percentage of rocks retained in the ditch was used to define "Good", "Moderate", "Limited", and "Poor" ditch effectiveness.

SLOPE PROFILES

In order to measure an accurate profile for each "A" ranked rock slope, numerous points on the rock face were measured using a Laser Technology Inc. Impulse 200 LR laser rangefinder with Slope Profiling software. The number of points recorded for each slope evaluated as part of this study ranged from about 20 to 80. The more points that are recorded, the more accurate the slope profile. Some of Vermont's rock slopes have excessive vegetation on them, making it difficult to obtain an accurate slope profile. When vegetation was too thick to take an accurate slope profile, profiling was postponed until the fall season when the foliage is sparser. Profiles were taken where the slope was highest or showed evidence of overhangs or where there was evidence of past rockfalls.

DITCH MEASUREMENTS

The geometry of the ditches at each "A" ranked rock slope was also measured. A section of ditch geometry was generated by measuring the ditch width, starting at the edge of pavement to the toe of the slope, and the ditch depth at each 1 foot increment. Excess vegetation in the ditches was cut down to assure accurate depth measurement. A cord line was marked in 1 ft increments and laid perpendicular to the roadway and rock slope face. The cord was fitted with a line level to assure measurements were referenced to a horizontal datum. The depth of the ditch was measured at each 1 foot increment and recorded in the field notebook (Figure 1). Because ditch geometries can vary across the length of a rock cut, measurements were taken at a location representative of the overall slope and ditch geometry and ideally where the slope profile was taken.

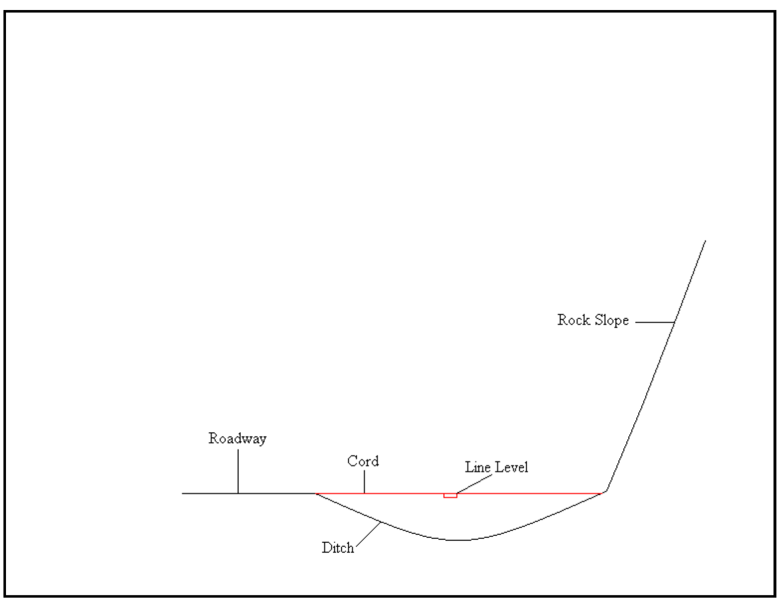

Figure 1: Diagram depicting basic setup of ditch measurement procedure.

SUBJECTIVE DITCH EFFECTIVENESS

RHRS scores from VTrans' 2007 RHRS study (Eliassen, T. D., and Springston, 2007) were assigned based on visual observations of ditch width, depth, shape and other properties that would have a bearing on the ability of each ditch to contain falling rocks. Effectiveness was assigned scores as follows:

- GOOD = RHR score 3 – Most rockfall occurrences expected to be contained in ditch. Ditch width and depth generally appear greater than expected rock block(s) size and volume.
- MODERATE = RHR score 9 – Ditch expected to contain rockfalls of moderate volume, but height, shape or size of rock materials raise concern for transport into roadway.
- LIMITED = RHR score 27 – Limited ditches appear to be inadequate in containing rockfalls.
- NONE = RHR score 81 – Either the toe of the rock cut is immediately adjacent to the roadway or there is a narrow flat ground surface at the toe of the cut or the ground surface slopes up from the roadway to the toe of cut.

The results of this subjective approach are shown below in Figure 2. Forty-seven ditches were rated as having "Good" ditch effectiveness, thirty-four were rated as having "Limited" ditch effectiveness, twenty-two were rated as having "Moderate" ditch effectiveness, and seven were rated as having "None" ditch effectiveness.

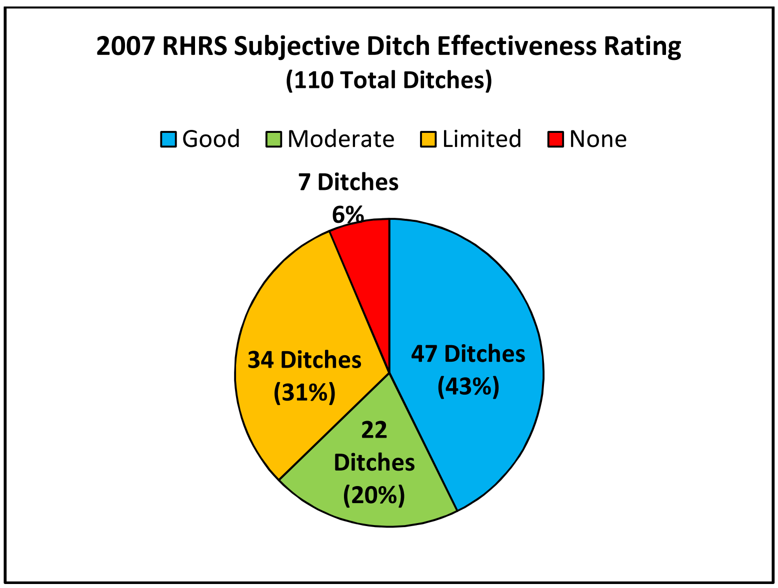

Figure 2: Results of Subjective Ditch Effectiveness Rating from 2007 RHRS

SECTION FACTORS

Section Factors (SF) were originally used by the New York State Department of Transportation (NYSDOT). SF's are a comparison of the ratio between the required dimensions based upon Ritchie Ditch Criteria (Ritchie 1963) and the actual ditch dimensions at the site.

The SF numerical value is calculated as follows:

SF = (DR + WR)/(DA+WA); where
DR = ditch depth in feet from Ritchie graph,
WR = ditch width in feet from Ritchie graph,
DA = actual ditch depth in feet, from field measurements, and
WA = actual ditch width in feet, measured from toe of the slope to the edge of pavement.

This numerical value can range from 1 or less in the best circumstances, to 11 in the worst circumstances. For the purposes of this study, we have defined ditch effectiveness performance (good, moderate, limited and poor) with corresponding SF value ranges:

- Good, SF = 0.00 – 1.00
- Moderate, SF = 1.01 – 2.00
- Limited, SF = 2.01 – 3.00
- Poor, SF = 3.01 – 11.00

The New York DOT Rock Slope Rating Procedure states that ditch geometry meeting the Ritchie criteria will reduce the number of rocks escaping the catchment area to a maximum of 15 percent (NYDOT *Rock Slope Rating Procedure: Geotechnical Engineering Manual No. 15*). This means that ditches with SF values of 1 should retain at least 85% of rockfalls, ditches with SF values of less than 1 should retain greater than 85% of rockfalls, and ditches with SF values greater than 1 are expected to retain less than 85% of rockfalls.

The Ritchie Design Criteria were created by Arthur M. Ritchie, Chief Geologist with the Washington State Department of Highways, in 1963. His study was the first attempt at measuring rockfall behavior on highway slopes. He simulated rockfall events by rolling rocks down a slope and measuring their impact distances and rollout distances. Ritchie drew several important conclusions from his study, including the following:

1. A rock's mode of travel down a slope, regardless of its size or shape, is a function of the slope's angle (Figure 3).
2. On steeper slopes, a rocks initial motion is rolling and this quickly changes to bouncing and even free fall, depending on the slope angle.
3. Rocks that are in free fall seldom have a high bounce height after impact.

In addition to these findings, Ritchie prepared an empirical design table of recommended minimum rock catchment width and depth, based on slope height and angle. This table was later adapted into a design chart (refer to Figure 7) in the FHWA publication "Rock Slopes: Design, Excavation, Stabilization" (*FHWA 1989*).

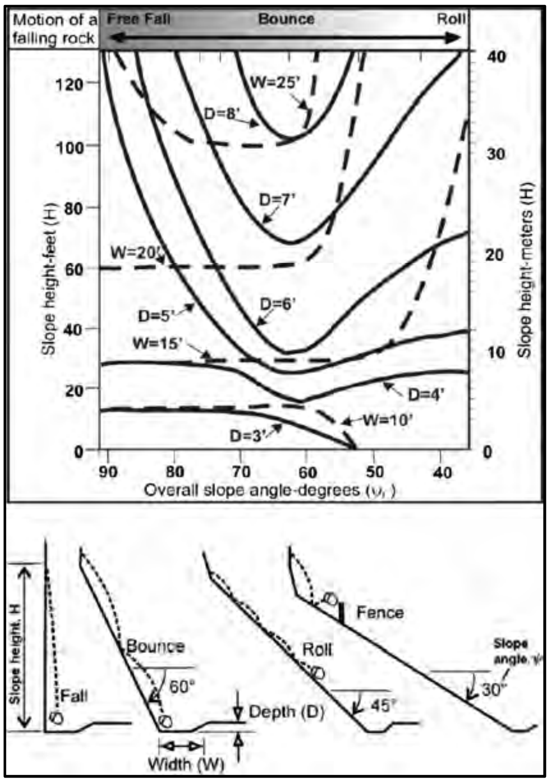

Figure 3: Ritchie's Rockfall Catchment Ditch Design Chart (FHWA 1989). All one needs to know to calculate proper catchment ditch width and depth is the overall slope angle and the slope height.

There are limitations with using Section Factors based on Ritchie Ditch criteria to evaluate ditch effectiveness. Section Factors rely heavily on the use of the Ritchie Design Chart. The ditches used to compile this chart were deep, flat-bottomed and had a steep 1V:1.25H fore slope (slope from the edge of roadway to the base of ditch). Ditches with such deep and steep fore slopes do not meet current American Association of State Highway and Transportation Officials (AASHTO) roadside clear zone safety requirements and may not drain properly. The AASHTO Roadside Design Guide states:

"*Embankment slopes between 1V:3H and 1V:4H may be considered traversable but non-recoverable if they are smooth and free of fixed objects. A clear run-out area is the area at the toe of a non-recoverable slope available for safe use by errant vehicles.* ***Slopes steeper than 1V:3H are not considered traversable and are not considered part of the clear zone***"

Also, the Ritchie criteria do not take into account massive rockfalls. A large volume rockfall could overwhelm a ditch that meets or exceeds the Ritchie criteria. The rock slopes studied by Ritchie were “rough” production blasted quarry, natural, and roadway slopes with numerous launch features (irregularities on the slope that could redirect falling rock toward the roadway). Today’s rock slopes are generally smoother due to controlled blasting techniques that produce fewer irregularities on the slope that can act as launch features.

The Ritchie Design Charts do not go above 130 ft for slope height and because of this six ditches could not be evaluated. These ditches were assigned the maximum score of 11.00 because it was assumed that the higher the slope, the wider and deeper a ditch would have to be to contain a rockfall.

The results of the SF evaluation are shown below in Figure 4. Fifty-four ditches were rated as having “Moderate” ditch effectiveness, twenty-three were rated as having “Good” ditch effectiveness, seventeen were rated as having “Limited’ ditch effectiveness, and thirteen were rated as having “Poor” ditch effectiveness.

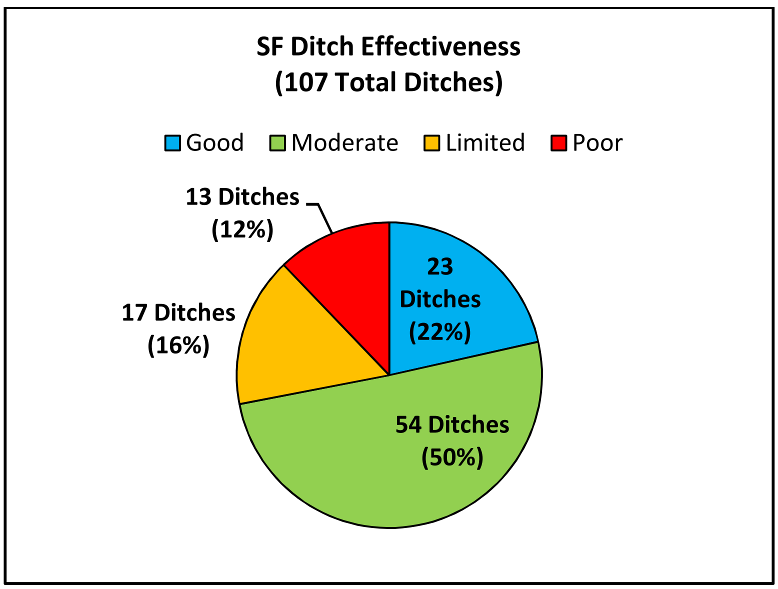

Figure 4: Results of Section Factor Ditch Effectiveness Analysis

ROCKFALL CATCHMENT AREA DESIGN CHARTS (RCAD)

The Rockfall Catchment Area Design Charts were created by the Oregon Department of Transportation (Pierson et al. 2001) as part of an FHWA pooled fund study. These design charts are the result of an extensive research project undertaken by the Oregon DOT. The project consisted of rolling more than 11,250 basalt boulders over quarry slopes of heights ranging from 40ft - 80ft and slope angles of vertical, 0.25H:1V, 0.5H:1V, 0.75H:1V, and 1H:1V. At least 250 rocks were rolled for each slope arrangement.

The RCAD charts provide quick and easy assessment of the effectiveness of a ditch by showing the expected percent retained of rock within that ditch based on rock slope height, rock slope angle and ditch slope angle (Figure 5).

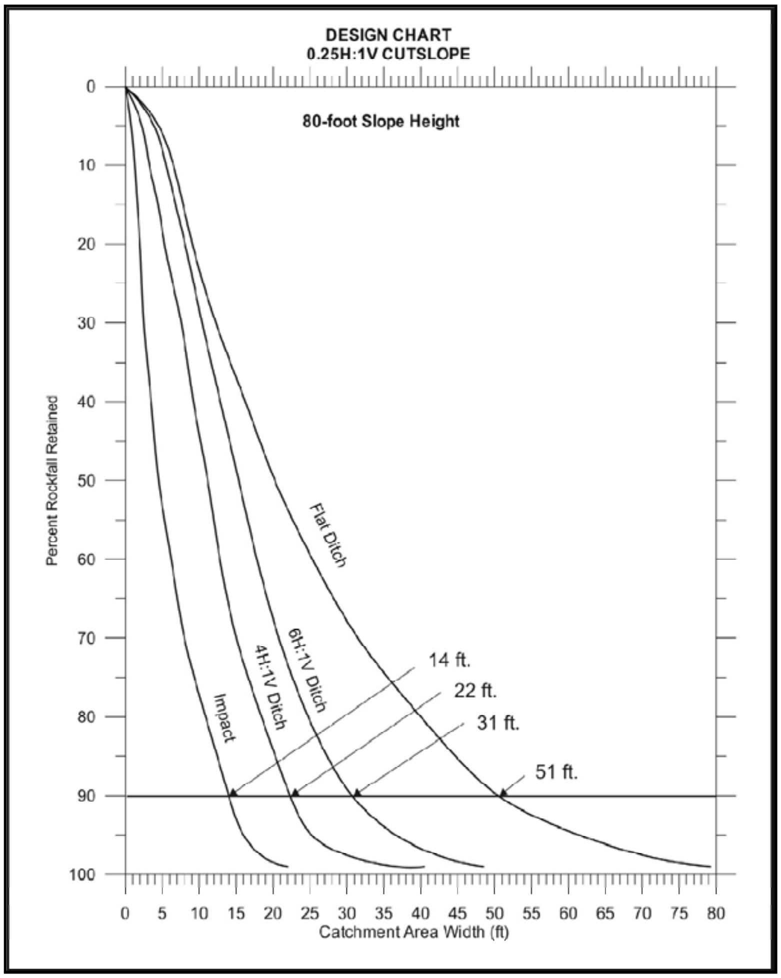

Figure 5: Example of RCAD chart for 80-foot 0:25H:1V cut slope.

The following criteria were used to assign a RHR Score for ditches that were evaluated with the RCAD charts:

- Good, 85% - 100% of rock was retained within the ditch. RHR score of 3.
- Moderate, 70% - 84% of rock was retained within the ditch. RHR score of 9.
- Limited, 30% - 69% of rock was retained within the ditch. RHR score of 27.
- Poor, 0% - 29% of rock was retained within the ditch. RHR score of 81.

The primary rock type tested was hard durable basalt that rebounds and rolls well after impact. Softer, less competent rock is expected to have smaller rebound values and shorter roll out distances. Another factor to consider is that not all rockfalls originate at the top of a rock cut, as was tested in the RCAD project. The results indicate that rocks that initiate from points below the maximum height of the cut may not need the entire catchment area width to achieve the same level of containment. The RCAD charts were made for slope heights between 40 ft – 80 ft. Extrapolation of the charts is possible for heights that fall below or exceed the height limits; however extrapolation should be performed with caution. Also, the quarry walls that the tests were conducted on were relatively smooth (although there were some narrow steps on the slopes resulting from drilling each lift). RCAD does not take into account launching features on a slope.

The results of the RCAD analyses are shown below as Figure 6. Thirty ditches were rated as having “Good’ ditch effectiveness, nineteen were rated as having “Limited” ditch effectiveness, sixteen ditches were rated as having “Moderate” ditch effectiveness, and five were rated as having “Poor” ditch effectiveness.

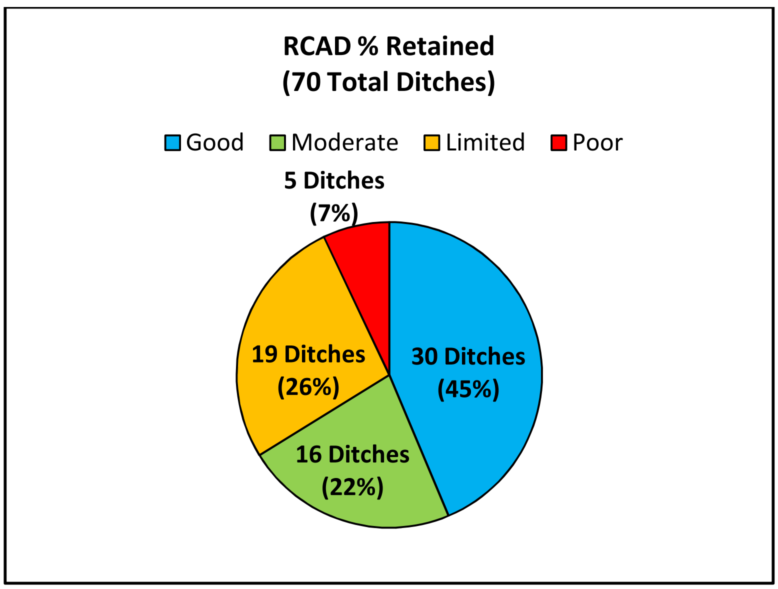

Figure 6: Results of the RCAD Ditch Effectiveness Analysis

ROCKFALL SIMULATION

A wide variety of rockfall computer simulation programs currently exist. Commonly used 2-D programs include the Colorado Rockfall Simulation Program (CRSP) initially developed by the Colorado Department of Highways and RocFall by Rocscience Inc. of Toronto, Canada. These programs were developed to provide a statistical analysis of probable rockfall behavior and to aid in the design of rockfall mitigation. Both programs use numerical input values assigned to slope and rock properties to simulate rockfall behavior. Empirically derived functions relating velocity, friction, and material properties are used to simulate the dynamic interaction of the rock and slope. The programs provide estimates of probable velocity, energy and bounce height at various locations on a slope.

Rockfall simulation was utilized during this study in developing ditch effectiveness criteria. Rock slope profiles generated in the field using the Laser Technology Slope Profiling equipment and software and ditch geometries measured in the field were collected, recorded in comma delimited format (file extension .csv) and imported into the program RocFall by Rocscience Inc. of Toronto, Canada to evaluate the ability of catchment ditches to retain fallen rocks.

The following steps were followed for each slope:

- Slope geometries were introduced to each simulation based on measured slope profiles and ditch geometries. Then, segments of each slope were assigned properties for specific materials which make up the slope. RocFall has assigned the following materials; Asphalt, Bedrock Outcrops, Clean Hard Bedrock, Soil with Vegitation, Talus Covered and Talus with Vegetation. The program provides corresponding values of slope roughness, friction angle and coefficients of normal and tangential restitution for these materials. For this study, *Asphalt* was assigned for the roadway, *Soil with Vegetation* for ditches and *Clean Hard Bedrock* for the rock slope faces.

- Initial starting points for falling rocks were selected by selecting line seeders within the program. Line seeders represent multiple locations where rock particles fall from the slope. Starting points were distributed randomly along the entire slope face. Initial horizontal and vertical velocities for each rock were set to the value of 0 (rock is at rest and upon running the simulation the rock is set in motion by the effects of gravity). A rock mass was also chosen. For this study, rock blocks with a unit weight of 170 lbs/ft^3 and measuring 3' by 3' by 3' were used (total mass of 2,750 lbs). The dimensions referenced were used only to calculate total mass. RocFall does consider cubical shaped rock in its computations.

- Next, the project settings were defined. A total of 100 rocks were chosen for each simulation using a scaling factor for Rn (coefficient of normal restitution) based on the velocities of each falling rock. The RocFall default value for the constant K=30 ft/sec. was used. A discussion of the determination of input parameters for use in the RocFall program is available in the tutorial (http://www.rocscience.com/downloads/rocfall/webhelp/pdf_files/tutorials/RF_adv_tutorial_1.pdf) available through the Rocscience web site.

- After each rockfall simulation, the distribution of rockfall endpoints (where rocks stopped rolling and came to rest) was evaluated and a percentage of rocks running out of the ditch and passing the edge of the roadway (closest to the slope) were noted.

Figure 7 shows a graphical representation of one of the slopes evaluated during this study. The red lines represent simulated paths individual rocks followed.

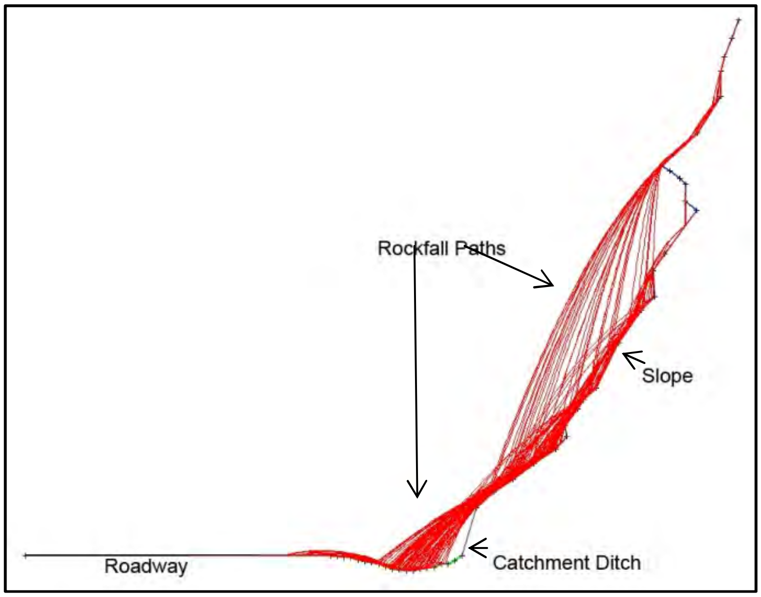

Figure 7: Graphical representation of a completed rockfall simulation analysis

Limitations and considerations when using RocFall to evaluate the ditch effectiveness include:

- RocFall does not simulate massive rockfall events; instead it simulates the trajectory of a single rock.
- The trajectory of a falling rock is highly reliant on the accuracy of the slope profile.
- RocFall does not compensate for vegetation on a slope face; all rocks were rolled down "clean bedrock". Vegetation on a slope is assumed to impede and lower the rock masses' kinetic energy during failure. Therefore, the "clean bedrock" that the rock was rolled down may represent a worst case scenario.

Percent Retained values were determined from the Rockfall Analysis for each ditch at each "A" ranked rock slope and the following ratings were assigned:

- Good, 85% - 100% of rock was retained within the ditch.
- Moderate, 70% - 84% of rock was retained within the ditch.
- Limited, 30% - 69% of rock was retained within the ditch.
- Poor, 0% - 290% of rock was retained within the ditch.

RHR Scores for the ditches were determined based on the following calculation:

RHR Score for Ditch Effectiveness = 100 - Rockfall % Retained Value

An explanation of why the Ditch Effectiveness RHR Score was calculated this way is discussed in the Results Section.

It is recommended that an experienced rock slope engineer/geologist make the determinations for the many variables that RocFall can simulate.

The results of the Rockfall Analysis are shown below in Figure 8. Rockfall rated fifty-two ditches as having “Good” ditch effectiveness, thirty-two as having “Limited” ditch effectiveness, thirteen as having “Moderate” ditch effectiveness, and twelve as having “Poor” ditch effectiveness.

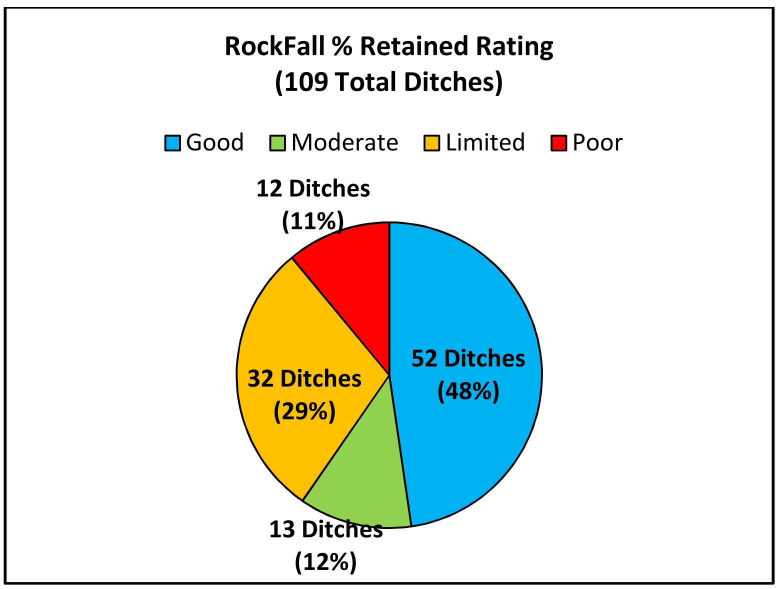

Figure 8: Results of the Rockfall Ditch Effectiveness Analysis

RESULTS OF DITCH EFFECTIVENESS COMPARISON

ROCKFALL vs. 2007 SUBJECTIVE METHOD

Fifty percent (55/110 total ditches) of the ditches evaluated with the subjective methods in 2007 matched favorably with the Rockfall analysis. Out of the remaining fifty-five ditches that did not match the Rockfall analysis ratings, 23% (25 ditches) were assigned better ditch effectiveness ratings than what the Rockfall analysis shows. 27% (30 ditches) were assigned worse ditch effectiveness ratings than what the Rockfall analysis shows. Fifteen ditches were evaluated as

“Moderate”, while the Rockfall analysis gives a rating of “Good”. Five ditches were evaluated as “Good”, while the Rockfall analysis gives a rating of “moderate”.

ROCKFALL vs. SECTION FACTORS

Fifty percent (54/107 total ditches) of the ditches evaluated with Section Factors match favorably with the Rockfall analysis. Out of the remaining fifty-three ditches that did not match the Rockfall analysis ratings, 15% (16 ditches) were assigned better ditch effectiveness ratings than what the Rockfall analysis shows. 34% (37 ditches) were assigned lower ditch effectiveness ratings than what the Rockfall analysis estimated.

It is interesting to note that out of all one-hundred and twenty five total ditches measured in the field, only one ditch (# 105, Montpelier) met the Ritchie Depth requirement. This suggests that Vermont’s ditches were not designed using Ritchie Criteria. It is also interesting to note that the only reason ditches received section factors of 1 and less than 1 was because the widths for these ditches were great enough to compensate for the lack of the required Ritchie Depth.

ROCKFALL vs. RCAD

Out of the seventy total ditches evaluated with the RCAD charts, 40% (28 ditches) matched the ratings assigned by the Rockfall analysis. Out of the forty-two remaining ditches that did not meet the Rockfall analysis ratings, 34% (24 ditches) were rated by RCAD as having better ditch effectiveness ratings than the Rockfall analysis estimates. Twenty-six percent (18 ditches) were rated by RCAD as having lower ditch effectiveness ratings than estimated by Rockfall analyses shows. One possible reason the RCAD study identified more ditches with better ditch effectiveness ratings is the lack of the ability to simulate launch features on slopes.

DITCH EFFECTIVENESS CONCLUSIONS

The following list shows the limitations and considerations associated with each ditch effectiveness rating procedure:

Subjective Method:

- Ditch Effectiveness is measured based on the field inspector’s observations of ditch geometry, rock slope angle, and rock slope height. Different inspectors of the same site may rate a ditch as having different ditch effectiveness – ditch effectiveness is based on rater’s experience and can be subjective.
- It is often difficult to determine the difference between “Good” ditch effectiveness and “Moderate” ditch effectiveness, and between “Moderate” ditch effectiveness and “Limited ditch effectiveness”.

Section Factors:

- Design charts used to calculate SF value are based on the Ritchie Study which used deep, flat-bottomed, steep 1V:1.25H fore sloped ditches. These types of ditches do not meet current AASHTO roadside clear zone safety requirements.
- Ritchie Design Charts do not exceed heights greater than 130 ft.
- Original Ritchie Study used "rough" production blasted slopes with numerous launch features. This can lead to overly conservative results.

RCAD:

- The design charts were made for slopes ranging from 40 ft – 80 ft. Extrapolation for heights below and above this range is possible but may result in less accurate assessments of risks.
- The RCAD study initiated rockfalls from the top of the rock slope. In reality, not all rockfalls originate from the top of slopes. Rocks that initiate from points below the maximum height of the cut may not need the entire catchment area width to achieve the same level of containment.
- The slopes used in the study lacked large launch features (although small steps left from drilling different lifts are present), - RCAD does not account for launching features on the slope.
- The rocks tested in the RCAD study were hard, durable basalt, softer rocks are expected to have shorter roll out distances and lower rebound heights.

Rockfall Analysis:

- The trajectory of the rock mass is only as accurate as the slope profile, algorithm and ditch profiles that are put into the simulation – vegetation on slope and in ditch may lead to inaccurate slope profiles and ditch profiles and therefore, create inaccurate ditch effectiveness ratings.
- Adjustments to the simulation for material properties allow the simulation to be calibrated for local geologic conditions.

A limitation associated with Section Factors, RCAD, and the Rockfall Analysis is that these methods do not consider massive rockfall events. A large volume of rock could overwhelm a ditch that has been rated as having "Good" ditch effectiveness. Only the Subjective Method takes this into account.

CONCLUSIONS

Based on the comparison of four ditch effectiveness rating procedures and their limitations, the authors believe that rockfall simulation provides an equally appropriate and reasonably accurate method to determine the RHR ditch score. The author's believe that, provided accurate slope profiles are used, rockfall simulation programs do a very good job of accurately simulating the path a falling rock will take down each slope. It is imperative that the most accurate slope profiles and most representative ditch geometries be obtained and proper rock property variables be chosen for each simulated rockfall, and that calibration field tests are performed whenever possible.

The author's recommend using the full range of percent passing values for the RHR score to allow for more accurate evaluations of a ditches' effectiveness where 100 points would represent no rocks were retained within the ditch while a score of 0 points would represent 100% retention within the ditch.

In FHWA SA-93-057 (Rockfall Hazard Rating System Participant's Manual), under 4.3 Scoring System, it is stated:

> "*When rating a slope, using the full range of points instead of only the set points listed above each column allows the rater greater flexibility in evaluating the relative impact of conditions that are extremely variable.* ***Continuing to use only the set points, however, is not an optimal use of the system, and is not recommended.***"

Vegetation on the slope limits the accuracy of the measured slope profile. Therefore, when possible, slope profiles should be taken in the fall when live vegetation is scarce. If there is some vegetation on the slope, it is up to the field inspector to decide to measure the profile or not. If the profile is measured, care should be taken to avoid tree limbs/grass/leaves that may distort the profile. Slope profile data, when returned to the office should be edited by the person who measured the profile as soon as possible, so that erroneous points caused by vegetation interference can be addressed.

It is important to reiterate that the Ritchie Catchment Ditch Design Charts and the RCAD charts were created to provide guidance on the adequate width and depth requirements for a catchment ditch design. They are excellent tools to use in this sense. They are also quite valuable in estimating ditch effectiveness, however as VTrans has learned, rockfall simulation using actual measured ditch and slope geometries can provide meaningful estimates of ditch effectiveness as well.

The Preliminary Survey used in the 2007 RHRS was based on subjective measures. It may be possible to use the Rockfall method of rating ditch effectiveness in the Preliminary Survey to assist in determining the overall rating of the slope. However, due to the sheer number of rock slopes that would need to be evaluated (3500+ rock slopes in Vermont's case); taking all of these measurements would be time consuming and therefore prohibitive. Perhaps future advances in slope profiling technology may allow for the cost effective profiling of all slopes.

The use of new technology will further the accuracy and efficiency of the RHRS. The use of LIDAR to evaluate discontinuities within a rock mass, measure slope profiles, and measure ditch geometries (2D and 3D) will greatly improve the assessment of the geologic score and ditch effectiveness in the future (Kemeny and Turner, 2008). Further advances in understanding the effect of vegetation on rockfalls and the incorporation of vegetation in computer-based rockfall simulations will create rockfall simulations that more accurately simulate natural behavior.

REFERENCES

Davis, Jesse W., and Shakoor, Abdul, *Evaluation of the Effectiveness of Catchment Ditches Along Ohio Roadways*. In Transportation Research Record: Journal of the Transportation Research Board, Geology and Properties of Earth Materials 2005, p. 196-204.

Drumm, E. C., M. Mauldon, W. M. Dunne, V. C. Bateman, and B. McCarter. *Rockfall Management System for Tennessee: Final Report—Phase II*. Tennessee Department of Transportation, Nashville, 2005. www.tdot.state.tn.us/longrange/reports/res1189.pdf.

Eliassen, T. D., and Springston, G. E., *Rockfall Hazard Rating of Rock Cuts on U.S. and State Highways in Vermont,* Research Project RSCH010-974, 2007, 31 p.

Federal Highway Administration; 1989; *Rock Slopes: Design, Excavation, Stabilization*; Publication No. FHWA-TS-89-045; Turner-Fairbank Highway Research Center; McLean VA.

Fish, Marc and Lane, Richard, *GIS and the New Hampshire Rock Cut Management System*. FHWA-NH-RD-12323V, New Hampshire Department of Transportation Bureau of Materials and Research, June 2002.

Geotechnical Engineering Bureau. *Rock Slope Rating Procedure, Geotechnical Engineering Manual GEM-15, Revision No.1*. New York Department of Transportation, April 2007.

Hopkins, Tommy C., Beckman, Tony L., Sun, Liecheng, Butcher, Barry, *Highway Rock Slope Management Program,* Research Report KTC-03-06/SPR-177-98-1F, Kentucky Transportation Center, College of Engineering, University of Kentucky. February 2003.

Hoppe, Edward J., and Whitehouse, Derek H., *Implementation of the Rock Slope Management Project at the Virginia Department of Transportation,* Report No. VTRC 06-R23, Virginia Transportation Research Council, June 2006.

Huang, Scott L., Darrow, Margaret M., and Calvin, Peter,. *Unstable Slope Management Program: Background Research and Program Inception Phase I Final Report*, Alaska State Department of Transportation, 2009.

Kemeny, J. and K. Turner. 2008. *Ground-Based LiDAR: Rock Slope Mapping and Assessment,* Report: FHWA-CFL/TD-08-006, Federal Highway Administration Central Federal Lands Highway Division, Lakewood, CO.

Maerz, N.H.; Youssef, A.; Fennessey, T.W.; 2005. *New Risk-Consequence Rockfall Hazard Rating System For Missouri Highways Using Digital Image Analysis,* Environmental & Engineering Geoscience*,* Vol. XI, no. 3, pp. 229-249.

Pack, Robert T., Boie, Ken, *Utah Rockfall Hazards Inventory Phase I*, Report No. UT – 03.01, Utah State University, Department of Civil and Environmental Engineering, April 2002.

Pack, Robert T., Boie, Ken, Mather, Stoney, Farrell, Jamie, *Udot Rockfall Hazard Rating System: Final Report and User's Manual*, Report No. UT – 06.07, Utah State University, Department of Civil and Environmental Engineering, January 2006.

Pierson, L.A., Davis, S.A., and Van Vickle, R. *Rockfall Hazard Rating System Participant's Manual*. FHWA, U.S. Department of Transportation, November 1993.

Pierson, L. A., F. G. Gullixson, and R. G. Chassie. *Rockfall Catchment Area Design Guide: Final Report SPR-3(032),* FHWA-OR-RD-02-04. Oregon Department of Transportation , January 2002.

Pierson, Lawrence A., Beckstrand, Darren L., Black, Brent A., *Rockfall Hazard Classification and Mitigation System,* FHWA/MT-05-011/8176, Landslide Technology for Montana Department of Transportation, September 2005.

Pierson, L. A., C. F. Gullixson, and R. G. Chassie. *Rockfall Catchment Area Design Guide, Final Report SPR-3(032),* Oregon Department of Transportation-Research Group; FHWA, U.S. Department of Transportation, 2001.

Ritchie, A. M. *Evaluation of Rockfall and Its Control*. In Highway Research Record 17, HRB, National Research Council, Washington, D.C., 1963, pp. 13-28.

Rocscience Inc., *RocFall Program*, http://www.rocscience.com/products/12/RocFall

Russell C. P., Santi, P., Humphrey, J. D., *Modification and Statistical Analysis of the Colorado Rockfall Hazard Rating System*. Colorado School of Mines, Golden.

Case Study: West Virginia US Highway 19 "The Narrows" Rockfall Mitigation

William F. Kane, PhD, PG, PE
President and Principal Engineer
KANE GeoTech, Inc.
7400 Shoreline Drive, Suite 6
Stockton, California 95219
209-472-1822
william.kane@kanegeotech.com

Frank Amend, PE
Regional Manager, Southeastern USA
Geobrugg North America, LLC
PO Box 7453
Rocky Mount, North Carolina 27804
252-937-3552
frank.amend@geobrugg.com

Prepared for the 63rd Highway Geology Symposium, May 7-10, 2012

Acknowledgments

The authors would like to thank Bob Forbes and Roger Moore of Ameritech Slope Constructors, Asheville, North Carolina for their excellent work on this project. Their attention to detail and quality of construction were greatly appreciated. We would also like to thank Doug Gould of the West Virginia Department of Transportation whose vision and understanding made this project so successful.

Disclaimer

Statements and views presented in this paper are strictly those of the author, and do not necessarily reflect positions held by their affiliations, the Highway Geology Symposium (HGS), or others acknowledged above. The mention of trade names for commercial products does not imply the approval or endorsement by HGS.

ABSTRACT

U.S. Highway 19 connects the city of Weston, West Virginia to neighboring counties. Along one cut-slope in Weston, there was little catchment along the highway and rockfall was a hazardous problem. KANE GeoTech, Inc., Geobrugg North America, LLC, and the West Virginia Department of Transportation worked together to develop rockfall mitigation system relying on new materials and technologies.

The cut slope was approximately 900-ft long with vertical slope heights varying from approximately 20-ft to 65-ft. The upper slope was composed of a 20-ft thick massive sandstone bed. Directly underneath the sandstone was a 35-foot thick layer of black to brown shale with coal seams and lenses. Just beneath the shale layer was a 5-ft section of massive sandstone. Massive rockfall was due to relatively large joint spacing in the sandstone combined with rapid weathering of the underlying shale and coal layers.

Rockfall on most of the slope was mitigated using a new type of heavy drapery system of high-strength 4-mm twisted steel wires forming rhomboids. This material was used, instead of more traditional cable nets, to prevent smaller sandstone blocks in the lower beds and slabs of shale from falling onto the road. The sandstone in the upper slope was approximately 55-ft above the roadway grade. These outcrops cantilevered up to 10-ft from the slope surface. The risk of massive rockfall in this area was significant and a drapery was considered inadequate. Instead, a tensioned high strength steel wire mesh system composed of twisted 4-mm wires in a diamond pattern was used. This system was designed to actively hold the sandstone blocks on the slope and prevent any movement.

The project was bid as a conceptual design with design-build aspects by the Engineer and the Manufacturer. The Owner, West Virginia DOT, and the Contractor, Ameritech Slope Constructors also worked to overcome design and constructability issues. The successful installation and on-time completion demonstrated the advantages of all stake holders working as a team rather than in adversarial relationships.

INTRODUCTION

U.S. Highway 19 connects the city of Weston, West Virginia primarily as commuter route to neighboring counties, Figure 1. The southern part of the Highway in Weston is along a cut-slope approximately 900-ft (0.2-mi) long where rockfall constituted an on-going and hazardous problem. This site parallels the New Fork River and is also known as "The Narrows," Figure 2 The approximate coordinate center location of the project was located at 39°2'4"N, 80°28'18"W. This section of U.S. Highway 19 trends generally from northeast to southwest. KANE GeoTech, Inc., Geobrugg North America, LLC, and the West Virginia Department of Transportation developed a rockfall mitigation system relying on several new technologies.

The West Virginia Department of Transportation Division of Highways (WVDOT) decided to install a rockfall protection system after multiple rockfall events occurred along this particular stretch of road. WVDOT developed a conceptual rockfall mitigation plan for the slope with bid documents that called for the winning contractor, Ameritech Slope Constructors (Ameritech) of Asheville, North Carolina to provide an experienced rockfall engineer to design a system meeting the project requirements. Ameritech utilized new technology developed by Geobrugg Protection Systems, Romanshorn, Switzerland and Algodones, New Mexico. Geobrugg retained KANE GeoTech, Inc. (KANE GeoTech) as its engineer to further develop the mitigation system design in collaboration with WVDOT.

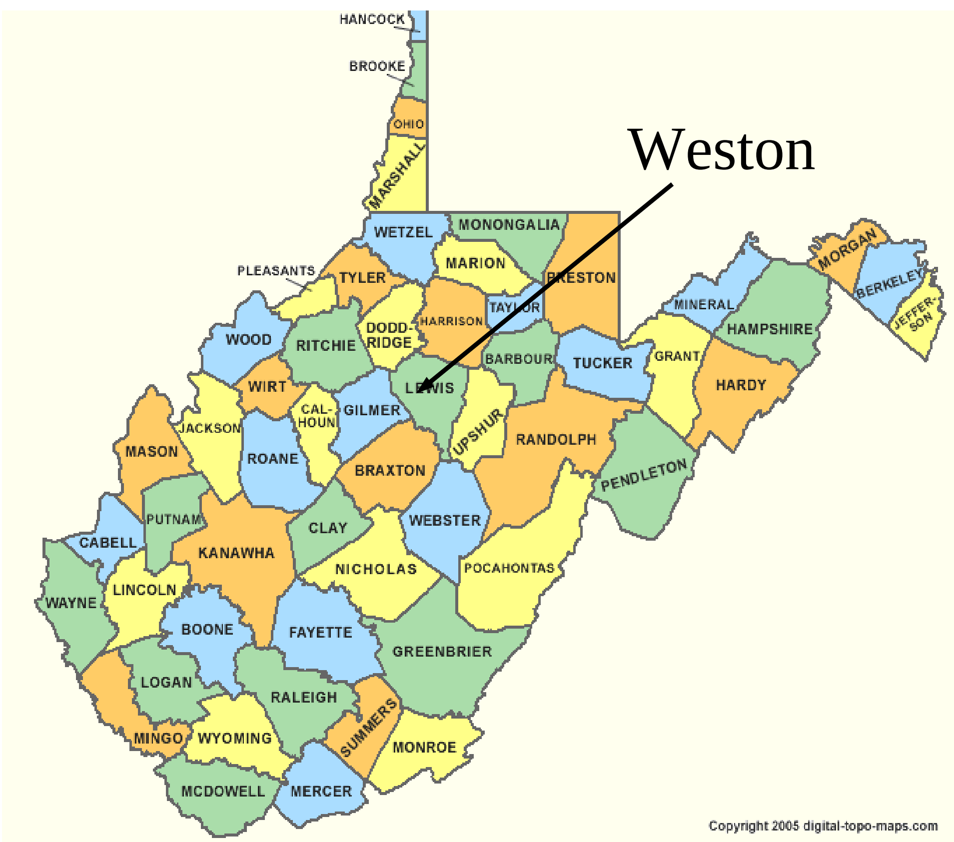

Figure 1. Project was located in Weston, Lewis County, West Virginia

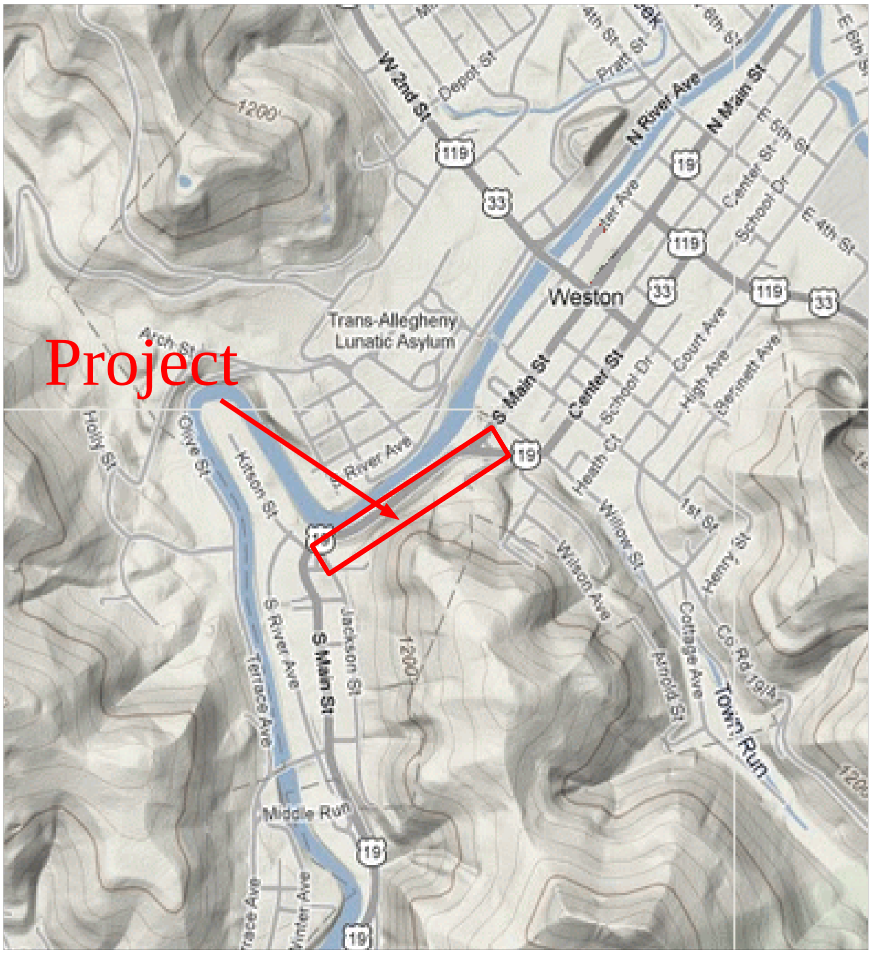

Figure 2. Project site just south of Weston, West Virginia

PROJECT APPROACH

The project approach consisted of a preliminary investigation prior to slope clearing to review and assess the original conceptual plans developed by WVDOT. Initial analyses and 90% design was accomplished. Preliminary construction drawings then were prepared. The slope was cleared of all vegetation and construction began. A second phase of investigation was then carried out to optimize the design and make refinements as a result of the better quality of information obtained. The Engineer was present during the entire construction process to ensure conformance to plans, make any necessary changes for constructability, and provide technical support to the contractor as necessary.

SITE DESCRIPTION

Weston, West Virginia is located within the Appalachian Mountain range and has a mostly continental climate characterized by hot, humid summers and cool to cold winters. Lewis County receives about 45-50 inches of precipitation annually. Almost half of the rainfall occurs during the months of May, June and July.

The Appalachian Plateau contains the most extensive area of slope failures in the eastern United States. This area most commonly experiences shallow earth flows in soil and weathered rock.

Due to the high amount of precipitation West Virginia receives, the state is covered by extensive colluvium that is highly susceptible to sliding. In addition, the geology of the area consists mostly of flat lying layers of Pennsylvanian Age interbedded sandstones, shales, and coal. Differential weathering of the shale and coal layers beneath massive sandstone beds can result failure of cantilevered sandstone beds. The relatively resistant sandstone beds become vertical cliffs and the relatively weak shale beds form recessed slopes, which pose potential rockfall hazard from the sandstone above the shale slope.

From the south along U.S. Highway 19, the project slope quickly increased in height and then slowly decreased towards the end of the project. Slope heights ranged from a maximum of 65-ft to a minimum of 20-ft. The slope was originally heavily wooded and vegetated making outcrops difficult to see, Figure 3.

Site characteristics were generally consistent along the slope, with alternating beds of sandstone and silty shale with a small amount of coal present. The top of the slope was composed of a 20-ft thick layer of thinly-bedded sandstone grading into massive sandstone in the lower part. Directly beneath the upper sandstone was an approximately 35-ft thick layer of black to brown shale with coal seams. Just under the shale layer was a relatively thin 5-ft section of massive sandstone. The latter sandstone layer was a lithic arenite with a more clay rich matrix, making it somewhat more susceptible to weathering. Since the shale present at this site was mostly composed of clay particles, it was highly weathered.

The roadcut had an azimuth trend of about 60°, roughly parallel with the sandstone bedding strike of 73°. Bedding had a dip of 8°SE, slightly into the slope face. Continuous vertical joints in the sandstone were perpendicular to the slope fact and spaced at about eight to ten feet. At the base of the slope under the thin massive sandstone was another 5-ft section of thin sandstone layers interbedded with brown shale, visible in Figure 3.

Figure 3. Project site at time of original investigation

FIELD STUDIES

Two field studies were performed. A preliminary, Phase 1, investigation was conducted prior to construction to collect data for analyses and design and to prepare working drawings. This included verifying the original WVDOT plans and evaluating the existing slope stability and potential rockfall hazard. The original concept divided the slope into three sections based on the nature of the hazards and relative risk of rockfall. The conceptual mitigation plan bid by the contractor was to have a drapery of Geobrugg Rolled Cable Net (RCN) with a secondary chain link mesh backing. The middle section was to have 76 rock bolts on a pattern to secure large, massive sandstone blocks at the highest portion of the cut. This section was also to be draped over the entire cut slope with RCN and conventional chain link mesh.

The slope was densely covered with vegetation at the time of the initial site investigation, Figure 4, so data collection was difficult and time-consuming. Standard field data collection procedures were used during this field study. These included recording slope height and angle, geology, potential rockfall sizes and shapes, surface conditions, and available rockfall run-out data. This data was collected in multiple areas along the entire project slope and incorporated as input in the analyses. Soil properties were determined for the site as well as the geologic characteristics of the slope. The larger outcrops in Section 2 were measured for analysis and mitigation design.

Figure 4. Dense brush made original site investigation difficult

Photographs

and notes were also taken of the slope and slope features.

The Phase 2 site evaluation was conducted after brush clearing to refine the drapery layout and anchor locations, Figure 5. At that time, it was observed that much of the slope was covered in loose soil and colluvium that was highly susceptible to sliding and additional loose material had to be removed, Figure 6. The slope clearing provided much additional insight into the project design although it did not change it significantly.

ROCKFALL AND SLOPE STABILITY ANALYSES

After the Phase 1 investigation, slopes were analyzed for kinematic global slope stability as well as with Geobrugg-developed software, RUVULOM Rock (Flum, et al., 2010; Roduner, et al., 2010). RUVULOM Rock is used to design tensioned rock block stabilization systems using Geobrugg SPIDER S4-230 mesh (Geobrugg Protection Systems. 2009). Nominal drapery and SPIDER anchor depths were determined using the Post-tensioning Institute (Post-tensioning Institute, 1996) guidelines for the design of grouted anchors. Because of the unknown depth of the large jointed sandstone blocks WVDOT specified that the SPIDER anchors be drilled a minimum of 25-ft into the sandstone. The goal was not only to anchor the tensioned mesh but also to have the anchors serve as rock bolts were they were inserted. Because loads on SPIDER anchors are relatively small, this resulted in pull-out safety factors on the order of 11 for anchors in shale to 18 for those in sandstone were achieved.

The RUVULOM Rock program utilizes limiting equilibrium analyses to determine the force vectors necessary to restrain a large block onto a slope face. The program output is a pattern of anchors around the block with the necessary tensioning forces to achieve a specified factor of safety. For the Phase 1 analyses, anchor patterns were developed for typical blocks anticipated from the initial data collection.

Figure 5. Phase 2 site investigation on cleared slope

Figure 6. Clearing slope of brush and light scaling created better conditions for collecting design data

All outcrops were visible once the slopes were cleared of all vegetation and debris. A final layout and anchor plan was then developed by dividing the slope into sections and specifying final mitigation plans for each section, as shown in Table 1 and Figure 7.

Table 1. Rockfall protection systems by Section

Section	Mitigation and Protection System(s)	Coverage
1	Rolled Cable Net Heavy Drape with Chain Link Mesh System	Entire slope
2	Tensioned SPIDER with Chain Link Mesh System	Outcrops
	Rolled Cable Net Heavy Drape with Chain Link Mesh System	Mid-slope
		Below outcrops
		Between Outcrops 8 and 9
3	Rolled Cable Net Heavy Drape with Chain Link Mesh System	Entire slope

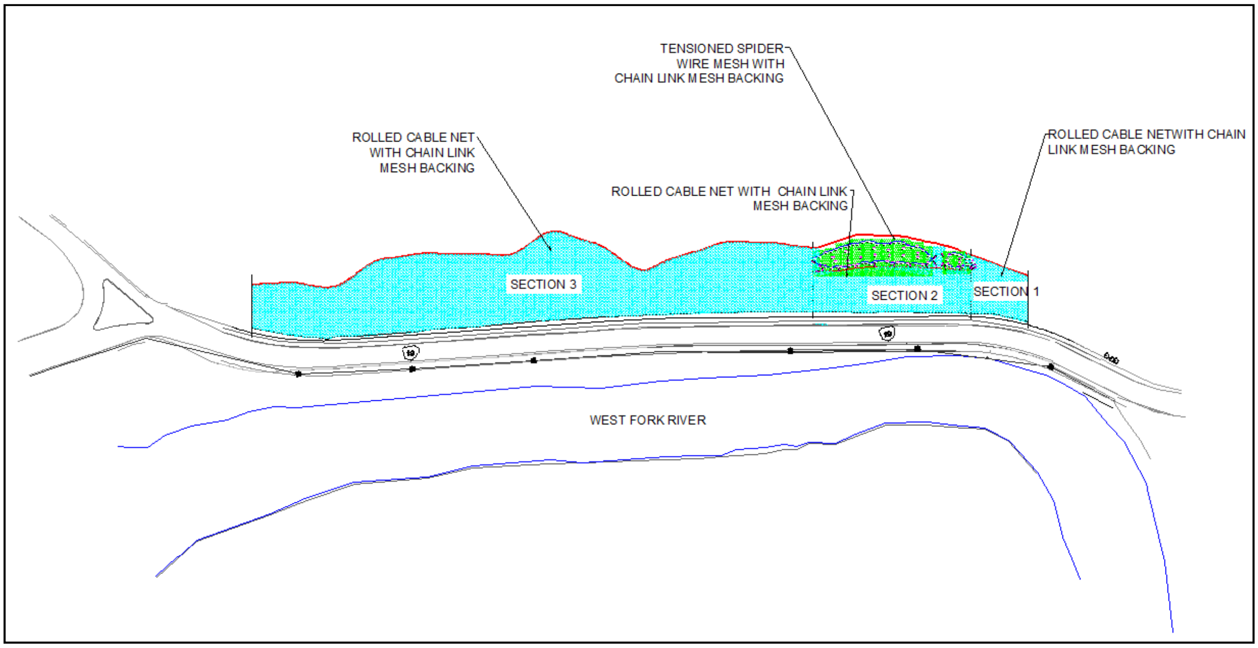

Figure 7. Slope Sections with final mitigation

ROCKFALL PROTECTION SYSTEM DESIGN AND INSTALLATION

The major difference between the original conceptual plan and the final plan, beside the detailed calculations and plans, was the change from a rock bolt and draped slope at the top of the middle section to a tensioned SPIDER system. This design was more effective for the purpose of full retention of the outcrops in Section 2. A RCN drape was also to be installed along the bottom of the slope below the SPIDER system. Combining these two mitigation methods effectively eliminated the rockfall hazard in Section 2. The final design also included covering Sections 1 and 3 with a RCN drape extending from the top of the slope to within approximately 5-ft from the toe of the slope.

The Engineer was retained by the Contractor to provide construction oversight to ensure conformance to the concept and design so that the systems would perform as intended. The Engineer was also able to provide technical expertise on construction details of the systems.

As described, prior to installation, the slope was cleared of all vegetation and debris. It was immediately determined that a thick layer of soil on part of the slope should be removed before the mitigation systems were installed. Topsoil removal decreased potential additional load on the drape system in the event of a landslide. This also reduced the overall landslide risk.

Wire rope drapery anchors were drilled in Sections 1 and 3 to a depth of 10-ft into competent bedrock. As described earlier all SPIDER anchors were drilled to a depth of 25-ft to provide rock bolting advantages and to serve as tension anchors for the mesh.

Load proof tests were performed on 20% of all system anchors using the industry standard practice of a yoke and jack. Wire rope anchors were tested to a load of 15-kips and all SPIDER threadbar anchors were tested to a load of 30-kips.

For the drapery sections, chain link mesh was hung on slope first to provide retention of smaller material before the larger-opening RCN was placed. Installation was accomplished using a crane. Each chain link panel (10-ft wide) was overlapped with the neighboring panel. The RCN panels were connected to the top rope with a 3/4-in shackle at every link to rope connection. Each RCN panel (11.5-ft wide) was laced vertically to the adjoining panel using a 5/16-inch wire rope. The RCN panels and the chain link panels were connected using Spenex rings on a 2-ft x 2-ft grid with a Spenex ring pneumatic gun.

In the tensioned SPIDER Section, chain link mesh first was hung around each outcrop. The contractor decided to hang these panels of chain link horizontally in order to get proper coverage and to better contour each outcrop. The SPIDER was then placed on top of the chain link at each outcrop. The Contractor was able to fit the system tightly around each outcrop because of the carefully prepared anchor design and layout. Spike plates were then placed over the anchors and SPIDER system with spherical washers and hexagonal nuts. A minimum of 18-in of SPIDER mesh was left at the bottom to be overlapped by the RCN drapery system installed below. Once the chain link and SPIDER were on the slope and contoured at each outcrop, a 3/4-in boundary rope was laced through each SPIDER mesh and attached to a wire rope anchor. After all components of the SPIDER system were properly installed, the nuts on the spike plates were tightened to tension the system.

Separate wire rope anchors were drilled at mid-slope, under the outcrops, to support the RCN system below the SPIDER system. Both systems were designed to act independently and not

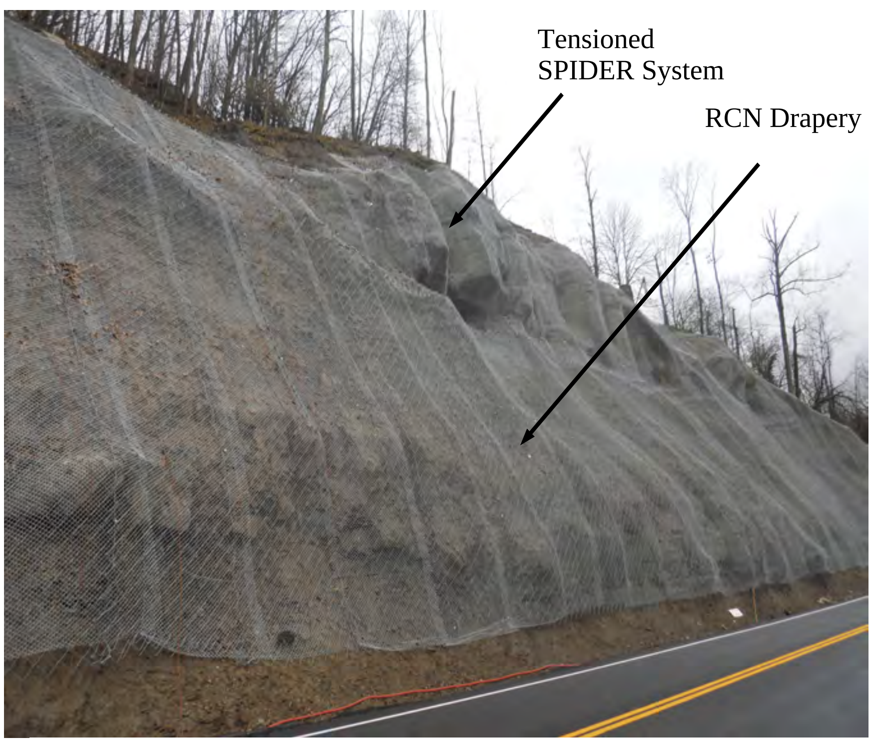

Figure 8. Completed Section 2 with tensioned SPIDER mesh and RCN drape below

share any anchors or other components. The completed middle Section is shown in Figure 8.

CONCLUSIONS

The abilities of the Owner, Contractor, Manufacturer, and Engineer to work efficiently and smoothly as a team led to the very satisfactory completion of the project, ensuring that the designed solution will perform as intended to protect U.S. Highway 19 infrastructure, traffic, and the traveling public.

Some conclusions from this project are as follows:

1. Initial rockfall project designs should be open to changes. Once slopes are cleared of vegetation, rockfall conditions are often quite different than initially thought. Initial designs should be general enough to allow for modification but also specific enough to allow a realistic bid process.

2. Consider design-build. Rather than design projects with personnel who rarely have the opportunity to do rockfall analyses and design, owners should consider design-build concepts by joint ventures between contractors, manufacturers, and engineers. Specialty professionals have a great deal of experience and expertise that they can bring to bear on projects.

3. Require engineered designs. Many rockfall mitigation projects in the past were designed and built using on-the-fly solutions. Methodologies for investigation have evolved as the discipline has developed over the years. In addition, many tools, based on sound engineering and scientific principles are available to provide well-engineered designs.

4. Retain the original design engineer for construction oversight and require that the contractor use the manufacturer's representative. Rockfall mitigation systems are not that commonplace. Inexperienced inspectors are not able to identify problems or irregularities during construction, or ensure conformance to the original design concepts. Retention of the design engineer for at least periodic inspections is essential to prevent large problems at the end of the project. In addition, reputable manufactures supply a certain amount of technical assistance with the sale of the products. Their expertise should be relied on whenever possible.

When all parties work together to overcome the problems inherent in the adversarial relationships between Owner, Contractor, Manufacturer, and Engineer, success is all but guaranteed. The Narrow project is a textbook example of what can be achieved in this atmosphere.

REFERENCES

Flum, D., Roduner, A., Engl, D., 2010, *SPIDER Rock Protection Systems*, Technical Documentation, Geobrugg AG., Romanshorn, Switzerland.

Geobrugg Protection Systems, 2009, *SPIDER Product Manual,* Geobrugg AG, Romanshorn, Switzerland.

Post-Tensioning Institute, 1996, *Recommendations for Prestressed Rock and Soil Anchors*, Post Tensioning Institute, Farmington Hill, Michigan.

Roduner, A., Rüegger, R., and Flum, D., 2010, *Summary of Published Technical Papers 2006-2010*, Technical Documentation, Geobrugg AG, Romanshorn, Switzerland.

Geotechnical Design of Supplemental Rock Anchors, Wurts Street Suspension Bridge, Kingston, NY

Priscilla Duskin
NYSDOT
50 Wolf Rd., Albany, NY
(518) 457-4731
pduskin@dot.state.ny.us

Matthew Charles
NYSDOT
50 Wolf Rd., Albany, NY
(518) 457-4725
mcharles@dot.state.ny.us

Prepared for the 63rd Highway Geology Symposium, May 7-10, 2012

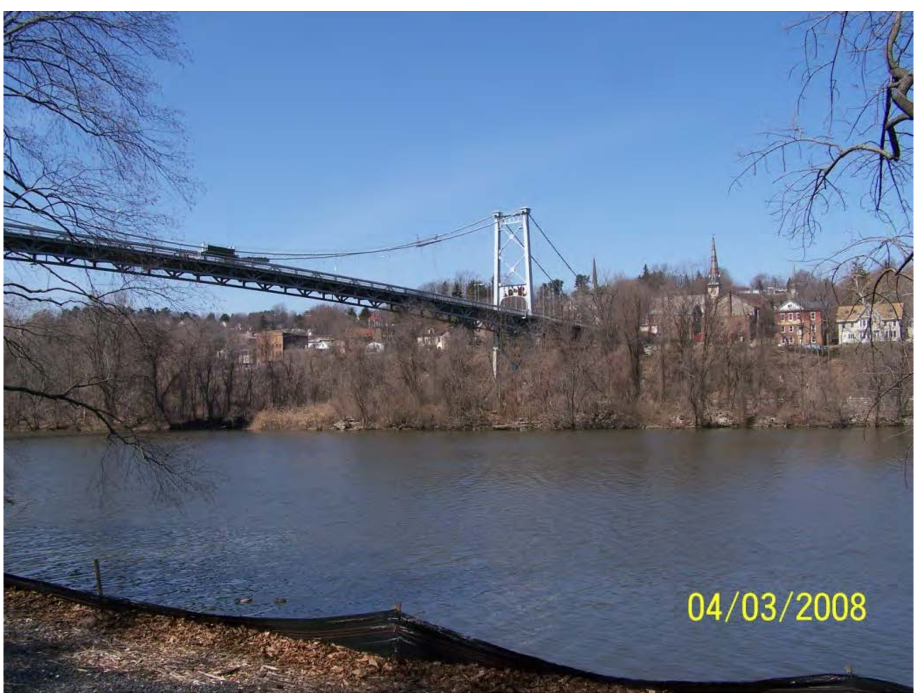

Acknowledgements

The authors would like to acknowledge Mike Grant of Hayward Baker Geotechnical Construction; Ray Ackerman of NYSDOT Region 8 Structures; Steve Borg of NYSDOT Geotechnical Engineering Bureau; and Blaise Blabac of Modjeski and Masters Bridge Engineering for their valuable contributions during the planning and design of this project.

Disclaimer

Statements and views presented in this paper are strictly those of the author, and do not necessarily reflect positions held by their affiliations, the Highway Geology Symposium (HGS), or others acknowledged above. The mention of trade names for commercial products does not imply the approval or endorsement by HGS.

Copyright Notice

ABSTRACT

The Wurts Street Bridge over Rondout Creek in Kingston, NY, is a two-lane steel cable suspension bridge built around 1920. The steel cables are connected to eyebars that transfer the load to a pair of vertical steel anchors embedded in concrete shafts on each side of the bridge. Recent measurements of deterioration of the steel eyebars led to a design to use supplemental rock anchors to partially offload the eyebars and remove a weight limit posting on the bridge. Subsurface exploration consisted of a dozen borings, each fifteen meters deep, which were nearly all rock core. The rock in the area consists of steeply dipping Devonian sandstone, interbedded with shale, that has zones of intense fracturing. The rock cores were evaluated and tested with a point load tester to derive unconfined compressive strength, and a design for the rock anchors was done based on these results. The rock anchors will consist of 1000 kN and 445 kN strand anchors installed at varying angles with staggered bond lengths and variable free lengths in order to spread stresses throughout the rock mass, and to avoid unfavorable geologic conditions encountered during exploratory drilling.

INTRODUCTION

The Wurts Street Bridge is a 213 m (700 ft.) suspension span over the Rondout Creek and Delaware & Hudson Canal in Kingston, NY, near the confluence of Rondout Creek and the Hudson River. It connects the City of Kingston, to the north, with the village of Port Ewen, NY, to the south, and was originally one of the bridges for State Highway 9W, the north-south highway which parallels the west side of the Hudson River. A new bridge was constructed for the Rte. 9W crossing over Rondout Creek in 1978, and the old suspension structure became a local bridge in Kingston.

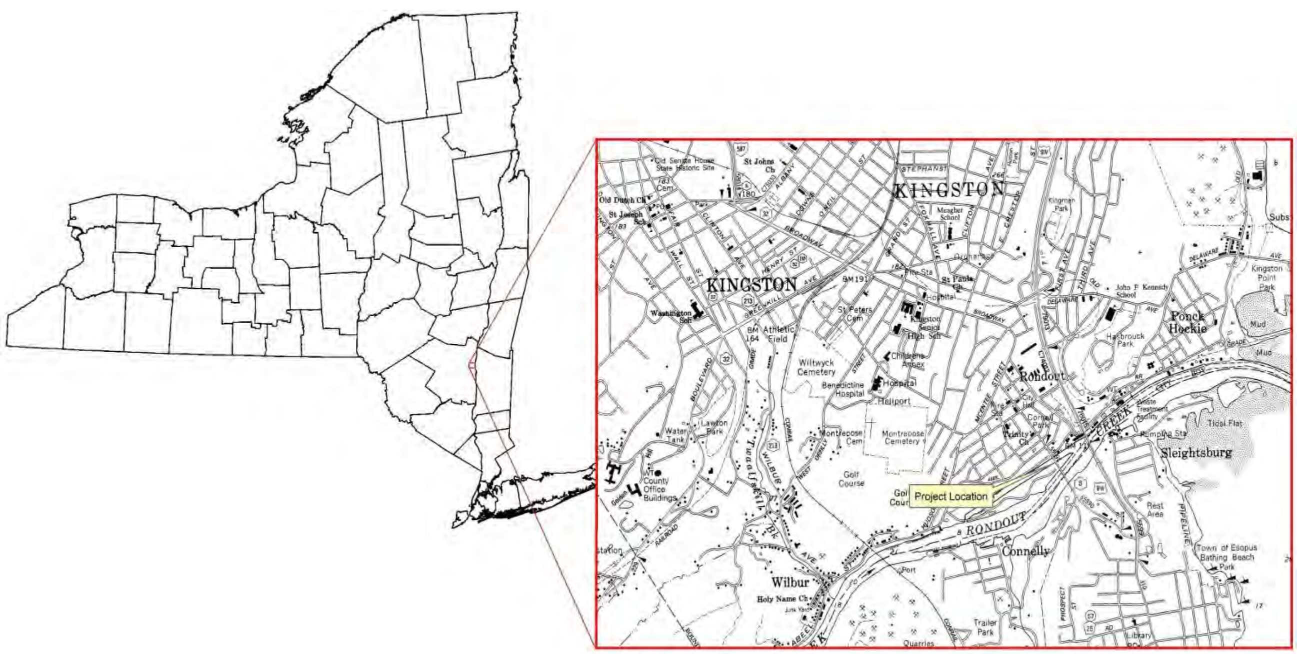

Figure 1. Project Location

Bridge inspection ratings performed by NYSDOT Region 8 Bridge Maintenance gave a poor rating to the bridge in recent years, which resulted in a posted weight restriction of five tons. Preliminary plans for bridge repairs were made, contingent upon an evaluation of the suspension cables. In 2007 the bridge engineering firm of Modjeski and Masters was selected to inspect the condition of the cables.

Surprisingly, the steel in the suspension cables was found to be in excellent condition. The cables go into concrete vaults at each end of the bridge and are connected to vertical anchorages by means of steel eyebars. Because of high humidity within the vaults, there was some corrosion deterioration of the anchorage eyebars. It was determined by the Modjeski and Masters structural engineers that installing rock anchors could serve to partially off-load the eyebars, and the weight restriction on the bridge could be lifted. The request was made of the DOT Geotechnical Engineering Bureau engineering geology section to design the rock anchors for this project.

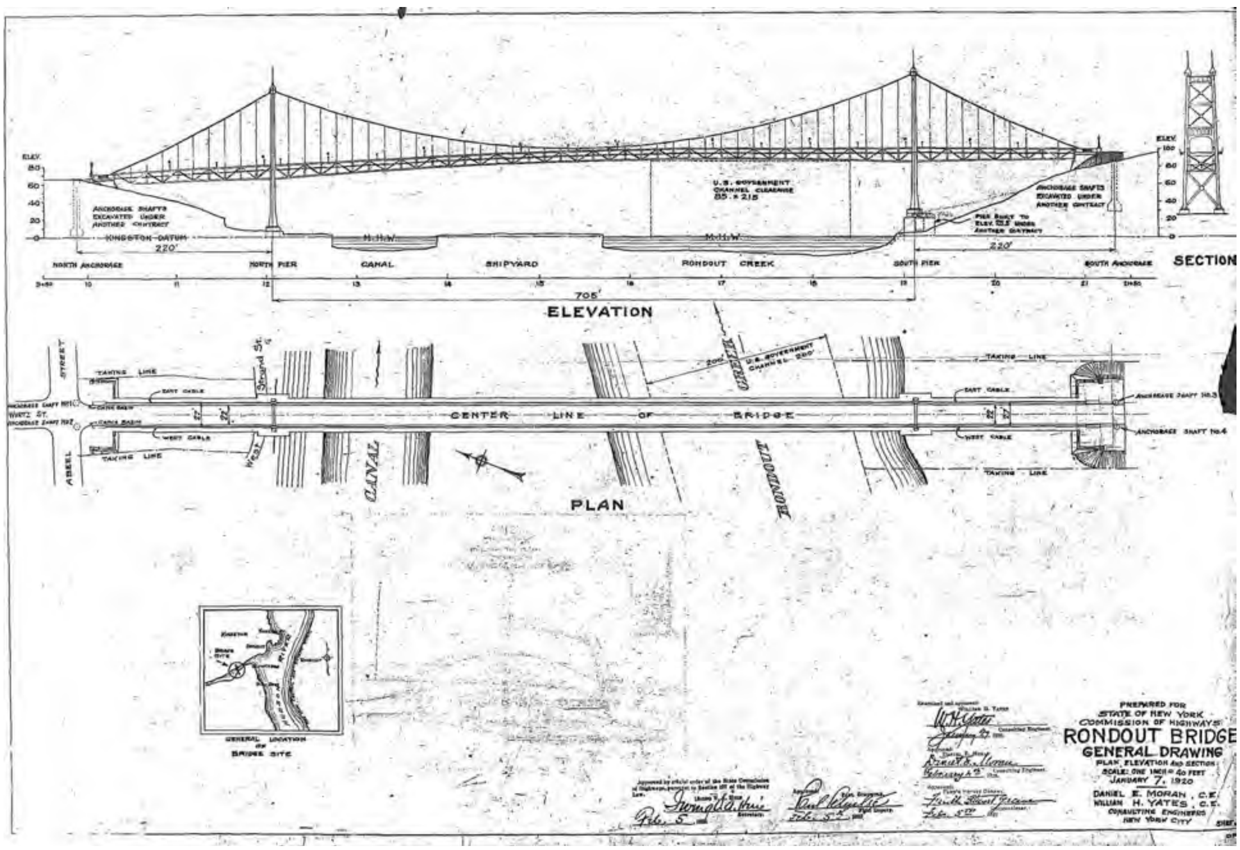

Figure 2 Original General Drawing of Wurts St. Bridge.

SITE GEOLOGY

The bedrock on both sides of the Wurts St. Bridge consists of steeply-dipping interbedded sandstones and shales of the Ordovician Austin Glen Formation, which underwent considerable deformation during Devonian orogenic events (Fig. 3).

Ten borings were drilled in the initial phase of subsurface exploration, five on each side of the bridge, at distances ranging from 8 to 27 meters (26 to 88 ft.) from the anchorage vaults. On the north side, by the Delaware and Hudson canal, there was considerable underground infrastructure that dictated the location of the drillholes. The rock cores were logged during drilling and later tested with a point load testing apparatus to determine their unconfined compressive strength.

Figure 3. Outcrop near bridge

Borings revealed that the rock on the north side of the bridge was in better condition than the rock on the south side, in that there were fewer fracture zones, higher RQD, and more massive sandstone layers. The cores tested by the point load tester showed greater unconfined compressive strength in the rock from the north side, an average of 240 MPa (34,800 psi) versus 100 MPa (14,500 psi) on the south side (Fig. 4).

Fig. 4 Rock Core From North (left) and South (right) Bridge Sides

EXISTING ANCHORAGES

The existing anchorages for the suspension cables consist of eyebar connections to vertical steel bars within a shaft in bedrock to a depth of approximately 15 m (50 ft.) below ground surface. This shaft was then filled with concrete (Fig. 5). The vertical shafts were excavated under a separate, earlier contract to the bridge construction contract, and no details could be found on the manner of the excavation work.

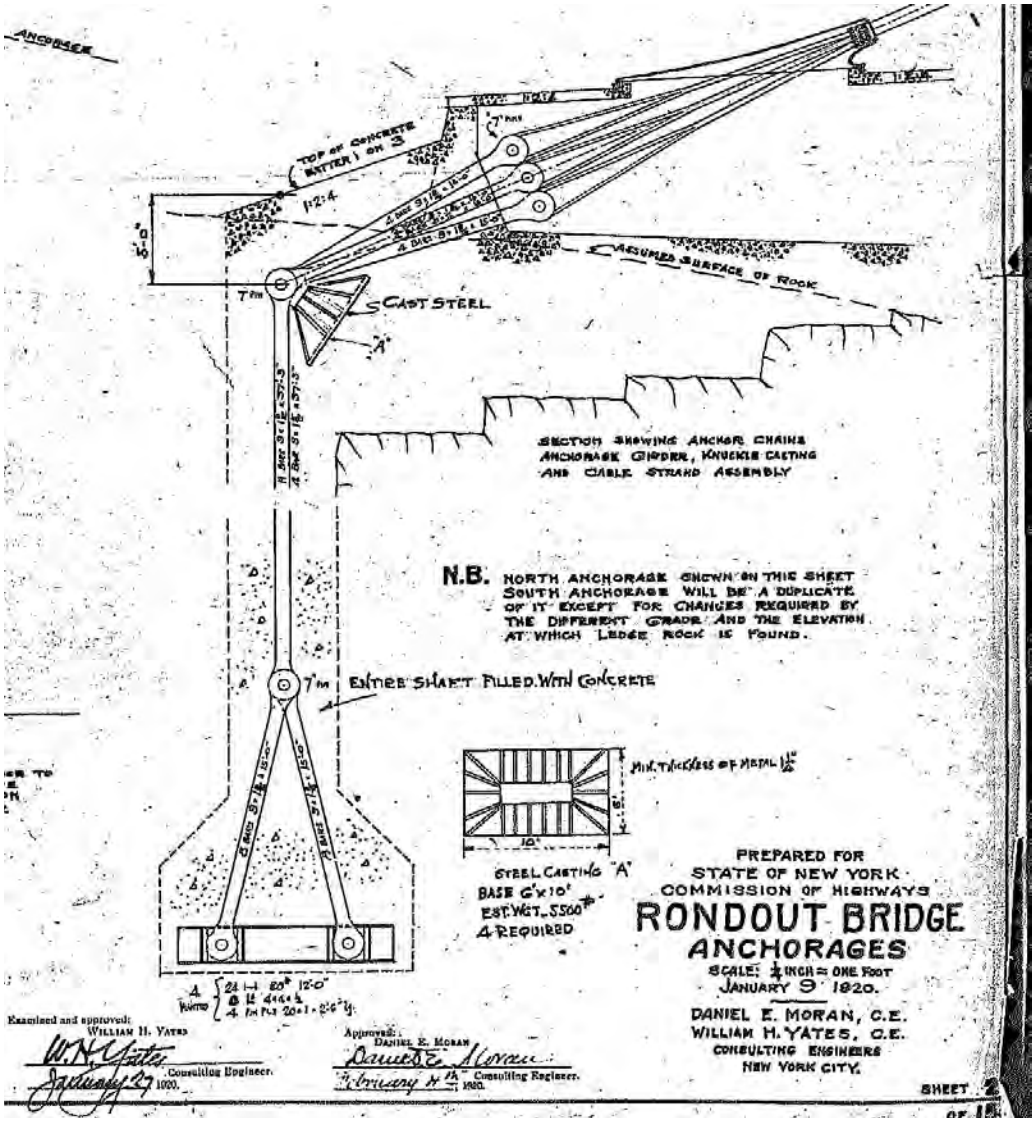

Fig. 5 Original drawing, anchorage detail

The four vaults containing the eyebar connections are located on each side of the bridge approaches. The suspensions cables are separated into three groups at the point of anchorage, with the top and bottom groups having two eyebar connections and the center group having three (Fig. 6). The designers wanted the supplemental anchorage rock anchors to be placed on each side of the eyebar rows, with the top two and bottom two anchors carrying a load of 445 kN (100 kips) each, and the center pair carrying 1000 kN (225 kips) each. This would offload about 25% of the total load on the suspension cable. A jacking beam will be installed at each row of eyebars to span between the corresponding pair of rock anchors, with flanges fitting between the cable strand loops. Jacks will then push the jacking beams against the strand shoes, using the rock anchors as reaction points.

Fig. 6 Eyebars and strand loops, SW anchorage inside vault

One issue that had to be resolved concerned access for the drilling equipment needed to install the rock anchors. A site visit was made into the anchorage vaults by NYSDOT personnel, accompanied by a drilling expert from Hayward Baker Geotechnical Construction. The concrete roofs and walls adjacent to the bridge will be removed as part of the bridge rehabilitation project, and because of this the specialized drilling equipment will have sufficient space to drill the rock anchors. The vaults will then be rebuilt, and will be made watertight and have dehumidifying equipment installed to keep the anchorage assembly dry.

ROCK ANCHOR DESIGN

General guidance for rock anchor design was found in "Recommendations for Prestressed Rock and Soil Anchors" (Post-Tensioning Institute, 2004) and more detailed guidance was obtained from "Foundations on Rock" (Wyllie, 1999).

The rock anchor design is a function of several variables:

1. Diameter of the strand or bolt necessary for the design load, and diameter of the hole
2. Bonded length of the anchor
3. Unbonded length of the anchor necessary to ensure that a large enough rock mass is mobilized
4. Bond stress between rock and grout
5. Physical characteristics of the rock mass

Using the design loads on each pair of rock anchors, a prestressed seven strand anchor, with 980 mm (1.52 square inches) cross-sectional area, was selected. This anchor requires a hole diameter of 140 mm (5.5 inches).

The bond length necessary for the design loads of 445 kN and 1000 kN is 2 m and 3 m, respectively, based on the uniaxial compressive strength of the rock and the working bond shear strength in this type of rock, using a factor of safety of three.

To determine the total length of the anchor needed, the mass of rock necessary to support the design load must be calculated. The mass of rock mobilized by the anchor tension can be considered to be conical, with the tip of the cone pointing into the earth and the apex angle at 90 degrees (Wyllie, 1999). The design of the anchor can be based on the weight of the rock mass alone, but this would be an excessively conservative design; instead, it should be based on a combination of the weight of the cone of rock as well as the strength of the rock on the cone's surface (Wyllie, 1999).

The rock weight was calculated assuming complete saturation for the buoyancy factor, as the borings had shown high water table conditions at the site. The tensile strength on the surface of the cone was calculated using the unconfined compressive strength of the rock and rock mass rating factors. By putting the various calculation elements into a spreadsheet, the variables could be changed and adjusted to derive the total anchor length. For the 445 kN rock anchors, a minimum bond length of 2 m and minimum free length of 7 m was required; for the 1000 kN anchors, the minimum bond length was 3 m and minimum free length was 8 m.

Some geologic and logistic factors had to be considered for the final anchor design. Because there was no information about the original vertical concrete anchorage shafts and how they were constructed, the exact location of sound rock past the shafts was unknown, and the rock anchors were lengthened to account for this. Also, as mentioned earlier, the rock quality on the south side of the bridge was not as consistent as on the north side, and there was more irregularity in the rock surface, with one noticeable dip in the surface that corresponded with a significant fracture zone (Fig. 7). The rock anchors for the south side will be two meters longer than those on the north side for this reason.

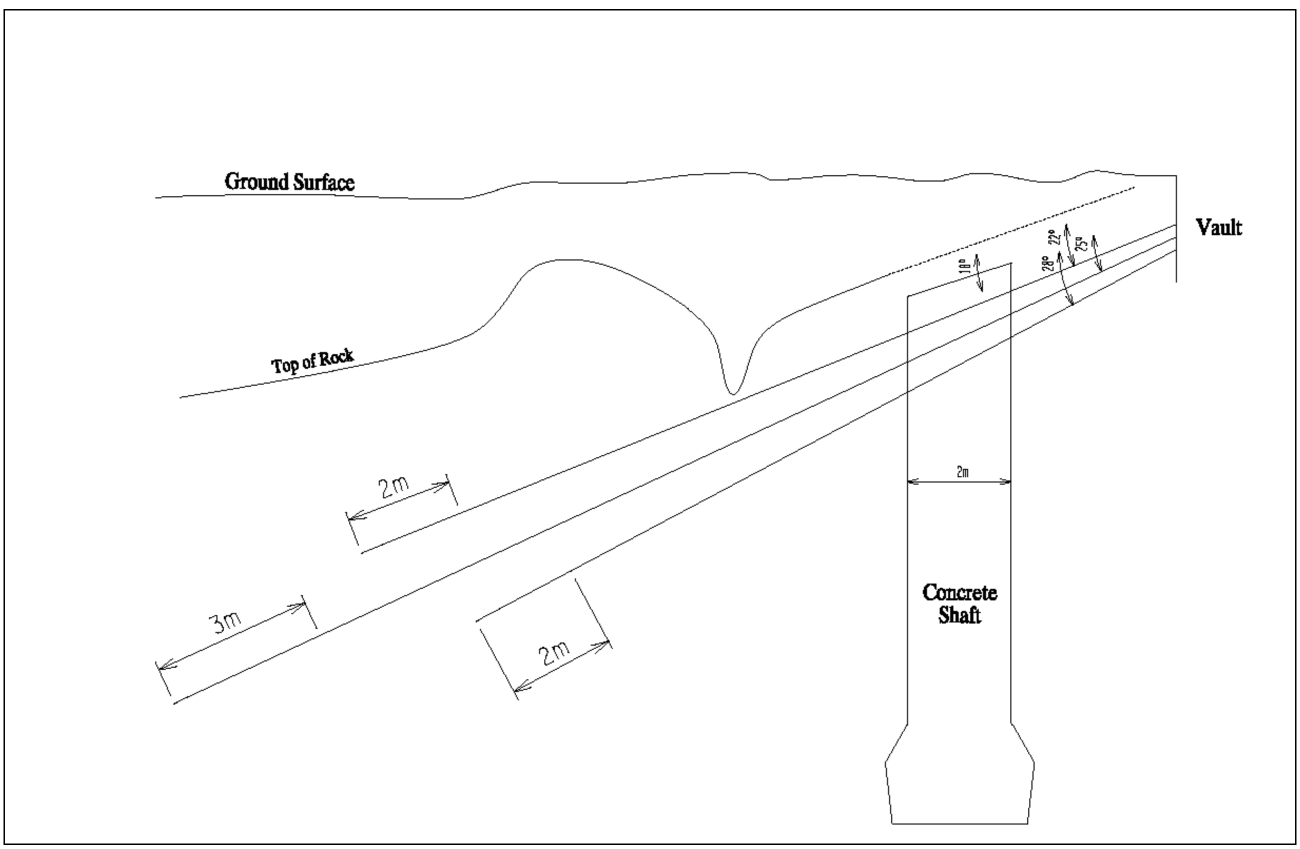

Fig. 7 Anchor design, south side (not to scale)

One other aspect of the rock anchor installation is that, because of the close spacing of the anchors, the drillholes should not be parallel to each other. This will avoid any intersection of the drillholes due to slight drilling deviations, and will also avoid concentrating stresses within a narrow cone of rock. The final design of the anchors stipulated that each row of rock anchor boreholes deviate from horizontal, increasing with depth by at least three degrees. The top row of anchors will be installed at 22 degrees from horizontal, the middle row at 25 degrees, and the bottom row at 28 degrees from horizontal. Also, the bonded zones of the anchors will be staggered by varying the length of the unbonded zone to avoid creating a tensile plane within the rock mass.

Rock anchor capacity cannot be improved after installation, and alternate locations will not be feasible if an anchor fails during testing. Therefore, one sacrificial test anchor, located away from the suspension cables, will be required at each vault. As of this writing, the installation of the rock anchors for the Wurts Street Bridge is scheduled for the year 2016.

CONCLUSIONS

An old suspension bridge that is scheduled to be rehabilitated needed a supplemental anchorage system for the suspension cables. Rock anchors were selected as the supplemental anchorage type. A design was proposed based on subsurface information and original as-built plans. This anchorage supplementation will make it possible to remove weight restrictions on the bridge and allow for increased local traffic to a popular and historic structure.

REFERENCES

Post-Tensioning Institute, 2004, *Recommendations for Prestressed Rock and Soil Anchors,* pp. 42-43.

Van Roosendaal, Danny J., and McKown, Andrew F., Haley and Aldrich, Inc., *Geological and Design Considerations for Replacement of Suspension Cable Anchorages, Bear Mountain Bridge, Hudson River, NY,* 2004, Proceedings, Highway Geology Symposium, Kansas City, MO, pp. 348-356.

Wyllie, Duncan C., 1999, *Foundations on Rock,* E&FN Spon, publishers, London, pp. 287-332.

Research into and Application of Attenuator Rockfall Protection Systems

Steve Mumma
Geobrugg North America, LLC
2050 Beavercreek Road
Suite 101, #325
Oregon City, OR 97045 USA
503-341-8251
steve.mumma@geobrugg.com

Prepared for the 63rd Highway Geology Symposium, May 7-10, 2012

Acknowledgements

Thank you to James Glover with the WSL Snow and Avalanche Research Institute in Davos, Switzerland for his assistance in the preparation of this paper.

Disclaimer

Statements and views presented in this paper are strictly those of the author, and do not necessarily reflect positions held by their affiliations, the Highway Geology Symposium (HGS), or others acknowledged above. The mention of trade names forcommercial products does not imply the approval or endorsement by HGS.

ABSTRACT

There are many rockfall mitigation scenarios in which traditional protection measures such as rockfall barriers, slope draperies, or earth dams are not applicable as a result of the slope geometry, catchment area, or other factors. One creative solution in such situations is the use of an attenuator rockfall system. These systems hybridize the best features of both a rockfall barrier and a slope drapery. They consist of netting lain on the rock slope with its top edge supported on posts, enabling the interception of bouncing rocks from above. At the tail the netting is open, allowing the rocks to pass through the system while reducing velocity and controlling trajectory.

Attenuator systems have been widely used for many years. Only recently have they begun to be studied in greater detail to provide rock fall engineers with guidance to optimum design and installation. While the research has already advanced the design and application of rockfall attenuators, there is still much scope for further research. Design features such as the range of feasible impact energies, attenuation of impact energy as a function of system configuration, system loading characteristics, and optimization of system components, are all important research questions. This paper shall provide an overview of current rockfall attenuator research aimed at assisting rockfall engineers in better tailoring the design of attenuator systems to specific mitigation scenarios. It shall summarize the key research findings, give examples of existing attenuator test systems, and identify and discuss the key areas for further research.

INTRODUCTION

Two of the most common solutions chosen to address rockfall problems are draperies and barriers. Both have their particular strengths and weaknesses, and can be efficient and cost-effective mitigation options for many scenarios. There are many situations, however, where neither option adequately addresses the issues raised by a particular site. Rockfall barriers can be impractical as a result of inadequate space at the toe of the slope to allow for the flex of the nets upon impact, or some slopes may have a cross section that will result in rocks bouncing with a height or trajectory that makes construction of an adequate barrier not feasible. Similarly, site topography can make drapery an unattractive option. For a drapery to be effective, the drape material must fully cover any potential source areas of rockfall. Draperies offer no protection against rockfall that originates outside the boundaries of the system. As a result, the cost required to drape some very high slopes can be so high as to make the project impossible. Generally, the topographical details of a particular site point readily to one of these two options as being the most appropriate solution. In some cases, however, the site conditions make both options impractical. One solution that is increasingly being employed in such cases is the attenuator system.

The attenuator system combines the best attributes of the drape and the barrier into one hybridized system. Attenuator design can vary from site to site, but a typical system will consist of a netting fabric that is draped freely on the surface of a slope with the top edge of the fabric being supported some height above the ground on a series of steel posts (Badger et al, 2008). The tail of the drape is open and typically extends down the slope, terminating just above an area that is designated for collection of the rocks (Fig. 1). The attenuator functions by having the post-supported top edge of the system intercept any rockfall that is initiated upslope of the system. As the rock passes through the drapery portion of the system, friction is generated as the rock impacts both the netting and the slope surface. This friction dissipates the kinetic energy of the rock such that it exits at the bottom of the system with an energy that is much lower than what it would otherwise have been if the system had not been present. The extent to which the system reduces energy is defined as its attenuation effect.

Another common type of attenuator system that will also be addressed in this paper is a hangar system. The hangar system consists of a top support rope that spans across a chute with a netting fabric hanging vertically down from the rope. Impacting rocks strike the netting, and are directed downward after the deflection of the netting has dissipated the horizontal kinetic energy of the rock. This type of system is particularly useful for sites with limited space to create catchment area at the toe of the slope. This scenario is common in Japan as well as numerous highway and railroad sites in North America.

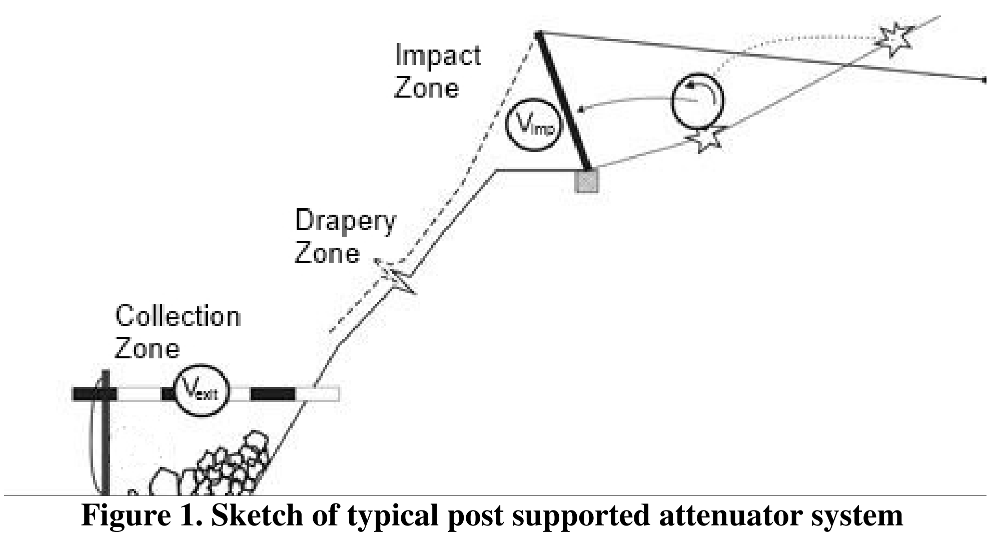

Figure 1. Sketch of typical post supported attenuator system
V_{imp} = impact velocity; V_{exit} = exit velocity

ATTENUATOR SYSTEM DESIGN ISSUES

The scope of this paper does not include a detailed analysis of the parameters that influence the design of site-specific attenuator systems,or how those design parameters affect the specifics of the system lay-out for a given site. These design parameters do, however, present many of the questions that must be answered by current and future research. It is important, therefore, to have a basic understanding of the design parameters before discussing the research and its application to the field setting.

The site characteristics that are important to understand include:

- Source area – height, location, design rock size, and rock shape
- Slope details – length, angle, surface roughness, catchment area
- System goal – slow rocks down, or stop rocks completely

The system characteristics that will affect performance include:

- Post height – based on expected bounce height of rocks
- System location – chosen to optimize issues such as: performance, cost, constructability
- Netting type –length, weight, opening size

The focus of this paper is on the interaction between the site characteristics listed above and the system netting. Understanding this behavior is of great importance because it is what provides the attenuation effect of the system. The complexity of this interaction makes analysis based strictly upon modeling and calculation difficult and unreliable. As a result, full scale and lab scale testing is necessary. This testing provides the baseline information necessary to understand system performance, and to enable further numerical modeling of the effect changes to the system design have on the attenuation effect.

FULL SCALE TESTS - SWITZERLAND

The location of the test site is in a quarry in St. Léonard, Switzerland. The test slope has a length of 164’ (50 meters) and an angle of 50^{o}. Launching of the test rocks is accomplished through the use of an adapted 66’ (20 m) high crane which supports a wire netting acceleration ramp that is attached to a purpose-built ramp located at ground level of the top of the test slope. Test bodies are lifted to the top of the acceleration ramp with a crane, and then launchedby means of an automated release mechanism. Upon release, they accelerate down the ramp structure to the point at which they impact the test barrier. A low deflection rockfall barrier is installed at the bottom of the slope as a safety measure (Fig 2). Rockfall experiments were conducted both with and without attenuator systems present (Glover, et al, 2010).

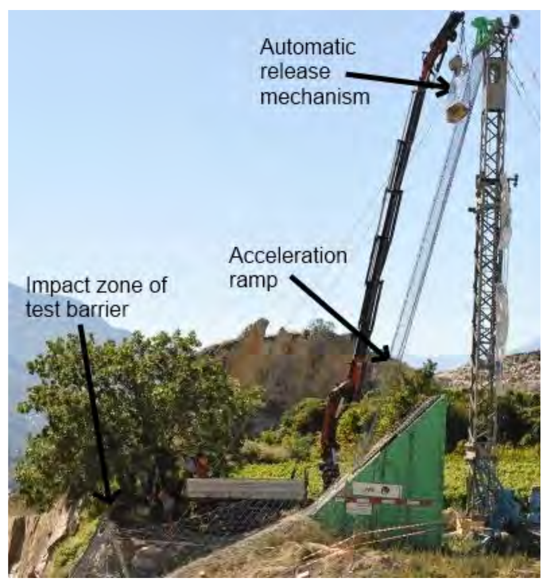

Figure 2. Release mechanism, acceleration ramp, and impact zone of test barrier

TEST BARRIER

The attenuator system used in the test series had a width of 57’ (17.5 m) across the top of the slope. The length of the netting tail running down the slope was 164’ (50 m). The top edge of the netting was supported on 10’ (3 m) posts that were braced with both upslope and lateral anchor ropes. The overall netting consisted of two different types of high tensile spiral rope netting (Figs. 3 & 4). The top 33’ (10 m) of the net that was located in the rock impact zone used a netting with a mesh opening size of 5” (130 mm). The drape section of the net used a netting with a 9” (230 mm) opening.

Figure 3.Impact zone of attenuator **Figure 4. Tail section of attenuator**

TEST INSTRUMENTATION

The instrumentation used for the experiments included:

- High speed video cameras recording at 250 frames per second to measure rock velocity at the impact and exit areas from the test barrier (Fig. 1), and to provide a qualitative assessment of the interaction between the rock and the barrier.
- Load cells to measure the forces in the support ropes of the system.
- A theodolite to provide precise positioning and calibration of the high speed video cameras as well as the starting and ending locations of the test rocks.
- Standard video cameras to analyze the trajectory of the rocks as they passed through the attenuator system.

RESULTS

The primary focus of the test program was to provide a comparative assessment of the difference between the energy of a rock reaching the bottom of the slope after passing through the attenuator system with that of an unattenuated falling rock. This comparison enables an analysis of the amount of energy that the system is able to absorb (attenuation effect).

In order to provide the required comparative data, rocks were dropped both with and without the test attenuator installed. The data from the unattenuated testing serves as a baseline indicator of actual behavior when rocks are allowed to move unimpeded down the slope, and provides a basis for comparison and assessment of barrier performance.

The data used here for analysis of the performance of the test attenuator includes two experiments each from the attenuated and unattenuated test series. The selected data have been chosen such that the total potential energy from rock release to the end of the slope is similar. Using the data from the unattenuated tests as a bench mark, the attenuation effect of the test system can be quantified. The exit velocity (V_{exit})

Figure 5.Test rock impact into the attenuatorFigure 6. Test rock exiting netting, with lowdeflection barrier at bottom for safety

was measured at the point at which the rock's center of gravity passed the scale bar located just beyond the end of the attenuator netting (Fig. 1). Exit kinetic energy (K_{exit}) is calculated as a function of rock mass and V_{exit} (Fig. 1). The attenuation capacity of the system is calculated as a percentage comparing the K_{exit} values of the attenuated and unattenuated tests. The results of this comparison are presented below in Table 1.

Table 1. Comparison between unattenuated and attenuated rock fall tests

	Comparison A		Comparison B	
	Unattenuated	Attenuated	Unattenuated	Attenuated
Mass	2,491 lbs. (1,130 kg)	2,623 lbs. (1,190 kg)	1,808 lbs. (820 kg)	1,918 lbs. (870 kg)
Drop height	148' (45 m)	164' (50 m)	115' (35 m)	115' (35 m)
V_{exit}	74.5 ft/sec (22.7 m/sec)	51.5 ft/sec (15.7 m/sec)	60.0 ft/sec (18.3 m/sec)	31.5 ft/sec (9.6 m/sec)
K_{exit}	108 ft-tons (292 kJ)	54 ft-tons (147 kJ)	51 ft-tons (138 kJ)	15 ft-tons (40 kJ)
System attenuation		50%		71%

The comparison data indicates that the test attenuator is capable of dissipating between 50% and 71% of the kinetic energy of a falling rock.

FULL SCALE TESTS – JAPAN

Hangar net attenuator systems have often been employed effectively in the field, but there has not been much field testing done specifically to assess their performance. The test site in Japan was constructed in order to analyze systems of this type. The test slope is approximately 100' (30 m) long at an angle of 45 □. A steel scaffold at the top of the slope supports the upper end of an H-beam monorail that extends down the slope. The test block is a fabricated concrete boulder 4' (1.2 m) x 4.5' (1.4 m) x 4.5' (1.4 m) with a weight of 7,900 lbs. (3,600 kg). The blockis mounted on wheels that are designed to fit onto the monorail (Fig. 7). The block is released at the top of the slope and slides to the bottom of the monorail where it is launched to strike the net freely at an impact angle of approximately 79 □.

Figure 7. Japan test siteFigure 8. Oblique view of netting

TEST HANGAR NET SYSTEM

The hangar net system used in the testing consisted of panels of high tensile spiral rope netting, and had overall dimensions of 88' (27 m) wide and 33' (10 m) high. The wide span of the netting was accommodated through the use of a catenary cable that provided vertical support to the top support rope and net panel (Fig. 7). Supplementary horizontal support ropes were installed at intervals of 8' (2.5 m) along the vertical plane of the netto help absorb impact energy and limit the horizontal deflection of the netting (Fig. 8). The net was attached to the supplemental horizontal ropes through the use of shackles at every other net opening. Braking elements were incorporated into the horizontal ropes on each side of the netting near the anchors.

RESULTS

The hanger net stopped the horizontal movement of the boulder in a braking time of 0.47 seconds, with a maximum horizontal net deflection of 17.8' (5.4 m) (Fig. 9). The velocity of the boulder at the time of impact was 62 ft/sec (19 m/sec) in the horizontal direction and 13 ft/sec (4 m/sec) in the vertical direction. The total energy dissipated by the hanger net system was 284 ft-tons (766 kJ). No load cells were used in the support ropes, but the forces can be calculated based on the maximum deceleration of 192 ft/sec^2 (58.5 m/sec^2) and the mass of the boulder. The resulting maximum anchor force is 47.2 kips (210 kN). Visual inspection of the netting and support

Figure 9. Side view of test impact to netting

system showed no damage after the test impact. This testing showed that the hangar net system is an effective means of absorbing impact energy in cases with this sort of challenging topography, and also provides empirical data with which to more effectively design site-specific real world systems of this type.

MODELING

Modeling as a stand-alone tool is not a reliable means with which to design rockfall protection systems. It is, however, a very useful and powerful tool with the proper incorporation of reliable input data from full scale field testing. The results of a large testing series (Glover et al., 2010) provided well-documented and detailed data regarding the system rope forces and the behavior of the drapery netting during rock impacts to attenuator systems. This data provides the means with which to calibrate a new finite element modeling tool (Fig. 10). A previously developed chain element model, FARO (Volkwein, 2005), gives a complete and reliable description of the complex behavior of high tensile, flexible steel mesh and netting when it is subjected to impact loading. Special care was taken in the development of this tool to ensure that it properly describes and numerically simulates the flexibility and elastic/plastic deformation capacity of the netting. The model has been calibrated and verified through comparison to mid-scale and full scale tests on typical rockfall barriers. By incorporating the empirical data gained in the field attenuator tests, it is now possible to perform a numerical investigation into the performance of flexible nettings used in attenuator systems.

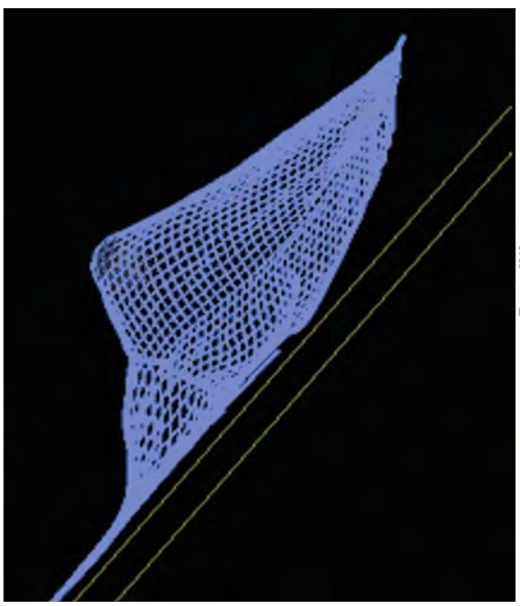

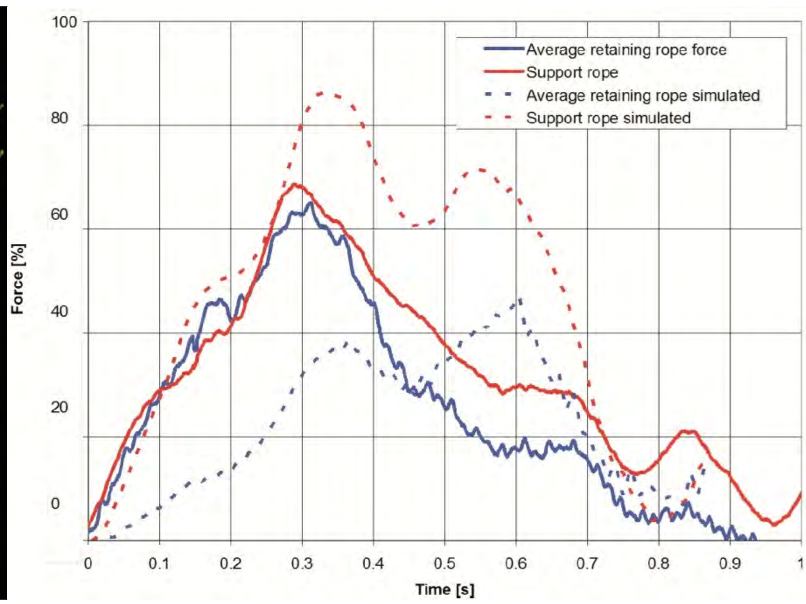

Figure 10.FARO simulationof St. Léonard attenuator impact

Figure 11. Simulated vs. measured rope forces

MODELED ATTENUATOR PERFORMANCE

Modeling confirms the field measurements and intuitive understanding that the loading within the attenuator barriers is significantly lower than that seen in conventional rockfall barriers. The strength of the system and the efficiency with which it dissipates energy is dependent upon slope topography and composition, impact energy at the entrance to the system, and the friction between the rock and the netting. Field tests have identified loading features such as an initial impact wave, mesh snagging, and tail drape exit wrapping. A further verification of the viability of the model is the fact that it also shows similar loading features (Fig. 10), as well as similar forces in the ropes (Fig. 11). The model has proven capable of measuring the attenuation capacity of a theoretical system including energy dissipated through ground contacts. This information provides a means with which to measure the effect of alterations on the system design, and provides invaluable guidance in making design decisions.

The current areas targeted for further investigation through modeling include the effects of net weight per unit area, changes in the length of the tail section of the drape, and changes to the size of the mesh opening. The initial calibration work in the modeling process has been done based on the barrier design used in the full scale testing program. With that as a starting point, design alterations can be made to the modeled barrier in order to investigate the effects on performance.

SMALL SCALE EXPERIMENTS

An additional part of the ongoing research into attenuator systems is small scale experiments. These experiments involved recreating field conditions as closely as possible in a lab setting. This allows experimentation in a tightly controlled setting with more frequent and extensive variation to the system components and inputs than is feasible in full scale testing.

A key element to small scale experiments such as these is proper scaling of the test equipment. For the attenuator model, scaling was done based on the physical similarity law which states that experiments with equal dimensionless parameters obtain equivalent results. The Pi-Buckingham theorem indicates which dimensionless parameters should be incorporated in order to ensure a complete and realistic representation of the environment. The test equipment is based on the St. Léonard test site described earlier. The scaling process indicated the following values for the small scale experiments (Table 2):

Table 2. Scaled test parameters

	St. Leonard test site	Small scale
Block velocity	34 ft/sec (10.4 m/sec)	34 ft/sec (10.4 m/sec)
Block mass	5,950 lbs. (2,700 kg)	1.1 lbs. (0.5 kg)
Net length	164’ (50 m)	4.3’ (1.3 m)
Net width	57’ (17.5 m)	1.9’ (0.6 m)
Net density	0.55 lbs/ft^2 (2.7 kg/m^2)	Varies

The test set-up has been constructed at the WSL Snow and Avalanche Research Institute lab facilities in Davos, Switzerland. The equipment consists of two primary frames – one supporting the launching system; and another that holds the test net, pressure cells, and high speed cameras. The outputs derived from the experiments include block trajectory, block velocity, edge motion of the net, and the forces exerted on the net’s support structure. The experiments are expected to lead to a better understanding of the interaction between the rock and the netting, and ultimately to an optimization of the energy dissipation that occurs as a result of the rock-net interaction. The small scale experiments are currently in the calibration phase.

CONCLUSIONS

Rockfall attenuators are a highly efficient and cost-effective means with which to address a variety of rockfall mitigation scenarios. The early designs have evolved in an organic way towards greater efficiency, and the current research has proven to be valuable in gaining an increased understanding of the performance of these systems. There is still ample room, however, for further research in supportof scientifically based design of attenuator systems. Effective research must include full scale field tests. Full scale testing provides both system validation and the empirical data necessary for modeling and small scale testing which are also valuable tools if properly applied. As long as they are founded on accurate and relevant empirical data, modeling and small scale testing offer the opportunity to perform a variety and quantity of test iterations that can greatly advance the understanding of the complex behavior of these systems. The primary areas for further research include a better understanding of the effects of unit net weight, the length of the tail section of the drape, and the size of the mesh opening. Obtaining a better understanding of the relationship of these parameters to overall system performance will enable more precise design of attenuator systems where the ultimate field performance can reasonably be expected to match the expected performance.

REFERENCES

Badger, T.C. et al, Hybrid Barrier systems for Rockfall Protection Proceedings of the IDWRP, Switzerland, 2008

Glover J., Volkwein A., Dufour F., Denk M., Roth A., Rockfall attenuator and hybrid drape systems – design and testing considerations, In: Darve, F.; Doghri, I.; El Fatmi, R.; Hassis, H.; Zenzri, H. (eds) Euromediterranean Symposium on Advances in Geomaterials and Structures. Third Edition, Djerba, 2010

Volkwein, A., Numerical simulation of flexible rockfall protection systems, Computing in civil engineering, Cancun, ASCE, 2005

CASCADE SUBDIVISION MILE 10.20 – ROCK FALL ANALYSIS AND PROTECTION OF RAILWAY WITH RING NET ATTENUATOR AND ROCK FALL BARRIER

A.J. Morris, P.Geol.
Canadian Pacific Railway
600-401 9th Ave SW
Calgary, AB T2P 4Z4
403-319-6617
tony_morris@cpr.ca

Duncan Wyllie, P.Eng.
Wyllie & Norrish Rock Engineers
1311 Howe St, Suite 200
Vancouver, BC V6Z 2P3
604-691-1717
dwyllie@wnrockeng.com

Tim Shevlin, PG
Geobrugg North America, LLC
4676 Commercial Street SE
Salem, OR 97302
503-423-7258
tim.shevlin@geobrugg.com

Dale B. Harrison, P.Eng.
Associated Engineering
1994 Comox Ave
Comox, BC V9M 3M7
250-339-9896
harrisond@ae.ca

Prepared for the 63rd Highway Geology Symposium, May 7-10, 2012

Acknowledgements

Geotechnical designs were provided by Duncan Wyllie of Wyllie & Norrish Rock Engineers. Structural engineering drawings were provided by Dale Harrison Associated Engineering Ltd. The installing contractor was Emil Anderson Construction Ltd.

Disclaimer

Copyright Notice

ABSTRACT

The unique requirements of operating a railroad combined with the need to cross extensive stretches of mountainous terrain present many challenges to the Canadian Pacific Railway (CP) in dealing with rock fall hazards. As part of CP's rock slope stabilization program, rock fall analysis indicated a potential hazard at Mile 010.20 of the Cascade Subdivision on the west side of the Fraser Canyon.

Rock fall records and site investigation identified a source area located approximately 270 meters above track level. The height of the source area combined with a slope topography that resulted in multiple potential paths to the track indicated that the most cost-effective overall solution for the site would be two separate mitigation systems. A 42 meter long attenuator using Geobrugg's ROCCO ring nets was installed at the location where it was possible to excavate catchment ditches. Just to the west of this system above a tunnel portal, a 32 meter long GBE-500A rock fall barrier was installed. After construction a LIDAR scan was performed in order to record the as-built condition of the site.

This paper will discuss the site investigation, the design process, and the installation of the systems. It will illustrate the ways in which both solutions were chosen relative to the site conditions and how the specific protection goals were met at the site.

INTRODUCTION

For nearly 40 years the Canadian Pacific Railway (CP) has carried out a comprehensive rock slope stabilization program on their continent-wide track system with the objective of reducing the frequency of rock falls and improving both safety and operational efficiency. The program comprises an annual inspection of every rock cut to assign a hazard rating, keeping rock fall records and carrying out stabilization work at selected sites. An important component of the program is the maintenance of a database of all inspections, stabilization work and rock falls in order to identify high hazard sites and implement pro-active remedial work.

The Cascade Subdivision on Canadian Pacific Railway's Vancouver Division extends for 129 miles from Mile 0.0 at North Bend to Vancouver, British Columbia, winding through some of the most rugged topography in British Columbia. An extremely narrow corridor through the steeply walled Fraser River Canyon has proven to be an active rock fall zone for many years affecting CP operations, particularly on the western side of the valley between Miles 2.0 and 14.0 (Figure 1). The annual inspection process identified a significant hazard at a location in the Fraser Canyon in British Columbia, designated as Mile 10.20 Cascade Subdivision. Rock fall analysis and mitigation design were undertaken resulting in construction of a hanging attenuator system using Geobrugg ROCCO ring nets and a GBE-500A rock fall barrier with TECCO mesh.

Figure 1. Cascade 10.20 - Project location

LOCAL GEOLOGY

Situated in the late Jurassic to early Tertiary primarily granitic Coast Mountains, the Fraser River Canyon was formed in the Miocene age by the river cutting into the uplifting Interior Plateau (Figure 2). The river follows the line of the north-south Fraser Fault system, which divides the Eastern Coast and Inter-montane belts of the southern Canadian Cordillera. Intermittent phases of thrust faulting, folding, volcanic, and plutonic events have created an extremely complex geologic evolution in the Fraser Canyon.

Rocks in the Cascade 10.20 area have been mapped as early and middle Cretaceous age grano-diorites with minor mafic rocks and gneissic phases of the Spuzzum pluton. Joint sets are well developed with at least 2 major orthogonal joint sets identified in intersections resulting in large blocks up to 1cubic meter.

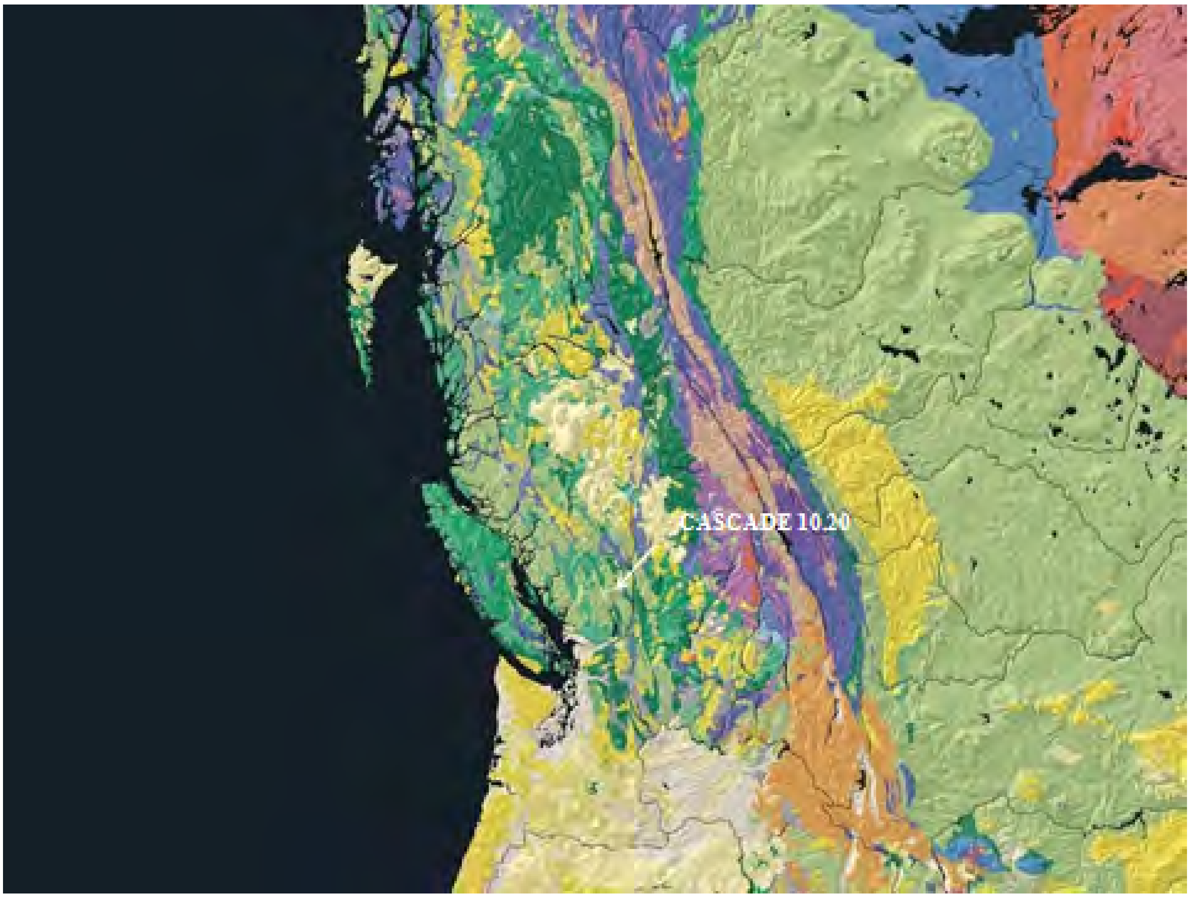

Figure 2. Geological map of southern Canadian Cordillera

CASCADE 10.20 ROCK FALL HISTORY

Rock fall problems have always been a problem at the Cascade 10.20 site. The CP database has over 110 recorded rock fall incidents between Mile 10.10 and 10.20 from 1975 to 2009 (Figure 3). During this time eight rock falls resulted in damage to trains, one derailment occurred, and over eight rock falls resulted in damage to the slide fence detector or track bed below. A dramatic increase in rock falls between 2003 and 2004 drew attention to this site resulting in a detailed rock fall mitigation study. Rock falls continued at the site on an annual basis and in 2007 a rock fall of nearly 17 cubic meters caused damage to the concrete retaining wall, many rails, and clips on a bridge at the site. In 2008 a rock fall caused damage again to the retaining wall below.

Figure 3. CP database records for all rock falls at Cascade 10.20

PREVIOUS MITIGATION AND STABILIZATION WORK

An electric rock fall detector fence of parallel wires was installed in the 1960's to alert approaching trains of a rock fall that triggers the fence and activates the signal system. Between 1976 and 2009 rock stabilization in the form of tree removal, hand scaling, rock bolting, drain installation, concrete buttress construction, shotcrete placement and mesh installation was carried out between Cascade 10.10 and 10.20 as per the following summary:

Table 1. Summary of Previous stabilization work at Cascade 10.20

Year	Mileage	Stabilization Work Description
1976	10.10	Scaled loose rock; 30m rock bolts
1978	10.10	Scaled loose rock; 30m rock bolts
1981	10.20	Scaled loose rock; 30m rock bolts
1984	10.10	Minor scaling following rock fall
1988	10.10	Trees removed; extensive scaling; 18m rock bolts
1991	10.10	Brush removed; drainage pipes installed; shotcrete placed; loose rock removed
1993	10.10	Trees removed; scaled 40m wide area; 50x3m rock bolts
2001	10.10	Scaled loose rock; 18x3m, 19x6m rock bolts; 24x1.8m dowels for catchment fence
2002	10.10	Brush removed; scaled; 8x5m rock bolts; drains; shotcrete
2006	10.10	Scaled; 78.5l.m. rock bolts; 3 concrete buttresses; shotcrete
2007	10.10	Brush removed; Scaled loose rock
2009	10.10	Scaled loose rock; 3x3m rock bolts

SITE DESCRIPTION AND ROCK FALL INVESTIGATION

The Cascade 10.20 site is a single track railway located on a 5 meter wide bench. Above the bench are near vertical rock cut faces up to 25 meters high and below the bench are retaining walls and steep rock slopes extending approximately 50 meters down to the Fraser River. The natural slopes above the crest of the rock cuts are about 500 meter high and have an overall angle of 40 to 50 degrees. In addition, tunnels are located at either end of this 200 meter long length of track making visibility to observe rock falls on the track very restricted. A further component of the hazard at this location is the high precipitation levels and frequent freeze-thaw cycles that tend to trigger rock falls in the winter.

The records for this site contained in the database indicated an increase in rock fall activity between 2003 and 2004. The damage to the track and structures from these incidents together with the severe consequences of additional rock falls identified the site as a high priority location for stabilization work. A detailed investigation involving both climbing the slope and observations from a helicopter were carried out in January of 2010 to determine the probable source, path, and trajectories of rocks falling above the track. The majority of all rock falls were believed to be concentrated down a chute situated 30 meters above the track side rock cut and below the natural talus slope angled at nearly 40 degrees (Figure 1, 4). Rock falls also have originated from the cut face immediately east of Mile 10.20 at the tunnel portal and from a relatively loose talus slope above this cut.

Figure 4. Cascade 10.20 rock fall source location, el. 270m above track

The field investigation identified an area of active movement about 270 meters above the track as the primary source of rock falls. A traverse was made above the chute to an elevation of about 200 meter above the track where the base of an outcrop was observed. The 40 degree slope below the outcrop rock face was found to be littered with rocks varying in size from 0.25 to 1.0 cubic meters leading to the conclusion that the rock fall source was from this rock face. Many large trees bore evidence of scarring by bouncing rocks. The helicopter inspection revealed a fresh rock fall scarp at the top of the exposed face with a large open tension crack (Figure 4). This scarp and loose blocks observed at an elevation of about 270 meter above the track was identified as the rock fall source. Based on both the site inspection and a topographic survey two separate cost effective rock fall protection measures were necessary to mitigate the hazard at Cascade 10.20.

ROCK FALL ATTENUATOR

Attenuation is the loss in intensity of any flux through a medium. In this respects the purpose of rock fall attenuator systems is to reduce the kinetic energy of rock fall and guide their trajectory. They function by intercepting rock fall trajectory, guiding it under a tail drape and dampening bounce heights. Through this there is the potential to dissipate large portions of the kinetic energy through barrier impacts deforming the netting and interaction with the slope during its transport to the base of slope. Rock fall attenuators systems are aimed at reducing the cleaning and maintenance requirements in comparison to standard rock fall barriers. They can also be applied where existing protection measures, such as rock galleries, do not meet the required energy level of rock fall hazard. The installation of an attenuator system can be used to dissipate the energy of rock fall to the design value of the existing installations (Wendeler and Vaero, 2011).

At the rock fall chute on the east end of the site a 40 meter length of slope was identified for mitigation by a hanging rock fall attenuator system made of Geobrugg's ROCCO ring nets (Figure 5). This portion of the site was well suited for an attenuator fence because of the space for a rock fall fallout zone at the toe of the track. The limited rockfall catchment area at the base of the chute was enhanced by drilling and blasting a larger ditch into the rock wall.

Figure 5. Completed Attenuator net 2010

The ROCCO ring net attenuator system was designed with three different net sections depending of the impact energy and the topography in relation to the likely rock fall trajectories. At the east end of the rock fall chute where the rock falls from the upper slope were concentrated a 1,100 kJ attenuator system was required. At the west end of this 40 meter long length of slope rock fall were only likely to occur from a height of about 20 meter the attenuator fence was designed for a 500 kJ impact.

Based upon the slope height, slope angle, observed block sizes and anticipated load conditions the potential rock fall trajectories were calculated (D.Wyllie) and the following design criteria for the structural design of hanging attenuator net were determined:

1. Rock Impact Load = 1,100 kJ
2. Dead Load on net = 8.6kg/sq.m
3. Ice Load (10mm Radial Ice) = 0.23 kPa
4. Wind Load (No ice) = 0.19 kPa (Gust 78-110 km/hr)
5. Wind Load (Ice) = 0.31 kPa (Gust 55-79 km/hr)
6. Top elevation of support posts 22m above top of rail

The final components of the attenuator net system consisted of three 5.5m high posts and an anchor bracket to support five net panels 3 x 20 m and nine net panels 3 x 17 m across a total length of 42m and located to span across both sides of the chute area (Figures 6 to 9).

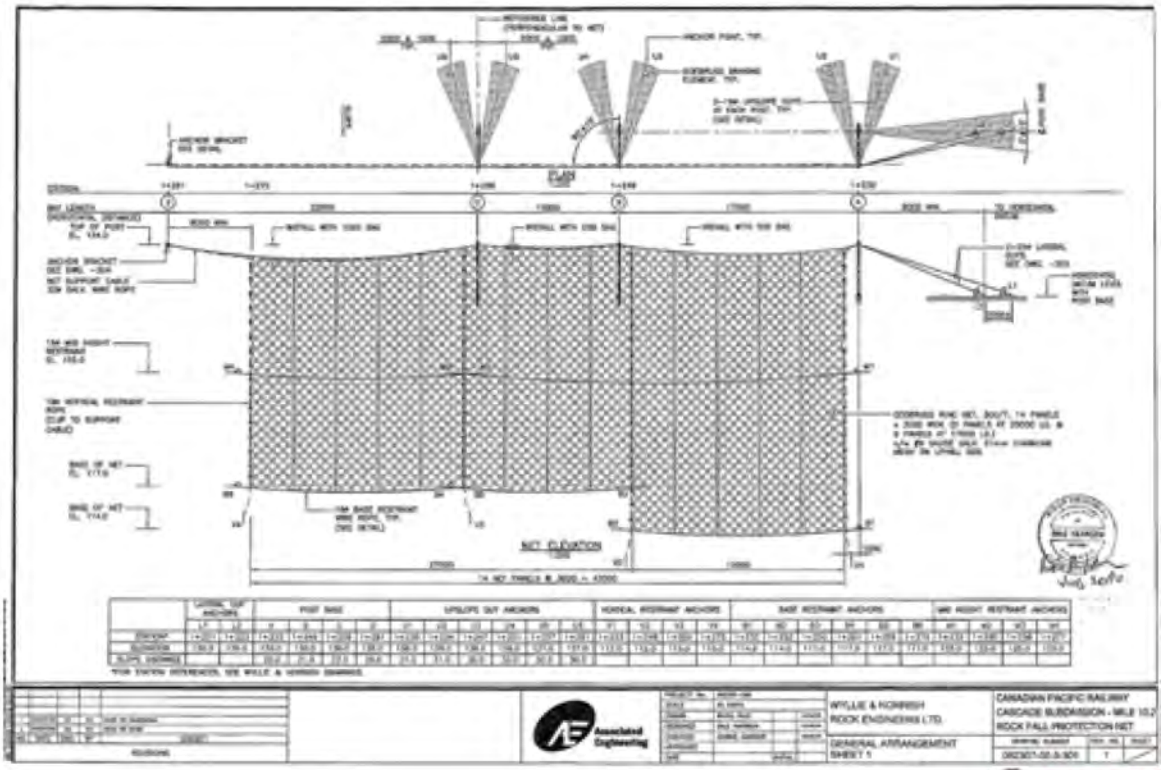

CANADIAN PACIFIC

Figure 6. Design drawing showing attenuator net layout (D.Wyllie & Associated Engineering)

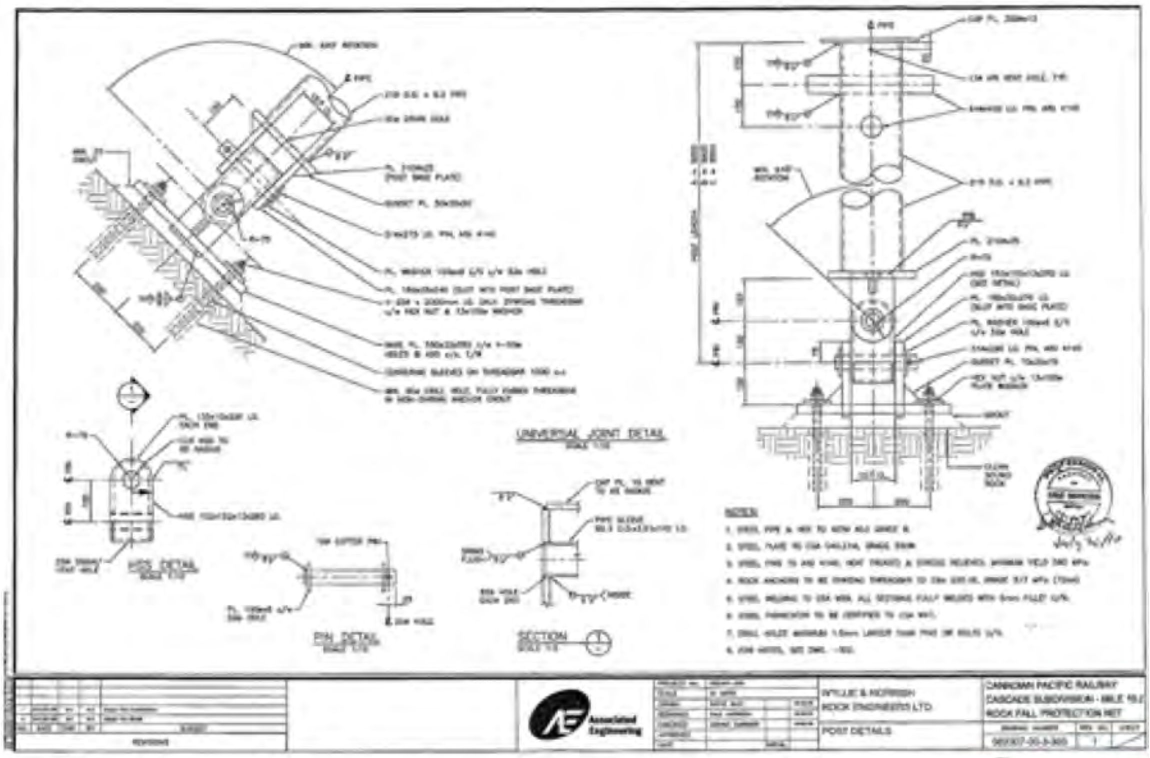

CANADIAN PACIFIC

Figure 7. Design drawing showing post hinge detail (D.Wyllie & Associated Eng.)

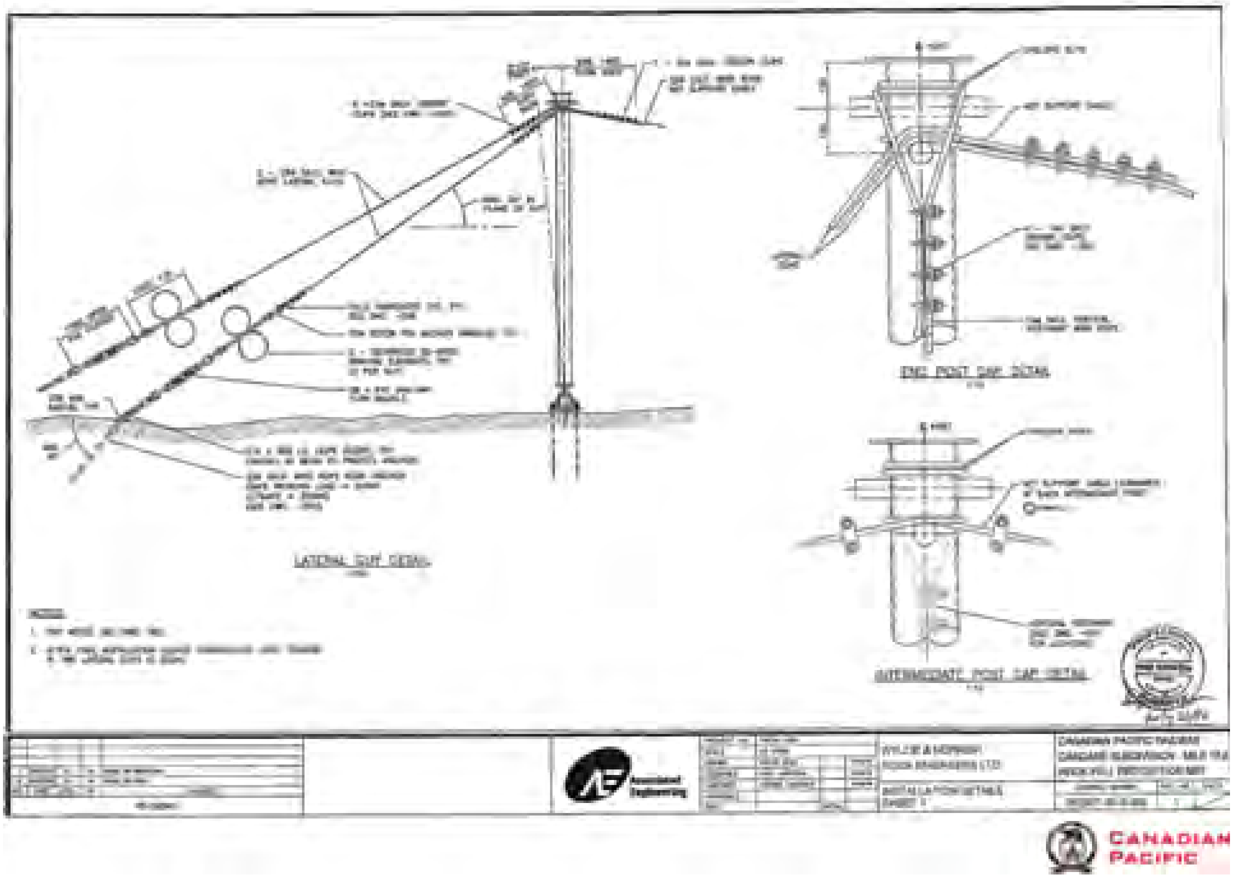

**Figure 8. Design drawing showing post and tieback details
(D.Wyllie & Associated Engineering)**

ROCK FALL BARRIER

A different solution was required immediately to the west of the attenuator net to mitigate the rock fall hazard from the rock face and talus slope above the tunnel. At this location a traditional rock fall fence that stops and catches rock fall was required. At this location a 32 meter long GBE-500A rock fall barrier with TECCO mesh was installed (Figure 9).

As rock fall barrier protection has become more widespread over the past several decades there are a number of different testing techniques for approval and certification. Since 2001 the standard for rock fall barrier certification was the Swiss Rock Fall Guidelines. In 2008 a new rock fall testing and approval guideline was implemented by European Organization for Technical Approvals (EOTA). The new European Technical Approval Guideline 027 (ETAG 027) is now becoming widely accepted. A favorable assessment of a rock fall barrier by a qualified testing body is indicated by a European Technical Approval (ETA) and the CE marking for product conformity (Amend, 2010).

Figure 9. Completed GBE-500A rock fall barrier

GBE-500A ROCK FALL BARRIER

Geobrugg's GBE suite of rock fall barriers fully complies with ETAG 027 fulfilling the most stringent requirements of EOTA barrier testing guidelines. The GBE line of rock fall barriers spans the complete spectrum of rock fall energy classes with barriers designed to stop rock fall from energies of 100 kJ now up to 8,000 kJ. All of these systems have the ETAG 027 "A" rating the highest of ETAG 27 for residual useful height (EOTA, 2008).

The rock fall barrier utilized at the Cascade 10.20 was the GBE-500A (ETA - 09/0085) rock fall barrier designed for a Maximum Energy Level (MEL) impact of 500 kJ. The GBE-500A has a residual barrier height of 66% after an MEL impact earning the "A" rating. In addition to having a valid ETA the GBE rock fall barriers are designed with a number of features making them efficient to install and cost effective. Owners and contractors realize cost savings with the use of GBE barrier system due to their:

1. Rapid installation through modular design,
2. Use of light-weight efficient components,
3. Simple anchorage thanks to lower force transmission,
4. No secondary mesh required

The primary structural netting of the GBE-500A rock fall barrier is TECCO mesh that factory attached to the post making a post-netting module that significantly reduces installation time and effort (Figure 10). At the Cascade 10.20 site the five post-mesh modules were installed on the anchor foundations with a helicopter in just 30 minutes. After seaming the top and bottom support ropes through the installation tube guide the TECCO mesh is quickly "curtained" between the posts and into place.

Figure 10. Installation of GBE barrier utilizing helicopter

The GBE rock fall barrier system is designed with other specialized components that increase system efficiency. One component is the running wheel that guides the support ropes smoothly along the posts reducing friction during an impact (Figure 11). A new brake system called the U-brake operates by pulling stainless steel bar 180 degrees around a hardened steel pin dissipating energy through deformation of the bar (Figure 11). The U-brake has a consistent flat deformation and braking process thereby making rock fall impacts more even. The brakes are installed completely outside the system making their replacement quick and easy after they are completely activated.

The efficiencies of the running wheel and U-brake help to keep the impact forces that are transferred to the foundation low in comparison to other system of the same energy. This in turn allows for smaller foundations with a single primary micropile anchor plus a small secondary anchor (Figure 11). Smaller foundation allow for easy fast installation of further reducing overall project costs.

The need for secondary mesh is eliminated on the 500 and 1,000 kJ GBE barriers by utilizing high-tensile strength TECCO (G80-4 mm) mesh as the primary structural netting (Figure 11). The high strength and flexible TECCO mesh (G80-4mm) has an in-circle opening of only 80 mm (3.14 inches). This is a much smaller opening compared to the 12 inch opening typical of other rock fall barriers. A barrier with a primary mesh opening of only 80 mm eliminates the need for using a low-strength secondary mesh backing for stopping small rock fall.

Figure 11. GBE Components clockwise from top right: Post and Running Wheel, U-Brake, TECCO Mesh (G80-4mm), Post Foundation.

CONSTRUCTION

The two main issues with construction of the rock fall mitigation at the Cascade 10.20 site involved train scheduling and access to the site. All the work was carried out under live track conditions with up to 40 train movements scheduled per day. Coordinating the work on such a busy track was a considerable undertaking considering the Fraser River Canyon is a primary rail corridor. The equipment needed for construction was a 50 ton crane and a 20 meter reach man-lift, both of which had to occupy the track during construction because of the narrow width of the bench on which the rails are located (Figure 12). This restricted work area and frequent train movements dictated that work could only proceed in short time windows between train movements.

Site access was further complicated due the rockfall hazard being on a stretch of track between two tunnels. The only available staging-laydown area for equipment and materials was to the west of the site, through a 150 meter long tunnel. Each time train movements occurred both the crane and man-lift had to boom up or down in order to mobilize and demobilize through the tunnel. The pre-attached modular design of the GBE barrier and helicopter installation reduced crane time providing valuable cost savings considering the unreliable track scheduling.

While the train schedule and site conditions limited the available work time per day, the expertise of Emil Anderson allowed much of the work to be carried out from ropes suspended at anchor points along the crest of the rock cuts. This allowed work to proceed on such tasks as drilling and installing rock anchors for the post base plates and guy wires without interruption by the passage of trains.

Figure 12. Construction of Attenuator net posts using 50T crane

CONCLUSION

Small foot print system such as rock fall barrier and attenuator systems are often times the only effective mitigation strategy for tight sites such as the Cascade 10.20 location. Using such mitigation strategies are integral in keeping construction costs down on railway projects where construction (Contract Work) costs can be high due to limited work windows and very difficult working conditions in an isolated area. In addition, material costs and time required for installation of these systems are extremely low compared to the high cost of rigid solutions such as rock fall sheds or large gravity structures. These considerations are extremely important when considering the high cost of construction along active railways.

Table 2: Cost breakdown of Cascade 10.20 Rockfall Mitigation

	Rock Fall Attenuator	Rock Fall Barrier/Bolts
Contract Work	64%	68%
Engineering	11%	6%
Supervision	5%	10%
Equipment Rental	11%	6%
Materials	8%	7%
Total Cost	100%	100%

As described in this paper the Cascade 10.20 site has a long history of rock fall. With increased weathering, rock fall intensity and frequency increased to a point that the existing rock fall detector signal fencing was not sufficient for preventing intolerable rock fall hazards to the railway. The use of rock fall attenuator systems using ROCCO ring nets are shown here to be an effective solution to rock fall hazard. With proper design by an engineer experienced in rock fall, relatively small attenuator systems can be placed at the toe of tall slopes providing maximum protection from hazards high above. At locations such as the Cascade 10.20 tunnel rock fall barriers, such as the ETAG approved GBE-500A, are the best solution for stopping rock fall from impacting a facility.

REFERENCES

Amend, Frank, 2009, *Innovations in rock fall barriers and the new European Standard ETAG 027*, Geobrugg North America Geohazard Solutions Technical Document, Romanshorn, Switzerland, 12.

EOTA, 2008, *ETAG 27GUIDELINE FOR EUROPEAN TECHNICAL APPROVAL Of FALLING ROCK PROTECTION KITS Edition 2008 - 02 – 0*, European Organization for technical Approvals, Brussels, 53.

Wendeler, Corinna and Cesar Vera Valero, 2011, *Rock fall attenuating system reduces the kinetic energy of rock fall and guides their trajectory*, Geobrugg AG, Geohazard Solutions Technical Document, Romanshorn, Switzerland, 12.

Geotechnical Investigation for the K-7 and I-70 Interchange
Bonner Springs, Kansas

Kyle Halverson
Kansas Department of Transportation
2300 Van Buren, Topeka, KS
785-291-3861
E-mail: kyleh@ksdot.org

Prepared for the 63rd Highway Geology Symposium, May 7-10, 2012

Acknowledgements

Recognition is given to Jim Burns: Engineering Technician Specialist, Sean Hudson Engineering Technician Senior for their assistance in completing the field work of this project. Also recognition should be given to Bob Henthorne: Kansas Department of Transportation Chief Geologist for his support organizing and facilitating each step taken to ensure the project has progressed efficiently.

Disclaimer

Statements and views presented in this paper are strictly those of the author, and do not necessarily reflect positions held by their affiliations, the Highway Geology Symposium (HGS), or others acknowledged above. The mention of trade names for commercial products does not imply the approval or endorsement by HGS.

Copyright Notice

ABSTRACT

The K-7 and I-70 interchange is a proposed project set forth to accommodate the growing city of Bonner Springs, KS as well as increase the traffic flow into Kansas City. Currently this is the second (2^{nd}) busiest interchange in all of Kansas City. Approximately 145,000 vehicles a day travel through the existing major system to system interchange. The design for the proposed interchange includes expansion of existing I-70 and K-7 to accommodate the traffic volume projected in the future as well as construction of new ramps and collector roads.

The project has ten (10) proposed phases. To date, KDOT has completed Phases 1 through 3, which are associated with the expansion of I-70 to six lanes, construction of new loop ramps in both the northwest and southwest quadrants of the existing K-7 and I-70 Interchange and two (2) bridge replacements at Riverview Ave. and 118^{th} St. We have portions of Phases 4 and 9 completed and are preparing to begin work on the remainder of Phase 4 and Phase 6.

The management of what has been done and what needs to be done has been a challenging obstacle that we faced since the project began. Since our geothechnical investigation has started, we have had to be flexible on which Phase we could work on due to landowner permission, right of way acquisition, designer needs, and information availability. We have also had to revisit and re-drill due to changes in design and site access. The geology of the site has posed many obstacles alone. In this area, the Tonganoxie Sandstone Member lies disconformably on the Stanton Formation where it cuts through the Iatan Limestone and Weston Shale Members. This disconformity developed by the infilling of existing deep erosional channels during the deposition. The Tonganoxie Sandstone encountered across the majority of the site contains thick sequences of fine grained, cross-bedded sandstone with several thin, non-continuous, interbedded sandy shales.

To date there have been over 200 power auger borings performed for approximately 5 miles of surface geology investigation and 3 bridge foundation investigations. KDOT's geotechnical investigation on the proposed infrastructure continues to be done as needed through this developing suburb of Kansas City. Construction is set to start early in 2013 on Phase 2 and letting date of mid 2013 for Phases 1 through 3. The remaining phases do not have let dates at this time.

As the state of Kansas grows, so does the need for development and improvement of our infrastructure. As geologists, we need to ensure that we provide the most accurate preliminary design information possible.

PROJECT DESCRIPTION

The K-7 and I-70 Interchange project was developed to upgrade an existing major system to system interchange. This project will have a significant impact to the traffic flow movement in and out of Bonner Springs as well as Kansas City. Currently the interchange is the second (2nd) busiest in all the Kansas City area. Approximately 145,000 vehicles a day travel through the existing interchange. The design for the proposed interchange includes expansion of existing I-70 and K-7 to accommodate the traffic volume estimated to triple by 2030 as well as construction of new ramps and collector roads.

The project has ten (10) proposed phases. Phases 1 through 3 are associated with the expansion of I-70 to six (6) lanes, construction of new loop ramps in both the northwest and southwest quadrants of the existing K-7 and I-70 Interchange and two (2) bridge replacements at Riverview Ave. and 118th St. Phases 4 through 10 are proposed construction of new loop ramps east of K-7, the widening of existing K-7 and construction of new collector distributor routes along both I-70 and K-7. Currently KDOT has funding for final design on Phases 1 through 3 and construction of the new bridges at Riverview Ave. and 118th St. associated with Phase 2.

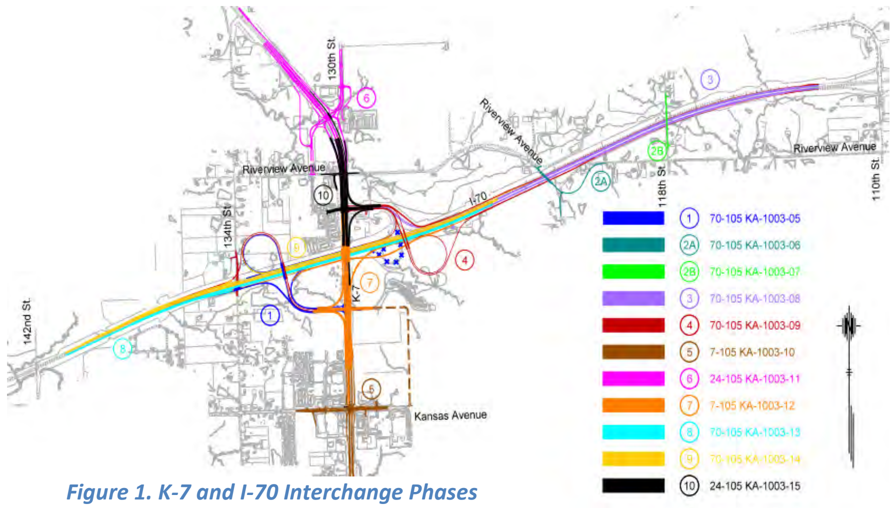

Figure 1. K-7 and I-70 Interchange Phases

PROJECT LOCATION

Figure 2. Project Location Map

The proposed K-7 and I-70 Interchange is located along the existing I-70 and K-7 corridor north of the city of Bonner Spring in Wyandotte County, Kansas. Bonner Springs has a population of 7,314 people according the 2010 US Census. It is a suburb of Kansas City, since only being located approximately 4 miles west of Kansas City, KS. The project area however is a traffic hub for three (3) counties: Johnson, Leavenworth, and Wyandotte. At 143 square miles, Wyandotte County is bound by the Missouri River on the north and east side, while the Kansas River marks the extent of the county to the south. Wyandotte is the smallest of the 105 counties in the state of Kansas and ranks fourth (4th) in population.

GEOLOGIC SETTING

The geologic setting of this area is unique as it represents the boundary from a regressive time with sub-arial exposure and severe erosion to a trend of deep water deposition. The bedrock units that have been encountered across the project are comprised of Pennsylvanian age rock. All of the units are Upper-Pennsylvanian and range between the Virgilian and Missourian Stages. The upper most stratigraphic unit encountered is part of the Stranger Formation. The basal section of the stratigraphic column on the project is the Merriam Limestone. This sequence represents approximately 112 feet of geologic section. The underlying geology is masked by glacial deposits from the Pleistocene Epoch. The extent of glacial advancement was just south of the project area approximately 11 miles. This has resulted in the topography of Wyandotte County being very similar to much of northeast Kansas. The topography ranges from low lying stream valleys to rolling upland hills cover by thick deposits of loess and glacial drift. The glacial deposits are characterized by thick deposits of till material with glacial erratic and loess.

Virgilian Stage
Douglas Group
Stranger Formation
<u>Tonganoxie Sandstone Member</u>

This member was encountered over much of the project. The sandstone stratigraphically "cuts" through the Iatan Limestone and Weston Shale Members and lies disconformably on the Stanton Formation. The Tonganoxie Sandstone was developed by the infilling of existing deep erosional channels. This unit contains thick sequences of fine grained, cross-bedded sandstone with several thin, discontinuous, interbedded sandy shales. Also at the basal portion of the Tonganoxie Sandstone, a lateral discontinuous sequence of shales and calcite cemented conglomerate have been observed. The conglomerate consisted of fragments of sub-rounded to sub-angular limestone and shale. The sub-angular edges of the limestone and shale are indications that the material has not traveled an extended distance from its origin and is locally derived from the erosion of the Iatan Limestone and Weston Shale just prior to the deposition of the Tonganoxie Sandstone. Locally, the distinction between the very competent basal conglomerate and the top of the South Bend Limestone has been very difficult using power auger soundings.

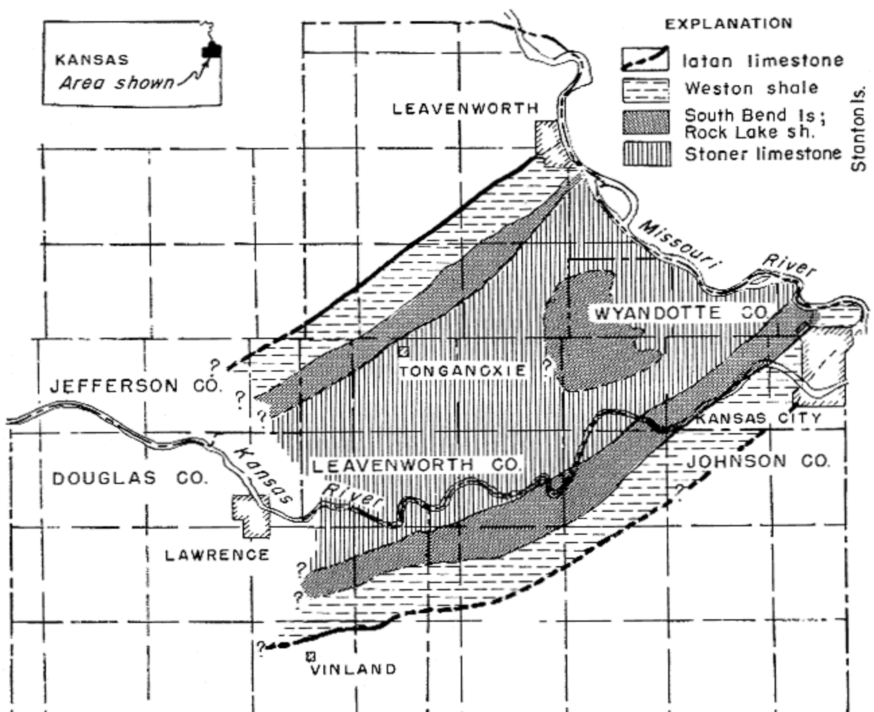

Figure 3: Tonganoxie Valley

Missourian Stage
Lansing Group
Stanton Formation
South Bend Limestone Member

The South Bend Limestone Member consists of 0 to 3.8 feet of unweathered to slightly weathered, greenish gray to brownish gray, well cemented, very hard, limestone. This limestone contains a broad assemblage of fossils ranging from *Echinodermata* to *Bivalvia*. Due to erosion, the "South Bend" may be replaced by the Tonganoxie Member.

Rock Lake Shale Member

The Rock Lake Shale Member varies from 0 to 7.5 feet of hard to medium hard, unweathered to slightly weathered, grayish green to olive green sandy shale. This shale weathers to a yellowish-gray, clayey shale. In this area, the Rock Lake is classified as a nondurable shale. The designation of nondurable or durable shale represents the unit's ability to maintain its structure and resist erosion when exposed to the elements. The Rock Lake was given to this classification because of its characteristics observed during our field investigation and from historical data. A backslope of 3:1 was recommended to ensure that the integrity of the slope would not be compromised over time.

Stoner Limestone Member

The Stoner Limestone Member consists of 0 to 14.0 ft. of gray to dark gray, well cemented, fossiliferous, very hard limestone. Occasional shale seams approximately .1 to .3 feet thick were observed interbedded within the limestone. Where covered by soil mantle, the Stoner Member tends to weather severely and develop large vertical joints that may extend through the entire unit. These joints are filled with expansive red-brown residual clay. This jointing and weathering will cause problems creating uniform lines along the backslopes and tends to form an irregular face, even when pre-split. During the construction and pre-splitting of the backslopes in the Stoner Limestone, the contractor must conduct a 100 ft test section. This will ensure that the backslopes are uniform and meet all recommendations associated with pre-splitting and backslope design.

Eudora Shale Member

The Eudora Shale Member observed across the site is composed of approximately 7.7 ft of gray to black fissle shale, non-weathered to weathered, hard to very hard, and well compacted. This unit is helpful in confirming the rock units in the stratigraphic column due to the unique black shale in this portion of the stratigraphic sequence. The Eudora Shale can be considered durable if unweathered. The Eudora Shale observed across the site will be considered as durable shale.

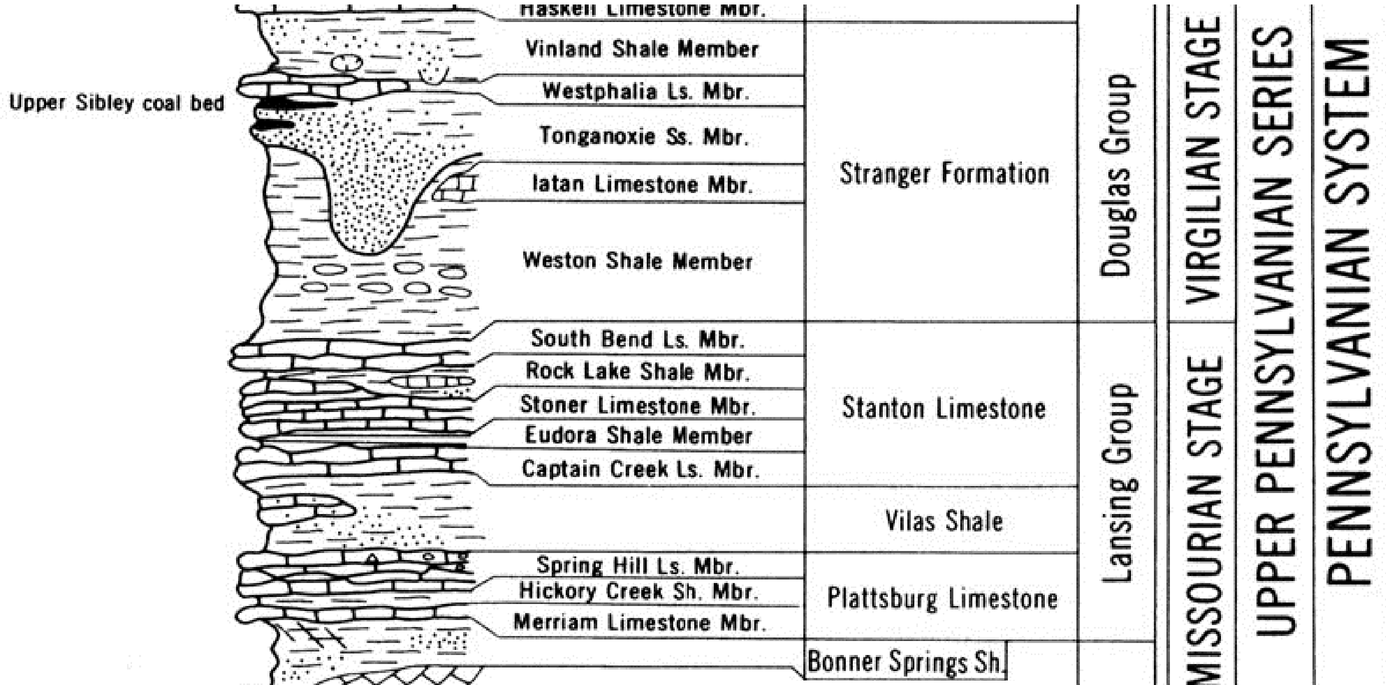

Figure 4: Stratigraphic Column through Project site

PROJECT INVESTIGATION TIMELINE

The K-7 and I-70 project has spanned more than three years of episodic field work. The initial surface investigation for Phase I began in March of 2009 along I-70 where the existing I-70 will expanded from four (4) lanes to eight (8) lanes and then continued to the proposed new ramps in the northwest and southwest quadrants.

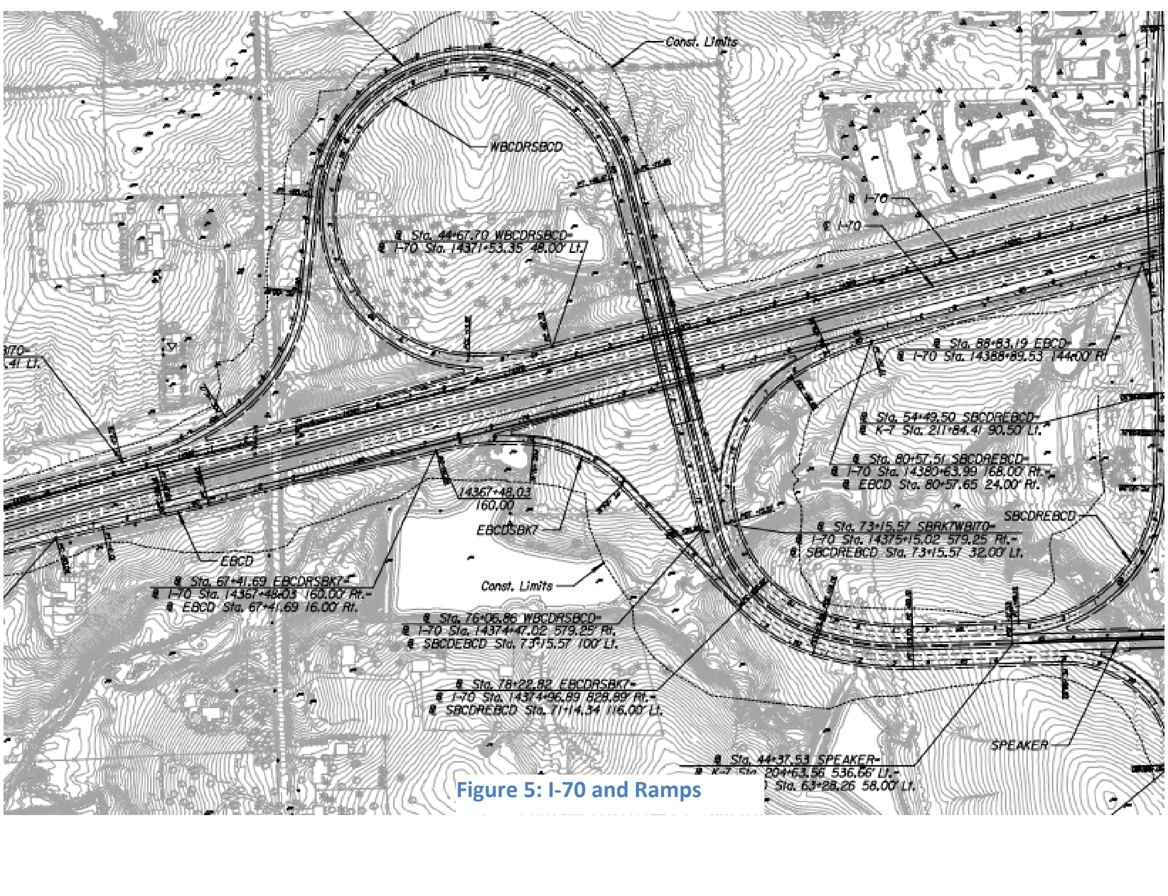

Figure 5: I-70 and Ramps

The second phase of the geotechnical investigation began in June 2010 and included surface geology and bridge replacements on Phase 2 at Riverview Ave and 118th St. These locations will be expansions of the existing roads from narrow two (2) lane road to a super two (2) lane with shoulders.

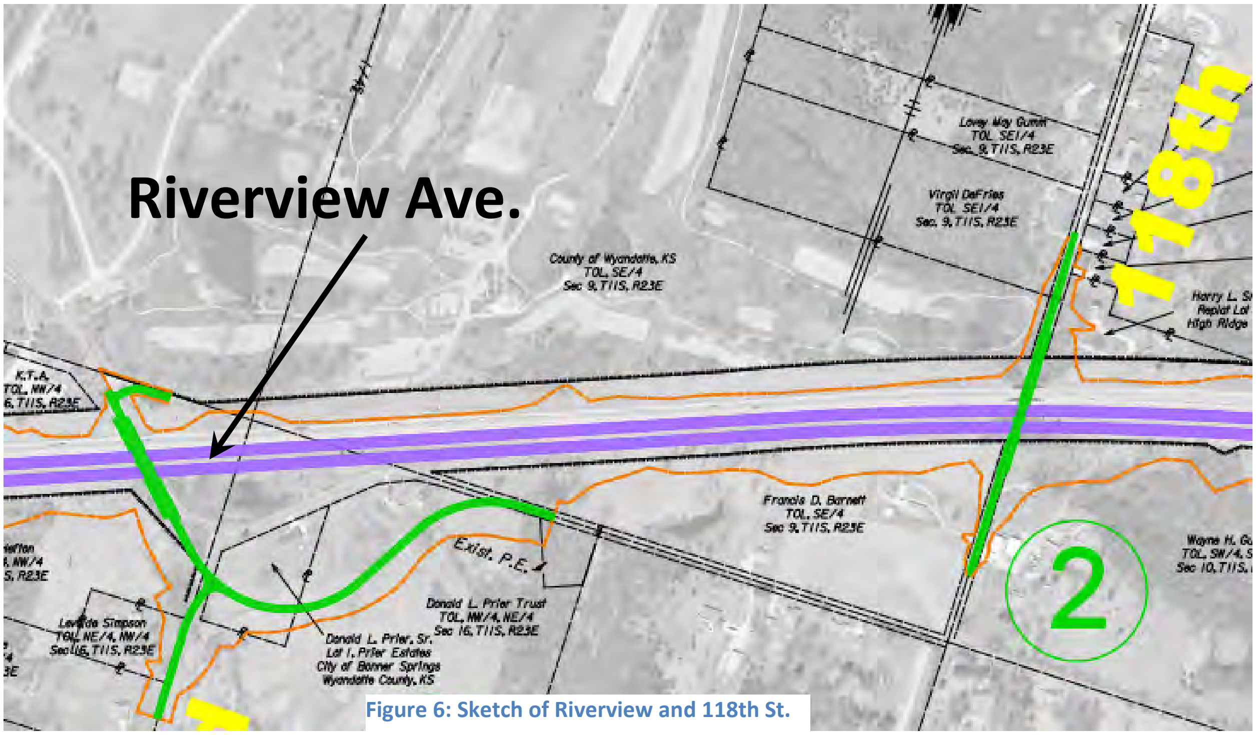

Figure 6: Sketch of Riverview and 118th St.

The third phase of drilling that has taken place was for a bridge foundation investigation along the proposed Ramp C in Phase 1. We also did the surface investigation for 134th St. realignment which is associated with Phase 4. The foundation investigation for the Ramp C bridge was conducted in March 2011 and the surface geology for 134th St was done in May of 2011.

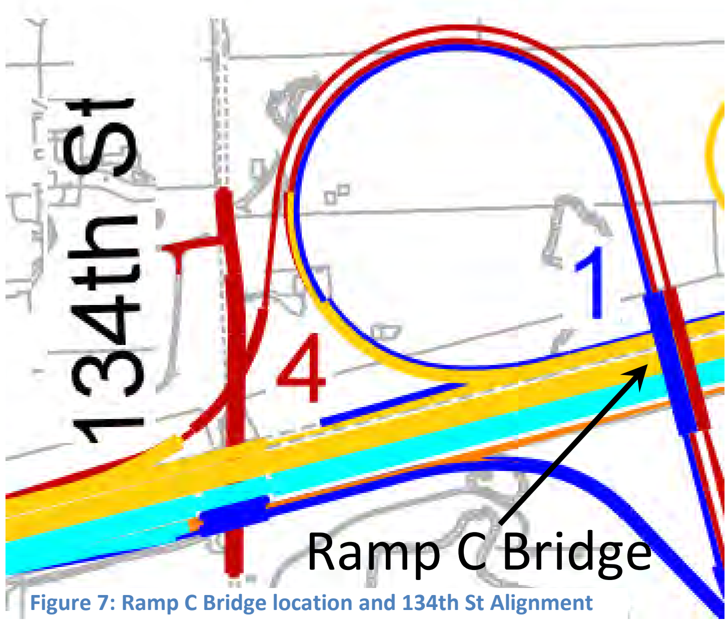

Figure 7: Ramp C Bridge location and 134th St Alignment

The next phase of field work is set to begin in March of 2012 on Phase 5. Work will be done along existing K-7 Highway and Kansas Ave. This intersection currently is a lighted four (4) way stop, however proposed plans call for a new Diverging Diamond intersection to replace it. This phase has a completion date August 2012.

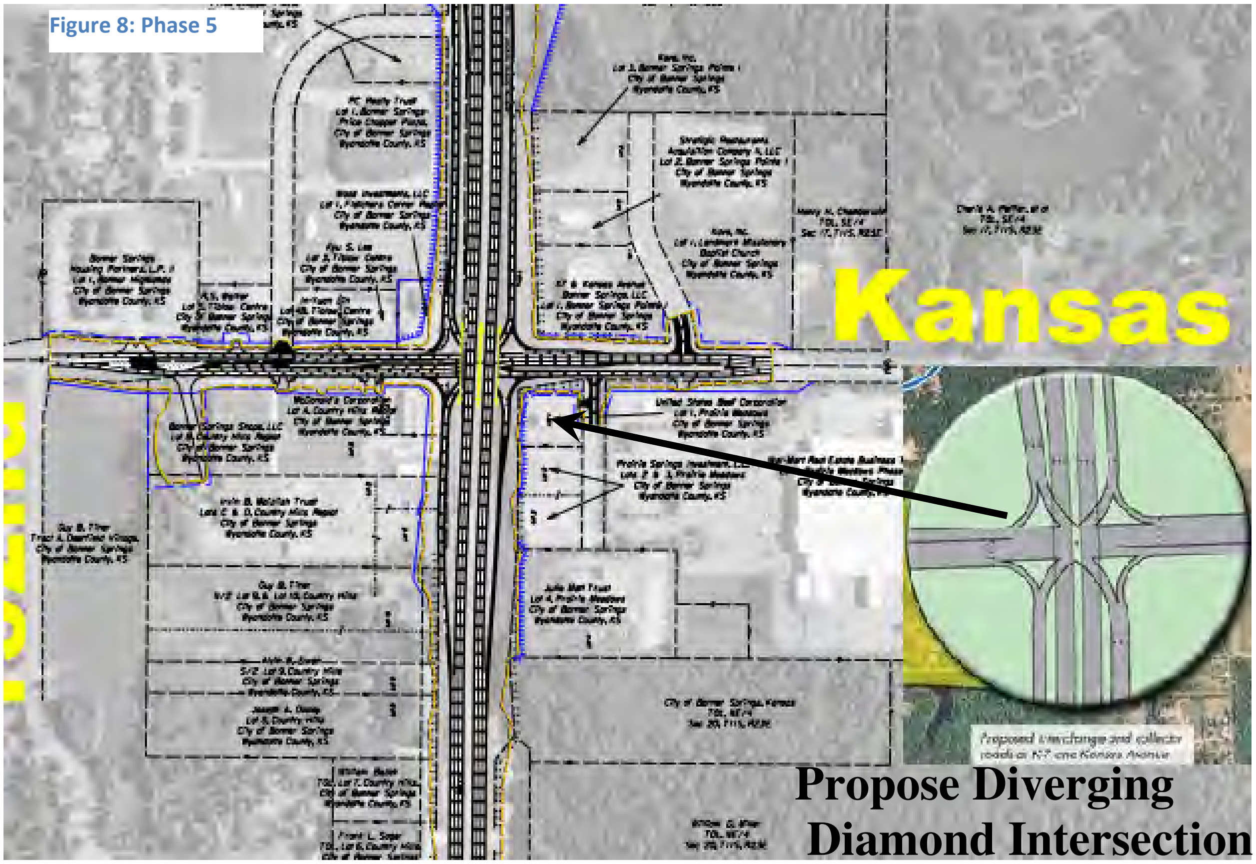

Figure 8: Phase 5

Currently we have all of Phases 1, 2A, 2B and 3 completed along with portions of Phases 4, 8 and 9 as well. To date there have been over 200 power auger borings performed for approximately 5 miles of surface geology investigation, and three (3) bridge foundation investigations completed so far for this project. The surface geotechnical investigation will provided designers with backslope recommendations, hydrology issues, excavation properties, along with detailed geologic cross-sections and plan profiles. KDOT bridge foundation investigations developed recommended foundation types along with load and resistance factored design parameters (LRFD).

PROJECT ISSUES

During our initial field investigation, the plans were to begin work along the expansion of I-70 and proposed new ramps in the northwest and southwest quadrants associated with Phase 1 of the project. However, as the field work was being completed for Phase 1, it was discovered that not only was work being done for Phase 1, but portions of Phases 4, 7, 8, and 9 had also been completed.

This has created a number of issues related to report submission, phase completion, organization of project, and changes in the alignments. The largest hurdle that we have had to face with our investigations is rearranging the order of completion for the various phases. As very few of the design phases have followed the proposed sequential order.

After the initial field work concluded, scheduling the field work to complete Phase 1 began; however, the road designers changed their priorities and now wanted information associated with expansion of I-70. This would encompass approximately four (4) miles of surface geology investigation and all or portions of five (5) different phases. This again presented the same issues that the initial investigation did, leaving portions of phases not completed and organization of the project very difficult.

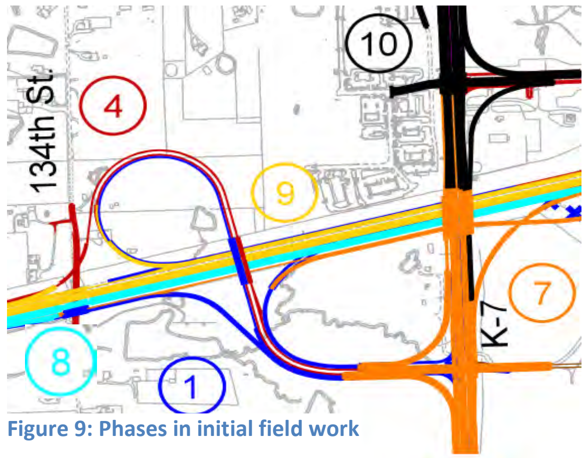

Figure 9: Phases in initial field work

KDOT developed a plan to eliminate; incomplete phases, multiple trips, and re-drilling of project areas. This was done by investigating all phase worked in a designated geographical area. However, this too has presented its own issues with alignment changes, changes in bridge design and funding issues.

LOOKING AHEAD

To date, 30% of the projects field work is completed and KDOT has funding for only Phases 1through 3 with construction set to begin on Phase 2A in March 2013. The next scheduled phase for field work is Phase 5 and is set to begin in March 2012 with a completion of August 2012.

Currently there are four (4) phases that have some portion completed with no completion date scheduled associated with those phases. Our plan is to move forward with what is scheduled and work through each phases as requested.

CONCLUSION

The K-7 and I-70 Interchange is vital to the growth and development of the state of Kansas. This interchange has presented many issues through its development, from alignment issues to geological disconformities. Though our geotechnical investigation we have provided designers with multiple design criteria critical to the completion of this project. It is fundamental that the geologist and designers must learn to work as a single unit to complete this type of project. The difficulties that this project has presented have given insight on how to better manage a project with this many phases, as well as a better understanding of the role that geologists play in the future of our infrastructure. Despite all the issues, the K-7 and I-70 Interchange is a much needed improvement and will greatly improve the traffic movements in this area.

REFERENCES

Zeller, Doris E, The Stratigraphic Succession in Kansas, Kansas Geological Survey, Bulletin 189, November 1998, Pages 33-34.

www.kgs.ku.edu/, Origin and Environment of the Tonganoxie Sandstone in Northeastern Kansas, August 7, 2006.

www.kgs.ku.edu/, Stratigraphic Succession in Kansas (1968), Plate 1-Classiffication of Rocks in Kansas, August 2005.

www.k7andi70interchange.org/, Sketches, Phases 1-10.

www.k7andi70interchange.org/, Sketches, Ultimate K-7.

www.k7andi70interchange.org/, Sketches, Phases 1-3 with construction limits.

www.k7andi70interchange.org/, Project Study Area, Project Fact Sheet.

www.census.gov/, State and County QuickFacts, Bonner Springs (city), Kansas.

Practical Estimation of Mohr-Coulomb Shear Strength for Cemented Conglomeratic Deposits in the Arid Western United States

William CB Gates, PhD, PE, PG, PEng
Jacobs Associates,
1109 1st Ave., Suite 501,
Seattle, WA 98101-2988,
206-496-4829
gates@jacobssf.com

Prepared for the 63rd Highway Geology Symposium, May 7-10, 2012

ABSTRACT

In the arid western United States it is not uncommon to observe slopes in weakly cemented alluvial deposits that stand at ½:1 (63 degrees) or steeper. These deposits are often conglomeratic in nature with clasts ranging in size from cobles to boulders enclosed in a matrix of finer material. Estimating accurate Mohr-Coulomb shear strengths for design presents a challenge because one cannot obtain a large enough sample to test in a standard shear box.

One of the best empirical methods to establish the shear strengths is back analysis of failed slopes coupled with general Hoek-Brown criterion. For back analysis, only one strength parameter can be used, I prefer friction. I have found that a practical method to estimate base friction is to measure the slopes of the small conical colluvial talus and scree fans of loose debris that have eroded from the slope face that are just at equilibrium and at the static angle of repose. The angle of repose represents the minimum angle of internal friction for these materials with cohesion at zero. I then employ a computer program such as SLIDE®Version 6 by RocScience®, to estimate the cohesion value assuming the slopes are in equilibrium and at a factor-of-safety of 1.0. The resultant shear strengths are compared to theMohr-Coulomb equivalent strengths developed using generalized Hoek-Brown criterion for the rock masses and charts developed by Hoek and Bray (1981) on back analyses of failed slopes of similar material. The results show that 34 degrees friction and 500 psf cohesive strength are conservative and therefore may be used for design of weakly cemented cut slopes in arid regions.

INTRODUCTION

Figure 1: Steep cut slope composed of partially cemented debris flow material, US 6, Utah.

The purpose of this paper is to discuss a practical method to establish base friction angles for a unsaturated weakly cemented alluvial and colluvial deposit that one would one observe along road cuts and cut banks in the arid southwest. Figure1is one example of a steep cut slopein a colluvial depositwhich is typical throughout the arid west. Most of these deposits are weakly cemented conglomerates and sandstones with various sizes of clasts. Cut slopes in these deposits tend to stand steeper because of apparent internal shear strength. It is not uncommon to observe road cuts and stream cut banks that have resisted erosion and stood for over 50 years or more. Highway engineers have taken advantage of these strength characteristics in design of the highway cut slopes. In addition, the performance of the old existing slopes is a good indicator of how new cut slopes will perform assuming the conditions remain the same. The big challenge that we have as engineers and geologists is to estimate an appropriate set of shear strength parameters (friction and cohesion) so that that we can establish an appropriate factor of safety for design.

In 2002, I was a member of a project team tasked to assess straightening a stretch of US-70 north of Ruidoso, New Mexico (PBQD, 2002).Along the present highway, we observed many older road cuts that had been constructed in weakly cemented alluvial soils that exhibited slope angles approaching ½:1 (horizontal to vertical) or about 60 degrees slope with heights over 50 feet. These road cuts were originally constructed over 25 years ago and were relatively stable except for shallow erosion. We assumed that performance of new excavated cut slopes would behave in a similar fashion to the present cut slopes with similar lithology.Therefore, to estimate the shear strength parameters for the new cut slopes our team first observed and catalogued the characteristics of present stable cut slopes along the highway and constructed a graph displaying each respective slope height and geometry. We also assumed that these slopes were at a factor of safety of one (1). In addition, for failed slopes we conducted back analysis to establish base shear strength parameters (friction and cohesion). As a result we estimated a friction angle and cohesion intercept of approximately 35 degrees and 300 psf (PBQD, 2002). The subsequent results were compared to charts by Hoek & Bray (1981) listing similar shear strength parameters of failed slopes of like lithology. It was noted that our results were conservative as compared to similar deposits.After inspection of the results, it was clear that the slopes maintained their present geometry not only because of the angle of internal friction but an apparent cohesion component of strength. Coupled with the above, triaxial and direct shear laboratory testing of similar coarse grained unsaturated samples was attempted with some degree of success to verify the shear strengths. In addition, Fisher and Hughes(2004) conducted pressure meter testing (PMT) on the same deposits coupled with numerical analysis and were able to estimate effective friction angles and cohesive strength that compared favorably to the results of the triaxial testing. Depending on the matrix, internal friction angles ranged between 25 and 35 degrees with attendant cohesive strengths ranging from 200 to 500 psf. These values were also conservative based on the table of reported values by Hoek & Bray (1981).

CASE HISTORY NOGALES, ARIZONA

BACKGROUND

Figure 2: Typical steep cut banks along a dry arroyo near Nogales, AZ.

In 2010, my team was contracted by a confidential client to evaluate the stability of similar conglomeratic oversteepened slopes in the Nogales, Arizona areaalong the border between US and Mexico.The Nogales area displays numerous steep road cuts and natural slopes in weakly cemented alluvial deposits(Figure 2). The steep cuts are prevalent as cut banks along the dry arroyos and constructed cuts along the highways and at the border crossing. One of the key issues was to establish appropriate shear strength values for these deposits to facilitate stability analysis and appropriate factors of safety.

ENGINEERING GEOLOGY

The specific deposits that we evaluatedare part of the lower member of the Nogales Formation and typically consist of light gray to brown, fine to coarse conglomerates with a fine-grained sandstone matrix. They are bound together with a weak to moderate calcium carbonate cementation. Bedding within the deposits is typically poorly defined and in these specific locationsdip into the slopes. In several areas the beds are transected by sub-vertical clastic dikes filled with silty-clay. Both slopes exceed 55 feet in height, are oversteepened and overhanging in places with an average slope of about 0.4:1 (vertical to horizontal) or 70 degrees.Because the cut slopes are composed of weakly cemented sandstones and conglomerates, with no clearly defined structure, they were considered a heterogeneous and isomorphic rock mass. The slopes showed areas of rill erosion and slope sloughing but no apparent tension fractures behind the brow suggesting imminent failure. Talus and scree deposits flank the toe of the slopes as a result of weathering and erosion.

In rock or soil slope evaluation or design, the rock mass is assumed to be a Coulomb material in which the shear strength of the sliding surface or failure surface is expressed in terms of the cohesion (c) and angle of internal friction (φ). Establishing the Mohr-Coulomb shear strengths for the rock mass in these cut slopes is difficult because of the very coarse conglomeratic nature of the rock mass.

PREVIOUS GEOTECHNICAL INVESTIGATIONS

Prior to our investigation, previous consultants had attempted to establish Mohr-Coulomb shear strengths of the conglomeratic material in the cut slopes and used the results to evaluate stability and factors of safety. Each consultant used a different approach to estimate the shear strengths and arrived at different conclusions with respect to the stability of the slopes.

One studyattempted to establish the shear strengths by selecting grab samples of the loose material from the cut slope face (less the large rock clasts) for laboratory shear strength testing. Before shear strength testing, the samples were remolded to the approximate in situ density of the rock matrix. The laboratory results of the peak shear strength values for the angle of internal friction ranged from 39 to 48 degrees with a mean peak friction value of 43 degrees. Similarly, peak cohesion ranged from 0 to 1800 psf. The residual strengths ranged as follows: angle of internal friction 36 to 44 degrees with a mean of 40 degrees; and cohesion 0 to 800 psf with a mean of 167 psf. Based on these shear strengths, the consultant estimated factors of safety ranging between 0.5 and 1.1 and concluded that the slopes were unstable.

In our opinion, the reported zero cohesion appeared inconsistent with the conditions observed in the cut slopes and was atypical for the geologic conditions. The cut slopes were standing and there was no apparent evidence of historical or pending global failure, though the inclination of the slopes was greater than the assumed angle of internal friction of the rock mass. Therefore, we assumed that there must be some apparent cohesivestrength to complement the friction.

Another study developed strength parameters of the rock mass on the basis of Hoek-Brown equivalent (Hoek and Brown, 1997) strengths and in situ pressure meter testing (PMT) of the rock mass within the bore holes behind the brow of the slopes. The following shear strengths were reported: angle of internal friction ranged from 31 to 44 degrees with a mean friction of about 34 degrees; cohesion ranged from 1100 psf to 4200 psf with a mean cohesion of 2132 psf. Based on the shear strengths, the stability analysis demonstrated factors of safety ranging from 1.9 to 2.3; and the consultant concluded that the slopes were stable.

It appeared that the PMT results yielded strengths that were on the high side. Based on our experience observing employment ofPMT in the alluvial gravel deposits along SR-70 in New Mexico,the coarser rock clasts in the bore hole tended to yield higher and false pressure meter readings suggesting higher strengths then the matrix. When Fisher and Hughes (2004) employed the PMT to test the alluvial soils, they insured that the PMT was located in the matrix between the large clasts.

Moreover, the exploratory borings drilled behind the open cut slopes probably did not show the most severe conditions for the slope. Weathering at outcrops tends to accentuate discontinuity orientations and decrease the strength of the rock mass exposed. Therefore, outcrop mapping rather than borings provides a more conservative estimate of the rock mass strength and other engineering characteristics (FHWA, 1998; Duncan &Mah, 2004). The best information on the rock mass characteristics of the cut or natural slope will typically come from scan line and window mapping of the exposed slope.

GEOTECHNICAL ASSESSMENT

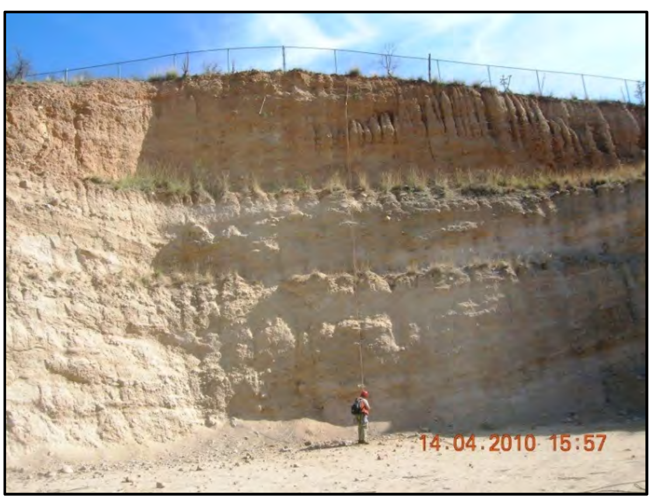

Figure3: Steep cut slope excavated in conglomeratic-sandstone. Vertical scan line follows rappel rope in center of photo.

In April 2010, our team conducted a geologic reconnaissance including limited geologic field mapping of the twocut slopes to verify the geologic conditions described by the previous consultants. We initially observed the slope for features, such as slumps in the face and toe and tension fractures behind the brow, that would suggest instability or pending failure, and found no apparent signs of global instability. In addition, at each slope we selected a vertical section that appeared to be the highest portion of the cut and represented the general lithology. Figure 3 displays the vertical line mapping location at one of the cut slopes. At both locations we conducted vertical line mapping using mountaineering techniques (rappelling). The geomechanical mapping was completed in accordance with The Rock Slopes Reference Manual (FHWA, 1998; Duncan &Mah, 2004). The purpose of the geomechanical mapping was to obtain geologic information on the rock mass and discontinuity data to be used in our assessment of the stability of the cut slopes.Because the cut slopes are composed of weakly cemented sandstones and conglomerates, with no clearly defined structure or discontinuities, we considered the deposits a heterogeneous and isomorphic rock mass. In addition, we assumed the exposed rock slopes represented the most weathered and weakest conditions for the rock mass.

GEOMECHANICAL ROCK MASS CLASSIFICATIONS

Our team classified the rock mass of the slopes usingBieniawski's (1989) Rock Mass Rating (RMR) and Hoek and Brown (1997) Geologic Strength Index (GSI). This approach by Hoek and others has been modified and improved over the last 10 years (Marinos and Hoek, 2001; Hoek and others, 2002; RocLab, 2012).

In general, because the rock mass is amorphous with no clear structure, it was difficult to establish an accurate RMR and subsequent GSI. We estimated a GSI of about 40; however, after review of Hoek and Brown's charts for GSI, we downgraded the value to about 35; which seemed more appropriate. The intact strength of the rock matrix ranged between 145 to 725 psi with a mean strength of about 483 psi. In addition, since the matrix of the conglomerate consisted of a weakly cemented sandstone, we selected a Hoek-Brown intact rock materials index of 17 for sandstone (conglomerate is 21 and not appropriate for this material; RocLab, 2012).The stability of the slope was very sensitive to the intact rock strength. To evaluate and select conservative strength data for the design, we used the "Three-Sigma Rule" described by Duncan (2000). This rule is based on the fact that 99.73% of all values of a normally distributed parameter fall within approximately three standard deviations of the mean value. Therefore, if HCV equals the highest conceivable value of the parameter, and LCV equals the lowest conceivable value of the parameter, these are approximately three standard deviations above and below the average value. One may elect to choose a value that is one to three standard deviations below the mean value to be conservative or in situations where there is limited data available. Therefore, for these slopes we estimated the strength as follows:

HCV = 725 psi, LCV = 145 psi.
Standard Deviation = σ = (725-145)/6 = 97 psi, 3σ = 290 psi
Mean = 483 psi
Mean - 3σ = 483 psi – 290 psi = 193 psi.

Therefore, intact rock strength of 193 psi was used to model the global stability of the cut slopes. This rock strength is probably conservative with respect to short term stability because it does not reflect the less weathered condition of the rock on the interior of the slope. However, we assumed that it was representative of the long term strength of the rock mass further into the slope if the rock mass is allowed to continue to degrade over time.

MOHR-COULOMB SHEAR STRENGTH BY BACK ANALYSIS

Weestimated the Mohr-Coulomb shear strength of the rock mass exposed in the cut slopes using back analysis. The geologic conditions of a rock mass at both cut slopes demonstrated there were no apparent distinct discontinuity surfaces on which sliding might take place during failure. The sliding surface in these rock masses will be along both natural discontinuity surfaces (indistinct bedding, joints or faults) together with shear through the intact rock or the matrix that holds the rock mass together. Two empirical methods have been established to establish the Mohr-Coulomb shear strengths; back analysis and general Hoek-Brown criterion. According to Wyllie and Mah (2004), the most reliable method to establish the strength of the rock mass is to back analyze a failed or failing slope. Only one strength parameter can be calculated in a back analysis. Typically, one would select a reasonable friction angle for the rock mass based on testing or the literature. The engineer would then employ a computer program such as SLIDE 6.0® by RocScience®, to estimate a cohesion value when the slope is in equilibrium and at a factor-of-safety of 1.0.

Figure 4: Measuring the angle of repose of the scree and talus at the toe of the slope.

At the base of both cut slopes, weobserved small conical colluvial talus and scree fans of loose debris (primarily sand with some large gravel and cobble sized clasts) that eroded from the cut slope face. These conical fans are just at equilibrium and at the static angle of repose (Figure 4). The angle of repose represents the minimum angle of internal friction for these materials with cohesion at zero. On each deposit, werecorded several measurements of the dip angle of repose; in all 77 measurements were recorded. Angles ranged from 25 to 38 degrees with a mean of 34 degrees. If the large angular material was included in the colluvial pile, the angle of repose would probably be higher by as much as 6 to 10 degrees. However, for back analysis purposes; we assumed 34 degrees as a conservative value. Also, it was assumed that the slope was dry, that is no ground water was observed discharging from the face.

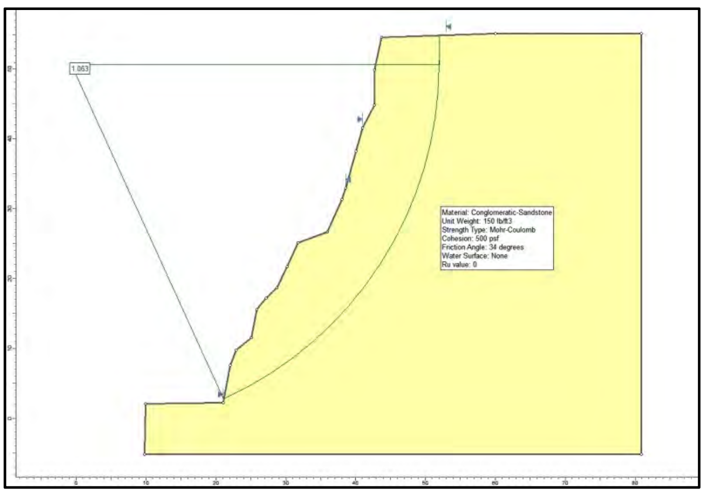

Figure 5: Limit of equilibrium analysis using Mohr-Coulomb shear strengths developed from back analysis of the slope.

Based on the back analysis using the angle of internal friction of 34 degrees; aided with the computer program SLIDE 6.0® by RocScience®, the cohesive strengthwas estimated at about 500 psf when the slope was at a static factor of safety of about 1.0 (Figure 5). According to a chart developed by Hoek and Bray (1981) on back analyses of failed slopes composed of sand or weathered soft rock, these values are reasonable. Since the cut slopesdid not appear to display evidence of global instability such as slumps in the face and toe and tension fractures behind brow, the static factors of safety are probably greater than 1.0.

GENERALIZED HOEK-BROWN CRITERIA

Because the presence of the oversize materials in the matrix of the conglomerate makes it difficult to characterize the Mohr-Coulomb strength, it was our opinion that analysis using the procedures of the generalized Hoek-Brown Criteria (Marinos and Hoek, 2001; Hoek and others, 2002; RocLab, 2012) might be a more appropriate approach for evaluating the global stability of these types of slopes.Assuming conservative intact rock strength of 193 psi and a GSI of 35 as part of the generalized Hoek-Brown criteria, the analyses indicatedthe existing slopeexhibits a static FS of approximately 1.0 for relatively shallow failure surfaces intersecting approximately 3 to 7 feet behind the brow of the slope (Figure 6). If the limits of the critical search are forced to mirror that of the Mohr-Coulomb failure circles, the factor of safety jumps up to about 1.2.

MOHR-COULOMB EQUIVALENTS FROM GENERALIZED HOEK-BROWN CRITERION

Hoek and others (2002) using the generalized Hoek-Brown strength coefficients and through a series of curve fitting equations have developed Mohr-Coulomb equivalent strengths. RocLab (2012) facilitates manipulation of the cumbersome equations (Figure 8). Assuming and intact rock strength of 193 psi and a GSI of 35, the equivalent shear strengths result in a friction angle of about 34 degrees and cohesion of about 1152 psf. These shear strengths yield a factor of safety of about 1.6 (Figure 9) which appeared high for the present slope conditions.

CONCLUSIONS

It appears that estimating the shear strengths for slopes composed of unsaturated weakly cemented alluvial and colluvial deposits by back analysis using a base friction angle developed by assessing the angle of repose at the toe of the slopes generate the most conservative values at a factor of safety of 1.0. Using generalized Hoek-Brown coefficients renders a factor of safety similar to back analysis for shallow failures. However, if the failure circles are pushed into the slope to mirror that of the back analysis, then the factor of safety goes up to about 1.2 accounting for the intact rock strength. Using Mohr-Coulomb equivalent strengths derived from the generalize Hoek-Brown criterion suggests the slopes are stable with a factor of safety greater than 1.5. It appears that this is too liberal and not useful for design.

When designing a new cutslope for these kinds of geologic conditions, it is a good idea to step back and evaluate how the old existing slopes have performed over time. These are good indicator of how new cut slopes will perform assuming the conditions remain the same.

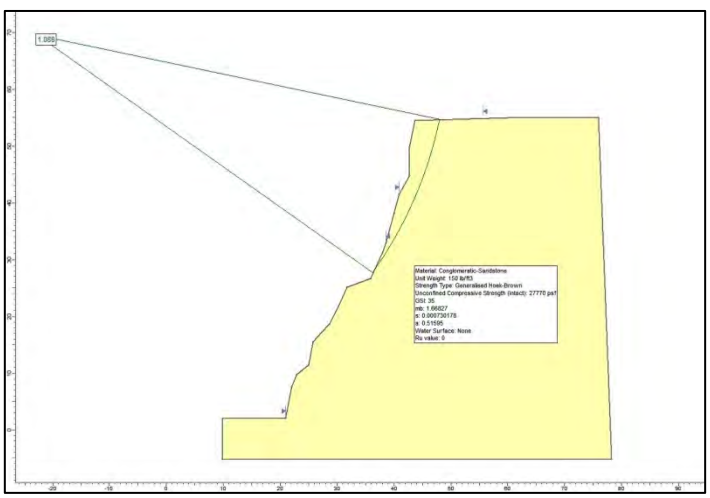

Figure 6: Limit of equilibrium analysis using generalized Hoek-Brown strengths. Note shallow critical circle of failure.

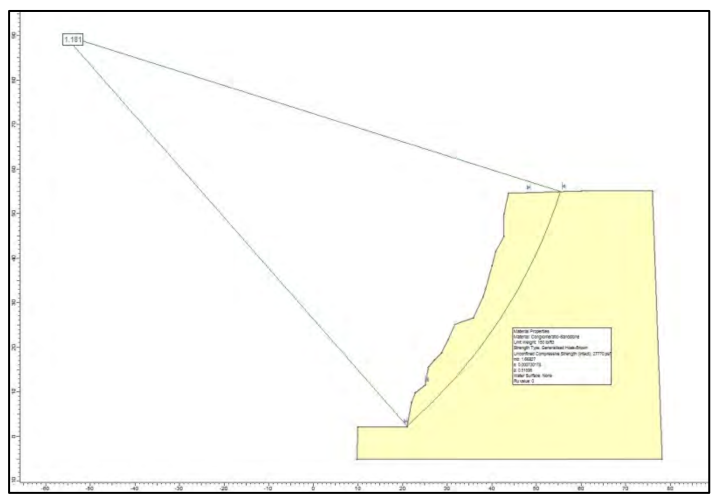

Figure 7: Limit of equilibrium analysis using generalized Hoek-Brown strengths. Note increased FS FS as search limits are changed to mirror Figure 5.

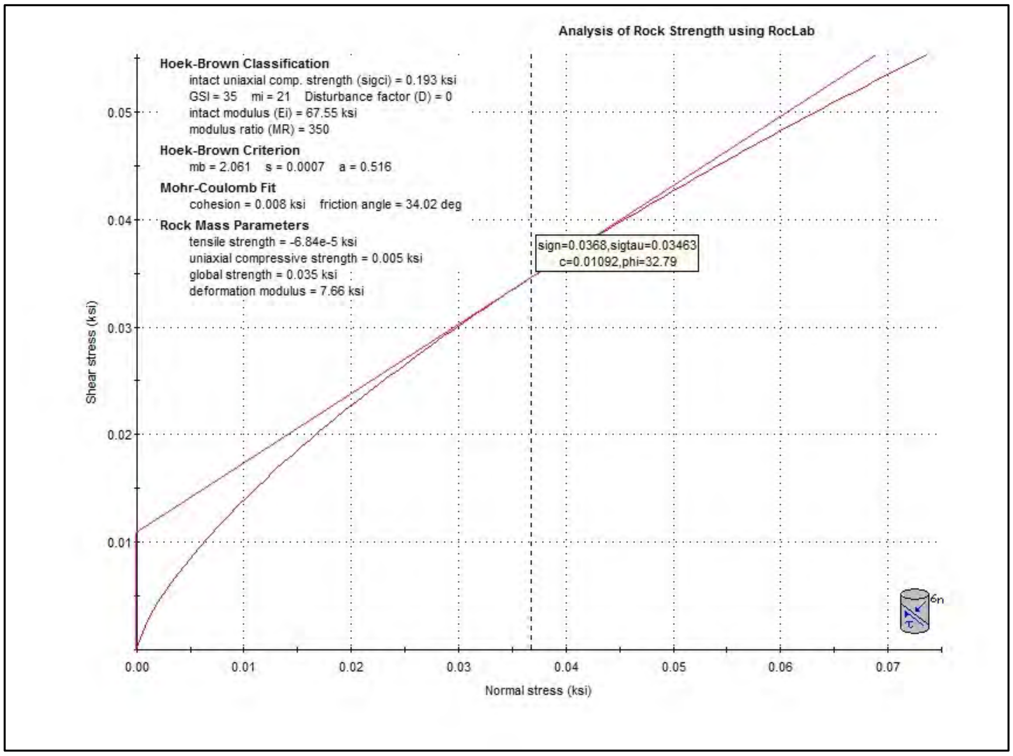

Figure 8: Analysis of rock mass strength using Mohr-Coulomb curve fit on Hoek-Brown strength criteria.

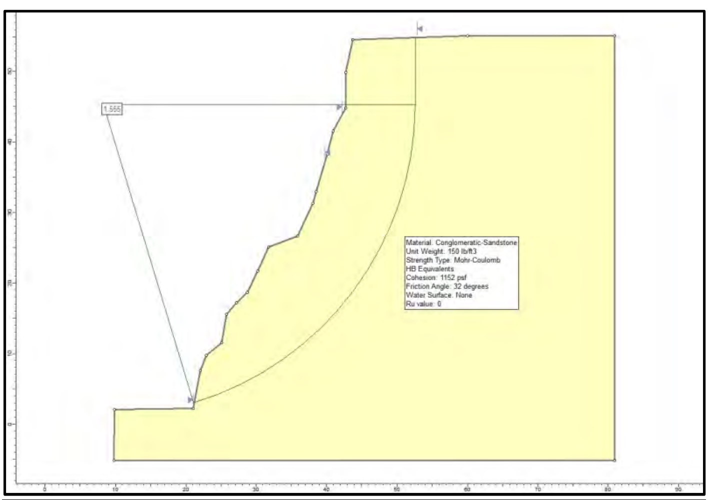

Figure 9: Limit of equilibrium analysis using Mohr-Coulomb shear strengths developed from equivalent generalized Hoek-Brown strengths

REFERENCES CITED

Bieniawski, Z.T., 1989,Engineering Rock Mass Classifications, New York: John Wiley, pp. 51-73.

Duncan, J.M., 2000, Factors of Safety and Reliability in Geotechnical Engineering: Journal of Geotechnical and Geoenvironmental Engineering, pp. 307-316.

FHWA, 1998,*Rock Slopes Reference Manual* (FWHA-HI-99-007)

Fisher, B.R. and J. M.O. Hughes, 2004, Cut Slope Design and Pressuremeter Testing in Weakly Cemented, Unsaturated Soil: ASCE, GeoTrans 2004.

Hoek, E., and Bray, J.W., 1981, Rockslope Engineering, Institution of Mining and Metallurgy, 357 p.

Hoek, E., and Brown, E.T.,1997, "Practical Estimates of Rock Mass Strength," International Journal of Rock Mechanics and Mineral Sciences, Vol. 34, No. 8, pp. 1165-1186.

Hoek, E, C., Carranza-Torres and B. Corkum, 2002, Hoek-Brown Failure Criterion-2002 Edition, In *Proceedings of 5th North American Rock Mechanics Symposium, Toronto, Canada, Department of Civil Engineering, University of Toronto*. 267-273

Marinos. P, and E. Hoek, 2001,Estimating the geotechnical properties of heterogeneous rock masses such as flysch. *Bull. Int. Assoc. Eng. Geol. (IAEG).* 60: 85-92

Parsons Brinckerhoff Quade and Doluglas, Inc., 2002, "US 70 Reconstruction, Ruidoso Downs to Riverside Preliminary Geotechnical Interpretive Report." Prepared for New Mexico State Highway and Transportation Department

RocLab by RocScience, 2012

Slide Version 6.0, 2011, Stability Analysis Software for Soil and Rock Slopes.RocScience Inc. Toronto, Canada

Wyllie, D. C. and C.W. Mah, 2004, Rock Slope Engineering: Civil and Mining, 4th Edition, Spon Press, 429 p.

Measurement of Ground Movement During Seismic Events

Pat Hipley

California Department of Transportation, MS 9-2/5i

1801 30th Street, Sacramento CA 95816

(916) 227-8608

Pat_Hipley@dot.ca.gov

Moh Huang

California Geological Survey, MS 13-35

801 K Street, Sacramento CA 95814-3531

(916) 322-9304

Moh.Huang@conservation.ca.gov

Prepared for the 63rd Highway Geology Symposium, May 7-10, 2012

Introduction

Understanding how ground surface movement is amplified from deep rock motions during seismic events has been a challenge to the earthquake engineering community for many years. Various soil types will increase the deep "rock like" material motions in varying degrees. Some soils can amplify the rock motions many times while others, such as thick peat layers, can actually de-amplify the surface motions.

Placing instruments at different depths at given locations will allow engineers and researchers to verify our theories and assumptions of deep ground and surface motions. This data will allow us to calibrate the current equivalent linear site response models available such as SHAKE and other fully non-linear models.

History

A typical downhole array consists of a series of drilled holes with different depths. Seismic instruments are placed at the bottom of each hole and at the ground surface. The California Geological Survey has worked with the California Department of Transportation since the early 1990’s to instrument soil and rock sites for seismic motions. There are currently 29 Downhole arrays located throughout California with more planned for the future (see Table 1).

The downhole instruments are 2g force balance accelerometers encased in a stainless steel cylindrical housing. These include two horizontal sensors and a vertical sensor set at defined depths below the ground surface. Four-inch diameter PVC pipe is grouted into drilled holes and utilize a specially designed end piece that locks the sensor package into place at the bottom of the hole. A compass is used to line up all the sensors in the north/south east/west orientation to more easily compare the readings at the different depths. Prior to placing the PVC pipe, various geotechnical tests are performed and data collected in the open hole for documentation and future studies. One of these tests is a P/S suspension log that determines the P-wave and S-wave velocities for the full length of the hole. These velocities are used as input for the dynamic site response models. Also, soil samples are taken from the deepest hole in the array and a geologist will prepare a boring report with photographs of the soil samples and a description of the soils at each level for future use. In addition, this data and the P/S suspension readings are studied to make minor adjustments to the depths of the shallower holes.

Figure 1 – Drilling a Downhole Array at the Napa River Bridge

Figure 2 – Preparing P/S Suspension Tool to be lowered into Borehole

Table 1 - Caltrans – CGS Geotechnical Arrays

Geotechnical Arrays Instrumented in the Caltrans/CGS Strong Motion Instrumentation Project, as of February 1, 2012

	Station Name	Station No.	No. of Sensors	No. of Depths (incl. surface)	Sensor Depths (m)	Local Site Geology
1	Alameda - Posey & Webster Geotech Array	58137	12	4	Surface, 5, 13, 40	Deep Alluvium
2	Antioch - San Joaquin River S Geotech Array	67266	15	5	Surface, 12, 24, 51, 102	Deep Alluvium
3	Benicia - Martinez Bridge N Geotech Array	68321	9	3	Surface, 16, 39	Shallow fill over bay mud
4	Benicia - Martinez Bridge S Geotech Array	68323	9	3	Surface, 11, 35	Thin alluvium over soft rock
5	Corona - I15/Hwy91 Geotech Array	13186	12	4	Surface, 8, 22, 42	Shallow alluvium over hard rock
6	Crockett – Carquinez Bridge Geotech Array #1	68206	9	3	Surface, 20, 46	Shallow clay over soft rock
7	Crockett - Carquinez Bridge Geotech Array #2	68259	9	3	Surface, 61, 125	Shallow clay over soft rock
8	El Centro - Meloland Geotechnical Array	01794	12	4	Surface, 30, 100, 195	Deep alluvium
9	Eureka - Geotechnical Array	89734	15	5	Surface, 19, 33, 56, 136	Deep soft alluvium
10	Foster City – San Mateo Bridge Geotech Array	58968	12	4	Surface, 16, 22, 35	Shallow alluvium over rock
11	Half Moon Bay – Tunitas Geotech Array	58964	12	4	Surface, 5, 12, 45	Alluvium over soft rock
12	Hayward - I580/238 East Geotech Array	58486	12	4	Surface, 9, 30, 91	Alluvium over rock
13	Hayward - I580/238 West Geotech Array	58487	18	6	Surface, 5, 9, 18, 37, 91	Deep alluvium over rock
14	Hayward - San Mateo Br Geotech Array	58798	15	5	Surface, 12, 23, 46, 91	Deep alluvium
15	Los Angeles - La Cienega Geotech Array	24703	12	4	Surface, 18, 100, 252	Deep alluvium
16	Los Angeles - Vincent Thomas Geotech Array East	14785	12	4	Surface, 18, 46, 91	Deep alluvium
17	Los Angeles - Vencent Thomas Geotech Array W1	14783	12	4	Surface, 30, 91, 189	Deep alluvium
18	Los Angeles - Vencent Thomas Geotech Array W2	14784	9	3	Surface, 15, 30	Deep alluvium
19	Novato - Petaluma River Geotech Array	68285	15	5	Surface, 10, 23, 54, 73	Shallow alluvium over rock
20	Oakland - Bay Bridge Geotech Array	58204	15	5	Surface, 17, 46, 91, 161	Fill, alluvium
21	Oxnard - Hwy 101 Bridge Geotech Array	25325	9	3	Surface, 18, 36	Deep alluvium
22	Palmdale - Hwy 14 Bridge Geotech Array	24206	9	3	Surface, 16, 35	Shallow alluvium over hard rock
23	Rohnert Park – Hwy 101 Geotech Array	68797	9	3	Surface, 11, 47	Alluvium
24	San Bernardino - I10/215 W Geotech Array	23792	12	4	Surface, 11, 35, 92	Deep alluvium
25	San Diego – Coronado East Geotech Array	03192	12	4	Surface, 13, 30, 91	Shallow alluvium over soft rock
26	San Diego – Coronado West Geotech Array	03193	15	5	Surface, 12, 23, 42, 103	Deep alluvium
27	San Francisco – Bay Bridge Geotech Array	58961	9	3	Surface, 14, 40	Fill, shallow alluvium oevr soft rock
28	San Rafael - Richmond Bridge Geotech Array	58267	6	2	Surface, 46	Thin alluvium over rock
29	Vallejo - Hwy 37/Napa River E Geotech Array	68310	9	3	Surface, 18, 45	Bay Mud

Humboldt Bay Bridges and Downhole Array Recordings

A magnitude 6.5 earthquake struck the Ferndale area on January 9, 2010. This event triggered the instruments at the Eureka Geotechnical Array and the three nearby Humboldt Bay Crossing bridges. The largest movement on the bridge structures was 10" back and forth longitudinally on the Somoa Channel Bridge. At this location seismic sensors were placed at the bottom of a new pile, at the mid-height of the pile, at the water level pier cap and at the superstructure deck level in both directions (see Figure 3). The recorded accelerations at Pier S-8 are shown in Figure 4. The acceleration spikes at the roadway level are due to the interaction (impacting) of the separate deck sections at the expansion joint. The amplitude of movement at the pile tip was 2", 5" at water level and 6" at the deck. This is an increase of three fold (see Figure 5). With the bridge pier being rather stiff the deck level and the water level readings were similar. Most of the flexibility was in the pile group and this was shown by the differential movement from the pile tip to the water level pier cap.

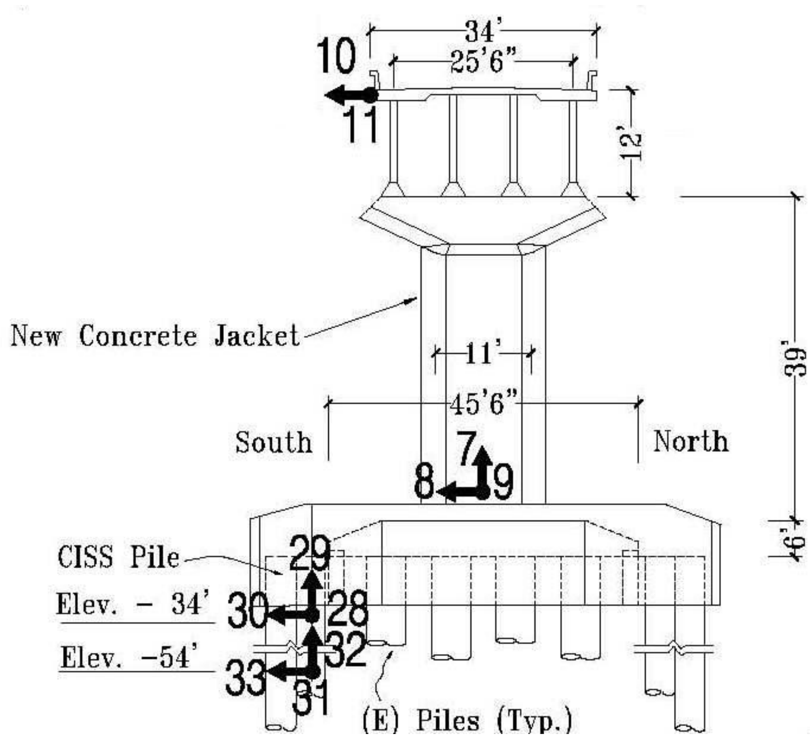

Figure 3 - Seismic Instrument Layout for Somoa Channel Bridge Pier S-8

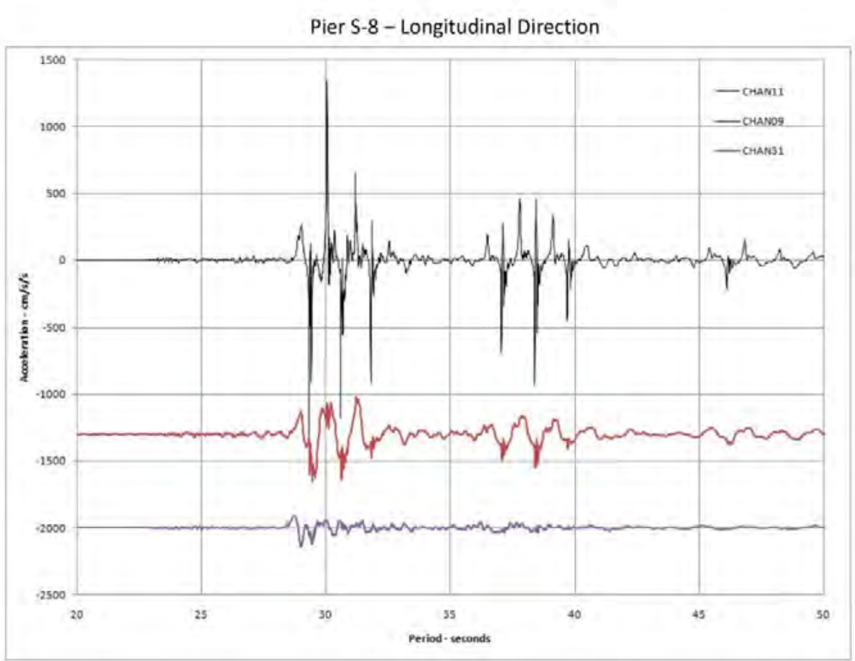

Figure 4 - Longitudinal Acceleration at Various Levels of Pier S-8

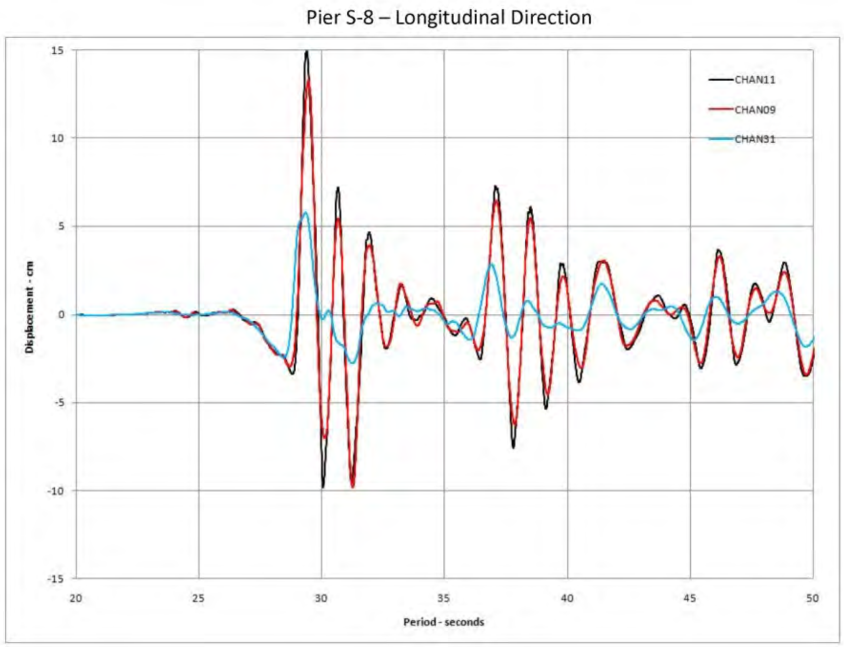

Figure 5 - Longitudinal Displacement at Various Levels of Pier S-8

Very near the Somoa Channel Bridge is the Eureka Geotechnical Array with sensors placed at depths of 446’, 185’, 109’ and 62’ below the surface along with ground surface instruments (see Figures 6 and 7). The accelerations recorded from the Array during the Ferndale Area earthquake are shown in Figure 8. The displacements integrated from the acceleration records are shown in Figure 9. The ground movement was amplified from 1.5” at 446’ below the surface to 4” at the surface. This is a very soft soil site with a high water table. The rock layer is assumed to be approximately 2000 feet below ground surface.

Figure 6 - View of Downhole Array at Somoa Channel Bridge near the City of Eureka, CA

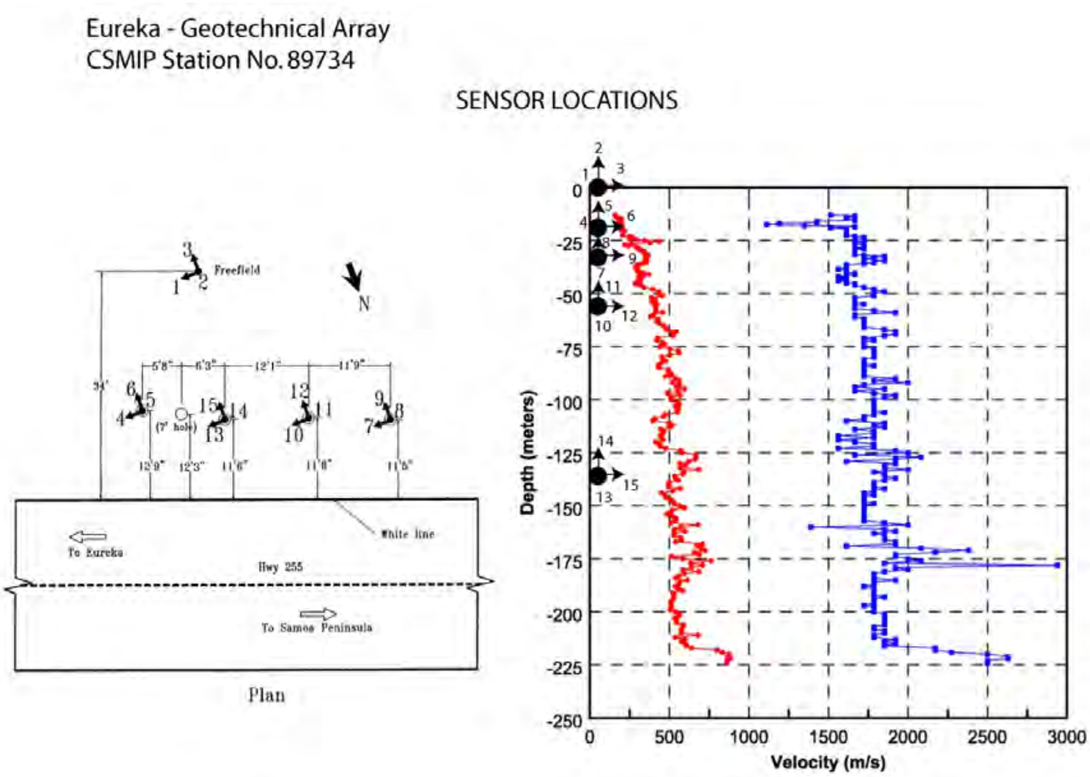

Figure 7 – Eureka Downhole Array Layout

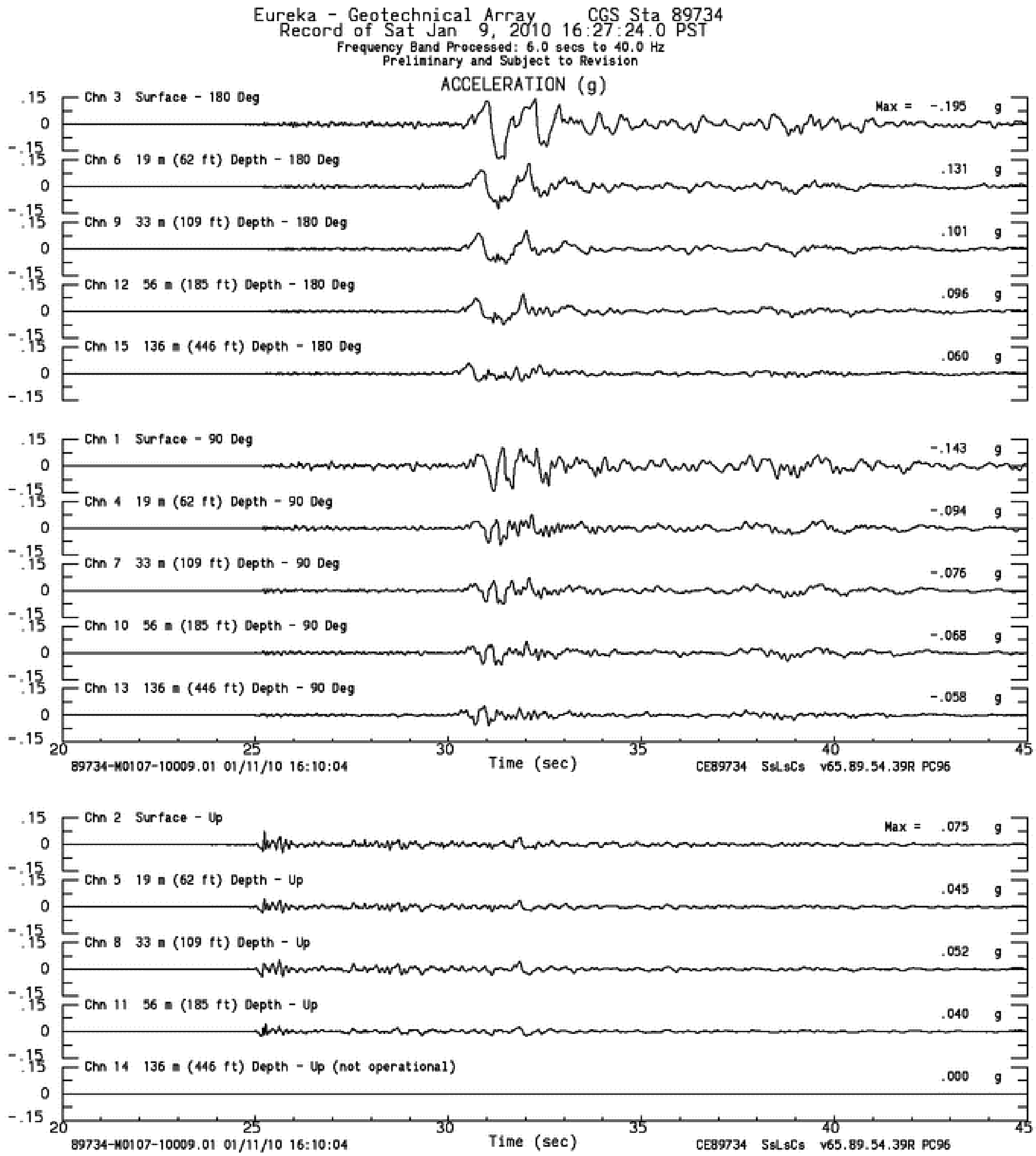

Figure 8 – Acceleration Readings from the Eureka Geotechnical Array

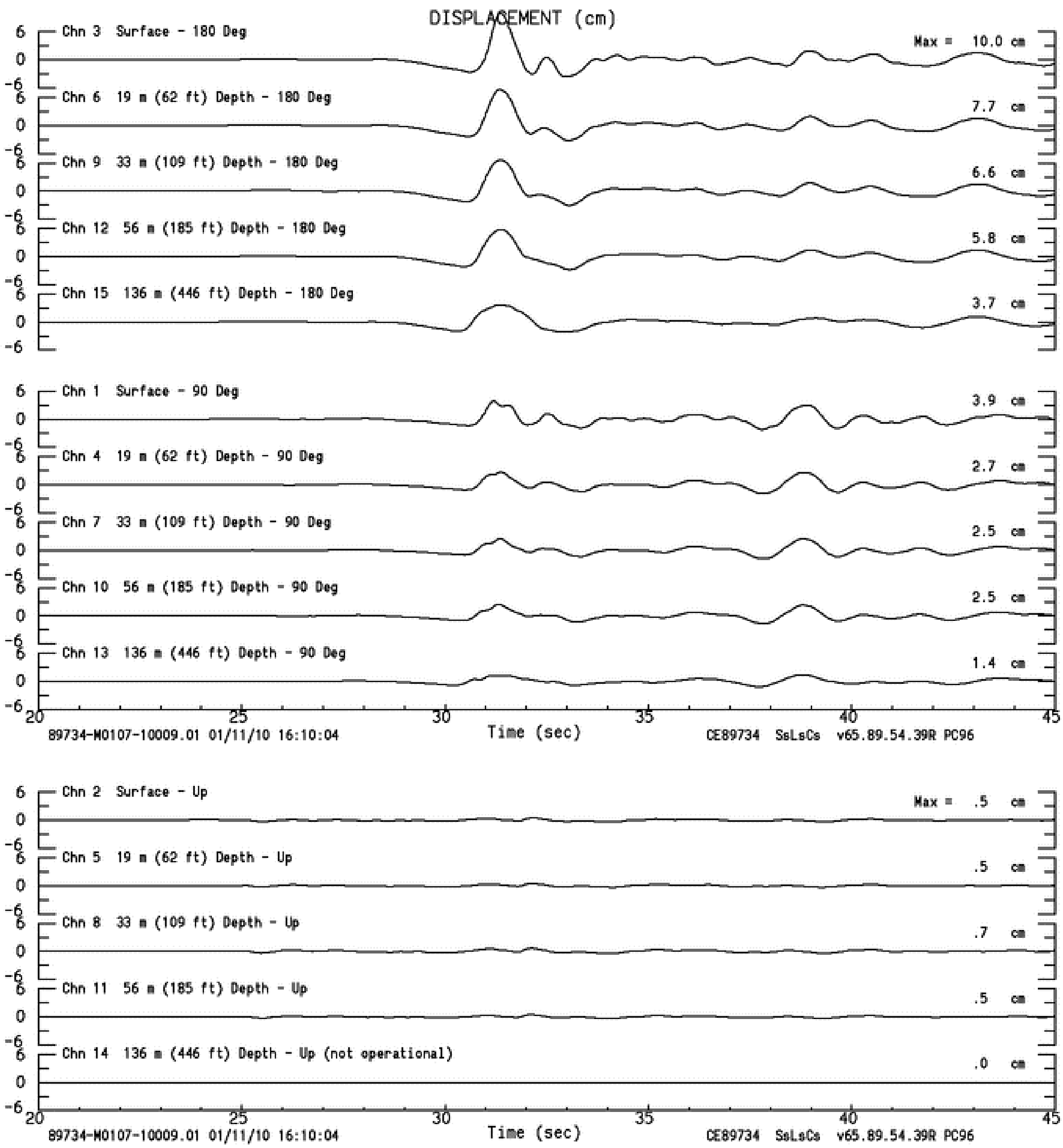

Figure 9 – Displacement Readings from the Eureka Geotechnical Array

Tectonic Setting

This region of the Northern California Coast is very seismically active with the San Andeas fault ending at the triple junction of various plates comprising the Cascadia Subduction Zone. These subducting plates are the reason the Cascade Range of volcanoes are still active. It is assumed that a magnitude 9.0 earthquake took place in the year 1800 in this region due to paleoseismilogical data from the coastline and records from Japan of the "Orphan Tsunami". The Tsunami occurred in Japan without any ground motion being felt thus the name given to this Tsunami by the Japanese people.

Near Fault Studies

The Caltrans/CGS project has recently started adding downhole arrays near major faults. These locations consist of two arrays with one on each side of a defined fault trace approximately ¼ mile from the fault. Near fault ground motion data is scarce for major earthquakes and some bridge designs, such as large outrigger bents, are likely very conservative in their design due to the unknown motions expected close to a rupture zone. We are trying to collect not only geophysical seismic data but are instrumenting bridges near these arrays to gather structural response information also.

The first near fault downhole array pair is along the Hayward Fault in the city of Hayward. The two arrays are on the shoulder areas along Highway 238 near the Highway 238/580 Interchange. The arrays consist of three depths and freefield sensors to the east and five depths and freefield sensors to the west. One of the interchange bridges nearby has been instrumented also. The soil conditions are radically different on each side of the fault with deep alluvium to the west and shallow rock outcropping to the east.

Conclusion

Deep soft soils tend to amplify the rock motion by many times at the ground surface and can be very destructive to large structures. Gaining an understanding of this phenomenon can help bridge and building owners better prepare for inevitable events in high seismic regions. The stability of land in California is unpredictable and being ready to record the surface and deep strata seismic movement is invaluable for the study of how structures and highways will react to strong ground shaking. The seismic data collected as part of this project will help us gain an understanding of how deep soft soil columns react to large earthquakes and will allow us to calibrate our dynamic modeling techniques.

Disclaimer

Statements and views presented in this paper are strictly those of the author, and do not necessarily reflect positions held by their affiliations, the Highway Geology Symposium (HGS), or others acknowledged above. The mention of trade names for commercial products does not imply the approval or endorsement by HGS.

Field Methods of Measuring Discontinuities for Rock Slope Stability Analysis on Price Mountain, VA

Nicholas J. Farny[1]
Department of Earth and Atmospheric Sciences, Purdue University
5550 Stadium Mall Drive, West Lafayette, IN 47907
812-550-0304
nfarny@purdue.edu

Terry R. West[2]
Department of Earth and Atmospheric Sciences, Purdue University
5550 Stadium Mall Drive, West Lafayette, IN 47907
765-494-3296
trwest@purdue.edu

Prepared for the 63rd Highway Geology Symposium, May 7-10, 2012

Acknowledgements

Nicholas would like to thank his adviser and committee chair, Terry R. West, for unwavering support during his time as an undergraduate and graduate student at Purdue. He would also thank Chester F. Watts, Radford University, for serving on the graduate committee and contributing many hours and resources to this project, and Thomas M. Tharp for also serving on that committee. Thanks are extended to thank Brendan Fisher, for providing helpful advice and consultation on this project. Lastly, Nicholas wishes to thank his family for their support and understanding.

Disclaimer

Statements and views presented in this paper are strictly those of the author, and do not necessarily reflect positions held by their affiliations, the Highway Geology Symposium (HGS), or others acknowledged above. The mention of trade names for commercial products does not imply the approval or endorsement by HGS.

ABSTRACT

Accurate and efficient measurement of rock discontinuities has great importance in rock slope stability analysis. To determine kinematic and kinetic stability of rock slopes, discontinuity orientations must be measured precisely, with cost and time efficiency. Several methods exist for taking field measurements of discontinuity orientations. The objective of this study was to compare the traditional method of hand measurements using a Brunton compass and satellite-based measurements to the modern methods of Sirovision stereo photography and LiDAR. The field site is a rock outcrop along Coal Hollow Road on Price Mountain, Virginia. The Price Mountain structure is a doubly plunging anticline window in the Pulaski Thrust Sheet. The rock outcrop consists of the Upper Price Formation, a Mississippian aged sandstone with frequent coal seams. The site features a set of bedding planes that dip steeply into the slope face, yielding toppling failures. In addition, three distinct sets of joints exist creating both planar and wedge failures. Rock slope stability analysis will consider a hypothetical widening of the road. Using window mapping and detail line methods, discontinuity orientations were taken for 200 feet of outcrop. Analysis underway includes Siriovison stereo photography and ground based LiDAR to provide discontinuity measurements compared to those of conventional mapping methods. These measurements will be analyzed using stereonets and probabilistic factor of safety calculations. Results will be used to determine the time required, cost efficiency and accuracy of the different methods.

INTRODUCTION

Rock slope stability is dependent on the accurate survey of unstable areas. To accurately predict the stability of a rock mass, the orientations and properties of discontinuities need to be evaluated in the field. Traditional surveying methods such as the detail line and window mapping methods require precise measurements using geologic compasses and surveying equipment. Rock mass characterization for rock slope stability analysis using these traditional methods is often a hazardous and time consuming endeavor, and comes with many inherit uncertainties from human error. Studying a rock slope with potential for falling or sliding block can place the surveyor in danger. Often rock outcrops are not readily accessible. For example, a rock outcrop along a highway may be accessible at the base, may be too high to collect data without the use of repelling equipment or cranes. Using detail lines, window mapping, and core logging in expansive areas such as tunnels through unstable rock and in open pit mines can take considerable time, manpower, and resources. Above all, discontinuity orientations and other properties are recorded by hand using geological compasses and field observations in traditional methods. This creates a significant source of human error. More modern methods, such as LiDAR and Sirovision terrestrial digital photogrammetry can be conducted at a safe distance from the slope with more accuracy and time efficiency. This study is a comparison between the traditional method of window mapping and the modern methods of Sirovision and LiDAR. This study is conducted on a rock outcrop along Coal Hollow Road on Price Mountain, Virginia. Discontinuity orientations from all three methods will be compared in stereonet analysis. These discontinuity orientations and other measurements will then be used in factor of safety probability analysis. From this analysis, a comparison of the accuracy, safety, time requirement, and cost effectiveness of the three methods can be made.

REGIONAL GEOLOGY

The field site for this study is Price Mountain, located south of Blacksburg, Va. Blacksburg is located at an elevation of 2,100 feet. It lies on the Continental Divide, with waters east of the divide flowing into the Atlantic Ocean via the North Fork of the Roanoke River. The field site is located near the junction of the Southern and Central Appalachians in the Appalachian Overthrust Belt, bounded by the Blue Ridge overthrust to the southeast. The Southern Appalachians trend N 60-65 E, while the Central Appalachians trend N 30-35 E (Lowry, 1979).

The Overthrust Belt of the Southern Appalachians includes all faults bounded by the Pulaski overthrust to the north and the Blue Ridge overthrust to the south (See Figure 1). Along the northeast edge of the Overthrust belt is the Pulaski thrust sheet. The width and horizontal displacement of the Pulaski thrust sheet is a minimum of 10 miles in Blacksburg, while in Roanoke it can reach 12 miles. The Pulaski thrust sheet spans a large amount of geologic history, with the Catawba syncline of the Salem synclinorium containing over 12,000 feet of strata ranging from the Middle Cambrian to the Early Mississippian. Based on seismic surveys, the Precambrian basement of the thrust sheet is located more than 25,000 feet below sea level. This thrust sheet is the northwestern expression of the Blue Ridge overthrust (Lowry, 1979).

Below the Pulaski sheet in the New River area is the Saltville thrust sheet, with the Saltville fault bounding it to the northeast. This thrust fault has a high angle dip of 50 – 55 E, and a stratigraphic throw of 4000 feet. The hanging wall is the Hoanaker Dolomite, a Middle Cambrian age formation . In the Blacksburg area, the Saltville is a low angle fault with an extensive stratigraphic throw of over 10,000 feet (Lowry, 1979).

Several Saltville structures, such as the Price Mountain and Christiansburg anticline windows, continued to develop after being overridden by the Pulaski Sheet as evident by their pronounced structural relief (See Figure 1). This is due to the transmission of deforming stresses northeastward during the process. Such post emplacement upwarping resulted in the base of the Pulaski thrust sheet being raised to an elevation of 2000 feet. The many windows of the Pulaski thrust sheet, which are part of underlying Saltville thrust sheet, show the occurrence of intense deformation (Lowry, 1979).

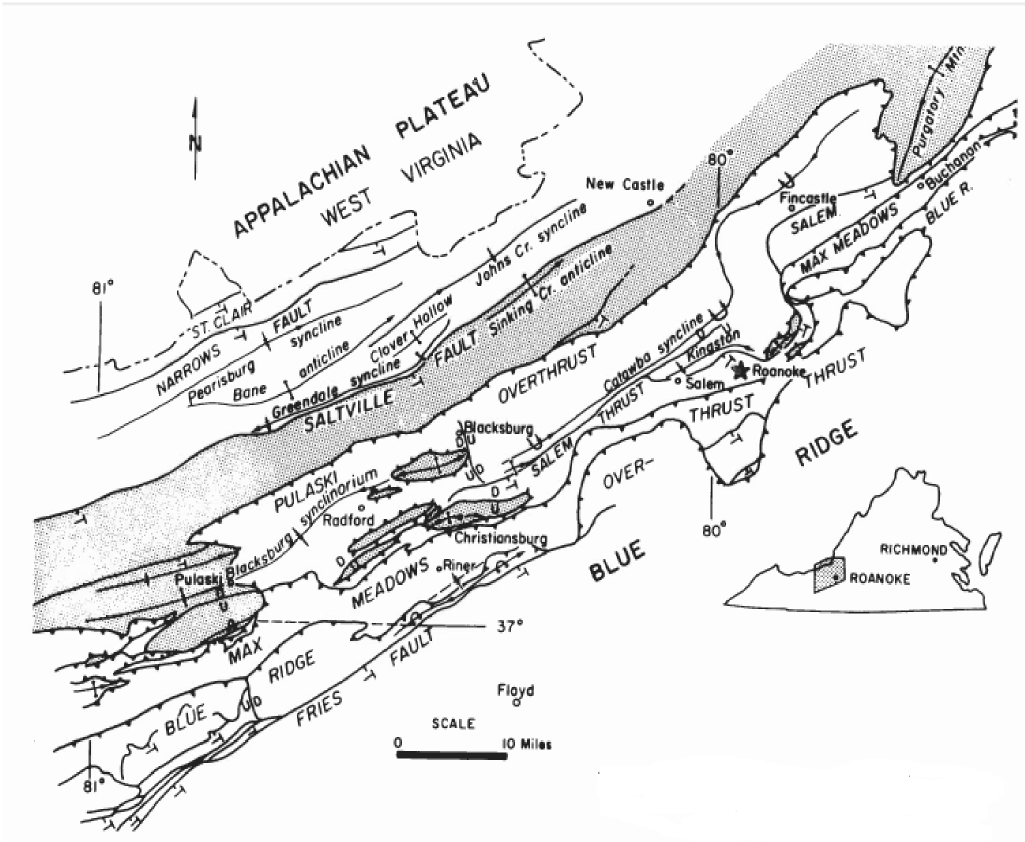

Figure 1. The major folds and fault of the Southern Appalachians near Blacksburg and Radford, VA. The stippled portions are part of the Saltville thrust sheet (Lowry, 1979).

The Price Mountain window is adjacent to Blacksburg, and is the largest and most northwesterly of the Pulaski thrust sheet windows (See Figure 1). The structure is a doubly plunging anticline with a northeasterly trend. In 1949 Calco drilled a 9,340 foot well for oil and gas exploration, ending in the Middle Ordovician Moccasin Formation. Price Mountain and the surrounding areas have been extensively mined for coal with an grade of semi-anthracite (Lowry, 1979).

The exposed portion of the Price Mountain anticline consists of the following Saltville thrust sheet formations, from oldest to youngest; Devonian Chemung, and Mississippian Price (Cloyd Conglomerate member), Lower Price, Upper Price, Lower Maccrady, and Upper Maccrady (Bartholomew et al., 2000).

The rock outcrop in this study lies entirely within the Mississippian Upper Price formation with a stratigraphic thickness of 350 meters in the Saltville thrust sheet. The basal 20 to 40 meters of this formation are a dark gray to black thinly laminated mudstone. This mudstone often contains plant fragments and lycopod tree stumps. Within the mudstones are several coal seams, the number varying locally from one to six. The black, laminated coal has a grade ranging from bituminous to semi anthracite, and exists in beds ½ to 6 meters thick (Bartholomew et al., 2000).

Above the basal mudstone and coal seams lies a cyclic nonmarine sequence of mudstone, siltstone, and sandstone. Within scour channels, the base of the cycle is an arenite sandstone that fining upward to siltstone. The arenite sandstone layers are thickly bedded, ranging from 30 to 120 centimeters thick. The upward fining sequence is often capped with a green and red, mottled mudstone. (Bartholomew et al., 2000).

TRADITIONAL METHODS OF ROCK MASS CHARACTERIZATION

The survey of rock masses requires extensive mapping to accurately record orientations and properties of the discontinuities. This section covers the traditional methods and tools utilized in the surveying of rock slopes for the purpose of rock slope stability investigation. These methods rely heavily on fieldwork and accurate observations by the surveyor.

The most important tool for the traditional methods of rock slope investigation is the geologic compass. This device allows for the measurement of discontinuity and slope face orientations in the field. The quality of data and interpretation is only as good as the ability to use a compass. There are two main geologic compasses, the Brunton transit compass and the Clar stratum compass. The Brunton compass contains two levels, a bullseye level for taking strike measurements, and the clinometer, which contains a barrel shaped level moved by using a lever on the backside of the compass and is used to take dip measurements. The Clar stratum compass contains only the bulleye level. It utilizes a graduated hinge scale between the box and the lid of the compass for taking dip measurements. This design allows the Clar compass to take dip direction/dip in one step, while the Brunton design requires two (Babaie, 2001).

There are several different procedures for measuring discontinuity orientations and properties in the field. The detail line method involves the use of a measuring tape stretched along the rock outcrop. This is usually placed at waist height or some other appropriate level, nailed to the outcrop at both ends. The typical traverse length of the tape is 100 feet, and is laid out clockwise around the site, so the line is always starts on the left of the surveyor. The ends of the tape is often marked with spray paint and/or flags so it can be seen at a distance or be used for correlation of structures between elevations. The surveyor then traverses the line, recording discontinuity data for every discontinuity that intersects the line (Piteau and Martin, 1977).

Discontinuity information is recorded in the field using simple data cards. The detail line method, because it records information for every discontinuity along the survey line, provides extremely detailed information of the rock slope. However, this can be a time consuming process, as recording information for every discontinuity becomes tedious when surveying large areas. Also, establishing detailed lines on high slopes are often dangerous procedures requiring climbing gear and/or cranes (Watts, 2003). The horizontal line used in detail line survey also adds sampling bias. This is because detail lines give preference to vertical discontinuities, while omitting those with a relatively horizontal orientation (Park, 1999).

A second traditional method for rock mass characterization is the window mapping procedure. This involves establishing “windows” on a rock slope. A window is a subset of the rock slope that has a consistent dominate structural regime throughout. The dimensions of a window are typically 5 feet by 25 feet long. The typical distance between windows is 10 to 25 feet. Once the window size and location is established, the surveyor identifies discontinuities based on his own judgment. For ease of identification, they are typically grouped into preliminary sets based on orientations. The data for the discontinuities is recorded similarly to the detail line method. The discontinuity spacing and spacing in joint sets cannot be accurately measured from this type of survey, as information for every discontinuity is not recorded. The number of discontinuities recorded is up to the surveyor, but it is imperative that the surveyor collect a statistically significant number of discontinuities (Priest, 1993).

The advantage of window mapping is that it is faster than the detailed line method, as data are not recorded for every discontinuity. However, because of this, the window mapping is not as extensive and yields less statistical knowledge and control of the surveyed site (Priest, 1993).

Cores from borehole logging can be used to acquire discontinuity data. This method is primarily used at sites where excavation has not begun, and therefore there are no exposed rock faces to perform detail line or window mapping surveys. Great care must be taken to adequately preserve the discontinuities in the cores (Priest, 1993).

Many problems exist when data from cores are used. The core sample is too small to provide sufficient information about the spacing, length, and continuity of discontinuities. Also, cores can rotate inside the borehole, misaligning the discontinuities. Sampling bias is also a problem with core logging, as the method gives preference to discontinuities with relatively horizontal orientations, while those with steeper angles are omitted (Park, 1999).

MODERN METHODS OF ROCK MASS CHARACTERIZATION

This section presents more modern tools and methods for collecting discontinuity orientations and other data. These allow for rapid and accurate scanning of rock slopes, often from a safe distance, which gives a certain advantage over the traditional methods.

Smartphones are high end electronics, mobile phones with higher processing power, memory, and functionality. They often contain features such as portable media players, digital cameras, GPS navigation systems, accelerometers, and web browsers. These features provide a powerful, mobile way of recording data in the field which is applicable to rock mass characterization (Sun et al., 2010).

The processing power and expanded memory of smartphones allows them to use application software (often shortened to applications or apps), computer programs designed to help the user carry out specific tasks. A variety of different application software has been developed to utilize the accelerometer to turn the smartphone into a geological compass. Using these applications, a smartphone can take strikes, dip directions, dips all in one step, in addition to measuring directions and the trend and plunge of a fold line. This provides a modern alternative to the geologic compass (Sun et al, 2010).

LiDAR (Light Detection and Ranging) is an active form of remote sensing, as opposed to passive forms that detect natural radiation that is reflected or emitted. It utilizes artificial light to illuminate a surface with lasers. The lasers hit the ground surface and scatter. The intensity of the scattered beams is detected by the LiDAR scanner, and the distance to the target can be measured using the travel time. LiDAR systems can be mounted on aircraft for airborne reconnaissance and on tripods for ground based surveys (Nayegandhi, 2007).

The use of LiDAR has a significant number of advantages over traditional methods of rock slope investigation. LiDAR scanning generates a tremendous amount of data, which allows for extremely accurate approximations of the the scanned object. Using multiple returns, it can also penetrate gaps in trees, allowing for accurate topography data in heavily forested terrains. Multiple returns can also provide detailed information on the distribution of vegetation in a forest canopy (Nayegandhi, 2007).

These advantages make it particularly applicable to the field of landslide investigation, which is hindered by hostile, inaccessible terrain that is difficult to accurately investigate. The traditional methods of rock mass characterization are also time consuming and expensive processes. Both of these problems can be solved by the prudent and skillful use of LiDAR technology.

Around 1998, the new ground based, near range LiDAR systems came into common use. The advent of ground based systems came in response to several problems with airborne LiDAR reconnaissance. Airborne LiDAR is a relatively time consuming process with significant costs. Taking accurate measurements of smaller structures and buildings can be done faster and cheaper using a ground based LiDAR system. These systems are also better for scanning a single site in higher detail. Examples include fault lines or unstable rock slopes (Kemeny and Turner, 2008).

Ground based LiDAR scanners weigh around 10 to 15 kilograms and typically have an effective range of up to a kilometer with an accuracy of 3 to 10 mm. Unlike the airborne versions, the ground based systems use a progressive scan of focused laser beams with gradually changing orientations. A recent addition is digital cameras which are bore sighted with the LiDAR scanner. These allows the taking of high quality photographs and allowing for photo draping (Kemeny et al., 2005).

The output data for ground based LiDAR consists of point clouds, sets of vertices defined by X, Y, and Z coordinates in a three dimensional coordinate system. The vertices are usually used to represent the external surface of an object. From these point clouds, discontinuities can be identified, and average orientations of these discontinuities can then be used for stereo net analysis (Kemeny and Turner, 2008)

There are several sources of error in ground based LiDAR scanning. The first of which is the accuracy of laser ranging. In order to minimize error, most laser manufacturers calibrate their products to be accurate to 1 to 5 cm (Kemeny et al., 2005). Other sources of error include atmospheric conditions and temporal lighting, which adversely affect the accuracy of the LiDAR scan. Point cloud registration and software processing errors can also occur, leading to inaccurate calculations of the size and orientation of scanned discontinuity planes. (Kemeny and Turner, 2008).

Terrestrial digital photogrammetry is a mapping method that uses overlapping photograph pairs to create a 3-D surface. The photographs used for terrestrial photogrammetry can be taken using off the shelf Digital single-lens reflex (DSLR) cameras, as opposed to metric cameras used in aerial photogrammetry (Haneberg, 2008).

The 3-D model is similar to the point cloud created by a LiDAR, but is created using stereo pairs of photographs instead of reflected lasers. A grid of the photographed surface is generated using algorithms that utilize the hundreds of thousands of XYZ data points from photograph pairs. The 3-D models generated can have scale and detail on a level approaching those created using LiDAR. The model or models can then be combined with others to produce 3-D mosaics to cover large field sites (Haneberg, 2008).

There currently are three software packages that can be used for rock slope stability analysis using terrestrial digital photogrammetry. These are 3DM Analyst (developed by ADAM Technology), ShapeMetrix3D (developed by 3G Software), and Sirovision (developed by CSIRO Mining and Exploration division), all with differing field procedures and computer analysis methods (Haneberg, 2008). This discussion will focus on the field procedures and computer analysis for Sirovision, because it is the terrestrial digital photogrammetry method used in this thesis.

Sirovision consists of two different programs. The Siro3D program is used to a generate 3-D models of the rock slope from digital photographs. These models are then analyzed in the Sirojoint program to identify discontinuities and find their orientations. In Siro3D, the photographs must first be processed and cleaned, in order to correct lens distortion. After this is accomplished, the control point and four corner points are identified in each picture. This is followed by automated pattern matching and then the generation of the 3-D surfaces that constitutes the model (Haneberg, 2008).

The 3-D model for the reference stereo pair is created first. Subsequent 3-D models created from subsequent stereo pairs of photographs can then be aligned to and daisy chained onto the reference 3-D model to create a mosaic of the entire surveyed site (Maconochie et al., 2010).

Once the 3-D models for the entire site have been created, mapping of discontinuities can begin in Sirojoint. The mosaic is used to identify discontinuities, which are then outlined using polygons or linear traces. Discontinuities can be identified either by hand using virtual mapping of the mosaic, or by an automated process. Planes are fitted to match these polygons and linear traces, and dip direction and dip of the discontinuities are taken from these planes. Information such as georeferenced locations and angular variance can also be obtain from the fitted planes (Haneberg, 2008)

Once the mosaic has been created and the discontinuities have been mapped, the file can be examined in the Sirovision 3-D Viewer. In the 3-D Viewer, the mosaic can be viewed as a 2-D orthophoto, a 3-D photographic surface model, a 3-D point cloud, a 3-D triangulated mesh, and a rose diagram or stereo-plot of diplines or poles (Haneberg, 2008).

Both the field and office procedures for Sirovision have several sources of error and uncertainty that can affect the accuracy and resolution of the generated 3-D models and mosaics. Most of the errors that affect the accuracy and resolution come from the camera. The type of camera and lens utilized greatly affects the quality and resolution of the photographs. Others factors such as the range from the camera to the outcrop, the precision of field measurements, and the atmospheric conditions such as precipitation, haze, and fog can also come into play (Haneberg, 2008).

COMPARISON BETWEEN LIDAR, DIGITAL PHOTOGRAMMETRY, AND TRADITONAL METHODS

LiDAR has several advantages over digital photogrammetry. The first is that LiDAR produces its own artificial light sources, while photogrammetry relies on the sun or artificial flash photography in underground surveys. This reliance on solar illumination can create lighting problems depending on the time of day and the weather, and LiDAR needs no artificial light source when performing underground scans. Second, photogrammetry needs two viewing angles in the form of a stereo pair of photographs to create 3-D data. LiDAR only needs one to generate a fully 3-D point cloud of data. However, the multiple viewing angles used in photogrammetry prevent creation of “shadow zones”, areas of no data obscured by dense vegetation, rubble, or topography (Kemeny and Turner, 2008).

However, terrestrial digital photogrammetry like Sirovision has several advantages over LiDAR. The first is the relative equipment and surveying costs of the two methods. The initial capital investment for a LiDAR scanner dwarfs that of the necessary photogrammetry equipment, which consists of an over the counter DSLR camera and lens, tripod, geologic compass, and basic surveying equipment. The price of a new ground based LiDAR scanner, based on 2008 prices, can range anywhere from $70,000 to an excess of $150,000. LiDAR scanners are also available used or for rent (Kemeny and Tuner, 2008). For comparison, a new DSLR camera with lenses can cost anywhere from $500 to over $5,000, depending on the quality and features of the camera itself and the lenses (Haneberg, 2008). Second, the LiDAR scanner itself is a large, fragile, and relatively bulky piece of equipment which cannot easily be transported over difficult terrain or by air. Photogrammetry equipment by comparison can be carried by one person and stored (with the exception of the tripod) in carry-on baggage for flights to the project site. The photogrammetry equipment is also very versatile, and has multiple geologic fieldwork applications, unlike the LiDAR scanner, which is a very specialized tool. A third advantage is the ease of integration of photographs into the models created by photogrammetry. Terrestrial digital photogrammetry creates models based on site photographs, and therefore the image is fully integrated into the models. This lies in stark contrast with LiDAR, where photographs must be draped over the point cloud of data created by the LiDAR scan (Haneberg, 2008).

The time needed to complete a survey by either method is approximately the same in the field. This is because both surveying types rely on similar principles, such as 3-D registration. The time to complete a ground based LiDAR scan depends on the size of the scanned area and the brand and type of scanner used. Phase shift scanner only takes approximately 30 seconds, while a time of flight scanner would require 5 to 45 minutes, depending on the area of the scanned area. (Kemeny and Turner, 2008). Maconochie et al., 2010 utilized the stand alone method for Sirovision surveying a 750 meter long, 45 meter high highwall. It took 15 minutes to position the camera, take the initial reference stereo pair of photographs, and record the GPS position and directional bearings. 12 more stereo pairs of photographs are needed to cover the entire highwall, and without the use of a tripod this took a total of 20 minutes to complete.

However, in-office computer analysis is much faster in a LiDAR survey, because a LiDAR scanner automatically outputs a 3-D point cloud of data. Photogrammetry software like Siro3D and Sirojoint takes several processing steps to create a 3-D model from digital photographs. The advantage to this is that photogrammetry creates a 3-D model fully integrated with a photographic image, while a LiDAR survey must take additional steps to drape photographs over the point cloud (Kemeny and Turner, 2008).

The cost of the software for either method varies greatly depending on the software package utilized. The software required for processing can range anywhere from $5,000 to an excess of $50,000, depending on the product (Kemeny and Turner, 2008). Due to the wide variety of LiDAR scanners, DSLR cameras and lenses, processing software packages, and field registration procedures, the final accuracy of the results from either method varies greatly. Based on the combination of equipment and field and office procedures, a LiDAR survey can be more accurate than a photogrammetry survey, and vice versa (Kemeny and Turner, 2008).

Both LiDAR and terrestrial digital photogrammetry can be utilized by a single person to survey a rock slope in a matter of hours. This is in stark contrast to the time and manpower necessary to complete the same survey using traditional methods. Based on the ground based LiDAR survey of a 300 meter section of Highway 93 in Arizona, Kemeny and Turner, 2008, estimate the following costs and resources:

- 1 person for 1 day to conduct six field scans and digital photography
- 1 day for data processing
- $1500 for scanner rental
- $200 for field equipment (camera, tripod, etc.)
- $800 for software costs
- <u>Total cost</u> - $4,500

For comparison, surveying the same section using traditional methods would have the following cost breakdown:

- 2 people for 2 days to conduct window (cell) mapping resulting in 350 discontinuity orientations
- 1 person for 1 day to process and graph the data
- 5 man days, estimated at $1000 a day with overhead
- $250 for equipment and software costs
- <u>Total cost:</u> - $5,250

As shown from the cost comparison of these two surveys, the traditional method takes five days and would cost more, with over 95% of the costs being manpower. In contrast, the LiDAR survey would take two days and the total cost of the LiDAR survey would be less than 50% manpower. The traditional method is assumed to be based on measurements at the bottom of the slope. If repelling or cranes/lift where to be used to increase the scale of the survey, the cost would increase significantly (Kemeny and Turner, 2008).

While the modern methods of LiDAR and terrestrial digital photogrammetry have significant time, safety, and in certain cases cost advantages over traditional methods, they do not completely eliminate the need for field observations by knowledgeable geologists. There are many properties of discontinuities that relate to the stability of a rock slope, and modern methods cannot measure all of them. Some of these properties include structure type, rock type, infilling materials, and rock quality and hardness. LiDAR currently has methods to measure discontinuity roughness and waviness, but photogrammetry currently has none that are in practice. With the current technology, field observation by experience geologists will be needed to supplement the information provided by LiDAR and photogrammetry, and such observations should always be used in comparison to results from modern methods (Haneberg, 2008).

FIELD METHODS

The following is the field methods conducted for the window mapping for this study. Based on field observations, the discontinuities where divided into four sets. These sets are as follows:

- Bedding planes, which dipped into the rock outcrop
- Two sets of large joints, differentiated by their orientations
- One set of small joints

For each discontinuity identified, information was recorded using a data sheet. The properties recorded are as follows:

- <u>Discontinuity number</u>
- <u>Traverse trend</u> – recorded using a Brunton compass
- <u>Distance</u>

- Rock Type
- Dominance – the numerical rating of the amount of control the structure has over the slope relative to other discontinuities. The dominance values used where 1 for bedding planes, 2 for large joint, and 3 for small joints.
- Structure
- Dip direction – two values were recorded per discontinuity. One was taken using a Brunton compass, and the other with an iPhone4 and using the eGEO Compass Application.
- Dip – like dip direction, two values were recorded per discontinuity using the Brunton compass and iPhone4 with eGEO Compass Application.
- Water
- Roughness – an estimate of the Joint Roughness Coefficient for use in Barton's equation. A value of A, B, or C was recorded.
- Remark – a place to record notes and observations.

Other pertinent information, such as the time, date, location, job title, and weather condition where recorded as well.

Two windows where utilized, each with a length of 100 feet for a total outcrop length of 200 feet. A total of 45 discontinuities where measured in window 1, and 55 in window 2, for a grand total of 100 discontinuities. As stated before, for each discontinuity, the dip direction and dip was measured twice; once with a Brunton compass and once with the iPhone4 eGEO Compass Application. This results in 200 total discontinuity orientation measurements. The major difference between the two windows was the traverse trend. Window 1 has a traverse trend of 50 degrees, and window 2 has a traverse trend of 56 degrees. The difference in trend of the road cut accounts for the change in the direction of Coal Hollow Road.

In window 1, the dip direction and dip measurements taken by both the Brunton compass and the iPhone4 eGEO Compass Application where taken on bare discontinuity surfaces. In window 2, a clipboard was introduced and placed along the discontinuity surface prior to Brunton and iPhone4 measurements. The purpose was to provide a level surface to take orientation measurement that are unaffected by the small scale roughness and waviness of the discontinuity. The metallic clip of the clipboard was removed prior to use, in order to prevent this clip metal from disrupting measurements by the Brunton compass.

Field procedures followed for the Sirovision survey where in accordance with those described by Maconochie et al. 2008, which is the stand alone method. For each photograph taken, the following information was recorded:

- Picture Number
- Distance to Outcrop – measured using a tape measure. This varied between an initial value of 21.5 and 25 feet.
- Distance Between Camera Points – a distance of three feet was used, measured using a tape measure. This length is approximately 1/7 of the initial distance to the outcrop.
- Azimuth Between Camera Points – this was kept at a constant 90 degrees
- Camera Height – the height from the road surface to the center of the camera lens. This varied between 58 and 59 inches over the course of the survey.

The DSLR camera was used in a Nikon D200, with a Nikon lens, focal length of 20 millimeters. All photographs were taken with the tripod attached and base leveling plate to ensure a level image. Latitude and longitude measurements were taken for every third photograph obtained. In addition to the initial reference pair of photographs, 35 stereo pairs of photographs were taken to cover the 200 feet of the outcrop, for a total of 72 photographs.

STEREONET ANALYSIS

Stereo-graphic analysis is used to determine the kinematic stability of planar, wedge, and toppling failure. Field observations of the dip direction/dip and the poles are plotted on stereo nets and are used to determine the geometry of discontinuities and the potential failures they may cause. Marklands Test is an examination of discontinuity great circles relative to the friction angle and the orientation of the slope. The space between the slope face great circle and the friction angle creates a critical zone, wherein any great circles of a plane (planar failure) or line of intersection of two planes (wedge failure) will daylight on the slope face, having a dip greater than the friction angle and less than the slope face (Hoek and Bray, 1981).

The Dips program by Rocscience was used to perform the stereonet analysis for this study. The poles of the discontinuities where contoured in order to determine the clusters for kinetic analysis. Figure 2 shows the contoured pole plot for the Brunton measured orientation data from the window mapping survey. The stereonet shows two clusters of large joints and one cluster of small joints along with a cluster of bedding planes. Considering the slope has a dip direction of 140 for window 1 and 146 for window 2, the large and small joints form potential planar and wedge failures, while the beddings plane form potential toppling failures. Figure 3 shows the contoured pole plot for the iPhone4 measured orientation data from the window mapping survey. This stereonet shows orientations very similar to the Brunton data, with two clusters of large joints with a cluster of bedding planes.

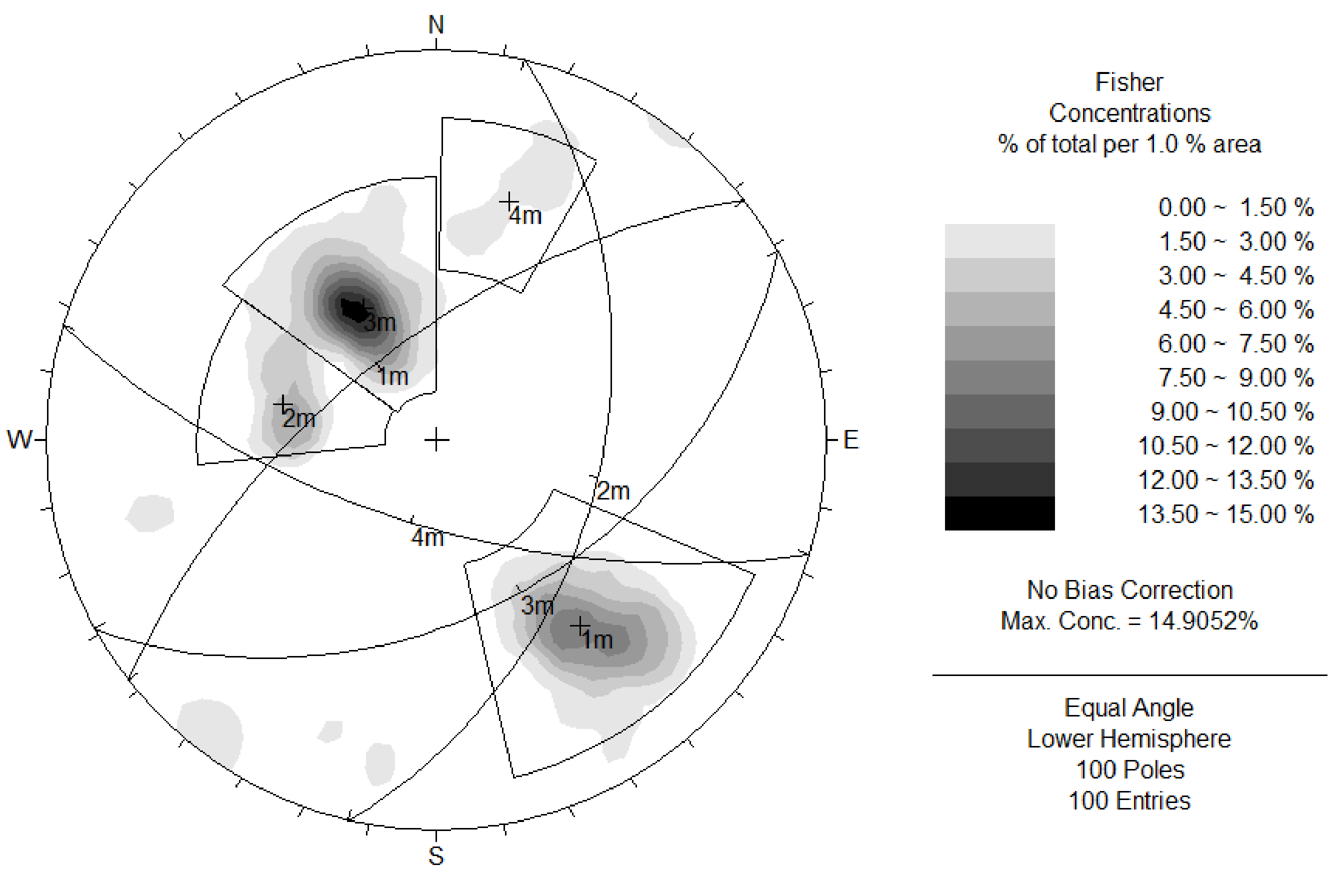

Figure 2. Clustered orientation data from Window 1 and 2 of the window mapping survey measured with a Brunton Compass, showing sets and major planes. Set 1m is bedding planes, sets 2m and 3m are large joint sets, and set 4 is small joint set.

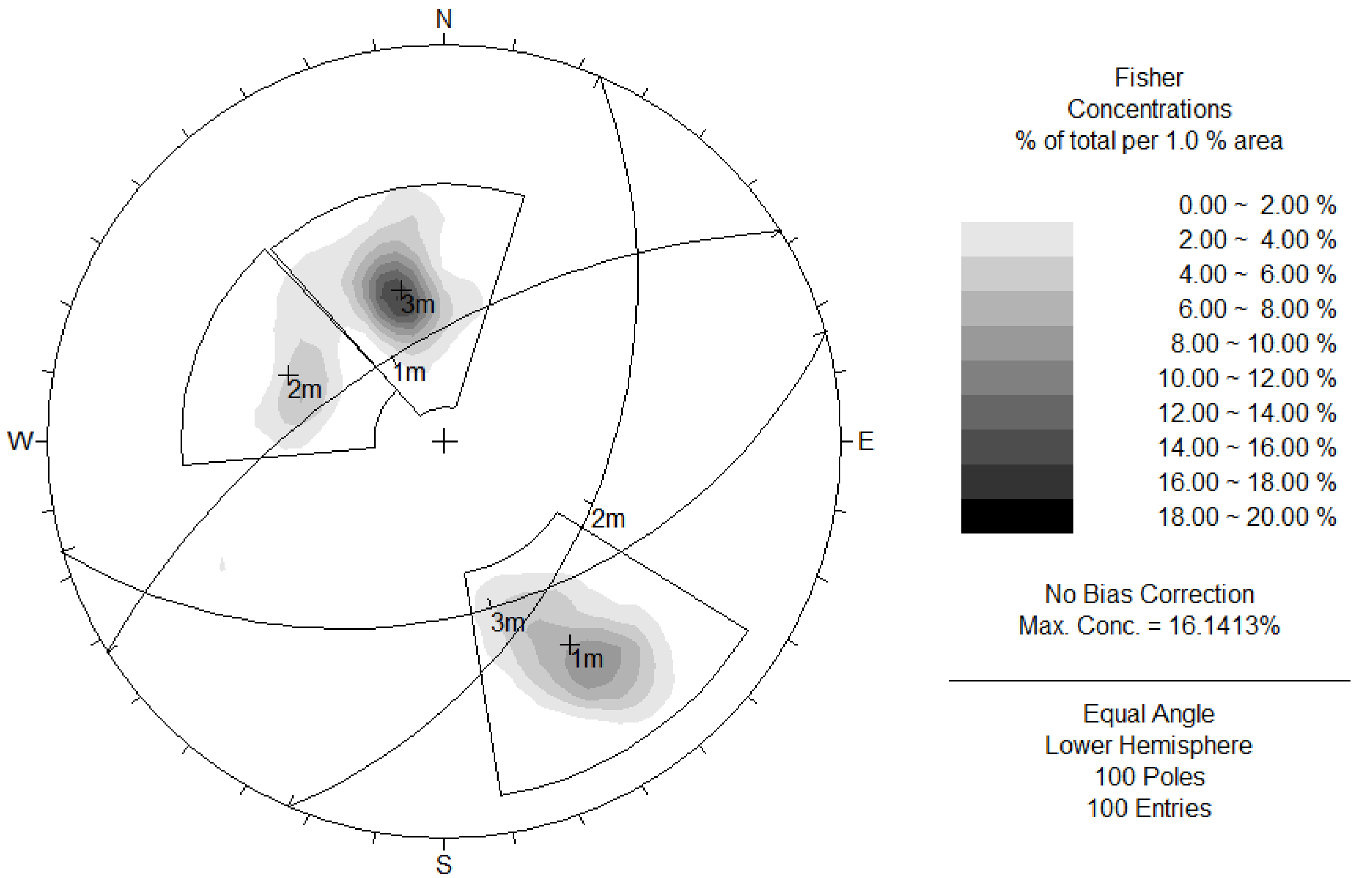

Figure 3. Clustered orientation data from Window 1 and 2 of the window mapping survey measured with an iPhone4 with the eGEO Compass application software, showing sets and major planes. Set 1m is bedding planes and sets 2m and 3m are large joint sets

PROBABILISTIC ANALYSIS

Limit equilibrium factor of safety analysis is used to determine the kinetic analysis. The traditional, deterministic analysis uses fixed values for the variables in the factor of safety equation, such as the mean value. The problem with deterministic analysis is that using fixed values for variables does not take into account their inherent uncertainty. Ignoring the uncertainty and inherent randomness of these values caused by differences in testing, models and spatial variation can drastically affect the accuracy of stability analysis. Values for variables may lie outside the mean, and may produce unstable conditions, but can be ignored if the deterministic method of analysis is used. This is because the factor of safety is very sensitive to scatter in the variables used (Park, 1999).

Probabilistic analysis is an alternative to the deterministic approach. In probabilistic analysis, the factor of safety is a random value based on the statistical deviation of its input variables. This analysis is preformed in two steps. The first is determining the mean and variance of the available data, and the probability density function (PDF) which is best for representing the random nature of each variable. In rock slope stability, variables such as discontinuity orientation, roughness and waviness, length, water content, and shear strength can be considered random variables The field observations of these properties can be used to find statistical parameters (mean and standard deviation) to generate a PDF to create random variables. The mean of the PDF is the best estimate of the value of the variables, while the standard deviation is the uncertainty (Park, 1999).

The second step is risk analysis which used the statistical parameters and PDF created in step one. The Monte Carlo Simulation is the method of risk analysis used in this study. In the Monte Carlo simulation, each random variable is generated using its respective PDF, and these random variables are used to calculate the Factor of Safety. This procedure is then repeated many times to create a probability distribution for the probability of failure, where the factor of safety is less than one. The advantage of the Monte Carlo Simulation is that a complete probability distribution can attain for the factor of safety. The disadvantage is that for the probability distribution to be accurate, a large number of calculations must be used. (Park, 1999).

The Monte Carlo simulation for this study was created using Excel and the built in Visual Basic (VBA) code. Excel itself has a wide variety of statistical functions that allows the Monte Carlo simulation to be easily run within the software. The built in Visual Basic programming environmental creates additional functionality, as it can be used to generate large number of random variables and factor safety calculations and output the results into an Excel spreadsheet. The Visual Basic code implemented in this study is based on similar work by Park, 1999.

CONCLUSIONS

In order to compare the traditional methods of rock mass characterization to modern methods, a series of surveys will be conducted at Price Mountain, VA. These include window mapping, Sirovision digital terrestrial photogrammetry, and LiDAR. The discontinuity orientations from these three methods will be used in both stereonet analysis and probabilistic factor of safety analysis. Currently, the window mapping and Sirovision surveys have been completed, as well as the direct shear testing. Further work includes the LiDAR survey, as well as stereonet and probabilistic factor of safety analysis for all three methods.

REFERENCES

Babaie, H.A, 2001, The Brunton Geologic Compass and Geological Objects, Georgia Geological Society Guidebooks, Vol 21, 1, October, 55-60.

Bartholomew, M.J., Schultz, A.P., Lewis, S.E., McDowell, R.C., and Henika, W.S., 2000, Digital Geologic Map of the Radford 30X60 Minute Quadrangle Virginia and West Virginia, Commonwealth of Virginia Department of Mines, Mineral, and Energy, Division of Mineral Resources.

Haneberg, W.C., 2008, Using Close Range Terrestrial Digital Photogrammetry for 3-D Rock Slope Modeling and Discontinuity Mapping in the United States, Bulletin of Engineering Geology and the Environment, Vol 67, 4, 457-469.

Hoek, E. and Bray, J.W., 1981, Rock Slope Engineering, 3rd Edition. Institute of Mining and Metallurgy, London.

Kemeny, J., and Turner, T., 2008, Ground Based LiDAR Rock Slope Mapping and Assessment, Central Federal Lands Highway division, Federal Highway Administration, U.S. Department of Transportation, Publication No. FHWA-CFL/TD-08-006.

Kemeny, J., Turner, K., and Norton, B., 2005, LiDAR for Rock Mass Characterization: Hardware, Software, Accuracy and Best-Practices, American Rock Mechanics Association, June 17-18.

Lowry, W.D., 1979, Nature of Thrusting Along the Allegheny Front Near Pearisburg and of Overthrusting in the Blacksburg-Radford Area of Virginia, Virginia Tech Department of Geological Sciences Guidebook Number 8, for the 11th Annual Virginia Geotechnical Field Conference, Blacksburg, Va., October 26-28.

Maconochie, P.A., Soole, P., and Simmons, J., 2010 Validation of a Simple One Person Method for Structural Mapping using Sirovision, Bowen Basin Symposium, 2010.

Nayegandhi, A., 2007, Lidar Technology Overview, Presentation for Airborne LiDAR Technology and Applications, Baton Rouge, LA, June 20-21.

Park, H., 1999, "Risk Analysis of Rock Slope Stability and Stochastic Properties of Discontinuity Parameters in Western North Carolina." Ph.D. Thesis, Purdue University.

Patton, F.D., 1966, Multiple Modes of Shear Failure in Rock, Proceedings of the 1st International Congress of Rock Mechanics, 1, Lisbon, 509-513.

Piteau, D.R., and Martin, D.C., 1977, Detail Line Engineering Geology Mapping Method, Field Manual, D. R. Piteau and Associates Limited, West Vancouver, B.C.

Priest, S.D., 1993, Discontinuity Analysis for Rock Engineering, Chapman and Hall.

Watts, C.F., 1983, "Development, Testing, and Evaluation of a Microcomputer System for Rapid Data Collection and Analysis of Geologic Structure Data Related to Rock Slope Stability." Ph.D. Thesis, Purdue University.

Watts, C.F., 2003, ROCKPACK III for Windows, ROCK Slope Stability Computerized Analysis PACKage, ROCKPACK III Users Manual.

West, T.R., 1996, The effects of positive pore pressure on sliding and toppling of rock blocks with some considerations of intact rock effects, Environmental and Engineering Geoscience, 2, 339-353.

Presidio Parkway Project Phase 1

Authors

Timothy J. Pokrywka
California Department of Transportation
111 Grand Avenue, Oakland, CA, 94623-0660
(510) 286-4840
Tim.Pokrywka@dot.ca.gov

Hossain Salimi
California Department of Transportation
5900 Folsom Boulevard, Sacramento, CA, 95819-4612
(916) 227-7147
Hossain.Salimi@dot.ca.gov

Mahmood Momenzadeh
California Department of Transportation
111 Grand Avenue, Oakland, CA, 94623-0660
(510) 286-5732
Mahmood.Momenzadeh@dot.ca.gov

Francis R. Greguras
Arup
560 Mission Street, San Francisco, CA 94105-2907
(415) 946-0255
frank.greguras@arup.com

Anna Sojourner
California Department of Transportation
111 Grand Avenue, Oakland, CA, 94623-0660
(510) 622-8839
Anna.Sojourner@dot.ca.gov

Tung Nguyen
California Department of Transportation
111 Grand Avenue, Oakland, CA, 94623-0660
(510) 622-1775
Tung.Nguyen@dot.ca.gov

Prepared for the 63rd Highway Geology Symposium, May 7-10, 2012.

Acknowledgements

We are thankful for the support and confidence of Caltrans District 4, Caltrans Structures Design and San Francisco County Transportation Authority management and design staff. Acknowledgment goes to Project Managers John Karn of Arup and Nidal Tuqan of Caltrans in addition to Lee Saage of SFCTA. We are grateful for all the Caltrans, Arup and Parsons Brinkerhoff staff that contributed to this project. In particular, thanks go to the Caltrans geotechnical design staff engineer Caroline Chen. Also from the Joint Venture, we acknowledge geotechnical design staff Terrence Carroll of Arup and Tom Lee of Parsons Brinkerhoff. David Nesbitt from Caltrans did an extraordinary job making sure the drilling program was conducted in a safe and efficient manner. We also want to thank Senior Engineering Geologist Grant Wilcox, in particular for his contributions to the Southbound Battery Tunnel subdrain design. We thank Malcolm Drilling for their work in the CDSM/CIDH project and R&L Brosamer for the lightweight fill, and Scott Taylor of Cell-Crete Corporation for his work on the detour.

Finally, thanks to our funding agency, the Metropolitan Transportation Commission. Without their financial support this project would not have been possible.

Disclaimer

Copyright Notice

ABSTRACT

The project is located in the 200 year-old Presidio, a National Park, in San Francisco, California. An integrated team consisting of Caltrans Geotechnical Services and the joint venture (JV) of Arup and Parsons Brinckerhoff provided geotechnical engineering services.

Originally constructed in 1936, the existing Doyle Drive needs design, seismic and traffic safety improvements. The project faces several significant challenges: highly variable and poor geologic conditions in a highly active seismic setting, preserving the natural and historical Presidio resources, providing extensive public outreach and inter-agency coordination for a large group of stakeholders and removing and replacing the existing facility while maintaining traffic during construction.

The many innovative ideas utilized in this project include: an integrated team of Caltrans drilling crews and local drilling subcontractors used for the subsurface exploration, a foundation contractor feedback meeting held for the Southbound Presidio Viaduct Bridge, a bridge foundation system design that includes a 12 foot diameter steel casing over a rock socket, a Cement Deep Soil Mixing and Cast in Drilled Hole Test Project, using separate excavation pay items for the different ground conditions, a special subdrain that maintains groundwater flow to the wetlands below a bluff while meeting the project needs of draining a tunnel, a soldier pile tangent beam retaining wall with steeply inclined heavy duty tiebacks used to avoid instability to adjacent facilities, and a lightweight fill combined with a retaining wall used for a temporary detour over soft soils in order to maintain traffic during the 3 to 4 year construction period.

INTRODUCTION

The Presidio Parkway, also known as Doyle Drive, is signed as U.S. Route 101 and serves as the southern access to the Golden Gate Bridge. Winding 1.5 miles along the northern edge of San Francisco, the project area extends from the Golden Gate Bridge Toll Plaza on the west to Broderick Street on the east (Figure 1). The roadway is the primary highway and transit linkage through San Francisco between counties to the south (San Mateo and Santa Clara) and the north (Marin and Sonoma) and provides access to historic and cultural landmarks, including the Golden Gate National Recreation Area, the Presidio, the Golden Gate Bridge, and the Palace of Fine Arts.

Originally constructed in 1936, the existing Doyle Drive needs design, seismic and traffic safety improvements. Located within the over 200 year-old Presidio of San Francisco, a National Park and a National Historic Landmark District, the project faces several significant challenges: highly variable and poor geologic conditions in a highly active seismic setting, preserving the natural and historical Presidio resources, providing extensive public outreach and inter-agency coordination for a large group of stakeholders (i.e. citizens' groups and other public agencies) and removing and replacing the existing facility while maintaining traffic during construction.

This paper discusses design and construction challenges for Phase 1 of the project, the components of which will eventually form the southbound Presidio Parkway. After all traffic is switched on to the completed Phase 1 project in early 2012, construction of Phase 2, the northbound Presidio Parkway will commence. The main project components of Phase 1 are the Cement Deep Soil Mixing (CDSM)/Cast-in-Drilled-Hole (CIDH) Test Project, temporary detour road, Retaining Wall No. 8, Southbound Battery Tunnel, and the Southbound Presidio Viaduct (Figure 2). The CDSM/CIDH Test Project was conducted in the detour road area before the temporary detour road was constructed. The detour road serves traffic through the eastern portion of the road until the proposed permanent roadways and structures are constructed under the second phase contract. Retaining Wall No. 8 is located between the proposed southbound Main Post Tunnel and the southbound Battery Tunnel. This tangent pile wall extends about 1,200 feet in length and varies in height from about 5 feet to more than 45 feet. The Southbound Battery Tunnel (SBBT) is a 1,036 foot-long, 66 foot-wide cut-and-cover tunnel, which required excavations up to 48 feet deep. It lies immediately north of the San Francisco National Cemetery. The Southbound Presidio Viaduct is 1,400 feet long and 80 feet high and connects the toll plaza with the SBBT.

An integrated team consisting of Caltrans staff and the joint venture (JV) of Arup and Parsons Brinckerhoff provided geotechnical engineering services for the project. The JV is under contract with the San Francisco County Transportation Authority.

GEOLOGY AND SEISMICITY

San Francisco lies in the California Coast Ranges, a northwest-trending range of fault-bounded mountains that roughly parallels the San Andreas fault system. The region is characterized by high seismicity and topography controlled by uplift and right-lateral shear on active fault systems. The San Andreas fault zone, considered capable of producing a maximum magnitude M_{max} 7.9 earthquake, lies over 5.9 miles southwest of the site. The highly active San Gregorio and Hayward faults also lie within several miles of the site and could produce strong shaking at the site.

The City of San Francisco is famously characterized by the block-in-matrix topography typical of the Franciscan Complex. Rugged, steep hills of the Cretaceous Franciscan Complex bedrock (chert, serpentinite, and greywacke sandstone) are surrounded by low-lying valleys of softer Franciscan matrix, filled with Quaternary sediments.

Medley (1994) defined block-in-matrix rocks (bimrocks) as geological mixtures of geotechnically significant harder blocks of rock within weaker, bonded rock matrices. In engineering practice, this means that rather than laterally continuous layers, bimrocks can be thought of as randomly sized and distributed blocks of hard rock in a highly sheared, softer matrix. Even closely spaced borings may fail to account for the distribution of hard rock if exploratory borings hit only matrix or only bimrocks. Different types of bedrock may be found adjacent to one another, as their borders are not depositional contacts, but blocks surrounded by matrix.

Serpentinite is metamorphic bedrock that can contain naturally-occurring asbestos (chrysotile). Because of the potential health hazard, excavation in serpentine triggers regulation by several agencies and requires additional safety plans, worker and public protection from dust, and additional measures for on-site storage and safe transport. Serpentine containing chrysotile must be treated and disposed of as hazardous waste.

Dune sand of the Colma and Merced Formations blankets much of western San Francisco. Low-lying areas along the Bay typically are filled with Bay Mud, a saturated, highly compressible, low-strength estuarine mud. Unengineered artificial fill was commonly placed along the Bay beginning in the late 1800s. This fill is highly susceptible to liquefaction during ground shaking, as was seen in the damage from the 1989 Loma Prieta earthquake.

GEOTECHNICAL EXPLORATION PROGRAM

The geotechnical exploration program included over 160 exploratory boreholes and cone penetration tests, and one horizontal boring for Retaining Wall No. 8, in-situ geophysical tests (suspension P-S velocity logging and seismic refraction method), oriented rock coring, and packer tests. In addition to a comprehensive laboratory testing program, over 50 standpipe piezometers were installed to monitor groundwater levels.

Conducting our exploration program in a national park, formerly a military base, in a densely populated urban area, required extensive coordination. Our program was overseen by the Presidio Trust, and fell under National Park and Federal regulations. The preliminary work required environmental documentation, three utility clearance processes, archaeological and biological monitoring, traffic control, California Highway Patrol traffic monitoring, lane and ramp closures, and public notification. Unexploded ordnance and unexpected contaminated soils were concerns.

This exploration program was conducted for Phase 1, the southbound component of the project, as well as Phase 2, planned to be designed and built by a Public-Private Partnership. Exploration results were provided to bidders for Phase 2 without guarantee or warranty. The Public-Private Partnership conducted extensive further subsurface investigation.

SITE SUBSURFACE CONDITIONS

The area of the CDSM/CIDH Test Project and Temporary Detour Road traverses low-lying former estuarine wetlands. A 5 to 7 foot layer of loose fill overlies 5 to 10 feet of very soft to soft clay (Bay Mud). Below the Bay Mud lie loose to medium dense marine sands, and dense to very dense Colma sand, and stiff to very stiff clay, underlain by sandstone and shale. Groundwater lies about 3 feet below the ground surface. The groundwater in the Colma sand is artesian in this area.

The eastern 700 feet of Retaining Wall No. 8 has a 0 to 7 foot layer of very loose to loose sandy fill and sandy silt that overlies a 20 to 25 foot layer of medium to very dense silty, clayey sand that overlies dense to very dense sands. The western 500 feet of Retaining Wall No. 8 has an 11 foot layer of very loose to loose sandy fill and sands that overlies 12 feet of soft to very stiff sandy clay that overlies dense to very dense clayey sand. Franciscan bedrock was encountered in preliminary borings at approximately 50 feet near the east end of the Southbound Battery Tunnel, but was not encountered in construction of Retaining Wall No. 8. Groundwater lay 25 feet below the ground surface on the east end of the wall and 45 feet below the ground surface at the west end of the wall.

The Southbound Battery Tunnel lies on an elevated bluff made up of Franciscan Complex bedrock overlain unconformably by Colma Sand. The bedrock surface dips to the east. At the northeast end of the site, approximately 60 feet of sand overlies the serpentinite bedrock, and no rock was encountered to the depth of tunnel excavation. At the west end, a large bimrock of greywacke sandstone lies nearly at the ground surface. Serpentinite was encountered in preliminary borings at the east end of the tunnel. At the east end of the tunnel, groundwater was encountered at 40 to 50 feet below the ground surface. At the west end, where the bedrock surface lay at a higher elevation, groundwater was perched at the soil/rock interface.

The San Francisco National Cemetery lies uphill of the tunnel, nearly 30 acres of irrigated lawn that contributed significantly to groundwater in the upper subsurface of the tunnel and Retaining Wall No. 8. Overland flow from the cemetery is not a significant factor at the site, even during heavy rain.

The Southbound Presidio Viaduct crosses a bedrock low filled with beach and dune sand deposits, Colma Formation and Old Bay Mud. The depth to bedrock varies from 5 feet to 140 feet. Bent 2, the focus of this paper, lies on the east end of the viaduct, and is seated in Franciscan shale and sandstone. The Franciscan bedrock was extremely variable in hardness, fracturing, and weathering, ranging from very hard to very soft, slightly to very intensely fractured, and slightly weathered to decomposed.

SIGNIFICANT PROJECT COMPONENTS

The following sections describe design challenges, issues that arose during construction and how they were addressed for the five significant project components.

Cement Deep Soil Mixing (CDSM) and Cast in Drilled Hole (CIDH) Pile Prototype Test

The tests were conducted in support of components of Phase 2: cut-and-cover tunnels, drilled shafts to support bridges, and to facilitate construction of a depressed roadway located in sand and Bay Mud under artesian conditions. The results were included in the bidding package for Phase 2. The tests were conducted with three objectives: to determine the best water/cement ratio for the site, to determine the amount of spoils generated from the deep mixing operation; and to determine the behavior of drilled hole in Colma sand under the artesian conditions for pile installation.

Two 10 foot by 10 foot solid blocks were constructed on the plan area, one by single shaft Deep Soil Mixing (DSM), and one by Cutter Soil Mixing (CSM). An additional 10 foot by 10 foot open cell was constructed with CSM (Figures 3 and 4). The DSM block and the cell were mixed to about 37 feet, about two feet into Colma sand. The CSM block extended to a depth of 60 feet, ending slightly above the Old Bay Mud. A water-to-cement ratio of 0.909 was used to achieve the average specified unconfined compressive strength (UCS) of 145 psi at 28 days and a maximum hydraulic conductivity of $5x10^{-6}\ ^{cm}/_{sec}$. The shallower mixing (37 feet) produced spoils varying from 19 to 37%. The deeper mixing (60 feet) produced 44% spoils.

Fifteen days after the deep soil mixing, a 5 foot-diameter hole was drilled to the specified CIDH pile tip elevation. Colma sand is dense to very dense, but under the artesian conditions at the site, the hole caved below the mixing depth. In contrast, 10 days after mixing, a 5 foot-diameter, 55 foot-long CIDH pile was successfully installed within the 60 foot-deep CMS block. The drilled hole was completely dry, therefore the inspection tubes were not necessary and removed from the cage.

Five 3.5 inch inside diameter drill cores were logged to verify the results of the mixing. UCS testing was conducted on representative samples at 5 foot depth intervals of four of the cores. The majority of samples reached and exceeded the required UCS.

Table 1: Unconfined Compressive Strength of Cores

Approximate Depth (ft)	Core # 1	Core # 2	Core # 3	Core # 4
	14 Day Break	28 Day Break	28 Day Break	46 Day Break
	CSM1B (psi)	DSM 3 (psi)	CSM1A (psi)	CSM3C (psi)
5	236	254	533	480
10	455	388	229	710
15	446	217	729	530
20	502	297	715	660
25	689	515	624	1000
30	588	584	501	970,660,900,510
35	555	222	326	620
40	582	316	442	
45	240		240	350,600
50	265		265	530
55	343		343	840
60	403		403	450

Grab samples from each of the constructed columns also had results consistent with those of the core samples. Grab samples were also tested for permeability. All of the measured permeabilities were lower than the design value.

Temporary Detour Roadway

The detour roadway lies on very soft ground that includes highly compressible Bay Mud. We calculated that ground settlement would occur with fill of 2 feet or thicker. We estimated that a 7 foot-high embankment would cause ground settlement of about 1.4 feet. Moreover, 90% of that settlement would occur in 90 days. We recommended expanded polystyrene (EPS) blocks, or GeoFoam, for the embankment fill, with a Hilfiker retaining wall system for the detour roads where the embankment is higher than 6 feet. For sections where the embankment was less than 5 feet, we recommended granular lightweight fill with a unit weight of around 60 pcf.

The contractor submitted a Cost Reduction Incentive Proposal (CRIP) to replace the EPS blocks with lightweight cellular concrete (LCC) in conjunction with a Hilfiker wall system (Figure 5). We worked with the contractor to delineate the area that required the LCC, developed the specifications and conducted oversight. The actual test densities ranged mostly between 25 and 28 pcf. The unconfined compressive strengths ranged from 118 to 242 psi.

Retaining Wall No. 8

The design of Retaining Wall No. 8 was broken into three segments and used 30 inch diameter piles. The 300 foot-long eastern portion of the wall was designed as a tangent pile wall to avoid impacting nearby historic buildings in the Presidio. The computed deflections at the top of the wall were 1.75 inch and 0.54 inch under seismic and static conditions, respectively. The 400 foot-long middle section was designed as a tangent pile wall, except for the section crossed by a 36 inch drainage pipe, where a reinforced concrete cantilever retaining wall supported by CIDH piles was used. The western 500 foot-long section of the wall was designed as a tangent pile wall with multiple levels of tiebacks. Due to the presence of very soft to stiff clay to the depth of 23 feet, the unbonded lengths of the first two rows was extended beyond that zone. Tieback length was about 85 feet for the first row. Where the available easement was not sufficient, 5 rows of tiebacks with 20 degree inclination and with variable horizontal and vertical spacing were used. For the 45 foot-high wall under temporary construction condition, an additional row of tiebacks was recommended.

Significant groundwater seepage occurred in the west end of the wall near the Battery Tunnel during construction, from a combination of heavy winter rains and irrigation in the adjacent cemetery. Horizontal drains were installed at three levels under contract change order to drain the wall backfill and to protect the finish of the cast-in-place reinforced panels between the soldier beams (Figure 6). These drains were designed with cleanouts to be maintained in the permanent wall. Drilled holes for the tiebacks and soldier beams frequently caved due to poor soil and high groundwater. Although temporary casing is often used in this condition, synthetic slurry was used for this project. Slurry is generally not used for soldier beam drill holes, because slurry film that remains on the beam can create a separation between the soldier beam and the concrete. Synthetic slurry, designed to prevent residue of the slurry film remaining on the beam, was successfully used in Retaining Wall No. 8, allowing expedited construction of the soldier beams.

To accommodate conforming of the tunnel grade with the adjacent roadway at the south end of the Battery Tunnel, an additional unsupported temporary excavation with 8 foot lifts was constructed below the lowest designed tieback along a section of the wall. This excavation caused a 1.5 inch deflection of the wall. After the required tiebacks were installed, the initial unsupported excavation and heavy rainfall caused an additional 0.5 inch deflection. Since the strands were already cut, a lift-off test to confirm the loads in tieback was not possible. Alternative analyses were conducted to check the loads in the tieback based on the estimated earth pressures and differential stretch of the unbonded length before and after the excavation. The results indicated a reduction of 20% in factor of safety for the tieback design load at the lower portion of the wall. This was judged to be acceptable because all tiebacks were loaded in performance testing to 1.5 times design loads.

Southbound Battery Tunnel (SBBT)

The tunnel alignment lay within 5 feet of the San Francisco National Cemetery property line. Criteria during the design phase did not allow for tiebacks extending into the cemetery, so the deflection of the temporary shoring needed to be limited to 1 inch. The shallow-depth cut-and-cover tunnel would be subjected to strong ground shaking during the design Safety Earthquake Event (SEE). The ground conditions at the tunnel invert consisted of Franciscan Complex at the west end and dense Colma sand at the east end. The field exploration indicated the presence of serpentine and greywacke bedrock. The tunnel invert elevation is below groundwater. Groundwater flows from the cemetery area to the west Crissy bluffs wetlands needed to be maintained.

Based on the criteria that tiebacks could not extend into the cemetery, the design for the temporary shoring for the tunnel excavation consisted of installing a dewatering system along the cemetery property line and using a temporary soldier pile and lagging retaining wall that would be braced internally with up to three levels of struts. Inclinometers were used to measure deflection of the temporary shoring walls.

Due to strong ground shaking under the SEE, it would be difficult to design a moment connection between a diaphragm wall and the tunnel roof, so this type of shoring/permanent wall for the tunnel was not considered. Also, a diaphragm wall system would impact groundwater flows to the west Crissy bluffs wetlands. Where the tunnel alignment lies very close to the cemetery, the temporary shoring consisted of tangent piles.

To provide uniform subgrade conditions below the tunnel invert slab, the bedrock in the west end of the tunnel was over-excavated two feet and replaced with compacted granular fill. Different pay items were used in contract documents for soil, rock, and serpentine that would require additional treatment and disposal.

Vertical drainage panels were specified behind the timber lagging. The vertical drainage panels were connected by HDPE pipes to strip subdrains on 24 foot centers below the tunnel invert slab to maintain groundwater flow under tunnel to the bluffs wetlands.

During the bidding phase the VA modified their criteria regarding use of tiebacks adjacent to the cemetery and allowed tiebacks 20 feet or more below the original grade at the cemetery property line. Based on this criterion, the contractor prepared a Cost Reduction Incentive Proposal (CRIP) for the two temporary shoring retaining walls. The CRIP eliminated the three levels of internal bracing, except for the first row at the pinch-point where the tangent pile wall was required, and at another location where the tieback depth criterion could not be met. The CRIP also replaced the original timber lagging with shotcrete lagging. The tiebacks were positioned between the soldier piles with internal walers.

The soldier pile drilling (180 piles on 6 foot centers) provided an opportunity to create a high-resolution geologic cross-section before excavation began. Despite a detailed preliminary investigation, additional geologic issues were encountered in construction. The serpentinite quantity was much less than expected. This can be explained both by the nature of drilling in bimrocks and because the estimates for bidding were conservative, extrapolated from the preliminary borings to encompass the largest possible amount of serpentinite. A large bimrock of Franciscan greywacke lay at the pinch-point where the alignment lay within 5 feet of the cemetery. This was not detected in the preliminary investigation because it lay between two borings. The bimrock lay within 5 feet of the ground surface. This coincided with the tangent pile section of the wall that was necessary to avoid tiebacks. Drilling the tangent piles was slower than anticipated, but the bedrock added strength to the subsurface at a critical section of the excavation. As excavation proceeded, the preliminary investigative conclusion that the Franciscan bedrock contained no dominant fracture orientation was verified. This source of water for the Crissy bluffs wetlands north of the project tunnel is not controlled by fracture orientation. However, significant quantities of groundwater are carried through the Colma sand to the wetlands.

Caving and blowouts occurred behind the south temporary retaining wall in the eastern portion of the tunnel during excavation (Figure 7). The caving and blowout became apparent when the excavation depth was about 16 feet. The caving and blowout conditions were related to an ineffective dewatering system, retaining non-cohesive Colma sand, heavy winter rains, and difficulty installing the internal walers and tiebacks between the soldier piles, which resulted in delays in shotcreting. The caving and blowout problems were addressed by backfilling the voids with slurry, increasing the width of drainage panels from 1 foot to 3 feet, limiting the excavation depth before shotcreting and installing tieback beams, and installing dewatering wells and sumps within the tunnel excavation.

Five of the six inclinometers showed results indicating that the cumulative deflections were less than the 1 inch criterion during excavation and placement of the tunnel invert slab. The inclinometer located in the transition area between the SBBT and Retaining Wall No. 8 exceeded the 1 inch deflection criterion. The measured deflection at the top of this inclinometer approached 2 inches, as discussed under Retaining Wall No. 8. Deflection was slowed and arrested when the excavation was limited to the next tieback level until the previous level of tiebacks was tensioned.

The ineffectiveness of the dewatering system, performing a deep excavation during the winter season, and having greater than normal rainfall produced a wet and softened subgrade that would not allow installation of the subdrain system or compaction of subgrade soils and aggregate base. To address the wet and softened subgrade conditions, a high-strength geotextile (Mirafi RS 580i) was used for stabilization. The aggregate base material placed above the geotextile was successfully compacted to 100 percent relative compaction (Figure 8).

Southbound Presidio Viaduct

The Southbound Presidio Viaduct is supported on drilled shafts. The pile lengths ranged from about 110 to about 190 feet. We drilled an exploratory hole in the middle of each support, and each support was analyzed separately. Both isolation casing to improve flexibility at Bents 2, 5, and 6, and permanent 12 foot-diameter steel casings in the soft upper strata were incorporated into the design. The High Viaduct Structure was classified as a District 4 Recovery Route facility, which is above Caltrans Ordinary Bridge and below Caltrans Important Bridge status. Two levels of earthquake performance, the Safety Evaluation Earthquake (SEE) and Functional Evaluation Earthquake (FEE), had to be considered. The seismic analyses of the structure were a two-pronged procedure. The static pushover analysis was performed for every bent with data provided by the Caltrans geotechnical personnel. The dynamic analysis was performed to verify the static pushover analysis, with data provided by the consulting firm Earth Mechanics Incorporated.

After the completion of the preliminary design, an outreach meeting was held, attended by dozens of potential contractors and subcontractors. Following the Caltrans presentation, contractors were allowed to make comments verbally and in writing, resulting in a very lively and helpful discussion. This helped everyone understand the project better and present ideas that were used to modify the design to improve the construction phase.

The Viaduct required large 12 foot diameter steel casings be placed as much as 150 feet into ground. A special oscillator rig was constructed to handle this task (Figure 9).

At Bent 2, a portion of the excavated rock socket caved in while it was left open over the weekend. The Contractor's position was that competent rock should not be subject to significant caving. Caltrans' position was that the material encountered was consistent with the descriptions in the LOTBs, and the specifications in the Foundation Reports and SSPs clearly described the rock. The hole was left open for several days at various stages of the drilling process prior to placing the rebar cage, which may have contributed to the cave-ins.

CONCLUSIONS - LESSONS LEARNED

From the CDSM / CIDH prototype test we learned that the unsupported Colma formation sands caved under artesian conditions. Unsupported holes could remain open for a limited time. It confirmed that CDSM is a viable tool to extend the time a drilled hole can remain open in these conditions and can create a dry hole. It provided strength, permeability and spoils data for the specific site conditions

In the construction of the temporary detour road we learned that the Hilfiker style retaining system could be successfully used in conjunction with cellular concrete. The placement of membrane along the face and the reinforcement is critical, due to the fluid nature of cellular concrete during placement.

In the construction of Retaining Wall No. 8 we learned that unusual external sources of groundwater, in this instance a cemetery and unusually high seasonal rains, need to be accounted for in design and specifications. Horizontal drains effectively control significant amounts of groundwater occurring at isolated locations during wall construction.

From construction of the SBBT we learned that greater emphasis must be placed on construction dewatering of deep excavations that extend below the groundwater table. An effective system for drawing down the groundwater level must be employed prior to the start of any excavation where a soldier pile and lagging wall is proposed for temporary shoring. Where non-cohesive soil conditions exist, the use of internal waler beams should be discouraged to prevent caving and blowouts. Where groundwater is significantly above the invert of a cut-and-cover tunnel, full-width drainage panels should be used between the soldier piles. Use of a high-strength geotextile, such as Mirafi RS 580i, is an effective way of combating wet and softened subgrades.

From construction of the southbound Presidio Viaduct we learned that wording in the specifications regarding payment is critical. The specifications stated that the contractor was responsible for all caving problems, however, there was no specific language requiring that they would be responsible for the costs. Specifications should give time limits for large-diameter holes to be left open. It is possible to construct very large diameter shafts in relatively weak ground conditions successfully while minimizing exposure to differing site conditions and other claims. The feedback meeting before final design with foundation contractors proved highly valuable for this large project with difficult ground conditions and extraordinary and challenging construction constraints and difficulties. The 12 foot diameter rotator oscillator equipment is now available locally to handle similar projects.

The highly cooperative partnership between Caltrans and JV staff proved very valuable. Each brought a unique set of experience and expertise that resulted in a positive and creative working environment that enhanced the project. Evidence was the successful completion of the large and complex subsurface exploration program and the critical construction support that was able to quickly address challenging field issues in an effective manner.

REFERENCES

Abrahamson, N., 2009, Seismic Hazard Assessment and Site Response Analysis for the Doyle Drive Project, report by AMEC Geomatrix, Inc., submitted to the ARUP-PB Joint Venture , Appendix A

ARUP-PB Joint Venture, 2009, Foundation Report: Southbound Battery Tunnel (Bridge no. 34-0161L), report prepared for the San Francisco County Transportation Authority Doyle Drive Replacement Project, variously paginated.

Baseline Environmental Consulting, 2009, Environmental Soil Investigation, Doyle Drive Replacement Project, Contract 4, San Francisco, California, for ARUP, variously paginated.

Blake, M.C., Graymer, R.W., and Jones, D.L., 2005, Geologic Map and Map Database of Parts of Marin, San Francisco, Alameda, Contra Costa, and Sonoma Counties, California, U.S. Geological Survey Miscellaneous Field Studies MF 2337, Online Version 1.0, http://pubs.usgs.gov/mf/2000/2337/.

Caltrans, 2009, Foundation Report: Retaining Wall No. 8, Doyle Drive Replacement Project.

Caltrans, 2009, Foundation Report: Southbound Presidio Viaduct (Bridge no. 34-0157L), Doyle Drive Replacement Project.

Malcolm Drilling Company, Inc., 2010, Deep Soil Mixing (DSM)/Cutter Soil Mixing (CSM) Testing Report.

Medley, E.W., 1994, The Engineering Characterization of Mélanges and Similar Block-in-Matrix Rocks (BIMrocks). Ph.D. dissertation, Dept. of Civil Engineering, University of California, Berkeley, California, USA,1994.

Figure 1. Location Map

Figure 2. Computer-generated graphic of completed Phase 1 construction, showing Temporary Bypass, Retaining Wall 8, Southbound Battery Tunnel, and Presidio Viaduct.

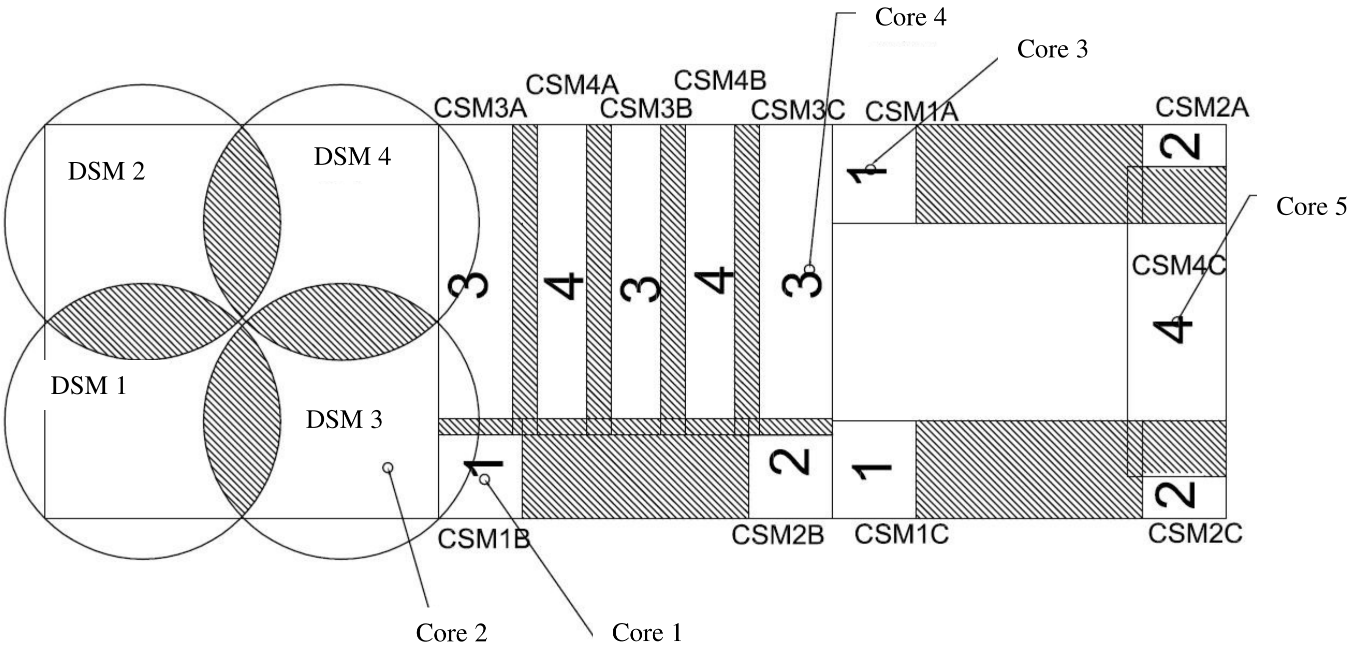

Explanation
DSM# - Number and sequence of DSM passes
CSM# - Number and sequence of CSM passes
Shaded areas are overlap of passes

Figure 3. Schematic of 10'x10' solid blocks constructed with Deep Soil Mixing (DSM) and Cutter Soil Mixing (CSM), and 10' x 10' open cell with Cutter Soil Mixing

Figure 4. CSM soil mixing tool (left) and DSM soil mixing tool (right)

Figure 5. Hilfiker wall/Lean Cellular Concrete (LCC) construction. There are two stacked layers of LCC surrounded by membrane and mesh. Mesh for a third layer has been placed on the top.

Figure 6. Retaining Wall No. 8 under construction with horizontal drains

Figure 7. Blowout in non-cohesive sand during construction of the Southbound Battery Tunnel

Figure 8. Southbound Battery Tunnel subdrain system under construction

Figure 9. 12 foot diameter oscillator

Multifaceted Approach for Evaluating and Treating Sinkhole Activity beneath Highways – Case Study: SR 0422 in Southeastern Pennsylvania

Sarah E. McInnes, P.E.
Pennsylvania Department of Transportation, District 6-0, Geotechnical Engineering Unit
7000 Geerdes Boulevard
King of Prussia, PA 19406
610-205-6544
smcinnes@pa.gov

Joseph T. Krupansky, P.G.
Gannett Fleming, Inc.
1010 Adams Avenue
Audubon, PA 19403
610-650-8101
jkrupansky@gfnet.com

Craig M. Benedict, P.E.
Gannett Fleming, Inc.
1010 Adams Avenue
Audubon, PA 19403
610-650-8101
jkrupansky@gfnet.com

Prepared for the 63rd Highway Geology Symposium, May 7-10, 2012

Acknowledgements

The authors would like to thank the following individuals/entities for their contributions in the work described:

Richard Lee, P.G., R. GP. - Quantum Geophysics (A Division of Gannett Fleming, Inc.)
TRC Companies, Inc., Test Boring Contractor
J.D. Eckman Construction Company, General Contractor
Structural Group, Inc., Grouting Specialty Contractor
B.L. Myers Bros., Drilling Subcontractor

Disclaimer

Statements and views presented in this paper are strictly those of the author, and do not necessarily reflect positions held by their affiliations, the Highway Geology Symposium (HGS), or others acknowledged above. The mention of trade names for commercial products does not imply the approval or endorsement by HGS.

ABSTRACT

In the overnight hours between September 30th and October 1st, 2010, several sinkholes developed along a heavily-traveled section of SR 0422 in southeast Pennsylvania. In conjunction with PENNDOT's geotechnical engineers, Gannett Fleming developed a sinkhole investigation program to identify the likely sources of the sinkhole activity amid the busy highway environment. The sinkhole investigation program consisted of a multifaceted approach incorporating three different geophysical survey methods; test borings within the travel lanes, shoulders, and median; a comprehensive review of available geologic data, including previous test borings performed adjacent to the investigation area; a visual pavement condition assessment; and visual and survey monitoring of the ongoing sinkhole and subsidence related activities across the site.

The geology of the project site is characterized by a variable bedrock surface consisting of pinnacles, solution cavities, fracture zones, and a localized thrust fault. Using a comprehensive investigation approach allowed for the analysis and consolidation of a large amount of data leading to a more detailed interpretation of the subsurface conditions. Based on the findings, a limited mobility grout program was designed and implemented to address the subsidence features at the site and mitigate future sinkhole activity.

Several logistical challenges were encountered during the investigation and subsequent construction phase of the project, including maintenance of traffic, limited work zone areas, and time constraints. Sinkhole activity in the carbonate belt of southeastern Pennsylvania is not unfamiliar to engineers and geologists, however, when sinkholes occur in a heavily-traveled highway corridor, they present unique challenges for investigation and remediation.

INTRODUCTION

Following an exceptional rainfall event in the overnight hours of September 30th, 2010 several sinkholes appeared along a heavily-traveled section of State Route (SR) 422 in Tredyffrin Township, Chester County, Pennsylvania. A total of seven sinkholes of various sizes were noted within the median and shoulders of the roadway and on an adjacent property west of the site. This section of 422, located between First Avenue and the Pennsylvania Turnpike (Turnpike) overpass, is four lanes (two in each direction) and carries more than 98,000 vehicles per day serving suburban communities of the Philadelphia metropolitan area.

After emergency repairs, the Pennsylvania Department of Transportation's (PENNDOT) Engineering District 6-0 requested Gannet Fleming develop a program to identify the limits and potential sources of the sinkhole activity and provide recommendations for remediation. A multifaceted approach to the investigation was employed, including a review of available geologic data and historic test borings performed in the area, geophysical surveys, test borings, a visual survey of existing pavement conditions, settlement monitoring, and routine observation of the ongoing sinkhole related activities on the site. Based on the findings of the sinkhole investigation, a program of limited mobility grouting (LMG) was conceived and implemented to address the subsidence features at the site and help prevent future sinkhole activity. Due to the high volume of traffic on 422, all investigation and construction activities were to take place while maintaining two lanes of traffic in both directions, which required both night and weekend work.

INITIAL EMERGENCY SINKHOLE AND HIGHWAY REPAIRS

The appearance of the sinkholes resulted in emergency closure of the eastbound right travel lane. At some locations, sinkholes along the shoulder extended beneath the adjacent lane by several feet causing subsidence of the roadway. The pavement section in this segment of 422 is ten inches of reinforced concrete overlain by two inches of bituminous asphalt. Fortunately, the reinforced concrete pavement (RCP) section was able to span the sinkhole cavities until the lane could be closed and the voids backfilled, thereby preventing collapse of the roadway and potential traffic accidents.

Utilizing the lane closure to protect traffic, PENNDOT crews performed emergency backfilling of the sinkholes with concrete. The roadway was subsequently reopened to traffic, but over the next two weeks, additional settlement and sagging of the pavement was observed at three locations in the eastbound lanes manifesting as longitudinal pavement sags. PENNDOT responded by initiating emergency limited mobility grouting via their on-call surface treatment contractor. This emergency grouting, conducted at night using lane closures and restricted work hours, focused only on the immediate areas where subsidence was present. Due to the limited work hours available and the need to reopen the roadway at the end of each work shift, the grout holes were limited to a maximum depth of 20 feet. Three grout holes, arranged in a longitudinal fashion at a spacing of 10 feet, were used to treat each sag area. The holes were placed roughly in the center of each affected travel lane, in an attempt to provide additional support to the overlying RCP slab. A total of 18 holes were grouted over a period of five nights in mid-October, with a total LMG injection volume of 204 cubic yards.

SITE GEOLOGY

To obtain a better understanding of the geologic conditions influencing the project area, a desktop study of geological publications and existing test borings was undertaken. The site lies within the Piedmont Lowland section of the Piedmont physiographic province and is underlain by Ordovician and Cambrian-age dolomite and brecciated dolomite bedrock of the Ledger Formation (see Figure 1). These geologic features trace their origins to a time of relative geologic quiescence more than 500 million years ago, when waters of the Iapetus Ocean were moving inland depositing shallow-marine carbonate sediments along the continental margin of Laurentia. Subsequent lithification of these sediments is responsible for the carbonate belt that extends across southeastern Pennsylvania today.

Along the southern boundary of the project site, in the area of the Turnpike overpass, the Ledger Formation carbonates meet the Triassic-age sandstone of the Stockton Formation at an unconformable contact and several faults have been mapped in the vicinity of this contact. The Pennsylvania Geological Survey's (PAGS) *Map 61* (Valley Forge quadrangle) shows a localized unnamed thrust fault striking northeast along the boundary of the unconformity (see Figure 1), evidence of which was not encountered during the subsurface investigation. A review was also performed of boring logs and data, obtained from the Pennsylvania Turnpike Commission (PTC), associated with the proposed widening of the Turnpike overpass.

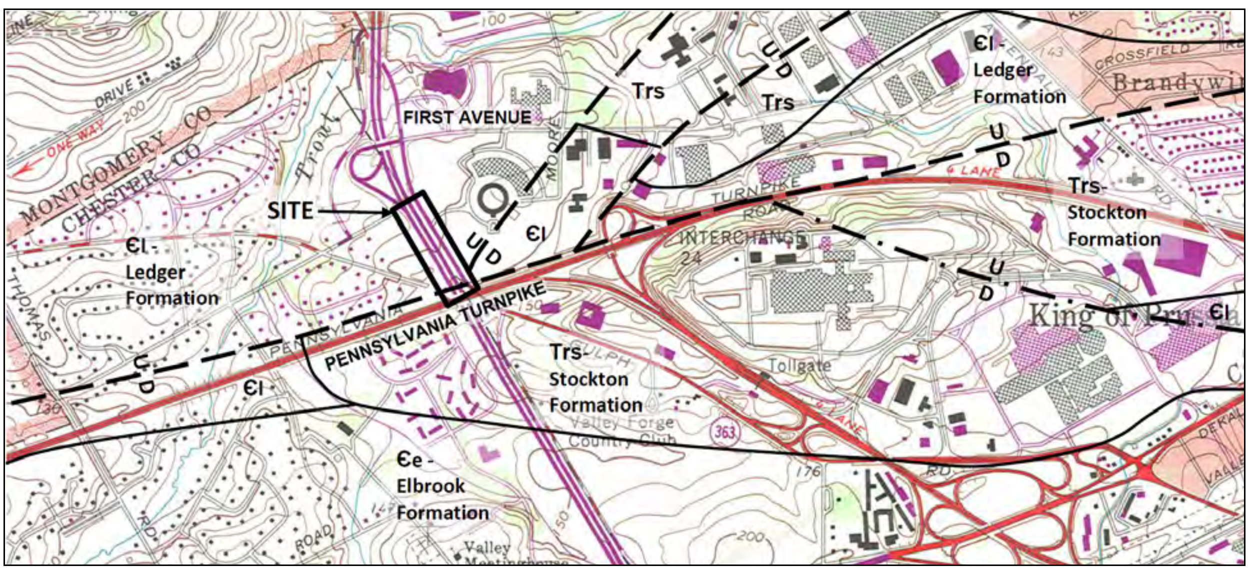

Figure 1. Combined Site Location and Geology Map (modified from PAGS Map 61 and after USGS Valley Forge, PA Quadrangle)

The Ledger Formation dolomite at the project site is characterized by karst features such as irregular bedrock surfaces, pinnacles, extensive interconnected fractures and solution cavities. Water transport in the rocks of this formation is dominated by secondary porosity (i.e., through fractures, joints, bedding planes, and solution features), which can be quite significant. The geological combination of karst features and disturbed geomaterials associated with disrupted zones along faults makes this area prone to hazards associated with sinkhole activity, including the potential for significant damage to buildings and infrastructure.

SUBSURFACE INVESTIGATION PROGRAM

Gannett Fleming personnel performed initial reconnaissance of the site concurrently with the emergency LMG repairs and used the surface indicators for subsidence to identify the affected area and plan the extent of the subsurface investigation. Ultimately, the subsurface investigation encompassed a 580-foot section of 422, with an area of approximately 65,000 ft^2, extending from the end of the First Avenue onramp (in the eastbound travel direction) to the Turnpike overpass. The investigation field work, performed between October 21st and November 22nd, 2010, (with subsequent site monitoring activities continuing through February 2011) included geophysical investigations, test borings, observation and documentation of on-going sinkhole-related activities, and review of available documents related to previous sinkhole activities on the site.

Geophysical Investigation

The geophysical investigation, performed by Quantum Geophysics, a division of Gannett Fleming, utilized a three-method approach, including multi-channel analysis of surface waves (MASW), microgravity, and ground penetrating radar (GPR). The geophysical investigation was performed in advance of any test borings in order to identify geologic anomalies or indications of potential voids that could be targeted with the borings, thereby maximizing their value.

Due to the vibration sensitivity of the microgravity and MASW equipment, geophysical surveys were conducted during off-peak nighttime hours from 9:00 PM to 5:00 AM. This also limited impacts of lane closures on motorists. MASW and microgravity methods were used to survey the extents of the project area (shoulders, travel lanes, and median), while GPR was exclusively used to survey the travel lanes to identify near-surface voids masked by the reinforced concrete pavement. PENNDOT Maintenance personnel supported the investigation by providing temporary lane closures and traffic control patterns.

The geophysical surveys revealed various types of anomalies within the limits of the site. Microgravity data collected using a 10-foot by 10-foot grid pattern revealed six relatively linear low gravity anomalies suggesting significant fracturing of the underlying bedrock. A sizeable low gravity anomaly was observed in the data, with a planimetric area of approximately 4,000 square feet, covering the eastbound outer shoulder, travel lanes, inner shoulder and a portion of the median, with a general east-west trend *(4)*. The anomaly may be a signature of the localized thrust fault shown on the PAGS *Map 61*. While the microgravity data indicates the planimetric projection of the gravity anomalies, it cannot be used to directly determine the depth or other characteristics of the features related to the anomalies. However, general trends of high or low gravity readings are typically indicative of relative changes in the top of bedrock surface and competency of the intact rock, with higher gravity readings indicating shallower intact bedrock, and lower readings indicating areas of significant weathering or a deeper rock surface.

The MASW data, taken in lines parallel to the roadway, revealed fifteen different low shear wave velocity (V_s) anomalies, located at depths estimated between 30 to 50 feet below the ground surface. The majority of the V_s anomalies appeared to be within the bedrock stratum, indicating areas of potential voids, soil-filled features or zones of highly fractured rock. The microgravity data and MASW data both revealed a relatively abrupt increase in the depth to bedrock in the southeastern portion of the site, approaching the Turnpike overpass (see Figure 2).

The GPR survey data collected showed several areas with signs of soil raveling or piping within the upper four feet of the ground surface, along with areas of potential voids at the base of the pavement. In addition, the GPR data identified three linear trench-like features within the roadway thought to have been the site of previous roadway repairs (see Figure 2).

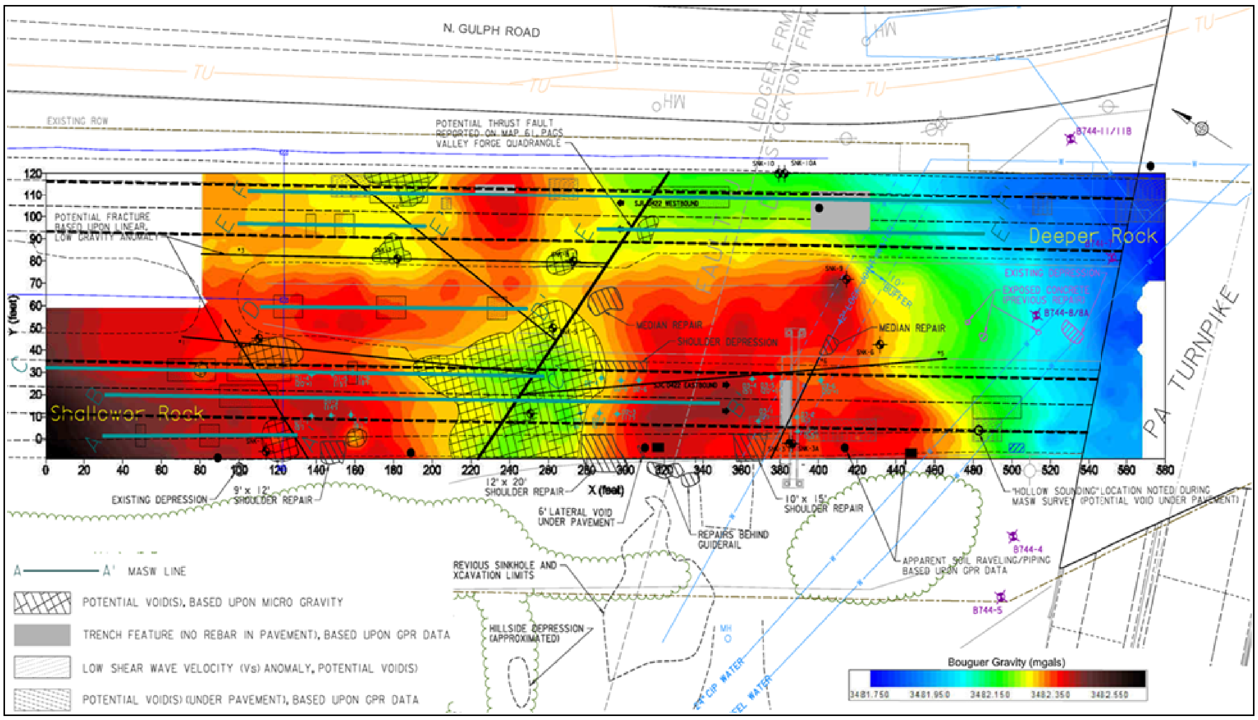

Figure 2. Geophysical data summary plan

Test Boring Program

Utilizing the results of the geophysical investigation, test boring locations were selected to target areas of interest, including several anomalies, and to provide additional subsurface data across the site to supplement planning of a sinkhole remediation program. A total of twelve test borings were performed, including one in the eastbound outside traffic lane (centered in the largest microgravity anomaly), five on the outside shoulders, three on the inside shoulders, and three in the median. The borings were advanced to depths ranging from 15 to 91 feet below grade, with the final depth determined by top of rock elevation, rock quality and whether or not any solution features were encountered within the rock mass. A temporary lane closure was required to drill the boring in the travel lane during the restricted daytime working hours of 9:00

AM to 2:00 PM due to the heavy traffic volume. Test borings on the shoulders utilized temporary shoulder closures to minimize traffic impacts.

Typically, the test borings encountered loose to dense silty sand (SM) and clayey sand (SC) residual overburden soils containing various amounts of gravel (rock fragments). Test borings in the eastbound outside shoulder and travel lane, near the original sinkhole activity, encountered very loose soils and low soil sample recovery within a zone of up to 13 feet above top of bedrock. In general, the overburden soils are underlain by light gray Ledger Formation dolomite, with localized brecciation. Half the test borings encountered significant voids and zones of very loose soil within the bedrock stratum, with the affected anomalous zones ranging from 13 to 32 feet in the vertical dimension within a particular boring (see Figure 3).

In general, the boring logs obtained from the PTC proved consistent with the conditions observed in the test borings. Specifically, the depth to bedrock is highly variable and is considerably deeper along the southern edge of the site, near the Turnpike overpass.

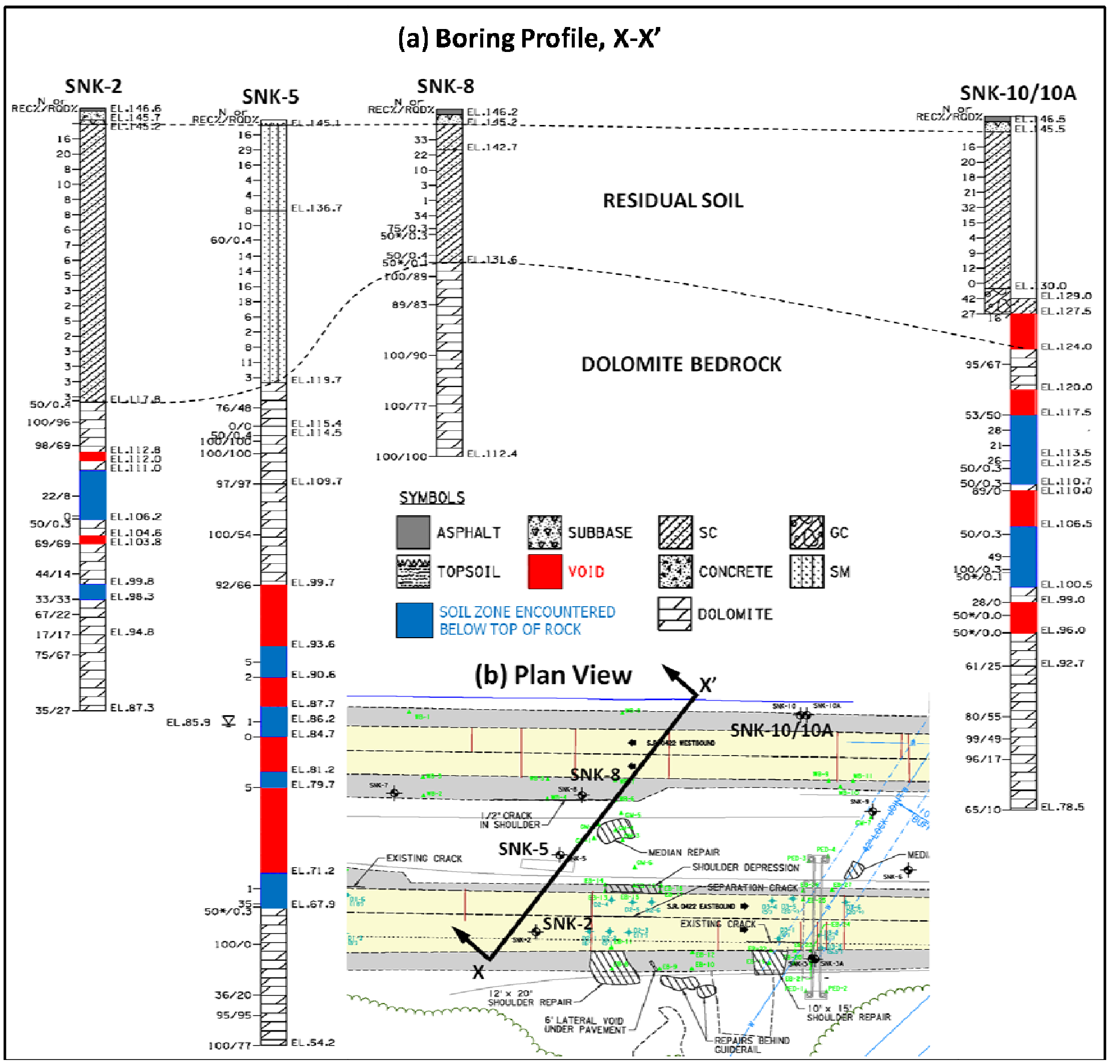

Figure 3. Typical subsurface profile trending along interpreted fault

Obtaining representative groundwater readings during the test boring program was difficult. To facilitate 24-hour groundwater readings in the borings, attempts were made to insert a small-diameter PVC conduit down each hole at the completion of drilling. Caving conditions in several of the borings made it impractical to insert conduit to the bottom of the hole. Where a groundwater level reading was obtained at the completion of the boring, it was unclear if the observed water level was influenced by the drill water circulated during rock coring. Two of the test boring logs obtained from the PTC provided long-term groundwater readings, and along with available well data in the area, suggest a groundwater table of 50 feet or more below the ground surface, which is consistent with regional groundwater levels. The deep groundwater table, which falls well below the top of rock elevation at several locations throughout the site, allows infiltrating water to transport soil into solution features within the underlying rock mass, leading to an increased risk of subsidence and sinkhole formation.

Site Surveying and Routine Monitoring

Surface indicators of impending sinkhole activity, such as shallow closed depressions, or settlement cracking of soils, pavements or structures, can be very subtle initially and may grow or show signs of movement over time, prior to the onset of a collapse. To help identify any developing or ongoing hazardous subsidence conditions, Gannett Fleming personnel visually monitored and documented anomalous surface features at the site from the beginning of the sinkhole investigation through completion of remediation activities.

To provide a quantitative evaluation of potential subsidence areas, a total of 50 settlement monitoring locations were established and surveyed every two weeks to look for indications of ongoing settlement. In the photograph below (see Figure 4), three settlement monitoring locations, indicated by the wooden survey stakes, can be seen adjacent to an active subsidence area in the median of the highway. Where survey results indicated possible settlement activity, an additional field reconnaissance was performed by personnel familiar with the site to see if any visual indicators of additional ground movement could be observed.

During the subsurface investigation and preceding primary construction activities, site observations identified two locations within the median exhibiting signs of continuing subsidence. The settlement progressed at these locations to the point surface repair methods were required, which consisted of overexcavating to competent soil strata and backfilling with flowable fill. This was an interim treatment measure to stabilize the areas until a permanent solution could be designed and implemented.

Figure 4. Evidence of ongoing sinkhole activity at a location of previous surface repairs

Visual Pavement Condition Assessment

In addition to settlement monitoring, a visual inventory of the existing pavement conditions was taken and evidence of past surface repair features that may have been related to previous sinkhole activity was documented.

The pavement condition assessment identified one area of significant pavement distress where abnormal slab settlement was present. This area was treated during the emergency LMG work, but continued to experience additional settlement prior to implementing the final treatment program. The depression, located eastbound approaching the Turnpike overpass, was readily apparent as vehicles passed over the area. In addition, the GPR survey identified that a portion of this area had been previously been excavated and repaired, possibly in response to a subsidence condition. Other areas of pavement distress were noted; however, they did not necessarily appear to be related to the subsidence activity at the site, but rather could have been a result of the advanced age of the pavement system in this segment of the roadway.

SINKHOLE TREATMENT PROGRAM

Based on the findings of the sinkhole investigation, a limited mobility grouting program was recommended to remediate the effects of the recent sinkhole activity to help prevent future sinkhole activity. Other ground improvement and structural support options were considered to stabilize the roadway and treat the subsidence features within the project area. However, none of the other options considered offered the relative economy of a grouting program while effecting a long-term solution. Other benefits realized are minimizing disturbance to the existing roadway, allowing for maintenance of traffic through the work zone, and treating the source of the ongoing sinkhole activity. The grouting program was developed with the following objectives in mind:

- fill voids in the bedrock into which significant amounts of overburden soils could migrate;
- choke off major openings, or “throats”, in the top of the rock mass through which soil could readily pass;
- fill voids and densify loose zones in the overburden soils caused by previous or incipient sinkholes; and
- create in-situ “columns” of grout in the overburden, which while not directly supporting the roadway, would allow for some arching of soil loading onto the grout columns and provide some densification of the overburden soils.

Limited mobility grout is a stiff, low-slump material, typically with a soil-cement composition designed to remain in a coherent mass and travel only a limited distance from the point of injection. When injecting LMG in a rock mass, the grout characteristics limit the size of fractures into which the grout can penetrate and the distance the grout can migrate in smaller solution features. Because solution features in carbonate bedrock can be interconnected over large distances, this helps prevent excessive grout takes that could occur with fluid grouts. The viscous nature of the grout also limits lateral migration of the grout during injection in soil overburden materials, allowing for controlled placement of the grout and reducing the risk of hydraulic fracturing of the soil mass, which can result in ground surface heave and weakening of the overlying soil mass.

The limits of the grouting program were selected as described above and encompassed the known subsidence features as well as areas of interest identified by the investigation. Areas of interest included: voids in the rock mass, fracture features, a potential fault, zones of loose overburden soils, and low gravity anomalies. The MASW and test boring data proved particularly valuable in establishing the minimum and maximum target treatment depths. Given the objectives of the grouting program, it was important for the grout holes to extend into bedrock to cut off the underlying solution features from the overburden soils. A minimum rock penetration of 10 feet was utilized, however, where voids or soil zones were encountered in the rock mass, grout holes were extended deeper in an effort to find the bottom of the anomaly, allowing a firm support zone from which the grout injection could commence upward. In the area of the large gravity anomaly, test boring and MASW data suggested that the problem areas would be encountered deeper within the rock mass and the 10-foot penetration might not be sufficient. To remedy this situation, a group of grout holes in this area was identified in which the contractor would be required to advance a minimum of 20 feet into the underlying bedrock. Based on the results of the subsurface investigation data, contract specifications were used to inform the contractor that grout holes of 80 feet or more in depth could be required so appropriate drilling and grouting equipment and casing would be selected for the work.

In addition, design of the grouting program needed to consider the overall cost and duration of the construction efforts, general sequencing of the grout holes, potential impacts to onsite structures and underground utilities, traffic staging requirements limiting the available work zones at any given time, and potential environmental impacts. The as-designed LMG program included a total of 425 primary grout hole locations on a grid pattern of 10 feet by 10 feet over the area of interest, with provisions to add intermediate secondary and tertiary holes where particularly large grout takes were encountered. The 10-foot grid spacing was selected as a balance between obtaining effective treatment of the soil mass between adjacent grout holes and maintaining a cost-effective grouting program.

Recommendations were also provided for the following: verification of the grouting program via test borings and geophysics; pavement repairs; and drainage and grading improvements. The latter included regrading of the grass median to direct stormwater runoff to a lowered inlet and installation of a geomembrane liner in the median swale to inhibit infiltration of surface water.

As a result of the pavement assessment, it was recommended that the bituminous overlay be milled off to expose the location of the longitudinal and transverse RCP joints prior to commencing the LMG program. The milling allowed for grout hole locations to be field adjusted to avoid problems associated with grouting too close to the edges of the pavement slabs, such as weakening the edge of the slab or causing differential movements between slabs leading to joint distress.

Along with the recommendations above, it was necessary for Gannett Fleming to prepare a construction cost estimate as part of the construction procurement process. The combination of MASW and test boring data significantly aided this process by providing a rational basis for estimation of average grout hole depths. The total grout injection volume was more difficult to estimate. Data was utilized from previous LMG projects at SR 309 and nearby SR 202, as well as grouting projects performed for private clients of Gannett Fleming, to estimate typical takes in the different strata encountered at the site. These estimated takes were then combined with the estimate of average hole depth and associated average rock depth to estimate the total grout injection required for the project. The final estimate incorporated an allowance for secondary and tertiary holes.

Role of Geophysics in Planning the Grouting Treatment Program

As found for this project, geophysical methods are useful when performing a subsurface investigation and planning an LMG treatment program in karst. However, the designer must keep in mind the limitations of any one geophysical method to get the most benefit from their investigation. Knowing the limitations of individual methods, multiple methods can be combined to create a more complete picture of the subsurface conditions and challenges that exist.

Test borings are a fundamental informational tool for the design of geotechnical solutions but are limited to providing reliable information only at the boring points, and thus represent a small percentage of the subsurface variability present at the project site. In a karst environment, where highly variable subsurface conditions are common, test borings provide a very limited picture of what is going on at a site. Geophysical surveys allow more complete spatial coverage of the site, while test borings are used as a calibration tool for data interpretation.

In this particular project each geophysical method contributed a unique aspect to the project. Microgravity provided grid coverage of the entire investigation area, allowing identification of anomalous features within the bedrock mass. A significant drawback of the method is the inability to determine the depth of the features of interest. MASW was utilized to gather longitudinal profile data of the site. The data was then processed in 2-D panels which showed the variation of top of rock. Due to considerations of cost and practicality, survey lines were performed at no closer than 10-foot spacing, meaning no direct data was available to interpret conditions between lines. Additionally, for reasons unknown, high-quality MASW data could not be obtained in all sections of each survey line. It is possible that the presence of LMG and concrete masses in the ground from previous sinkhole repair efforts interfered with the collection and processing of the data. Lastly, GPR was used to determine if there were any open voids directly beneath the pavement section that were being bridged by the RCP slabs. GPR is limited to relatively shallow penetration depths and is therefore not normally used for large-scale sinkhole investigations; however, it proved useful in a niche role in this case.

CONSTRUCTION PHASE

As a result of ongoing surface subsidence during the investigation phase, PENNDOT assigned emergency status to the project which allowed construction of the project to be bid and let under an accelerated procurement process. The bid period of the project was reduced from the five-week period normally allowed for PENNDOT projects to one week. The successful bidder was general contractor J.D. Eckman, Inc. (JDE), of Atglen, Pennsylvania, who teamed with specialty subcontractor Structural Preservation Systems (SPS), now known as STRUCTURAL, of Hawthorne, NJ, to perform the LMG grouting work.

Staging of Traffic Control and Resulting Impacts on the LMG Program

Maintaining four lanes of traffic (two in each direction) through the work zone during the execution of the LMG program was particularly challenging for the construction team. As part of the project design, a traffic control plan was developed to maintain traffic through the work zone and protect the traveling public as well as construction personnel within the work zone. The plan included three separate stages of traffic control patterns, with each stage customized to allow for logical partitioning of grouting work in the travel lanes and shoulders. Traffic control patterns were implemented in both the eastbound and westbound directions of the highway concurrently, allowing LMG crews to work on both sides of the highway at the same time thereby expediting the grouting operations. The traffic control patterns, which encompassed the work zone and staging areas, along with lane shift tapers, covered more than 1,700 linear feet of the 422 corridor.

By shifting traffic lanes onto either the inner or outer shoulders through the work zone, both lanes of traffic could be maintained in each direction; however, the resulting work areas available within these traffic control patterns were long linear zones that presented a challenge for design and construction of the grouting program. Within the confines of the work areas provided by the traffic control, typically only one or two rows of grout holes were available to the contractor at a given time in each direction. As a result, the contractor was forced to progress much of the grouting in a linear fashion, making it a challenge to move equipment within a work area.

LMG work typically progresses from the periphery of a planned treatment area towards the center; however, this approach could not be utilized under these circumstances. In general an attempt was made to grout the holes in a given line by progressing from either end towards the middle but this was not always possible due to the challenges of positioning the drill rigs, pumps and grout trucks within the linear work areas, particularly when more than one crew was working concurrently on a line of holes. Because the use of an onsite batch plant would have been impractical under the circumstances, all grout was provided from a local ready-mix concrete plant.

Limited Mobility Grouting Program

The final limited mobility grouting program consisted of drilling and grouting a total of 605 production holes, including 436 primary holes, 161 secondary holes and 8 tertiary holes, with total grout injection of more than 85,000 cubic feet of grout. The production grouting work was performed over a period of 17 weeks between February and June of 2011. SPS provided between one and four full-time crews during the course of the LMG work, while Gannett Fleming provided full-time inspection of the grouting operation.

Production drilling was controlled using a set of termination criteria established during the design phase of the project. The criteria established limits for drilling depths under the various subsurface conditions anticipated across the site. In general, an attempt was made to terminate holes in a competent rock stratum, however this was not possible at all locations. Where competent rock was not encountered, maximum drilling depths were limited to no more than 100 feet below ground surface. Only 2.5 percent of all grout holes ended up reaching 100 feet, and less than 11 percent reached depths of 70 feet or more. Average drilling depths were much shallower at only 45 feet, correlating very well with the design estimates based on the geophysical and test boring data. Twenty-four percent of the grout holes were terminated at 30 feet or less below ground surface, serving as another indicator of the large variation in top of rock encountered within the project limits.

The grout mix selected by SPS consisted of water, Portland cement, Class F fly ash, clean sand, and admixtures including a combination water reducing agent and retarder, and an air entraining agent. Over the course of the project the grout slump averaged 1-3/4 inches and 28-

day compressive strengths typically ranged between 3,000 and 6,000 psi, or higher in some cases, well in excess of the required strength of 400 psi.

Grouting was performed using a bottom-up, or upstage, approach with injection intervals, or stages, of two feet. A maximum injection rate of two cubic feet per minute was selected, except where large anomalies were encountered in the rock mass when a maximum injection rate of four cubic feet per minute was permitted. The intent of limiting the grout injection rate was to prevent uncontrolled lateral and vertical movement of the grout which could lead to hydraulic fracturing of the overburden soils and increased potential for heave at the ground surface. Grout injection stage termination criteria were also established in the design phase, providing specific limits for injection pressures, volume cutoffs, combinations of intermediate pressures and volumes, surface heave and structural movement. More conservative stage termination criteria were utilized when grouting adjacent to structures and subsurface utilities, because damage to these facilities could not be tolerated.

Once grouting of primary hole locations was completed in a particular area, grouting and drilling log data for each hole were reviewed to determine where secondary and tertiary hole locations should be added. For each line of grout holes, a conditionally-formatted (color-coded) summary spreadsheet was prepared showing the grout takes for each stage. The summary spreadsheet was updated daily so timely recommendations for secondary and tertiary holes could be provided to PENNDOT for review, and subsequently passed on to the contractor once approved. Conditionally formatting the large body of data into an easily readable summary table made it manageable for the design engineers and reviewers to quickly evaluate grouting progress and supply the contractor with updated recommendations in a timely manner.

In general, secondary holes were added where the following grout take conditions were encountered in an adjacent primary hole(s):

- a single stage with a take of 50 cubic feet or more,
- two consecutive stages with a combined take of 60 cubic feet or more,
- any series of five stages with three or more stages exceeding 25 cubic feet each.

Depths of secondary grout holes were tailored using information from the drilling logs for nearby holes and depths of the exceptional grout takes in adjacent holes. The need for tertiary holes was evaluated on a case-by-case basis given the available drilling and grouting data. A total of 161 secondary grout holes were incorporated into the project, while only 8 tertiary holes were required. The total number of added secondary and tertiary grout holes represented just under 30 percent of the total number of production holes grouted, correlating very well with the design estimates used to develop anticipated construction costs. In a few instances, additional primary holes were added when high grout takes were encountered at the perimeter of the treatment area to confirm a significant subsurface anomaly was not left partially untreated. Eleven primary grout holes were added as a result of this approach.

Due to construction impacts on the traveling public and potential hazards associated with sinkhole activity, the project was under a strict construction schedule. The contractor and subcontractors faced daily challenges associated with working in a high traffic area with a limited work zone and compressed time schedule. Inclement weather interspersed throughout the timeline, including significant snowfalls at the start of the project, resulted in less-than-ideal working conditions that hampered grouting efforts. Effectively managing these conditions was a major contributor to reaching the timely conclusion of the project.

Estimated total drilling and grouting quantities, which served as the basis for the contract bid process, compared favorably with the total quantities used on the project. Total grout hole drilling quantities were within less than 1 percent of the estimate, while grout injection quantities were within 15 percent.

Figure 5. Grouting and traffic control arrangement during weekend lane closure

Quality Control

Full-time inspection of all LMG activities was implemented to establish and maintain quality control, to assure compliance with the specifications, and maintain detailed records of the grouting operations. The inspectors maintained drilling records for each hole, identifying strata changes and taking special note of zones with voids or very loose materials to be targeted during the grout injection, and were also responsible for determining the termination depth for each hole based on the depth and condition of rock encountered. During the grout injection, inspectors recorded the volume and the range of injection pressures for each stage, injection rate, stage termination criteria (pressure surge, volume cutoff, etc.), slump, and start and stop times, along with any unusual occurrences that might affect the work. The inspection staff for the drilling and grouting operations were geotechnical engineers or geologists familiar with the site conditions and objectives of the grouting program. This was a contributing factor in providing a successful oversight and quality control effort.

Special attention was paid to monitoring ground movements during the course of the grout injection, with the goal of minimizing ground surface heave and associated impacts to the highway infrastructure. In general, no injection of grout under pressure was allowed within eight feet of the ground surface. Survey laser targets equipped with alarm features were used to establish real-time monitoring at various locations near each active injection site. Additionally, vertical "tell-tale" indicators were installed at regular intervals above a 42-inch diameter concrete lock-joint pipe water main traversing the site. The tell-tales allowed for direct monitoring of movements at the pipe, preventing a situation where pipe movements might be masked by the overlying soils.

Additional quality control measures included regular testing of the grout slump, daily calibration of the grout pump stroke volumes, confirming grout hole layout and spacing, pre- and post-grouting verification test borings and careful documentation of all pay quantities associated with the LMG program. Prior to allowing grout to be injected, the slump of each ready-mix batch delivered to the site was tested. On rare occasions when the grout slump came up low (between ½ and 1 inch), the concrete truck driver was allowed to add a small amount of water to the batch to increase slump and aid pumpability of the mix. If the slump exceeded the maximum allowable of 3 inches, the grout batch was automatically rejected. Consistency of the grout was also monitored during placement of each batch to make sure no issues arose if the truck was onsite for more than approximately four hours (the contractor utilized a set-retarding admixture to extend the working time of the grout).

CONCLUSIONS

To date, several months after completion of the grouting program and associated pavement repair work, the site appears to be performing well with no obvious visual indicators of active subsidence, even after the region experienced record monthly precipitation levels during August and September, 2011, including the remnants of Hurricane Irene, which dumped more than five inches of rain on the region.

Several factors contributed to the successful implementation of the limited mobility grouting program.

1. A combination of methods were utilized during the investigation phase of the project, allowing subsurface factors contributing to subsidence to be clearly identified and targeted for treatment. The investigation included a test boring program, multiple geophysical methods, review and analysis of geologic resources including historic test boring and groundwater well data, and reconnaissance and regular visual monitoring of

the site.

2. Drilling termination criteria were implemented, based on the objectives of the grouting treatment program, to limit the overall drilling and grouting depths required while targeting specific areas of concern. This helped control the total project cost and schedule.

3. Comprehensive limited mobility grouting criteria were employed, including continuous evaluation of grout injection rates, monitoring of grout takes and pressure behavior for each stage of each hole, and monitoring for ground and structural movements.

4. Primary grout hole parameters were reviewed and evaluated daily to determine the need for secondary and tertiary grout holes, with the goal of providing consistent grouting treatment throughout the project area.

Meeting the investigation, design, and construction challenges was facilitated through constant communication between Gannett Fleming, PENNDOT, and the Contractors, along with detailed attention to documentation and implementation of field activities.

REFERENCES

Berg, T.M. and C.M. Dodge, 1981, *Map 61*, *Atlas of Preliminary Geologic Quadrangle Maps of Pennsylvania*, Valley Forge Quadrangle, Pennsylvania Geological Survey.

Gannett Fleming, Inc., 2010 (January), *SR 0422 Sinkhole Investigation Report prepared for the Pennsylvania Department of Transportation, District 6-0*, Audubon, PA (LT-9449-1).

Shultz, C.H., et. al., 1999, *The Geology of Pennsylvania*, Pennsylvania Geological Survey, Harrisburg, PA and Pittsburgh Geological Society, Pittsburgh, PA.

United States Department of the Interior Geological Survey, 1966 (Photorevised 1981), *Valley Forge Quadrangle, Pennsylvania,* 7.5 Minute Series.

Dani Creek Landslide: Anchored Soldier Pile Wall in Franciscan Mélange

by

Ryan Turner P.E.
California Department of Transportation
50 Higuera St, San Luis Obispo, CA 93401
(805) 748-1706
ryan_turner@dot.ca.gov

Prepared for the 63rd Highway Geology Symposium, May 7-10, 2012

Acknowledgments
California Department of Transportation Geotechnical Design North Branch D
Mike Finegan, Mike Jurasius, Dan Appelbaum, John Duffy, Zeke De Llamas, Wade Hoon

Disclaimer
Statements and views presented in this paper are strictly those of the author, and do not necessarily reflect positions held by their affiliations, the Highway Geology Symposium (HGS), or others acknowledged above. The mention of trade names from commercial products does not imply the approval or endorsement by HGS.

ABSTRACT

Prepared for the 63rd Highway Geology Symposium, May 7-10, 2012

Dani Creek Landslide: Anchored Soldier Pile Wall in Franciscan Mélange

by
Ryan Turner P.E.
California Department of Transportation
50 Higuera St, San Luis Obispo, CA 93401
(805) 748-1706
ryan_turner@dot.ca.gov

The topic of this case history is the Dani Creek Landslide and some of the issues associated with the design, construction, and on-going monitoring of the landslide and constructed anchored soldier pile wall including:

- Identification of the boundaries of active landsliding within a larger dormant landslide through surface monitoring and installation of slope inclinometers and time domain reflectometer instrumentation
- Characterization of the strength and index properties of highly heterogeneous geologic materials encountered in Franciscan Mélange for use in limit equilibrium slope stability modeling
- Characterization and modeling of a complex groundwater regime defined by multiple zones of perched groundwater
- Challenging construction access including design and construction of a temporary soil nail shoring wall and construction and maintenance of working benches on a moving landslide
- Highly variable drilling conditions and mitigation measures to overcome groundwater infiltration and caving into soldier pile and ground anchor excavations
- Instrumentation of ground anchors with load cells to monitor long term performance of ground anchors within the retained mass

Introduction

Landslides and slope instabilities on State Highway 1 along the Big Sur Coast of California are abundant and varied in nature. The highway is often closed for weeks or months during the winter as state maintenance forces and state-hired contractors work to remove slide material from slope instabilities above the road and rebuild the highway when slides occur below the road. Dani Creek Landslide, near the small town of Lucia in Monterey County, presented annual maintenance and safety issues due to the dropping roadway and edge failures. A rapid increase in the rate and magnitude of movement during the winter of 2009-2010 prompted the California Department of Transportation (Caltrans) to design and construct a permanent mitigation.

State Highway 1 was constructed as a two-lane highway perched several hundred feet above the ocean on a side-hill cut and fill. The highway consists of 10-to-12-foot lanes with 2-to-6-foot paved and unpaved shoulders. The highway crosses an active landslide, as evidenced by the dropping roadway and observed movement. During the El Nino winter of 1997-1998, the historically very slow moving landslide accelerated and the roadway began dropping more rapidly than had been observed in the past, increasing maintenance efforts required to keep the highway open. A project to study the landslide and provide alternatives to mitigate the dropping roadway was initiated, and exploratory drilling within the landslide began in 1999. Slope inclinometers (SI) were installed at the roadway elevation and read periodically. From 1999 to 2009 the roadway was maintained by placing imported fill and paving in an effort to offset drops in road elevation. During wet winter months, the roadway was observed to drop as much as 6 inches in a 24 hour period. Maintenance costs for materials and labor grew, often requiring daily attention in the winter months.

Heavy rains and high groundwater levels in the winter and spring of 2009-2010 further increased the rate of landsliding below the roadway and caused migration of a near vertical scarp across the southbound lane of Highway 1. Daily maintenance was required to maintain one passable lane; an unpaved, uneven dirt road approximately 12 feet wide at its narrowest point. K-rail and an earthen berm were placed above the advancing headscarp to prevent vehicles from going over the edge. The berm, K-rail, and sections of the remaining roadbed required daily maintenance to prevent them from falling below the road and for the road grade to remain passable to motorists. The deteriorating highway conditions prompted Caltrans to commit to constructing a permanent solution.

The headscarp of the active portion of the landslide impacting the highway roughly followed the southbound lane of Highway 1 and extended for a width of approximately 600 feet. Pavement and shoulder cracking parallel to the highway were observed from approximately the toe of the upslope cut in the worst case, and to the shoulder of the outside lane above the landslide elsewhere. Vertical and near-vertical slopes up to 30 feet high were visible at the headscarp below the highway and continued to advance inland as toppling type failures occurred in the over-steepened scarp.

Figure 1: Caltrans maintenance forces placing fill to maintain roadway elevation, May 17, 2010.

Landslide Investigation

An investigation including field reconnaissance and surface mapping, comparison of historic and recent aerial oblique photography, slope inclinometer and time-domain reflectometer (TDR) instrumentation, ground surface monitoring via a survey grid, groundwater level monitoring, and subsurface sampling was performed for this project. Twenty-five mud-rotary borings were drilled at the site between 1999 and 2010 to determine the subsurface conditions. Seventeen slope inclinometers and five TDR cables were installed to determine the depth of sliding of the active portions of the landslide and locate stable features. Off-road drill rigs, a helicopter transported drill rig, a large air rig, several on-road mud rotary drill rigs, and years of work by Caltrans forces and a consultant drilling contractor were utilized in the investigation. Twelve slope inclinometers were installed at the highway elevation, one above the cut slope adjacent to the highway, and four below the roadway. Three TDR cables were installed at the roadway elevation and two were installed below the roadway in the body of the slide.

In addition to the subsurface monitoring, Caltrans surveyors and geotechnical personnel installed a total of 58 ground surface monuments, constructed by mounting a survey prism on a post above the vegetation and clearing line of site to a monitoring point. Surveyors periodically monitored direction and magnitude of movement with the use of a total station from a stable point to the north of the landslide. Monuments placed below the roadway and within the visible headscarp of the active portion of the slide all exhibited significant movement over the course of about a year of monitoring, from approximately 23 feet near the toe of the slide at the bluffs above the beach, to several feet at the base of the fill just below the roadway. Monuments installed above the roadway and behind the visible headscarp on the roadway exhibited minimal movement.

Results of the surface and subsurface monitoring programs indicated the active sliding zone begins at the roadway headscarp and toes out in the bluffs near sea level. Geomorphologic features identified in the investigation indicated the presence of a now stable paleo-slide extending far above the road. Insignificant movements were measured on the ground surface above the highway, and no sliding surface was identified in the slope inclinometers installed above the highway or behind the visible scarps on the road. No cracking was visible on the paved and unpaved roads or cleared areas on the private property above the highway. No historic damage to the numerous structures on the private property above the cut slope was observed or reported. In addition to the recent monitoring and field reconnaissance, observation of the cut slope over the years and review of historic photographs of the cut slope and natural slopes above the roadway show very little change, indicating relative stability above the highway.

Figure 2: Oblique aerial view of Dani Creek Landslide limits

Geology

The Dani Creek Landslide is located in the Santa Lucia Mountain Range, part of the northwest-southeast trending Coast Range Geomorphic Province. Geology of the province is dominantly comprised of Franciscan Complex basement rocks, characterized by a mixture (mélange) of metamorphosed igneous and sedimentary hard rock (blocks), embedded within softer metamorphosed mudstone and siltstone (matrix). For the purpose of geotechnical characterization, the Franciscan Mélange is classified as block-in-matrix rocks, or “bimrocks”. Within the project limits the Franciscan Complex is overlain by colluvium and surficial landslide deposits of variable composition and age. Imported fill placed over the colluvium and surficial landslide deposits underlies the roadway along the current highway alignment. The variable-depth fill is composed of imported aggregate base, native soils and rock from on-site, and layers of cold-mix asphalt. A prominent vertical scarp near the center of the landslide showed exposure of more than 20 feet of alternating layers of fill and cold-mix asphalt, typical of the fill unit. Movement of the landslide below the roadway continues to transport the fill down slope towards the ocean.

Colluvium and surficial landslide deposits overlie Franciscan Mélange within the landslide limits. The colluvium is characterized by loose, gravity-transported sediments, and varies at the road elevation in thickness from a few feet to about 40 feet thick. Surficial landslide deposits extend up to 125 feet thick in the active portion of the landslide, and are projected to be up to 200 feet thick on the upper dormant portion of the landslide. The unit is comprised of hard, intact meta-greywacke blocks within a meta-siltstone matrix pervasively sheared to a soil-like consistency.

Franciscan Complex underlies all surficial deposits in the project area. The two primary rock types encountered in the unit were meta-greywacke blocks and meta-siltstone matrix. The sandstone-siltstone sequence has undergone high-pressure-low-temperature metamorphism and tectonic shearing. Intense shearing is observed dominantly in the weaker meta-siltstone matrix material. Blocks of meta-greywacke are dispersed randomly in the matrix rock and vary in size from a few inches to tens of feet.

Groundwater

Open observation wells and vibrating wire piezometers were installed throughout the site. Fluctuations in groundwater levels were monitored to determine the influence of groundwater on construction and foundation design. Groundwater head pressures measured at several depths in the borings by piezometers varied widely, indicating a complex perched groundwater regime. Groundwater generally resides in fractured blocks of meta-greywacke and seeps into the less permeable, fine-grained matrix materials. Oxidation on fracture surfaces in block zones recovered during drilling indicate that water is moving through fractures in blocks in perched zones bounded by lower permeability matrix material. Perched groundwater can also be observed in spring activity daylighting through the slopes above and below the road during the rainy season.

Structure Alternatives

Caltrans engineers considered and evaluated several structure alternatives on the basis of cost, constructability, and traffic constraints. Viable alternatives considered included: a side-hill viaduct with a retaining structure, a bridge, an anchored soldier pile wall, and a gravity type retaining wall. An anchored soldier pile wall was the chosen alternative, primarily because the highway could remain open during the construction and economic feasibility.

Slope Stability and Strength

Slope stability of the Dani Creek Landslide was evaluated using geometry from defined failure surfaces determined from the SI and TDR installations, and ground profiles generated from a LIDAR based topographic map with a two-foot contour interval. Sliding surface points were defined using the headscarp observed in the roadway, discreet sliding depths from the slope inclinometer and TDR installations below the road, and the toe of the slide visually observed in the bluffs at the beach. The limit equilibrium model computer program SLOPE-W was used to model the existing slope geometry and material properties to back-calculate a static global slope stability factor of safety. Several cross sections were analyzed to determine the critical landslide geometry and material strengths. Due to uncertainty in defining the groundwater regime, a high groundwater surface was assumed in the analyses to model the potential for excess pore pressures in the sliding mass and on the slide plane. Mohr-Coulomb strength parameters were back calculated to result in a factor of safety of 1.0 for the active slide geometry at the critical cross section. Because the landslide has undergone significant displacement, it was assumed that the residual shear strength along the slip surface has no component of cohesion. The following soil parameters were determined from the slope stability modeling of the existing slope:

$\phi' = 27^\circ$ $c' = 0$ psf Total Unit Weight = 135 pcf

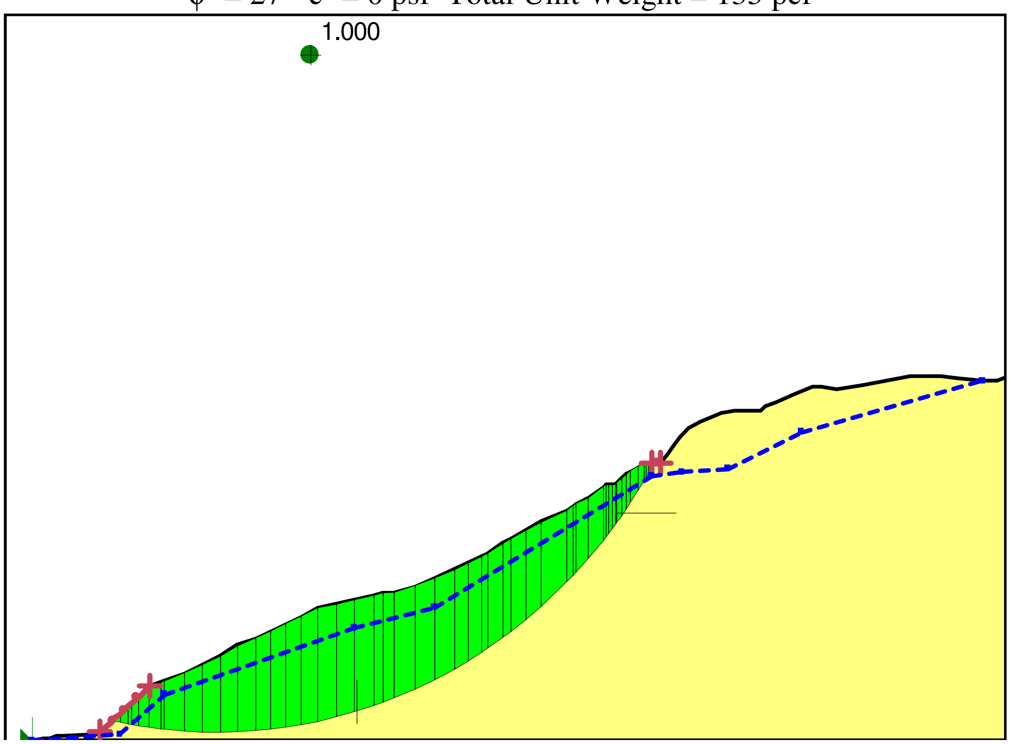

Figure 3: Slope stability model results

An additional slope stability model of the proposed retaining wall was then analyzed with the same soil strength properties and used to determine the required resisting force to be applied to the ground anchors to provide a static factor of safety of 1.3. Slope stability of the wall was also evaluated for pseudo-static seismic conditions with an applied horizontal force at the slide mass centroid calculated using a horizontal seismic coefficient of 0.16.

Anchored Soldier Pile Retaining Wall Design

Material strength parameters were back calculated from a limit state equilibrium analysis of the existing slope in the computer program SLOPE-W, as described in the Slope Stability and Strength section. Resisting forces provided by the ground anchors required to achieve a global stability FOS of 1.3 were determined from the slope stability analysis, and compared to the resultant lateral earth pressure force calculated using an apparent earth pressure distribution with a Coulomb lateral earth pressure coefficient and the same material strengths and unit weight. Landslide forces resulted in higher anchor forces and controlled the design.

Design of pile spacing, diameter, and depth considered the horizontal and vertical load effects generated by retaining the landslide mass behind the soldier piles. Final soldier pile design consisted of two side-by-side steel W14x68 sections on 10-foot spacing with 4 rows of anchors drilled between adjacent flanges of the W-sections, embedded in a 42 inch diameter drilled shaft below the lagged portion of the wall. The wall is lagged to a depth of 45 feet from the top of the wall, 8 feet below the observed sliding surface, in an effort to prevent material from sliding below the lagging as has been observed at similar nearby structures. The drilled shaft portions of the piles extend 35 feet below the lagged height of the wall, for a total pile length of approximately 80 feet. The final wall design is 754 feet long, with the lagged height at each end of the wall tapering back up to meet the highway grade.

Typically, an anchored soldier pile wall is best suited to top-down construction methods, with anchors installed through lifts excavated in native material. Due to the narrow remaining roadway width at some locations in the slide, some portions of the wall were required to be constructed in a bottom-up manner. Fill had to be placed behind the lagging in order to build up the required roadway width; some locations required nearly 15 feet of fill, extending below the second row of anchors. Particular attention was paid by designers to specify strict compaction and backfill height requirements above the anchor elevations prior to stressing to ensure that the lateral resistance provided by the fill was adequate to prevent deflection of the piles into the fill during anchor stressing. A minimum height of 3 feet of compacted fill above each anchor level was required before stressing was permitted.

Temporary slopes or shoring required for construction were left to the contractor to propose and design. Caltrans designers anticipated that some type of temporary retaining wall or shoring system would be required to support the existing portion of the highway to remain open during construction.

An estimation of the percentage of anticipated hard rock drilling was made using Dr. Edmund Medley's theories (Medley, 1998) developed for predicting the volumetric proportion of blocks to the entire rock mass volume of a bimrocks mélange unit. Dr. Medley was consulted in the field (April 26, 2010) and provided guidance on the applicability and use of his theories after visiting the site and reviewing some of the subsurface data collected in the exploration. The estimated percentage of hard rock drilling was calculated by correlating the linear proportion of blocks to matrix encountered in the borings to a volumetric proportion in the three dimensional mélange unit and adjusting for sources of error.

Based upon the preceding method, it was estimated that 35% of the foundation drilling in the rock unit would be in hard rock blocks. The remaining 65% of the drilling was predicted to be in intensely weathered and fractured matrix rock between block zones. This information was provided in the construction documents to contractors for use as a bid basis and to allow for planning of drilling methods.

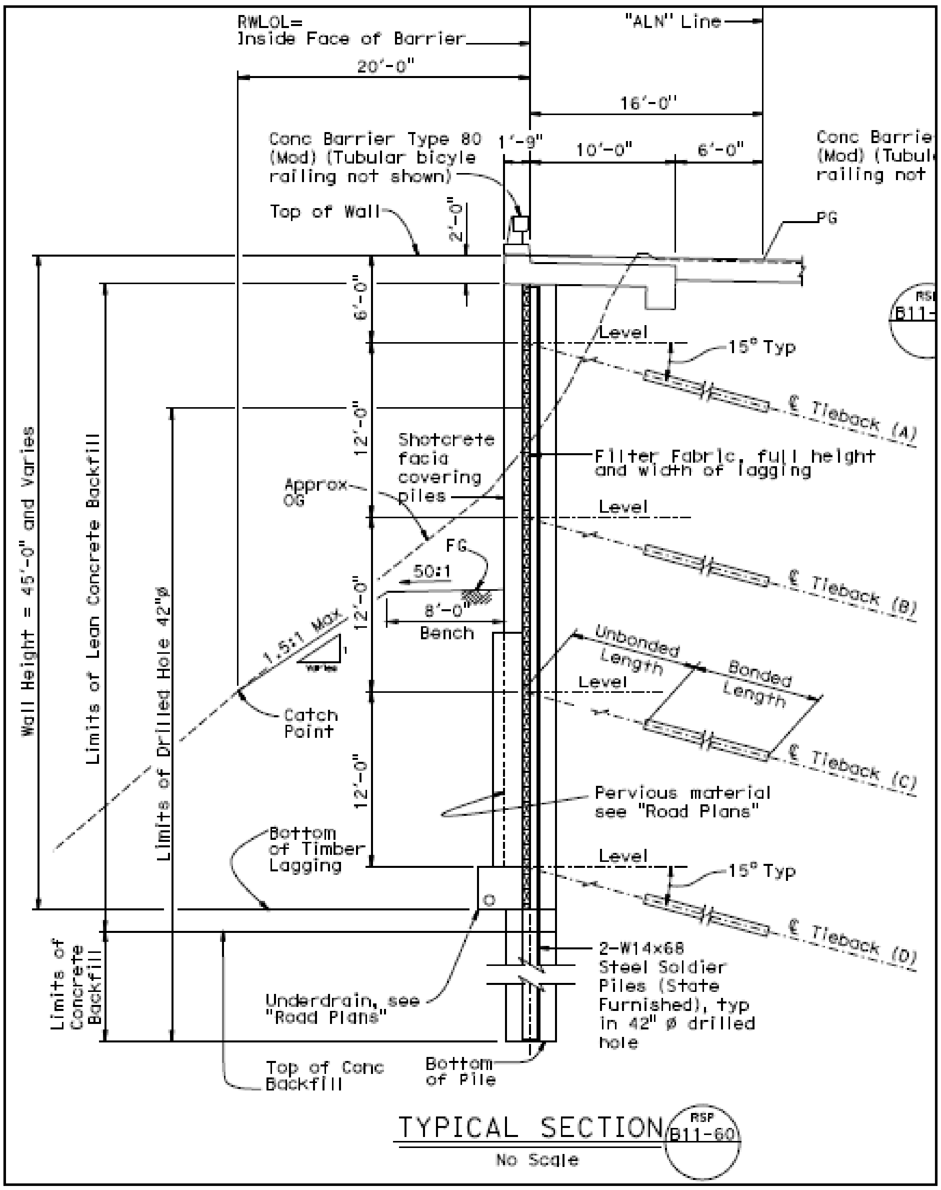

Figure 4: Anchored soldier pile wall typical cross section

Construction

Difficult drilling conditions encountered in the subsurface investigation borings were also anticipated during the drilling for the piles and ground anchors. The Franciscan Complex consists of very intensely to moderately fractured rock ranging from extremely hard to very soft, and fresh to decomposed. The varied nature of the rock condition and perched groundwater were identified and described in the construction documents, with emphasis placed on the difficult drilling conditions in an effort to alert contractors to plan drilling methods and bid accordingly.

Condon Johnson and Associates (CJA) was awarded the contract to construct the wall in early September, 2010. The awarded bid was $7,641,152.90, or approximately $250 per square foot of lagged wall. Construction began in November of 2010.

CJA proposed and constructed a temporary soil nail wall at the existing highway centerline to support the roadway while the piles were drilled from a bench between the temporary wall and the new retaining wall alignment. Some of the piles were drilled entirely in the dry with little or no caving and were able to be drilled, the piles placed, and concrete poured within a single day. Other piles, sometimes directly adjacent to more-easily installed piles, required over-drilling the hole diameter and the use of several lengths of telescoping casing in conjunction with placement of lean concrete plugs to control caving and groundwater seepage leading to caving. Ground conditions were highly variable on a small scale. Some holes took several days to drill, and required the use of many toolings, including multiple diameters of soil augers, rock augers, core barrels, digging buckets, and cleanout buckets. Hard blocks of the meta-greywacke identified in the subsurface investigation took significant time and effort to advance through with bullet-toothed core barrels. Groundwater was controlled by pumping from the base of the piles prior to pouring concrete, precluding the use of drilling fluids and allowing all of the drilled shafts to be constructed utilizing the dry method.

Concrete was mixed at a remote concrete batch plant constructed several miles north of the project site. The distance and time to the closest available commercial concrete plant exceeded the allowable trucking times specified by Caltrans. Concrete was batched during drilling of the final feet of each pile and transported the short distance to the project in ten-yard mix trucks. Water was pumped from the holes if present, and concrete was placed by free-falling from the rear of the mix trucks. If used, temporary casing was removed by crane after establishing a head of concrete above the base of the casing to prevent caving as the casing was withdrawn.

Pile construction was completed in May of 2011, with only minor issues. The stability of the bench between the soil nail wall and soldier pile tieback wall was marginal during the wet winter months of 2011, and cracking was observed at the rear of the bench as it continued to be transported by the landslide. CJA often had to place fill to maintain the bench elevation and provide a stable drilling platform. The pile drilling was done entirely with a Soilmec SR-70, which provided the high crowd and torque capacity required for the subsurface conditions. As the pile installation progressed and the rainy season ended, the temporarily cantilevered piles began to provide resistance to the slide movement and the stability of the bench improved. Tension cracks developed between the piles at the retaining wall alignment, indicating soil arching between the piles and stabilization of the bench behind the wall.

Excavation in front of the wall to construct the working bench and the vertical face at the lagging encountered many layers of cold mix asphalt and aggregate base, particularly at the northern end of the wall. Horizontal layers several inches thick were encountered to depths of over 30 feet below the existing road elevation. Much of the vertical excavation at the face behind the wall was in asphalt, serving as a reminder of the magnitude of movement and cost of maintenance required to keep the road open in previous years.

Figure 5: Excavation of the face behind the lagging encountered layers of asphalt and aggregate base well below the existing roadway elevation.

In addition to the difficult construction conditions, landslides to the north and south of the Dani Creek construction site closed Highway 1 for several months in the spring of 2011, making access difficult for construction monitoring and presenting difficulties in transporting supplies and personnel to the site for the contractor.

Anchor construction was concurrent with pile installation after enough room was established for the anchor drill rigs to work behind the pile drilling operation. Sub-horizontal holes for anchors were drilled using Klemm air-rotary rigs from the bench in front of the wall, and a reach-over air rig from the bench behind the wall to install the top row of anchors. The same hard rock and groundwater issues encountered in the pile excavations affected the anchor drilling, requiring casing for the full length of the ground anchor holes. Typical production drilling rates of 3 to 4 anchors per day were achieved when installed in the softer matrix material. Anchor excavations that encountered hard rock conditions took longer to drill and required much higher volumes of grout, due to grout loss into fracture zones in the hard block material. Several drill holes near the center of the landslide intersected perched groundwater zones and released thousands of gallons out of the holes under pressure, flooding the working bench in front of the wall.

Figure 6: Installation of soldier piles between temporary soil nail wall and final anchored soldier pile wall alignment. Note soil arching in front of soldier piles in foreground.

Anchors are 7 and 9 strand tendons, with maximum design loads of 190 kips at the first and fourth rows, and 250 kips at the second and third rows. Anchors were tested to 150% of the design load and locked off at 75% of the design load. Secondary grouting was performed on all of the anchors at the contractor's discretion, although not required, in an effort to reduce the risk of failing anchors in tension. All of the anchors met load testing criteria and no additional anchors were required. Minimal issues with lateral pile deflection into the fill sections of the wall during anchor stressing were observed, with the success of the bottom-up method of construction method attributed to the strict compaction and height requirements above anchors in fill situations, and the quality of work and attention CJA paid to meeting the specifications. Anchor installation was completed in mid-August of 2011.

Figure 7: Near completion of four rows of anchors prior to placement of shotcrete fascia.

The final wall design includes a vertical, rectangular shotcrete fascia at each soldier pile to protect the steel pile sections and anchors from corrosion. In addition to the shotcrete fascia, a contract change order was employed to add grout caps over the exposed anchor tails and anchor heads within the shotcrete to provide additional corrosion resistance due to the proximity of the structure to the Pacific Ocean and highly corrosive environment.

In order to balance the quantity of excavation and fill on the job, material excavated during construction of the wall was stockpiled on site and used to construct a bench of compacted fill in front of the wall. The bench also serves to provide coverage of the lagging during future movement of the unrestrained portion of the landslide below the wall. A chimney drain was designed and constructed in front of the wall to the bottom of the lagging elevation to allow water that drains through the buried face of the wall to be carried through the bench. The drain consists of a slotted 8” PVC pipe at the bottom of a 2-foot wide zone of permeable aggregate base encapsulated in nonwoven geotextile filter fabric. The pipe and chimney drain are sloped to drain to solid outlet pipes that extend through the bench.

Figure 8: Construction of the chimney drain and bench in front of the wall

Construction Monitoring and Instrumentation

Observation of the retaining wall construction was performed primarily by Caltrans Structure Construction personnel. Geotechnical personnel made weekly site visits or as required when issues or questions arose. At the request of the contractor, slope inclinometers were installed on several piles to quantify the stability of the working bench behind the retaining wall during pile construction. Significant magnitude of movement was measured in the slope inclinometers on the piles, but movement was gradual and eventually stopped as the wall construction began to stabilize the portion of the landslide behind the wall. Pile movement ceased after installation of anchors on the instrumented piles. Maintenance of the bench behind the wall by placement of fill where required and the use of lagging and trench plates to support pile drilling equipment was successful.

Movement of the bench in front of the wall continued throughout construction as the excavation and anchor installation proceeded. Maintenance of the bench by placement of fill was sometimes required to access anchors, but for the most part did not impede operations. Continued movement of the portion of the landslide not retained behind the wall was anticipated and continues to occur. Future maintenance of the finished bench may be required if sliding occurs beneath the bottom of the lagging and material continues to be displaced vertically.

Permanently installed vibrating wire strain gauge load cells on twelve of the anchors were added to the project under a contract change order. Previous experience with construction and long-term performance of anchored soldier pile walls on the Big Sur Coast has indicated issues with roadway deformation behind the walls, slide material moving below the lagged portion of the wall, and possible changes in landslide forces and direction after wall construction. Underlying causes of these issues have been unknown and require significant time and money to study without any information other than observation of ground surface deformation. Installation of load cells on anchors throughout the wall provides information about the load distribution on the wall, and may be a valuable tool for determining the cause of continued movement or changing landslide conditions, should they occur.

Initial anchor tension load readings were taken during or soon after installation and stressing of instrumented anchors, and a monitoring program of instrumented anchors began in July of 2011. Twelve Geokon model 4900 load cells with three vibrating wire strain gauges per load cell were installed between the anchor head and bearing plate, with 1½” machined plates on either side, then sealed in a cap longer than the production grout caps to accommodate the load cell assembly.

Figure 9: Installed load cell.

Initial load cell readings on five of the twelve installed load cells indicated that the load cells were eccentrically loaded at the anchor head/bearing plate assembly. The contractor and Caltrans construction inspectors made efforts to ensure that the load cells were centered over the hole in the bearing plate and that the anchor head was bearing on the center of the plate on the outside of the load cell, but very slight deviation from the exact center resulted in eccentric loading of the load cell. Individual readings of the three vibrating wire strain gauges within the load cells typically showed one gauge reading well above the design lock-off load, while the other two gauges read well below the design lock-off load. The direct load reading feature of the load cell readout box computes the average of the three gauges and reports the result as a load in force units. Due to the eccentric loading of the load cell, the direct load readout values were significantly below the design lock-off loads. Load cells were calibrated with the hydraulic jack and strain gauge used to test the anchors to ensure that the low readings were a result of eccentric loading, and not a malfunction in the load cell assembly or readout box. Although the direct load values on five anchors do not accurately reflect the magnitude of the total tension load in the anchors, monitoring of the change in load readings is still a valuable tool in assessing the long term performance of the anchors.

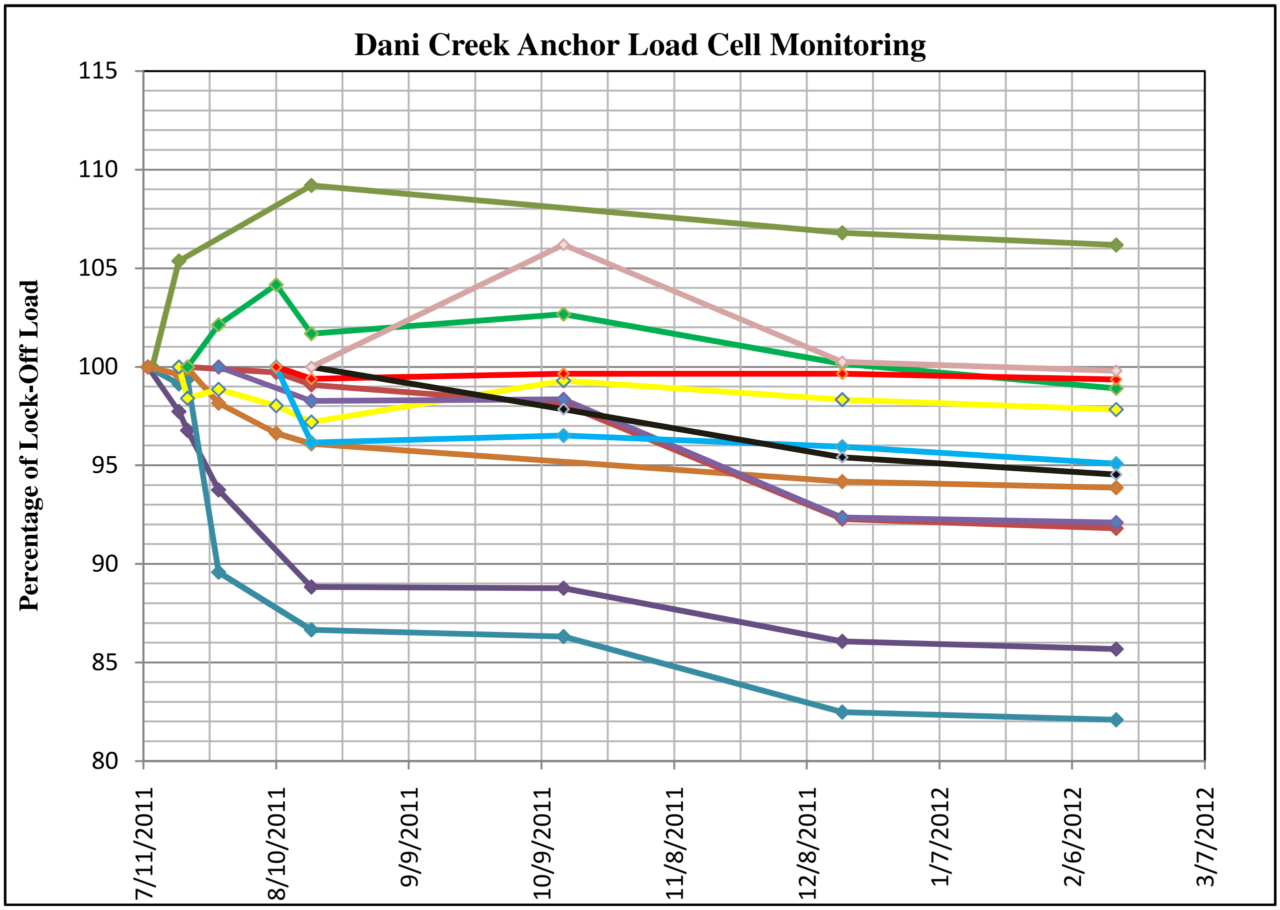

Figure 10: Load Cell Monitoring Results

Results of the on-going load cell monitoring are presented in Figure 10. Ten of the twelve load cells indicated relative stability in the measured load after the initial load lock-off, varying from approximately 92% to 106% of the lock-off load. Fluctuations in the readings taken during construction of the wall due to changing earth pressure distribution were observed as excavation and anchor installation proceeded downward. After completion of construction, minimal fluctuations in the readings have been observed, indicating that the wall forces are approaching equilibrium. Two of the load cells, 65A and 67B, exhibited load loss to approximately 87 to 89% of the lock-off load in the month immediately following initial lock-off. The decline in measured tension load is likely due to reduction in the anchor force due to stressing of anchors adjacent to and below the instrumented anchors. Following the initial decline, the load cells on anchors 65A and 67B have stabilized in a manner similar to the other instrumented anchors at approximately 85% of the lock-off load.

Summary and Conclusions

Organization and deduction of raw data including landslide feature mapping, instrumentation data, laboratory data, subsurface material properties, and interpretation of geology and groundwater regime were critical in constructing a simplified model of the landslide geometry, geology, and material strengths that accurately represented complex field conditions. Analyses of multiple two-dimensional landslide geometries and varying material strength properties using several limit equilibrium slope stability analysis methods resulted in a critical condition that was used to calculate the geotechnical and structural loads and resistances used to design the wall. The use of slope stability analysis software is an excellent tool for conducting sensitivity studies of analyses inputs and narrowing the results to an efficient design.

Figure 11: Final Constructed Structure.

Years of maintenance, field study, research, instrumentation, subsurface exploration, design, and finally construction of a structure were invested to mitigate effects of Dani Creek Landslide on Highway 1. The completed anchored soldier pile wall has performed well through the first year of service, with no signs of deformation behind the wall. Despite a relatively dry winter in 2011-2012, movement of the unrestrained portion of the landslide below the wall continues; cracks in the completed bench developed just days after final compaction. The complex geology and groundwater regime will likely continue to change and shift with seasonal fluctuation and as landslide forces come to equilibrium. Installed anchor load cells will provide a valuable tool in assessing the magnitude of change in landslide and anchor forces throughout the life of the structure, and provide insight into the direction and magnitude of changing landslide forces should they begin to cause deformation of the structure.

References

Big Sur Coast Highway Management Plan. (2004). California Department of Transportation, San Luis Obispo, CA.

Hall C.A. Jr. (1991). *Geology of the Point Sur-Lopez Point Region, Coast Ranges, California: Part of the Southern California Allochthon.* Geological Society of America, Special Paper 266.

Medley E. (1998). *Order in Chaos: The Geotechnical Characterization of Mélange Bimrocks.* Proceedings, First International Conference on Site Characterization, Atlanta, GA.

Turner K.A., Schuster R.L. (1996). *Landslides Investigation and Mitigation.* Transportation Research Board Special Report 247. National Academy Press, Washington DC.

Wills C.J., Manson M.W., Brown K.D., Davenport C.W., Domrose C.J. (2001). *Landslides in the Highway 1 Corridor: Geology and Slope Stability along the Coast between Point Lobos and San Carporforo Creek, Monterey and San Luis Obispo Counties, California*. California Department of Conservation, Division of Mines and Geology.

Estimating Landslide Losses to State Highways: a general approach for a winter storm scenario

Chris Wills
California Geological Survey
801 K Street, ms 12-32, Sacramento CA 95814
(916) 324-7324
E-mail: Chris.wills@conservation.ca.gov

Florante Perez
California Geological Survey
801 K Street, ms 12-32, Sacramento CA 95814
(916) 324-7324
E-mail: Ante.Perez@conservation.ca.gov

David Branum
California Geological Survey
801 K Street, ms 12-32, Sacramento CA 95814
(916) 324-7324
E-mail: Dave.M.Branum@conservation.ca.gov

Prepared for the 63rd Highway Geology Symposium, May 7-10, 2012

ACKNOWLEDGEMENTS

The compilation and analysis of landslide hazard data described here benefited from the help of Jonathan Stock, Jeff Coe and Jonathan Godt of USGS and Jerry Treiman of CGS. GIS assistance was provided by David Strong of USGS. Dale Cox provided guidance and inspiration throughout the project.

DISCLAIMER

Statements and views presented in this paper are strictly those of the author, and do not necessarily reflect positions held by their affiliations, the Highway Geology Symposium (HGS), or others acknowledged above. The mention of trade names for commercial products does not imply the approval or endorsement by HGS.

COPYRIGHT NOTICE

ABSTRACT

ARkStorm is a statewide emergency planning scenario hypothesizing severe storms that entrain huge amounts of moisture from the tropical Pacific and dump it on California over a few days. The storm is projected to be similar to but more intense than storms that have struck California in recent decades, and approach the massive storms of 1861-1862 in total rainfall. Estimating the numbers and impact of landslides from the ARkStorm requires models relating rainfall to the numbers and distribution of landslides and detailed records of the impact of landslides in past storms. Neither of these basic data sets exist. Models that estimate the areas with the greatest susceptibility to landsliding do exist, however. These can be combined with records of landslide damage and areas likely to be damaged and total damage can be projected. Quality of the projection depends on the amount of data. This study is based on landslide damage data developed by Caltrans over the past ten years. This data is enough to develop a general method for estimating landslide damage but not sufficient to give us confidence in the results. The general pattern of statewide landslide susceptibility is similar to the pattern of landslide damage to state highways, as recorded by Caltrans emergency opening and SHOPP repair projects. The amount of damage is correlated with the total statewide annual rainfall. Emergency opening costs are higher in years of greater than average rainfall. SHOPP landslide repair costs show a similar pattern, but lag a year or two behind the rainfall. We have extrapolated the incomplete records of damage from landslides in past storms to the ARkStorm. Projecting damage estimates from a short data set leads to significant uncertainty in the result. Using the highest recorded intensity estimates, damage to infrastructure due to landslides triggered by ARkStorm could approach two billion dollars.

INTRODUCTION

The United States Geological Survey (USGS) Multi-Hazards Demonstration Project (MHDP) uses hazards science to improve communities' resiliency to natural disasters (Jones, et al, 2007). The project engages emergency planners, businesses, universities, government agencies, and others in preparing for major natural disasters. The first public product of the MHDP was the ShakeOut Earthquake Scenario in November 2008. This detailed depiction of a hypothetical magnitude 7.8 earthquake on the San Andreas Fault in southern California served as the centerpiece of the largest earthquake drill in United States history, involving over 5,000 emergency responders and the participation of 5.5 million citizens.

The second major public project of the MHDP is a hypothetical winter storm scenario, called ARkStorm. AR stands for atmospheric river; a narrow corridor of concentrated moisture in the atmosphere (Ralph & Dettinger, 2011), the meteorological phenomenon that leads to most intense winter rainstorms in California. ARkStorm, like ShakeOut, is a large but scientifically realistic event. Description of the event is followed by an examination of the secondary hazards (e.g., landslides and flooding), physical damages to the built environment, and social and economic consequences (Porter et al, 2010).

Like many of the major storms in California history, the ARkStorm would begin by entraining moisture in the tropical Pacific and streaming that moisture in an atmospheric river directly to California. The rainfall totals for the storm approach those of the California winter storms of 1861 and 1862 that left the Central Valley impassible. High rainfall totals, usually averaged over a month or over an entire rainfall season, are needed to trigger the types of large, deep-seated landslides that underlie large areas and cause extensive damage to property. An atmospheric river storm also results in very intense rainfall. High intensity rainfall, usually measured in inches per hour, can trigger fluid, fast-moving landslides that cause most casualties. Estimates of landslide damage for the ARkStorm can be made based on a new map showing the susceptibility of California to deep-seated landslides and new correlations between rainfall and total landslide damage from past storms. Other aspects of landslides and landslide consequences of ARkStorm are described by Porter et al (2010) and Wills et al (in prep.).

SUSCEPTIBILITY TO DEEP-SEATED LANDSLIDES

In order to estimate the spatial distribution of landslides in the ARkStorm, the relative susceptibility to landslides of the area affected by the storm had to be determined. A new statewide map of susceptibility to deep-seated landslides (Wills et al, 2011) (Figure 1) is based on available landslide inventory maps, geologic maps, and topographic data, in the context of published and unpublished literature and the experience of scientists working on California landslides. Preparation of the map followed the general procedures that Ponti et al (2008) used for the ShakeOut Scenario. The susceptibility map describes the relative likelihood of future landsliding based solely on the intrinsic properties of a site. Prior failure (from a landslide inventory), rock or soil strength, and steepness of slope are the most important site factors that determine susceptibility.

This landslide susceptibility map allows for statewide estimation of landslide potential and costs in a major event like the ARkStorm. Although the simplified geologic classifications and lack of digital landslide inventory maps in many areas result in generalized landslide susceptibility estimates, this statewide map is the most detailed yet developed. Using the susceptibility map to estimate the overall distribution of landslides, historic records of landslides triggered by individual storms can be used to estimate the effects of landslides in the ARkStorm. As discussed below, this calibration of the susceptibility map using historic data is the key to estimates of future landslide losses.

CALCULATION OF LOSSES

The ARkStorm scenario should depict the effects of the landslides that are triggered by the sustained, intense rainfall; where those landslides are, and how much damage they cause. This analysis requires a loss estimation system or model. Such a model exists for earthquakes, hurricanes, and floods: the HAZUS program developed for FEMA by the National Institute of Building Sciences (NIBS, 2009). Although HAZUS does not calculate landslide losses, this study represents a first step towards developing a model using the general approach and some of the background data included in HAZUS to estimate landslide losses.

In HAZUS, a hazard with a measured or estimated intensity acts on an inventory of structures with estimated values and vulnerability. The result is an estimate of loss, expressed as the dollar value of direct losses or as a loss ratio: the amount of damage divided by the value of structures. For earthquakes, the intensity is measured by the strength of ground shaking, the numbers of structures of different types are estimated from census data and the vulnerability of each type of structure is estimated based on structural engineering evaluations from past earthquakes. For landslides, the intensity of a storm can be measured or, like the ARkStorm, a detailed scenario model can be developed. Landslides are a secondary hazard and can be related to the intensity of the triggering storm and the susceptibility of a site to landsliding. For past storms, and for the ARkStorm, storm intensity is known and susceptibility is estimated from the map described above. Estimated landslide losses are based on the value of structures exposed to a given level of storm intensity, the landslide susceptibility and the vulnerability of those structures. The values of structures of different types are included in HAZUS for each census tract. Census tracts are areas designated by the U.S. census bureau and designed to have similar population, so they are small in urban areas and large in rural areas. Census tracts in relatively low-density, hilly, suburban areas are small enough so that they commonly include a limited range of topography as well as a limited range of building types. The value of a single building type, light wood-frame structures, was used by Wills et al (2012) as the value of structures exposed to landslide losses for private property. HAZUS also includes values of infrastructure, so calculation of loss ratios is possible for highways and other facilities. To calculate vulnerability of an inventory of structures, landslide damage from past storms must be known and correlated with storm intensity and landslide susceptibility. The lack of data on losses in previous storms is the primary impediment to the development of a landslide loss model, as is discussed below. If losses are known for a given storm intensity and landslide susceptibility, vulnerability can be calculated and used to estimate losses for different intensities. Unfortunately, there is no generally accepted measure of storm intensity for estimating landslide losses, nor is there an established correlation between susceptibility and loss. For the ARkStorm project, available landslide loss data have been used to develop relations between susceptibility and loss to the extent that is supported by the data. Losses to private property are detailed separately (Wills et al, 2012), potential losses to the state highway system are estimated here.

DAMAGE TO INFRASTRUCTURE

Landslides damage highways, local roads, pipelines and many other facilities. As with private property, there is no centralized compilation or reporting of the number of landslides that damage infrastructure or the amount of damage caused. Especially large or disruptive landslides are reported in the news media, sometimes with estimates of the cost of repairs. Very rarely, reports of individual landslides will include both the cost to repair the slide and associated economic costs. In cases where indirect costs of a landslide are reported, they may be several times the direct repair costs. Two examples of this are the landslide that closed Highway 50 between Sacramento and Lake Tahoe in 1997 and a small landslide east of Watsonville in 1998. The Highway 50 slide cost over $4.5 million to repair. Indirect economic costs were over $28 million (Reid and LaHusen, 1998). The 1998 slide east of Watsonville cost under $1 million to repair the local road and drainage facilities. Repair of a natural gas pipeline and restoration of gas service to a large area cost over $10 million. Half of the restoration costs were for personnel to re-light approximately 60,000 pilot lights in the affected area (Schuster et al, 1998). We found no consistent data on indirect economic costs of landslides and so do not include indirect costs in any of our analysis. Data from owners and operators of roads, railroads, pipelines, water, wastewater, electrical, gas and other infrastructure systems was compiled and summarized by county for Bay Area storms (Taylor et al, 1975; Taylor and Brabb 1972; Nilsen et al, 1976; Shearer et al,1983; Creasey, 1988; Crovelli and Coe, 2009). This data is valuable, but because it is compiled at the county level, does not allow a comparison with the landslide susceptibility map. Additionally, many infrastructure repair projects take significant time to plan and the cost is not known immediately following a storm. Two cases where landslide damage developed over many storms and the total cost of repair was not known until long after the storms had passed are Devil's Slide on the San Mateo County coast and Confusion Hill along Highway 101 in northern Mendocino County. At both these locations, Caltrans damage records include the cost of short-term repair needed to re-open the road. Eventually, long term repairs involved construction of new highway alignments. Construction costs of these new alignments was reported to be $325 million for Devil's Slide and $70 million for Confusion Hill. This type of landslide cost is very difficult to associate with a triggering storm or storm season, so is difficult to include in a system that correlates storm intensity with damage. As with damage to private property, we would like to project from detailed records of damage that include the date, location and amount of landslide damage. We would also like to include an estimate of costs for landslide repair beyond the immediate return to service. The only data set that meets these requirements is the records of landslide damage to the state highway system compiled by Caltrans.

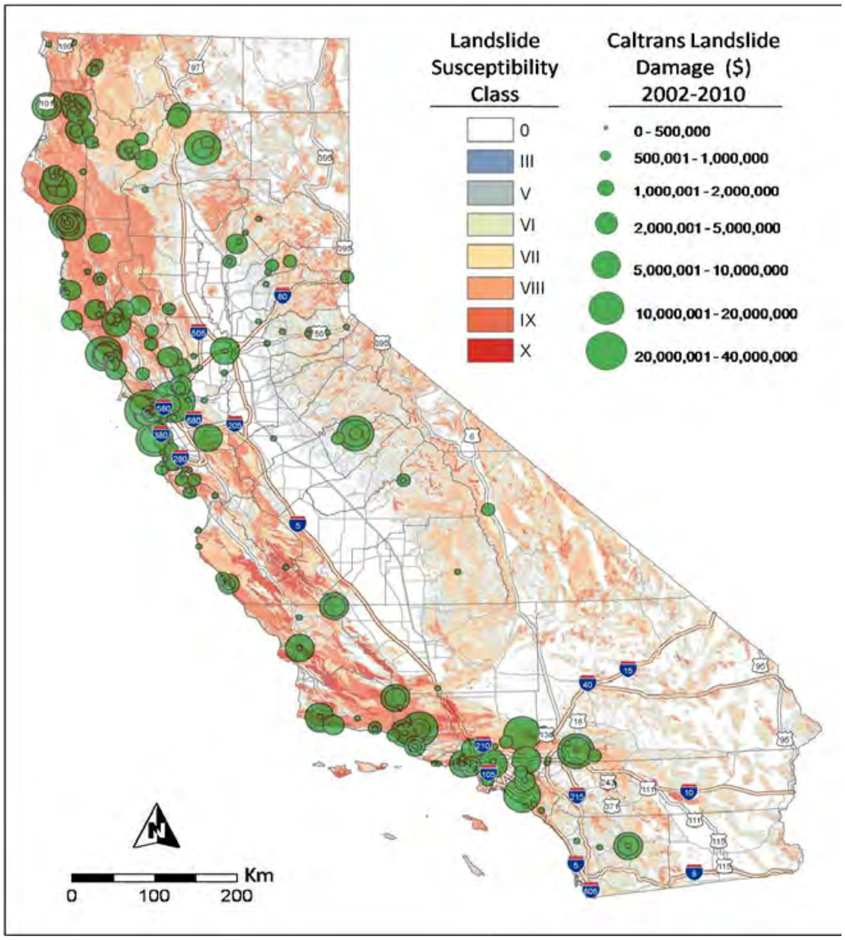

Figure 1. Caltrans 'Emergency opening" projects from 2002-2010 compared to statewide landslide sucseptibility.

Caltrans keeps records of landslides in each of their 12 districts statewide. In addition, a statewide compilation of major landslides is maintained at the headquarters office in Sacramento. This compilation shows the funds expended for "emergency opening" projects, the immediate response to emergencies. Additional repair projects that involve longer term planning are included in the "State Highway Operation and Protection Program" or SHOPP. These projects are included in lists and descriptions of projects voted on by the California Transportation Commission. Still longer term landslide repair projects, optimistically called "permanent restoration", are also included in the SHOPP listing. The Confusion Hill new highway alignment construction described above is an example of a project in the SHOPP listing. For the ARkStorm project, we obtained landslide records from Caltrans District 5 in San Luis Obispo, 7 in Los Angeles, 8 in San Bernardino and 12 in Orange County. We also obtained spreadsheets of the statewide "emergency opening" and "permanent restoration" projects from Caltrans headquarters and SHOPP listings from the Caltrans web site at http://www.dot.ca.gov/hq/transprog/shopp.htm and http://www.dot.ca.gov/hq/transprog/SHOPP/SHOPP_Prior_Doc.htm .

Overall, the geographic distribution of Caltrans "Emergency Opening" projects is similar to the distribution of landslide susceptibility, with more damage in areas of high susceptibility and a denser highway network (Figure 1). Landslide damage is most extensive in the western Transverse Ranges and the northern Coast Ranges, though there are notable landslides along highways that follow canyons through the Sierra Nevada.

There is extensive overlap between the records kept at the Caltrans district offices and those at headquarters. Only those "emergency opening" repairs with a total cost above $250,000 are compiled at headquarters, so the district records include more landslides and the amount of recorded damage is higher. We compiled the landslide damage data and calculated annual totals for each rainfall-year (July 1 through June 30). Unfortunately, we were not able to obtain landslide records from all Caltrans districts, so the only data set we have that covers the entire state is the records from Caltrans headquarters. That data set is relatively complete from 2003 through 2010. We also obtained records from Caltrans District 7 (Los Angeles and Ventura Counties) for 1996 through 1999, with additional records from 2005. The combination of the statewide data with the data from district 7 shows that landslide damage is very strongly correlated with rainfall (Figure 2). Rainfall for this comparison is simply the statewide average from the Western Regional Climate Center of the Desert Research Institute and NOAA. We downloaded the annual rainfall for "water years" (July through June) for comparison with statewide landslide costs from http://www.wrcc.dri.edu/monitor/cal-mon/frames_version.html . Figure 2 shows rainfall and the cost of landslides from Caltrans headquarters and Caltrans District 7 as mean values and deviations from mean. Rainfall for the past 15 years has been most commonly below the mean annual rainfall calculated for the past 115 years, with 1998, 2005 and 2006 notably above average. Each year when rainfall was significantly above average, cost of landslide repairs was also significantly above average.

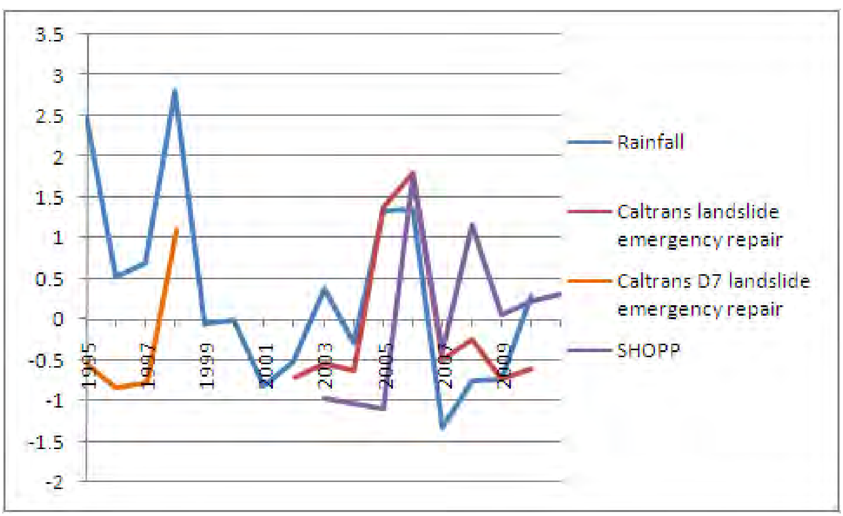

Figure 2. Comparison of variability in annual rainfall with variability in landslide repair costs to state highways. Both rainfall and costs are expressed as difference from mean values. Differences expressed as standard deviations. Years with higher than average rainfall have higher than average emergency repair costs. Landslide repairs that require longer term planning included in the SHOPP plan increased in cost in 2006, following heavy rains in 2005, but have not yet decreased to pre-2005 "background" levels.

The SHOPP listing shows a similar pattern for the past eight years, but with a delayed response to rainfall. Landslide repair projects listed in the SHOPP were under $10 million in 2003-04, 04-05 and 05-06, even though 05-06 had high total rainfall. SHOPP landslide repairs jumped to over $150 million in 06-07, reflecting the response to the 05-06 winter as well as the $70 million Confusion Hill realignment project. Average cost of landslide repairs listed in SHOPP has been about $60 million, which includes the low costs preceding 05-06, high costs for the next few years and continuing costs for projects scheduled to be completed in 10-11 and 11-12.

Showing the statewide data in another format, with rainfall in inches plotted against costs of "emergency opening" landslide repair projects in millions of dollars (Figure 3) allows a projection to higher rainfall levels than have been recorded historically, such as the ARkStorm. The data, however, do not plot along a neat line, but rather suggest that there is a typical rainfall year, with around $20,000,000 damage and an exceptional rainfall year, with around $150,000,000 damage. The "step" between a typical year and an exceptional year is between 25 and 30 inches of rainfall, about 0.5 to 1 standard deviation over the statewide average.

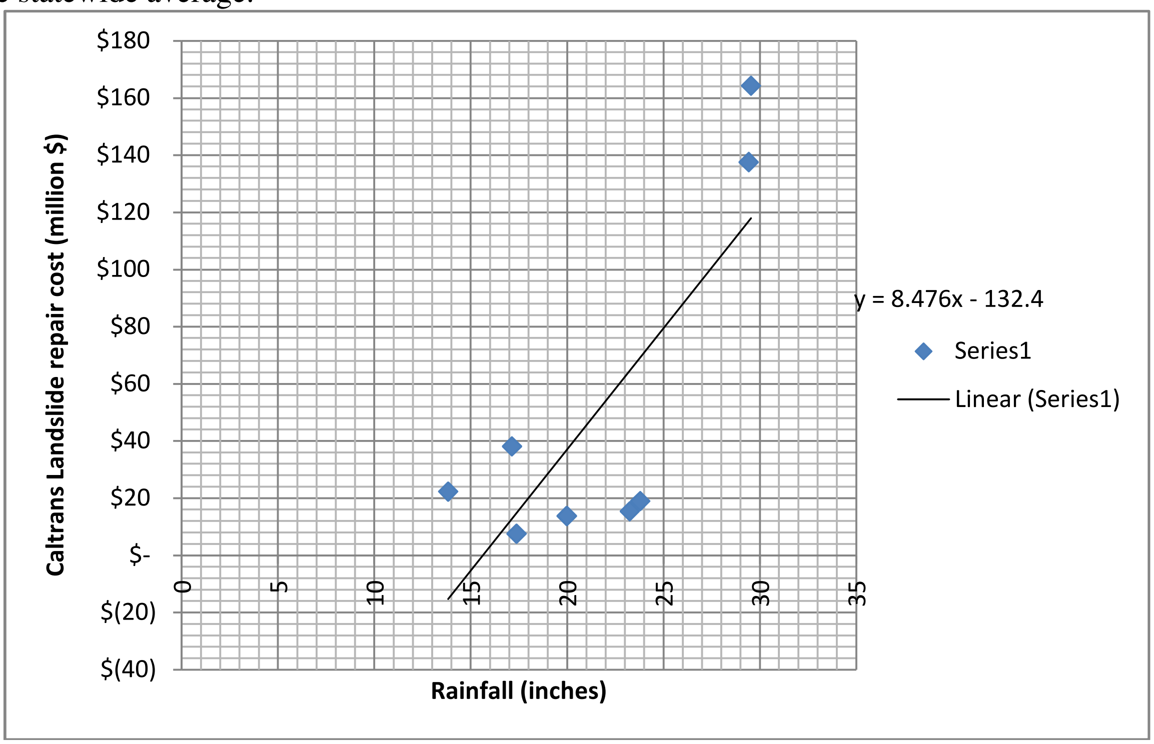

Figure 3, Statewide Caltrans "Emergency Opening" costs due to landslides compared with statewide annual rainfall. In typical rainfall years with less than 25 inches of rainfall, Caltrans spends $20 to$40 million on landslide repairs. In the years of substantially above 25 years of rainfall, Caltrans has spent an average of $150 million.

Projecting landslide costs to infrastructure for the ARkStorm requires a projection from the data that we have to the amount of rainfall for the ARkStorm. The last 9 years of data relating the amount of rainfall to the cost of landslide to the state highway system do not form a clear linear pattern that can project to larger rainfall amounts. The data suggest an exponential increase in damage with increasing rainfall or possibly a step function. With this small amount of data we can't develop a formula to project from typical years to high-cost years. In particular, if the data forms a step function, we cannot determine how much rainfall could trigger the next step up in landslide costs, and how high that step would be. Lacking further data, the simplest projection to higher rainfall values is a linear relation from the existing data. That linear relation suggests that, for the ARkStorm statewide average rainfall of about 47 inches the state highway system will sustain landslide damage approaching $300 million in cost for “emergency opening” projects. This immediate expense would be followed by planned repair and “permanent restoration” projects in succeeding years that would cost at least as much. In addition to the State Highway system, landslides would damage local roads and utilities. For the 1982 storms in the Bay Area, Creasy (1988) reports that state roads accounted for 31% of damage to infrastructure. County roads accounted for 40% of infrastructure damage and utilities accounted for 13% of infrastructure damage. These proportions suggest that total losses to infrastructure from a storm of the intensity of the ARkStorm would approach $2 billion.

CONCLUSIONS

A landslide loss estimate can be developed using the general methodology and some of the input from the HAZUS program, which is a standard system for estimating earthquake or flood losses. The landslide loss can be expressed as a loss ratio, the amount of damage compared to the value of existing structures that can be damaged. An evaluation of loss ratio and rainfall for private property resulted in a method for estimating landslide damage as a function of the peak 2-day rainfall averaged over a county or peak 30-day rainfall averaged over a county (Wills et al, 2012). Preliminary analysis shows similar variation in losses to the state highway system with landslide susceptibility and with rainfall. Although detailed estimates of loss ratios for the highway system have not been completed, rough projections from past damage are possible. None of the data that these projections are based on are complete or comprehensive, so the resulting estimates are highly uncertain. As additional data on landslide damage become available, the general approach described here can be repeated and the estimates can be progressively refined.

REFERENCES

Creasy, C.L., 1988, Landslide Damage, A costly outcome of the storm, in Ellen, S.D., and Wieczorek, G.F., editors, Landslides, floods, and marine effects of the storm of January 3-5, 1982, in the San Francisco Bay region, California: U.S. Geological Survey Professional Paper 1434, p. 195 – 203.

Crovelli, R.A. and Coe, J.A., 2009, Probabilistic estimation of numbers and costs of future landslides in the San Francisco Bay region: Georisk, Vol. 3, No. 4, p. 206-223

Jones, L, R. Bernknopf, S. Cannon, L. Gaydos, J. Keeley, M. Kohler, H. Lee, D. Ponti, S. Ross, S. Schwarzbach, M. Shulters, A. W. Ward, and A. Wein, 2007, Increasing Resiliency to Natural Disasters: A Strategic Plan for the Multi-hazards Demonstration Project in Southern California, USGS administrative report, Pasadena, CA, 31p.

National Institute of Building Sciences (NIBS), 2009, Multi-hazard Loss Estimation Methodology, Earthquake Model, HAZUS-MH MR3, User Manual and Technical Manual, developed by Department of Homeland Security, Emergency Preparedness and Response Directorate, Federal Emergency Management Agency (FEMA), Mitigation Division, Washington, D.C., under a contract with National Institute of Building Sciences, Washington, D.C. (Available online: http://www.fema.gov/plan/prevent/hazus/hz_resources.shtm, downloaded in May 2009)

Nilsen, T.H., Taylor, F.A., Brabb, E.E., 1976, Recent landslides in Alameda County, California (1940–71) an estimate of economic losses and correlations with slope, rainfall, and ancient landslide deposits. US Geol Surv Bull 1398.

Ponti, D.J., Tinsley, J.C. III, Treiman, J.A., and Seligson, H., 2008, Ground Deformation, section 3c in Jones, L. M., Bernknopf, R., Cox, D., Goltz, J., Hudnut, K., Mileti, D., Perry, S., Ponti, D., Porter, K., Reichle, M., Seligson, H., Shoaf, K., Treiman, J., and Wein, A., 2008, The ShakeOut Scenario: U.S. Geological Survey Open-File Report 2008-1150 and California Geological Survey Preliminary Report 25 http://pubs.usgs.gov/of/2008/1150/.

Porter, K., Wein, A., Alpers, C., Baez, A., Barnard, P., Carter, J., Corsi, A., Costner, J., Cox, D., Das, T., Dettinger, M., Done, J., Eadie, C., Eymann, M., Ferris, J., Gunturi, P., Hughes, M., Jarrett, R., Johnson, L., Le-Griffin, H., Mitchell, D., Morman, S., Neiman, P., Olsen, A., Perry, S., Plumlee, G., Ralph, M., Reynolds, D., Rose, A., Schaefer, K., Serakos, J., Siembieda, W., Stock, J., Strong, D., Wing, I., Tang, A., Thomas, P., Topping, K., and Wills, C., 2010, Overview of the ARkStorm Scenario: U.S. Geological Survey Open File Report 2010-1312, 183 p.

Ralph, F.M., and Dettinger, M.D., 2011: Storms, floods and the science of atmospheric rivers. EOS, Transactions, AGU, v. 92, no. 32, p. 265-66.

Reid, M.E., and LaHusen, R.G., 1998, Real-time monitoring of active landslides along Highway 50, El Dorado County: California Geology, v. 51, no. 3, p. 17-20.

Schuster, R.L., Baum R.L., and Highland, L.M., 1998, The April 1998 El Nino-triggered Anzar Road landslide, San Benito County, California: AEG News, v. 41, no. 4, p. 5 -7.

Shearer, C.F., Taylor, F.A., and Fleming, R.W., 1983, Distribution and costs of landslides in San Diego County, during the rainfall years of 1978-79 and 1979-80 U.S. Geological Survey Open-File Report 83-582, 22 p.

Taylor, F.A., Nilsen, T.H., and Dean, R.M., 1975, Distribution and cost of landslides that have damaged manmade structures during the rainy season of 1972-1973 in the San Francisco Bay region, California U.S. Geological Survey Miscellaneous Field Studies Map MF-679, scales 1:500,000 and 1:1,000,000.

Taylor, F.A., and Brabb, E.E., 1972, Maps showing distribution and cost by counties of structurally damaging landslides in the San Francisco Bay region, California, winter of 1968-1969 U.S. Geological Survey Miscellaneous Field Studies Map MF-327, scales 1:1,000,000, 1:500,000.

Wills C.J., Stock, J., Perez, F., Bellugi, D., Lancaster, J., Cannon, S., Branum, D., Morton, D., Alvarez, R., In preparation, Estimating landslides triggered by ARkStorm: proposed as U.S. Geological Survey Open File Report and/or California Geological Survey Special Report.

Wills C.J., Perez, F., Gutierrez, C., 2011, Susceptibility to deep-seated landslides in California: California Geological Survey Map Sheet 58.

Wills, C. J., Perez, F., Branum, D., 2012, Estimating Landslide Losses: a General Approach for a Winter Storm Scenario.in Eberhardt, E., editor, Proceedings of the International Symposium on Landslides/North American Symposium on Landslides.

Effects of postfire debris flows on California Highway 395 - geologic factors and assessment tools

Jeremy T. Lancaster
Engineering Geologist
California Geological Survey,
801 K Street, Sacramento, CA
(916)-322-9309
Jeremy.Lancaster@conservation.ca.gov

Prepared for the 63rd Highway Geology Symposium, May 7-10, 2012

(Photo by Tony Symanovich, Caltrans District 9)

ABSTRACT

On August 26, 2010 in Inyo County, CA, at about 2:30pm, a thick slurry of boulders, trees, ash, organic soils, and water issued out of Haiwee Creek (Figure 1) after an intense, short duration cloud burst on a drainage basin that burned in July 2008. From the topographic apex of the Haiwee alluvial fan, the debris flow traveled in pulses for over 3 miles before crossing Highway 395 (US 395) at approximate Post Mile 23.7, then carrying a semi tractor and trailer into a catchment basin just east of northbound lanes. The flow overwhelmed highway drainage structures and overtopped both the south and northbound lanes with debris 3 to 4 feet thick. As the flow proceeded east past the highway it traveled through a box culvert in an abandoned railway fill, then continuing nearly another mile out to the valley floor.

Although this event was generated in a steep mountain canyon and flowed on an alluvial fan, flow was confined within an incised channel (Haiwee Creek) on the fan with the exception of a location approximately 1,000 feet west of US 395. At this location the debris flow exceeded channel bank capacity and deposited sediment and debris in a 150 ft. wide zone extending to the east of the highway. While debris cleanup was underway by California Department of Transportation (Caltrans) maintenance crews the southbound lanes remained blocked for over 7 hours, and the northbound lanes were not reopened until 9:45 am the following morning. Debris removal within the basin and areas surrounding the highway continued for an additional week.

Effects of this debris flow on the built environment included: 1) the cost associated with debris removal on and adjacent to US 395; 2) long delays to local residents and travelers on the primary arterial route into Owens Valley; 3) the destruction of a Los Angeles Department of Water and Power 8-inch water collection pipeline to the Los Angeles Aqueduct (Jim Campbell, personal communication.), and 4) the nearly complete removal of the Haiwee Canyon trail.

Postfire flood flows, such as the Haiwee event, often result in disastrous consequences to the built environment, and while the processes that generate these destructive flows are well understood, watershed-scale frequency and magnitudes that can be used for design purposes are not. Because of this, highway drainage structures are rarely sized to accommodate such dramatic increases in flow, along with associated sediment and debris. Should a watershed burn, several methods are available to assess the potential for flood flows to impact values at risk. These include, among others, alluvial fan flooding susceptibility maps (AFTF, 2010); postfire debris flow probability and volume modeling (Cannon et al., 2008), and postfire watershed assessments (Longstreth, 2012). These types of assessments can be used to aid in determining where postfire flood flows are most likely to occur, and may assist highway maintenance crews in planning efforts following a fire. This paper focuses on the documentation of the Haiwee event, and the use of Quaternary maps to identify the susceptibility of an area to flood flows on alluvial fans.

Figure 1: General location map of the Haiwee watershed showing the schematic distribution of debris flows in relation to US 395. Shaded relief base developed from USGS National Elevation Dataset, 10 meter digital elevation model.

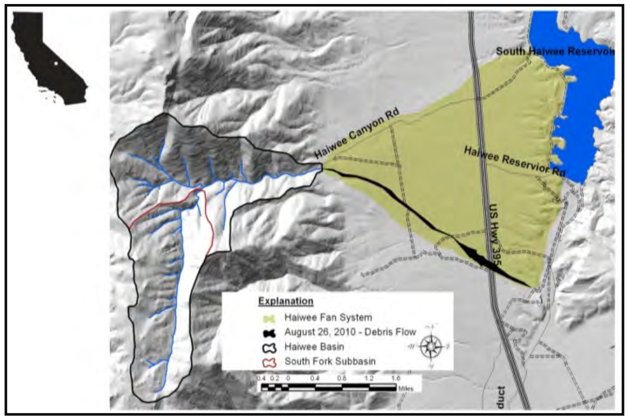

INTRODUCTION

The Haiwee Creek watershed encompasses both confined mountain drainage networks within the eastern Sierra Nevada, and a broad series of coalescing alluvial fans in the Haiwee-Rose Valley area that form below the Sierran escarpment. The upland drainage basin is formed in a steep mountainous environment ranging in elevation from 4,920 feet at the topographic apex of the Haiwee alluvial fan, to 9,400 feet at the drainage divide. Below the apex, a prominent incised channel (Haiwee Creek) traverses the fan system to the toe of the fan at an elevation of 3,600 feet. Several first order streams in the upper portions of the basin are fed by spring sources. These tributaries head from the west and south merging into a third-order stream at an elevation of 5,920 feet. For convenience, this paper terms the tributaries upland of this junction as the north and south forks of the Haiwee Creek system (Figure 1). The upland drainage basin is 5.55 square miles in area, with slopes ranging from 8-15 percent measured along channel reaches to over 100 percent measured along canyon side slopes. Roughly 40 percent of the Haiwee basin contains slopes of between 30 to 50 percent, whereas a majority of slopes (56 Percent) are steeper than 50 percent.

Climate is variable across the study area, with the Sierra Nevada influenced by precipitation originating as moisture-laden air masses in the Pacific, and the Haiwee-Rose Valley lying within a rain shadow produced by the high sierras. Roughly 60-80 percent of the average annual precipitation occurs between October and April, with infrequent thunderstorms occurring during summer months (Hollett et al., 1991).

Cursory review of published literature and aerial photography reveals that the majority of the alluvial fans along the eastern Sierra Nevada are debris flow or composite alluvial fans (Beatty, 1963; Hubert and Filipov, 1989; Whipple and Dunne, 1992; and Dunhforth et al., 2007). These fans are the result of thousands of years of accumulation of debris and hyperconcentrated flow deposits. While alluvial fan flooding occurs on an annual scale in this environment, postfire flood flow occurrence is more random in time and space. Factors that influence the initiation of postfire flood flows in this region are rainfall intensity and duration, burn severity, basin geometry, slope, and soil and rock erosion characteristics. Factors that control debris flow depositional patterns below the fan apex are channel slope, and geometry. On debris flow and composite fans, flood flows have a tendency to avulse from a channel where they exceed conveyance capacity, or at abrupt channel bends. This did not occur during the Haiwee event, primarily because Haiwee Creek is deeply incised into older geomorphic surfaces at the fan apex, with incision continuing downfan for approximately 2.5 miles. Because of this, the Haiwee debris flow maintained its course in channel until just above US 395 (See cover photo and Figure 2).

This paper documents both the factors that lead to the debris flow event and the Quaternary depositional patterns of the Haiwee fan system; it relates debris flow deposition to Quaternary geologic mapping, and provides an approach to aid in determining where flood flows on alluvial fans are most likely to occur.

Figure 2: Panoramic view looking east toward South Haiwee Reservoir from the apex of the Haiwee alluvial fan. Vehicles parked on Haiwee Canyon Road are situated on late Pleistocene alluvial fan deposits. Haiwee Creek channel has incised deeply into this older surface, primarily due to changes in local base level. (All photos by author)

BACKGROUND

As is well documented in California (See Chawner, 1934; Troxell and Peterson, 1937; Rowe et al. 1954; Wells, 1987; Spittler, 1995; Cannon, 2001; Cannon and Gartner, 2005, and Cannon et al., 2008), fires greatly increase both the probability of debris flow occurrence and the volume of material transported from mountain canyons to alluvial fan surfaces. Research in recently burned areas in California, Colorado, and Utah (Santi et al., 2008) shows that most postfire debris flows are initiated by increased runoff and grow in size through erosion and scour in channels by moving debris. Most commonly, postfire debris flows occur within two years after a fire (USGS, 2005) and can be triggered during storm events with return periods of two years or less (Cannon, 2008). The primary triggering mechanism is the severe increase in runoff as a result of wildfire related factors, including, reduction of rainfall interception due to the loss of soil mantling vegetation and litter, development of hydrophobic soils, and vegetative ash.

Documentation of the Haiwee event provides another example of debris flow occurrence on alluvial fans in Owens Valley region of California. Beatty (1963) documented debris flow distribution, avulsion processes, and characterized deposit textures of debris flows generated from rainfall events in 1918 and 1952 in the northern Owens Valley. Hubert and Filipov (1989) built on Beatty's study characterizing these deposits as being inversely graded with a sandy mud matrix, having entrained air bubbles, and forming elongate-lobate shapes and marginal levees with coarse boulders. Based on stratigraphic analyses and Carbon 14 dating of debris flows on three different alluvial fans, Hubert and Filipov also developed a mean recurrence interval of 320 years for several watersheds. In July 2008 a catastrophic debris flow occurred on the Oak Creek alluvial fan, north of Independence, California, after portions of the watershed were burned and then inundated by a cloudburst. These debris flows also caused damage to highway drainage structures, and closed US 395 for a week. Wagner and DeRose (in press.) documented the volume and distribution of debris flow deposits from this event, and related the distribution to Quaternary geologic deposits.

Hyperconcentrated Flows and Debris Flows

Flood flows consisting of water, sediment, and debris mixtures moving through channels have been identified by a number of terms including, but not limited to, debris flow, hyperconcentrated flow, mudflow, debris torrent, mud flood, debris avalanche, and water flood (Pierson and Costa, 1987). Water floods are characterized by turbulent flow and behave as Newtonian fluids, generally having sediment concentrations of less than 20 percent by volume. Sediment concentrations in hyperconcentrated flows typically range from about 20 to 60 percent by volume (depending on grain-size distribution), overlapping in range with debris flows (Pierson and Costa, 1987; Costa, 1988). The transition from turbulent Newtonian phase streamflow to non-Newtonian hyperconcentrated flow is strongly dependent on sediment concentration and particle size distribution because of particle interactions (Cannon et al., 1995). Clay concentrations as low as 3 to 13% by volume may cause particle interactions to occur, the dampening of turbulence, and the development of yield strength in the flow. In contrast, water floods absent of fines (silt and clay) may not develop particle interaction and yield strength at sediment concentrations as high as 50% by volume (Pierson and Costa, 1987). Sediments are deposited from hyperconcentrated flows while the remaining fluid continues to flow resulting in clast-supported deposits that exhibit some sorting (Cannon et al., 1995).

Sediment-water mixtures with sediment concentrations above 60% by volume are defined as debris flows (Pierson and Costa, 1987). Debris flows are a form of mass wasting which may initiate as landslides along steep slopes, or in stream channels, as a result of scour and bank collapse, and the progressive entrainment of sediment (bulking) in floodwaters. Debris flow properties vary with water and clay content as well as grain size distribution (Costa, 1984; Pierson and Costa, 1987; Costa, 1988; Cannon, 1995), forming thick viscous granular flows with a wide range of particle sizes (but very little fines content) to fluid flows dominated by fine-grained matrix traveling as thinner flows with longer runout distances (Iverson, 2003). In contrast to hyperconcentrated flows, in viscous granular debris flows only the largest particles (i.e. boulders) are deposited from suspension, and the mixture typically comes to rest en masse (Cannon et al., 1995).

GEOLOGIC CONDITIONS AND DEBRIS FLOW OBSERVATIONS

Bedrock and Quaternary Geology

Bedrock geology of the Haiwee drainage basin is mapped by Duffield and Bacon (1981) as undifferentiated basement rocks; primarily as granitic intrusives of Mesozoic age composed of granite, and gabbro. While bedrock mapping was beyond the scope of this study, general field observations indicate weathering and discontinuity characteristics are highly variable, with zones of intensely fractured, weathered rock forming broader channel reaches, and areas of relatively intact bedrock forming narrow constricted channel reaches with steep canyon side walls.

The Haiwee fan system is composed of a series of moderate to deeply incised, coalescing alluvial fans mapped by Stinson (1977) as Holocene age (Qf) and by Duffield and Bacon (1981) as latest Quaternary age (Qya). However, Wills (1989) evaluated the expression of different geomorphic surfaces related to active faulting of the Sierra Nevada fault, and concluded based on the presence of abandoned fan segments that both Pleistocene and Holocene fan deposits exist. Furthermore, Wills observed fanglomerate at the toe of the Haiwee fan system containing deeply pitted and decomposed granitic boulders and a well developed B horizon. These factors lead to the postulation that the deposits are late Pleistocene and possibly equivalent to Tahoe stage glacial deposits (60,000 to 100,000 years before present). Younger Pleistocene fan deposits (possibly Tioga stage equivalent) were also identified as light brown silty sand with granitic cobbles and boulders. These deposits were found to be unconsolidated, with boulders on the surface showing signs of pitting and spalling.

Fire Effects

The Clover wildfire was contained on Sunday July 15, 2008 after burning more than 15,300 acres (766 acres, and/or 21.6 percent within the Haiwee drainage basin), with fuels composed of Pinion Pine, Juniper, Mountain Mohagany, and Sage (InciWeb.com, 2008). Burn severity mapping was conducted by the Monitoring Trends in Burn Severity (MTBS) program jointly implemented by the USGS and USFS, and utilized 30 meter resolution Landsat imagery from June 30, 2007 and July 5, 2009. Review of MTBS data indicates <2% of the Haiwee drainage basin was burned with low severity, and 19.7% at moderate, to high severities.

Rainfall

Rainfall occurred as an isolated cloudburst resulting from a convective system traveling from the southwest. Remote automated rain gage records were searched for precipitation data in the near vicinity to Haiwee Creek watershed, including Bear Peak (BPKC1) and Black Rock (BKRC1), but these gages recorded no rainfall from the event. Other gages reviewed were either not in the path of the convective cell, or were of limited use in establishing short duration intensities, consistent with the event that occurred. National Oceanic and Atmospheric Administration (NOAA) NEXRAD (Next Generation Radar) doppler radar at Edwards Air Force Base (Station ID# KEYX) recorded rainfall intensity and storm totals over the Haiwee watershed on a 1 kilometer grid. While it has been well established NEXRAD radar can both under and overestimate rainfall intensity with distance, and requires validation with physical rainfall gages (Mazari et al., 2009), these data are all that are available for the immediate area. Peak 1-hour rainfall intensity recorded by NEXRAD radar on the burn area was 1.25 inches/hour at 2:26pm on August 26, 2010. Total rainfall accumulations in the basin ranged from 1.5 to 2 inches for the total duration of the cloud-burst, a period between 2:26pm and 3:54pm. Rainfall accumulation data for the 1.46 hour period were averaged yielding 1-hour intensities between 1- and 1.3- inches per hour.

Precipitation frequency estimates in the southwest are established in NOAA Atlas 14 (Bonnin, 2006). These estimates are based on annual maximum, or partial duration data, and are used to compute the statistical recurrence of different precipitation depths at short and long period durations (e.g. 1-hour to 24-hour). Based on NOAA "point" estimates for the latitude and longitude corresponding to the Haiwee creek watershed, the "60-minute" depth/duration storm indicates depths for median average recurrence intervals of 100-years and 200-years as 1.0- and 1.29- inches, respectively. Therefore, if the NEXRAD recording is accurate, it would be reasonable to conclude that the 100-year precipitation frequency estimate for a 60-minute duration storm was exceeded during this event.

Haiwee Debris Flow Genesis and Character

Field observations and aerial photographic interpretation were used to identify the mechanism by which the Haiwee flow occurred. Low altitude oblique aerial photographs were taken immediately after the event on August 28 by Caltrans District 9 Maintenance (Patricia Sanders) and on September 4 (Andrew Brandt and Tony Symanovich). Based on these observations it is apparent the Haiwee flow originated from the Clover Fire burn area in the south fork of Haiwee Creek. These photos reveal that concentration of runoff within steep canyon swales caused erosion, increased sediment loading in the south fork channel, and the progressive increase in flow depth leading to channel scour and the entrainment of sediment and debris. There are no features apparent from the photos to suggest that slope-derived debris flows contributed substantially to flow in the south fork. Field observations of the north fork indicate flow from this drainage just west of the confluence with the south fork was normal streamflow (water flood), and not bulked with sediment and debris.

Figure 3: Observation location map

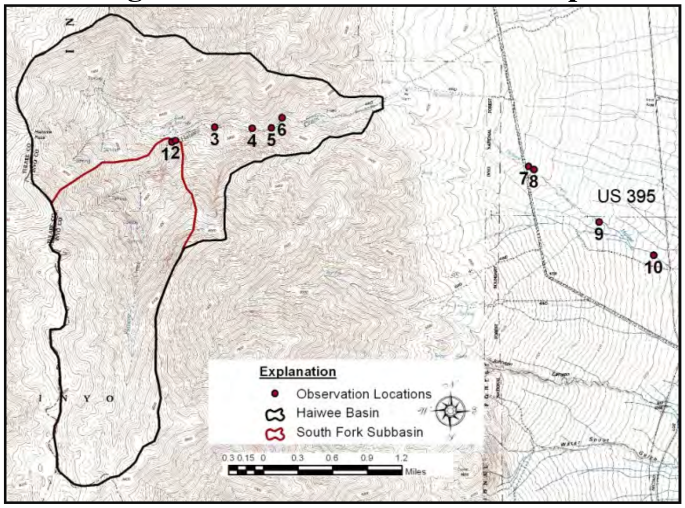

Several features identified in the field illuminate unique characteristics with respect to how the flow was generated, including apparent changes in its viscosity along the length of flow. Primarily, flood flow issuing out of the south fork was laden with sediment and debris, as indicated by the presence of channel scour, bank collapse, super-elevation, and a mudline containing soil and tree fragments. Flood flow emanating out of the north fork behaved as normal streamflow, perhaps in the lower range of sediment-water concentrations, and no channel scour was observed. At observation location 3 (Figure 3), less than 1,000 feet east of the confluence, a 4.5-foot thick marginal levee composed of matrix supported cobble and boulder clasts was deposited just before a southward channel bend (Figure 4). This deposit is suggestive of a viscous granular debris flow. However, further east within Haiwee Canyon, and along the incised channel traversing the fan, similar deposits were not observed. Where the flow became unconfined, and more broadly distributed just west of US 395, the deposits were relatively thin (0.5 to 2 feet in thickness), and consisted of clayey silt with sand including scattered cobbles and boulders (Figure 5). In general, the deposit showed little to no grading and contained numerous 1-2 millimeter size voids indicative of the entrainment of air bubbles in the flowing mass.

Figure 4: 4.5 foot thick marginal debris flow deposit consisting of angular to subrounded cobble to boulder size clasts, supported by a fine-grained matrix, and resting on the former channel bank.

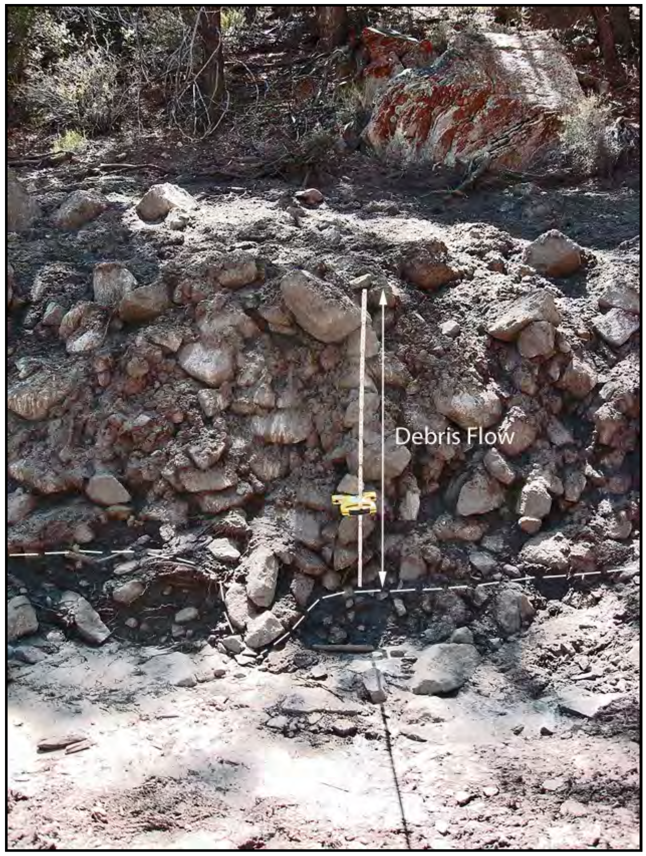

Figure 5: View along Haiwee Creek looking southeast toward US 395, showing remains of fluidized debris flow deposit. Boulder in middle foreground is approximately 2.5 feet in diameter

In addition to the textural changes observed between the upper canyon and midfan areas, measured cross sections provide additional insight into locations where flow continued to gain in volume, and where dissipation occurred. Cross sections measured at locations 1, 2, and 5 suggest a progressive increase in flow volume (assuming a constant velocity) with a maximum cross sectional area of 545 $feet^2$ at location 5. Progressive increase in volume is supported by the observation of channel scour, bank collapse and slope failure noted at locations 3, 4, and 6. Flow volume dissipation was most dramatic in the lower reaches of Haiwee Canyon, where broad channels exist, and deposition as opposed to channel scour was noticeably widespread.

QUATERNARY MAPPING

Existing geologic maps and imagery were compiled in ArcGIS to identify the general distribution of Quaternary-age alluvial deposits based on remote sensing. Interpretations of geomorphology from aerial photography were digitized, and limited field observations were utilized for preliminary mapping purposes. Detailed soil and lithologic descriptions are planned for future site visits. Mapping indicates the Quaternary alluvial fan and associated alluvial channel deposits are distinct enough based on their surface expression that they can be differentiated on a relative age basis. Pleistocene deposits of the Haiwee fan system consist of several interlayered Late Pleistocene debris flow and fluvial deposits that are combined into the general map unit Qof (Figure 6a). The older parts of these fan units have exposed soil-stratigraphic profiles with intensely weathered and pitted granitic clasts, and locally well developed carbonate morphology consistent with soil-stratigraphic profiles found in Pleistocene-age deposits of the southwest. These soils are primarily developed in subangular to subrounded matrix supported debris flow deposits. Along the apex and medial portions of the Haiwee fan, numerous debris flow tracts are observable with moderate to strongly diffused marginal levees. Clearly the topographic position occupied by these Qof deposits suggests the processes forming the deposits are no longer active, and the geomorphic surface has been abandoned. As the Haiwee Creek channel has been progressively eroding headward into the Pleistocene fan surfaces due to changes in local base-level, Holocene deposition occurs at a lower topographic position. Late Pleistocene to latest Holocene-age alluvial fan deposits are mapped as Qyf and Qf, respectively. These younger fans are composed of a mixture of debris and hyperconcentrated flow deposits, and particularly, the Qyf unit is traversed by several debris flow tracts that have emanated from Haiwee Creek. The marginal levees associated with these past flows are shown on Figure 6a as a black stippled pattern. The August 26, 2010 debris flow deposit primarily stayed within the Haiwee creek drainage (mapped as Qfdf), but became unconfined from the channel banks just west of US 395.

Figure 6a and 6b: 6a. Quaternary geologic map of the southern portion of the Haiwee fan, inset square superimposed on shaded relief map (bottom left corner) shows extent of mapping. Map units, Qof, medium yellow = Pleistocene-age alluvial fans; Qyf, pale yellow = Latest Pleistocene to Holocene –age alluvial fans; Qf, very pale yellow = Latest Holocene-age alluvial fans; Qa, pale gray = alluvial channels; Qfdf, bright yellow = August 26, 2010 debris flow event; black stipples represent Holocene-age debris flow marginal levees interpreted from aerial photography. 6b. Debris and flood flow susceptibility map developed from Quaternary geology. Red = High susceptibility; Green = Low susceptibility. Topographic contour interval 10 feet.

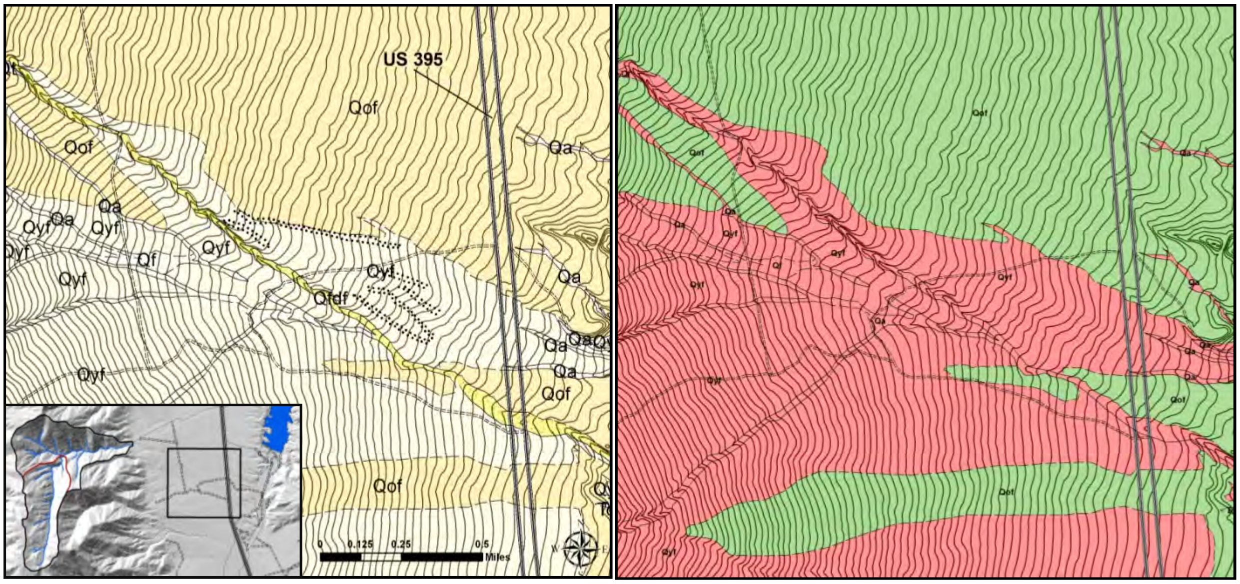

DEBRIS FLOW HAZARD MAPPING

Geologic maps of Quaternary units that comprise alluvial fans are useful in characterizing the location of active channels, their drainage divides, and in the differentiation of relict, abandoned, and active geomorphic surfaces that allow for first order identification of flood and debris flow hazards (Rhoads, 1986; House, 2005, 2007; Giraud, 2005; and Robbins et al, 2009). Comparisons of Quaternary geologic maps with the boundaries of historic floods on alluvial fans indicate that historically flooded areas correlate well with the most geologically recent alluvial fan surfaces (Pelletier, et. al., 2005; and AFTF, 2010).

For debris flow susceptibility studies, high hazard areas are those underlain by Holocene-age debris flow deposits because they are reflective of debris flow activity under the current climate regime (Giraud, 2005), and are more likely to experience future debris flow deposition than older fan surfaces. Following this approach, Figure 6b shows a relative debris and flood flow susceptibility map developed from a Quaternary geologic map for a portion of the Haiwee fan system adjacent to US 395.

CONCLUSIONS

A combination of field observations, review of aerial photography, rainfall data, drainage basin morphology, and published literature, were used to characterize the geologic factors contributing to the Haiwee Creek debris flow event. The debris flow occurred as a result of an intense cloud burst falling on a partially burned drainage basin with average rainfall intensities on the order of between 1- and 1.3-inches per hour, and may have exceeded the 100-year precipitation frequency estimate for a 60-minute duration storm. Sediment and debris were entrained by channel scour and bank collapse as the flood waters traveled down the south fork evolving into a viscous granular debris flow. As the storm progressed from south to north across the basin, flood waters from the north fork introduced relatively clear water at the confluence, increasing the volume of water, but perhaps reducing the viscosity and depth in subsequent surges. The result of this apparent reduction in viscosity was a long-runout debris flow that traveled 3 miles from the mouth of Haiwee Creek Canyon before it clogged and damaged highway drainage structures at US 395, destroyed a semi tractor and trailer, and caused closure of a major highway.

The Haiwee debris flow traveled in surges, but stayed within the confines of the mapped Holocene-age alluvial fan and channel deposits - an observation consistent with the hypothesis that Quaternary geologic maps can be used in the identification of debris flow hazard areas on alluvial fans (Giraud, 2005; AFTF, 2010).

REFERENCES

Alluvial Fan Task Force (AFTF) 2010, *The Integrated Approach: for Sustainable Development on Alluvial Fans*. Water Resources Institute, California State University, San Bernardino, for the CA Department of Water Resources. 183 p.

Beaty, C. B. 1963. *Origin of alluvial fans, White Mountains, California and Nevada*. pp. 66–73 in Modern and Ancient Alluvial Fan Deposits, T. H. Nilsen, ed. New York: Van Nostrand Reinhold Co.

Bonnin, G.M., Martin, D., Lin, B., Parzybok, T., Yekta, M., and Riley, D., 2006, *Precipitation-frequency atlas of the United States: NOAA Atlas 14*, v. 1, version 4, NOAA, National Weather Service, Silver Spring, Md., accessed online October, 2009, at http://hdsc.nws.noaa.gov/hdsc/pfds/sa/sca_pfds.html

Cannon, S.H., Powers, P.S., Pihl, R.A., and Rogers, W.P., 1995, *Preliminary evaluation of the fire-related debris-flows on Storm King Mountain, Glenwood Springs, Colorado*: U.S. Geological Survey Open-File Report 95-508.

Cannon, S.H., 2001, *Debris-flow generation from recently burned watersheds*: Environmental & Engineering Geosciences, Vol. VII, No. 4, pp 321-341.

Cannon S.H., and Gartner, J.E., 2005, *Wildfire-related debris flow from a hazards perspective*, Chapter 15 in: Jakob, M., and Hungr, O., (eds), Debris-flow Hazards and Related Phenomena: Praxis Publishing LTD., Chichester, UK.

Cannon S.H., and Gartner, J.E., Wilson, R.C., Bowers, J.C., and Laber, J.L., 2008; *Storm rainfall conditions for floods and debris flows from recently burned areas in southwestern Colorado and Southern California: Geomorphology*, Vol. 96, pp. 250-269.

Cannon S.H., and Gartner, J.E., Rupert, M. G., Michael, J. A., Rea, A. R., and Parrett, C., 2010, *Predicting the probability and volume of postwildfire debris flows in the intermountain western United States:* Geological Society of America Bulletin v. 122: 127–144.

Chawner, W. D., 1934, *The Montrose-La Crescenta flood of January 1, 1934, and its sedimentary aspects*, Caltech Masters of Science Thesis, 78p.

Costa, J.E., 1984, *Physical geomorphology of debris flows*, in Developments and Applications of Geomorphology, edited by J.E. Costa and P.J. Fleisher Springer-Verlag, Berlin Heidelburg, p. 268-317.

Costa, J.E., 1988, *Rheologic, geomorphic and sedimentologic differentiation of water floods, hydperconcentrated flows, and debris flows*, in Baker, V.R., Kochel, R.C., and Patton, P.C., eds., Flood Geomorphology, Wiley, New York, p. 113-122.

Duffield, W.A. and Bacon, C.R., 1981, *Geologic map of the Coso volcanic field and adjacent areas, Inyo County*, California:U.S. Geological Survey, Miscellaneous Investigations Series Map I-1200, scale 1:50000.

Dűhnforth, M., Densmore, A.L., Ivy-Ochs, S., Allen, P.A., and Kubik, P.W., 2007, Timing and patterns of debris flow deposition on Shepherd and Symmes creek fans, Owens Valley, California, deduced from cosmogenic 10Be. Journal of Geophysical Research. 112:F03S15, doi:1029/2006JF0240-256.00562, p. 1-11.

Gartner, J.E., Cannon, S.H., Santi, P.M., and Dewolfe, V.G., 2008, *Empirical models to predict the volume of debris flows generated by recently burned basins in the western U.S.: Geomorphology*, Vol. 96, pp 339-354.

Giraud, R.E., 2005, *Guidelines for the Geologic Evaluation of Debris-Flow Hazards on Alluvial Fans in Utah*: Miscellaneous Publication 05-6, Utah Geological Survey, 16 p.

Hollet, K.J., Danskin, W.R., McCaffery, W.H., and Walti, H., 1991, *Geology and water resources of the Owens Valley, California.* U.S. Geological Survey Water Supply Paper2370-B, 77 p.

House, P.K., 2005, *Using geology to improve floodplain management on alluvial fans: an example from Laughlin, Nevada*. Journal of the American Water Resources Association, v. 41, n. 6, p.1-17.

House, P.K., 2007, *Geologic assessment of piedmont and playa flood hazards in the Ivanpah Valley area, Clark County, Nevada*. Nevada Bureau of Mines and Geology Map 158, scale 1:50,000.

Hubert, J. F., and Filipov, A. J., 1989, *Debris-flow deposits in alluvial fans on the west flank of the White Mountains, Owens Valley, California, U.S.A*. Journal of Sedimentary Geology. Vol. 61, no. 3-4, pp. 177-205. Feb 1989.

Iverson, R.M., 2003, *The debris-flow rheology myth, in Rickenmann, D., and Chen, C.-l., 3rd International Conference on Debris-Flow Hazards Mitigation*: Mechanics, Prediction, and Assessment: Davos, Switzerland, American Society of Civil Engineers, v. 1, p. 303-314.

Inciweb, 2008, Incident Information System website accessed September 2010: http://www.inciweb.org/

Longstreth, D. L., 2012, *Assessing post fire landsliding and flooding along highway corridors, an example from US Highway 1, Monterey County, California, 2008*: Program with Abstracts, 63rd Annual Highway Geology Symposium, Redding California.

Mazari, N., Xie, H., Wang, X., Zeitler, J. W., and Sharif, H., 2009, *Validation of NEXRAD DSP product with high accuracy rain gauges network*, 34th Conference on Radar Meteorology, Abstract with programs.

NOAA, Next Generation Radar (NEXRAD) website accessed September 2010: http://www.roc.noaa.gov/WSR88D/

Pelletier, J. D., Mayer, L., Pearthree, P. A., House, P. K., Klawon, J. E., and Vincent, K. R., 2005, *An Integrated Approach to Flood Hazard Assessment on Alluvial Fans Using Numerical Modeling, Field Mapping, and Remote Sensing*, Geological Society of America Bulletin, vol.117, no. 9/10, pp.1167-1180.

Pierson, T. D., and Costa, J. E., 1987, *A Rheologic Classification of Subaerial Sediment-Water Flows*, Geological Society of America, Reviews in Engineering Geology, Vol. VII, pp.1-12.

Rhoads, B. L., 1986, *Flood hazard assessment for land use planning near desert mountains*. Environmental Management, 10(1) pp. 97-106.

Robbins, C. R., Buck, B. J., Williams, A. J., Morton, J. L., House, P. K., Howell, M. S., and Yonovitz, M. L., 2009, *Comparison of flood hazard assessments on desert piedmonts and playas: A case study in Ivanpah Valley, Nevada*, Geomorphology, vol. 103, pp. 520-532.

Rowe, P.B., Countryman, C.M., and Storey, H.C., 1949, *Probable peak discharges and erosion rates from Southern California watersheds as influenced by fire:* U.S. Department of Agriculture, Forest Service, 270 p.

Santi, P.M., deWolfe, V.G., Higgins, J.D., Cannon, S.H., and Gartner, J.E., 2008, *Source of debris flow material in burned areas*: Geomorphology, v. 96, p. 310–321.

Spittler, T.E., 1995, *Fire and debris flow potential of winterstorms*, in Keely, J.E., and Scott, T., eds., Brushfires in California Wildlands—Ecology and Resource Management: Fairfield, Washington, International Association of Wildland Fire, p. 113–120.

Stinson, M.C., 1977, *Geology of the Haiwee Reservoir 15'quadrangle, Inyo County, California*: California Division of Mines and Geology, Map Sheet 37, scale 1:62500.

Troxell, H.C., and Peterson, J.Q., 1937, *Flood in La Cañada Valley, California, January 1, 1934*: U.S. Geological Survey Water-Supply Paper 796-C. 98 p.

USGS, 2005, *Southern California – Wildfires and Debris Flows*, Fact Sheet 2005-3106, 4p.

USGS and USFS, Monitoring Trends in Burn Severity (MTBS) website accessed September 2010: http://www.mtbs.gov/

Wagner, D. L., and DeRose, (In Press), *The Oak Creek Debris and Mudflows of July 12, 2008 Inyo County, California: A Geologic Investigation*.

Wells, W.G., II, 1987, *The effects of fire on the generation of debris flows in southern California*, *in*, Costa, J.E., and Wieczorek, G.F., editors, Debris flows/avalanches: Process, recognition, and mitigation: Geological Society of America Reviews in Engineering Geology Volume VII, p. 105-114.

Whipple, K.X, and Dunne, T., 1992, The influence of debris-flow rheology on fan morphology, Owens Valley, California, Geological Society of America Bulletin 104:887-900.

Wills, C.J., 1989, *Sierra Nevada Fault Zone – Haiwee Segment, Inyo County California*: California Division of Mines and Geology Fault Evaluation Report FER-208, 6 p.

Impacts of the Double Draw Landslide (debris flow) in

Wyoming's Snake River Canyon

Lincoln County, Wyoming

Kirk Hood, P.G.
Wyoming Department of Transportation
5300 Bishop Blvd., Cheyenne, Wyoming
307-777-4418
kirk.hood@wyo.gov

Mark Falk, P.E, P.G.
Wyoming Department of Transportation
5300 Bishop Blvd., Cheyenne, Wyoming
307-777-4202
mark.falk@wyo.gov

Prepared for the 63rd Highway Geology Symposium, May 7-10, 2012

Acknowledgements

The authors would like to thank WYDOT-Geology and District 3 for their efforts on this landslide as well as Holly Daniels for reviewing the content of this paper.

Disclaimer

Statements and views presented in this paper are strictly those of the author, and do not necessarily reflect positions held by their affiliations, the Highway Geology Symposium (HGS), or others acknowledged above. The mention of trade names for commercial products does not imply the approval or endorsement by HGS.

Copyright Notice

Impacts of the Double Draw Landslide (debris flow) in Wyoming's Snake River Canyon

Lincoln County, Wyoming

Kirk Hood, P.G.
Wyoming Department of Transportation
5300 Bishop Blvd., Cheyenne, Wyoming
307-777-4418
kirk.hood@wyo.gov

Mark Falk, P.E, P.G.
Wyoming Department of Transportation
5300 Bishop Blvd., Cheyenne, Wyoming
307-777-4202
mark.falk@wyo.gov

Prepared for the 63rd Highway Geology Symposium, May 7-10, 2012

ABSTRACT

The winter of 2011 was an extremely wet year in Wyoming. Snow pack in some areas of the state exceeded 300 percent of normal. The Snake River Canyon area, south of Jackson Wyoming, was no exception with a snowpack of 171 percent of normal. On May 14, 2011, a debris flow at M.P. 127.4 on Highway 26/89 began flowing onto the road. By the end of the day, Maintenance personnel were having trouble keeping up with the removal of the material and the road was closed. By the early morning hours of May 16, 2011, a 25 to 30 feet high wall of debris, approximately 300 feet long, had covered the road. When WYDOT Geology personnel arrived on site to assess the area on May 16, 2011, the debris flow was still active with no end to the movement in sight.

The road closure had an immediate impact to the traveling public. Several hundred daily commuters from the Star Valley area and all other eastbound traffic into Jackson were routed on an 80-mile detour over a steep mountain pass, with a 60,000 lb load limit. Because the Snake River Canyon remained closed, due to the debris flow, several stake holders became involved. These stake holders included the U.S. Army Corps of Engineers, the U.S. Forest Service, residents of Jackson and Star Valley, several rafting companies, and Governor Matt Mead. Each of these parties was affected differently by the road closure. WYDOT's plan to wait until the debris flow stopped moving, before beginning some type of mitigation, became more unpopular locally and from a political standpoint with each day of closure. The WYDOT Geology Program was tasked with determining when the cleanup of the roadway should begin. This is when the struggle between politics and engineering judgment began.

INTRODUCTION

The Snake River Canyon, where the Double Draw Landslide occurred, is located south of Jackson, WY on Highway 26/89. The areas on either side of the Double Draw Landslide have been active in the past in terms of embankment failures and large landslide complexes. The area of the Blue Trails Landslide located west of and adjacent to the Double Draw Landslide (Figure 1) was addressed in 1997, by Hayward Baker, using a Micro-pile insert wall. This area has been stable ever since this remediation and was presented at the 49th HGS conference in 1998. Adjacent to the Blue Trails Landslide, is a large backslope (Force Account Mt.) that required a million dollar change order for excavation costs during construction to address a separate failure. Just recently in 2011, approximately one quarter mile from the Double Draw Landslide, an embankment failure (TM Slide) was remediated using micro piles and expanded polystyrene (EPS). The Little Blue Landslide located east of the Double Draw Landslide has yet to be addressed.

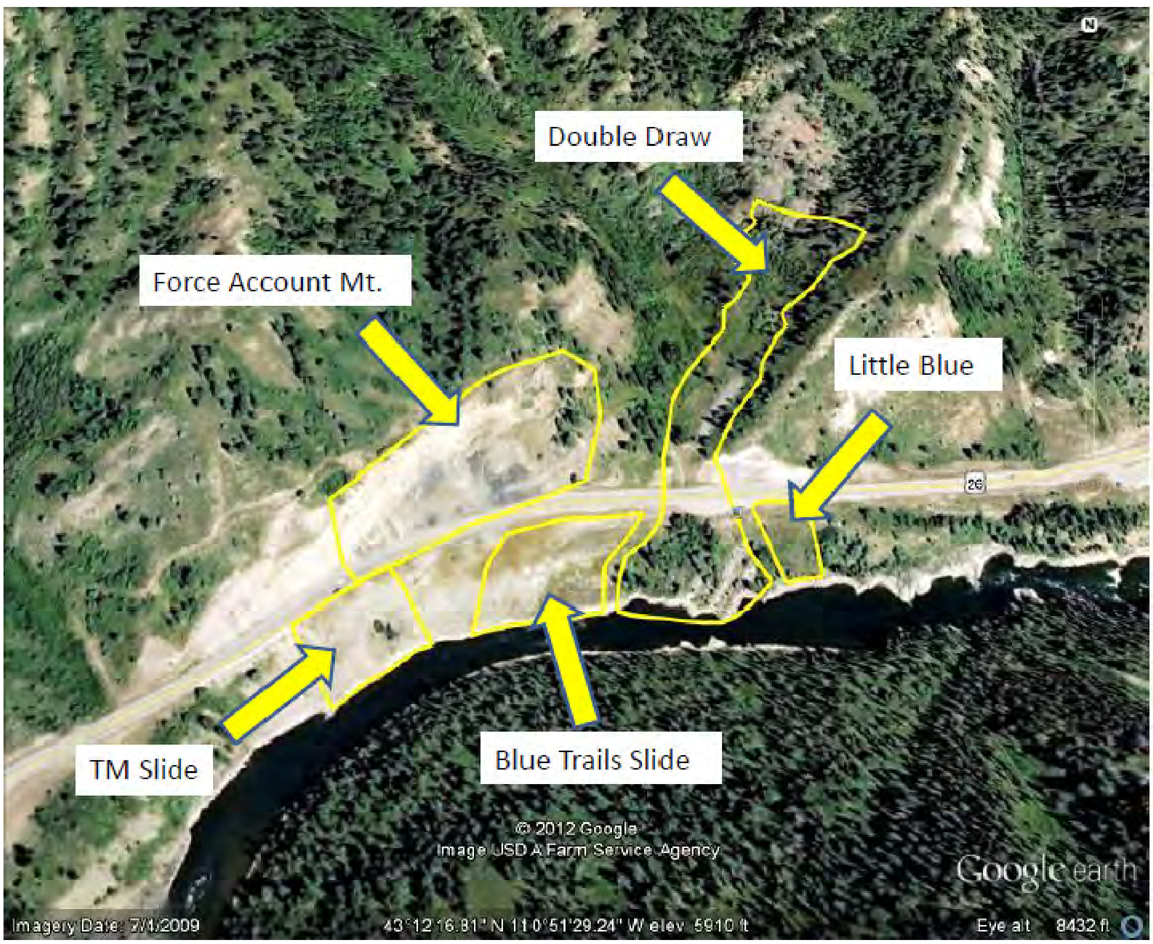

Figure 1. Area Instability

All of these failures can be attributed to two distinct geologic bedrock layers present in Snake River Canyon: the Aspen Shale and the Bear River Formation. The Aspen shale is made up of light to dark-gray siliceous tuffaceous shale and siltstone, thin bentonite beds, and quartzitic sandstone. The other problematic bedrock layer is the Bear River

Formation. It is made up of black shale, fine-grained brown sandstone, thin limestone and bentonite beds (Schroeder, 1973). The common depositional feature shared by the two bedrock formations is the presence of bentonite layers sourced from the local the Yellowstone volcanic complex. Although beautiful in every way and a must see when touring the state of Wyoming, Yellowstone has created problematic soils and bedrock throughout the state during its active volcanic history.

MOBILIZATION TO THE SITE

May 14, 2011, was a Saturday and it is common for Jackson Maintenance to send Maintenance personnel down Snake River Canyon to plow rocks off the road if necessary and address wildlife that may have been struck by traffic. On this Saturday, Jackson Maintenance forces noted the backslope ditch at M.P. 127.4 was full of debris and that a lot of water was flowing out of the backslope (Figure 2). The debris had plugged the ditch and the culvert under the road, forcing all of the water coming out of the backslope across the road (Figure 3). The backslope at this site consisted of a colluvial filled valley between two resistant rock outcrops: the Bear River Formation and the Gannet Group. The Gannet Group (Draney Limestone, Bechler Formation and the Peterson Limestone) consists of hard, grayish-blue white weathering limestone interbedded with calcareous shale (Schroeder, 1981).

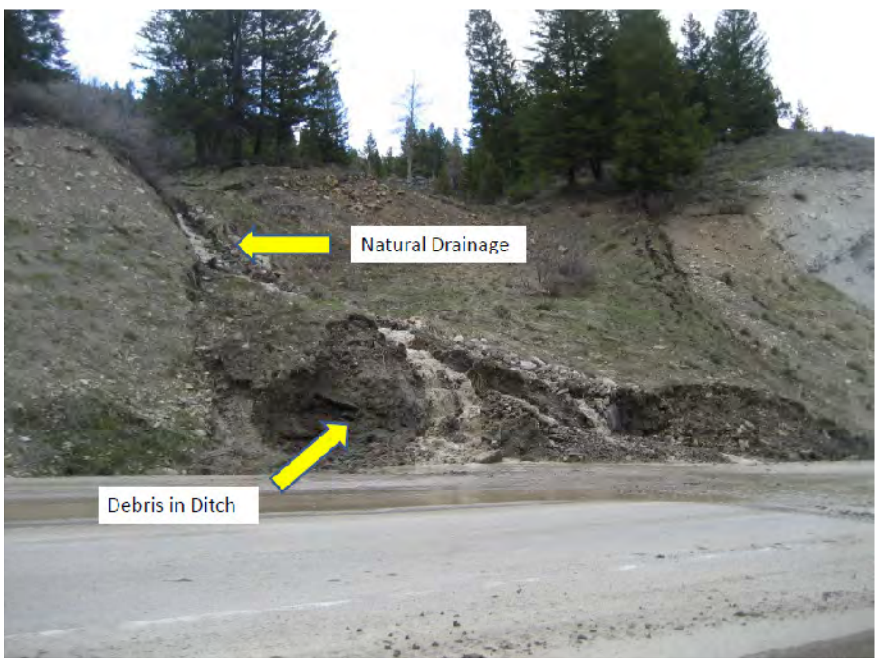

Figure 2. Initial Debris Flow

Figure 3. Initial Impacts to Highway 26/89

Maintenance decided to mobilize to the site and began cleaning out the ditch. Once excavated, the material was wasted on the opposite side of the highway onto an existing traffic pullout. However, after several hours of excavating, Maintenance personnel appeared not gaining on the debris as more material flowed into the excavation created by the front-end loader. Over time, the debris began not only to fill the ditch, but both lanes of Highway 26/89 as well. The Resident Engineer (R.E.) in Jackson, who was aware of the situation, contacted the District Engineer (D.E.) about how Maintenance was not keeping up with the debris flowing into the ditch and onto the roadway. The D.E. then drove three hours to the site to assess the situation. By 10:00 pm, it was determined that it was futile for Maintenance forces to try and keep the highway open, as the debris flow across the highway was growing wider and coming down faster. Highway 26/89 was closed.

On Sunday, May 15, 2011, Maintenance returned to the site and began to remove debris from the EBL in the hopes of maintaining at least one lane of traffic through Snake River Canyon. As the day went on, it was obvious that the removal of material was not keeping up with the flow of debris and once again, Highway 26/89 was closed later in the evening.

Maintenance's intention on Monday morning (May 16, 2011) was to arrive at the debris flow early, remove material from the EBL and maintain one lane of traffic. However, when they returned to the site at 5:00 am, the road had an approximately 30 foot thick layer of debris, which covered approximately 300 feet of the highway (Figure 4).

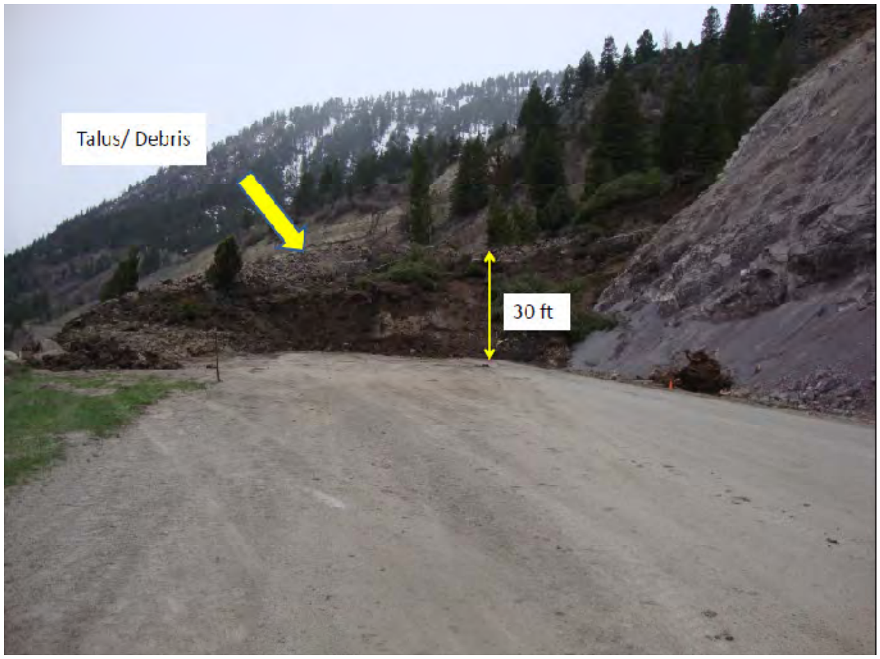

Figure 4. Debris on Highway

Figure 5. Debris at Toe of Embankment Impacting Snake River

The debris was flowing over the roadway and down the embankment into the Snake River (Figure 5). WYDOT-Geology was notified, early Monday morning of the situation and mobilized to the site: Highway 26/89 remained closed.

INTIAL ASSESSMENT AND MAPPING

After arriving on-site at 3:00 pm on Monday, all thoughts of another "typical" Snake River Canyon landslide failure were extinguished. This was a classic debris flow that was similar to the Wolf Mtn. Slide (debris flow) that occurred in 1997 (Figure 6) which completely closed Highway 26/89 at M.P. 135.4 for three weeks. However, the Wolf Mtn. slide was on a very steep slope (35 degrees) with 1500 feet of vertical relief in contrast to the relatively flat 14 degree slope (1:4, rise: run) and 300 feet of vertical relief at Double Draw (Figure 7). The result of both were the same though; ROAD CLOSED!

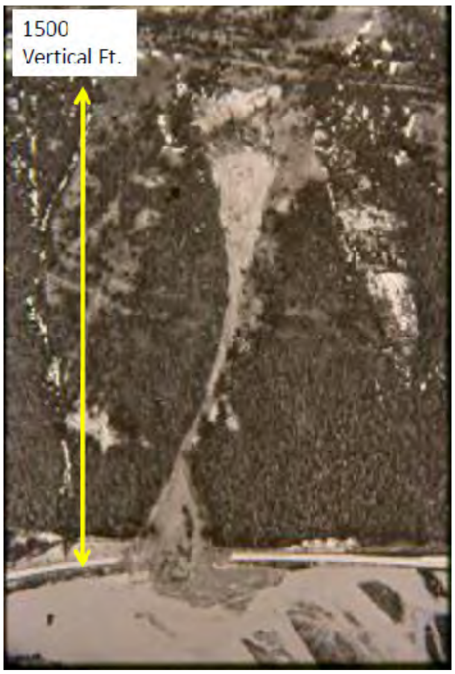

Figures 6 and 7. Wolf Mountain Debris Flow and Double Draw Debris Flow

At the time of initial observation, the entire debris flow mass was still very active. At the outside margins of the flow, the debris was capped with a 7 to 10 feet thick layer of very angular limestone talus, which had once armored the colluvial filled valley floor above the roadway. Movement of the material was very obvious with rocks continually rolling off the edges of the debris pile. In the middle of the flow, the material was much more viscous and consisted of finer grained material and large amounts of vegetation. Trees that were still standing upright in the slide debris flowed across the roadway and down the slope into the Snake River (Figure 8).

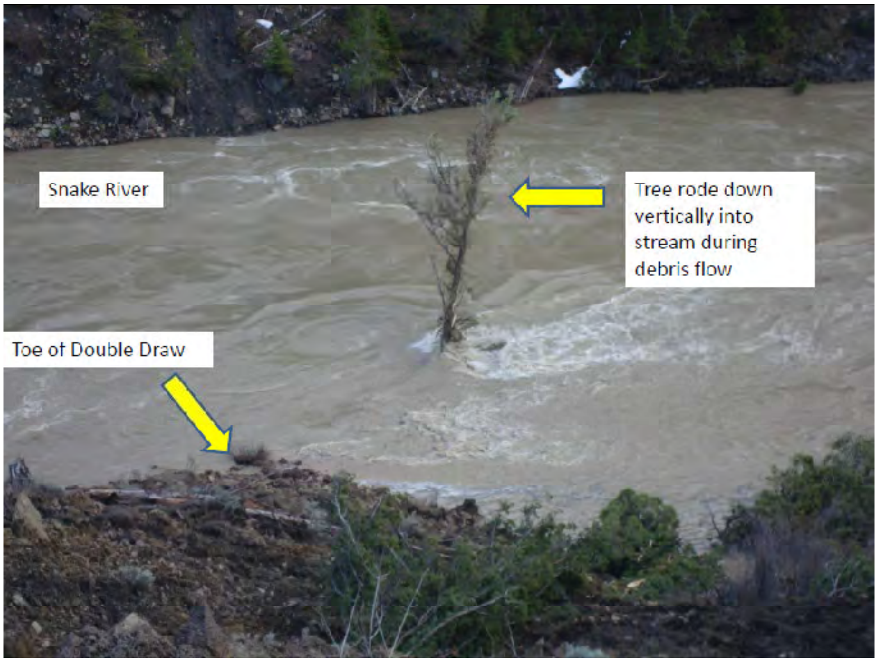

Figure 8. Tree Standing Vertical in Snake River

The initial observations noted that the failure in the backslope was 300 feet wide and extended from the centerline approximately 1100 feet up an unnamed draw. The debris flow extended down the highway embankment another 400 feet from centerline to the Snake River. The head scarp was 60 feet in height while the outer limits of the debris channel were 30 feet high (Figure 9). An adjacent draw to the west of the debris channel was flowing significant quantities of water into the main channel approximately 400 feet up the slope from the roadway.

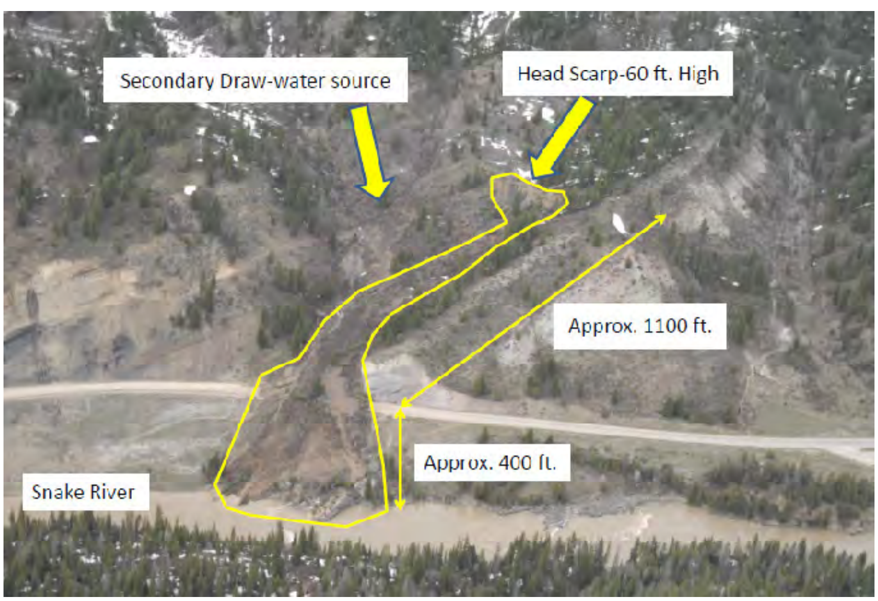

Figure 9. Double Draw

On the morning of May 17, 2011, it was evident that the outside margins of the slide, which were covered with the talus, had stabilized and that the debris flow had stopped spreading laterally. The movement of the material in the middle of the flow appeared to have slowed and it was decided to try to get rough measurements of the rate of movement of the material in the center portion of the slide mass. Using a line of lathe, a Brunton and painted talus boulders for reference, measurements were taken across the channel to estimate the rate at which the debris was flowing across the highway. At that time, the initial measurement of the debris flow channel's speed (1 foot/minute), seemed insignificant, just another mapping tool. However, it would end up being the key element for determining when the removal of the debris could begin and when the highway could open.

Mapping was a daily occurrence with two trips a day up the mountain to measure and map the entire site (Figure 10). The speed of the debris flow was continually measured and ranged from 1 to 2 feet/minute. Trees that were near the head scarp or along the edges were marked with flagging to determine the progress of the migration of scarps. Specific photo locations were marked around the entire site to record changes from day to day. The photos were shot each morning. However, the photos taken from the specific locations proved not as useful as planned. The photos were shot from different angles by different people so enough variation occurred between the photos that they could not be used to determine specific changes at the site. The best tools used throughout the two weeks of daily mapping, was a Brunton, a range finder, flagging tape along with paper and pencil. Technology was not completely abandoned, as the WYDOT public affairs department arrived on site (May 17, 2011) and used a HD video camera located on the now stable talus to video across the moving portion of the debris flow for 30 minutes. The video was later compressed to 45 seconds and posted on WYDOT's website. The video went viral and was shown on the Weather channel and several other news media outlets. The video showed that the debris was still moving and showed the rate at which it was traveling. It was also noted that as the temperature rose during the day, water flow increased in the channel and the rate of the debris flow across the highway similarly increased.

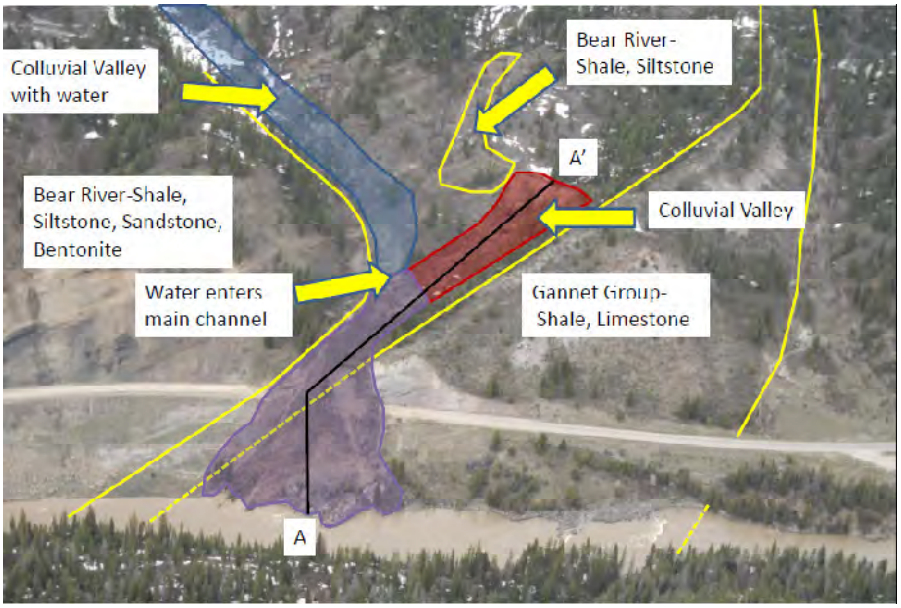

Figure 10. Mapping of Double Draw

The Jackson Survey crew was also involved in assisting with the mapping and monitoring of the debris flow. Where possible, several points were marked in the center of the flow and followed the unnamed draw to the head scarp of the failure. Each point was shot daily to gain an understanding of the dynamics of the movement (i.e. was the material at the top moving faster than the material on the highway, etc.) In one instance, a point that had been marked near the head scarp had moved a total of 380 feet downhill in approximately 48 hours.

After a couple of days of observation, the characteristics of the movement of the debris became evident. The debris flow was divided into 4 distinct zones. The first zone was the furthest upper portion of the slide, which extended up the slope from the convergence of the main slide channel, and the adjacent draw (which was supplying the significant water flow into the debris) to headscarp of the failure. The movement of material in this area was the slowest. Typical measurements on the scale of feet per day were observed in this portion of the slope. The second zone was an approximately 350 feet length of channel between the convergence of the two draws and the roadway. At the convergence of these draws, where the water poured into the slide channel the material became super saturated and began to flow quite rapidly, on the order of 2 to 4 feet per minute. As the flowing debris reached the roadway (zone 3), and the slope flattened across the width of the roadway (approximately 60 feet), flows slowed to a typical 1 foot per minute. This slowing resulted in accumulation or a “heaping” action of material on the roadway. On the river side of the roadway or zone 4 where the slope became very steep, the rate of the flow increased significantly typically on the scale of being in excess of 4 feet per minute. Once the debris flow crossed the road, the velocity increased which created a flushing action of the material down the slope to be carried away by the Snake River.

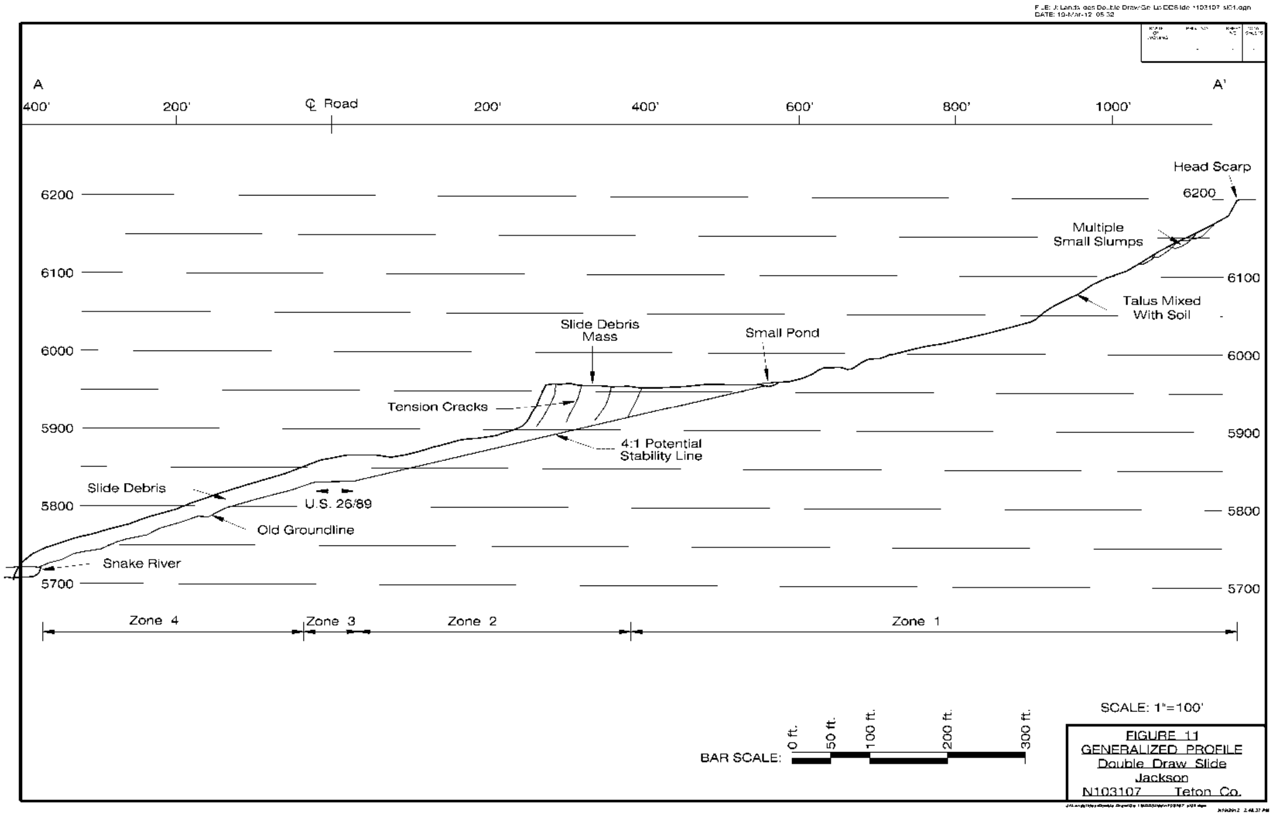

Figure 11. Cross Section

POLITICS 101

Once the highway closed on the evening of May 15, 2011, the impacts were immediate. Several hundred commuters, who live in the Star Valley area because of lower housing costs, commute to the Jackson area daily for work. Normally they travel 35 miles up Snake River Canyon from Alpine to Jackson, which depending on traffic and weather conditions, takes 30 to 50 minutes. However, since the highway was closed, commuters had to take an alternate route which added 38 miles to their commute one-way. The detour took commuters to Victor, ID, and then over Teton Pass in Wyoming, a treacherous mountain pass with steep grades and switchbacks (Figure 12). This added 50 minutes each way to the commuters' daily travels. Since Teton Pass is steep and difficult to navigate, commercial truck traffic has always been limited to 60,000 lbs. GVWR. During the closure of Snake River Canyon truck traffic over Teton Pass was restricted to non commuter hours. The majority of the freight into the Jackson Hole comes from the west, off the I-80 corridor, and through Snake River Canyon. After the Double Draw Landslide, all commercial vehicles that were over 60,000 lbs. GVWR had to take even longer alternate routes over Togwotee Pass, which is northeast of Jackson, or through Hoback Canyon and down to Pinedale, Wyoming.

May is also the time of year that several of the commercial rafting companies begin preparing and training personnel to take clients down the Snake River. It did not take long for the public to begin to voice their opinion that WYDOT needed to open the highway sooner than later.

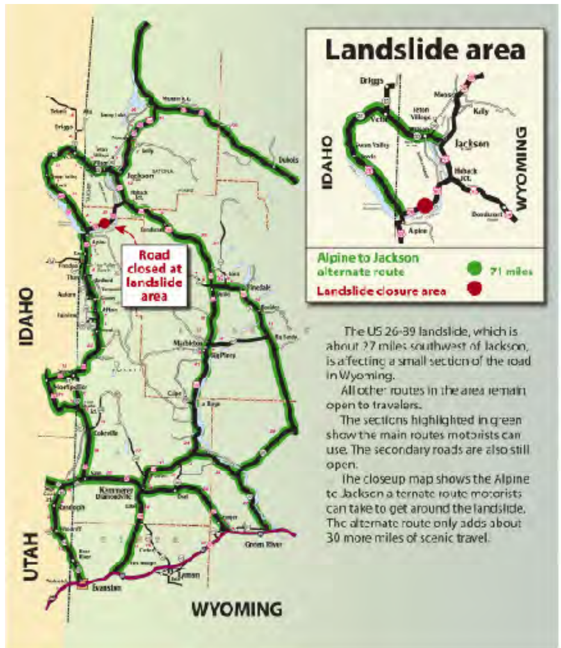

Figure 12. Required Detour

Without information from the mapping taking place at the slide, it was difficult for WYDOT's Public Affairs department and other entities to keep informed. It was determined that the Geology program would submit daily reports via email to the District Engineer's office. The D.E. would then forward the information to the Governor's office and Homeland Security and press releases would be developed based on the information provided. Initial press releases stated that the slide was still moving faster across the highway than what an entire fleet of equipment could move. Based on Geology's observations in the field, WYDOT had no choice but to wait until the debris stopped moving before any sort of debris removal could be effective.

As the road closure dragged on, several parties became involved. The USFS Supervisor, the Assistant USFS Supervisor, the District Ranger, and two local legislators visited the site May 19, 2011, to better understand why the road was closed and why WYDOT had to let Mother Nature take its course. Between May 20 and May 25, 2011, there were similar visits to the site by Governor Matt Mead, several more legislators, Wyoming Geological Survey, the U.S. Army Corp of Engineers, several media outlets and BYU-Idaho College Geology students.

MORE OBSERVATIONS

The characteristics of the flow channel, where it crossed the roadway, began to change after the first two days of observation. Initially, the viscous material flowing through the center of the debris mass was flowing at an elevation which was approximately level with top of the entire mass of material covering the road. As the volume of the material being carried down the channel began to decrease, and with the amount of water flowing into the channel remaining the same, the channel began to down cut through the debris and a narrow (50+ ft. wide) U-shaped channel formed. With the formation of this channel, all of the flowing material was being contained within this channel and the material at both edges of the slide mass began to dry out and stabilize.

As of this date, the highway had been closed for almost six days and observations from Geology's mapping showed that the debris began to slow as it crossed the road to 1.0 ft/hour on May 20, 2011. It was decided between Geology and the District Engineer along with the Director of WYDOT, who were present on site, to begin some test excavations on the east side of the debris pile on the highway. These test excavations were done to verify the stability of the debris. The goal was to remove as much material as possible from the roadway on the edges of the slide, while still maintaining the U-shaped flow channel through the center of the mass to contain the flowing material. There was concern that if the U-shaped channel were breeched, the material could flow toward the west and encroach on the original Blue Trail Landslide repair or flow in the direction of the Little Blue Landslide on the east margin of the flow mass. A large addition of material to either of those sites could potentially cause additional instability to the highway adjacent to the Double Draw Landslide.

To help keep the public informed, there were also two public meetings held; one in Jackson and one in Alpine. The timing of the test excavations was fortuitous; WYDOT was able to report to the public at these meetings that steps were being taken to begin material removal from the roadway. The tone of public meetings at the two different sites was an interesting contrast. The public's concern in the Jackson meeting seemed to focus on getting the road open and ensuring stability so there would be no further closures after Memorial Day, which is the beginning of the large tourist season in the area. Since this was typically one of the slowest times of the year in Jackson, most people and businesses in the community had not yet suffered significant impacts.

At the meeting in Alpine, the public's concerns were different and had a more urgent tone. The commuters from the Alpine/Star Valley area had seen an immediate impact to their lives in terms of adding 2 to 3 hours to their work day (depending on traffic conditions), many additional miles, and extra fuel costs due to the detour over Teton Pass. Additional issues that surfaced were such things as the detour over Teton Pass requiring local delivery trucks and contractors, to now pass through Idaho which required stops at the port of entry to incur additional fees for permits. The general consensus of the public at the Alpine meeting was to open the road as soon as possible even if it was just for limited commuter hours. Various WYDOT officials, at the meetings, sought to reassure the public that everything possible was being done to open the road in a timely manner. Other state and local officials who had visited the site were very helpful in supporting WYDOT's position to the public.

On Monday May 23, 2011, the removal of material from the roadway began in earnest as construction crews began attacking the pile of debris from both edges hauling materials to waste sites (Figure 13). The contractor worked 20 hours a day with 15 trucks to haul debris. Working from the edges toward the middle was very effective because it allowed more time for the material remaining in the channel to pass over the roadway, resulting in the need for less material to be removed from the road.

Figure 13. Begin Removal of Debris Off Highway

When all of the material had been removed to roadway level, it was discovered that the debris flow had cut a channel approximately 10 feet deep and 50 feet wide across the roadbed. Since the existing culvert at this location had been destroyed and there was still significant water flowing, it was necessary to install a new culvert under the road. A 60 inch CMP was installed on a steep grade to help prevent the culvert from plugging (Figure 14). A headwall made of large concrete blocks and a dirt catchment berm was constructed at the inlet of the culvert to protect the culvert and allow access for equipment to clean the end of the culvert if necessary (Figure 15).

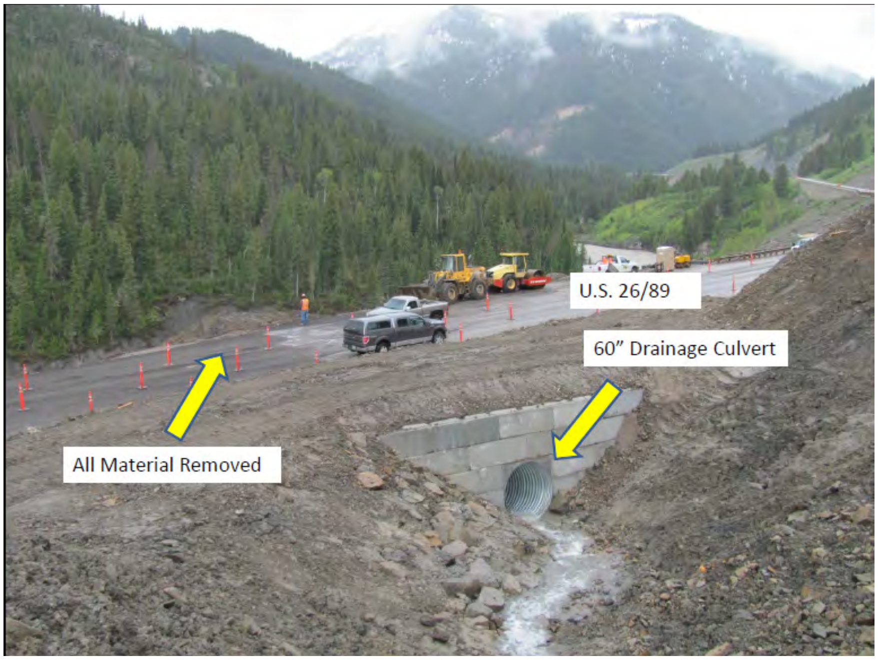

Figure 14. Repaired Highway with Drainage Culvert

Figure 15. Looking up Debris Chute

The road was opened to traffic on Sunday May 29, 2011 during the Memorial Day weekend, two weeks to the day after it was closed.
It was noted that as material from the Double Draw, entered the Snake River it had narrowed the channel considerably; possibly by half. The water began to erode the southern river bank which slightly changed the river's course. As the river exited the southern embankment it came across and began to erode the toe out of the slope 1000 feet downstream of the Double Draw Landslide (Figure 16). This area was already quasi-

stable and the erosion at the toe started making matters worse. A separate emergency contract had to be let, to install embankment protection downstream of the Double Draw to ensure the highway would remain in place (Figure 17). This required coordination between WYDOT, U.S. Army Corps of Engineers and the USFS.

Figure 16. Erosion at Toe of Embankment

Figure 17. Required Downstream Embankment Protection

SUMMARY

The large debris flow that caused the closure of US Highway 26/89 for two weeks beginning on May 14th 2011, was caused by a combination of factors. The snowpack of 171 percent of normal with a snow water equivalent in excess of 30 inches was the second highest in recorded history (Figure 18).

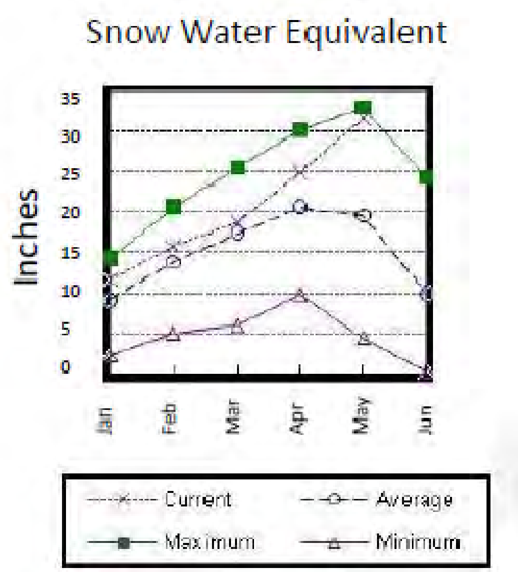

Figure 18. Snowpack (Snow Water Equivalent) May 2011 Snake River Basin

A quick spike in temperatures between May 11 and 14, 2011, (Figure 19) caused rapid melting of the heavy snowpack and saturation of the upper portion of the material on the slopes.

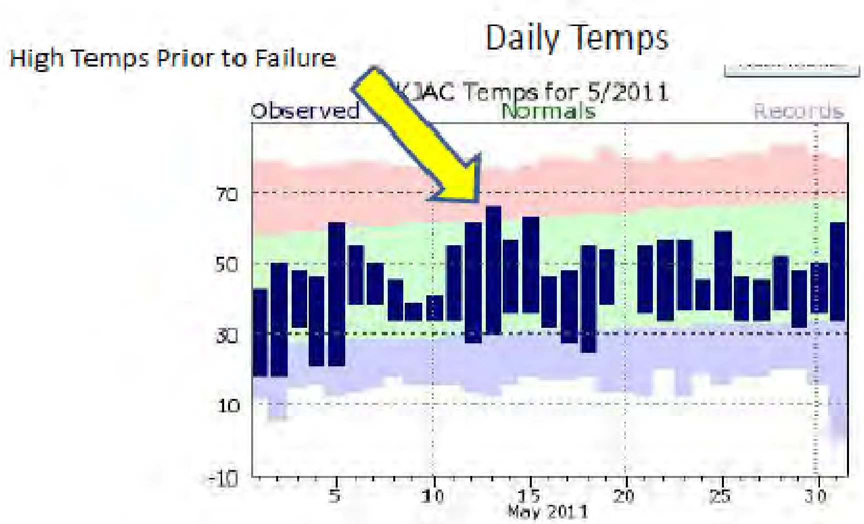

Figure 19. Daily Temperatures Jackson Wyoming May 2011

The topography at the site was such that significant runoff was generated, dumping large quantities of water into a quasi-stable colluviam filled valley with the toe of the valley located in the backslope of the roadway. This colluvial-filled backslope was virtually the "plug", which held back the colluvial material in the valley. As the excessive meltwater entered into the valley from the adjacent drainage, the backslope became saturated and failed. Once the "colluvial plug" had failed it allowed the material in the valley to flow downslope, carrying away everything in its path and covering the roadway.

Due to significant flows of material for several days it was not possible to begin clearing the roadway until the flow subsided significantly. Removal of material began seven days after the initial road closure and it took seven days of working around the clock to remove the material to get the road open to traffic at a cost of $694,500. It is estimated in excessive of 75,000 cubic yards of material was generated by the debris flow and in excess of which 40,000 cubic yards was carried away by the Snake River with the balance being hauled to waste areas or left on the slope below the roadway.

In addition to the direct impact that the debris flow had in closing the highway, it also set off a chain of events that impacted the highway in another way. The amount of material, which flowed into the Snake River, changed the course of the river temporarily and created significant erosion at the base of a slope approximately 1000 feet downstream from the debris flow. This erosion destabilized the slope and accelerated the movement of an existing landslide, which affected a retaining wall that supported the highway. It was necessary to place rock embankment protection at this site under an emergency contract to stabilize the slope.

The road closure, caused by the Double Draw failure, had a significant impact on the people in the area particularly the commuters from Star Valley that work in Jackson. There was significant public pressure to open the road in a timely manner. The communities of Jackson, Alpine, and all smaller communities in Star Valley came together to help each other during this situation. Motels and restaurants offered discounts to commuters who chose to stay in Jackson during the road closure. Some people in Jackson opened their homes to weary commuters and different stores shared inventory to ensure that there were adequate supplies of necessities. The City of Jackson used its busses to help transport commuters from Star Valley to Jackson.

CONCLUSIONS

Although this was not a typical landslide for the WYDOT Geology Program, which requires a geotechnical drilling investigation, soil testing, stability analysis and some type of design to stop or prevent the movement of a landslide. The observation, monitoring, and trying to predict potential scenarios for movement of the material provided a series of new and unique challenges. In summary, the WYDOT Geology Program was tasked with determining when it would be safe and effective to clear the slide debris from the road. This was a decision that had far-reaching, economic and personal impacts, for a large percentage of the population in this area of the state. In this type of situation, it is imperative that judgment (engineering and geological) of the experts analyzing the situation not be overridden by political pressure, which could result in decisions that could jeopardize the safety of the traveling public or result in significant unnecessary costs. WYDOT was fortunate to have the backing of Governor Matt Mead and his administration and other local and state officials in this regard.

REFERENCES

Marvin L. Schroeder, 1973, Geologic Map of the Davis Quadrangle Teton County, Wyoming, USGS

Marvin L. Schroeder, Howard F. Albee and Robert A. Lunceford, 1981, Geologic Map of the Pine Creek Quadrangle Lincoln County, Wyoming, USGS

National Weather Service, 2011, Western and Central Wyoming Weather Forecast Office, Riverton, WY

J. Xavier Montoya, 2011, State Conservationist, National Resources Conservation Service, Casper WY

WYDOT, Public Affairs, Headquarters, Cheyenne WY

Civil Air Patrol, May 2011.

Challenges Faced During the Emergency Response to the Bear River Canal Failure

Darren A. Mack, P.E., G.E.
Sanders & Associates Geostructural Engineering, Inc. (SAGE)
4180 Douglas Blvd., Ste. 100, Granite Bay, CA, 95746
(916) 729-8050
E-mail: dmack@SAGEengineers.com

Drew G. Kennedy, P.G., C.E.G.
Sanders & Associates Geostructural Engineering, Inc. (SAGE)
4180 Douglas Blvd., Ste. 100, Granite Bay, CA, 95746
(916) 729-8050
E-mail: dkennedy@SAGEengineers.com

Ken Leung, P.E.
Pacific Gas & Electric, Power Generation Department
245 Market St., San Francisco, CA 94105
(415) 973-3493
E-mail: KKL2@pge.com

Robert McManus, P.E., G.E.
Pacific Gas & Electric, Geosciences Department
245 Market St., San Francisco, CA 94105
(415) 973-1623
E-mail: RAM8@pge.com

Prepared for the 63rd Highway Geology Symposium, May 7-10, 2012

Acknowledgements

We would like to thank everyone who participated in this important project, including PG&E, PCWA, NID, SAGE, northwest hydraulic consultants, PACE Engineering, REY Engineers, NORCAL Geophysics, Taber Drilling, GeoTest Unlimited, Syblon Reid Construction, American Crane, Camblin Steel, Capital Engineering Laboratories, Dees Hennessey, KNG Concrete Pumping, Neil's Controlled Blasting, and RJ Miles, for their professional contributions and excellent team work.

Disclaimer

Statements and views presented in this paper are strictly those of the authors, and do not necessarily reflect positions held by their affiliations, the Highway Geology Symposium (HGS), or others acknowledged above. The mention of trade names for commercial products does not imply the approval of or endorsement by HGS.

CHALLENGES FACED DURING THE EMERGENCY RESPONSE TO THE BEAR RIVER CANAL FAILURE

A landslide caused failure of a section of PG&E's Bear River Canal near Colfax, California. The canal failure disrupted a major source of water for western Placer County, affecting thousands of residents. Pacific Gas & Electric retained Sanders & Associates Geostructural Engineering, Inc. to evaluate the landslide failure and perform expedited engineering design to repair the failed canal on an accelerated schedule.

The failure occurred on very steep slopes in a remote area with limited equipment access. The emergency response required the development of a unique engineering design to rapidly repair the canal in this potentially dangerous terrain. The selected repair method consisted of placing approximately 2,000 cubic yards of unreinforced cementitious fill to replace the slope materials lost in the failure. This created a stable subgrade for a new at-grade reinforced concrete flume section, while reducing the need for personnel or equipment within the potentially unstable failure zone. Global stability for the fill mass was achieved using a reinforced concrete waler and five multi-strand tieback anchors post-tensioned to 350 kips each. The anchors were installed concurrently with the flume construction using limited-access drilling equipment winched down the slope face. Engineering and construction of the repair were substantially completed in just over six weeks and 10 days ahead of schedule, allowing full canal operation and delivery of water supply.

This paper shares experiences from the geological and geotechnical investigation, the alternatives evaluation and selection, the engineering design process, the construction process, and lessons learned from this fast-track project.

.

INTRODUCTION

The Bear River Canal is a water conveyance canal owned by Pacific Gas and Electric (PG&E) that runs along the south slope of the Bear River Canyon. The canal is used to convey water over 22 miles, from the Bear River Diversion Dam Impoundment to Halsey Forebay, where it is used to generate power at PG&E's Halsey Powerhouse. In addition to power generation, the canal supplies domestic and irrigation water to Nevada Irrigation District (NID) and Placer County Water Agency (PCWA). The canal has a maximum rated flow capacity of approximately 490 cubic feet per second (cfs).

On April 19, 2011, a landslide caused the failure of a 55-foot-long section of the canal near Colfax, California. Colfax is located in the western foothills of the Sierra Nevada mountain range, along Interstate 80, about 50 miles northeast of Sacramento, California. The flow of approximately 400 cfs out of the canal caused considerable erosion downslope before it could be stopped. This resulted in an eroded ravine with a head scarp in excess of 30 feet tall at the canal and that extended approximately 110 feet vertically down to the Bear River, leaving large boulders and exposed bedrock in its path (Figures 1, 2).

Figure 1. Breach in the Bear River Canal, Colfax, CA, observed April 21, 2011.

Figure 2. Boulder pile and erosional scar resulting from breach, observed April 21, 2011.

In response, PG&E rapidly mobilized a team of consultants and contactors to address this emergency condition. The failure disrupted the water supply downstream and had the potential to greatly impact the residents of Placer County. The emergency response to the failure required developing a unique engineering design to quickly repair the damaged canal in a steep and potentially dangerous terrain with very limited access. When selecting the repair method, the team was cognizant that the surrounding land was heavily forested private property and, therefore, any impact to surrounding lands needed to be minimized to the greatest extent possible. The owner, engineer, contractor, resource agencies, landowners, and regulatory agencies joined efforts to complete the canal structure repair and restore full water delivery ahead of schedule and one month ahead of the start of the critical irrigation season.

CANAL GEOMETRY

The failed canal section consists primarily of a trapezoidal channel with a thin shotcrete liner. Average dimensions in the vicinity of the break are on the order of 9 feet wide at the base, 18 feet wide at the top, and 8 feet deep. The canal, which was first built in the late 1800s, appears to have been constructed in a conventional side-hill fashion, with inboard cuts used to build a fill berm to the outboard edge of the canal. The canal section was lined with gunite. Canal side slopes are nominally ½:1 (horizontal to vertical).

EVALUATION OF REPAIR ALTERNATIVES

In light of the emergency and urgency, a team of engineering consultants, general contractors, and key PG&E personnel was formed immediately after the failure to evaluate alternatives for repair of the canal, while simultaneously performing the subsurface characterization. The team's goal was to restore full water service as soon as possible while ensuring the safety of construction crews and maintaining interim water supply to the affected communities. Multiple alternatives were evaluated, including:

- suspending bypass pipes from the slope above the canal with cables
- constructing an elevated pipe bridge that spanned the break and gained support on intermediate bents supported on drilled piers
- constructing bulkheads in the canal and using bypass pumps and a multi-pipe manifold to pump several hundred cubic feet per second around the toe of the failure
- excavating a stabilized bench in the slope adjacent to the eroded zone
- filling the scarp with various kinds of fill materials or mechanically stabilized earth (MSE) fill

For several of these alternatives, it would have been necessary to at least partially fill the scarp with loosely placed fill material to provide a working platform for construction or to stabilize the side walls of scarp in-place (e.g., by installing soil nails with a shotcrete facing). Some alternatives were dismissed because of their potential operational risks, environmental impact, or unacceptable construction safety risks from the unsupported "excavation."

The general contractor, Syblon Reid Construction (SRC), provided constructability review and input to cost and schedule from the beginning of the design process. Including the contractor this early on proved invaluable to the project. The design team received real-time input regarding construction concepts, methods, equipment access or limitations, and estimated construction durations. As a result, the team selected the alternative that could be constructed as quickly as possible while meeting all of the project goals.

SELECTED ALTERNATIVE

The selected alternative consisted of re-establishing the eroded slope and canal foundation by filling the scarp with unreinforced cementitious fill and replacing the open ditch embankment type canal section with a reinforced concrete flume structure (Figure 3). The fill material was constructed at a 1H:1V inclination from the toe of the fill to El. 2460 (project datum), and then continued at an inclination of ¾H:1V to El. 2490. A flat, 15- to 20-foot-wide bench at El. 2490 feet served as the foundation for the concrete flume structure. The overall height of the fill is approximately 60 feet. One advantage of the cementitious fill over granular materials such as rock or soil is it is self compacting and has minimal settlement after placement. In comparison with the other alternatives, the cementitious fill alternative had the shortest construction duration with limited site excavation, smaller total fill volume, and simpler construction methods.

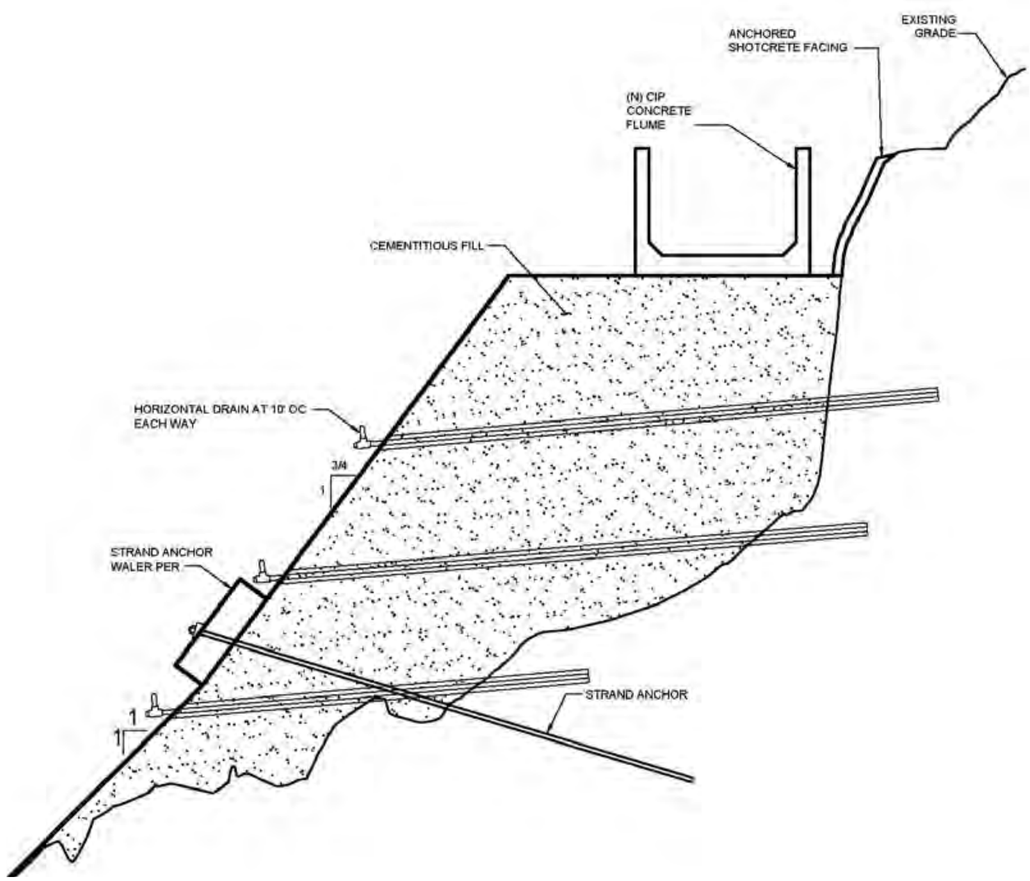

Figure 3. Cross section through cementitious fill and new flume structure.

The cementitious fill consisted of a 5-sack sand and gravel mix with the maximum aggregate size limited to a 1-inch maximum to improve pumpability. Twenty-five percent of the Portland cement was replaced with fly ash in the upper portions of the fill (where it is thicker) to help control heat of hydration and reduce thermal cracking within the unreinforced fill. The minimum required design strength of the cementitious fill was 300 pounds per square inch (psi), although the actual strength averaged about 3,000 psi. Five 350 kips capacity tie-back anchors were installed through the cementitious fill block to provide adequate stability. Thirteen horizontal drains were drilled through the face of the cementitious fill to reduce potential hydrostatic pressures behind the impermeable fill mass.

The new canal structure consists of a 116-foot-long cast-in-place (CIP) reinforced concrete flume constructed atop of the cementitious fill. The flume has an 18-inch-thick mat slab and 12-inch-thick vertical walls. A flared transition structure was constructed at the downstream end of the new flume to tie into the existing channel section. Control joints were constructed at a maximum center-to-center spacing of 16 feet, with an expansion joint constructed mid-length. The new flume was constructed using conventional concrete forming methods.

Another advantage of the selected alternative was the ability to accommodate a temporary bypass to deliver limited interim water to the downstream water agencies. Once the concrete flume slab was constructed, a steel bulkhead was constructed in the upstream existing flume and a 48-inch-diameter smooth-walled HDPE pipe was run through the center of the work zone. The flume walls were then constructed alongside the bypass pipe. This allowed approximately 50 cfs of water delivery to the downstream water users about 10 days before resumption of full canal operations.

SITE CHARACTERIZATION

The canal is situated on a steep slope and generally runs parallel to the Bear River. The natural slope inclination is between 1H:1V and 1.5H:1V. Site conditions are generally rugged with heavy tree and vegetation growth (Figure 4). The erosional scarp exposed a combination of fill, colluvium, and weak, deeply to moderately weathered intrusive bedrock. At the time the break was first observed, the erosional scar was filled with debris, downed trees, and rock/ boulders of varying sizes. Some loose fill had also been pushed into the upper part of the scarp during initial efforts to secure the site.

The site is located in the western foothills of the Sierra Nevada, within a geologic region commonly referred to as the Western Metamorphic Belt (WMB). Located west of the plutonic granitics of the Sierra Nevada batholith and east of sedimentary basin of the Great Valley, the WMB is comprised of north-trending bands of Upper Paleozoic and Middle Mesozoic marine sedimentary and volcanic rocks tectonically emplaced along the western margin of the continent (Dickinson, 1981; Day, 1992).

Review of regional geologic maps (Chandra, 1961; Tuminas, 1983; Saucedo and Wagner, 1992; Loyd, 1995) indicates that the site vicinity is underlain by Jurassic-age igneous rocks, specifically gabbro of the Lake Combie Complex. Gabbro is a dark-colored, intrusive igneous rock composed principally of plagioclase and clinopyroxene. Where little weathered to fresh, the gabbro is easily recognized by its coarse-grained "salt and pepper" appearance. The gabbro bedrock is locally cut by fine-grained intrusive dikes and sills that are comprised of dark-gray to black, fine-grained mafic rocks.

Figure 4. Steep, heavily wooded topography surrounding failure.

A geotechnical and geological investigation was performed to explore and characterize the site. Due to the water emergency posed by the canal outage, the field investigation was performed on an accelerated schedule and concurrent with alternatives analysis and engineering design. Prior to the investigation, regional and local geologic maps were reviewed to understand the geologic setting of the site. In addition, aerial reconnaissance of the site was performed via helicopter to obtain post-failure aerial photographs of the site vicinity.

The investigation consisted of drilling 8 exploratory borings, including 4 borings on the downstream side of the failure from within the canal; 2 borings on the slope above the canal failure; and 2 borings on the upstream side of the failure from within the canal (Figure 5). The borings were drilled using solid-stem auger and rotary-wash triple-tube HQ rock coring methods, and were continuously logged by a geologist. The borings were drilled vertically, with the exception of Boring BR-4, which was drilled at an inclination of 40° below horizontal oriented N62°E to explore behind the scarp. Downhole caliper, optical televiewer, and/or acoustical televiewer surveys were performed to obtain discontinuity orientations within the boring. Laboratory testing included unconfined compressive strength and multi-stage direct shear on samples of intact joints.

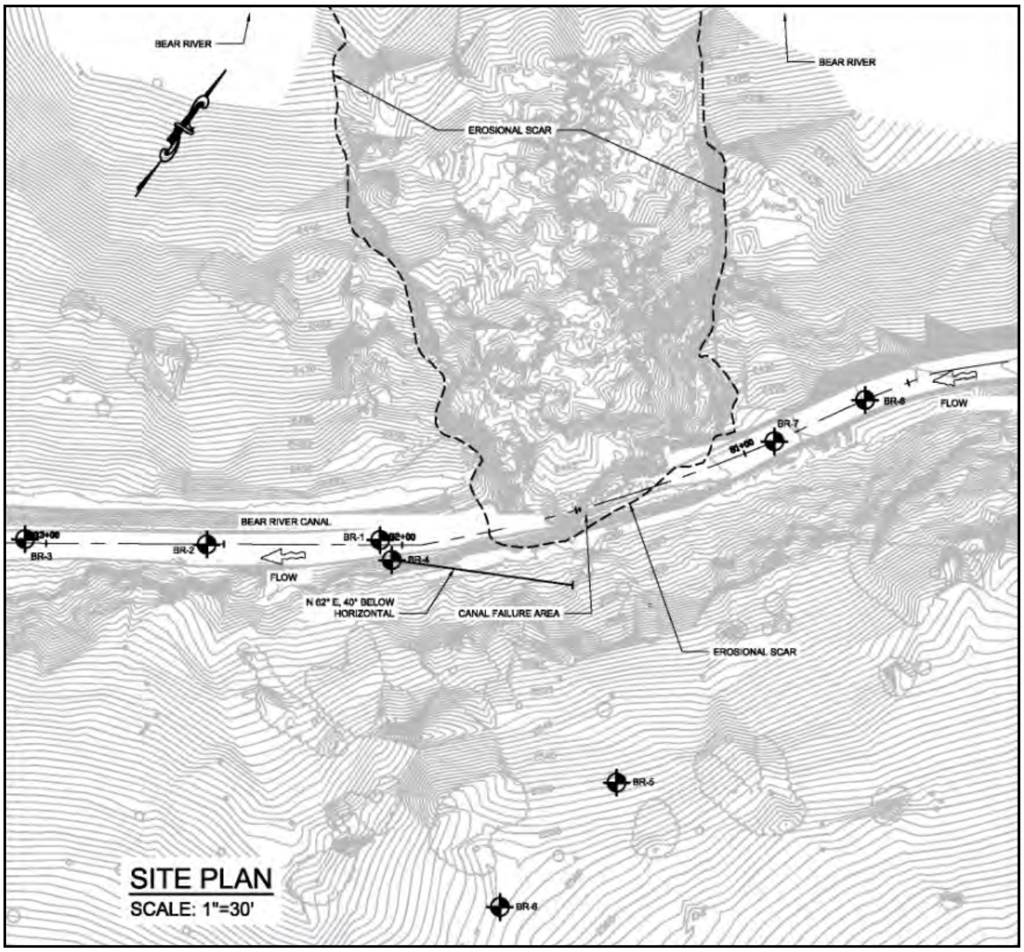

Figure 5. Exploration site plan. Not to scale.

Geologic mapping of the canal failure and surrounding areas was completed concurrent with the exploratory drilling activities. Surface exposures surrounding the failure, and outcrops within the erosional scar, were observed as part of the geologic mapping, which included recording rock discontinuities, degree of weathering, rock quality/type, presence of seepage, and pre-existing areas of instability. The project geologic map is presented as Figure 6.

Consistent with the regional geologic maps, the site is characterized by gabbro bedrock (Jgb) which is locally blanketed by surficial deposits. The surficial deposits consist of the following units:

- Fill (Qf) – Present along the outboard edge of the canal. Consists of locally derived materials that were placed during canal construction.

- Boulders/Debris (Qbd) – Includes boulders, concrete debris (from the failed canal section), and tree trunks within the erosional scar. There are little to no fine-grained materials present, except in the upper portion of the erosional scar where soil material was pushed in shortly after the canal failure to address temporary scarp stability concerns.
- Landslide Deposits (Qls) – Localized slope failures on the inboard canal cut slopes and native slopes upstream of the erosional scar. The landslide deposits on the inboard canal cut slope appear to be dormant, heavily vegetated, remnant scarps from shallow debris slides.
- Colluvium (Qc) – Slope deposits on the inboard canal cut slopes and the surrounding native slopes. Generally composed of gravity transported soil, debris, and rock fragments. Also includes residual soil materials formed by in-place weathering of rock.

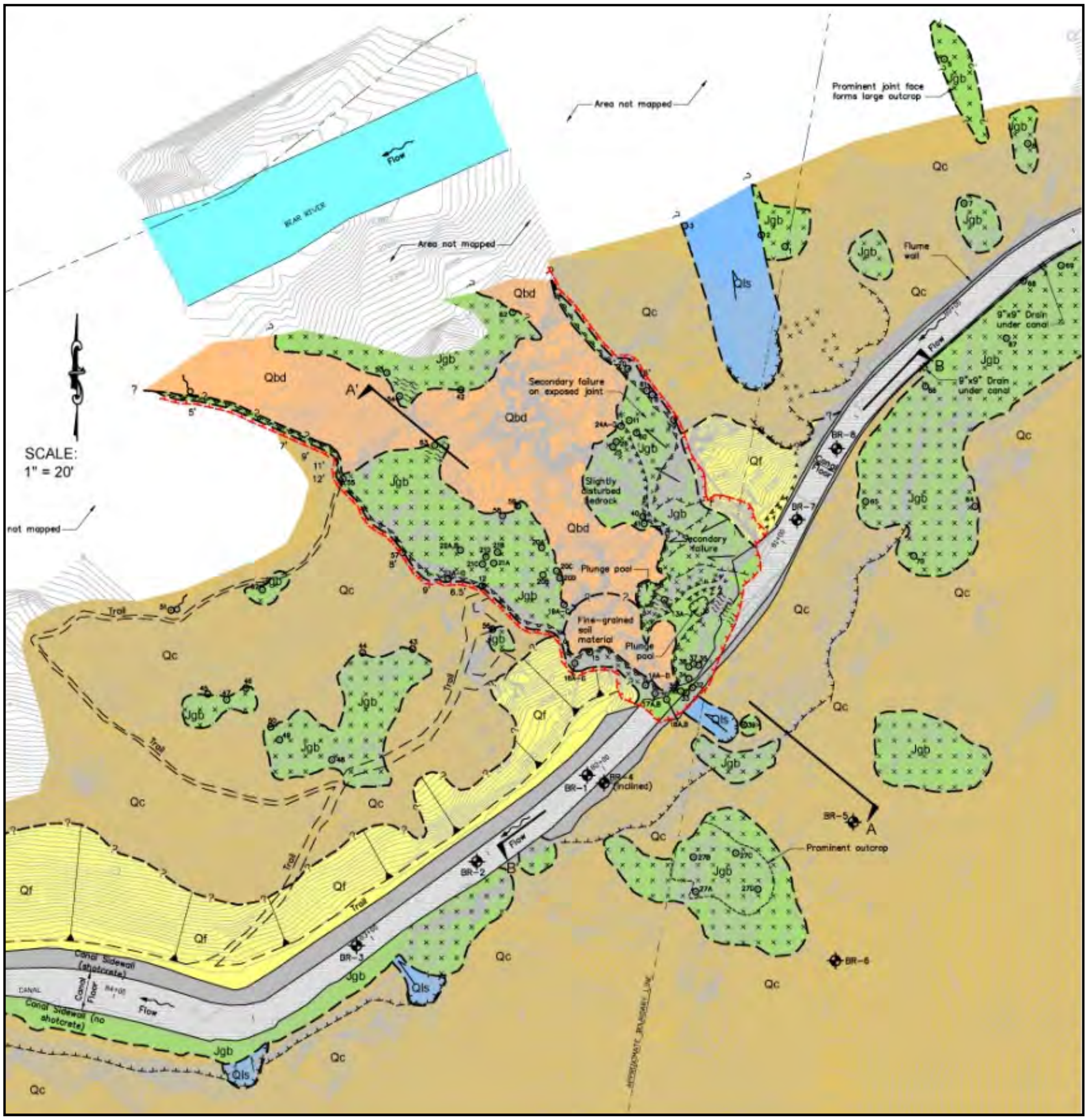

Figure 6. Surficial geology of Bear River Canal repair project. Not to scale.

The site area is located below the Pleistocene glaciation line and, therefore, the gabbro bedrock was not scraped clean of weathered material by glaciers. Consequently, the results of the investigation indicated most of the slope is mantled by a layer of decomposed (weathered) bedrock that retains the original rock structure. The thickness of this layer varies considerably across the site, from approximately 10 to 60 feet. Fractures, joints, shears, and other discontinuities in the bedrock act as preferential pathways for the effects of weathering. As a result of preferential weathering pathways, the degree of weathering varies considerably within the deeply weathered materials, and locally contains moderate or little weathered core stones.

In general, the engineering properties of the gabbro bedrock are directly related to the degree of weathering. Where observed on surface exposures and in rock core samples collected from eight geotechnical borings, the engineering properties vary widely in the upper 30 to 60 feet of material. Rock hardness and strength properties range from low hardness to very hard, and friable to very strong, with significant variability over depth.

SAGE attempted to correlate weathering subunits (deep, moderate, little, and fresh) between the borings and surficial exposures, but specific correlations were limited by the highly variable nature of the weathering. For the purposes of slope stability analyses, we simplified the materials into two primary units: weathered and unweathered (Figure 7). The "weathered" subunit includes moderately to deeply weathered rock with strong discoloration and low strength. The "unweathered" subunit includes little weathered to fresh rock that is strong to very strong and characterized by discoloration along localized joint surfaces. The strengths of these units are highly variable, with unconfined compression strengths ranging from 26 psi (deeply weathered) to 18,000 psi (fresh).

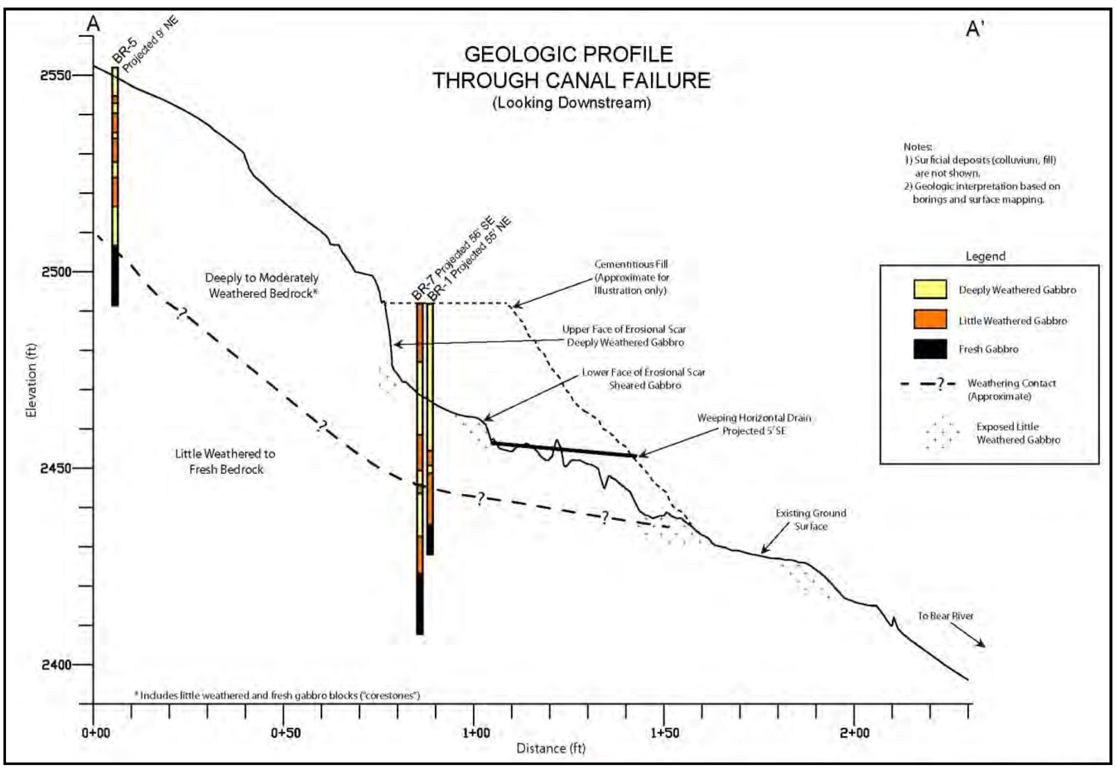

Figure 7. Geologic profile through failure showing weathering variability vs. depth.

Rock cores obtained from borings at the site indicate that the rock in the upper 30 to 40 feet is typically intensely to closely fractured. Maintaining fluid circulation during rotary wash drilling was problematic, with much of the drilling performed with partial or complete water loss. In addition, the borings were difficult to grout, with several of the borings requiring up to three times the amount of grout anticipated for the given diameter and depth. The degree of fracturing combined with the loss of water and grout during the drilling operations suggests that overall permeability of the rock mass is high.

STABILITY EVALUATION

The cementitious fill has the advantage of quickly stabilizing the most critical portion of the erosional scar without exposing site workers to safety risks from working below the near vertical, unstable slopes. However, this also required that the cementitious fill be placed on an unprepared, boulder-strewn foundation (Figure 8). To evaluate the required dimensions of the fill that would result in acceptable slope and canal stability, we performed slope stability analyses using the program SLOPE/W (GeoStudio 2007, v7.17) by Geo-Slope International.

Figure 8. Boulder pile left in the bottom of the erosional scarp.

The preliminary results of the geotechnical and geologic investigation were used to develop the cross sections required for the slope stability analyses. The variability in weathering, along with the critical nature of the structure, suggested that a conservative, two-layer stratigraphic model be used, as shown previously in Figure 7.

In order to meet the aggressive project schedule, design began before the field investigation and laboratory testing of the soil and rock samples was complete. It was necessary to make conservative assumptions regarding material strengths to advance the design and begin construction. Then the slope stability was re-analyzed when lab testing results were available to validate the adequacy of the design. This approach was necessary in view of the emergency and fast-track nature of the project.

Back calculation of the erosional scarp was performed to conservatively estimate the strength of the variably-weathered materials. Average strength envelopes were assumed for the generalized stratigraphy. As the scarp did not continue to retrogress, we solved for a factor of safety just greater than 1.0 (1.05) in our back calculation. Although the groundwater encountered was likely fracture flow, all analyses were performed with a conservative estimate of phreatic surface based on the measured water surface elevations. Based on the results of our back calculation, two sets of weathered rock strength parameters were estimated for the initial stability analyses. These parameters were used to bound the range of factor of safety for stability calculations and to define the geometry of the fill mass.

When the laboratory test results were available, the mass properties of the weathered rock were estimated using the generalized Hoek-Brown (H-B) Failure Criterion (Hoek and others, 2002; Rocscience, 2002). In general, the rock mass strengths are reduced, relative to the unconfined compressive strengths, based on the fabric, interlock, and strength of the mass. The amount of reduction increases as the unconfined compressive strength decreases or as the number of discontinuities increases. The Hoek-

Brown criterion utilizes five input parameters for estimation of the H-B failure envelope – Unconfined Compressive Strength (UCS), Geologic Strength Index (GSI), disturbance factor (related to disturbance to blasting or excavation), a tabulated material parameter (m_i), and Young's Modulus. The back-calculated and equivalent H-B failure criteria strength parameters are presented in Table 1.

Table 1. Summary of H-B Parameters

Parameter	Back Calculated Values		"Weathered" Gabbro	"Unweathered" Gabbro	Cementitious Fill
Unconfined Compressive Strength, psi	--	--	82	13,808	3,000
Geologic Strength Index (GSI)	--	--	36	82	55
mi (material parameter)	--	--	27	27	19
Disturbance factor, D	--	--	0	0	0
Young's Modulus, ksi	--	--	36.9	6,213.6	3,100
phi, degrees	37	44	*33*	*67*	*60*
cohesion, psf	460	240	*720*	*71,000*	*5,000*

Notes: 1. Young's Modulus values estimated using the modulus ratio (MR) feature within RocLab software.
2. Values in italics represent equivalent Hoek-Brown Failure Envelope parameters.

Because of the variability of the weathered material, which contained layers of moderately weathered and unweathered corestones, the upper bound UCS for deeply weathered material was utilized in the Hoek-Brown analysis to represent the overall rock mass strength of the weathered gabbro. For unweathered gabbro, we computed H-B strength parameters using the average of all UCS tests for unweathered gabbro.

Due to the placement methods, the cementitious fill was assumed to have small voids, imperfections, and localized cracks that would be present through the mass. Therefore, the cementitious fill was not analyzed as a monolithic structure. Instead, the strength for this material was also estimated using the H-B approach. However, the resulting H-B strength envelop was sufficiently high that failures through the cementitious fill mass were not expected and it could be assumed to be monolithic for the purposes of design. The input parameters used for the cementitious fill are also summarized in Table 1.

The computed factors of safety using the H-B rock mass properties were compared to those computed initially using the back-calculated strengths. The use of the rock mass properties resulted in a factor of safety around 1.25. Given the fact the deep-seated global slope stability failures had generally not been observed in immediate area, we considered this factor of safety to be compatible with the previously performed back-analysis of the slope. Therefore, we concluded that the results of the H-B analysis validated the preliminary analysis and initial submittal to the regulatory agency.

The required factors of safety for the design are 1.3 for temporary construction conditions, 1.5 for long-term static conditions, and 1.15 for seismic conditions. The cementitious fill alone has an estimated static factor of safety of 1.35. Five 350-kip post-tensioned tiebacks were installed at Elevation 2463 raising the factor of safety to around 1.92. To transfer the anchor loads to the cementitious fill, a 3-foot-thick by 8-foot-tall continuous concrete waler was designed across the front of the fill mass.

The site is in an area of relatively low seismic activity. For seismic conditions, we estimated a peak ground acceleration (PGA) for the site consistent with ASCE 7-05 using the USGS on-line seismic calculator. This resulted in a PGA of 0.16 g and represents an approximate 10% probability of exceedance in 50 years. For seismic stability analyses, we selected horizontal and vertical coefficients of 0.08, which are one-half the PGA value. This is conservative, as the vertical coefficient is routinely neglected in these analyses. The resulting factor of safety is 1.38.

Because the cementitious fill was placed over unprepared subgrade, the sliding stability of the fill block mass on the boulder pile/exposed bedrock was also evaluated by using a simple hand calculation that treated the mass as a simplified rigid block with an inclined base and a reduced base friction angle of 33 degrees. Given the roughness of the foundation, exposures of in-place rock in the scarp, and some favorable three-dimensional geometry, we believed this value to be conservative. The sliding block analyses showed that the concrete fill block with the five tiebacks is stable with a computed factor of safety above 2.0.

In view of the urgency in restoring water supply, the canal was returned to full operation once the concrete for the fill and the flume structure reached the design strength and two of the five tie-backs were installed and tested. This provided a short-term factor of safety of at least 1.4 while installation of the other three tiebacks continued to provide long-term stability.

CONSTRUCTION

Construction of the cementitious fill began on May 9, 2011, approximately three weeks after the break. A new access road and lay down pad were developed into the hillslope above the canal to allow access for concrete trucks, the concrete pump, and construction equipment. A 164-foot-long concrete boom pump and a 300-ton mobile crane were used to deliver and place concrete into the fill area (Figure 9). The use of the boom pump reduced the need for personnel or equipment within the potentially unstable scarp created by the failure.

Figure 9. 164-foot boom pump placing cementitious fill in scarp (left); 300-ton mobile crane (right).

The first layer of cementitious material was placed in and around the boulders to make sure the fill was keyed in well to the existing boulder field and underlying less weathered bedrock. Concrete with a slump of around 3 inches was initially used to ensure material would flow into the smaller crevasses. However, this slump would not maintain the required outside slope face of 1:1. After the concrete level rose above the irregularities of the boulder field, the slump was reduced to 1 to 1-1/2 inches at the point of discharge. This allowed the cementitious material to be "stacked" in a slope that is as steep as about ¾H:1V (Figure 10). Surveyors were on site full time during the placement of the fill to check line and grade. The cementitious fill topped out on May 12, 2011, with approximately 2,000 cubic yards of unreinforced cementitious fill placed in the scarp to replace the slope materials lost in the canal failure (Figure 11).

Figure 10. Appearance of cementitious fill during placement. Steepened slope in background was buttressed with rockfill later in construction.

Figure 11. Topping out of cementitious fill beneath former canal lining, May 12, 2011.

After completion, the cementitious fill created a stable working platform for demolition of the former canal lining as well as a subgrade for the new, 116-foot-long, reinforced concrete flume section. Because the new flume could be constructed using conventional concrete forming methods, construction of the canal invert was performed quickly during the 24/7 shifts, with formwork and rebar for each panel placed at night, the panel of concrete placed the next day, and then the forms stripped the next night.

The 12-strand tiebacks anchors were installed through the face of the cementitious fill by winching an air-track drill rig down the face of the slope (Figure 12). Cable anchors were drilled and set into the cementitious fill and grouted into place and served as tie-off points for the equipment and personnel accessing the face of the slope. Drilling was sometimes slow because of the potential for hitting loose soils or small voids at the back of the cementitious fill. Voids results in a loss of air circulation for clearing the holes. Because installation of casing through the cementitious mass was very difficult, the drilling issues were generally resolved by grouting and redrilling the holes to seal the voids so that the holes could be cleaned. For two of the tiebacks, two rounds or regrouting were required to adequately seal the holes.

Since the tieback anchors were constructed concurrently with the canal, a monitoring program was implemented during construction to confirm that the cementitious fill was not moving prior to tieback lock off. Survey monitoring points were set on the outside edge of the cementitious fill and monitored daily. In addition, two 30-foot-deep, open standpipe piezometers were installed vertically at the back of cementitious fill and penetrated into the weathered bedrock foundation. The piezometers were monitored daily, and an emergency action plan was put into place with steps to be taken if the water levels in the piezometers reached certain action levels. However, neither piezometer reported appreciable amounts of groundwater, even though they were near the boring locations where groundwater was encountered. This provided further proof of fracture flow, rather than piezometric head, with the rock mass.

Figure 12. Limited access drilling through face of cementitious fill.

Several steps were taken through the design and construction process to accelerate construction so that water could be reintroduced to the canal and provided to the community. The flume was designed with cantilevered walls designed for low short-term (green) concrete strengths that could be loaded within days of concrete placement and well before the concrete was fully cured. The project team worked 24/7 to accelerate completion of the project, including daily conference calls between the field crews, design engineer, and owner to address issues and questions in real time and prevent delays. The strong communication, dedication of the field crews, and atmosphere of cooperation between the engineer and contractor resulted in a resumption of canal flows on June 3, 2011. Flow of 450 cfs was restored to the canal on June 7th, just over six weeks after the failure occurred, and 10 days ahead of schedule.

Site restoration work continued throughout the summer to restore the site to pre-failure conditions to the extent possible. Site restoration activities included:

- Installation of the remaining three tiebacks and completion of the waler beam.
- Excavation of a temporary access road from the upslope staging area to the canal and construction of a large rockfill access road below the canal, on the steep native slopes, to provide access to restoration areas below the canal.
- Construction of a low-rise, single span, temporary steel girder bridge for crossing the canal during restoration efforts. Bridge abutments comprise permanent cast-in-place concrete abutments founded on micropiles. The 48-foot-long, W18x211 wide-flange beams had to be shipped to the site on articulated logging trucks.

- Construction of soil nail stabilization for the earthen slopes to remain below the flanks of the new flume section, adjacent to the erosional scarp.
- Regrading of scarps and/or buttressing of scarps with rockfill (Figure 13), as appropriate and as access allowed. The rockfill was also topped with a soil "planting berm" that would allow new trees to be planted in the scarp area and that, once mature, can screen the cementitious fill when viewed from the river and reduce the visual impact of the repair.
- Covering the cementitious fill and soil nail walls with an overlay of integrally-colored shotcrete designed to blend into the surrounding soil and rock exposures, which also reduced the visual impact of the repair.
- Restoring areas disturbed by construction, including the partial removal of the rockfill access road to reduce its footprint and visual impact, site revegetation, and tree replanting.

Figure 13. Completed fill, waler, tiebacks, flume, soil nail walls (downstream shotcrete in progress), and rockfill. Photograph shot prior to application of colored shotcrete.

CONCLUSIONS

The emergency situation at the Bear River Canal failure prompted the unconventional application of concrete, a common construction material, to quickly stabilize the slope and repair the canal, filling a large, steep void. The cementitious fill and concrete flume design facilitated an expedited construction schedule that restored the canal structure and brought it to full operation despite the limited access and steep terrain. In the case of the Bear River Canal failure site, the overburden material had been scoured down to resistant rock and large boulders that were suitable for the cementitious fill foundation. The pumped cementitious fills is a simple design and construction method that may have applications in similar emergency response situations, such as quickly reopening roadways or highways to service after a landslide.

Selecting reasonable and conservative geotechnical design parameters concurrently with the field investigation was also a key to addressing the emergency nature of the project. Real-time data from the investigation was provided to the design engineers, allowing reasoned back-analysis of the slope to be performed and a design to be prepared prior to completion of the subsurface investigation. The investigation and laboratory testing program was still critically important; however, it was used to validate the initial assumptions and analysis prior to resumption of flow in the canal.

One key to success was the extraordinary teamwork, dedication, cooperation, and coordination among the project owner, engineer, contractor, and regulators. All parties worked together on the design, scheduling, and construction to keep the project moving. The early involvement by the contractor was instrumental in identifying and implementing a constructible solution that could be quickly constructed given the site access constraints and safety concerns. The 24/7 schedule required the owner and engineer to respond quickly to field changes and questions so that crews were not left idle while waiting for answers. The implementation of a daily conference call between the design and construction team was invaluable to early identification and resolution of potential issues, as well as the complex coordination required to keep so many crews working simultaneously.

REFERENCES

Chandra, D.K., 1961, *Geology and Mineral Deposits of the Colfax and Foresthill Quadrangles, California*: California Division of Mines and Geology, Special Report 67.

Day, H.W., 1992, *Tectonic Setting and Metamorphism of the Sierra Nevada, California* in Schiffman, P., and Wagner, D.L., eds., Field Guide to the Geology and Metamorphism of the Franciscan Complex and Western Metamorphic Belt of Northern California: California Division of Mines and Geology Special Publication 114, p. 12-28.

Dickinson, W.R., 1981, *Plate Tectonics and the Continental Margin of California*, in Ernst, W.G., ed., The Geotectonic Development of California: Engelwood Cliffs, N.J., Prentice Hall, Inc., p. 1-28.

Hoek, E., Carranza-Torres, C., and Corkum, B., 2002, *Hoek-Brown failure criterion – 2002 Edition*: Proc. 5th North American Rock Mechanics Symposium, Toronto, July 2002, p. 267-273.

Loyd, R., 1995, *Mineral Land Classification of Placer County, California*: California Division of Mines and Geology, Open File Report 95-10, scale 1:100,000.

Rocscience, 2002, *RocLab: Rock mass strength analysis using the Hoek-Brown failure criterion – User's Guide: Rocscience, Inc.*, 25p.

Saucedo, G.J., and Wagner, D.L., 1992, *Geologic Map of the Chico Quadrangle*: California Division of Mines and Geology, Regional Geologic Map Series Map No. 7A (Geology), scale 1:250,000.

Tuminas, A., 1983, *Structural and Stratigraphic Relations in the Grass Valley – Colfax Area of the Northern Sierra Nevada Foothills, California:* Ph.D. dissertation, U.C. Davis.

Case Studies in Roadway Landslide Repair and Rock Slope Stabilization in California

James Chinchiolo, B.S.
Landslide Solutions, Inc.
1809 S Street Ste. 101-203, Sacramento, CA 95811
(916) 913-0748
james@landslidesolutions.com

Colby Barrett, J.D., E.I.T
Soil Nail Launcher, Inc.
2841 North Avenue, Grand Junction CO 81501
(970) 210-6170
colby@snl1.com

Nate Beard, PE
Soil Nail Launcher, Inc.
2841 North Avenue, Grand Junction CO 81501
(970) 210-6170
nate@snl1.com

Prepared for the 63rd Highway Geology Symposium, May 7-10, 2012

Acknowledgements

Disclaimer

Statements and views presented in this paper are strictly those of the author, and do not necessarily reflect positions held by their affiliations, the Highway Geology Symposium (HGS), or others acknowledged above. The mention of trade names for commercial products does not imply the approval or endorsement by HGS.

ABSTRACT

The challenges associated with roadway landslide and rock slope failures along California's roadways can introduce a series of difficult problems to solve. Not only is the design and construction associated with the repair of these landslides and rock slope failures challenging, many of the traditional contracting and review processes available either present too long of a time frame or are not flexible enough to handle the field level decisions often required with emergency landslide and rock slope repairs.

This paper outlines some landslide and rock slope design build mitigation methods and technologies that are both relatively lower cost when compared to traditional repairs methods and robust enough to achieve standard design life and seismic criteria. Relevant technologies include soil nailing (including hollow injection anchors), high capacity tensioned wire rock mesh, micropiles, post-tensioned rock bolts, and various types of drilled horizontal drains.

The case studies for this presentation include a rock slope stabilization using tensioned rock bolts and high capacity wire mesh for the United States Army Corps near Chowchilla, CA; a Pacific coast bluff repair using hollow bar soil nails, micropiles, and shotcrete for CalTrans District 4 near Pescadero, CA; a landslide repair using self drilling soil nails, micropiles and shotcrete for CalTrans District 2 near Weaverville, CA; and a landslide repair using self drilling soil nails and shotcrete for Santa Clara County Public Works near Los Gatos, CA, and a series of landslides repaired using an innovative combination of the "Deep Patch" method and micropiles for the USDA Forest Service near Fresno, CA.

INTRODUCTION

Landslides and rock slope failures along California's roadways are common in mountainous areas throughout the state. Often these sites are activated by periods of substantial rainfall and require immediate remediation. Time and cost are always constraining factors and it is rare that complete subsurface data is available to designers in emergency situations.

The challenges associated with the repair of roadway landslides and rock slope failures is compounded by the desire to minimize the impact to the traveling public and often precludes the use of more traditional landslide repair methods such as rock buttressing, mass excavation, soldier piling, crib walls and reinforced soil slopes.

The case studies outlined below highlight the use of soil nailing (including hollow injection anchors), high capacity tensioned wire rock mesh, micropiles, post-tensioned rock bolts, and various types of drilled horizontal drains to repair the areas while minimizing cost, construction time, and impact to the traveling public.

ROCK SLOPE STABILIZATION - UNITED STATES ARMY CORP OF ENGINEERS

Eastman Lake Park is approximately 48 miles north east of Fresno, California in Madera County and is a United States Army Corp of Engineers (USACE) reservoir providing irrigation and flood prevention for local Agribusiness. During the early 1970's the hillside along the southern side of the park was cut to its existing grade of 65 degrees (0.5:1) to construct an access road.

The exposed rock on this slope is systematically jointed and has very blocky characteristics. In general the rock blocks are little to moderately weathered, strong to very strong and moderately hard to very hard. Weathering in the rock mass is concentrated along discontinuity planes, where the rock is generally highly weathered to locally completely decomposed. The rock mass is generally closely to moderately fractured, with mean joint spacing of about 3 to 10 feet. The dominant rock structures were characterized by 4 systematic joint sets and the mean orientations of each of these joint sets are presented in Table 1.

Table 1 - Mean Discontinuity Orientations

Discontinuity Set	Mean Orientation (dip, dip direction)	Comments
J_1	69, 58	Foliation
J_2	79, 300	Joint Set
J_3	48, 143	Joint Set
J_4	21, 9	Joint Set

The 90-ft tall rock cut slope exhibited episodic failures since its construction and generally occurred following periods of substantial rainfall (Figure 1). Some failures had been large enough to block road passage and raise concerns regarding both impending rock fall hazards and the long term stability of the cut slope.

Figure 1. Wedge failure in 2005 following substantial rainfall (photo provided by USACE).

The rock cut slope consists of 980-linear feet of weathered schist and sandstone broken into a lower, middle and upper benches. The lower bench runs the entire 980-linear feet and the middle and upper benches run along 280 linear feet. A concrete v-ditch bench separates the lower and middle section. The average vertical height of each bench is 30 feet. The lower and middle benches are inclined at an average angle of 65 degrees and the upper bench is inclined at an average angle of 45 degrees (Figure 2). Total estimated area of all three benches is 50,000 square feet.

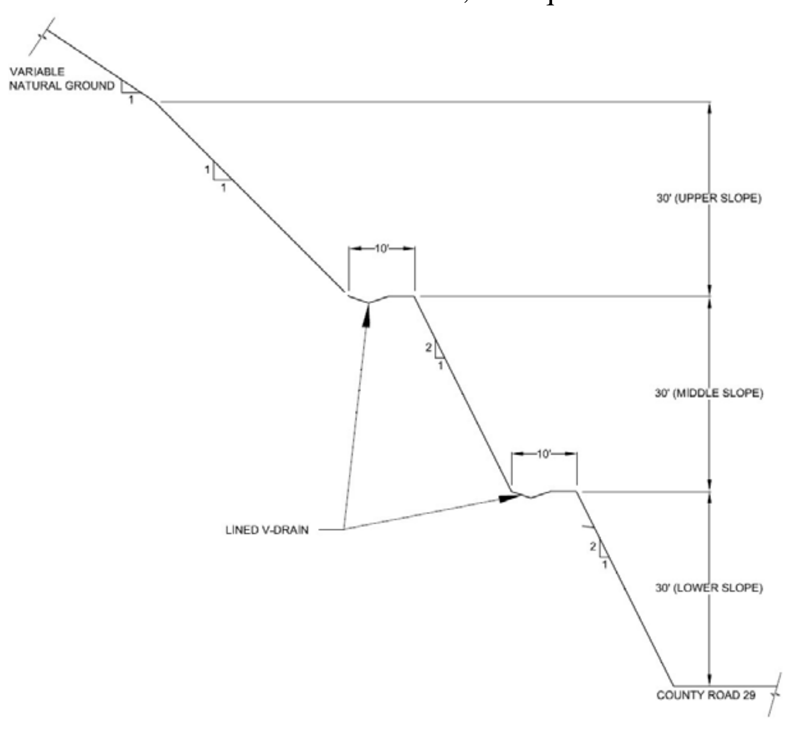

Figure 2: Slope Cross Section

Following heavy rains during the 1996-97 winter season portions of the slope failed. The USACE immediately commissioned a crew to clear debris from the road and scale the slope. In August of 1997 a consultant was asked to prepare a slope evaluation study to include remediation recommendations. Phase one recommendations called for scaling of all loose rock blocks and talus debris and phase two recommendations included rock bolting and surface protection, adding a debris ditch and barrier, mass grading or abandonment of existing alignment.

Upon receipt of the consultants recommendations, the USACE sought out a specialty contractor to scale the rock cut slope. Following the scaling effort the slope continued to exhibit failure and in 2005 produced a large wedge failure that completely blocked the access road (Figure 3). The material was removed and no other remediation measures were employed at the time. During the 2010-11 winter season park officials reported that several large rock blocks up to 30-ft in height and 20-ft in width had fallen on the road and were concerned about the apparent dilatation of some of the rock blocks within the slope.

Figure 3. Failure in 2005 showing rock blocking the access road (photo provided by USACE).

The rock fall during the 2010-11 winter season coupled with the dilation of rock blocks within the slope prompted the USACE to decide on a phase two remediation plan and proceed with implementation. Cost and time directed the USACE to choose rock bolting and surface protection.

A specialty subcontractor worked in conjunction with the USACE to optimize the USACE design to minimize time and cost. The friction strength of the rock blocks were not tested, however the average joint friction angle is likely in the range of about 20 to 30 degrees (Keiffer, 1997). Considering the sensitivity of required bolt spacing to discontinuity strength, bolt orientation and work load, a staggered square bolt pattern with 7-ft spacing between bolts in a single row was recommended. The consultant's report originally assumed a bolt working load of 42 kips with bolts installed horizontally to inclined upward 10 degrees into the hill slope. The USACE choose to use rock dowels with a bond breaker as opposed to "spin-lock" type mechanical rock bolts because of concern that the rock was not hard enough to properly lock the bolts in place. A rock dowel offers a longer grout to rock bond hence is able to insure a stronger overall bond in soft rock when compared to mechanical rock bolts. In the time between the consultant's report date and 2011 rock block failures suggested that the original 10-ft and 14-ft recommended bolt length would need to be lengthened to 20-ft and 24-ft. The additional length was determined by size of failed blocks. The working load of each dowel was increased to 59.3 kips and the dowels were installed at a 10 degree sub-horizontal angle to minimize safety concerns and allow for the use of cement grout. A double twist wire mesh cable system with a tensile strength equal or greater than 15,000 lbf/ft and 5,500 lbf/ft transverse strength was selected as the surface treatment.

Construction started in May 2011 with a scaling operation then followed by installation of the rock dowels and double twist wire mesh cable system (Figure 5 & 6). To date the USACE reports no further dilation or failure of the rock slope.

Figure 4. Scaling and rock dowel installation in progress.

Figure 5. Rock dowel post tensioning and double twist wire mesh cable system.

PACIFIC COAST BLUFF REPAIR – CALTRANS DISTRICT 4

Sliding at Pescadero Creek Road in San Mateo County, began in the early 1970's and intermittent movement continued until final remediation measures were installed in 2010. Boring logs showed mudstone, shale, and sandstone overlain by approximately ten feet of sand and silt. The headscarp started at the centerline of the 24-ft wide highway and terminated outside the shoreline (Figure 7). The movement from the slide resulted caused roadway cracking and differential settlement along 140-ft of roadway. CalTrans maintenance staff would typically level the drop with hot mix asphalt to temporarily maintain a safe travel way for the motoring public. At some point in time between the early 1970s and 2010 CalTrans maintenance staff excavated the top of the slide to an approximate depth of 5-ft and replaced the sliding material with a light weight volcanic backfill. In early 2010 CalTrans maintenance staff reported that the slide exhibited an increased rate of movement, requiring them to return to the site on a daily basis to add asphalt to the road surface. CalTrans Geotechnical Design West installed an inclinometer casing at the slide location. Inclinometer data showed that the slip plane at the outboard edge of pavement was in a weathered mudstone formation at approximately 35-ft below the roadway elevation. Within two weeks the inclinometer had moved 1.29-inches and subsequently sheared. CalTrans Geotechnical Design West recommended emergency action to make permanent repairs to the slide and an emergency contract was issued to a local prime contractor.

Figure 6. Cracking in road platform is beyond centerline.

CalTrans Construction required the prime contractor to select a specialty design/build contractor to design the repair and conduct the specialty geotechnical construction activities. During the design phase of the project CalTrans provided a cross section, a plan view sketch of the slide, inclinometer and bore log data, and a listing of design requirements. Due to the importance of the roadway and the proximity to the ocean, CalTrans required that the repair operations keep the highway open to traffic, limit activities to the 30-ft right of way (measured from center line), and be virtually invisible from offshore when completed. The design was based on a 75 year service life with a minimum factor of safety of 1.1 under seismic loading and 1.5 under static conditions. From this information the specialty design build contractor conducted a back analysis to determine assumed soil properties (Figure 8 & 9). With this predictive modeling the design build contractor then designed a repair scheme that required 13-FT excavation just outside of the edge of pavement, a 1400-SF hollow bar soil nail wall tied to a reticulated micropile and a reinforced micropile cap (Figure 10). The excavated soil was then placed back over the repair and hydroseeded with a native seed mix (Figure 11).

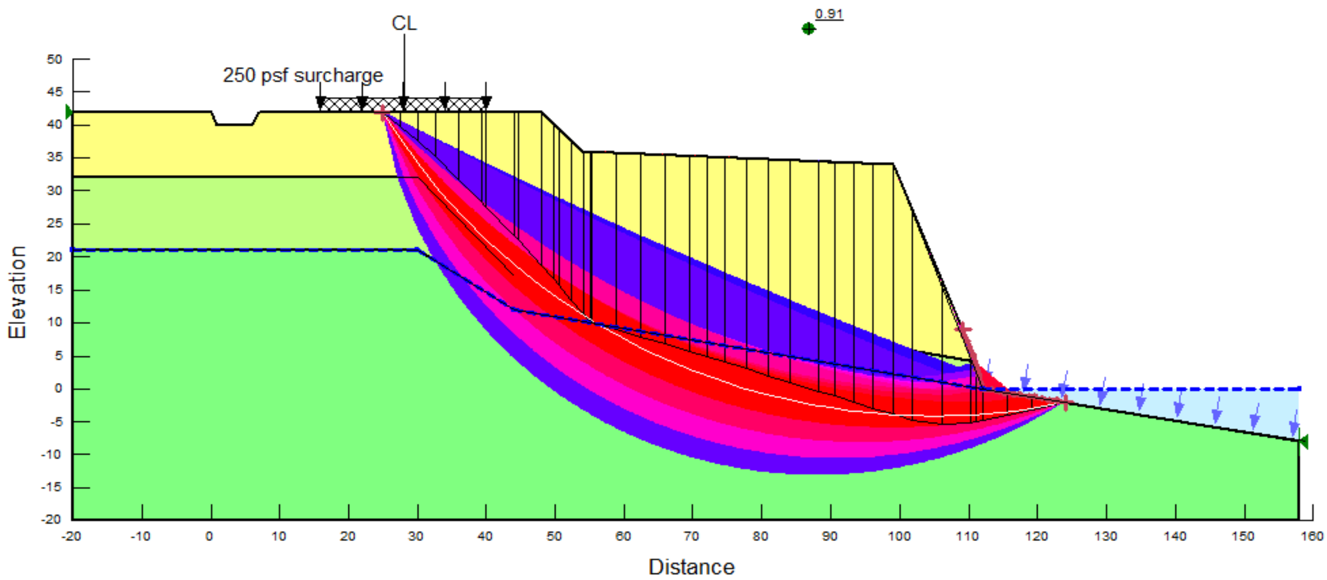

Figure 7. Back calculation analysis indicating unity.

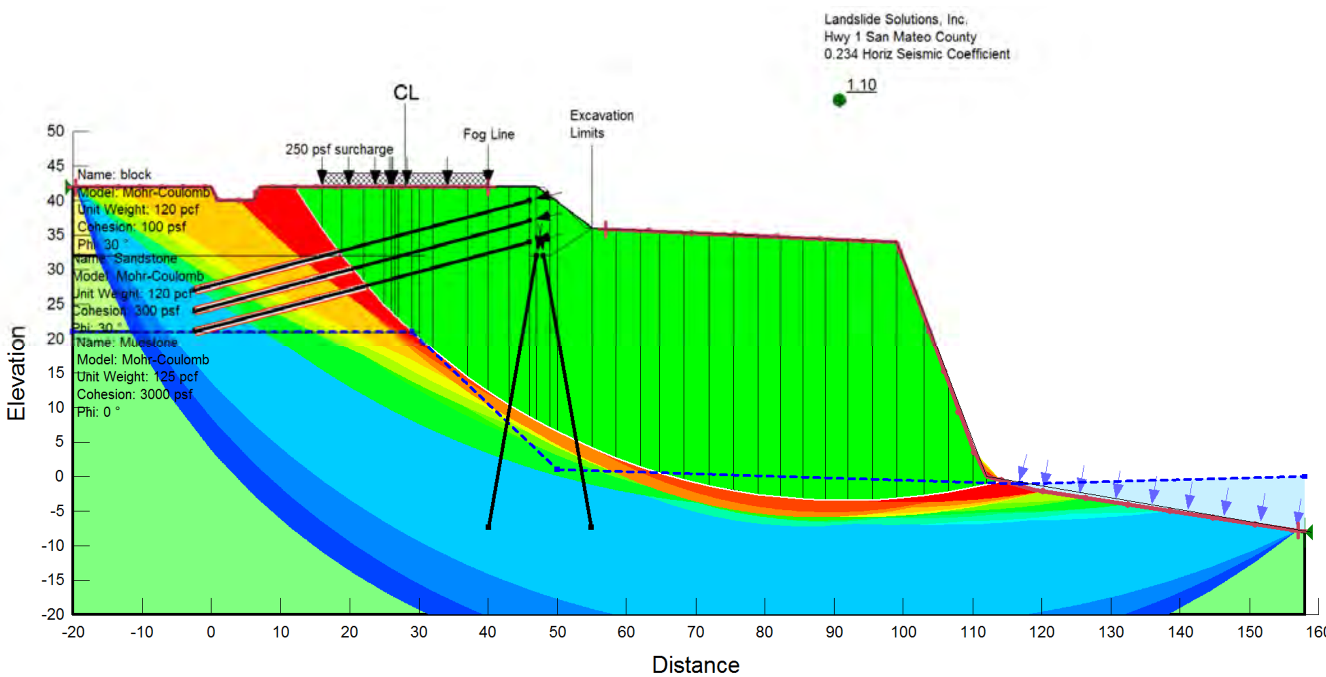

Figure 8. Repaired slide indicating 1.1 FOS under seismic.

Figure 9. During construction - showing excavation of the second cut.

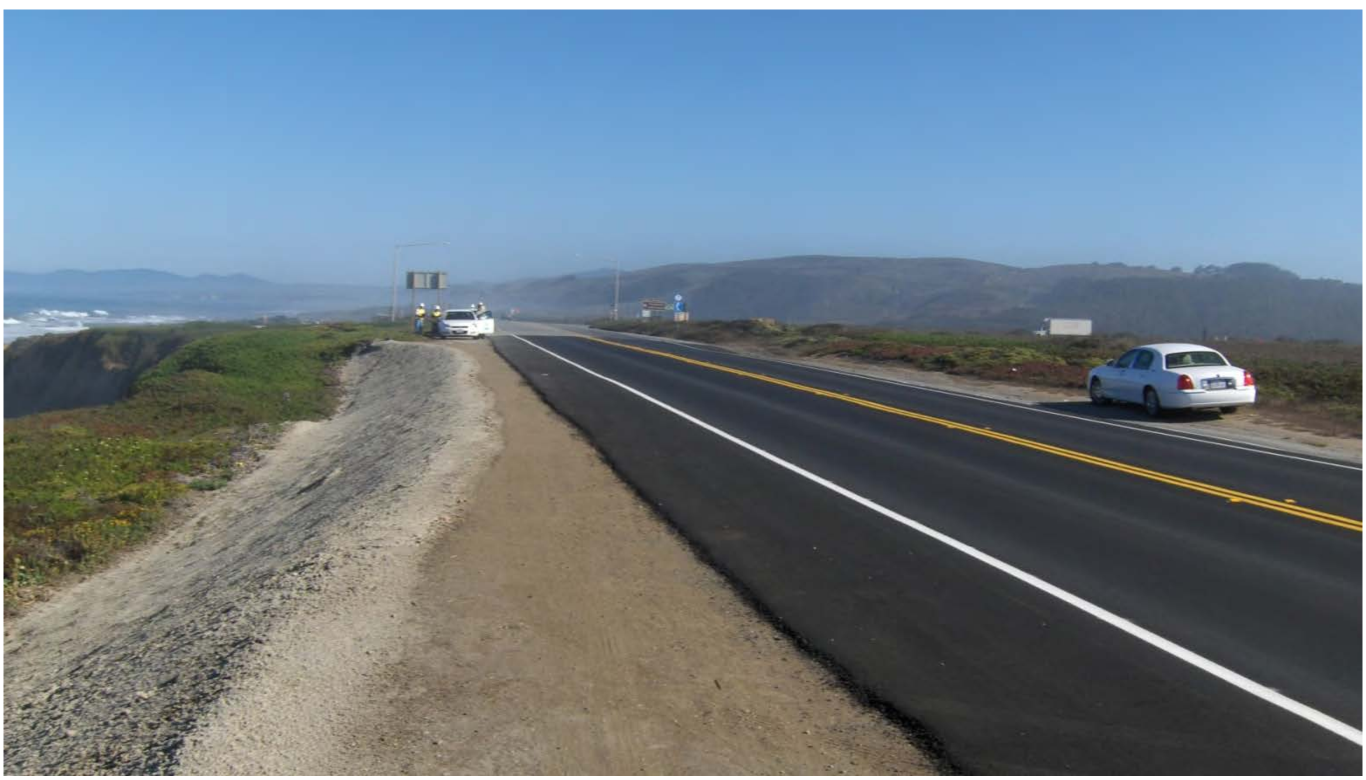

Figure 10. After completion of the repair - note that repair was completely covered and what looks like shotcrete is hydroseed (photo provided by CalTrans District 4).

Five weeks after mobilizing to the site, the specialty design/build contractor stabilized the slide. Cal-Trans reported a cost savings of over 2 million dollars when compared to improvement conventional piling wall project planned for the site. Inclinometer casing was installed to verify performance. Movement rates suggest that the landslide movement has decreased from over 50 inches per year to under 0.08 inches per year (Figure 12).

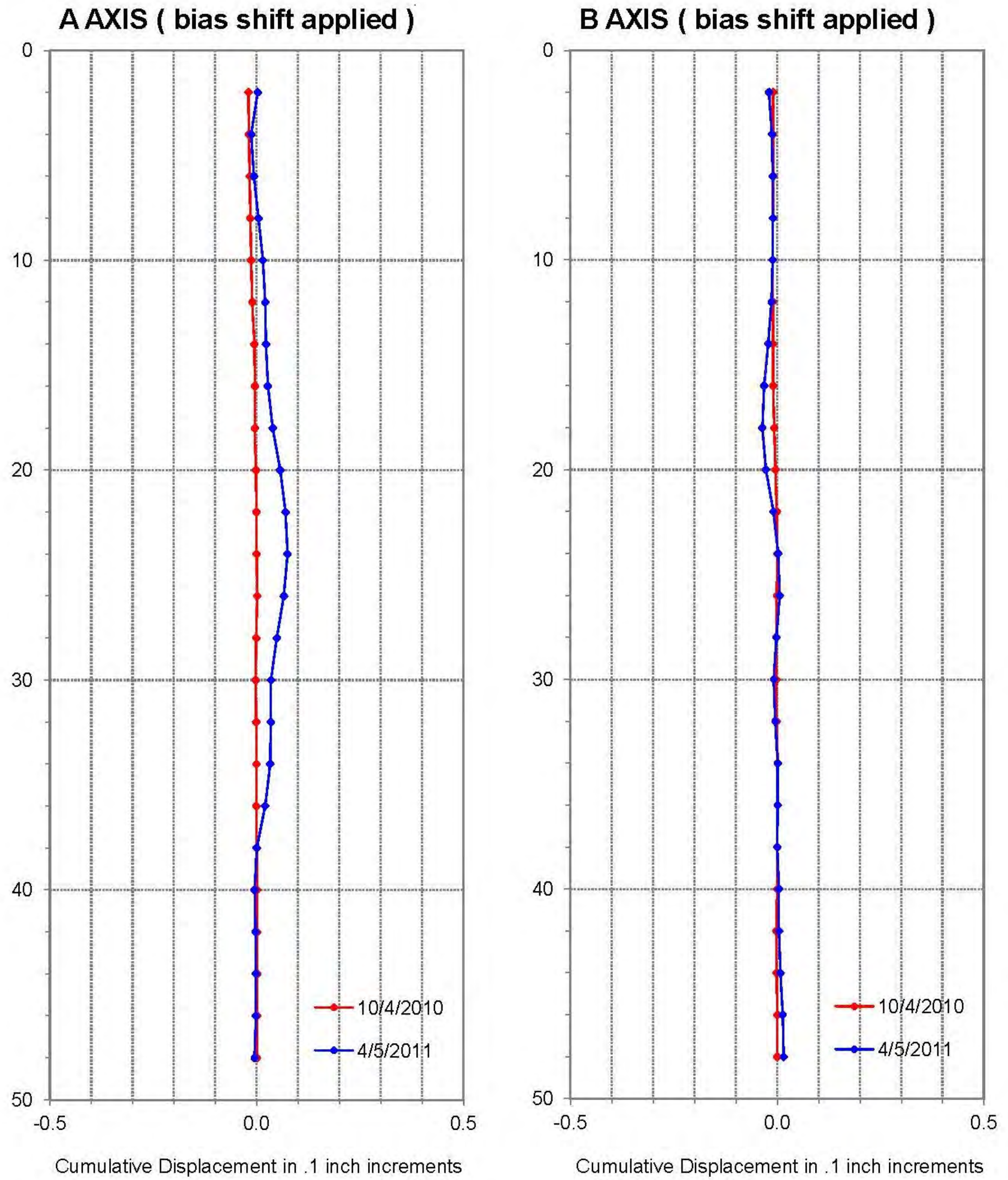

Figure 11. Inclonometer data showing less than .08 inch movement 6 months from installation of the repair.

LANDSLIDE REPAIR – CALTRANS DISTRICT 2

During the 10-day deluge of rain in March of 2011 an existing landslide on Hwy 299 in Trinity County California reactivated and exhibited accelerated movement of up to 3-inches a day (Figure 13). CalTrans District 2 Maintenance Engineering staff asked a specialty design build firm to provide a design and cost estimate to repair the slide. The design was formulated using a cross section survey of the slide coupled with back calculation analysis. The outboard fill slope was modeled with a fairly deep-seated failure plain with zero cohesion. Within days after receiving a formal notice to proceed the specialty contractor mobilized to the slide and started the repair process.

Figure 12. 3-inch tension crack developed over the course of 24-hours.

As-built records as far back as 1983 indicated that CalTrans had been challenged by a fairly deep seated landslide on Hwy 299 in Trinity County California at mile 49.1. Initial efforts to stabilize the slide included the installation of a stab drainage trench at the uphill edge of road and several horizontal drains. At some point in time between 1983 and 2011 the road was widened and a third passing lane was added. Until the permanent repair was installed in the spring of 2011 local maintenance crews continued to struggle with the slide and were forced to maintain the travel way with regular repaving efforts.

The specialty contractors repair design included a combination of self drilling soil nails with self drilling micropiles and the road was open throughout the entire of construction process (Figure 14 & 15). The soil nails with a design load of 1,500 lbs/ft were embedded twenty feet past the failure zone into silty sand. According to CalTrans this system saved the agency over half the cost when compared to traditional landslide repair techniques.

Figure 13. Excavation of second cut to accept soil nails - note that all construction is taking place on the shoulder of the road.

Figure 14. Completed project after 5 weeks of construction.

LANDSLIDE STABILIZATION – SANTA CLARA COUNTY

High in the Santa Cruz Mountains Santa Clara County is responsible for several precarious cut / fill roads with inherent slope stability issues. Once such road fell victim to the 2010-11 storm year after a landslide left a 13-ft tall near vertical head scarp on the outboard side of the road (Figure 16). The slide consisted of a stiff clay block failure. This road services several multimillion dollar mountain homes and is the only way in and out for critical services. The local fire department was particularly concerned about the road because of the surcharge their equipment places on the road system and the reduction of road width caused by the slide. Santa Clara County instructed their on-call contractor to hire a specialty contractor to design and construct the slide repair.

Figure 15. 13-ft tall head scarp.

Upon arriving onsite the specialty design build contractor conducted an onsite cross section survey above and below the road. Within days from notice to proceed construction activities started. The design called for four rows of 30-ft long self drilling soil nails embedded into bedrock with a design load of 1,500 lbs/ft and a shotcrete facing (Figure 17). The shotcrete facing was installed in such a fashion to regain two additional feet of roadway width to accommodate fire equipment. Construction was complete within 2.5 weeks (Figure 18). An inclinometer casing was installed to verify performance and to date the repair has shown deformation commensurate with a traditional soil nail wall (Figure 19).

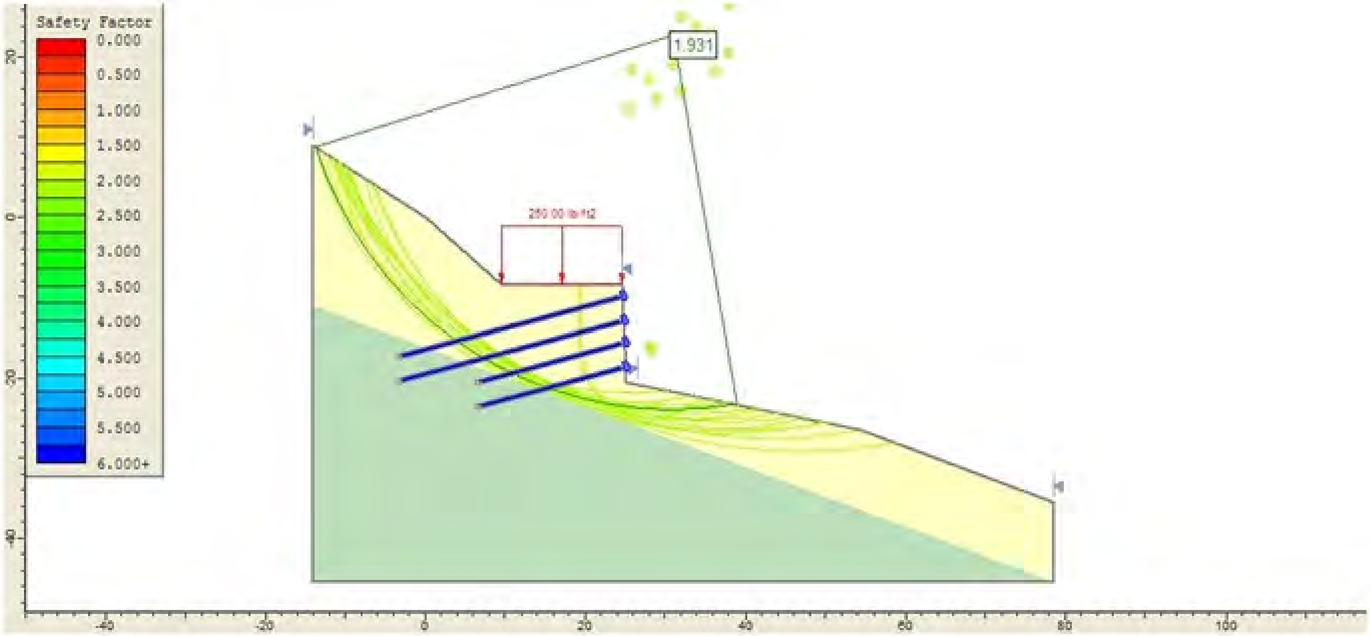

Figure 16. Stabilized head scarp above 1.9 FOS under static.

Figure 17. Completed project after 2.5 weeks of construction.

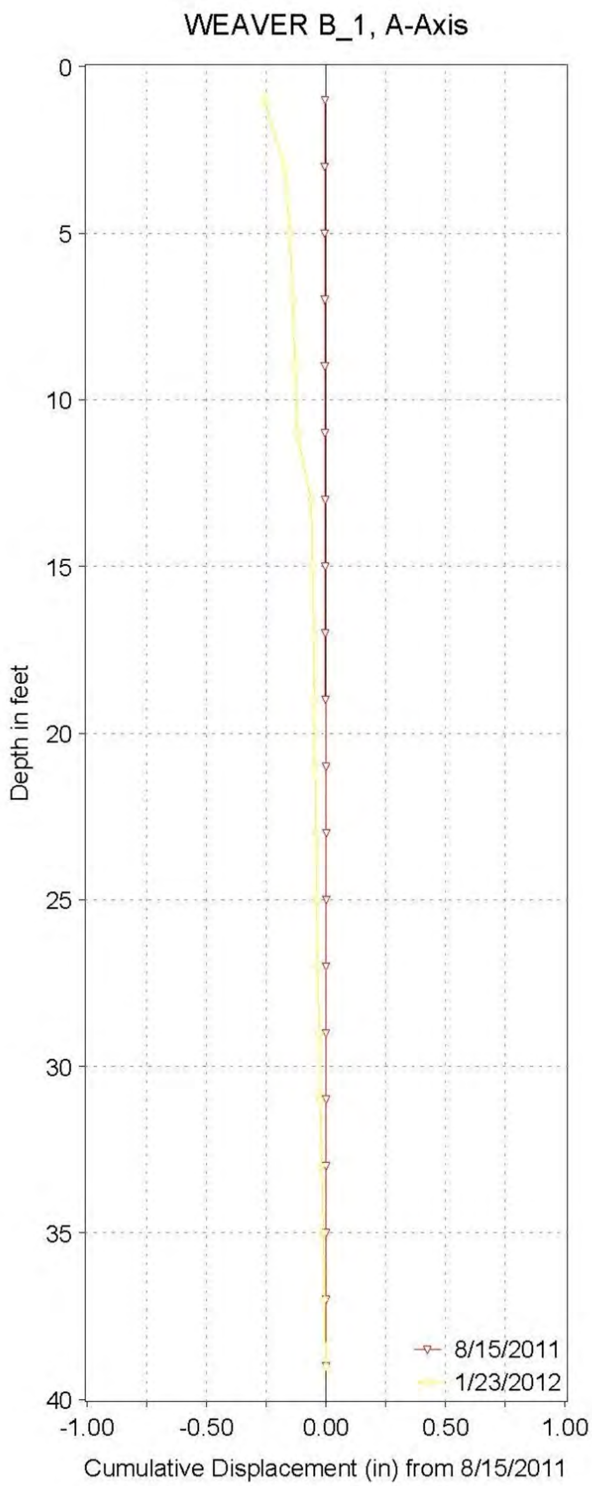

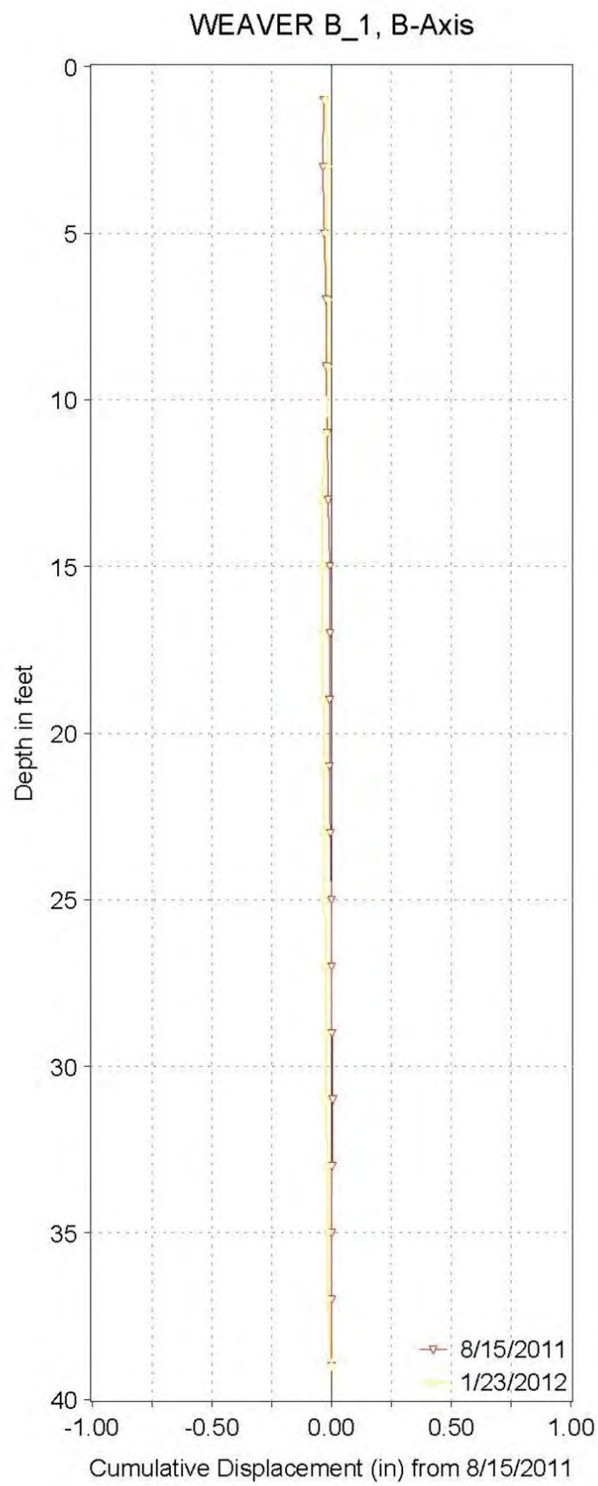

Figure 18. Inclinometer data showing marginal movement 5 months from installation of the repair.

LANDSLIDE STABILIZATION – USDA FOREST SERVICE

Thirteen slides were stabilized along a one lane, one way access, four mile long, unpaved forest road in the Stanislaus National Forest. Conventional side cast construction was used along most of the road. The slides developed at the interface between original ground and the cast material (Figure 20).

This road was constructed to access Tuolumne River at the bottom of the cannon. The river cannon is now registered as a “Wild and Scenic Corridor” requiring specific detail to maintaining its natural look and function.

Figure 19. Slip line at the interface between original ground and side cast.

The Forest Service categorized the slide repairs depending on funding source and severity of the slides. These categories where then associated with specific mitigation regimes which included; deep patch, deep patch with micropiles, and soil nails with shotcrete facing. The deep patch method was prescribed on ERFO (Emergency Relief Federal Owned) funded sites where the slide slip line was less than three feet from the edge of roadway. Deep patch with micropiles was prescribed on ERFO funded sites where the slide slip line was three feet or more from the edge of roadway (Figure 21). The patching method is generally described as over excavating a slide area then replacing the soil with geosynthetic reinforcements. Soil Nails with shotcrete facing were prescribed on CIP (Capital Improvement Project) funded sites (Figure 22).

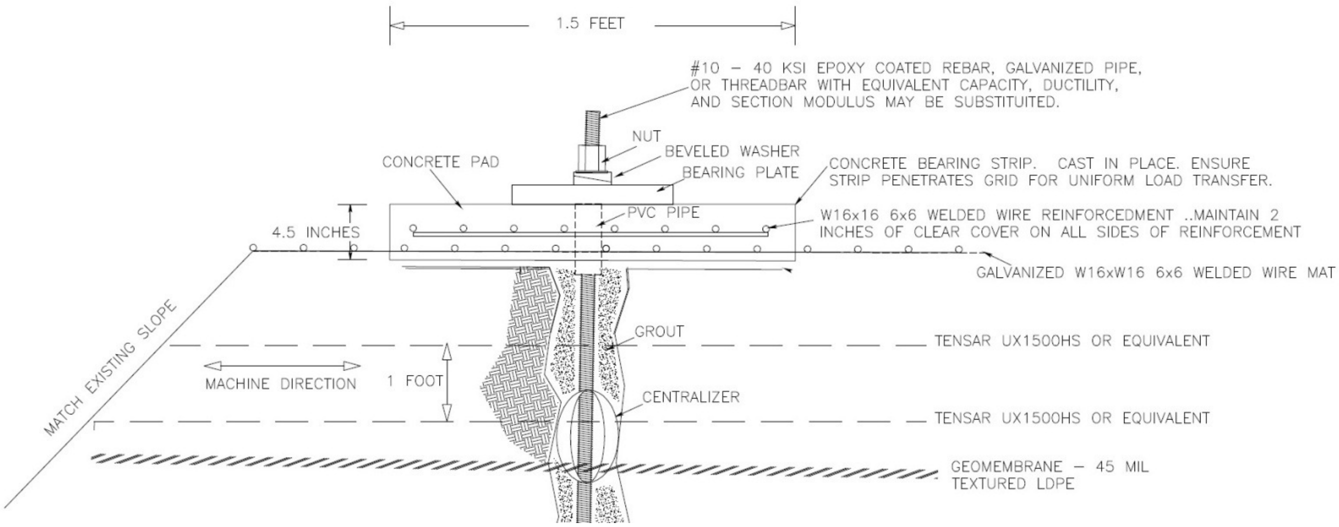

Figure 20. Plan indicating micropiles being installed through a deep patch. The purpose of the micropiles is to add lateral resistance to the deep patch system.

Where soil nails and shotcrete were to be installed the Forest Service sought the expertise of a specialty design build firm to develop the design and plans for each individual site.

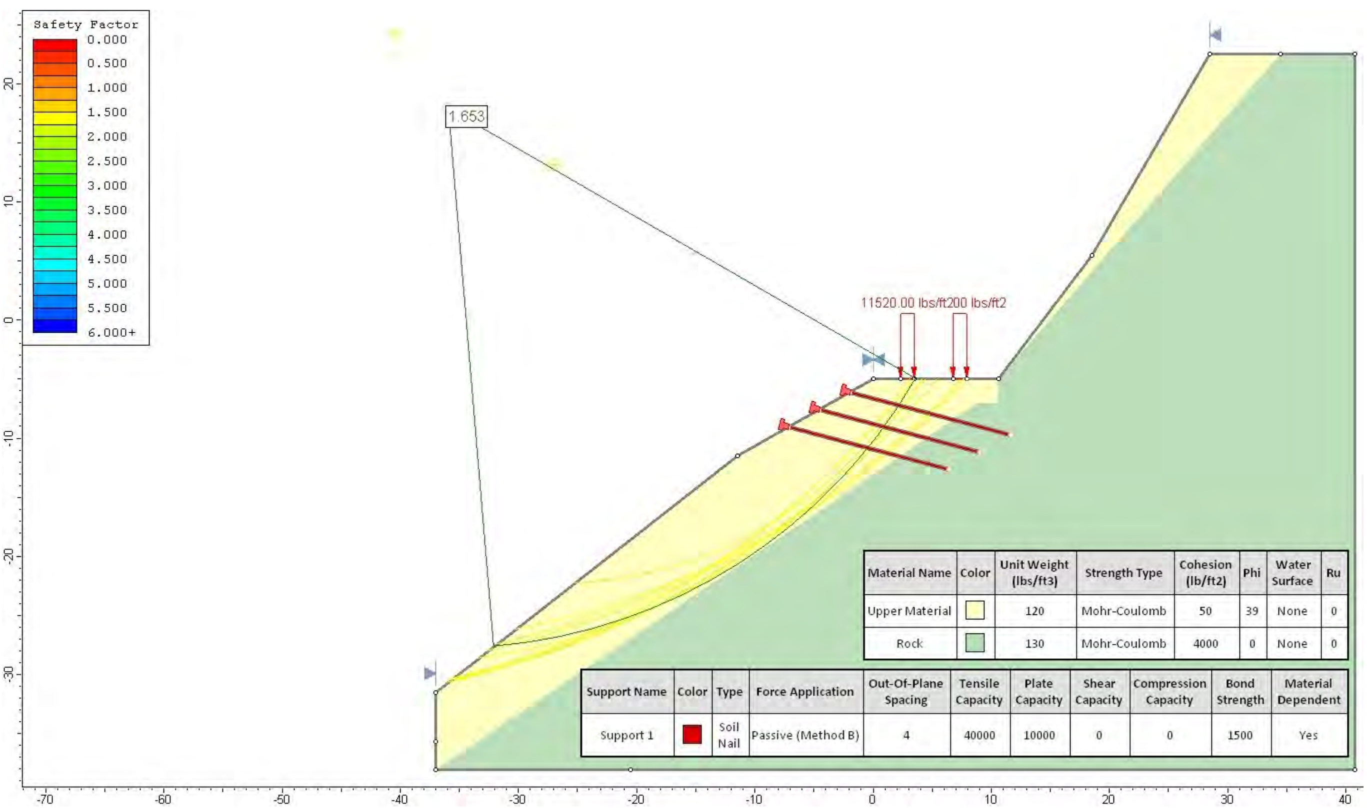

Figure 21. Repaired slide indicating above 1.5 FOS under static.

In addition to traditional shotcrete the design build company choose to install sculpted and stained shotcrete at several high visibility sites (Figure 23).

Figure 22. Sculpted and Stained Shotcrete.

CONCLUSIONS

Road maintenance, engineering and geotechnical practitioners have many options to choose from with respect to landslide and rock slope repair tools and techniques. The more versatile the tools and techniques are with respect to varying soil and rock types certainly makes a positive time and cost impact. Many of the tools and techniques discussed in the case studies can rapidly be deployed to emergency type situations.

REFERENCES

Musser, S. and Denning, C, 2005, Unites States Department of Agriculture Forest Service, Deep Patch Road Embankment Repair Application Guide, Introduction, Page 1

Rocscience Inc., 2011, Slide, Rocscience Inc., Version 6.0

Kieffer, S., 1997, Cut Slope Stability Evaluation Eastman Lake Access Road (County Road 29, STA 92+00 to 101+00) Madera County, California, Independent Consultant, Site Conditions and Discussion and Recommendations, Pages 2-4 and 9-13

I-40 along the Cumberland Escarpment
Highway Instability, Historic Reviews, and Remedial Concepts

Deana Sneyd, PG, Anthony Sak, PE & Harry Moore, PG
Golder Associates Inc.
3730 Chamblee Tucker Road
Atlanta, Georgia, USA
(770) 496-1893
dsneyd@golder.com; *tsak@golder.com*; *hmoore@golder.com*

David H. Barker, PE
Tennessee Department of Transportation
Knoxville, Tennessee, USA
(865) 594-2702
david.h.barker@tn.gov

Len Oliver, PE
Tennessee Department of Transportation
Nashville, Tennessee, USA
(615) 883-8930
Len.Oliver@state.tn.us

Prepared for the 63rd Highway Geology Symposium, May 7-10, 2012

Acknowledgements

Disclaimer

Statements and views presented in this paper are strictly those of the author, and do not necessarily reflect positions held by their affiliations, the Highway Geology Symposium (HGS), or others acknowledged above. The mention of trade names for commercial products does not imply the approval or endorsement by HGS.

Copyright Notice

ABSTRACT

The eastern Cumberland Plateau Escarpment, separating the Cumberland Plateau and the Valley and Ridge Physiographic Provinces, has a record of hampering highway construction in central East Tennessee, due to a combination of steep natural slopes, thick accumulations of colluvium, and the presence of swelling clay from the Pennington Formation. In that record is the 1968 construction failure of approximately 370 meters of eastbound Interstate Highway 40 embankment. Planned as an up to 43-meter high embankment across the Escarpment, the Tennessee Department of Transportation (TDOT) responded to the landslide and embankment failure through geometric modifications and slide mass drainage using dewatering wells and horizontal drains. Even with these mitigation measures and periodic installation of additional horizontal drains, movement of the slide mass has continued through the ensuing decades. Measurements in 2010 had shown displacement on the order of 25 millimeters per year, requiring annual resurfacing of the pavement.

Interstate Highway 40 (I-40) is a heavily-traveled, east-west interstate through the mid-section of the United States. Traffic safety concerns with a traffic-disruption threat led TDOT to request a detailed review of the available project documentation by Golder Associates Inc. Since the initial slide, limited topographic, geologic, and geotechnical data have been gathered and assimilated for evaluation of the slide. As a result of Golder's review, additional slope inclinometers and automated vibrating-wire piezometers were installed to better define the conditions and their variation with time. A limited laboratory testing program was conducted for evaluating potential remediation options. Installation of a system of dewatering wells and horizontal drainage was initiated in late 2011 in an effort to mitigate further displacement. Implementation of these drainage measures was still underway at the time of publication.

This paper presents the historical background, results from the first year of slope and groundwater monitoring, dewatering program, and feasible remediation options available to TDOT in order to improve the margin of safety on this career-spanning slope failure.

INTRODUCTION

The Mississippian-age Pennington Formation has been associated with numerous slope stability problems throughout the Southeastern United States since modern road building began. This geologic formation is predominantly comprised of calcareous, marine shale that weathers deeply in a subtropical climate due to both physical and chemical degradation. The weathered product is a fine, residual clay that readily absorbs water. The Pennington is typically overlain by massive sandstones and siltstones which are pervasively undercut in scarp slopes as the Pennington weathers, resulting in a heterogeneous mass of colluvial material overlying the residual soils. Surface and groundwater flows through the relatively permeable colluvium and tends to perch along the interface between the colluvial and residual soils. The clayey soil tends to absorb water, becoming very weak and unable to resist the downward pressures of the overlying colluvial material. Slope movements within this geologic environment range from the occurrence of progressive creep spanning decades to abrupt, catastrophic failure, associated with sliding along the unstable interface between the colluvial and residual soils as well as within the residual soil/weathered rock mass. Placement of roadway embankments over these deposits exacerbates the destabilizing conditions.

I-40 crosses the eastern Cumberland Plateau Escarpment in central East Tennessee, between the folded and thrust-faulted Valley and Ridge to the east and the relatively flat-lying Cumberland Plateau to the west. The escarpment is draped with colluvium, consisting of boulder through clay-sized soils that originated as "talus" material accumulated at the front edge of the plateau and has weathered through time. Steep natural slopes, thick accumulations of colluvial material and the presence of weak weathered rock/clay within the Pennington Formation have collectively hampered construction performance of the east bound lanes (EBL) near Roadmarker (Mile Post) 342 in Roane County, Tennessee, located on Figure 1, for over 44 years. Problems began with a catastrophic failure during construction in 1968 and continue with ongoing down-slope creep that has caused frequent maintenance issues for the highway pavement.

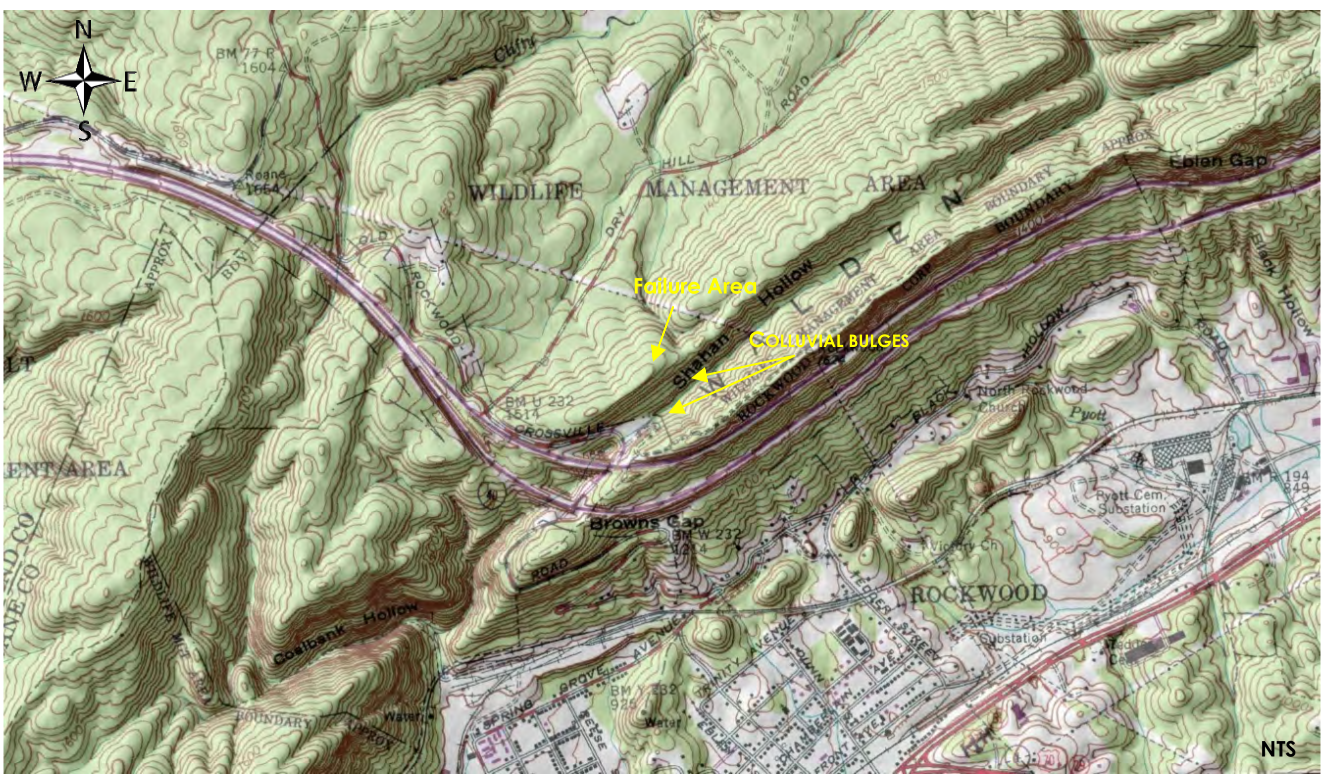

Figure 1. Site Location

REVIEW OF HISTORICAL RECORD: 1968-2003
Failure During Construction

Construction of an up to 43 meter high embankment for the EBL of I-40 began in August 1967. Initial failure of a 370 meter section of the embankment occurred in January 1968 when the fill placement had reached 27 meters in height (Royster, 1973). The fill slide was referred to by TDOT as the Original Fill slide or Major Fill slide and later designated as Slide E-1. A total of 20 major slides developed within a 6.5-kilometer interval during I-40 construction in this area. Construction of the fill was halted in March 1968. Initially, it was assumed that the movement was related to settlement of the embankment fill, so additional fill was placed on top of the embankment. When the embankment did not stabilize, the roadway design was revised to move the alignment further north and lower the road grade of the eastbound lane substantially. With a smaller embankment, the rapid large-scale movement ceased, but smaller movements continued.

FIRST RESPONSE
Geotechnical Evaluation

Law Engineering & Testing Company (Law) was retained following failure of the embankment to evaluate the slide and develop remedial options for slope stabilization (Law 1969). A grid of survey markers were initially installed in July-September 1968 on the slope of the Major Fill Slide on 30-meter centers. Based on survey results from August 1968 to May 1969, down-slope displacements of up to 2.3 meters were measured, with most of the movement occurring near the head scarp and middle portion of the slide area. Law also evaluated aerial photographs that TDOT collected during construction, performed surface geologic mapping, advanced nine geotechnical borings, installed six inclinometers and four piezometers, and conducted limited geotechnical laboratory testing. The geological structure, depth, orientation and nature of the sliding surface in the middle of the slide mass beneath the embankment, geotechnical characterization of the units, and nature of the groundwater conditions, however, were not well defined for the bulk of the slide mass and at depth.

Initial Remedial Action: 1968-1972

TDOT initially responded to the landslide and embankment failure through roadway geometric modifications and slide mass drainage. The redesign primarily consisted of lowering the vertical grade 12 meters below the original planned grade and shifting the alignment to the left (north). Uphill of the east-bound lanes, a perforated 200 mm diameter, corrugated metal pipe was placed in an excavated drainage trench backfilled with crushed stone in April 1968. The intent of this drain was to catch surface water sheet flow upslope of the slide mass to limit infiltration of water into the ground. The pipe drained into a catch basin and a 1 meter diameter pipe that was subsequently removed in August 1968 after it was damaged by continuing slope movement. The location of this movement indicated that the headscarp of the landslide occurred further north than previously understood.

In June 1968, a series of 0.9 meter diameter, 10.7 to 12.2 meter deep, stone-filled shafts were installed right of the toe (at that time) of the fill slope within the slide mass. It was anticipated that this would relieve water pressure within the mass, thereby reducing slide movements but not prevent them from continuing. While no major movements occurred when the embankment was constructed to the redesigned grade, minor movements continued to occur that totaled 150 to 200 mm vertically per year between 1968 and 1972.

In March 1972, a large slide developed in the west end of the Major Fill slide as a result of excessive loading in the area. Consequently, the embankment was again lowered to its present grade. In July 1972 construction of a small rock buttress was initiated to stabilize the west-end slide. The buttress was completed in September 1972.

REMEDIAL EFFORTS: 1972-2009

Movement continued but on a lesser scale from 1972 to 1975. Vertical movement during that time was on the order of 75 to 125 mm per year. The slide movement, however, was significant enough to disrupt pavement along the adjacent Airport Road necessitating repairs to that roadway. Forty-four horizontal drains were installed in December 1972 most of which were dry initially and became active during wet periods (Trolinger, 1980; Royster, 1977, 1979). Seven slope inclinometers were installed during March and April 1974 below the toe of the embankment. Detailed measurements at the time indicated horizontal movement of 75 to 150 mm with 150 to 200 mm of vertical displacement. Due to this additional movement, multi-level piezometers were installed within the slide to better define the depth and lateral continuity of water-bearing zones within the mass. Additionally, a well point and several deep piezometers were installed in the slide in an effort to determine if the slide mass could be dewatered. Water was encountered at only two locations, and correlations between these could not be made.

On August 19, 1974 the EBL's were opened to traffic. In September, a total of 3,000 meters of horizontal drains were installed from two pad setups; ten holes at Pad "A" and twenty-three at Pad "B" (Royster, 1977). Eventually, the dewatering system reduced movement of the slide mass to about 15 mm per year. From approximately 1977 to 1994 the Major Fill slide area only required routine maintenance that involved periodic overlays of asphalt to seal the slide cracks that would show in the roadway driving surface.

Through the 1990's, additional horizontal drains were installed along with geomembrane-lined drainage ditches below the toe of the embankment to limit infiltration of stormwater and horizontal drain discharge into the slope. In June 2003 three additional slope inclinometers were installed by TDOT below the roadway fill as a result of movements in the embankment and resulting pavement cracking. Numerous readings were taken and all showed distinct movements at depths from near 12 to 23 meters below ground surface. In about 2005, TDOT maintenance forces performed some ditch work at the fill slide site to help alleviate runoff drainage issues thought to potentially be contributing to the slide movement. The ditches along the fill toe area were cleaned out and rip-rap was placed in the ditches to help prevent excessive erosion.

Even with these mitigation measures and installation of additional horizontal drains, movement of the slide mass has continued. Asphalt-pavement overlays continue to be required on a periodic basis to compensate for the vertical displacement experienced at the I-40 Major Fill slide site.

CURRENT EVALUATIONS: 2009-PRESENT

TDOT decided to solicit an independent evaluation of work performed to date that would result in short- and long-term recommendations for remedial action. Golder Associates Inc. (Golder) was retained in 2009 to review over 270 documents related to the site, including geotechnical engineering files, reports, tests, and monitoring results pertinent to the subject landslide and provide recommendations concerning additional data needs and potential remedial measures. However, given the long chronology of geotechnical issues at the site, much of the actual data collected during construction and initial remedial response had been lost.

During the document review, relevant geotechnical boreholes, instrumentation, geologic mapping, geomorphic interpretations from aerial photography, and location of horizontal drains were compiled on a base map and cross section constructed through the slide mass. Based on these graphics, it became evident that the vertical and horizontal distribution of the geotechnical data did not adequately characterize ground conditions associated with the slide mass. Only two inclinometers were functional, the efficiency of the horizontal drains to perform their intended design function had been reduced, current pore water pressure on the sliding surface was unknown, geotechnical characterization of the fill, colluvium, residuum, and rock was lacking, and geotechnical laboratory data available to characterize the slide was modest by current standards. Consequently, additional geologic and geotechnical evaluations of the slide mass were performed.

Remote Sensing and Geologic Mapping

The TDOT archive contained two sets of black and white vertical aerial photographs with stereo pairs for 1969 and 1974 (i.e. during construction of I40). Golder's review of the TDOT aerial photographs indicated a lot of earthwork construction in the area of the embankment. In order to gain an appreciation of the preconstruction topography, black and white aerial photographs with stereo pairs were obtained from the USDA at 1:20,000 scale, dated October 1961 and November 1967. A series of elongate, arcuate-shaped or curvilinear features were observed to occur upslope of the current location of the EBL on both sets of USDA photos. As shown on Figure 2, the largest arcuate feature extends about 1,285 meters laterally and appears to be locally oversteepened as compared to the relatively shallower-dipping topographic slope observed along the ridgeline northeast and the slope southwest of the feature. Several minor arcuate-shaped features and a large topographic bulge were also identified on the aerial photographs downslope of the large arcuate-shaped feature. The topographic bulge occurs in an area of two colluvial lobes identified by Law in the area of movement, shown on Figure 1.

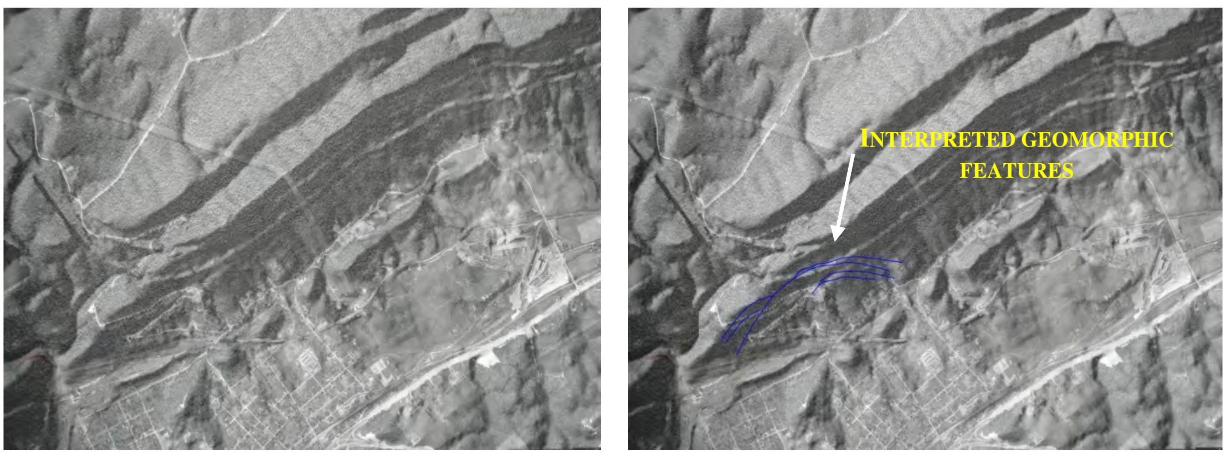

Figure 2. Pre-construction imagery showing interpreted headscarps in area of proposed highway construction. The 1961 photos in these images have been draped over the USGS DEM, which has resulted in I40 being shown on the images, despite the fact that construction had not begun until 1968.

Geologic mapping was conducted in the area around the Major Fill slide, shown on Figure 3. In general, shale with interlayered sandstone of the Pennington Formation was observed in conformable contact with overlying sandstone, shale and coal of the Pennsylvanian-age Gizzard Group.

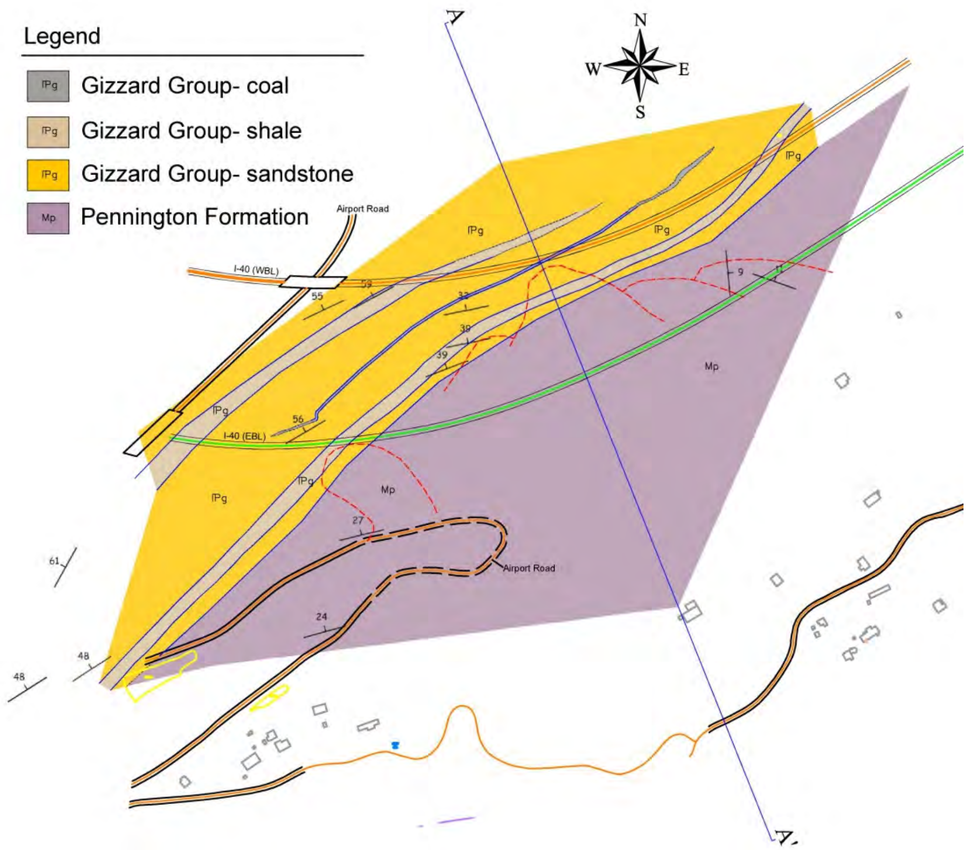

Figure 3. Geologic Plan of Site showing interpreted lithologic and formational contacts. Red curvilinear lines represent scarp slopes observed during geologic mapping.

Mississippian-age Newman Limestone is shown to occur beneath the Pennington Formation south of the site (Jewell and Swingle, 1965), illustrated schematically on Figure 4, a conceptual geologic cross section A-A', location shown on Figure 3. The geologic contact between the Pennington and overlying units along with the contact for mappable sandstone and coal bed are also shown on Figures 3 and 4.

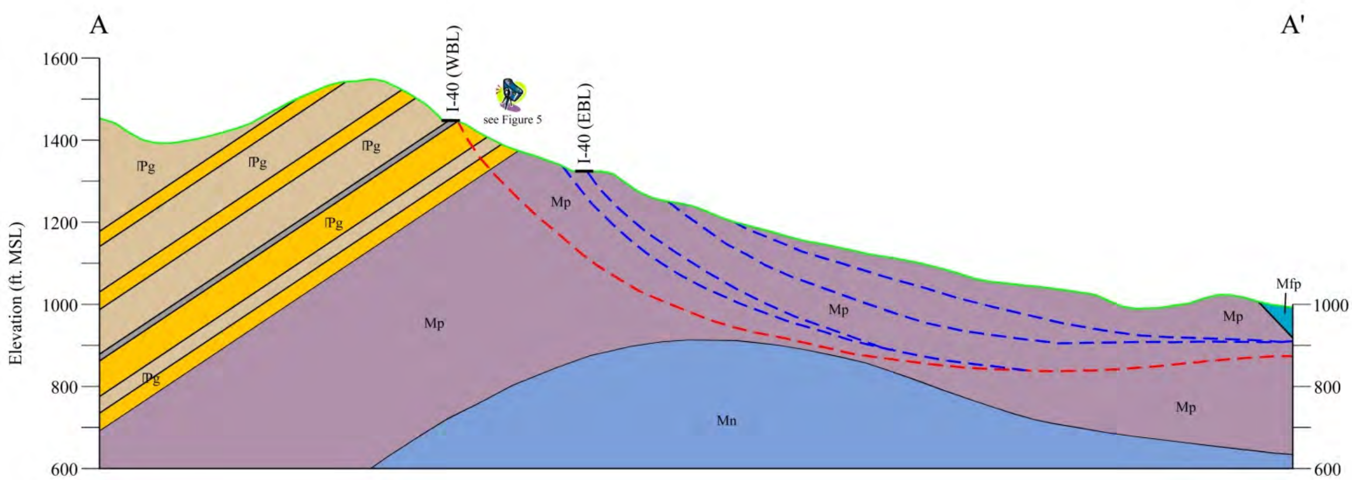

Figure 4. Conceptual Geologic Cross Section of Site. Dashed blue lines represent historic slip surfaces through slide mass interpreted from 1961 imagery. Dashed red line represents recent slip surface observed during geologic mapping in 2010.

In-situ bedrock was observed on the eastern and western flanks of the slide mass, but absent within the slide mass. Bedding planes were observed to generally dip to the northwest or into the slope indicating that the slope on which the embankment was constructed is a scarp slope. Although the site occurs in a structurally complex area within the footwall of the last major thrust fault in the Valley and Ridge, disruption of bedding due to faulting outside of the slide mass was not observed in available exposures during the mapping. Several scarps, shown on Figure 3, were observed upslope of the EBL during geologic mapping and on 2011 imagery. These scarps appear to be more recent than those identified on the 1961 imagery (Figure 2).

A well-developed strike joint set was observed dipping to the southeast, orthogonal (dip direction) to bedding in the Gizzard Group sandstone layers overlying the Pennington Formation. Release along this joint set was observed within sandstone bedrock underlying the WBL, resulting in the headscarp of the failure occurring adjacent to the south shoulder of the WBL, as shown on Figure 5. The new headscarp post-dates those identified on the pre-construction aerial photographs (Figure 2) and is also shown in plan view on Figure 3 and schematically in cross section on Figure 4.

Figure 5. Photograph of Recent Slope Failure beneath WBL, looking east

Landforms identified from the remote sensing evaluation and geologic mapping, including the large- and small scale arcuate features shown on Figures 2 and 3, and the topographic bulge shown on Figure 1, are considered to represent relict (historic) dormant landslide headscarps and an associated colluvial debris pile that predates highway construction. The minor scarps shown on Figure 2 are interpreted to represent displaced material of the landslide downslope of the main headscarp, produced by differential movements within the displaced mass. The topographic bulge observed on the imagery and topographic maps potentially represents the foot and toe of the relict slide mass, now consisting of two colluvial bulges downslope of the EBL. The bulges were likely a single mass following initial slope movement. Springs emanating from the mass may have followed a radial crack, resulting in development of a perennial surface-water drainage dissecting the mass into two lobes, as shown on Figure 1. The topographic surface on the bulges is currently characterized by hummocky terrain with local, discontinuous transverse ridges. Structural orientation of rock exposure observed within the slide mass does not follow local trends observed on the flanks of the mass.

The spatial relationship of the geomorphic features identified on 1961 imagery (Figure 2) and scarps identified during geologic mapping (Figure 3) with respect to the constructed EBL and associated embankment is shown on Figure 6. Based on this spatial relationship, it appears that the EBL embankment was constructed on top of the weathered mass of a historic landslide. Although interpretation of the mechanism of slope movement was inconclusive based on results of remote sensing analysis and geologic mapping, a failure mechanism can be surmised from the following observations:

- Interpretation of historic landslide scarps on pre-construction aerial photographs. The size of the scarp, along with observed bedrock cropping out along the ridgeline adjacent to the scarp, suggests that slope failure may have extended down into the bedrock
- Interpretation of colluvial bulges with hummocky terrain present downslope of the landslide scarps on historic aerial photographs and topographic maps
- Identification of a strike joint dipping and observed, recent failure along this joint set within the overlying sandstone
- Deeply weathered calcareous shale of the Pennington Formation occurs underlying massive sandstone

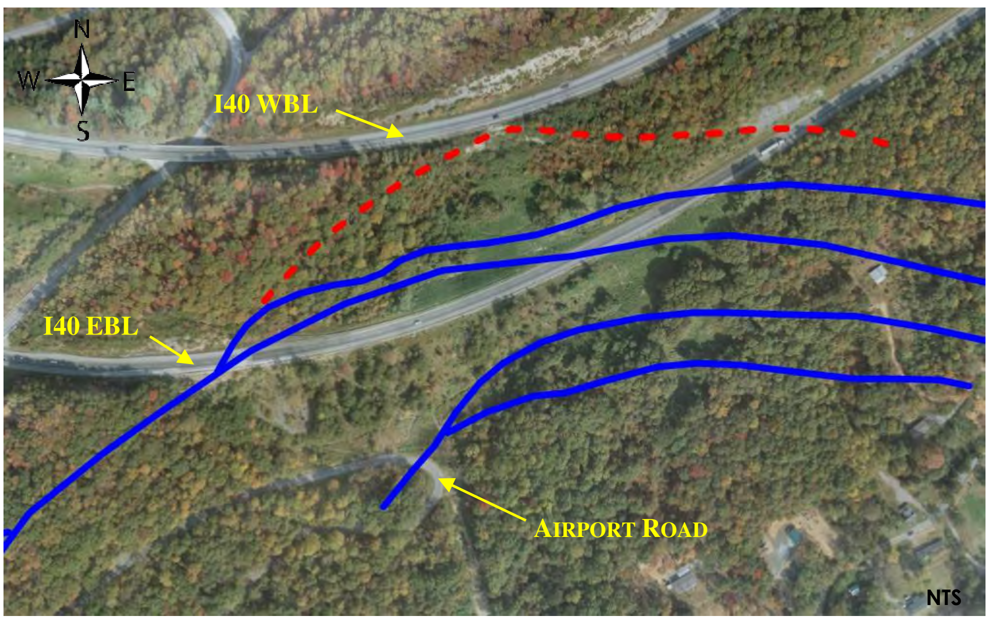

Figure 6. Post Construction Imagery showing historic headscarps (in blue) interpreted from 1961 imagery and recent headscarp (in red) interpreted from 2011 imagery.

It is conceivable that sandstone bluffs cropping out along oversteepened topographic slopes were progressively undercut and put in tension by deep weathering of underlying weak shales. Although bedding dips into the slope as shown in the geologic cross section presented as Figure 4, large scale release could occur along the adversely dipping strike joint observed to occur in the rock mass. Failure through the sandstones along this joint set would result in the headscarp shown in red on Figures 3 through 6. Because the underlying shales are calcareous, they would be subjected to deep, pervasive chemical and physical weathering. The weak, deeply weathered nature of this unit would allow the shale to behave more as a mass, allowing slip surfaces related to slow, progressive downslope movement to cut through the mass. Further downslope and to the south, bedding dip is interpreted to be folded and reverses direction, dipping to the southeast, as shown schematically on Figure 4. In this portion of the mass, slip surfaces would likely follow the bedding surfaces, which are interpreted to have very shallow dips to the southeast. Failure through the shale was likely manifested as multiple discreet slip surfaces that are listric, becoming flatter with distance downslope of the headscarp, as illustrated on Figure 4. Movement of the underlying shale would result in undercutting of the overlying sandstone bluffs with rapid, large-scale release eventually occurring along the strike joint, resulting in development of the large headscarp observed on 1961 aerial photography (Figure 2). The landslide likely remained dormant until placement of the EBL embankment during road construction reactivated movement of the relict debris mass along pre-existing slip planes. New headscarps resulting from this reactivated movement are shown in red on Figures 3 through 6.

Instrumentation Installation and Monitoring

To gain a better understanding of geotechnical conditions related to the failed mass, including groundwater characteristics within the mass and information regarding the depth and surface characteristics of the slip surfaces as well as rate of continued movement, additional drilling and installation of instrumentation was performed. Accurate, detailed topography for the site was not available; consequently, prior to mobilization for the field investigation in December 2010, a Light Detection and Ranging (LIDAR) survey was conducted. Instrumentation and drain locations and slide analyses are based on data from the survey.

Golder used sonic drilling techniques as a means to install monitoring instrumentation along two cross-sections parallel to the slope. Sonic drilling uses high frequency vibrations, down pressure, and rotation to extract continuous samples from the ground. This method was selected for use on this project due to its ability to advance quickly through highly variable, mixed (soil and rock) ground conditions anticipated in fill and colluvial soils, while retrieving intact disturbed and periodic undisturbed samples. Based on samples collected from seven borings advanced in the slide mass, located on Figure 7, fill material for the embankment was observed to occur to depths of up to about 14 meters in borings advanced adjacent to the EBL. Colluvial and residual soils of the Pennington Formation were encountered at depths up to 20 and 35 meters, respectively. The colluvium was very heterogeneous, generally ranging from clay and clayey gravel to gravel with clay to clayey sand to poorly graded sand. Residual soils were more homogeneous, occurring primarily as clay, clayey sand and gravel, and poorly graded sand that are locally saprolitic where relict structural fabric was preserved in the soil.

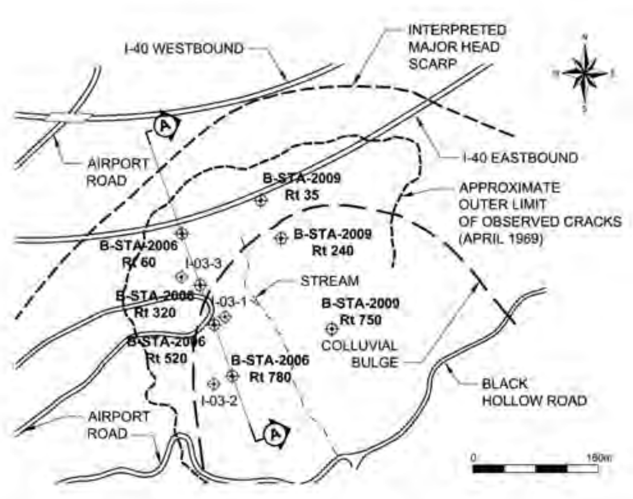

Figure 7. Alignment and Instrumentation Layout Plan

Transitionally weathered bedrock occurred at depths between 15 to 42 meters below ground surface. Highly to completely weathered layers of dark gray, weak, intensely fractured, calcareous shale and moderately to highly weathered, variably gray, white, brown and red, strong to very strong, course to very course grained, moderately fractured, thinly bedded calcareous sandstone was encountered with variably thick interlayers of residual clay and sand. Slip planes were identified to occur as discreet lenses primarily within the residual soils as well as in soil layers within the differentially weathered bedrock. Distinctive characteristics of the slip planes included the presence of deeply weathered, mottled, moist to wet clay with very contorted relict fabric.

An inclinometer casing and between one and three vibrating wire piezometers with data loggers were installed in the seven boreholes up to 240 meters down slope of the highway. Loss of fluid grout backfill was observed during several inclinometer installations, requiring multiple grouting phases. A weather monitoring station, including a thermometer, barometer and rain gauge, was also installed. Data from instrumentation and geotechnical borings are illustrated on Figure 8, a generalized cross section showing interpreted subsurface conditions through the slide mass. The location of an interpreted failure zone on which the mass is moving is also depicted on the cross section, oriented at 5° from horizontal, which is consistent with what would be expected based on the working hypothesis developed for the failure mechanism. From the Lidar and inclinometer data, the estimated volume of the landslide is on the order of 2.5 million cubic yards.

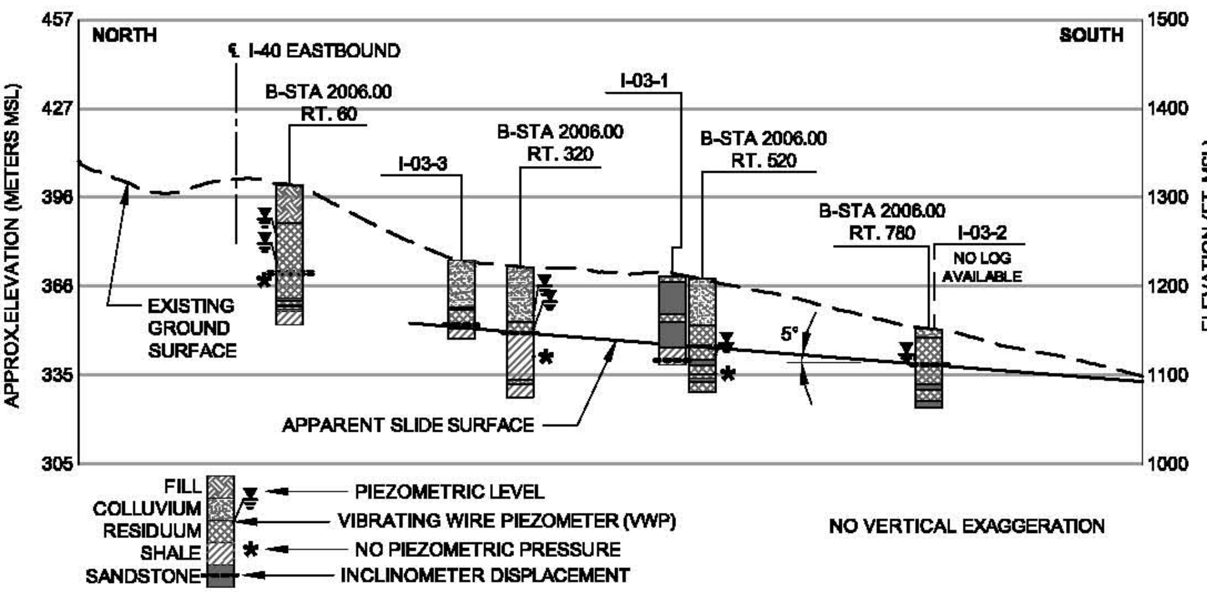

Figure 8. Geotechnical Cross Section A-A (located on Figure 7) - Generalized Subsurface Characterization

Traversing inclinometer readings indicate that between approximately 6 and 20 mm of displacement has occurred since monitoring began in February 2011. As an example, shown on Figure 9, inclinometer data collected since 2003 at the toe of the highway embankment near the western end of the slide indicate about 80 mm of displacement, at a depth of 22.9 meters below ground. Note the change in the displacement rate from approximately 8 mm per year prior to 2009 to 16 mm per year after 2009. These recent movements, while comparatively small, have impacted the highway such that TDOT is now resurfacing the pavement that traverses the slide scarp on a biennial basis.

Vibrating wire piezometers located between 11 and 33 meters below the ground surface indicate perched water within the slide mass, with pressures ranging from about 0 to 150 kPa. These perched groundwater horizons are likely related to the heterogeneous distribution of laterally discontinuous, low permeability lithologic layers located within the colluvium, residuum and differentially weathered bedrock. Water pressures were measured near 0 kPa at four locations below the failure plane. The onsite weather station and piezometer logging do not indicate a strong correlation between precipitation and piezometric response in all piezometers.

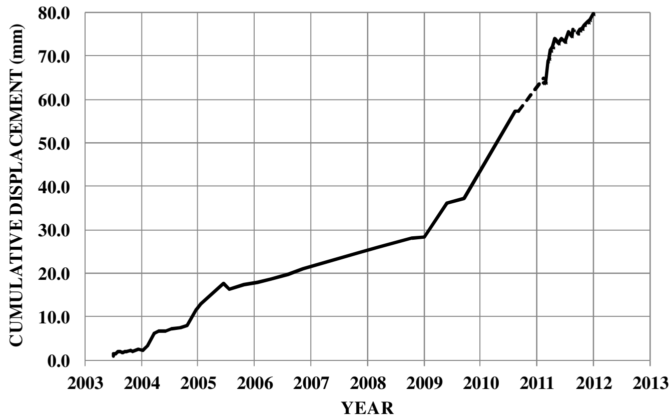

Figure 9. Cumulative Displacement since June 2003 at Inclinometers located at ± B-2006-Rt 320

Nine disturbed samples recovered during the instrumentation installation were selected for classification testing according to the Unified Soil Classification System (USCS), data shown in Table 1. These samples were located within or near the slide zone. Only two of the 9 samples were classified as high-plastic clay, while the rest were CL to ML. Given the long-term displacements that have occurred on the slide planes, it may be assumed that the shear plane materials have reached the residual shear strength. Assuming no cohesion, correlation of residual friction angle as a function of material properties, as reported by Mesri and Shahien (2003), indicate values between 12° and 28°. These discrete data points indicate that the slide plane is a zone in a heterogeneous mass.

Table 1. Laboratory Sample Summary

Borehole	Sample Depth (m)	USCS	Natural Moisture Content (%)	Liquid Limit (%)	Plasticity Index (PI - %)	Approx. clay fraction, (CF - %)	PI/ CF
B-STA-2006-RT-780	12.2-12.3	CL	18.2	37	18	33.6	0.54
B-STA-2006-RT-320	22.6-23.2	CL	12.4	35	13	29.1	0.46
B-STA-2006-RT-60	29.9-30.2	CH	26.8	59	31	42.9	0.72
B-STA-2009-RT-750	17.7-18	CH	30.0	60	34	60.8	0.56
B-STA-2009-RT-240	29.9-30.2	CL-ML	14.1	26	7	14.8	0.45
B-STA-2009-RT-35	36-36.3	CL	18.6	31	12	21.8	0.56
B-STA-2009-RT-750	14.9-15.5	ML	22.7	45	17	29.75	0.58
B-STA-2009-RT-240	29.3-30.2	CL	14.4	28	8	10.7	0.76
B-STA-2009-RT-750	17.5-17.7	CL	22.9	44	17	35	0.49

SHORT TERM REMEDIAL OPTIONS

Because of accelerated movement within the slide mass over the past several years, an emergency construction contract has been implemented by TDOT. Two rows of vertical dewatering wells, one near the crest and the other near the toe of the highway embankment (Figure 10), are currently being installed in an attempt to dewater the head of the slide mass. Planned depths are up to 46 meters below ground. The wells are designed to fully penetrate the materials with a continuous sand filter pack from the bottom of the well to within 2 meters of the ground surface.

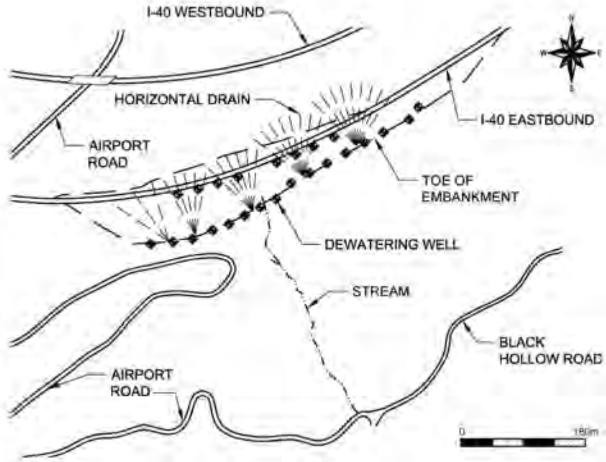

Figure 10. Dewatering Wells and Horizontal Drains Layout Plan

As previously described, the vibrating wire piezometers indicate perched groundwater conditions with minimal lateral continuity in the slide mass. To illustrate this point and the heterogeneity of the ground conditions, measured ground water levels in dewatering wells prior to the start of dewatering are shown in Figure 11. Compounding these conditions, during drilling of the dewatering wells, loss of drilling air circulation was documented from at least one dewatering well into an adjacent, completed dewatering well and reported excess quantities (2X the estimated quantity) of sand filter pack indicate there are open fractures or cavities related to the heterogeneous nature of the material and / or openings as a result of the downslope movement. Additionally, horizontal drains are being installed through the embankment toe to replace and/or supplement drains installed 15 to 20 years ago (Figure 10).

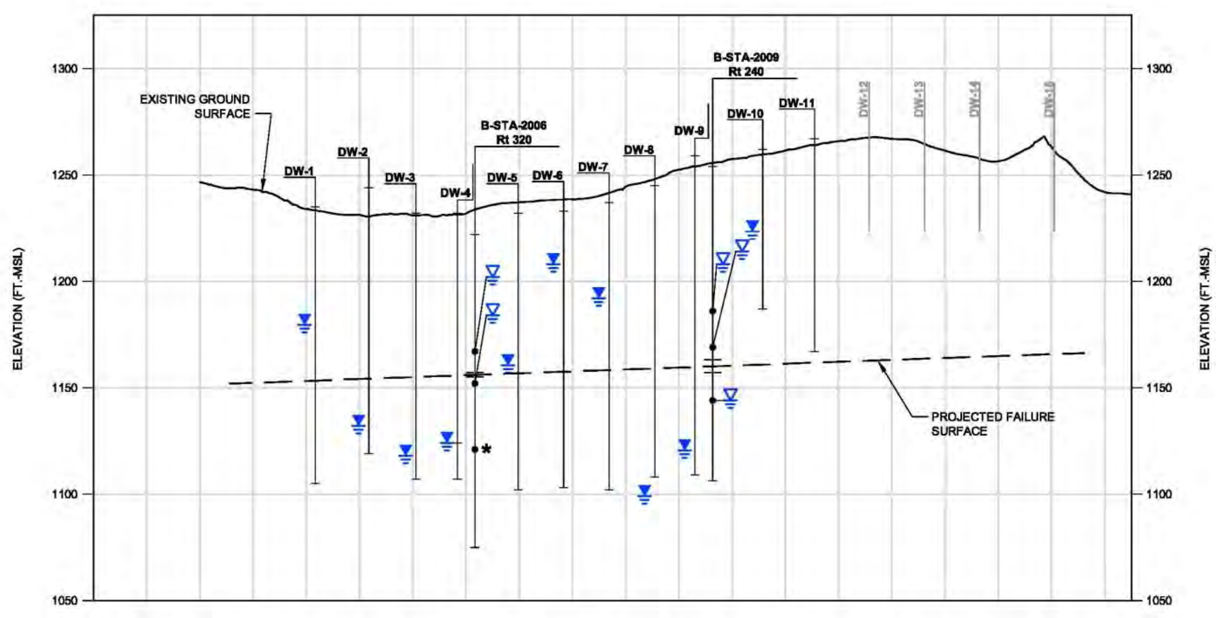

Figure 11. Measured Water Levels in Dewatering Wells and Vibrating Wire Piezometer – Toe of Embankment

Completion of these short-term measures, anticipated in early 2012, is intended to mitigate further displacement while TDOT considers permanent remedial alternatives. As described above, horizontal drains and dewatering wells have been utilized over the years by TDOT, however, they were typically applied only in the western half of the slide. Based on the inclinometer monitoring, no horizontal drains have been installed below the apparent slide surface

LONG-TERM REMEDIAL OPTIONS

Active dewatering may be considered a permanent long-term remedial option depending on the performance of the dewatering wells system. Other remedial options may be considered in coordination with TDOT. These may include one or more of the methods in the following categories:

<u>Earthwork</u>

- Realignment
- Lower grade
- Maintain grade - excavate and replace with lightweight material
- Flatten the slope
- Toe berm

<u>Structural</u>

- Bridge and remove embankment

<u>Drainage</u>

- Drilled-in horizontal drains
- Drainage trench (parallel to toe of slope)
- Slot trenches (perpendicular to toe of slope)
- Drainage adits with radial drains
- Dewatering wells

<u>Ground Modification / External Force</u>

- Stone columns
- Soil –cement columns / barrettes (jet or soil-mixed)
- Drilled shafts
- Reticulated micropiles / piles
- Ground anchors
- Soil nails

In order to develop these, slope stability back-analyses were conducted relying on the data described in this paper. Assuming residual shear strength is mobilized on the apparent slide surface, the back analyses estimated average residual friction angles between 12 and 19 degrees for dry and fully-saturated ground conditions, respectively, with a most likely value of 16 degrees. Using the 16 degree friction angle, the estimated horizontal resisting force needed for a slope stability factor of safety equal to 1.3 is approximately 7,000 kN per meter (500 kips per foot). To give a sense of the magnitude of resisting force, one row of 15-strand, high capacity anchors spaced at every 30 centimeters (1-foot) is required to stabilize the slope for the apparent slide surface shown in Figure 8.

All these options, whether individually or in some combination, are intended for permanent stabilization. Some of the options identified above, such as a bridge, lightweight material, and lowering the grade are not feasible because the remaining slope would still be marginally stable. At this time, it is unknown how effective drainage measures, specifically the dewatering wells, will be in mitigating future displacement.

If they are effective, radial drains installed from drainage adits could be excavated under the slide mass to effectively drain the ridge under the slide mass.

TDOT may elect to continue monitoring and perform periodic pavement repairs. Past monitoring has been on a periodic, infrequent basis. TDOT may consider implementing an active remote system of in-place inclinometers, vibrating wire piezometers, and weather station to give real-time monitoring. Such a system can be utilized to notify TDOT should increases in movement be detected so TDOT can rapidly respond to any changes and alert maintenance forces and the traveling public, as needed.

Selection of the most appropriate remedial measure will depend on a variety of factors, such as, cost, time to implement, long-term reliability, selection of an appropriate factor of safety, and perhaps most important, impacts to the traveling public. The analysis of available measures will rely heavily on the back-analysis of the existing slide mass, as the variation in the limited laboratory data and groundwater levels indicate the heterogeneity and overall size of the slide mass will make it infeasible to fully characterize the slide mass into a neat slope stability model.

CONCLUSIONS

For over 40 years, the Tennessee Department of Transportation has been dealing with a slow deformation of a fill embankment founded on colluvium and residual soil supporting the eastbound lanes of Interstate 40 in central East Tennessee. The deep-seated, ongoing slope movement responsible for the embankment deformation appears to be occurring along discreet slip planes located within the colluvium, residuum, and differentially weathered bedrock. Recent monitoring indicated acceleration in movement, requiring annual pavement repairs. As a result, new and replacement instrumentation was installed and a limited laboratory testing program was conducted in order to characterize the dimensions and properties of the mass and slide surface. This information and reliance on back analyses will be used to evaluate long-term remedial options that will allow TDOT to continue to provide a safe highway for the travelling public.

REFERENCES

Jewell, J.W and Swingle, G.D. 1965. Geologic Map of thee Cardiff quadrangle, Tennessee. *Tennessee Division of Geology*, GM 123-NW.

Law Engineering Testing Company 1969. Landslide Investigation, Interstate Highway Project I-40-6 (40)340, Roane County, Tennessee. *Report issued to Tennessee Department of Highways*, June 25, 1969.

Mesri, G. and Shahien, M. 2003. Residual Shear Strength Mobilized in First-Time Slope Failures. *Journal of Geotechnical and Geoenvironmental Engineering*, 129 (1): 12 – 31.

Royster, D. L. 1973. Highway Landslide Problems along the Cumberland Plateau in Tennessee. *Bull. Assoc. Eng. Geol.* 10, No.4 (Fall): 255-87.

Royster, D. L. 1977. Some Observations on the Use of Horizontal Drains in the Correction and Prevention of Landslides. In *Proceedings. 28th Annual Highway Geology Symposium:* 137-45.

Royster, D. L. 1979. Landslide Remedial Measures. *Bulletin. Association of Engineering Geology. Eng. Geol.* 16, no. 2 (May): 301-52.

Trolinger, W.D. 1980. Rockwood Embankment Slide between Stations 2001+00 and 2018+00: A Horizontal Drain Case History. *Transportation Research Record*, 783: 26 – 30.

DISTRIBUTION OF WEATHERED GEOLOGIC BEDROCK UNITS CONTROLS SLOPE MOVEMENT, GREEN POINT SINK, STATE ROUTE 299, HUMBOLDT COUNTY, CALIFORNIA

Dawn J. McGuire, CEG
Engineering Geologist
California Department of Transportation
1656 Union Street
Eureka, CA 95501
dawn_mcguire@dot.ca.gov

Prepared for the 63rd Highway Geology Symposium, May 7-10, 2012

Acknowledgements
California Department of Transportation Geotechnical Design North: Reviewers and Eureka drill crew

ABSTRACT

Green Point Sink is one of many locations in Humboldt County where State Route 299 is damaged by active landslides. For decades, the highway has been settling excessively at the locations of two active landslides at post miles 20.2 (Location 1) and 20.4 (Location 2). This paper is a discussion about Location 1, where movement has accelerated in recent years on a relatively gentle slope of 14°-18°. Movement at Location 2 has continued more slowly, though the slope is steeper: 25°-30°. Geologic maps show the Redwood Creek schist (Eastern Belt of the Franciscan Complex) as the only bedrock unit at Green Point. During a geotechnical investigation borings encountered the Redwood Creek schist at both locations. However, seven of the eight borings at Location 1 encountered clay above the schist. The clay is a weathering product of an unmapped unit of mélange, rather than part of the engineered road fill as investigators initially thought. Inclinometers showed displacement in the clay, near the contact between the schist and mélange.

The residual shear strength of the clay-rich decomposed mélange involved in the actively moving landslide was based on a correlation of liquid limit (48%), clay size fraction (35%), and an estimate of the effective normal stress at the active failure zone of 3,7393 lbf/ft^2 (Stark and others, 2005). The estimated friction angle of 18° and the relatively weak shear strength along the landslide failure surface are consistent with failure of a relatively gentle slope.

INTRODUCTION

Beginning as a pack trail and a wagon route to gold fields in the 1850's, State Route 299 (SR 299) now is a major east-west highway connecting the Pacific Coast (U.S. Route 101) with the northern Sacramento Valley (Interstate 5) (Figure 1). SR 299 traverses mountainous terrain with moderate to steep grades, providing access to and from the north coast for tourism, recreation, industry, and residents of the coast and valley.

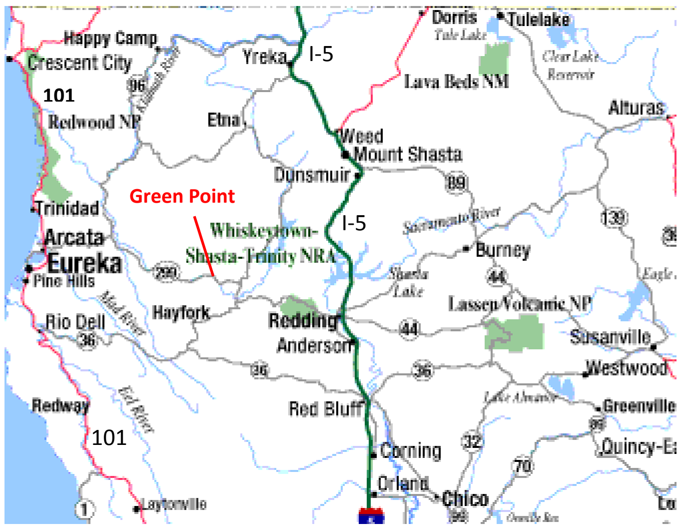

Figure 1. – Map showing the location of Green Point.

The current alignment of SR 299 at Green Point was constructed in the early 1960's. The roadway has been settling for decades due to landslide movement on the north side of Green Point. Storm events of 2008-2009 accelerated the settling of the roadway and maintenance repairs became so frequent that a longer term repair was needed. A study of alternative repairs resulted in the selection of a soldier pile wall with ground anchors. Slope movement following storms in 2010-2011 nearly closed the roadway at Location 1. An emergency drainage system was constructed to slow highway settling, but the deformation is continuing.

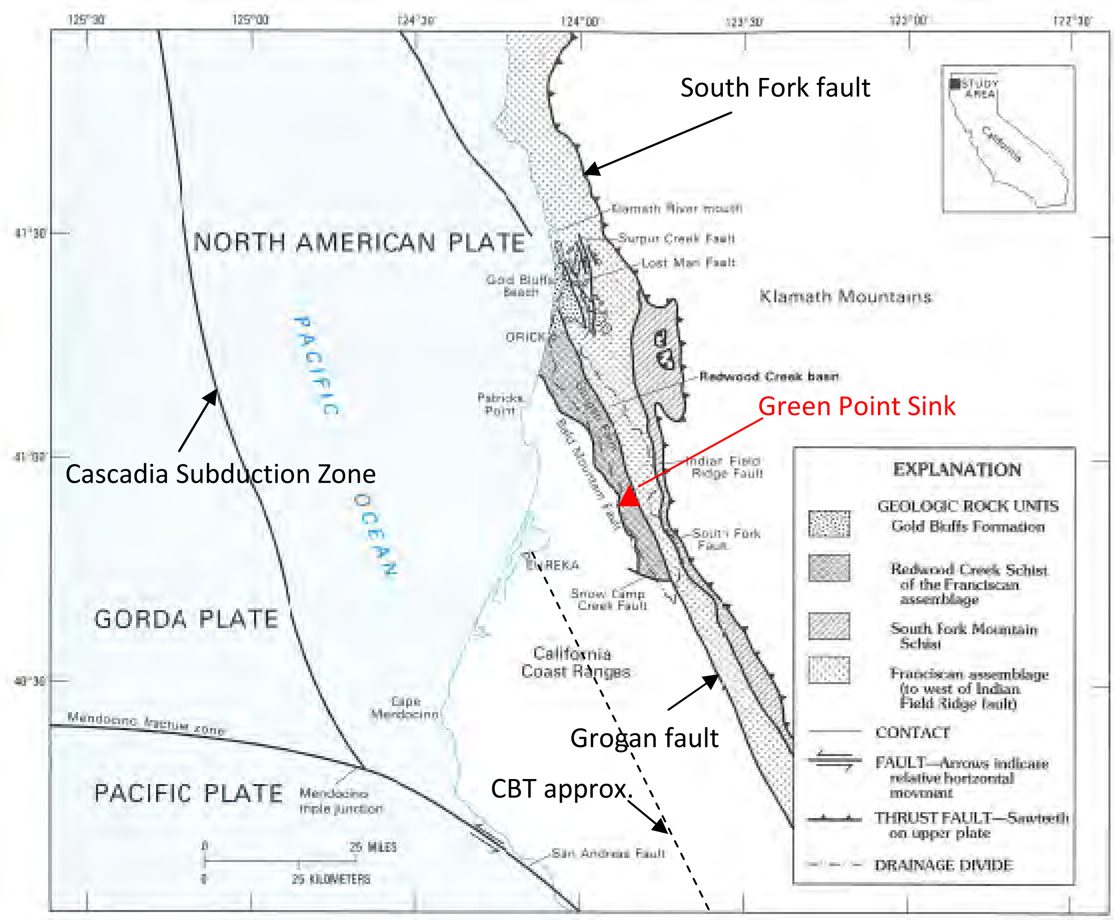

Figure 2. - Map showing Redwood Creek drainage basin and Green Point Sink in the California Coast Ranges (from Cashman and others, 1995). The Cascadia Subduction Zone and Coastal Belt thrust (CBT, approximate) are labeled.

REGIONAL GEOLOGY

Green Point Sink lies in the Coast Ranges Province, which is underlain by Mesozoic and Cenozoic rocks of the Franciscan Complex. The Franciscan Complex is subdivided into three broad fault-bounded belts: the Eastern (oldest), Central, and Coastal belts (Irwin, 1960; McLaughlin and others, 2000). East of Green Point, the Grogan fault separates the Eastern and Central belts of the Franciscan Complex (Figures2 and 3); the South Fork fault (part of the Coast Range thrust fault) separates the Eastern belt from the Klamath Mountains to the east;

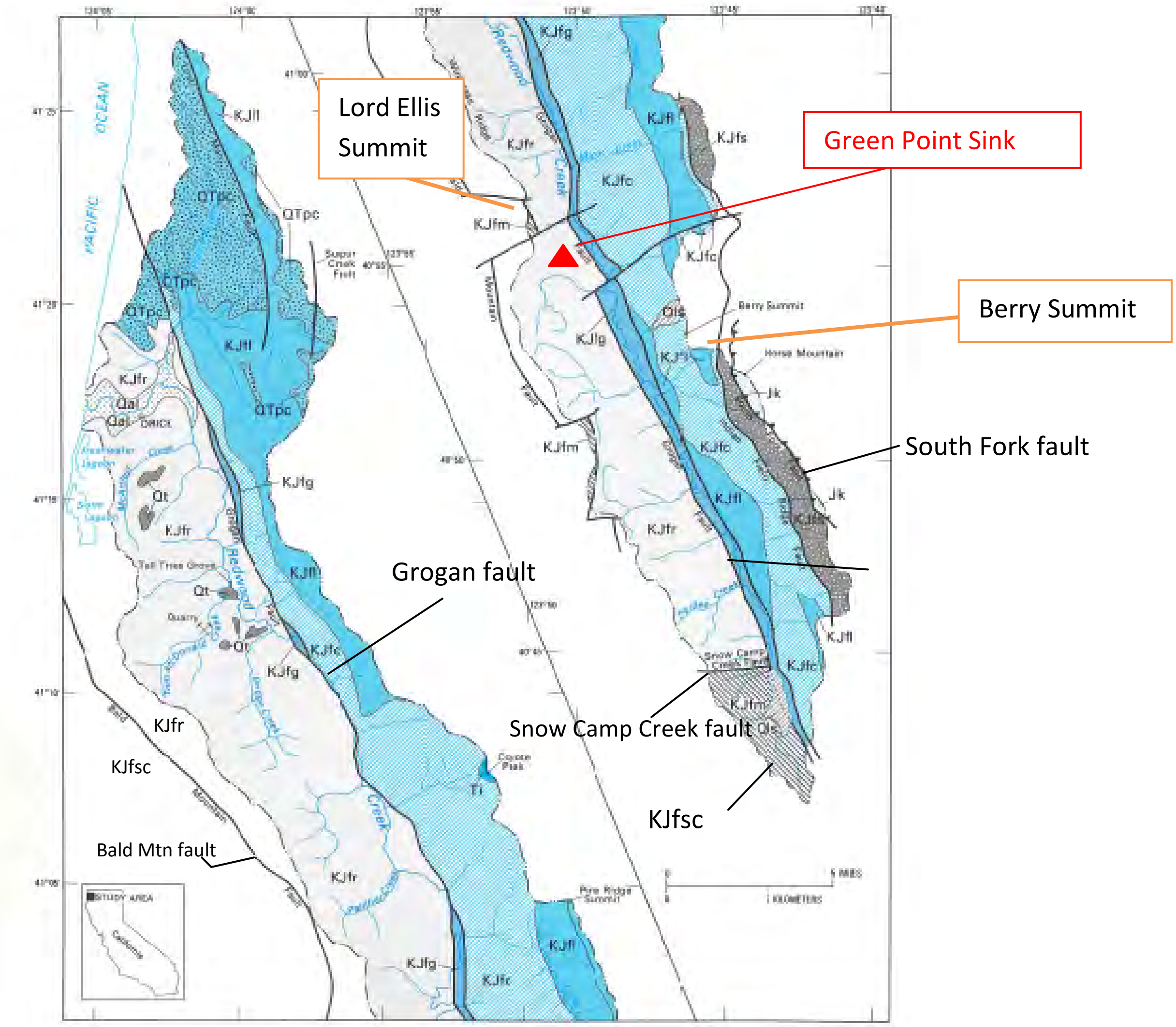

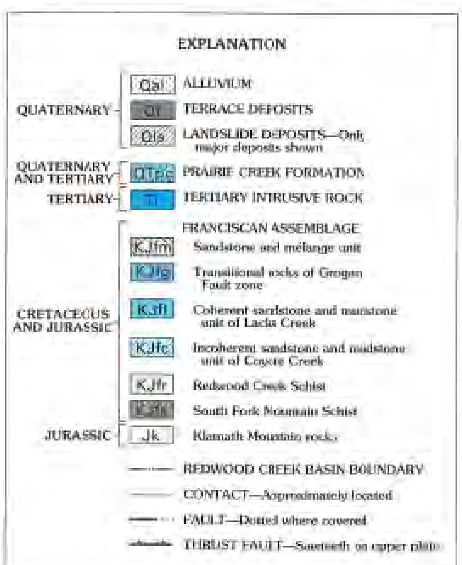

Figure 3. - Geology of Redwood Creek basin (from Cashman and others, 1995). In Redwood Creek basin, KJfm is the sandstone and mélange of Snow Camp Mountain (KJfsc).

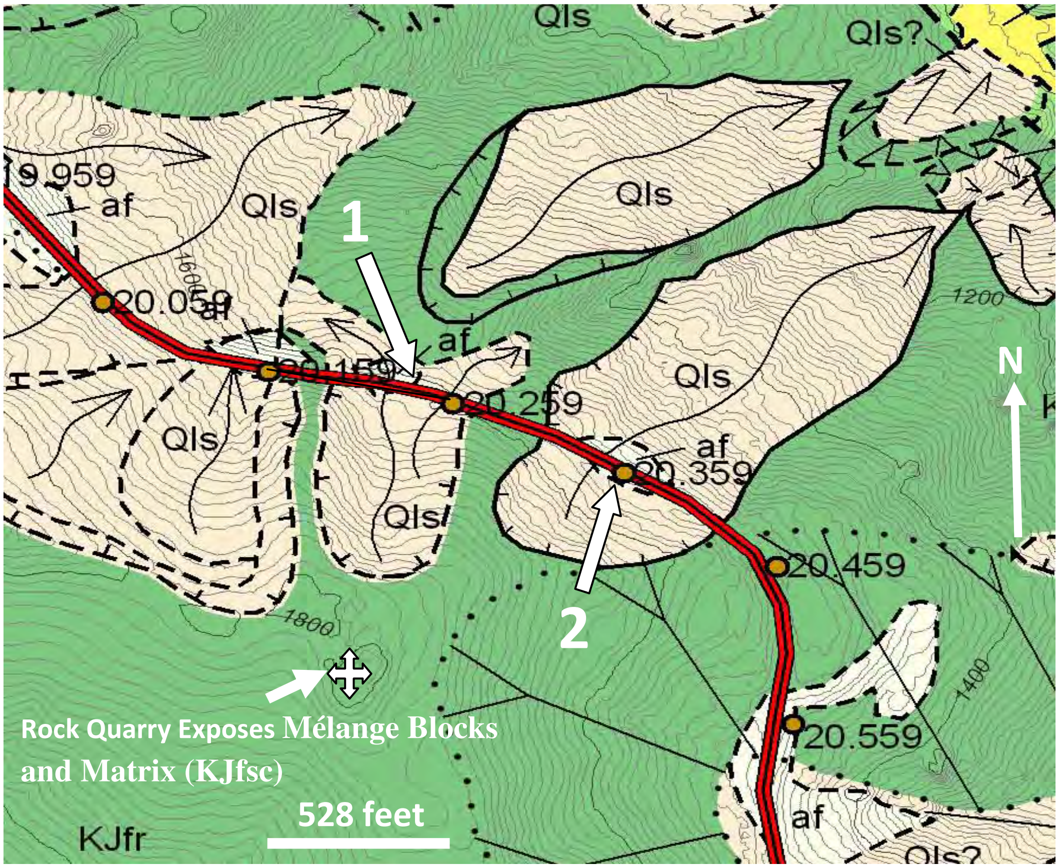

MAP UNIT DESCRIPTIONS

af	Artificial Fill
Qrt	Quarternary River Terrace Deposits
Qls	Quarternary Landslide
KJfr	Redwood Creek Schist

Figure 4. - Geologic map showing Locations 1 and 2 (in white), the Redwood Creek schist (KJfr), and landslides at Green Point Sink (Falls and others, 2006). Though existing geologic maps show no mélange, a rock quarry above Location 1 exposes mélange blocks and matrix (KJfsc) and SR 299 exposes the same mélange at PM 21, on the southeast side of Green Point.

The Coastal Belt thrust fault separates the Central belt from the Coastal belt to the west (Figure 2). The contacts between the geologic bedrock units are faults at Green Point.

LOCAL GEOLOGY AT GREEN POINT

As SR 299 descends eastward from Lord-Ellis Summit into the Redwood Creek basin, it passes through two mapped, informal, geological units: the sandstone and mélange unit of Snow Camp Mountain (KJfsc), then the Redwood Creek schist (KJfr) to the east (Harden and others, 1981). The Redwood Creek schist is part of the Eastern belt of the Franciscan Complex; the sandstone and mélange unit of Snow Camp Mountain is part of the Central belt. The belts are separated by faults.

On geologic maps, the schist dominates the western half of the Redwood Creek basin and the mélange is distributed only locally (Figure 3). Maps of Green Point show the Redwood Creek schist, but no mélange unit (Figure 4). At the beginning of the geotechnical investigation, it was assumed that the bedrock was entirely schist; it was unclear why the gentle slope (14^{o}-18^{o}) at Location 1 failed. The schist is decomposed to granular material having a friction angle of approximately 30^{o}. Discovery of the unmapped mélange, decomposed to clay-rich soil, helped to explain the failure of the slope.

Falls and others (2006) mapped more than 200 landslides along SR 299, over the 18 air miles and 33 road miles between Blue Lake (PM R5.9) and Willow Creek (PM 38.8). Figure 4 shows the Quaternary landslides they mapped at Green Point Sink.

Redwood Creek schist (Eastern belt of the Franciscan Complex)

The Redwood Creek schist (Eastern belt of the Franciscan Complex) consists of fine-grained schist, metagraywacke, greenstone (laminated to massive), and metatuff. The most common lithology is the fissile, light-green to dark-gray, fine-grained schist containing quartz, chlorite, white mica, albite, epidote, actinolite, and lawsonite, with or without opaque graphitic material (Cashman and others, 1995). The schist is foliated and crenulated by numerous small folds. Large dormant landslide complexes are common within the Redwood Creek schist.

In the subsurface at Green Point, the schist is fine grained, medium-dark gray, foliated, very intensely weathered to decomposed to silty sand and silty sand with gravel (SM), and very intensely fractured. The schist includes thin “layers” of green metatuff and fragments of hard vein quartz.

Mélange units in Redwood Creek drainage basin

Geologic maps show only one unit of mélange exposed in the western half of Redwood Creek drainage basin: the sandstone and mélange unit of Snow Camp Mountain (Central Belt of the Franciscan Complex). The Snow Camp Mountain mélange consists of bodies of bedded graywacke intermixed with a pervasively sheared argillite-matrix mélange. The matrix contains blocks of chert, metabasalt, volcanic breccia, metavolcanic rocks, and glaucophane-lawsonite blueschist (Cashman and others, 1995). At Green Point Sink, the matrix of the mélange is decomposed to sandy lean clay, sandy fat clay, clayey sand with gravel, and clayey gravel with sand. The sandstone and mélange unit of Snow Camp Mountain is lithologically and structurally similar to mélange exposed over extensive areas to the south in the Mad, Van Duzen and Eel River basins; it is contiguous with the sandstone and mélange unit in the Mad River basin (Harden and others, 1981).

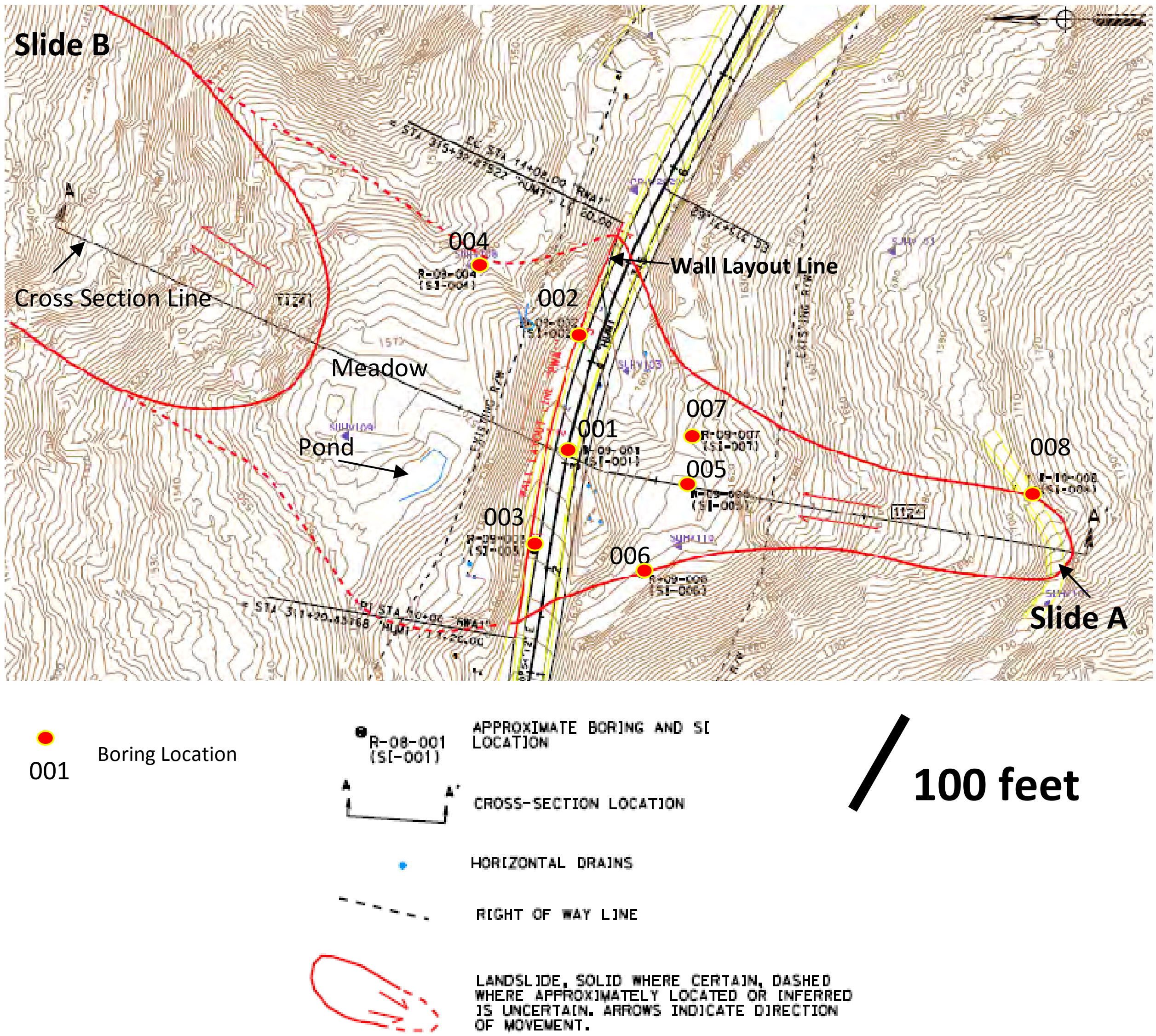

Figure 5. - Map showing the outlines of the active landslides in mélange decomposed to clay-rich soil, Green Point Sink Location 1.

The mélange of Snow Camp Mountain forms rounded hilltops with gentle slopes. Active earthflows and deep landslides are the main modes of mass wasting, while debris slides typically occur on slopes oversteepened by stream erosion or grading. Cashman and other (1995) noted that the largest landslide in the Redwood Creek basin is an ancient earthflow formed on this same mélange unit at the southern headwaters of Redwood Creek basin (see map by Harden and others, 1981). The matrix of the mélange generally underlies grasslands and lightly wooded hillslopes. Cashman and others (1995) observed that the mélange of Snow Camp Mountain forms more hummocky landscapes than other hillslopes in Redwood Creek basin.

Figure 6. - Photo showing lush vegetation where water ponds in a closed depression on the meadow below SR 299 at Green Point Sink, Location 1. The location is shown in Figure 5. The embankment of SR 299 is to the right.

The incoherent unit of Coyote Creek (Eastern Belt of the Franciscan Complex) was mapped in the eastern half of Redwood Creek basin (Harden and others, 1981). This unit has been described as tectonic blocks of chert, greenstone, and sandstone, and isolated bedded sequences of sandstone and chert. The greenstone blocks contain chlorite, pumpellyite, prehnite, and mica, and are commonly immersed in a sheared mudstone matrix. A lesser degree of shearing distinguishes this mélange from Snow Camp Mountain mélange at Green Point.

GEOTECHNICAL FIELD INVESTIGATION AT LOCATION 1

Surface

Surface mapping helped to identify the limits of the active landslides (Figure 5). Surface evidence for Slide A is visible above SR 299. The headscarp is located above a watercourse crossing on a ranch road. Irregular lateral scarps were traced downslope in 2010, across the highway, and along the unpaved shoulder on the north side of SR 299. Lateral scarps mark the flanks of the slide in the pavement of SR 299 (Figure 5). A meadow, deformed into ridges and swales, is located below the highway embankment. The swale nearest to the embankment contains a pond in a closed depression (Figure 6). Air photos indicate that the access road to the cabin was more or less continuous to the meadow in 1973 (Figure 7). Today, the access road ends at a ridge that has grown along the eastern flank of Slide A (Figure 5).

The outer edge of the meadow is cut by the headscarp of Slide B (Figures 5, 7, and 8). The headscarp exposes clay-rich soil decomposed from the mélange. Below the headscarp, tree tops have fallen upslope toward the scarp during 2009 -2010 as the ground surface moved downslope to the north (Figure 8).

Subsurface

Drilling and Borings

The California Department of Transportation drilled eight rotary borings at Location 1 between November 2009 and March 2010 to help determine the limits of the landslide. The borings were drilled using a truck-mounted Acker MPCA and a CME 750 drill rig with a 94-mm HXB casing equipped with a diamond impregnated core bit. Slope-inclinometer casings were installed in all borings and perforated in the bottom 20 feet (well below the slip surface) to allow monitoring of water levels. Slope inclinometers were monitored between December 2009 and July 2010. The inclinometer in boring 005 showed cumulative displacement of 2 inches over two months in early 2010. The boring is located where the clay-rich soil is relatively thick (see Figures 9 and 10).

During drilling, seven of eight borings encountered the clay-rich soil above the Redwood Creek schist. The clay was relatively thin beneath SR 299, most likely due to excavation during construction of the alignment.

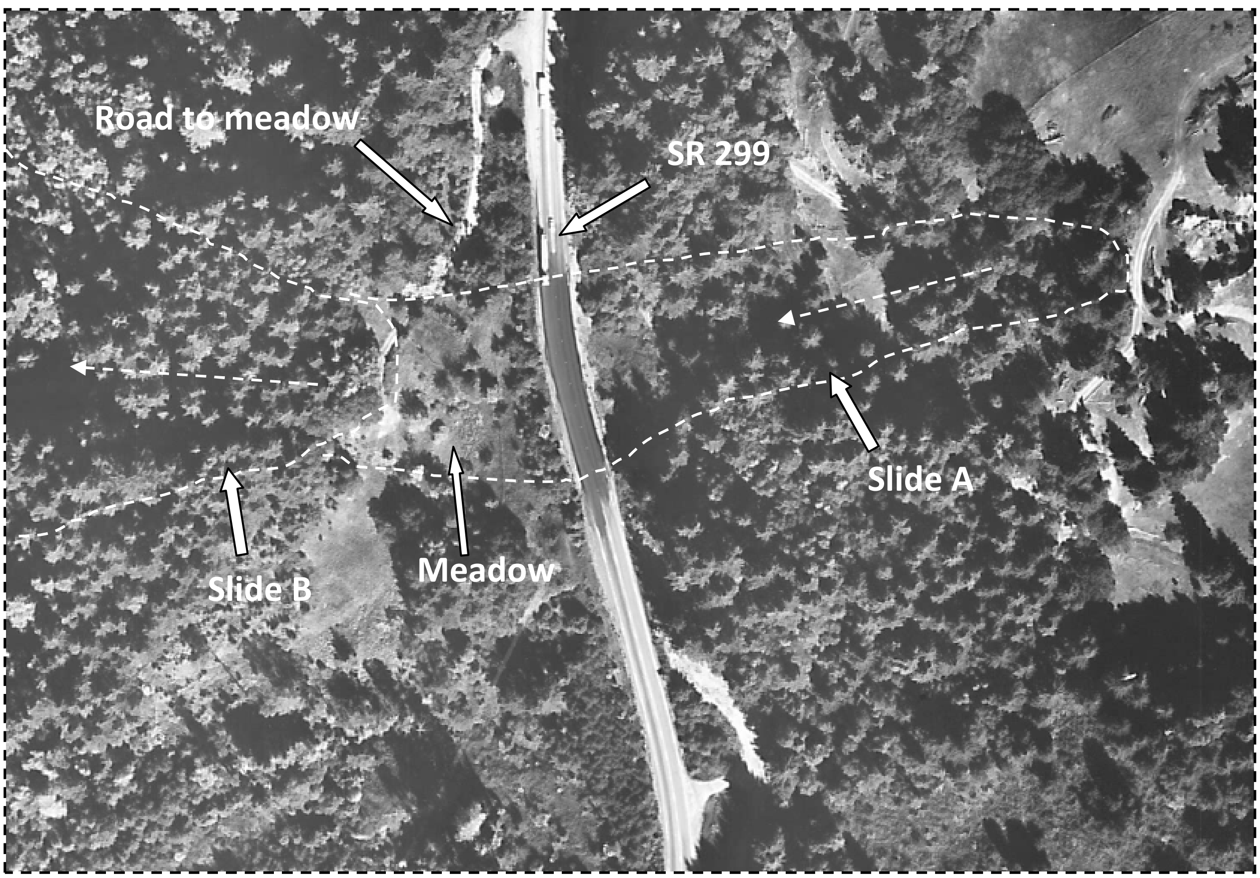

Figure 7. – 1973 air photo showing a repaved section of SR 299 at Location 1, the meadow below SR 299, the access road to the meadow, and the approximate locations of the two landslides labeled A and B.

While thinner beneath the highway, the clay is as thick as 57 feet off the highway in boring 006 (Figure 5). Near the headscarp of Slide A (Figure 5), boring 008 encountered 30 feet of decomposed mélange above less weathered mélange; no schist was found below mélange to a depth of 70’ (Figure 10). Inclinometers show deflections within decomposed mélange (borings 002, 003, 005, and 007) and in the contact zone between mélange and schist (001). Figure 9 shows inclinometer deflections in borings 003 and 005, while Figure 10 shows the various units, locations of deflections within units in six of the eight borings, and total depth of each boring.

Figure 8. - Photo view to the west showing trees that fell counterclockwise at the base of the headscarp of Slide B as the ground moved downslope to the right.

All but one boring (008) encountered decomposed Redwood Creek schist beneath the mélange. The schist is weathered to silty sand and silty sand with gravel (SM). The intense weathering lowered the consistency of the fine-grained schist and standard penetration tests were performed to depths of nearly 100 feet. For example, in boring 001 the apparent density was loose to dense to 12 feet (mélange clay), medium dense to 37 feet (mélange clay to weathered schist at 30 feet), very dense to 88 feet (weathered schist), and refusal from 90 feet to 100 feet (weathered schist).

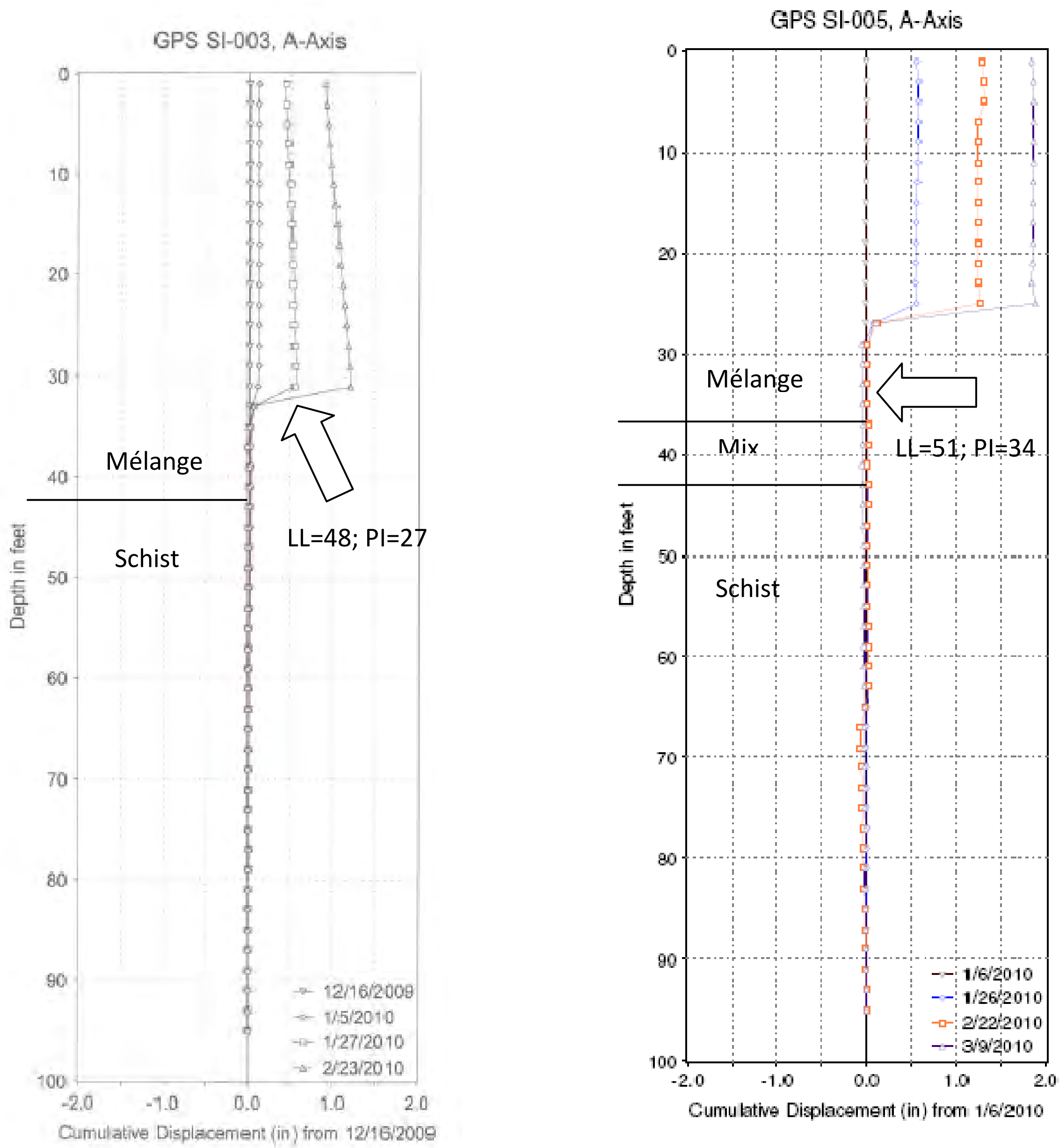

Figure 9. – Graphs showing slope-inclinometer results from borings 003 and 005 and lab results from samples collected in the two borings. Note two inches of movement in two months recorded in boring 005. Clay of the decomposed mélange was found in seven of eight borings.

Figure 10. - Chart showing slope-inclinometer deflections (red lines) within geologic units encountered within Location 1. Boring 004 encountered no mélange and showed little deflection, while the casings sheared off in other borings 001, 002, 003, 005, and 007 (red lines). No schist was encountered in boring 008. Total depths are listed below each boring.

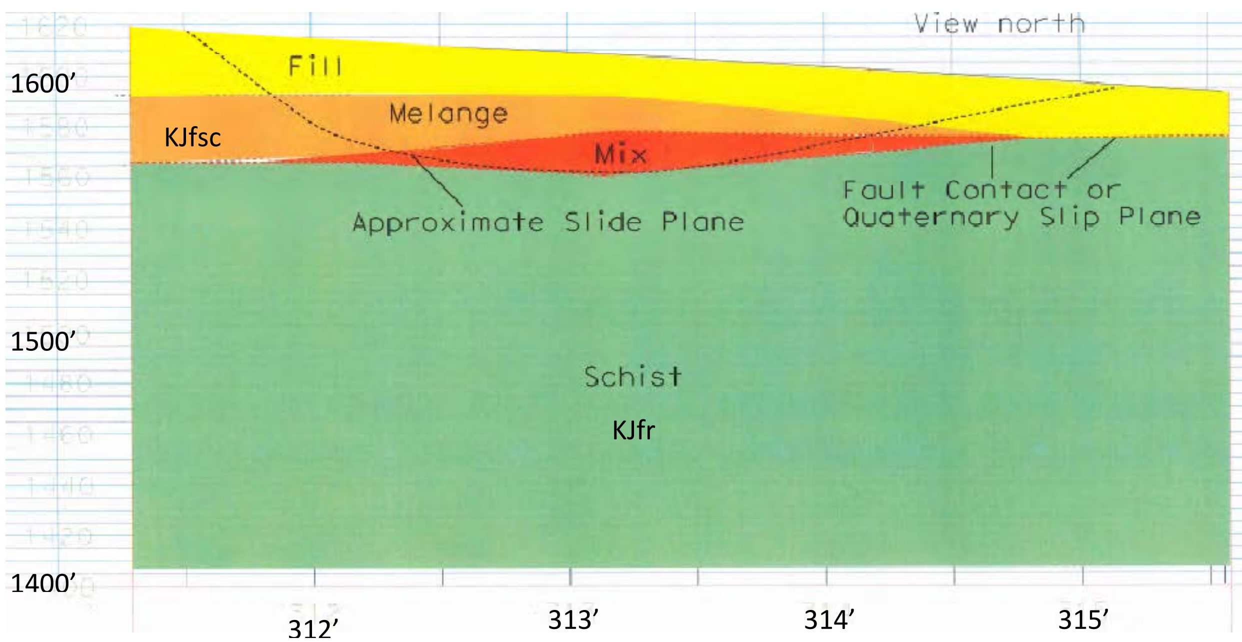

Figure 11. – Profile along the layout line of the proposed wall (Figure 5) showing fill (yellow), decomposed clay rich mélange of Snow Camp Mountain (light brown), a mixture of decomposed mélange and schist along and between the red-dashed contact (red brown), and Redwood Creek schist (green; mostly decomposed to granular material). To the west the fill and mélange are thicker.

LAB RESULTS

Soils

Results from gradation analyses indicate the decomposed mélange consists of sandy lean clay, sandy fat clay, clayey sand with gravel, and clayey gravel with sand. All samples tested contained more than 25% clay-size fraction. Figure 9 shows that near the slip plane in boring 003, the sandy lean clay (CL) has a liquid limit of 48 and a plasticity index of 27 (41% clay <0.002 mm). Below the slip plan in boring 005, the sandy fat clay (CH) has a liquid limit of 51 and a plasticity index of 34.

No clay was found in the weathered schist, which is decomposed to silty sand (SM) with and without gravel, and locally to sandy silt (ML).

Interpretation of Lab Results

Empirical data indicate a friction angle of 18^{o} in weathered mélange, based on a correlation of liquid limit (48%), clay size fraction (35%), and estimated effective normal stress at the active failure zone of 26 lbf/in^2 (Stark and others, 2005). The higher the liquid limit and clay-size fraction, the lower the friction angle (Stark and others, 2005). The friction angle on the slip plane depends on clay mineralogy and the degree of shearing and particle reorientation along the slip plane (Skempton, 1985). The clay-size fraction in the weathered mélange is high enough (>25%) to facilitate particle reorientation. Multiple landslide shearing events have occurred near the contact between the mélange and schist.

The Redwood Creek schist is decomposed to granular material having an estimated friction angle of 30^{o}. No samples submitted for gradation analysis were clay (CL).

PROFILE AND CROSS SECTION

Figure 11 is a profile located along the line of proposed the wall (line is shown in Figure 5). Figure 12 is a cross section through Location 1. The cross-section line is shown in Figure 5. The roadway is underlain by fill consisting mostly of silty sand with gravel (SM) and silty gravel with sand (GM). The fill is underlain by clay-rich soil weathered from mélange. The mélange is underlain by a fault contact with the schist. The contact is locally a mixture of decomposed mélange and decomposed schist. Beneath the contact zone is weathered schist.

CONCLUSIONS

Initially, it seemed unusual that a gentle slope of 14^{o}-18^{o} would fail within Redwood Creek schist, because the schist decomposes to a granular material (SM and GM) with a friction angle of approximately 30^{o}.

Geotechnical investigations showed a widespread, unmapped unit of mélange weathered to clay-rich soil above the schist at Green Point Sink Location 1. The decomposed mélange clay beneath SR 299 is original hillslope material and not engineered fill. The upper contact of the clay is the base of engineered fill and the limit of excavation during construction of SR 299.

The matrix of the mélange is decomposed to clay having a friction angle of 18^{o}. The low friction angle and low residual shear strength of the material along the slip plane help to explain the slope failure. For decades, the reactivated landslide (Slide A) has been moving intermittently and is patched as needed. Air photos from 1973 show that SR 299 was being patched at Location 1 thirty-nine years ago.

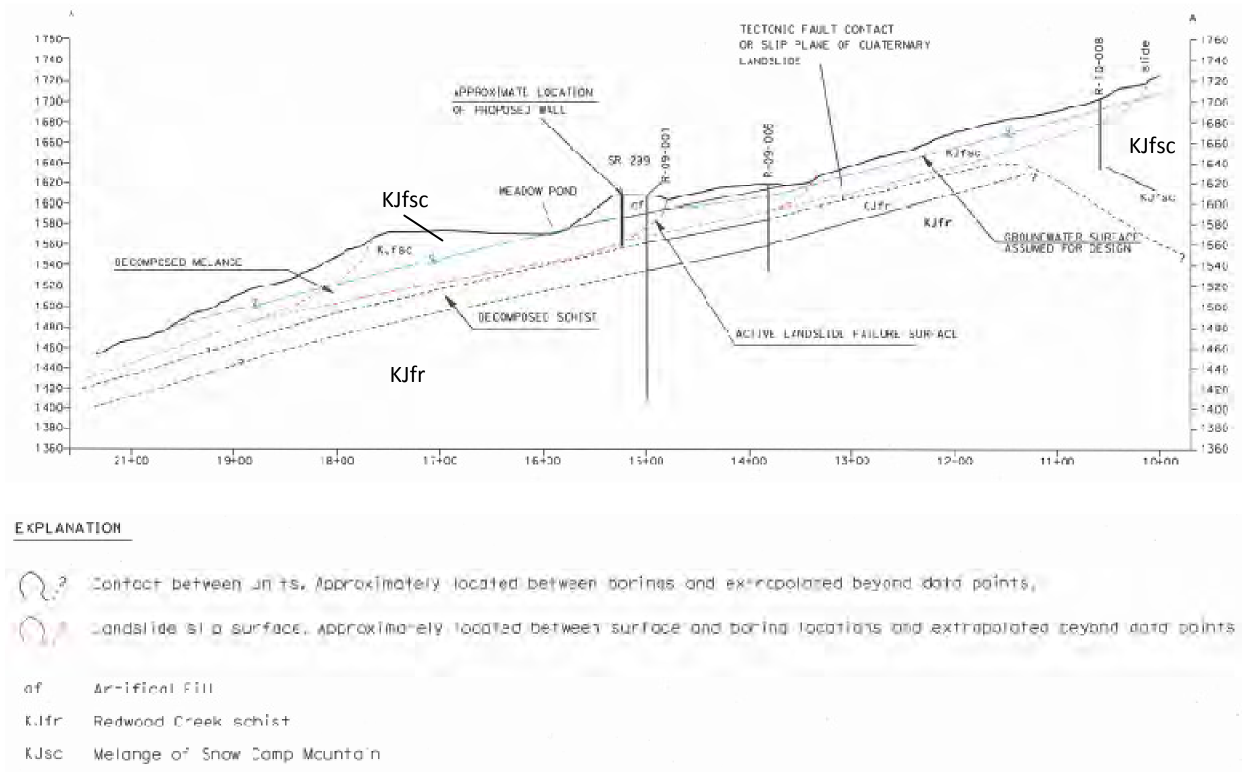

Figure 12. – Cross section through location 1, facing toward the east. Geologic contacts and landslide slip surfaces are extrapolated between outcrops and borings. Boring 008, projected into the cross section, encountered no schist and showed no deflection.

The contact between the two bedrock units is a fault, according to regional rock relationships. Landslide maps indicate Green Point Sink is underlain by Quaternary earthflow features. Slides are active today within the older Quaternary earthflow features. The combination of soil containing more than 25% clay-size fraction and multiple events of shearing have led to the low residual shear strength along the shear plane. Pre-existing shear causes the residual shear strength of a clay-rich material to drop due to the reorientation of particles along the shear plane (Skempton, 1985). The effects of particle reorientation are more pronounced when the clay-size fraction is 25% or greater (Stark and others, 2005), as in the weathered mélange. Gradation analyses showed all samples of decomposed mélange contained >25% clay. The nature and geometry of the weathered bedrock and pre-existing shearing during landslide movement exerted a controlling influence on the slope at Location 1.

REFERENCES

Cashman, S.M., Kelsey, H.M., and Harden, D.R., 1995, Geology of the Redwood Creek basin, Humboldt County, California: in Nolan, K.M., Kelsey, H.M., and Marron, D.C., Eds., Geomorphic processes and aquatic habitat in the Redwood Creek basin, northwestern California: U.S. Geological Survey Professional Paper 1454, B1-B13.

Falls, J.N., Wills, C.J., and Harden, B.C., 2006, Lanslides in the Highway 299 corridor between Blue Lake and Willow Creek, Humboldt County, California: California Geological Survey Special Report 195, 57 p., 1:12,000.

Harden, D.R., Kelsey, H.M., Morrison, S.D., and Stephens, T.A., 1981, Geologic map of the Redwood Creek drainage basin, Humboldt County, California, U.S.G.S. Open File Report 81-496, 1:62,500.

Irwin, W.P., 1960, Geologic reconnaissance of the northern Coast Ranges and Klamath Mountains, California, with a summary of mineral resources: California Division of Mines Bulletin 179, 80 p.

McLaughlin, R.J., Ellen, S.D., Blake, M.C. Jr., Jayko, A.S., Irwin, W.P., Aalto, K.R., Carver, G.A., and Clarke, S.H., Jr., 2000, Geology of the Cape Mendocino, Eureka, Garberville, and southwestern part of the Hayfork 30 X 60 minute quadrangles and adjacent offshore area, northern California: Miscellaneous Field Studies MF-2336, 27 p., 1:100,000.

Skempton, A.W., 1985, Residual strength of clays in landslides, folded strata and the laboratory: Geotechnique, vol. 35, no. 1, p. 3-18.

Stark, T.D., Hangseok, Choi, and McCone, Sean, 2005, Drained shear strength parameters for analysis of landslides: Journal of Geotechnical and Geoenvironmental Engineering, vol. 131, no. 5, p. 575-588.

Rock-Socketed Foundations for the Bridge at Pitkins Curve

John P. Turner
Dan Brown & Associates, PC, and Professor Emeritus, University of Wyoming
Civil & Architectural Engineering
Laramie, WY 82071
(307) 286-2958
E-mail: jturner@danbrownandassociates.com

John D. Duffy
California Department of Transportation
50 Higuera St., San Luis Obispo, CA 93401
(805) 527-2275
E-mail: John_D_Duffy@dot.ca.gov

Reid Buell
California Department of Transportation
5900 Folsom Blvd., Sacramento, CA 95819-4612
(916) 227-1012
E-mail: reid_buell@dot.ca.gov

Xing Zheng
California Department of Transportation
5900 Folsom Blvd., Sacramento, CA 95819-4612
(916) 227-1036
E-mail: xing_zheng@dot.ca.gov

Prepared for the 63rd Highway Geology Symposium, May 7-10, 2012

Acknowledgments

The authors wish to thank the California Department of Transportation for permission to publish this work and their support during design and construction of the bridge at Pitkins Curve. The general contractor is Golden State Bridge and the foundation contractor is Case Pacific, Inc. Mr. Ryan Turner, P.E., Caltrans District 5 geotechnical engineer, reviewed this paper and provided valuable input based on his first-hand site observations.

Disclaimer

Statements and views presented in this paper are strictly those of the authors, and do not necessarily reflect positions held by their affiliations, the Highway Geology Symposium (HGS), or others acknowledged above. The mention of trade names for commercial products does not imply the approval or endorsement by HGS.

ABSTRACT

A case history is presented on the design, construction, testing, and performance of drilled shafts for a bridge located at a difficult site on Highway 1 along California's Big Sur Coast. The purpose of the bridge is to traverse a landslide that has been a long-term maintenance challenge for Caltrans. The site is underlain by rock of the Franciscan Formation and consists of metamorphosed siltstone and sandstone with inclusions of metabasalt. The rock is highly folded and fractured, difficult to sample in some locations, and exhibits wide variations in strength and quality. Construction challenges included the need to place bridge piers on a steep slope just outside the limits of active sliding and installation of drilled shafts into highly fractured rock prone to caving. The presence of perched water tables caused variable inflow of water to drilled shaft excavations. This paper describes how these constructability issues were addressed and how they influenced the selection and design of the foundations. This paper demonstrates a rational approach to a difficult design and construction problem, including: (1) the use of careful engineering geologic studies to design a structure with difficult access while traversing a major landslide (2) the need for careful attention to constructability for drilled shafts in highly fractured rock with variable groundwater, and (3) the interaction between load testing and site investigation and its application to LRFD design of rock-socketed drilled shafts.

SITE CONDITIONS AND GEOLOGICAL SETTING

Pitkins Curve is located on Highway 1, approximately 1.5 miles south of Lucia, on the Big Sur Coast in Monterey County, CA. This area lies in the Santa Lucia Mountain range in the Coast Ranges geomorphic province. The area is characterized by rugged, steep terrain with steeply incised drainages and narrow crested ridges.

Figure 1 is a photograph of Pitkins Curve and adjacent sections of Highway 1. Immediately south of Pitkins Curve is a major rockfall area referred to as Rain Rocks. The area is underlain by the Franciscan complex, consisting of metamorphosed sedimentary and volcanic rocks. A matrix of dark gray, highly sheared siltstone and shale, metamorphosed to argillite or phyllite, contains blocks of medium-grained fractured meta-sandstone and greenstone (metabasalt). The metabasalt (greenstone) is relatively hard and erosion resistant.

Quaternary colluvial and debris flow deposits overly the Franciscan rocks, forming a thick sequence of crudely bedded silty sand with numerous angular cobbles and boulders. Below the roadway, fill is intermixed with this material where it was used to construct and maintain the roadway embankment. This material is derived from the upper adjacent slopes and is therefore similar to the colluvium and in most cases indistinguishable.

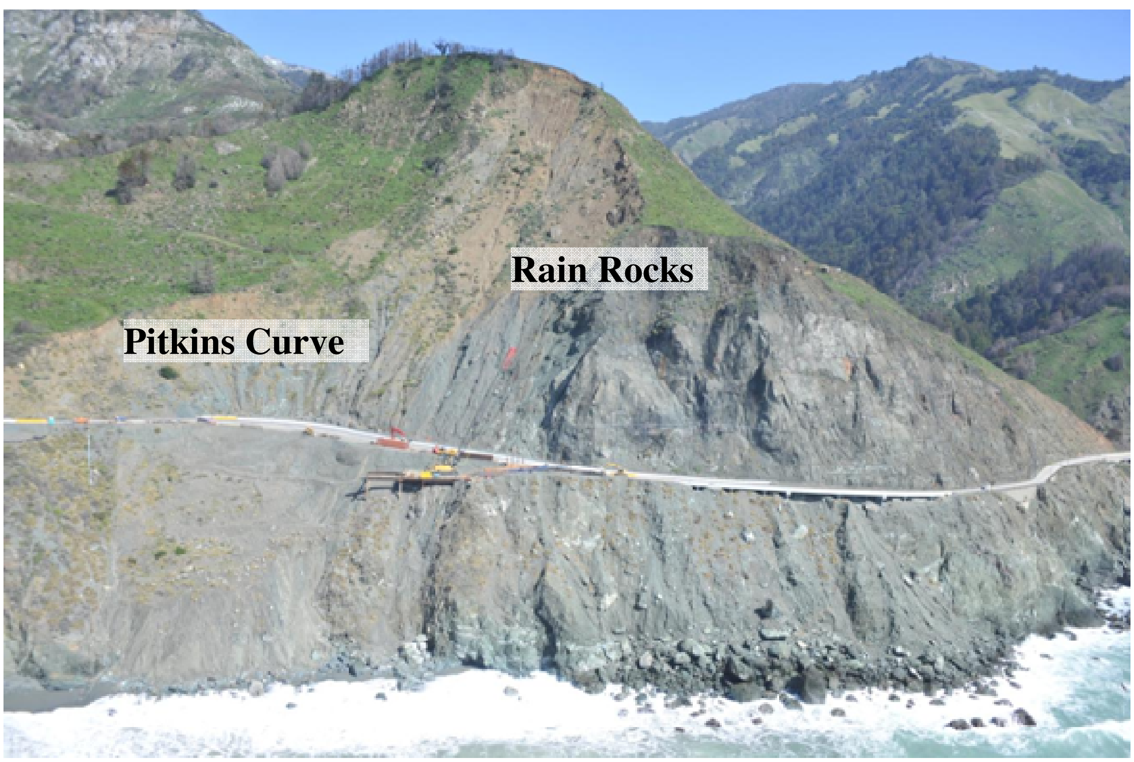

Figure 1. Pitkins Curve and adjacent sections of Highway 1, Big Sur Coast (View is to the east).

Pitkins Curve Landslide. In the Pitkins Curve section (Figure 1) the roadway embankment has been creeping since its original construction in the late 1930's. Largely the sliding was restricted to shallow failures receding up into the traveled way. Repairs were made by end dumping slide debris over the side. The slopes below the roadway are subject to constant erosion by high surf at beach level and full exposure to oncoming Pacific storms. In 1998 a landslide below the roadway caused the loss of one lane. In February of 2000, 130,000 cubic yards of material translated down slope, undermining and destroying three hundred feet of roadway. Pitkins Curve Landslide is a combination translational/rotational movement, slipping above competent bedrock at depth. Based upon surface features and subsurface borings, the depth to sliding is approximately 65 ft below the roadway grade. The slide material consists of pre-existing landslide deposits, side cast materials, and roadway embankment. Triggering mechanisms included high groundwater levels, surface water infiltration, and toe erosion by high surf leading to undermining.

A variety of repair strategies were considered to remediate effects of the 2000 slide and later that year the roadway was relocated inland, away from the landslide into the cut slope above the road. Approximately 100,000 cubic yards of material was excavated to cut-slope angles varying between 1:0.75 and 1: 1 (V:H). This strategy reduced driving forces from the head of the slide and diverted a portion of infiltrating groundwater and surface runoff away from the slide area. This was supplemented by the installation of horizontal drains above and behind the slide. A wire mesh drapery system was placed on the slopes above the roadway to control post-construction rockfall.

Pitkins Curve Rockslide. In February 2001, heavy winter storms again hit the site accompanied by development of rockfall and small rock slides in the new cut slopes above the roadway. These rockfalls and rock slides rapidly progressed upslope to the ridgeline. Daily rockfalls, 1 foot to 10 foot in dimension, and rockslides of 50 to 100 cubic yards destroyed the wire mesh drapery system placed on the cut slopes to prevent smaller rockfalls from hitting the highway. To maintain traffic safety the roadway was shifted seaward away from the hillside and a rockfall catchment ditch was constructed. This roadway alignment was close to the pre-2000 alignment. The ditch was approximately 33 feet wide and 13 feet deep. Slope movement was so regular and consistent that ditch cleaning was required daily. The total accumulation of these small events totaled more than 20,000 cubic yards in three months.

Immediately south and adjacent to Pitkins Curve are the high cliffs known as Rain Rocks (Caltrans, 1995). Since the road was constructed in the 1930's Rain Rocks has been a known rockfall location. Rockfall has occurred regularly during heavy rains and high winds. Mitigation historically consisted of warning signs, rock patrols, and rock scaling. In January 1993 a rockfall of approximately 20 ft in dimension damaged a concrete crib wall supporting the roadway. The crib wall failed and was repaired in 1995. In 1997/1998 a sidehill viaduct was constructed. During construction of the viaduct falling rocks traveled beyond the catchment area and into the construction zone. In response, additional rockfall mitigation measures were implemented by covering the slope with a wire mesh drapery system.

Following the 2000 repair the slopes above Pitkins Curve continued to recede, eventually reaching the ridge crest where Pitkins Curve and Rain Rocks transition. This triggered an increase in rockfall in the most northern chute of Rain Rocks, which at the time was covered by wire mesh drapery. A 350 cubic yard rockfall destroyed the wire mesh drapery in the chute. Slopes above the chute continued to destabilize and fall onto the roadway. Caltrans maintenance crews were continually interrupting traffic to clear the roadway of rockfall and scale the slopes of loose rock. In spite of these efforts, several vehicles were struck by falling rock. A temporary rockfall barrier was installed, which required narrowing the roadway to two 10-foot lanes. In 2001 the temporary at-grade barrier was replaced with a cable net drapery system on the cut slope above the highway, restoring the roadway to its original width.

The slope instability issues described above made the Pitkins Curve/Rain Rocks section of Highway 1 one of the most costly sections of roadway in the United States (Wills et al., 2001). As a result of frequent landsliding, Caltrans maintenance costs became excessive, roadway closures were frequent, and emergency work posed a risk to highway workers and the traveling public. To address these challenges, an interagency task force recommended a long-term engineered solution consisting of: (1) a bridge across the Pitkins Curve landslide and (2) a rock shed at Rain Rocks. A rendition of the roadway with the two proposed structures is shown in Figure 2. The bridge superstructure consists of a cast-in-place, pre-stressed concrete segmental box girder with a total length of 620 feet and central span of 311 feet. An important feature of the bridge at Pitkins Curve is the location of the two bridge piers. The piers are located just outside the lateral limits of movement of the Pitkins Curve Landslide. These limits were established on the basis of long-term monitoring of aerial photos and satellite imagery by the U.S. Geological Survey and detailed site characterization by the California Department of Transportation involving borings, geological mapping, and monitoring of surface movements. The bridge is designed to span the landslide while allowing the slide material to continue moving down slope in response to natural geologic processes. This approach solves a civil engineering problem, *i.e.*, providing reliable transportation, while accommodating the challenging geology of the Pitkins Curve site. That is to say, *match the structure to the ground conditions*.

Figure 2. Proposed bridge and rock shed at Pitkins Curve/Rain Rocks.

GEOTECHNICAL FEATURES

Site characterization included extensive core sampling at the sites of the bridge piers. Detailed subsurface profiles were developed from core logs. Rock mass characteristics, including core recovery, RQD, and uniaxial compressive strengths, varied significantly with depth. The detailed profiles were used to assess both constructability issues and design parameters for potential foundation schemes. Based on the degree of fracturing and observations of perched water tables with locally high water inflow, the potential for caving and seepage were identified as construction challenges for foundations requiring excavation. From a design perspective, rock uniaxial strengths were considered favorable for developing side and base resistance of rock socketed foundations.

FOUNDATION SELECTION

Foundation types considered for the bridge piers ranged from a single large-diameter drilled shaft (14-ft diameter) to drilled shaft groups of (2 to 4 shafts) supporting a footing at each pier. The most critical load combination resulted from analysis of the bridge for Extreme Event I (earthquake) loading and resulted in significant lateral and overturning forces at the foundation level. One of the site factors that favored a larger number of smaller diameter shafts is the steepness of the slope on which the piers are located. Larger diameter shafts require larger and heavier equipment (drilling rigs and cranes). Positioning of the required equipment on the steep slopes required either (a) construction of temporary trestles out over the slope, or (b) construction of stabilized benches cut into the slope. While both means were considered feasible, both could be achieved more cost-effectively if the loads to be supported were minimized. Accounting for the steep (and potentially unstable) slopes, the lateral and overturning loads, and the characteristics of the rock mass, a four-shaft group supporting an 8-ft thick concrete footing at the top-of-rock elevation was selected as the most efficient and cost-effective foundation system.

DRILLED SHAFT LOAD TEST

Several factors created a high degree of uncertainty with regard to the application of predicted values of side and base resistance to the design of drilled shafts deriving their support from the Franciscan rocks underlying the Pitkins Curve bridge site. First is the large degree of variability in rock mass characteristics observed in core logs. Features such as degree of weathering, degree and orientation of fracturing, characteristics of the fracture surfaces, and the strength of intact rock specimens exhibit wide ranges both vertically and horizontally. Second, it had been Caltrans policy to neglect base resistance of drilled shaft in rock due to uncertainties about the quality of rock mass beneath the tip and uncertainties about the effectiveness of contractors' cleanout procedures, particularly for shafts placed under water or slurry. Water, in the form of perched groundwater with potential for inflow to the drilled shaft excavations, created further uncertainty due to its potentially adverse impacts on both side and base resistance due to disturbance and caving.

To address these issues and to obtain valuable information on constructability, Caltrans conducted a pre-design Osterberg Cell (O-cell) load test on a prototype drilled shaft constructed just on the inboard side of the roadway and upslope from Pier 2. A boring was made at the exact location of the test shaft and carefully logged to provide a detailed profile of the rock. Core samples that were sufficiently intact were tested for uniaxial compressive strength. At a depth corresponding to the tip of the test shaft (35.5 ft) the rock is described as very hard metabasalt.

The test shaft was 42-inches in diameter and 35.5 ft deep. The O-cell was placed at a distance of approximately 3 ft above the base of the shaft. The test shaft was drilled using a rock auger without casing or other support. Seepage of water into the excavation was observed during drilling. Water at the base was mixed with cement and re-excavated just prior to the final concrete pour in order to minimize potential adverse base conditions. Strain gages placed at a depth of 20 ft were used to determine the magnitude of load transfer over the depth intervals from 0 – 20 ft, 20-ft to the O-cell, and O-cell to the base of the shaft.

O-cell test results are presented in a report prepared by Loadtest Inc. (2007). The maximum load applied to the test shaft was 5,200 kips. Corresponding axial displacements above and below the O-cell were 1.02 and 0.76 inches, respectively. Table 1 presents values of unit side resistance measured at the maximum test load. In addition, base resistance was mobilized under very small displacement, clearly showing that base resistance could be relied upon for design, provided that proper cleanout and inspection procedures were employed as part of the construction process. Mobilized base resistance was calculated to be 396 ksf.

Table 1. SUMMARY OF UNIT SIDE RESISTANCES FROM O-CELL TEST

Depth Interval	**General Material Description**	**Unit side resistance (ksf)**
1.6 – 20.0	top 2-3 ft pavement base course underlain by interbedded metasediments/metabasalt rock	5.51
20.0 – 32.3	metasediment and metabasalt	29.43
32.3 – 37.0	metabasalt	27.0

ANALYSIS AND DESIGN

Drilled shafts were designed to satisfy AASHTO LRFD criteria for all applicable limit states. For design under lateral loading, the *p-y* method of analysis was used to evaluate the drilled shaft response to combined lateral, moment, and axial force effects predicted by structural modeling of the bridge. User-specified *p-y* curves were input to the program LPILE (Ensoft, 2007). The user-specified curves were developed using the hyperbolic model proposed by Liang et al. (2009). This model requires the following parameters to define each hyperbolic curve: (1) the initial slope, which is the subgrade modulus K_h and (2) the asymptote, which is the ultimate lateral resistance p_{ult}. Both of these are approximated on the basis of empirical correlations given by Liang et al. (2009) to rock mass characteristics, in particular the Geological Strength Index (GSI) and uniaxial compressive strength of intact rock, q_u. GSI was evaluated from examination of rock core and photos of rock core. Lateral loading considerations and the resulting moment demand governed the final shaft diameters (5 ft).

Design for axial loading incorporated both side and base resistances for evaluation of strength, extreme event, and service limit states. This approach was validated by results of the O-cell load test. Values of side resistance (f_s) measured in the load test were fit to the following expression relating f_s to uniaxial compressive strength of intact rock (q_u):

$$\frac{f_s}{p_a} = C\sqrt{\frac{q_u}{p_a}} \qquad (1)$$

in which: p_a = atmospheric pressure in same units as f_s and C = fitting coefficient. For the inerlayered meta-sedimentary rock and basalt observed in the test location, this yields an average value of $C = 0.62$. For highly fractured rock this agrees well with the lower-bound value of 0.63 reported by Kulhawy et al. (2005). The back-calculated value of $C = 0.62$ was then used to evaluate design values of side resistance based on uniaxial compressive strengths measured for core samples taken from the borings at each of the pier locations. For tip resistance, two factors were considered: (1) results of the O-cell test, in which the tip was bearing on a layer of metabasalt, and (2) careful evaluation of the boring logs so that tip elevations of the production shafts corresponded to high quality rock, i.e., high RQD material. The final design, considering LRFD criteria and the objective of high quality rock at the tip elevations, resulted in 50-ft long rock sockets at Pier 3 (south) and 60-ft long rock sockets at Pier 2 (north).

Service limit state design was based on a tolerable settlement for individual shafts of ½ inch under a nominal axial force of 2,300 kips, as established by the bridge structural engineer. A load-displacement model was developed from the O-cell load test results, as described by the authors in an earlier paper (Turner et al., 2009). A simplified model of rock socket load-settlement behavior given by Kulhawy and Carter (1992) is fit to the measured axial load-displacement curve from the load test through trial values of the rock mass elastic and strength properties. Where borings verify that the rock mass has similar lithology, strength, and discontinuity characteristics, the analysis can then be used to evaluate load-deformation behavior of trial designs (Turner, 2006). Figure 3a shows the O-cell curve and the resulting modeled curve, while Figure 3b shows the curve extrapolated to the conditions at Pier 2. For an axial compression load of 2,300 kips, the predicted displacement is approximately 0.07 inches and the shaft response is in the linear elastic range. By this analysis, the proposed trial design easily satisfies the service limit state criterion that limits settlement to ½ inch. The final shaft dimensions are governed by strength and extreme event load considerations and not by the axial settlement criterion.

CONSTRUCTION

Construction began in January of 2010 with the erection of trestles to support construction equipment for drilled shaft construction. Two trestles were erected, one from the north abutment and one from the south, as shown in Figure 4. Trestles are supported on 24-inch diameter pipe piles driven into rock using a downwhole hammer.

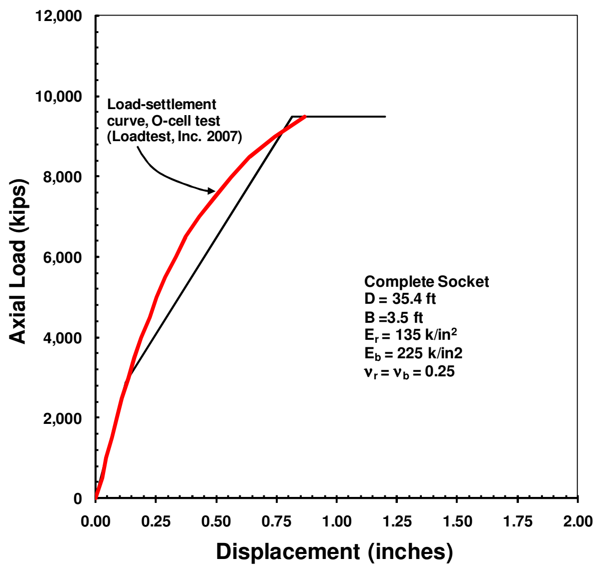

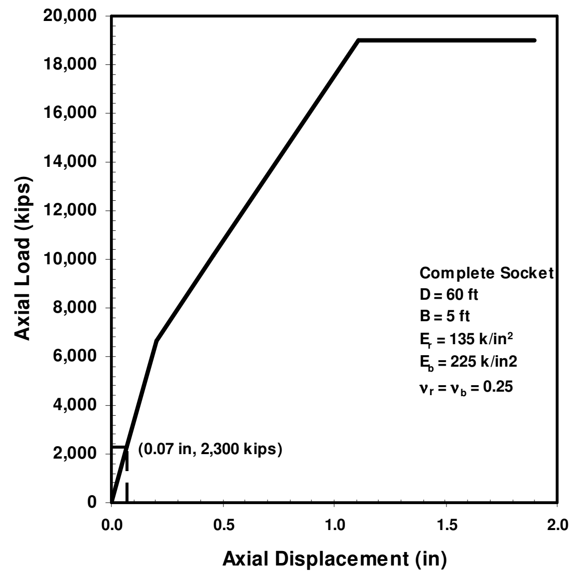

(a) O-cell Load Test Results (b) predicted for shafts at Pier 2

Figure 3. O-Cell equivalent top-load versus settlement curve and modeled curve.

Figure 4. Trestles extending from north and south abutments.

At each pier location, a temporary shored excavation was extended to the top of rock. Shoring consisted of trench plate between H-pile sections placed inside of driven 24-inch pipes, backfilled with pea gravel, and the pipes withdrawn using a vibratory hammer. A group of four 5-ft diameter drilled shafts was then constructed inside each excavation by drilling from the trestle (Figure 5).

Figure 5. Drilled shaft excavation from south trestle.

Difficulties encountered during drilled shaft construction were those anticipated during the planning phases, namely caving of fractured rock and inflow of water upon encountering pockets of perched water. The contractor addressed these difficult conditions by first drilling into the caving material with slightly oversized tooling (augers and core barrels) and removing as much material as possible. A low-strength sand-concrete mix was then placed to the bottom of the excavation. When the lean concrete plug was sufficiently hardened, the socket was re-drilled to the design diameter. At Pier 3 (south) this technique made it possible to extend the shafts through the zones of caving and water inflow to the target tip elevations. Figure 6a shows conditions at the bottom of the shored excavation for construction of the foundations at Pier 2, while Figure 6b shows the excavation of one of the cement-stabilized zones.

(a)

(b)

Figure 6. (a) Drilled shaft construction inside shored excavation, (b) cement-stabilized excavation in caving rock.

At Pier 2 (north), use of the lean concrete plugs was not entirely successful in controlling water and caving. The plug was poured and allowed to harden, but when the contractor drilled into the plug, the thin layer of remaining lean concrete caved and water inflow caused further caving of the fractured rock. The contractor then switched to the use of bentonite slurry and the shafts were completed without further caving.

SUMMARY AND CONCLUSIONS

The bridge at Pitkins Curve provides a case history of foundation design and construction that required the unique and challenging aspects of site geology to be taken into account properly. The primary purpose of the bridge is to avoid a landslide that has impacted Highway 1 since its construction in the 1930's. Location of the bridge foundations was dictated by the slide geometry and characteristics, requiring long-term monitoring, detailed site characterization, and understanding of the geologic processes. Design of the foundations to meet LRFD criteria required very detailed characterization of rock mass characteristics and was made feasible by conducting a pre-design axial load test. Construction difficulties were anticipated by conducting the site investigation for constructability as well as for establishing geotechnical design parameters.

Figure 7 is a photo of the Pitkins Curve site in January of 2012, immediately following completion of the main span of the bridge. Rock shed construction is underway to the south of the bridge (right side of photo).

Figure 7. Pitkins Curve Bridge and Rain Rocks Rock Shed, January 2012.

REFERENCES

California Department of Transportation (1995). *Geologic Report, 05-Mon-001-PM21.1, Rain Rocks Rockfall*, Office of Structural Foundations, Engineering Service Center.

Loadtest, Inc. (2007). Report on Drilled Shaft Load Testing (Osterberg Method), Pitkins Curve Bridge – TSI, Big Sur, CA (LT-9357), Gainesville, FL, 52 p.

Kulhawy, F.H. and Carter, J.P. (1992). "Settlement and Bearing Capacity of Foundations on Rock Masses," Ch. 12, *Engineering in Rock Masses*, F.G. Bell, Editor, Butterworth-Heinemann, Oxford, pp. 231-245.

Kulhawy, F.H., Prakoso, W.A., and Akbas, S.O. (2005). "Evaluation of Capacity of Rock Foundation Sockets," *Alaska Rocks 2005,* Proceedings, 40th U.S. Symposium on Rock Mechanics, American Rock Mechanics Association, Anchorage, AK, 8 p.

Liang, R., Yang, K., and Nusairat, J. (2009). "P-y Criterion for Rock Mass," *J. Geotech. and Geoenvir. Engrg.*, ASCE, 135(26), 11 p.

Turner, J.P. (2006). *NCHRP Synthesis 360: Rock-Socketed Shafts for Highway Structure Foundations*, Transportation Research Board, National Research Council, Washington, D.C., 148 p.

Turner, J.P., Buell, R., and Zheng, X. (2009). “Axial Load-Settlement Behavior of Rock Sockets from O-Cell Testing”, *Proceedings, 60th Highway Geology Symposium*, Buffalo, N.Y., Sep 29 – Oct 2, 2009.

Wills, C.J., Manson, M.W., Brown, K.D., Davenport, C.W., Domrose, C.J. (2001). *Landslides in the Highway 1 Corridor: Geology and Slope Stability along the Coast Between Point Lobos and San Carporfora Creek, Monterey and San Luis Obispo Counties, California,* California Department of Division of Mines and Geology.

Numerical Analysis of Rockfall Sheltering Structures

Francesco Calvetti
Politecnico di Milano, Dipartimento di IngegneriaStrutturale
Piazza L. da Vinci 32, 20133 Milano, Italy
+39-0341-488819
francesco.calvetti@polimi.it

Thomas Frenez[1] and Francesco Tondini[2]
Rockfall Defences.r.l.
Piazza delleErbe 1, 38017 – Mezzolombardo (TN), Italy
+39-0461-605528
E-mail[1]: thomas.frenez@rockfalldefence.com
E-mail[2]: francesco.tondini@rockfalldefence.com

Prepared for the 63rd Highway Geology Symposium, May 7-10, 2012

Acknowledgements

The Authors acknowledge BetonCostruzioniS.p.A. for the information provided about the prototype modular tunnel, and HSH s.r.l. for the support in performing numerical analyses with the FE code Straus 7.

Disclaimer

Statements and views presented in this paper are strictly those of the author, and do not necessarily reflect positions held by their affiliations, the Highway Geology Symposium (HGS), or others acknowledged above. The mention of trade names for commercial products does not imply the approval or endorsement by HGS.

ABSTRACT

This paper concerns the numerical analysis of rockfall shelters covered by an absorbing layer of soil.

The evaluation of the actions on the shelter is derived from a recent design approach introduced by one of the Authors. This approach allows one to evaluate the time history of stresses acting on the upper face of the roof of the shelter (usually a reinforced concrete slab) during an impact, starting from the evaluation of the impact force acting at the boulder-soil interface, and subsequently considering the stress propagation through the soil stratum.

Starting on this basis, the design approach can be conveniently used to simulate the effects of a number of impacts by performing a series of dynamic numerical analysis of the behavior of the shelter where the stress increments are directly applied to the structure itself as input loads.

These simulations are particularly useful for highlighting some relevant aspects of the behavior of the shelter, particularly the importance of the size (longitudinal extension) of the structure.

INTRODUCTION

This paper concerns the application of the uncoupled design approach for rockfall protection tunnels that has been recently introduced by Calvetti and di Prisco (2011) to evaluate the time history of stresses acting on the upper face of the roof of the shelter. This approach has already been tested by comparing the design diagrams with the results of impact experiments performed on different types of granular layers (namely loose and dense sand), as shown in the aforementioned publication. Considering the dynamic nature of the phenomenon, the complete description of time evolution of both impact force and stress increments is given in the form of synthetic curves whose parameters depend on the design impact (size of the block, falling height) and on the geometrical and mechanical properties of the absorbing layer (thickness of the layer, stiffness of the soil layer). All of these parameters are available to the end-user in the form of design charts, as a function of the mentioned factors.

Starting on this basis, the design approach can be conveniently used to simulate the effects of a number of impacts by performing a series of dynamic numerical analysis of the behavior of the shelter, where the synthetic stress increments are directly applied to the structure itself as input loads. In particular, the FE code Straus is used for modeling a modular structure made up of a series of precast cantilever modules (courtesy of BetonCostruzioniS.p.A.). Each module of the structure is anchored to the mountainside by tendons, and a reinforced concrete (RC) plate is cast in-situ on the modules to connect them and, to provide continuity in the longitudinal (parallel to the tunnel axis) direction (Figure 1).

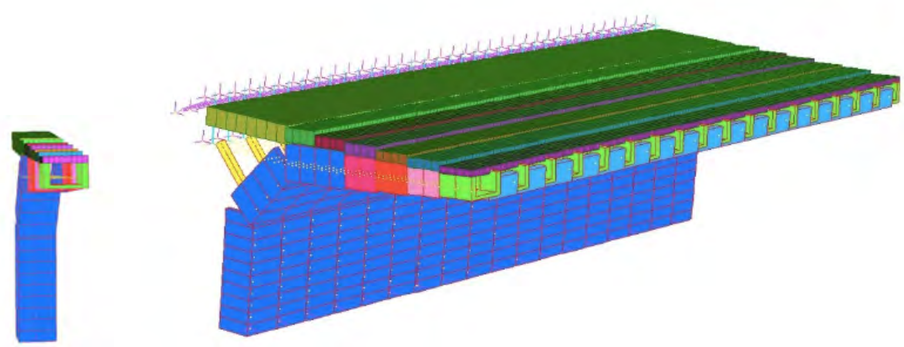

Figure 1. Numerical model of the shelter; one module (left) and assembled structure (right)

NUMERICAL SIMULATIONS

Numerical simulations are particularly useful for highlighting some relevant aspects of phenomenon such as the non-linear relationship between the duration of the impulse and the natural period of the structure, the separate influences of structural stiffness and mass, and the importance of the size (longitudinal extension) of the structure, which heavily affects the 3D response. This effect is due to the behaviour exhibited by the plate under impacts, as qualitatively shown in Figure 2. When only a few modules are assembled, the structure essentially behaves as a cantilever beam. On the contrary, for longer shelters the bending stiffness of the upper plate contributes to diffusing the propogation of stresses transversally (which reduces the maximum deflection, see Figure 3).

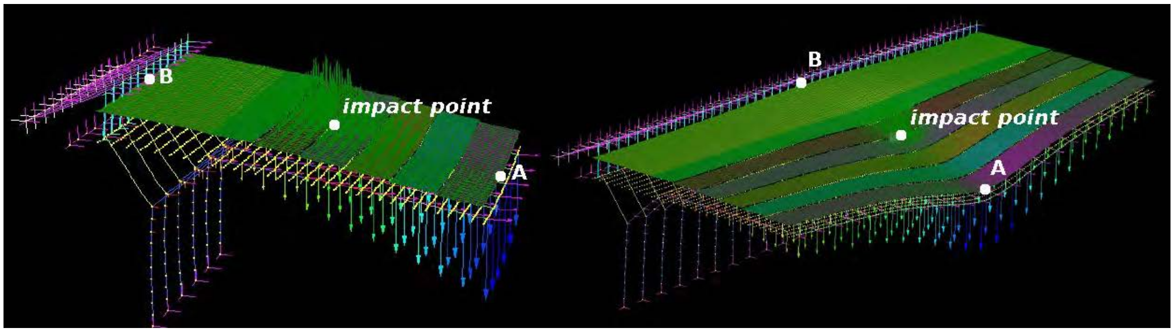

Figure 2: Shelter deformation under impact loads; 6 modules (left) and 24 modules (right)

These effects can be quantitatively studied by plotting the displacements of the plate during impacts as a function of time (Figure 3). Besides the progressive reduction of the maximum deflection at point A, which rapidly becomes constant for shelter length larger than about 30 m (more than 18 modules), it is worth noting that the horizontal displacement of the plate is reduced significantly as the larger number of modules is increased. This is due to the increased number of collaborating anchors.

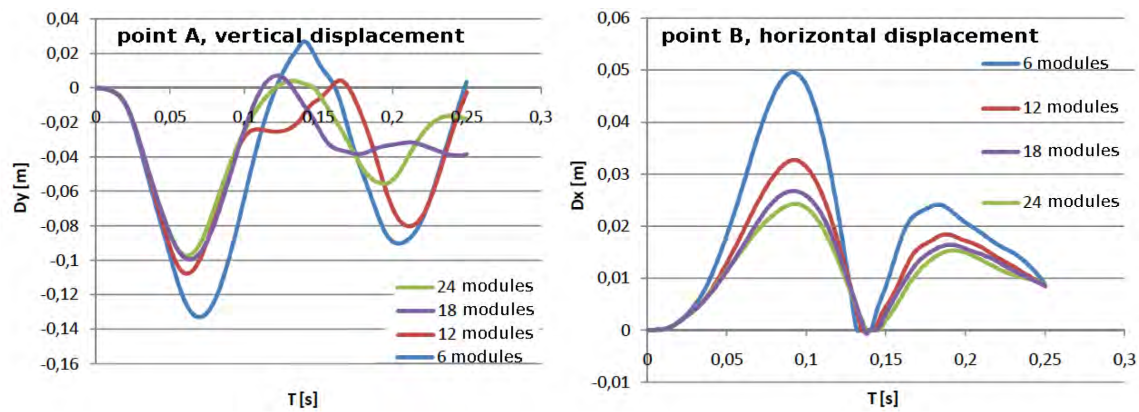

Figure 3: Plate displacements as a function of time

It is worth noting that in both cases the in-plane stiffness of the plate is such that the plate itself moves horizontally as a rigid body. This evidence can be illustrated by plotting the displacements recorded at the tip of the slab at various longitudinal distances from the impact point, as schematically depicted in Figure 4 with reference to the 24 modules case.

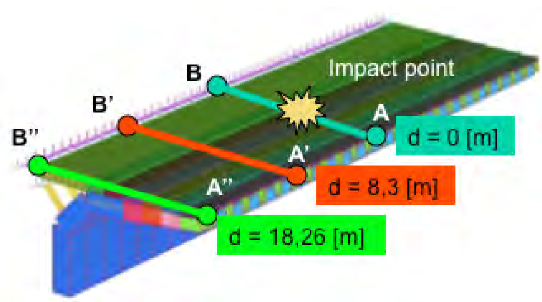

Figure 4: Schematic view of measurement points

The evolution with time of the vertical and horizontal displacements recorded at points A, A',A'' and B,B',B'' of Figure 4, is plotted in Figure 5. It is clear from the plot of vertical displacement with time that the maximum deflection decreases with distance from impact point., In addition, the time instant when the maximum value is recorded is progressively delayed. This evidence is also reported by Calvetti and di Prisco (2011), on the basis of experiments performed on a real tunnel. On the contrary, the observed horizontal displacements are independent of the distance from impact point. This evidence is justified by the high in-plane stiffness of the plate, which makes the structure move horizontally as a rigid body.

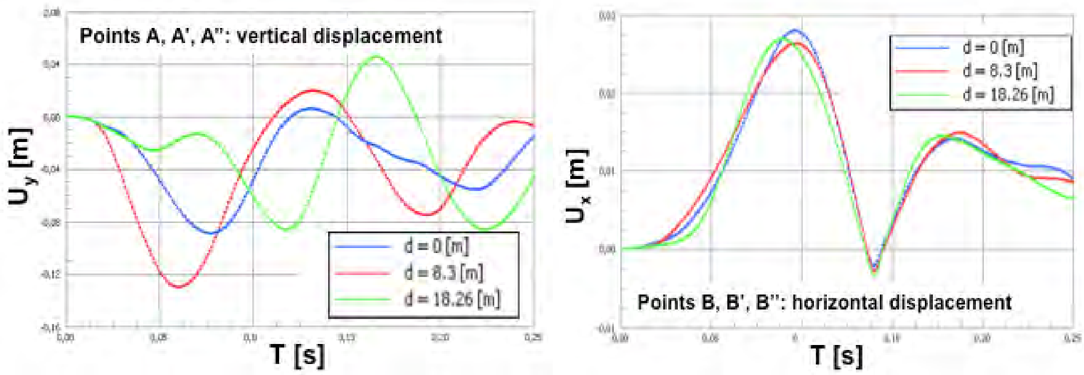

Figure 5: Plate displacements as a function of time, at various distances form impact point

CONCLUSIONS

In this short note results of numerical simulations are shown in order to highlight some features of the structural behavior of shelters under impact loads. The main point considered concerns the importance of the size (longitudinal extension) of a prototype structure made of a series of modules. In fact, as the number of modules increases, the deflection pattern of the roof plate changes from that typical of a cantilever beam to that of a plate. As a consequence, the deflection of the tip of the plate decreases. The in-plane stiffness of the plate is such that the structure moves horizontally as a rigid body, which decreases the horizontal displacements (and the loads on the tendons) as the number of modules increases.

REFERENCES

F. Calvetti and C. di Prisco, 2011, *A New Design Method for Rockfall Shelters Covered by Granular Layers*, in Rockfall Engineering, Wiley, 343-373.

WSNs for rockfall protection assets tracking and maintenance

Andrea Danzi[1]
Rockfall Defence Srl
Mezzolombardo (TN) ITALY
+39 0461 605528
andrea.danzi@rockfalldefence.com

Prepared for the 63rd Highway Geology Symposium, May 7-10, 2012

Acknowledgements

This paper is the one of outcomes of “Natural Risk Sensing (NRS)”, a research project funded by the Autonomous Province of Trento and the European Regional Development Fund (ERDF)

ABSTRACT

This paper investigates the indicators required by a Wireless Sensor Network (WSN) for defining a Condition-Based Maintenance (CBM) plan for rockfall protection assets. The approach described in this paper is one of the outcomes of Natural Risk Sensing (NRS), a research project with the aim of applying condition based maintenance techniques to perform non-destructive testing techniques and performance data management to assess rockfall protection assets condition. The paper illustrates two main components of the NRS project: the WSN component, dedicated to the calibration of sensors, and the CBM component describing a more general asset management approach with its underling technological platform.

After describing some background related to CMB and WSN, this work proposes some inputs coming from Euro-norms useful for understanding the requirements in term of maintenance of the assets addressed. Managing structures that are designed for absorbing huge impacts is not the same as managing structures that have a relatively “quiet” life, like those composing buildings, bridges and other construction works. Rockfall protection systems have some specific performance indicators that should be addressed to plan maintenance and assess their performance efficiency. These performance indicators are strictly linked to the highly non-linear dynamic behavior that can be evaluated only through full-scale tests (1:1). For this reason during the NRS project a huge amount of effort was spent to compare data coming from different types of sources, like load-cells, micro-electromechanical accelerometers and visual inspections. The objective of the test program was to calibrate and compare the loads (kN) retrieved from the load-cells and the acceleration (g) retrieved from the accelerometers with the hope of finding some correlation with the data gathered from visual inspections.

The last part of the paper introduces an IT platform that should be able to transform the raw data retrieved from WSN to information useful for the people in charge of managing the maintenance activities of the assets spread around the country. This last component of the NRS project is still under development and for this reason this paper cannot go deeper in details about the complete and definitive implementation of a CBM approach.

INTRODUCTION

This paper investigates the indicators for defining a Condition-Based Maintenance (CBM) plan for rockfall protection assets with the support of Wireless Sensor Networks (WSNs). In Italy, every year, more than $32M of new rockfall protection related assets is installed to protect roads, railways and buildings. It's understandable that sooner or later all the related structures (rockfall barriers, drape netting, embankments, concrete structures, etc.) will be subject to damages, reducing the protection efficiency level for which they were designed. Moreover, rockfall protection systems are installed in harsh environments, like steep slopes, rock cliffs, and in areas that are difficult to reach, and with a high level of risk for the people that should do visual inspections. For this reason, once the construction of rockfall protection measures is completed, the main issues that public administrations should address are the management of those assets and the maintenance of the related structures. Some local agencies have attempted to apply asset management procedures, starting from creating asset inventories and geo-referencing the structures. Some national agencies also applied the principles of condition assessment, but only on major assets, like bridges and tunnels, ignoring the multitude of relatively small geotechnical works. In the middle of 2010, Rockfall Defence Srl started a research project with the aim of applying Condition-Based Maintenance techniques to perform non-destructive testing techniques and performance data management to assess rockfall protection system condition.

THE BACKGROUND

Condition-Based Maintenance (CMB) is a maintenance approach developed mainly by industrial companies to actively manage the health condition of their equipment, tools, and mechanical devices in order to perform maintenance only when it is needed and at the most opportune times. The components of CMB are a weighted mix of:

- Maintenance Principles (reliability-centered maintenance performance monitoring, etc.);
- Techniques (diagnostics, sensor data management, etc.);
- Enablers (IT infrastructure, assets inventories, geo-referenced data, etc).

Well-designed CMB processes can be used for almost all industries, like: Department of Defense (DoD) weapons systems, turbine generators, jet engines, circuit card manufacturing, etc.

One of the techniques which CMB can leverage is the management of data coming from a micro-sensor designed to survey a specific asset. Wireless Sensor Networks (WSNs) are systems composed of spatially distributed autonomous sensors that cooperatively monitor physical or environmental conditions. WSNs are applied in many scenarios, each with unique characteristics in terms of features, displacement, and connectivity. Some applications of WSNs are the following: area monitoring, for enemy intrusion detection inside restricted areas; environmental monitoring, state of permafrost assessment in mountainous areas like the Alps; machine health monitoring, machinery condition-based maintenance in small machinery spaces.

Ideally CBM performed with the support of WSNs allows the maintenance staff to make the most informed decisions thereby minimizing the level of risk, system failures and time spent on maintenance. It can drastically reduce operating costs and increase the safety of assets requiring maintenance.

The main problems with this approach are the following:

- Define performance indicators to assess the rockfall protection assets maintenance status;

- Retrieve and distribute the data from the sensor network located in harsh environments;
- Manage the considerable amount of data collected by the WSN and implement algorithms to transform raw numbers into performance indicators.

ROCKFALL PROTECTION ASSETS AND MAINTENANCE ACTIVITIES

Referring to Euro-norm design and construction standards, European Technical Approval Guidelines and Italian local norms, rockfall protection systems are construction products that should meet the first essential requirements: mechanical resistance and stability. In other words, they are products which are produced for permanency and should guarantee performance with an acceptable probability during an economically reasonable working lifetime.

Citing the Interpretative Document related to Council Directive 89/106/EEC of 21 December 1988:

"*. . . maintenance is a set of preventive and other measures which are applied to the works in order to enable the works to fulfil all its functions during its working life. These measures include cleaning, servicing, repainting, repairing, replacing parts of the works where needed, etc. Normal maintenance generally includes inspections and occurs at a time when the costs of the intervention which has to be made are not disproportionate to the value of the part of the works concerned, consequential costs being taken into account.*"

Considering what the Interpretative Document states, it is easy to believe that the maintenance measures applied to works to fulfill all their functions should make it such that the loads that are liable to act on the structures will not lead to:

- Collapse of the whole or part of the works;
- Major deformations to an unacceptable degree;
- Damage to other parts of the works or to fittings or installed equipment as a result of major deformation of the load-bearing construction;
- Damage by an event to an extent disproportionate to the original cause.

The points listed above are clearly understandable for structures used in standard construction works, like reinforced concrete walls designed for buildings, steel structures for bridges, and reinforced soil walls for landfills.

In the case of rockfall protection measures the loads that are liable to act on the structures (impacts of one or more boulders) can lead to partial collapse and deformations on its components that are unacceptable for other standard structures. At the same time there are components of rockfall protection assets that are designed to dissipate the impact energy through plastic deformations that lead to irreversible damages. For this reasons those assets should be maintained with two main objectives:

- Monitor all the events that can produce irreversible damages;
- Measure the deformations occurred.

Currently maintenance activities are performed by direct visual inspections, where people, annualy in the best cases, visit inaccessible construction sites and report any visible damages. Traditional maintenance activities are expensive and consume a lot of technical and economic resources. Furthermore there is an aspect related to the uncertain nature of rockfall events for which visual inspections are inadequate: rockfall may occur anytime, including after an inspection has taken place. This means that a protection system can be irreversibly damaged right after inspection and consequently the damage will not be discovered until the next inspection

SEARCHING FOR PERFORMANCE INDICATORS

Asset management and maintenance plans, whether they are performed with innovative methodology or not, need a set of broadly accepted metrics which reflect the efficiency level of the structures. The approach followed during the NRS project for defining such indicators starts from the background stated ETAG 027, the European Technical Approval Guideline for Rockfall Protection Kits.

The guideline first clarifies terms and definitions, such as the nature of the construction product, the classifications of its structural components, the intended use of the system (no avalanche, no active protection, etc.), and the assumed working life. The main source inside the guideline useful for defining performance indicators is the section “Assessment of Fitness for Use”. In the case of rockfall barriers, the assessment of the fitness for use also includes the characteristics of the assembled system which are relevant to its fitness for use with the expression of the respective performances, i.e. Energy absorption (Class), Deformation characteristics (Value, Class), Actions on foundations (Value) and Durability (Value), Table 1.

System Characteristic	**Expression of System Performance**	**Example**
Energy absorption	Class ranging from 0 to 8	2000 kJ <=> Class 5
Deformation characteristics	Class (A, B or C) and Value	Residual height > 50% <=> Category A
Actions on foundations	Value	250 kN
Durability	Value	Values accroding to ISO 1461

Table 1. Characteristics of the assembled system (ETAG 027)

The method of verification of energy absorption consists of testing the system with impacts at different energy levels: Maximum Energy Level (MEL) and Service Energy Level (SEL). To pass the test, the rockfall protection systems should first stop the block without any contact with the ground until the system has reached the maximum elongation. There are also other performance requirements such as the absence of ruptures and the residual height in some acceptable range.

Figure 1: test site for crash-test

For the work described in this paper, the important information is the set of measurements that should be performed for assessing the performance of the system foundations.. The forces must be measured throughout the time of impact and the peak force shall be recorded., and In addition, the time-force diagrams Must be provided. The measured values must be declared in the European Technical Approval (ETA).

As stated before, for the purpose of maintenance activities it is important to know if the loads acting on the structure during its working life are compatible with the forces measured during testing for each Energy Absorption Level. Because of technical constraints and huge economic impact, a generic system installed outside the test site, on a real construction site, cannot be provided with load cells that measure the forces acting on the foundations.

A force is any influence that causes an object to undergo a change in speed, a change in direction, or a change in shape. In other words, a force is that which can cause an object with mass to change its velocity (which includes to begin moving from a state of rest), i.e., to accelerate, or which can cause a flexible object to deform. This last statement gives the idea that with knowledge of the acceleration of a structural component of a barrier, and the data measured during full-scale tests, it is possible to estimate the magnitude of the loads acting during an impact event which occurred on the construction site.

The reason to choose acceleration as a performance indicator is sustained by the fact that now there is a large set of low cost Micro-electromechanical systems (MEMS) available for constructing embedded devices (sensor nodes) that measure the proper acceleration of a body. Single- and multi-axis models of accelerometers are available to detect magnitude and direction of the actual acceleration (or g-force) as a vector quantity, and can be used to sense orientation (because direction of weight changes), coordinate acceleration (so long as it produces g-force or a change in g-force), vibration, shock, and falling (a case where the acceleration changes, since it tends toward zero).

TESTING WSNS IN HARSH ENVIRONMENTS

Wireless sensor networks (WSNs) are applied in many scenarios, each with unique characteristics in terms of connectivity and sensing requirements. Assessing the specifics of a target environment is usually complex, and often entails a preliminary pilot deployment. In this paper we report about such a pilot deployment, which took place on two test sites located in northern Italy. The objective of the pilot deployment was to test the behavior of wireless sensor devices working with different protocols (ZigBee, GPRS), and frequencies (2.4GHz, 868MHz, 900MHz) capable of getting links to distance of up to 12km. The sensors were a 3D 8g-range accelerometer and a GPS sensor. The features implemented in the sensor node are the following:

- High-performance, low-power 8/16-bit Atmel® AVR® XMEGATM Microcontroller
- High-performance RF-CMOS 2.4 GHz Radio Transceiver targeted for IEEE 802.15.4TM, ZigBee®, 6LoWPAN, RF4CE, SP100, WirelessHARTTM and ISM Applications
    - Ultra-Low Current Consumption: SLEEP= 0.02 μA, TRX_OFF = 0.4 mA, RX_ON= 12.3 mA
- Ultra low-power high performance 3-axes accelerometer with ±2g/±4g/±8g dynamically selectable full-scale
    - Sleep to wake-up function
- Low-Power High-Performance 65 Channel SMD GPS Module

The features listed above enabled the netork to measure and transmit data related to

- 3D Acceleration with a full-scale of 8g
- Global position with differential correction

Harsh environments require the absence of cables and any physical connecting medium and the use of wireless technology for transmitting the data measured by the sensors. For these reasons the transceiver adopted by the NRS project supports ZigBee, a specification developed for a suite of high-level communication protocols using small, low-power digital radios based on an IEEE 802 standard for personal area networks. ZigBee is targeted at radio-frequency (RF) applications that require a low data rate, long battery life, and secure networking. This industrial specification is a low-cost, low-power, wireless mesh networking standard. The low cost allows the technology to be widely deployed in wireless control and monitoring applications. Low power usage allows longer life with smaller batteries. Mesh networking provides high reliability and more extensive range.

Sensor nodes were tested with different types of impacts and loads. The objectives of the crash tests were to compare the loads retrieved from the load-cells and the acceleration retrieved from the accelerometers.

Tests were performed with two different configurations:

1. Full-scale test on a rockfall barrier, accordingly to ETAG 027 procedure. In this case the block impacted the barrier net and the loads were transmitted to the accelerometers through the cables and the posts.
2. Stress-test on ropes and dissipators. In this case the block was connected through a single rope to a dissipator with no interception structure (barrier net) involved in the dissipation of the energy.

The second case, compared with the first one, is more severe, because the block and the sensor nodes are directly connected with a steel wire rope and there is no intermediate dissipation (barrier net).

Figure 2: crash-test

Figure 3: stress-test

In the case of the full-scale tests, the nodes were placed in 4 different positions (see red bullets in Figure 4)

1. Top of the Post
2. Retaining rope
3. Lower bearing rope
4. Interception structure

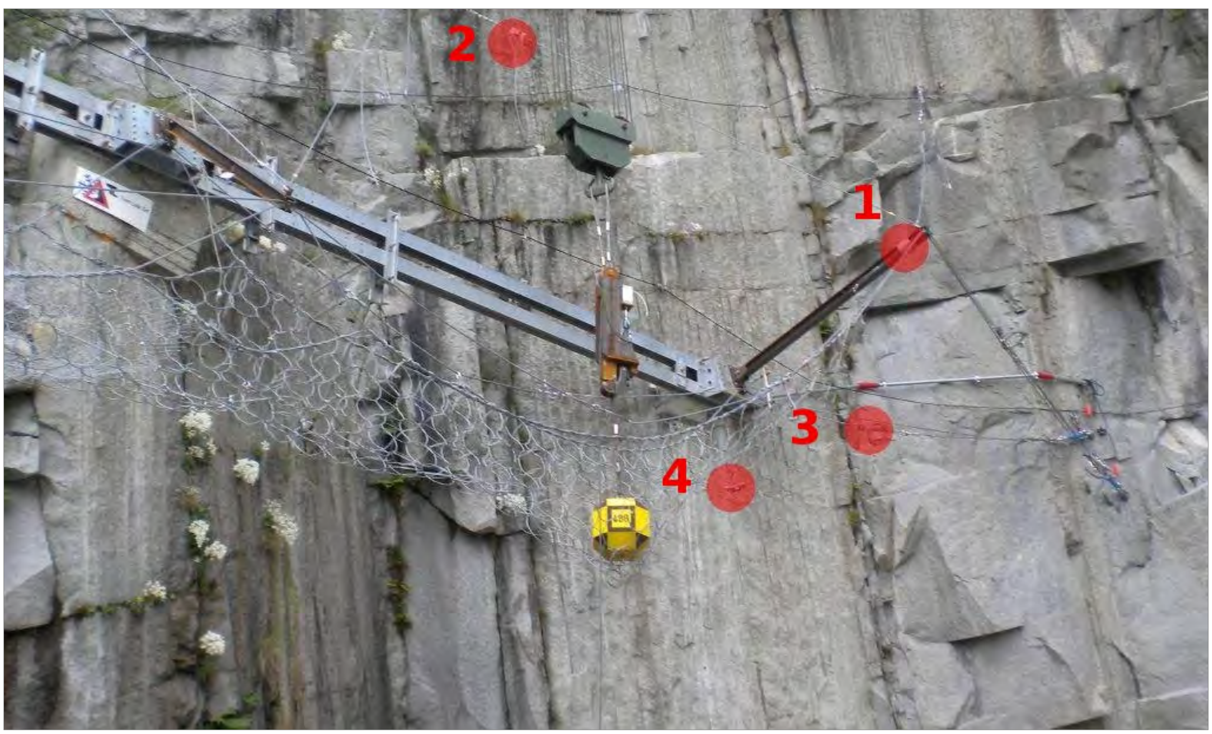

Figure 4: position of the nodes during crash-test

To understand the correlation between energy impact, forces measured from the load cells, and acceleration measured from the sensor nodes, the tests were performed with blocks with increasing mass:

- 530 lbs (240 kg)
- 1,060 lbs (480 kg)
- 2,120 lbs (960 kg)
- 7,100 lbs (3220 kg)

Figure 5: blocks with different sizes

In the case of stress-tests, the nodes were placed in 5 different positions (see red bullets in Figure 6)

1. Before the dissipator (N1)
2. After the dissipator (N2)
3. Near the block (N3)
4. On the retaining rope (N4)
5. At the top of the supporting post (N5)

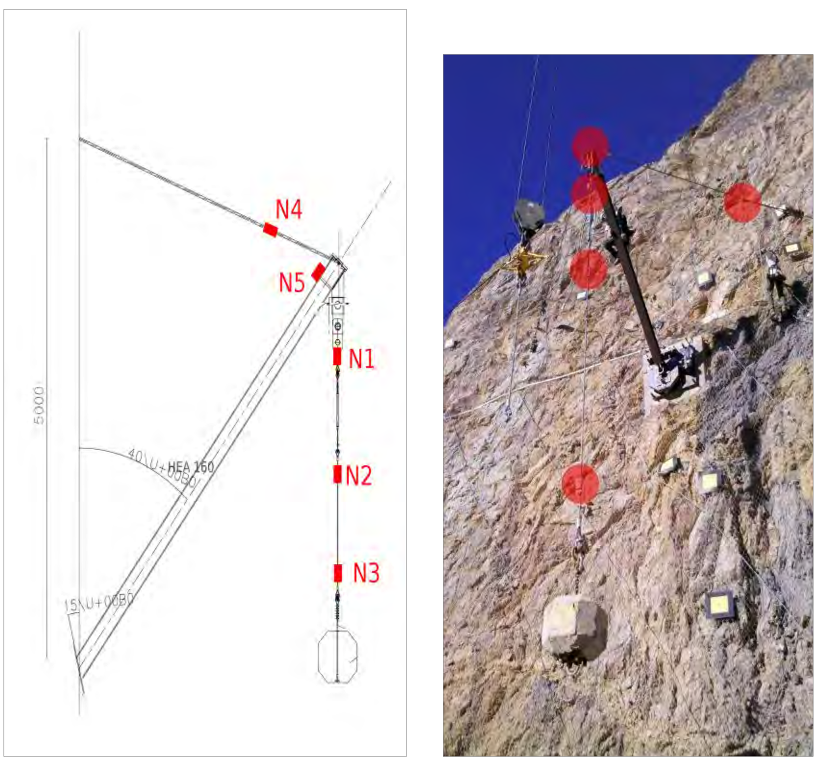

Figure 6: position during stress-test

To understand how the nodes behave in different configurations, the load tests were performed with 3 different types of dissipators:

1. Plastic deformation of three aluminium pipes
2. Plastic deformation of one aluminium pipe
3. Friction between ropes and steel plate

The scope of this type of test was to understand if the measures of the accelerometers change when the configuration of the system changes (the weight of the block was obviously constant).

During the NRS project a significant amount of data was collected and the results of the related analyses were useful for establishing the threshold levels for the sleep-to-wake-up function, optimizing energy consumption. Moreover, by implementing advanced data filtering, it was possible to classify different types of events which occurred to the structures. These included:

1. Impact on the interception structure;
2. Impact of the block on a single post;
3. Impact on other components (ropes, anchors, etc);
4. Shocks caused by the activity of people interacting with the system;
5. Shocks caused by the failure of the foundations (soil/rock);
6. Static load of the block inside the net.

FROM RAW DATA MANAGEMENT TO CMB

It is possible to design and develop micro-devices that are able to measure, collect, and transmit condition-related data from rockfall protection assets'. Now it is important to investigate how that data can be transformed into useful information for personnel in charge of managing the assets conforming to CMB's principles. The main job should done by an IT platform that aggregates all the data and shows on detailed maps the status of each asset (see Figure 8 in the next page). The main features of the envisioned IT platform are the following:

1. Implement a digital geo-localized asset inventory;
2. Integrate data coming from remote acquisition (WSNs);
3. Integrate data coming from traditional means (visual inspections) ;
4. Provide rich informational mapping tools;
5. Track asset-related reports on the map but also over time;
6. Collect information via text messages, email, web-forms and other innovative channels.

The digital inventory is the first step to organizing and sharing information related to any kind of assets. Without a well-organized database it is impossible to manage huge amounts of data, whether they come from sensor devices or from manual data entry. In general the "*integration*" keyword is the most important feature that a specialized platform like the envisioned one should be able to implement. Many agencies already have implemented digital inventories as well as GIS tools, so one of the main requirements of the platform is the possibility to integrate with existing databases, maps and geo-localized content in general.

In figure 7 there is an illustration of the data model proposed for managing assets, events and maintenance related activities. The main entity represented in the model is "*incident*", an abstraction of all possible events that can occur to a defined asset. An "*incident*" is identified in space (location) and time (incident_date) and can has one or more associated "*media*" (images, video and digital contents in general) inserted by one "*reporter*". *Reporte*s can be human, in the case of visual inspections, or WSN related services, in the case of CMB supported by digital devices. Every "*incident*" has a rating, depending on the performance indicators, and can raise alerts ("*alert_send*") if pre-defined thresholds are reached. The model considers also the possibility to share incident with other platforms as well as implementing a verification process where some kind of supervisor can approve or discard the notification of the "*incident*".

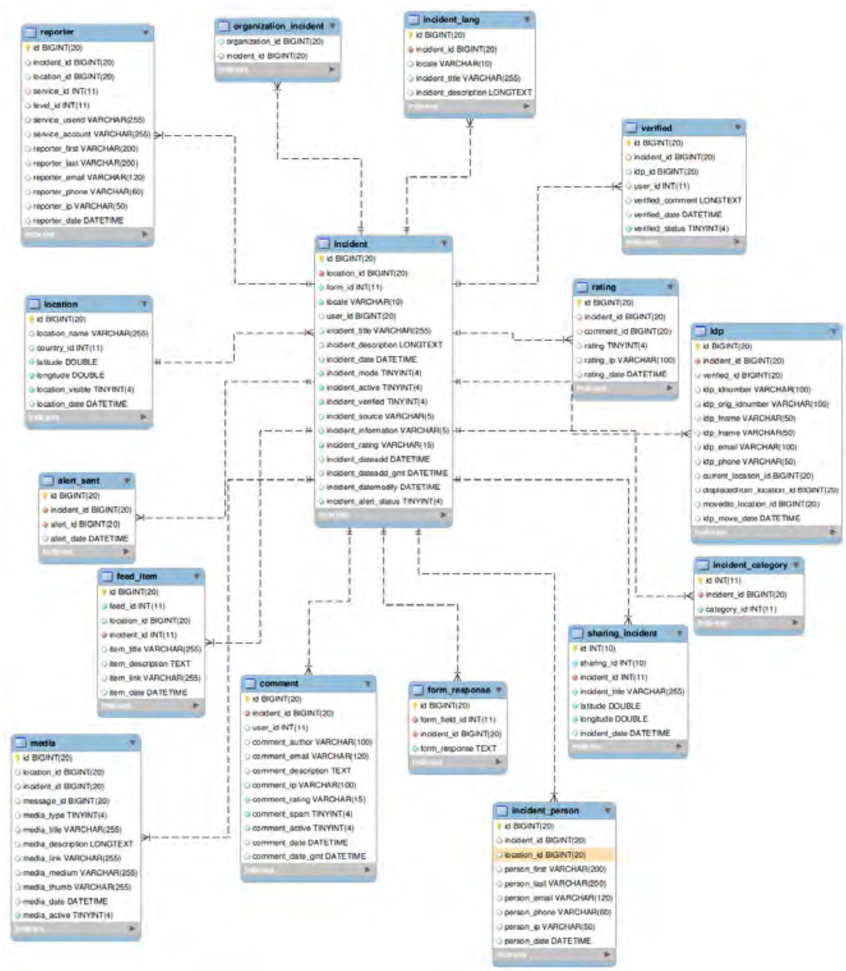

Figure 7: asset management data model

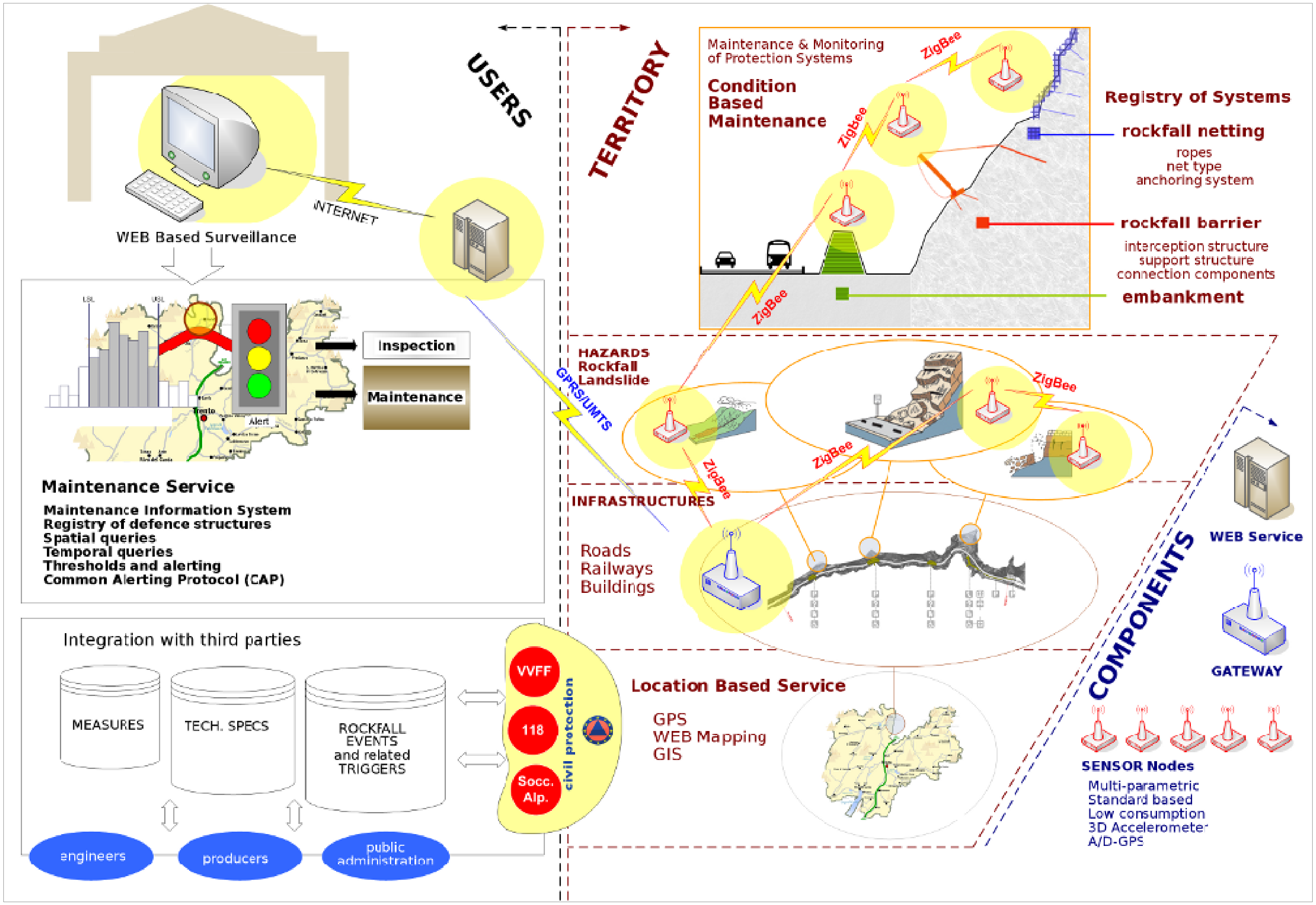

Figure 8: illustration of the NRS platform

CONCLUSIONS

The NRS project is still ongoing and the main results currently come from the tests executed on the sensor nodes. Initially this activity was underestimated, but during the testing, many issues and opportunities arose. The main issues were related to the reliability of the sensor node hardware. Due to the large accelerations, the devices suffered damage to the enclosures and the batteries. This was the because batteries are the components with the highest mass, and due to acceleration moved from their original location destroying all the electronic components encountered.The opportunities that pushed further investigation of full-scale tests were those related to establishing proper relationships between the configuration of the systems after different types of events and the data retrieved from the sensors.

In conclusion, despite their usefulness, there are several challenges to the use of WSNs for monitoring the maintenance status of rockfall protection assets. First of all the introduction of a new technology will invoke a major change in how maintenance is performed, and potentially in the whole maintenance process. For this reason the WSN should be supported by easily adopted software, enabling the efficiency of distributing and using huge amounts of data. Secondly, the cost of a complete system should be comparable with the costs related to periodic inspections performed by humans. Also, the technical side of building a WSN is not always simple. Even if the status of rockfall barriers can be easily assessed by measuring simple values such as displacement or acceleration, it is not trivial for other types of structures, to turn this data into actionable knowledge about status of the whole system. As performance requirements (e.g. CE marking and ETAG 027) cause rockfall mitigation measures to become more costly, micro-electro-mechanical instrumentation and software tend to become cheaper and more reliable. WSNs and related information systems become important tools for defining innovative and optimized maintenance processes.

FIELD TRIP GUIDEBOOK

Compiled By

Chris T. Higgins
California Geological Survey
Brian Rasmussen
National Parks Service
Brandon Badeker, Scott Lewis, Ed Speer, Jim Morris,
Richard Rusnak, Al Trujillo, Tom Graves
California Department of Transportation

63rd HIGHWAY GEOLOGY SYMPOSIUM

www.HighwayGeologySymposium.org

Redding, California
May 7-10, 2012

Hosted and Coordinated By

The California Department of Transportation
Division of Engineering Services – Geotechnical Services

Table of Contents

Field Trip Logistics

Welcome to the Field Trip for the 63rd Highway Geology Symposium, headquartered in Redding, California. All participants will be travelling in deluxe, 50 passenger coaches.

Lunch will be catered at the Oregon Mountain Lookout by Fat Daddy's Barbeque.

The lunch is sponsored by **Geobrugg** and the field trip refreshments sponsored by **Golder Associates**.

Field Trip Itinerary

Wednesday, May 9, 2012

7:30 AM	Busses arrive at Red Lion Inn
8:00 AM	Busses leave Red Lion Inn
8:30 - 9:00 AM	Stop 1: Whiskeytown Lake (Brian Rasmussen - National Parks Service)
9:15 - 9:45 AM	Stop 2: Bottom of Buckhorn Grade (Scott Lewis)
10:30 - 11:00 AM	Stop 3: Rocky Point (Tom Graves)
11:30 - 1:15 PM	Stop 4/Lunch: Oregon Mountain (Ed Speer)
1:15 - 2:00 PM	Stop 5: Storm Damage Locations (Jim Morris/ James Chinchiolo)
2:45 – 3:30 PM	Stop 6: Top of Buckhorn Summit (Al Trujillo)
4:00 PM	Arrive at Red Lion Inn

Field Trip Overview

Figure 1: State Route 299 south of Weaverville.

The geology of California is extremely complex, exhibiting in different places, parts of Earth's history over the last 2 billion years or so. Evidence of early quiescence is juxtaposed against later active tectonics that produced several orogenic events. In some areas, both extensional and compressional tectonic regimes have overlapped and fundamentally established the natural landscape that we see today. This complex geology has also provided the foundation for many industries that have flourished over time, from mining and timber harvesting that helped build the American West to the tourism/recreational industry that thrives today. The field trip will be a view through history, both geologic and anthropogenic, offering a glimpse into the challenges that our State faces, as well as the beauty it displays.

California History

California's history was rich well before its acquisition to the United States as a free state in 1850. The first European exploration of California by Juan Rodriguez Cabrillo took place in 1542 when his party landed in San Diego. In 1769; Gaspar de Portola (governor of the Californias) established a colony and California's first mission in San Diego; he later established the Presidio at Monterey. Spanish explorers established settlements there in the late 1770's. In 1776 the first colonizing party founded La Mision de San Francisco de Asis (Mission Delores) which is the oldest intact building in San Francisco. The first mass was celebrated at the mission on June 29, 1776 which was five days prior to the signing of the Declaration of Independence.

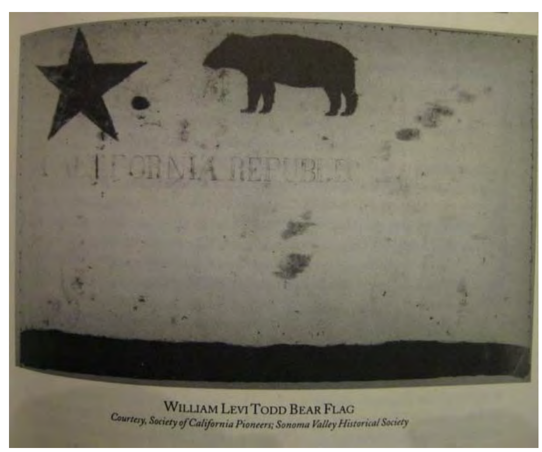

Figure 2: The flag of the 'Bear Flag Revolt' and California's first flag.

In 1846, the Mexican-American War began when Mexico declared war on the United States after numerous small battles along what is now the current border between the two countries. In California, American settlers revolted against Mexican rulers with the raising of the "Bear Flag", the precursor of California's current state flag. The war ended in 1848 with the signing of the Treaty of Guadalupe

Hidalgo, which required Mexico to give up California, several other future states, and the Rio Grande area, in exchange for fifteen million dollars.

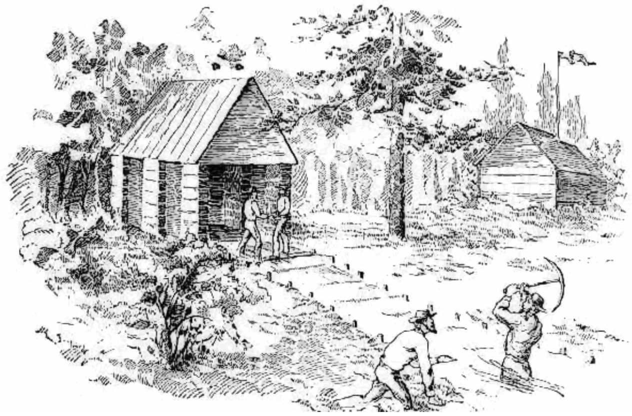

Figure 3: Sketch of Sutter's Mill in Coloma, California in 1849.

James Marshall discovered gold at Sutter's Mill in Coloma in 1848 leading to California's famous gold rush of 1849. In 1850, California was admitted as the 31st State. As part of the transcontinental railroad, the Central Pacific began installing tracks through the Sierra Nevada in 1863. In 1869, the first westbound train arrived in California. This achievement led to significant increases of population and economic expansion in California. By 1870, San Francisco was the tenth largest city in United States.

Figure 4: View of Post and Grant Avenues after the 1906 San Francisco earthquake.

In 1892, the Sierra Club was founded with John Muir elected as its president. At that time, its first conservation effort, the fight against the decrease in size of Yosemite National Park, was successful.

In 1899, Oil was discovered in the Kern River field, which lead to the great expansion of oil production in Southern California during the early twentieth century.

In 1906, a tremendous earthquake with an estimated moment magnitude of 7.9 hit San Francisco. The earthquake and resultant fire severely damaged or destroyed over 28,000 structures, and killed about 3,000 people. It is considered one of the worst natural disasters to strike the United States. Some of the damaged buildings can still be seen today in downtown San Francisco.

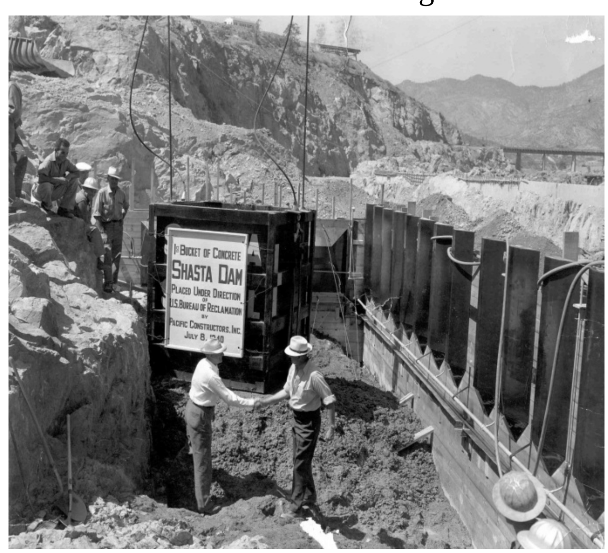

Figure 5: View of the placing of the first bucket of concrete in Shasta Dam. July 8, 1940.

Franklin Roosevelt's New Deal in the 1930's helped create much larger infrastructure in California, including a number of roads that are now state highways. In 1937, the Golden Gate Bridge was completed and opened to pedestrian traffic, a dream for the City since the late 1800's. Shasta Dam, just north of Redding, was completed in 1940 to provide water, electric power and flood control for Northern California. With increases in water and transportation infrastructure, California then became an agricultural giant, known as the breadbasket of the world.

Today, many aspects of the culture and economy of California still thrive despite global competition and budgetary challenges.

Shasta and Trinity County History

The first people to inhabit California and the local area were American Indians. In this area, five tribes coexisted and eventually intermingled with European Explorers and settlers who first arrived in the early 1800's. Disease struck the tribes, however, and may have caused further inroads for European settlement. The first commercial industry was trapping, which lasted until the late 1840's when beavers became nearly extinct. When gold was discovered in the local area during the late 1840's, the gold rush flourished. Subsequently, copper mining was a major industry in the 1880's, and in 1897, replaced gold as the top mineral produced in Shasta County. The fumes (sulfur dioxide produced by open-air heat roasting) produced by the smelting of the copper ore, however, killed vegetation as far away as Anderson, 15 miles distant. Orchards with ripened fruit died literally overnight due to the toxic fumes. By 1919 all smelters shut down due to violent protests by local citizens and farmers against the mining companies. Much successful litigation against the mining companies was also commenced. The area is still feeling the environmental effects of mining, i.e., heavy metals in soil and water that have to be continually mitigated. The Iron Mountain Mine northwest of Redding is the most prominent example.

Figure 6: View of the heat roasting piles at the Mammoth Mine, on the flank of iron Mountain.

As the easier gold deposits became exhausted, the mining industry faded early in the twentieth century and gave way to agriculture. The timber industry was strong since the mining days as large amounts of timber were required to shore the mines and build infrastructure. As the population increased and mining decreased, the timber industry continued, providing the raw materials for development. Slowly, with continued environmental regulation and increasing competition from a global economy, the timber industry has since declined. One of the largest industries currently active in this area is recreation/tourism, through the form of many water activities (boating fishing, etc.) as well as terrestrial activities (hiking, camping, bird watching, etc), has found a beautiful area to thrive.

California's Geologic History

Few areas of equivalent size in the world match the geologic diversity and complexity of California. Situated along a continental margin, the state has a long and dynamic geologic history. Episodes of passive sedimentation and major tectonism along this margin have produced many types of metamorphic, plutonic, volcanic, and sedimentary rocks that range in age from Precambrian to Cenozoic. All four types are distributed throughout California. Some radiometrically dated rocks in the state are at least 1.8 billion years in age.

Structurally, California has experienced significant changes through geologic time. Major tectonism, as demonstrated by accretion of exotic terranes along plate boundaries, development of extensive marine sedimentary basins, eruption of volcanic materials, and periods of major folding and faulting, has most notably constructed the California landscape. Following the Paleozoic when the state was part of a passive continental margin, a period of compressional tectonics began in the early Mesozoic. This regime dominated the state's tectonic development through the Mesozoic into the mid-Cenozoic and was the most important period of geologic assembly in California when successive terranes were accreted to the North American continent. About 28 million years ago, this regime began transition to one of translational and extensional tectonics, which led to formation of the San Andreas system of strike-slip faults and companion Basin and Range-type normal faults. Since then, this tectonic regime has increasingly dominated the geologic history of the state and is responsible for much of the high earthquake activity we experience today. In northernmost California, including the Redding area, however, convergent tectonics are still dominant today as the offshore Juan de Fuca-Gorda Plate plunges down the offshore Cascadia Subduction Zone beneath coastal California and continues to generate volcanic activity in the Cascade Range. Aside from the present great variety of landscapes and climatic regimes we see today, relatively recent tectonism has produced the highest (Mt. Whitney, 14,505 feet) and lowest (Death Valley, -282 feet) points in the continental United States, which are only about 80 miles apart.

From a practical perspective, this geologic history has spawned a variety of geologic hazards and earth resources. Earthquakes, landslides, tsunamis, volcanic eruptions, and floods comprise a set of historic and potential natural disasters that require constant vigilance and preparation. Although famous for its gold-mining history, California has an abundance of other metallic and non-metallic mineral deposits that have aided, and will continue to aid, development of the state. Similarly, California also contains world-class petroleum and geothermal resources.

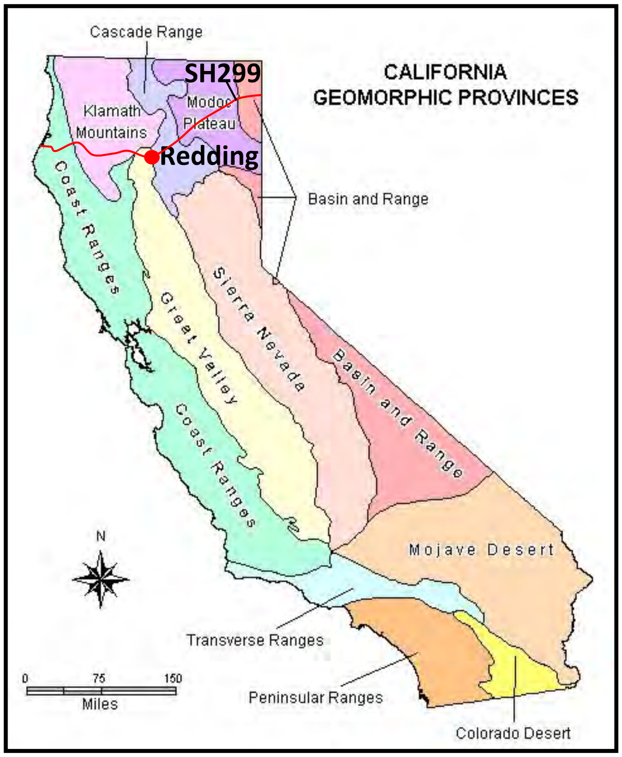

Figure 7: Map showing the Geomorphic provinces of California with the locations of Redding and State Route (SR) 299 indicated.

GEOLOGY OF THE REDDING AREA

The city of Redding (population 90,000) is nestled at the intersection of several geomorphic provinces. Surrounded by mountains on three sides, its location allows access via several highways, including State Route 299 (SR299), to many features that highlight the region's geology. Although our field trip is almost exclusively within the Klamath Mountains Province, SR299, which extends from the Pacific Ocean to the Nevada border, actually traverses six of California's eleven geomorphic provinces (Figure 7). No other highway in the state, except for Interstate 5, crosses as many provinces. From west to east these are: Coast Ranges, Klamath Mountains, Great Valley, Cascade Range, Modoc Plateau, and Basin and Range. Of these, the first four will be described briefly below because of their proximity to Redding.

Great Valley Province

Redding is within the northernmost end of the Great Valley Province. This province consists of a NNW-trending alluvial plain almost 450 miles long and 25-60 miles wide that extends through central California. The northern part, the Sacramento Valley, is drained by the Sacramento River. The province's relatively flat topography, favorable climate, sufficient water resources, and variety of soils have made it one of the most productive agricultural areas in the world.

The Great Valley is a structural trough in which marine, and later, continental sediments have been deposited almost continuously for the last 150 million years or so. The youngest of these sediments are largely unconsolidated or weakly consolidated coalesced alluvial-fan materials deposited by rivers and creeks, which drain the mountains that surround the Great Valley. Redding itself is mostly underlain by Holocene deposits of the Sacramento River and older dissected alluvial deposits of Quaternary and Pliocene age.

Klamath Mountains Province

West of Redding and extending northward into Oregon, the Klamath Mountains Province has rugged irregular topography with peaks and ridges that reach 6,000-9,000 feet in elevation. Actually comprising many individually named mountain ranges, this topography is a reflection of the underlying complex structure and many different lithologic units that comprise this province. Two main rivers, the Klamath and Trinity, drain the province; their channels and adjacent terraces have been extensively mined for placer gold. The Trinity, a short segment of which we will follow on the field trip, is the subject of a major restoration program by the U.S. Bureau of Reclamation (http://www.trrp.net/) to remediate the effects of this mining as well as historic logging in the surrounding terrain. Northwest of (and partially visible from) Redding is the Iron Mountain Mine, a major producer of copper, zinc, and pyrite from volcanogenic sulfide deposits. This mine is being remediated through the U.S. EPA Superfund Program.

Geologically, this province is considered to be a northwestern extension of the Sierra Nevada Province. The province as a whole is characterized by a complex assemblage of northerly-trending arcuate oceanic terranes of metamorphic and plutonic rocks of Paleozoic-Mesozoic age. These were attached to the North American continent by amalgamation and accretion, probably during the Cretaceous. They have been intruded locally by post-amalgamation Mesozoic plutonic rocks, most of which are intermediate in composition. By traversing the province in an east-west direction, SR299 offers an outstanding cross-section through many of these terranes. Generally, the terranes are sequentially younger from east to west and are bounded by major east-dipping thrust faults. The metamorphic rocks in these terranes are mostly island-arc sedimentary and volcanic rocks, ophiolitic (oceanic crust/mantle) complexes, and mélange belts, all of which are highly disrupted. Career-long study of these rocks led the late USGS geologist Porter Irwin to introduce the concept of "terranes," which eventually helped define the intricate assemblage of distinct packages of rocks by accretionary tectonics. Younger episodes of extensional detachment-type faulting have been superimposed on some of these terranes as well as overlying Tertiary sedimentary rocks. The highly disrupted metamorphic/plutonic units and some of the post-amalgamation plutonic rocks are subject to instability where slopes are steep and precipitation abundant. Along SR299, rockfalls are common in these settings and thus a topic of main interest on our field trip.

Cascade Range Province

Depositionally overlapping the Klamath Mountains Province on the east is the Cascade Range Province, which is also mountainous, but generally more arid. Extending northward into Oregon and Washington, it is a forested constructional volcanic highland of Cenozoic age built by numerous volcanoes, some of which have been recently active. Mount Shasta, a spectacular stratovolcano 14,179 feet high north of Redding, is the dominant landform in this province. Lassen Peak, a plug-dome volcano southeast of Redding and much lower than Shasta in elevation at 10,462 feet, erupted as recently as 1914-1921. This activity led to establishment of Lassen Volcanic National Park in 1916. Both peaks are visible from Redding.

The province consists dominantly of calc-alkaline (mafic-intermediate composition) volcanic rocks erupted along a north-trending continental magmatic arc that began forming about 36 million years ago. This arc developed in response to subduction of the Farallon Plate and its remnant, the Juan de Fuca-Gorda Plate, beneath the North American Plate off the coast of California to the west. Numerous NNW-trending normal faults cut the volcanic rocks. At least some of these faults may be related to structural subsidence caused by east-west extensional stresses associated with westward migration of the Basin and Range Province into this region.

Coast Ranges Province

Although it extends over 500 miles along the coast from the Oregon border to Santa Barbara County in southern California, only a very small portion of this province is present in the Redding area. Overall, the province is mountainous with many basins and valleys, particularly in the central and southern parts of the state. Many of these features trend north-northwest, a reflection of the underlying geologic structure.

The small portion of the province near Redding is underlain by a wedge of forearc marine sedimentary rocks that are part of the Mesozoic Great Valley Complex. This wedge overlaps the Klamath Mountains Province to the north and in turn is overlapped by sediments of the Great Valley Province to the east. In parts of the Coast Ranges Province, these rocks depositionally overlie a metamorphic basement called the Coast Range Ophiolite, which is also part of the Great Valley Complex. Age-equivalent to the Great Valley Complex and underlying it along the Coast Range Fault is the Jurassic-early Tertiary Franciscan Complex. This unit is a chaotic assemblage of dominantly marine sedimentary and volcanic rocks characterized by mélange belts, broken formations, and high-pressure/low-temperature metamorphic facies. The Franciscan Complex is notable as the first rock unit recognized in plate-tectonic theory as a subduction complex.

Structurally, the rocks of the Coast Ranges Province have undergone pervasive folding and faulting. Subduction driven by compressional tectonics dominated the early history of this province. Since the mid-Cenozoic, however, translational tectonics have become increasingly dominant as major strike-slip faults formed, including the San Andreas, which extends for about 400 miles through the province. Within this translational setting, elements of transpression and transtension have locally formed compressional and extensional features, such as anticlinal hills, thrust faults, and pull-apart basins. Many of the faults are active today, and some are responsible for significant historic earthquakes during the last 50 years.

SR299 Geology

Figure 8: View of the Devonian Copley Greenstone.

The following will provide an overview of the generalized geology along the SR299 corridor between the City of Redding and the town of Junction City. The guidebook is contains two fold out maps showing the generalized geology along the field trip route.

The geology of the SR299 corridor between Redding and Junction City is composed of parts of two major juxtaposed Paleozoic geologic terranes, the Eastern Klamath Terrane and Central Metamorphic. These terranes were accreted to the North American continent by compressional tectonics and later affected by episodes of extensional tectonics. The history has created an interestingly complex riddle that has yet to be fully solved.

Heading west from the start of the trip in Redding, SR299 travels over alluvium of the Sacramento River. At about PM 23, we enter the Eastern Klamath Terrane by crossing into rocks of the Devonian Copley Greenstone, which consists chiefly of metamorpohosed island-arc volcanic rock, of mafic and intermediate compositions. A small portion of the Copley Greenstone is of sedimentary in origin converted to slate and phyllite, through subsequent metamorphism.

Continuing west on SR299 up the ridge near PM 20, the Copley Greenstone is intruded by plutonic rock of the Devonian Mule Mountain Stock. Recognized by its light color in roadcuts, this rock unit is silicic to intermediate in composition, consisting of primarily of albite granite and trondhjemite. At the edge of the stock, is Whiskeytown Lake, Stop 1.

Continuing along the north shore of Whiskeytown Lake, SR299 resumes its traverse of metamorphic units of the Eastern Klamath Terrane. At about PM 15, we pass by steep roadcuts in Devonian Balaklala Rhyolite, which is composed of metamorphosed volcanic rock that may have formed in the same island arc as the Copley Greenstone. The Balaklala (Figure 9) is the main host for volcanogenic sulfide mineralization in this area, including the large massive copper-zinc deposits north of here at Iron Mountain. Oxidation of sulfide minerals has produced the extensive discoloration of the roadcuts.

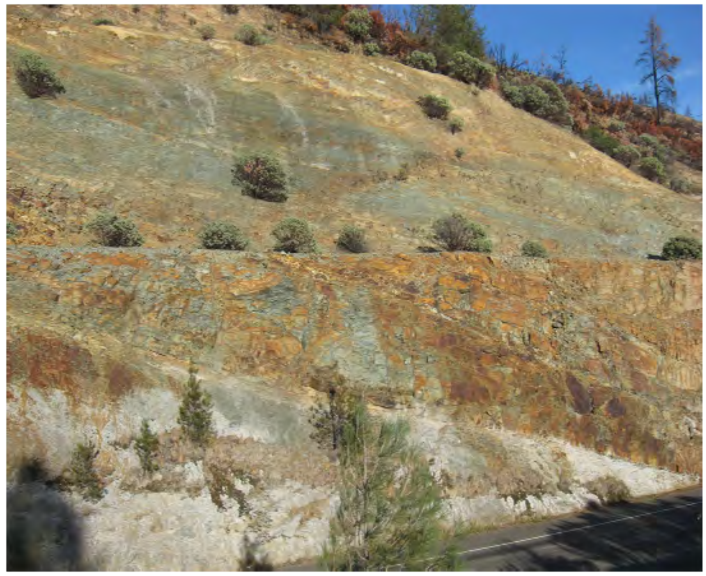

Figure 9: View of the Devonian Balakala Rhyolite near Whiskeytown Lake.

At approximately PM 9, before the turnoff to the historic gold-mining town of French Gulch, the route passes into the Mississippian Bragdon Formation, a silicic marine metasedimentary rock; in this area it contains gold-bearing quartz stringers and veins, and is a good example of the typical auriferous metamorphic terrain of the Klamath Mountains. Stop 2 at PM 5.35 affords a close-up view of this formation in roadcuts that expose black argillite and white quartz veins as well as small intrusions of intermediate-composition dikes.

Figure 10: View of a road cut in decomposed granite at Buckhorn Summit.

From Stop 2, we begin climbing Buckhorn Grade. In the canyon to the left are tailings from the Greenhorn Mine, which was developed in a massive-sulfide deposit of the Balaklala Rhyolite. At about PM 3.5, we cross into the intermediate composition plutonic rock of the Cretaceous Shasta Bally Batholith. The quartz diorite and granodiorite here are highly fractured and intensely decomposed by weathering. Cut slopes in the decomposed granitics (Figures 10 and 11) which we will view later today at Stop 6 on our return to Redding, are susceptible to erosion and shallow slides.

West of Buckhorn Summit, the batholith gives way to a complex assemblage of gneiss, ultramafic rock, and mafic intrusive rock, portions of which have been affected by landslides. At approximately PM 64, we cross the major thrust fault between the Eastern Klamath Terrane and the Central Metamorphic Terrane.

Figure 11: Photograph showing the Shasta Bally Batholith on the west side of Buckhorn Summit.

At about PM 63, the Tertiary Weaverville Formation is well-exposed in roadcuts (Figure 12). It consists of fluvial sandstone, mudstone, siltstone and conglomerate that were derived from mixed sources, including serpentinite, and was a major source of placer gold.

Between PM 58 and 61, the route passes next to alluvium of the Trinity River.

The metasedimentary Devonian Abrams Schist, a quartz-mica schist, is extensively exposed in this area along with small exposures of Devonian Salmon Schist and ultramafic rock. Stop 3 at Rocky Point is located along a 5-mile-long body of serpentinized ultramafic rock that is in contact with the Abrams Schist. Many areas of serpentinized ultramafic rock in California host asbestiform accessory minerals; Rocky Point is such a location. Unfortunately, due to the sheared and slickensided nature of the rock, it is problematic for cut slopes in mountainous terrain. The hazardous nature of asbestos in this serpentinized rock greatly increases its excavation costs and the costs of offhauling destabilized material that has come down on the road.

Figure 12: View of a road cut in the Tertiary Weaverville Formation.

Several miles north of Rocky Point, we enter the town of Weaverville, the county seat for Trinity County and once a major center of gold mining. It is underlain by rocks of the Weaverville Formation, through which we will ascend to Oregon Mountain Summit, the location of Stop 4. At Stop 4, the Weaverville Formation is faulted against the Devonian Salmon Schist, which was probably derived from mafic volcanic rock.

At Stop 4, just west of Oregon Mountain Summit, the Weaverville Formation (and some older rock units) is again faulted against the Salmon Schist, this time along the La Grange Fault, a large-scale detachment fault. Stop 4 is also the lunch location. Additional information is presented for that location in the guidebook on page 21. During lunch, individuals may choose to view the La Grange Fault, and/or the La Grange Mine, one of the largest hydraulic mines in California.

Field Trip Stops

STOP 1: Whiskeytown Lake

Figure 13: View of Whiskeytown Lake.

Central Valley Project (CVP)

Whiskeytown Lake is one in a series of reservoirs "plumbed" together as the Central Valley Project (CVP). Other local reservoirs include:

- Trinity Lake
- Lewiston Lake
- Shasta Lake
- Keswick Lake - the convergence point in which most water flows within the system, although water leaves Lewiston Lake down the Trinity River and Whiskeytown Lake down Clear Creek.

Trinity Lake flows into Lewiston Lake, which is an after-bay where water level is controlled for maximum power generation from the Trinity Lake Powerhouse. Water can pass through the plant at a maximum of 4,000 CFS with peak power output at 140 MW.

After leaving the Trinity Lake power station, water flows through Lewiston Lake to be discharged into the Trinity River after generating power (350 kW) at the Lewiston Dam Powerhouse, or is diverted to pass through the 10.8 mile Clear Creek Tunnel to the Carr Powerhouse on the west side of Whiskeytown Lake. The tunnel can pass 3,200 CFS and generate 154,000 Kw at the powerhouse. The water then discharges into Whiskeytown Lake, an after-bay to the Carr Powerhouse. Up to 50 percent of all Trinity River waters entering Lewiston Lake can be diverted to Whiskeytown Lake, and eventually to the Sacramento River.

Water passes through Whiskeytown Lake to be discharged into Clear Creek through the Whiskeytown Dam, or else diverted to pass through the 2.4 mile Spring Creek Tunnel to the Spring Creek Powerhouse on Keswick Lake. The tunnel can pass 3,500 CFS and generate 180,000 Kw at the powerhouse. The water then discharges into Keswick Lake, an after-bay for the Spring Creek Powerhouse and the Lake Shasta Powerhouse. Whiskeytown Dam can only discharge 1,200 CFS in a controlled release, and generates very little power. A total of 4,700

CFS can be discharged from Whiskeytown Lake and when input exceeds discharge and the lake rises above 1210 feet above sea level, the glory hole spillway releases the excess water down Clear Creek.

Finally, water passes through the Keswick Powerhouse, generating 117,000 kW at peak efficiency and discharges directly into the Sacramento River. Keswick Powerhouse does not have an after-bay.

In theory, a single drop of water precipitated in the watersheds upstream of Trinity Lake could have power generated from it at four different points: Trinity, Carr, Spring Creek, and Keswick Powerhouses before finally discharging into the Sacramento River. Then the water is used for municipalities, agriculture, and manufacturing on its way to the Pacific Ocean.

Water releases from Whiskeytown Lake and Shasta Lake are coordinated by the Bureau of Reclamation (BOR) to achieve cooler water temperatures for salmonids in Clear Creek and the Sacramento River.

STOP 2: Bottom of Buckhorn Grade

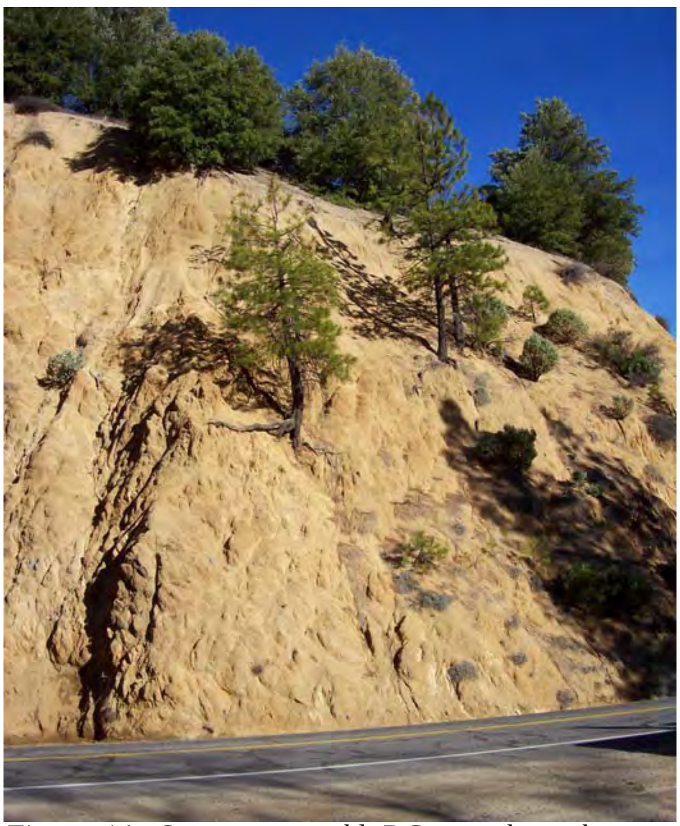

Figure 14: Seventy-year old DG cut slope that was originally cut planar at 0.75:1. The planarity is gone due to differential erosion and sloughing, but the overall slope ratio remains the same.

<u>Geotechnical Challenges and Solutions Involved in Highway Straightening and Widening on the Buckhorn Grade, Northern California</u>

J. Scott Lewis, M.S., PG, CEG, RGP,
California Department of Transportation,
1657 Riverside Drive, MS# 85, Redding, CA, 96001

Realignment of the upper 7.25 miles of the sinuous, rugged narrow Buckhorn Grade on SR299 in the Klamath Mountains west of Redding, California began in 2008 and is scheduled for completion in 2016. Studied and proposed as a single large-scale project for over 50 years, yet never put on track, the realignment is now being accomplished by linking a series of 6 separate safety projects, each with relatively restrained budgets, through a combination of creative and iterative designs, tailored geotechnical solutions, calculated geotechnical risks, two-year construction periods, geotechnical construction support, and problem solving (problems resulting from calculated risks) during construction.

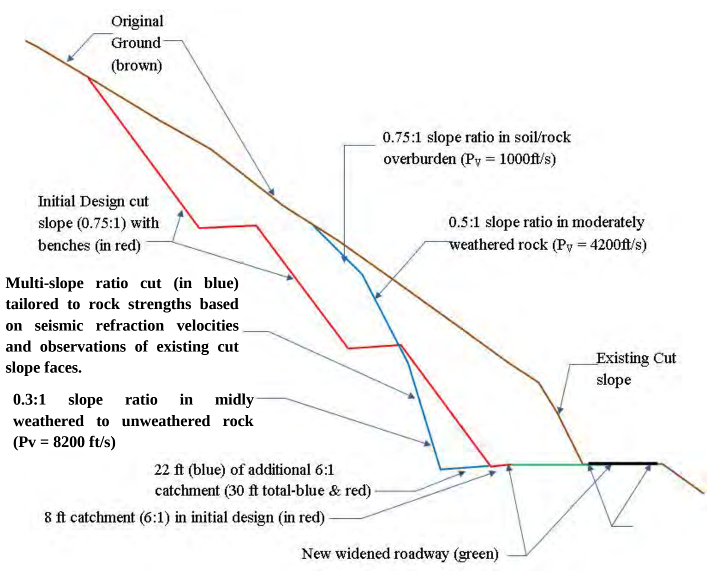

Figure 15: Cross section of multi-slope-ratio cut slope (blue) that reduces excavation quantities and greatly widens rockfall catchment area relative to the preliminary cut slope (with benches) shown in red. Slope ratios are based on field observations of existing cut slopes, correlations between the rocks exposed on these faces, seismic velocities determined from seismic lines shot above existing cut slopes, and geological experience with the rock types and their performance in cuts.

The upper half of the realignments, from the western end of the westernmost project at the summit (PM 0.0) to about PM 3.7, occurs in varyingly decomposed granite (DG) of the Shasta Bally Batholith, which is composed primarily of granodiorite and quartz diorite within the realignment areas. Decomposition is fairly deep in most places, with a few drill cores near the summit going over 150 ft without hitting relatively unweathered rock. Decomposition varies with depth and location, with the upper areas of the alignment appearing to be the most deeply weathered, while some areas lower down the grade appear to have harder granitics (probably only slightly weathered) less than 50 feet below road grade as evidenced by seismic refraction.

The lower half of the realignments, from approximately PM 3.4 to the eastern end of the easternmost project occurs in sedimentary, volcanic, metasedimentary, and metavolcanic rocks. These include: gneiss and amphibolites derived from rocks of the Bragdon Formation, Copley Greenstone, and Balaklala Rhyolite; phyllite derived from the Bragdon Formation; slightly metamorphosed to non-metamorphosed rocks of the Bragdon Formation and Balaklala Rhyolite; and Copley greenstone, which mainly consists of keratophyre, spilite, and metaandesite. The area between approximately postmiles 3.4 and 3.7 is a zone where chunks and slices of the Shasta Bally Batholith are intermixed with slices of the gneiss and amphibolite, likely as a result of the batholith emplacement.

Figure 16: Geogrid Reinforced Buttress constructed at the toe of a spring-induced slide activated during construction.

Cut slopes in the DG are designed up to 130 feet in height at a slope ratio of 0.75:1. This ratio was considered optimum, considering erosion, the relative steepness of the native slopes, and the 60 to 70 year performance of existing DG cut slopes. Although the literature and a mix of professional opinions regarding the optimum DG cut slope ratio with respect to minimizing erosion was indecisive, our opinion is that the 0.75:1 ratio was the best approach for the Buckhorn Grade. Flatter slopes result in significantly more excavated and denuded surface area, while exposing more surface area to rainfall impact and surface flow rilling. Based on the performance of existing cuts on the Buckhorn Grade we considered that reducing the exposed surface area more than offset the greater erosive power of higher surface flow velocities. Our observations indicated that a considerable portion of DG particles are dislodged by freeze-thaw processes rather than surface flow, an observation which favors steeper slopes that reduce exposed surface area. In addition, due to the relative steepness of the native slopes on the Buckhorn Grade, flattening slopes even slightly would result not just in significantly greater exposed surface area, but would also result in huge increases in excavation quantities. It was estimated that flattening the DG cut slopes to 1:1 would more than double the excavation quantities, which would have made the job unaffordable.

Cut slopes in the non-DG rocks vary up to 150 feet in height with slope ratios ranging from 1:1 to as steep as 0.25:1. Slope ratios were designed based upon the strength and structural orientation of the rock, and the nature and thickness of the soil overburden, as determined by field mapping, sampling, structural geology measurements, and seismic refraction surveys.

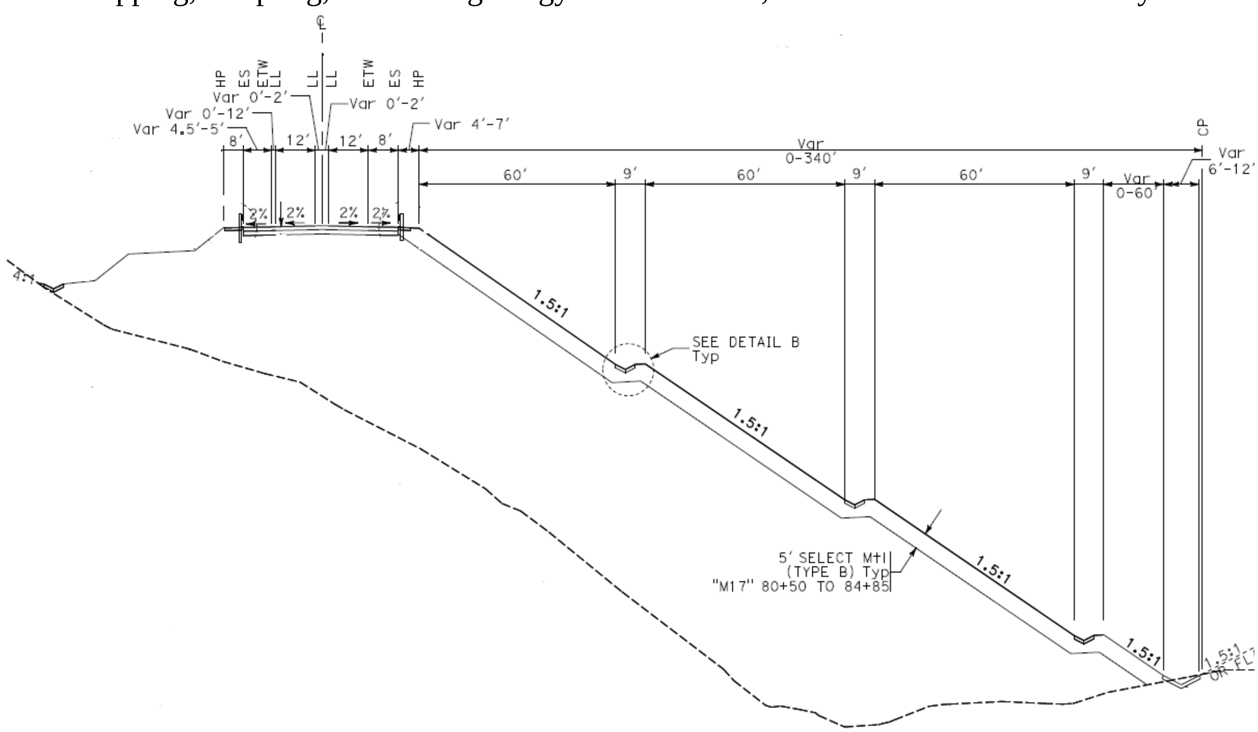

Figure 17: Cross Section of typical fill constructed at 1.5:1 showing outer layer of select rock material (5 ft thick perpendicular to slope face) and drainage ditches that are lined with gabion mattresses underlain by impermeable geomembrane. Some fills are up to 270 ft in height and extend horizontally up to 340 ft from hinge point to toe.

Many cut slopes were designed with 2 or 3 slope ratios, with the top soil overburden being typically cut at 1:1, the underlying upper rock being cut at a ratio somewhere between 0.75:1 and 0.5:1, and the lower portion of the cut being cut even steeper where seismic refraction velocities indicated sufficiently competent rock (Figure 15).

Embankment and fill slopes were designed up to 270 ft in height at a slope ratio of 1.5:1. Slope ratios flatter than 1.5:1 were untenable because such fills would extend so far down their respective valleys that they would impinge upon Willow Creek below, which would create significant engineering problems and greatly increase cost. In all but one of the projects, where cuts involve at least some DG material, fills were designed with an outside encapsulation of rock taken from select locations (select material) within the rock cuts in order to protect the fills, particularly those containing highly erosive DG material, from erosion. This encapsulation, which is 5 feet thick perpendicular to the face of the slope (or 9.3 ft horizontally), is laid out lift by lift with the other fill material and compacted at the same time lift by lift (Figure 17). In addition, sloping drainage ditches, lined with gabion mattresses underlain by impermeable linear low density polyethylene geomembranes, are constructed on the rock face as the fill is built up. This approach to encapsulation and ditch construction provides assurance that there will be no destructive erosion issues on these fills during the overwinter period (between two consecutive construction seasons), or during a potential summer squall, or after construction is complete. In order to attain the maximum phi angle on the DG-containing fills, fill compaction on those projects involving at least some DG is specified at 93%, which represents the best balance between dense compaction and avoiding excessive flooding during wetting.

STOP 3: Rocky Point

Naturally Occurring Asbestos (NOA) in California Highway Construction-Overview

Figure 18: View of asbestos at the Rocky Point location.

Naturally Occurring Asbestos (NOA) is present in specific minerals and geological formations that are common in California. When soil or rock of ultramafic origin is disturbed, particularly under conditions where rock is broken or crushed, there is a potential for releasing NOA in the form of asbestos fiber containing dust. The primary source of NOA in California soil is serpentinite, which is a variety of ultramafic rock. The asbestos in serpentinite is a specific type called "chrysotile," which is the most common type of asbestos found in

California. The other broad category of asbestos minerals falls under the classification of "amphiboles" and includes crocidolite, amosite, anthophyllite asbestos, tremolite asbestos, and actinolite asbestos.

In California, NOA is regulated by federal, state, and local agencies. Agencies with enforcement responsibilities including the following:

1. **U.S. EPA –** The Clean Air Act section known as National Emission Standards for Hazardous Air Pollutants (NESHAP) [40 Code of Federal Regulations (CFR) Part 61, Subpart M] established asbestos as an airborne contaminant that is known to be hazardous to human health.
2. **OSHA** – Established worker standards for permissible exposure limits to asbestos, enforceable at the state level by Cal/OSHA.
3. **State of California-California Air Resources Board (CARB) –** Responsible for airborne releases and enforces protection of the public from asbestos-related health hazards, including the management of asbestos risks to workers. In designated areas local Air Quality Management District's will be the primary regulatory agency.
4. **State of California Department of Toxic Substances Control (DTSC)** – The Hazardous Substance Account Act [Chapter 6.8 of the California Health and Safety Code] regulates material containing NOA.

Figure 19: View of a small rockslide at the Rocky Point location.

California Air Resources Board (CARB) Method 435, *Determination of Asbestos Content of Serpentine Aggregate*, measures asbestos quantitatively. The method uses Plain Light Microscopy (PLM) and a point counting method to determine the percentage of asbestos fibers in a bulk sample, and is the primary analytical method for measuring percent NOA in samples collected from project sites. Additional analysis using Transmission Electron Microscopy may be used for confirmation.

NOA is considered to be present at the project site if the percent asbestos, as determined using CARB Method 435, is 0.25% or greater, according to the Airborne Toxic Control Measure (ACTM) for Construction, Grading, Quarrying, and Surface Mining operations [California Code of Regulations, Title 17).

The Department of Toxic Substances Control sets a threshold of 1% for classifying NOA as a hazardous material. Material composed of 1% or more NOA is considered a “hazardous waste” when disposed of outside the right-of-way and must be removed, hauled, and disposed of in accordance with federal, state, and local laws and regulations.

Under the CARB ACTM, an Asbestos Dust Mitigation Plan (ADMP) is required for construction or grading projects where the area to be disturbed is greater than 1 acre. The ADMP is to be submitted to and approved by the Air Quality Management District/Air Pollution Control District (AQMD/APCD) before the initiation of any construction or grading activity. An ADMP typically will be prepared by a contractor/consultant and will detail the installation of engineering controls to mitigate potentially NOA containing dust. The ADMP will address track-out control, storage, dust mitigation, off-site transport, post-construction stabilization, air monitoring, etc.

"Rocky Point" Passing Lane and Highway Widening Project-Postmile 56.0, State Route 299 in Trinity County, CA

The Rocky Point Project was a passing lane and highway widening project on SR299, east of the City of Weaverville in Trinity County, implemented in 2006 at an estimated cost of 4.2 million dollars. Controlled blasting in ultramafic serpentinite bedrock cuts above the highway was required. Testing of the material indicated that NOA was present as high as 12.5% (ARB Method 435). During the construction, local media was alerted and significant public outcry occurred regarding the potential for dust containing asbestos to impact the travelling public and nearby residents. A dust mitigation control plan was prepared and implemented. A Health and Safety plan including air monitoring for workers was prepared by a Certified Industrial Hygienist. The air samples were collected using personal air sampling pumps worn by construction personnel during operations. The data collected indicated that none of the workers monitored were exposed to a concentration of airborne filters above the 0.1 fibers/cc permissible exposure limit (PEL) as established by OSHA.

All excavated NOA material was placed with a minimum cover of 4-6 inches on slopes no greater than 20%. In 2007, the year after construction a 1200 cubic yard slide occurred in the new cut slope. The slide debris was removed and the material was appropriately disposed of.

LUNCH: Oregon Mountain

Figure 20: Photograph showing the La Grange Mine area and the La Grange Fault crossing SR299 (CGS County Report 4).

Oregon Mountain holds interest on several geologic occurrences. The La Grange Fault, identified early on as a normal fault, has been more specifically identified as a large scale detachment fault. Detachment faults are low-angle (about 20 degrees) normal faults, where large sections of overlying geologic material have extensionally separated from the underlying units, creating a fenster where underlying formations are exposed. The highway crosses the fault just west of the large cutslope (Figures 20, 21 and 22).

Another item of interest in this area is the La Grange Mine, which encompassed much of the area along the highway just west of Oregon Mountain Summit (Figure 23). The La Grange Mine was one of the largest hydraulic mines in the State. During the Tertiary, rivers eroded the gold-bearing veins of the metamorphic and plutonic rocks and deposited the gold in the streambeds. Subsequent tectonism elevated these placer deposits, which were recognized by the early miners. Hydraulicking, or jetting of water through water cannons, was utilized as the most efficient way of removing both the overburden and these auriferous gravels. The water broke down the gravels, and gravity segregation of the high-specific-gravity gold was accomplished by large-scale sluicing.

Figure 21: Photograph looking roughly parallel along the La Grange Fault.

Figure 22: Photograph showing the cataclasite on the La Grange Fault surface.

Although hydraulic mining proved to be the most efficient way of extracting the placer ore, it was also very efficient at clogging the rivers, affecting habitat and causing extensive damage to agricultural fields in the valleys below these areas. Eventually, in 1884, a court decision was handed down, which forbade the release of hydraulic debris from mines when it would adversely affect downstream citizens and habitat. Although this decision did not specifically ban hydraulic mining, it effectively ended its use in the Sierra Nevada because of the expense and impracticality of building structures to retain the massive quantities of debris. In some parts of California, however, hydraulic mining continued into the 1900's.

The La Grange Mine can be seen to the east of our lunch location.

Figure 23: View of hydraulic mining at the La Grange mine in 1914.

STOP 4: Oregon Mountain

This location has experienced local and global instabilities since it was first constructed in 1920. The original roadway consisted of 10-foot wide lanes with little to no shoulder. Cut slopes were 1:1 with heights up to 40-feet, which contributed to much of the local instabilities observed.

The geology of the area, as well as the high rainfall amounts, assisted in causing the slides and slip outs observed at this location. The lithologies here consist of Devonian metamorphic rocks (Abrams Schist and Salmon Schist) as well as younger sedimentary rocks (Weaverville Formation). At this location, the La Grange Fault intersects two additional, unnamed faults.

The roadway at Oregon Mountain was experiencing heave in the late 1990's and early 2000's. The heave was associated with a large landslide situated on the left (east) side of the roadway that incorporated the roadway section. A fatality collision occurred due to the heave and other factors. Frequent maintenance was required to clean earth material off of the roadway, often during storms in the middle of the night. These problems prompted a roadway safety rehabilitation project in 2001.

A large slip out was reconstructed and buttressed against the opposite side of Oregon Gulch. The existing shoulder was widened to a catchment area for the deposition of slide material without affecting the roadway. Full depth asphalt concrete reconstruction was performed to buffer the continuing heave and allow Maintenance to cold plane, keeping the road smooth. The curves were improved. Ditches both upslope and down slope were lined with Rock Slope Protection (RSP) or gabions to help prevent future erosion.

The results indicate that the previously repaired slip out is stable. In general, slides occur with less frequency, and can be cleaned in a routine fashion as opposed to emergency. Although heave still occurs, the roadway is less affected due to the realignment. The roadside ditches are traversable and stable, making a safer roadway in this section.

Figure 24: Views showing storm damage at the Oregon Mountain location

STOP 5: Storm Damage Locations

Figure 25: Series of photographs (left and above) showing roadway settlement at post mile 49.2. The settlement was due to loss of lateral stability in the embankment fill. The embankment was stabilized utilizing a system designed and manufactured by Landslide Solutions, Inc.

Figure 26: Series of photographs (below) showing roadway settlement in 2003 due to a slide at post mile 49.8. The slide depth at the wall location was 35-feet. In this case, a soldier pile wall with two levels of ground anchors and timber lagging was utilized to stabilize the slide. The lagging was installed to a 20-foot depth and the anchors were installed on 8-foot centers. The wall was founded on double steel H-piles in 3-foot drilled shafts.

STOP 6: Top of Buckhorn Summit

The realignment of the Buckhorn Grade will require reconstructing over seven miles of California SR299. Over the seven plus miles, the elevation ranges from 3280 feet down to 1460 feet. The soil type within the project limits ranges from decomposed granite in the upper reaches to metasedimentary rocks at the eastern end. When the entire Buckhorn Grade is realigned, approximately 2.8 million cubic yards of earth will have been excavated and new embankments constructed. To date, three projects have been completed, one major contract is currently under construction, another will be advertised shortly, and the last contract will begin construction in 2015. Balancing earthwork within the individual project limits and staging construction to minimize traffic delays has been a driving force throughout the design process. Cooperation between the Highway Engineers and the Geotechnical Engineers is critical to successfully managing the many risks associated with the complexity of the materials and terrain while remaining within the overall project funding limits.

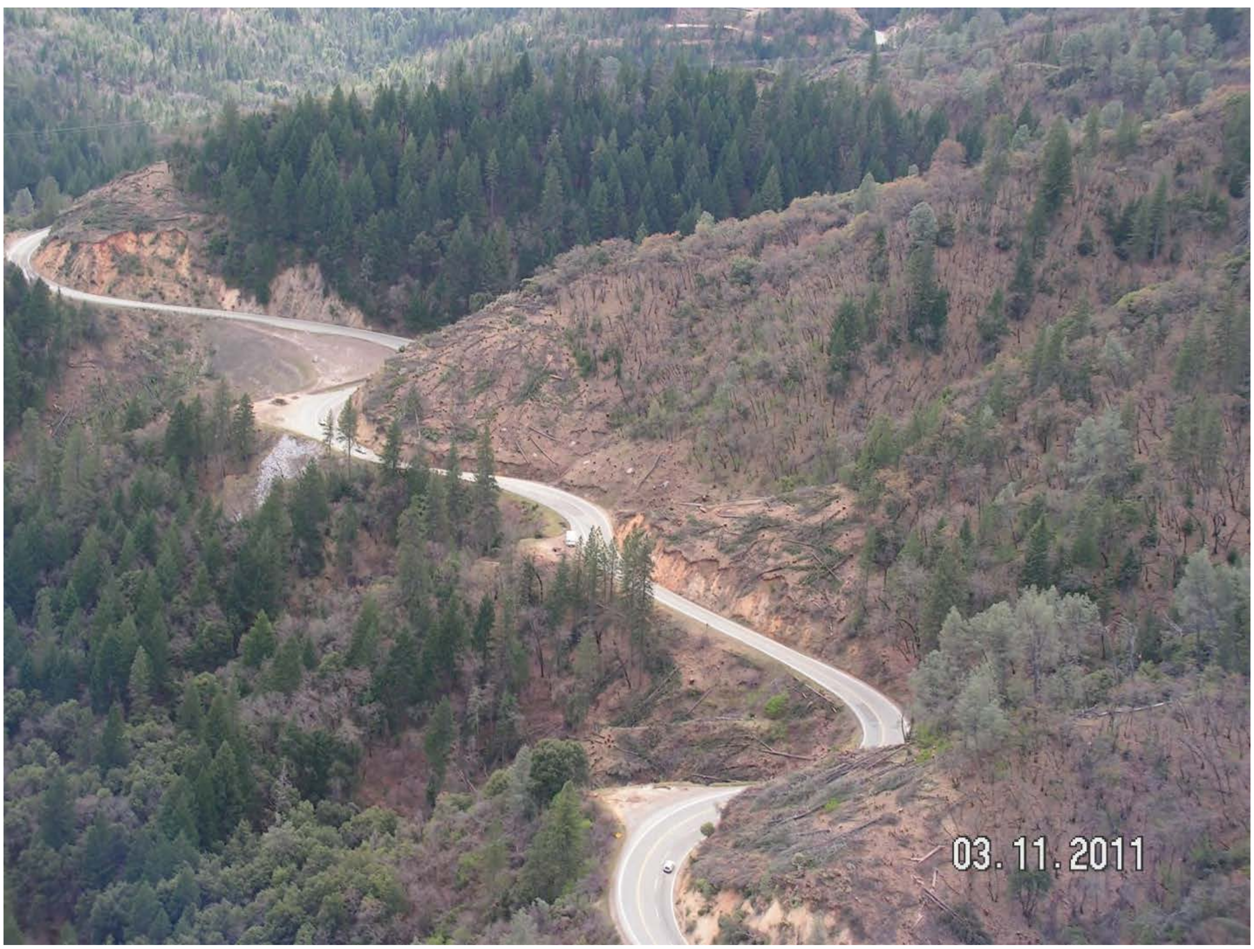

Figure 27: View of SR299 west of Buckhorn Summit.

References

Alpers, C.N., Hunerlach, M.P., May, J.T., and Hotham, R.L., Mercury contamination from historical gold mining in California: United States Geological Survey, Fact Sheet 2005-3014 Version 1.1, November, 2005.

Cashman, S.M. and Cashman, K.V., Cataclastic textures in La Grange fault rocks, Klamath Mountains, California:, Geological Society of America Special Paper, , Vol. 410, pp.443-450, 2006.

Cashman, S.M. and Elder, D.R., Post-Nevadan detachment faulting in the Klamath Mountains, California: Geological Society of America Bulletin,; v. 114, no. 12; pp. 1520-1534, 2002.

Clinkenbeard, J.P., Churchill, R.K., and Lee, K., Guidelines for geologic investigations of naturally occurring asbestos in California: California Geological Survey Special Publication 124, 70 p., 2002.

Fraticelli, L.A, Albers, J.P., Irwin, W.P.,and Blake, M.C., Geologic map of the Redding 1x2 degree quadrangle, Shasta, Tehama, Humboldt, and Trinity Counties, California:United States Geological Survey, Open File Report 87-257, 1987.

Harwood, D.S. and Helley, E.J., Late Cenozoic tectonism of the Sacramento Valley, California, United States Geological Survey, Professional Paper 1359, 1987.

Higgins, C.T., Churchill, R.K. and Downey, C.I., Preliminary assessment of mineral occurrences and mining-related substances along SR299 between Buckhorn Summit and Montgomery Creek, Shasta County, California: California Geological Survey technical report prepared for the California Department of Transportation under Interagency Agreement No. 43A0185, 161 p., 2009. (Source of fold-out geologic map, from Redding to Buckhorn Summit.)

Higgins, C.T., Downey, C.I. and Churchill, R.K., Preliminary assessment of mineral occurrences and mining-related substances along SR299 between Arcata and Buckhorn Summit, Humboldt and Trinity Counties, California: California Geological Survey technical report prepared for the California Department of Transportation under Interagency Agreement No. 43A0185, 183 p., 2009. (Source of fold-out geologic map, from Buckhorn Summit.to Junction City.)

Hollister, V.F. and Evans, J.R., Geology of the Redding quadrangle, Shasta County, California, California Geological Survey, MS004, 1965.

Irwin, W.P., Preliminary geologic map of the Weaverville Quadrangle, California: U.S. Geological Survey Miscellaneous Field Studies Map MF-275, scale 1:62,500, 1963.

Irwin, W.P., Geologic Map of the Klamath Mountains, California and Oregon: U.S. Geological Survey Miscellaneous Investigation Series Map I-2148, scale 1:500,000, 1994.

Irwin, W.P., Field guide for a Geomar and University of Kiel trip across the accreted terranes of the southern Klamath Mountains, California: U.S. Geological Survey Open-File Report 97-288, 1997.

Note 36, California Geomorphic Provinces, California Geological Survey, 2002.

Silberman, M.L., Hassemer, J.R., Force, J.,and Tripp, R.B., Assessment of the mineral resource potential of the Redding 1:250,000 Quadrangle, Northwestern California:, United States Geological Survey, Open File Report 93-0296, 1994.

Silberman, M.L.and Danielson, J., Geologic setting, characteristics, and geochemistry of gold-bearing quartz Veins in the Klamath Mountains in the Redding 1x2 degree quadrangle, Northern California: United States Geological Survey, Open File Report, 91-595, 1991.

Strand, R.G., Geologic map of California: Redding Sheet, California Geological Survey, GAM011, 1962.

The Robinson Library, Important Dates in California, http://www.robinsonlibrary.com/america/uslocal/pacific/california/history/dates.htm

e-Reference Desk, California History Timeline, Important Dates, Events, and Milestones, http://www.e-referencedesk.com/resources/state-history-timeline/california.html

California History, Resources for Teachers and Students, http://www.debbiesthemes.com/calhistory/

Dam Builders Celebrate Memories of Shasta Dam, United States Department of Reclamation, May 4, 2011, http://www.usbr.gov/newsroom/newsrelease/detail.cfm?RecordID=36122

Acknowledgements

63rd Highway Geology Symposium Local Committee

Bill Webster CEG	Caltrans, Engineering Geologist
Roy Bibbens GE	Caltrans, Chief, Office of Geotechnical Design North
Charlie Narwold CEG	Caltrans, Senior Engineering Geologist
John D. Duffy CEG	Caltrans, Senior Engineering Geologist
Thomas Whitman CEG	Caltrans, Senior Engineering Geologist
Brian Hinman PE	Caltrans, Senior Transportation Engineer
Scott Lewis CEG	Caltrans, Engineering Geologist
Brandon Badeker CEG	Caltrans, Engineering Geologist
Chris Koepke CEG	Caltrans, Engineering Geologist
Richard Rusnak PE	Caltrans, Transportation Engineer

California Geological Survey Local Organizing Committee

Chris Wills CEG	CGS, Supervising Engineering Geologist
Chris Higgins PG	CGS, Senior Geologist

Symposium Sponsors

Gannett Fleming, Inc.
Geobrugg North America, LLC
Golder and Associates
HI-Tech Rockfall Construction
Landslide Solutions Inc.
Maccaferri, Inc.
Zonge Geophysics

Symposium Exhibitors

AIS Construction Company
Carlsons Construction
Central Mine Equipment
Chama Valley Production
Gannett Fleming, Inc.
Geobrugg North America, LLC
Geodaq
Geokon, Inc.
Golder and Associates
HI-Tech Rockfall Construction
Horn and Associates
Janod Inc.
Kane GeoTech Inc.
Kleinfelder
Landslide Solutions Inc.
Maccaferri, Inc.
Shannon&Wilson Inc.
Trumer Schutzbauten
Williams Form Engineering Corp.
Zonge Geophysics

Special Thanks to

John Parrish PG	CGS, California State Geologist
James Davis PE	Caltrans, Acting Division Chief, Division of Engineering Services
Phil Stolarski PE	Caltrans, Chief, Materials Engineering & Testingand Geotechnical Services
John Bulinski PE	Caltrans, District 2 Director
Stephen Most	Keynote Speaker
Brian Rasmussen	National Parks Service

California Geological Survey
Caltrans District 2 Maintenance
Mount Lassen Motor Transit, Inc.
Fat Daddy's Barbeque